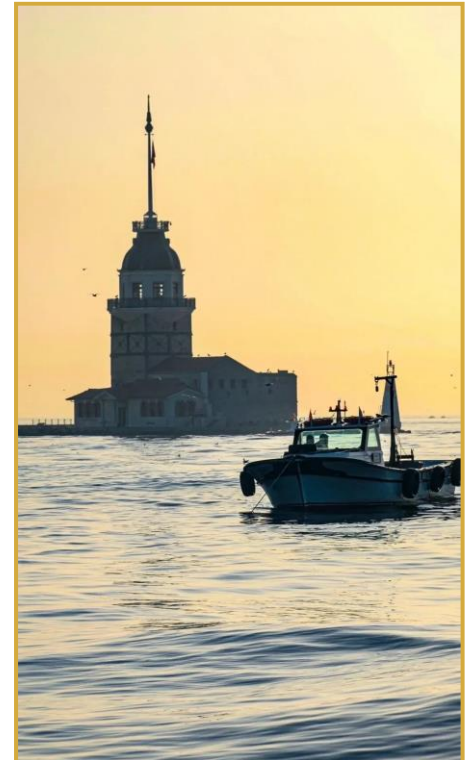


IWA 4th Regional Conference on Diffuse Pollution & Eutrophication



Proceedings Book

24-28 October, 2022
İstanbul, Türkiye



ODTÜ METU

www.iwadipcon2022.org



IWA DIPCON 2022

October 24-28, 2022 İstanbul-Türkiye

**Proceedings of the 4th IWA Regional Conference on
Diffuse Pollution & Eutrophication**

DIPCON 2022
İstanbul, Türkiye

EDITORS

Prof. Dr. Cevza Melek Kazezyılmaz-Alhan

İstanbul University-Cerrahpaşa

Prof. Dr. Nadim Copty

Boğaziçi University

Compiled by

Kavsar Bako

İstanbul University-Cerrahpaşa

ISBN: 978-605-7880-13-0

Table of Contents

Preface	11
Local Organizing Committee	13
International Programme Committee	14
Organizers	15
Sponsors	16
Keynote Speakers	19
Detailed Program	23
Climate Change Adaption and Mitigation	29
Modifying the RUSLE Factors to Develop Site-Specific Land Management Practices against Rainfall-Induced Erosion	30
<i>Denzel Keith G. Urieta, Kirk Dominick P. Bautista, Adrian Vaughn L. Noriega, Michael Irvin H. So, and Marla Maniquiz-Redillas</i>	
Analysis of Cooling and Heating Effects During Heat Waves and Cold Waves Using Blue-Green Roof Technology	33
<i>Mun Soo Na, Sung Min Cha, Seung Won Lee, Jung Min Lee and Sang Rae Kim</i>	
Resilience in Water Supply Systems: Towards a Water-Wise City	37
<i>Tuğba Akdeniz, I. Ethem Karadirek</i>	
Climate Change Induced Water Scarcity Risk Assessment: Coupling of MCDA-AHP Methods with QGIS	43
<i>Sena Ödensoy and Başak Güven</i>	
Mitigation of Diffusion Pollution through Circular Economy	49
<i>Ece Demir, Emre Alp</i>	
Estimation of Infiltrated Runoff Coefficient for Predicting Infiltrated Water of the Permeable Pavement LID System Considering the Cross Section	54
<i>Jaerock Park, Kyungmo Im, Youngjae Seo and Hyunsuk Shin</i>	
Development of a Steady State-Analytical Watedbody Network Modeling Tool to Identify the Individual Impacts of Multiple Point and Diffuse Nuntrient Emissions	61
<i>Ali Ertürk, Cenk Gürevin, Natalja Čerkasova</i>	
Water Footprint Concept and Forests	64
<i>Gafura A. Özdemir and Batın Mehmet Yer</i>	
Ecological Protection and Restoration	65
Using System Dynamics Modelling to Visualize the Effects of Resource Management and Policy Interventions on Biodiversity at a Regional Scale	66
<i>Chrysi Laspidou, Konstantinos Ziliaskopoulos</i>	
Characteristics of Vegetation Succession in the Exposed Land Caused by the Opening of the Floodgate in Sejong Weir, Geumgang River, South Korea	70
<i>Kim YoonSeo, Park Jae-Hoon, Kim Eui-Joo, Lee Jung-Min, Park Ji-Won, Kim Se-Hee, and You Young-Han</i>	
Vegetation and Flora of Gongju and Baekje Weir in Geumgang River, Korea	77
<i>Jung-Min Lee, Jae-young No, Eui-joo Kim, Ji-won Park, Yoon-seo Kim, Se-hee Kim, Jae-hoon Park and Young-han You</i>	

Development of an Algorithm for the Detection of Forest Fire Spread in Areas without Internet Connection	81
<i>Çağdaş Tari, Elçin Tan, and Sevinç Asilhan Sırdaş</i>	
Estimation of the Soil Erodibility Factor (K) for the Marmara Region of Turkey with the RUSLE Model Using GIS Techniques	82
<i>Ezer A., Guven B.</i>	
Plant Community, Net Primary Production and Soil Environment Factors in Estuary, Korea	115
<i>Ji-won Park, Eui-joo Kim, Jung-Min Lee, Yoon-seo Kim, Jae-Hoon Park Se-hee Kim and Young-han You</i>	
Ecological Assessment of Waterfront Space Using Plants of Weirs in the Nakdong River Basin, Republic of Korea	119
<i>Eui-Joo Kim, Young-Sub Han, Jae-Hoon Park, Ji-Won Park, Jung-Min Lee, Yoon-Seo Kim, Se-Hee Kim and Young-Han You,</i>	
The Study on the Exotic Plant Management Considering on the Plant Life Form and Bird Population Characteristics at the Exposed Floodplain by Drawdown in South Korea	125
<i>Jae-Hoon Park, Ho-Joon Kim, Ji-Won Park, Jung-Min Lee, Eui-Joo Kim, Yoon-Seo Kim and Young-Han You</i>	
Characteristics of Habitat Environment and Population of Mankyua Chejuense, Endangered Endemic Fern in Korea	132
<i>Eui-Joo Kim, Ji-Won Park, Jung-Min Lee, Jae-Hoon Park, Yoon-Seo Kim, Se-Hee Kim and Young-Han You</i>	
Evaluation of EPA SWMM Modeling Performance of Infiltration Trench	138
<i>Kaan İlker Demirezen and Cevza Melek Kazezyılmaz-Alhan</i>	
Wetland Construction and Management	142
A Case Study of South Korea: Current Status and Performance Assessment of Treatment Wetlands	143
<i>Hyeseon Choi, Boram Kim, Nash Jett Reyes, Minsu Jeon and Leehyung Kim</i>	
Designing the Sizing Criteria for Free Water Surface Flow Constructed Wetland Based on River Flow Interpolation	147
<i>Miguel Antonio Campos, Nicanor Chan, John Kristoffer Chua, Sophia Claudette Gaudia, Sergi Garbanzos, and Marla Maniquiz-Redillas</i>	
Literature Analysis about Changing and Influence Factors in Wetland	151
<i>Younghoon Yoo, Jong-Gu Hwang Bo, Kisung Lee, and Soojun Kim</i>	
An Overview of Diffuse Pollution Management through Stormwater Treatment Wetlands	154
<i>Nash Jett DG. Reyes, Franz Kevin F.Geronimo, Heidi B. Guerra, Minsu Jeon, Lee-Hyung Kim</i>	
Nature Based Solutions and Implementations	157
Determining the Optimal LID Combination through Hydrological Performance Modeling and Cost-Effectiveness Analysis	158
<i>Sergi Garbanzos and Marla Maniquiz-Redillas</i>	
Comparison of Urban Stormwater Flow Reduction Using LID under a Centralized and Decentralized Scheme	162
<i>Marla Maniquiz-Redillas and Sergi Garbanzos</i>	
Hydraulic Behavior and Performance of Soil with Varying Infiltration Rates for Green Stormwater Infrastructures	165
<i>Heidi Guerra, Nash Jett Reyes, Franz Kevin Geronimo, Minsu Jeon, Lee-Hyung Kim</i>	

Development of Remediation Design for the <i>in-Situ</i> Treatment of Highway Runoff: Self Cleansing Ditches	168
<i>Ayush Pokharel</i>	
Evaluation of the Unit Pollutant Loads and Urban Heat Island Mitigation Function of Low Impact Development (LID) Technologies	178
<i>Md Tashdedul Haque, Nash Jett DG. Reyes, Heidi B. Guerra, Minsu Jeon, Lee-Hyung Kim</i>	
Modeling of the Rainfall-Watershed-Swale Experimental System by EPA SWMM	182
<i>Kebir Emre Saraçoğlu and Cevza Melek Kazezyılmaz-Alhan</i>	
Introduction and Review of Preliminary Consultation System for Low Impact Development to Reduce Outflows and Non-Point Source Pollutions	186
<i>Hyojeong Lee, Hyunsuk Shin, Jihyun Moon, Jaemoon Kim, Youngsu Jang</i>	
Evaluation of Water Balance for Green Roof Based on K-LIDM	189
<i>Jihyun Moon, Jaemoon Kim, Hyojeong Lee, Jaerock Park and Hyunsuk Shin</i>	
Investigating the Efficiency of Infiltration Trenches for Stormwater Peak Flow and Outflow Reduction Using SWMM	192
<i>Sergi Garbanzos, Johaimin Panalondong , Karlo Bryan Ng Cha, and Marla Maniquiz-Redillas</i>	
An Evaluation of Green Roof Modeling Performance of EPA SWMM	195
<i>Kavsar Bako, Cevza Melek Kazezyılmaz-Alhan</i>	
The Impact of LID Implementation on Surface Runoff by Using EPA SWMM	199
<i>Merve Dinçer, Sezar Gülbaz</i>	
A Land-Suitability Analysis for Low Impact Development Applications in Ankara, Turkey	200
<i>İlksen Şenocak, Hayrettin Onur Bektaş, Yasin Erkan, Gül Şimşek, Aysun Tuna, Sermin Çakıcı Alp, Mehdi H. Afşar, Emre Alp</i>	
Urban/Industrial Water	204
A Graph-Based Monitoring Framework of Sludge Bulking in Industrial Wastewater Treatment Plants via Dynamic Graph Embedding and Bayesian Networks	205
<i>Jorge Loy-Benitez, Shahzeb Tariq, SungKu Heo, Taeyong Woo, Sangyoun Kim, ChangKyoo Yoo</i>	
Novel Porous Geopolymer Granules to Control Diffuse Pollution and Eutrophication Related to Ammonium Nitrogen	211
<i>Yangmei Yu, Tero Luukkonen,</i>	
Rainwater Reuse Evaluation by Design Capacity of Rainwater Utilization Facilities	214
<i>Changyeon Won, Inkyeong Sim, Jeongyong Lee , Heeman Kang</i>	
Evaluation of Heavy Metal Sorption Capacities of Cellulose Based Adsorbents with Ionic Functional Groups – Aqueous Cobalt (II) Ion Removal –	217
<i>Abdifatah A. Hashi, Buket Erdoğan, Yağmur Kuzucu, Serdar Şam, Gül G. Hacıosmanoğlu, Abdelhadi F. M. Deghles, Othman A. Hamed, and Zehra S. Can</i>	
Sustainable Cities for the Future with the Sustainable Urban Water Management	224
<i>Rouhollah Nasirzadehdizaji</i>	
Emerging Pollutants	228
Kinetics of the Photolytic and Photocatalytic Degradation of Veterinary Antibiotics	229
<i>Johanna Zambrano, Pedro Antonio García-Encina, Juan José Jiménez, Rebeca López-Serna, Rubén Irusta-Mata</i>	

Pharmaceuticals Residues and Biocides from Biosolids and Manure Spread as Fertilizers: First Results after One Year Field Study	239
<i>Pernin Noémie, Benoit Pierre, Patureau Dominique, Wiest Laure , and Bertrand-Krajewski Jean-Luc</i>	
Modeling of Regionalized PFOA and Pfos Emissions in Austria	243
<i>Steffen Kittlaus, Matthias Zessner, and Ottavia Zobolia</i>	
Estimation of Biodegradation Potential of Pharmaceuticals by Biowin Models and Comparison with Experimental Data	246
<i>Başak Kılıç and Ferhan Çeçen</i>	
Resistance to Benzalkonium Chlorides Favors Antibiotic Resistance	249
<i>Gökçin Gül, Ulaş Tezel</i>	
Vuv Induced Photo-Oxidation of Imidacloprid in Aqueous Solution	255
<i>S.L. Sanin, H. Derin</i>	
Integrated Watershed Management	259
Decision Support System for Selective Withdrawal in Water Supply Reservoirs: an Approach Based on Thermal Stratification	260
<i>Elif Soyer, Haluk Bayram, Nalan Canigeniş, and Onur Eren</i>	
Estimating Diffuse Nutrient Loads of Melen Watershed by Using Soil and Water Assesment Tool (SWAT)	266
<i>Gokhan Cuceloglu, Alpaslan Ekdal, Melike Gurel and Nusret Karakaya</i>	
Investigating Applicability of Grassed Waterway Practice with Geographic Information System	269
<i>Mehmet Kalfazade, Alpaslan Ekdal</i>	
Integrating Protected Area Management with River Basin Management Plans as a Measure to Address Diffuse Pollution	272
<i>Cronin Lisa, Regan Fiona, and Lucy Frances</i>	
Compliance Checking for Modelled N and P Loads in Surface Waters and Gap Analysis for Reaching MSFD and WFD Targets	278
<i>Venohr Markus, Nguyen Hong Hanh, Kunkel Ralf and Tetzlaff Björn</i>	
Coupled Modelling Application for Climate Change Impact Assessment in the Nemunas River Watershed – Curonian Lagoon – Baltic Sea Continuum	281
<i>Natalja Čerkasova, Georg Umgieser, Ali Ertürk, Rasa Idzelytė, Jovita Mėžinė</i>	
A Study on the Selection Method of Water Cycle Priority Management Basin Based on HSPF	284
<i>Jaemoon Kim, Jongseok Baek, Hyojeong Lee, Jihyun Moon and Hyunsuk Shin</i>	
A Novel Design for Sediments' Filtration/Entrapment System at Decentralized Infiltration Facilities	287
<i>O. Dawoud</i>	
The Characteristics of Distribution and Environmental Factor of Vegetation in Western and Southern Coast in Korea	292
<i>Ji-won Park, Eui-joo Kim, Jung-Min Lee, Yoon-seo Kim, Jae-hoon Park, Se-hee Kim, and Young-han You</i>	
Monitoring and Modeling	298
Systemic Hydraulic Fracturing Chemical Risk Indicators for Assessing Relative Hazard Levels to Water Supply	299
<i>Christopher Hill, Om Prakash Yadav, and Eakalak Khan</i>	

Development of a Microfluidic System for the Colorimetric Detection of the Diffuse Pollution of Phosphate in Fresh Water Systems	300
<i>Rachel Bracker, Harry Beggy, Louis Free, Joyce O'Grady, Sean Power, Karen Daly, Nigel Kent, Fiona Regan, Blánaid White</i>	
Diffuse N- and P-Inputs into Surface Waters of Germany	302
<i>Kunkel R., Kreins P., Nguyen H., Tetzlaff B., Venohr M., Wendland F., Wolters T., Zinnbauer M.</i>	
Investigation of Thermal Discharge Dilution at River Mouth Using Hydrodynamic Tools	305
<i>Fatih Yorgun, Mehmet Erbişim, Murat Aksel, Oral Yağcı and Şevket Çokgör</i>	
Optimizing the Annular Photocatalytic Reactor Configuration for the Degradation of Perfluorooctanoic Acid (PFOA) Using an Immobilized Titanium Dioxide (TiO ₂): a Computational Fluid Dynamics (CFD) Analysis	306
<i>Mikaila Denise H. Loanzon, and Joseph Albert M. Mendoza</i>	
Application of Machine Learning Classification and Regression Algorithms for Quantifying Nutrient Transport Considering Groundwater-Surface Water Interactions in an Agricultural Watershed in Canada	312
<i>Ahmed Elsayed, Sarah Rixon, Jana Levison, Andrew Binns, Pradeep Goel</i>	
Real Time Monitoring of Temperature Stratification to Respond to Eutrophication	314
<i>Özge Yücel-Bilen, Emrehan Berkay Çelebi, Utku Berkalp Ünalın, Emine Betül Şanlı, Serbay Şimşir, Süleyman Kazım Sömek, Aydoğa Kallem, Reza Ahmadian, Şimşek Demir, Ayşegül Aksoy</i>	
Model Based Eutrophication Assesment of Köycegiz Lake	320
<i>Elif Atasoy Aytuş, Elif Soyer, Ali Ertürk</i>	
Long-Term Spatial-Temporal Monitoring of Eutrophication in Lake Burdur Using Remote Sensing Data	324
<i>Serra Salgut, Gizem Tuna Tuynun, and Alper Elçi</i>	
Examining the Use of Gemstat Global Data Source for a Water Quality Model	333
<i>İsmail Bilal Peker, Sezar Gülbaz</i>	
Particulate Phozzylogic Index: Towards a More Accurate and Transparent Identification of Critical Source Areas to Mitigate Phosphorus Emissions	341
<i>Gerold Hepp, Ottavia Zoboli, Eva Strenge and Matthias Zessner</i>	
Meta-Research on Nutrient Transport in Surface Water and Groundwater Using a Text Mining Algorithm	344
<i>Ahmed Elsayed, Sarah Rixon, Christina Zeuner, Jana Levison, Andrew Binns, Pradeep Goel</i>	
Assessment of RUSLE's Cover Management Sub-Factors for Unidentified Urban Land-Use Classes	346
<i>A. Eljamassi; O. Dawoud; M. Davud</i>	
Modelling Potential Impacts of Climate Change on Heavy Metal Transport in Drainage Basins	351
<i>Kamil Çöllü, Muhammed Aslan, Zeynep Akdoğan, and Başak Güven</i>	
The Application of Atmospheric and Soil Sensors for Monitoring Nature-Based Stormwater Treatment Facilities	357
<i>Minsu Jeon, Nash Jett Reyes, Hyeseon Choi, and Leehyung Kim</i>	
Correlation Analysis Between Wetland Water Level and Rainfall in Janggün Wetland	360
<i>Junhyeong Lee, Jong-Gu Hwang Bo, Kisung Lee, and Soojun Kim</i>	

Groundwater Hydrology and Quality	362
A Laboratory Scale Examination of Salinity Intrusion Using Underground Dam <i>Akif Epcin, Ayse Nur Karayel, Babak Vaheddoost, Egemen Aras</i>	363
Assessing the Spatiotemporal Variability of Groundwater Level and Quality Using Hybrid VMD-DSE-K-Means Thechnique <i>Roghayeh Ghasempour, V. S. Ozgur Kirca, Seyed Mahdi Saghebian</i>	364
Engagement of Wash Entrepreneur to Address Groundwater Contamination <i>Shah Riazur Rahman,</i>	375
On Numerical Modeling of Groundwater Flow in Stream-Wetland-Aquifer Systems <i>Uğur BOYRAZ, Cevza Melek KAZEZYILMAZ-ALHAN</i>	376
Investigation of Lake-Aquifer Interactions with Experimental Methods <i>İnci Yalçın and Cevza Melek Kazezyılmaz-Alhan</i>	377
Nexus Approach	381
The Impact of Renewable Energy on Economic Growth in CEE Countries <i>Prof. Assoc. Dr. Doriana Matraku (Dervishi), Ph.D. student Kamela Selenica</i>	382
Prolonged Droughts Effects on Stream Nitrogen Dynamics in Central Germany <i>Seifeddine Jomaa, Xiangqian Zhou, Xiaoqiang Yang and Michael Rode</i>	391
Forecasting the Water Consumption of Hydroelectricity Power Plants in the Context of the Water-Energy Nexus Based on an Artificial Intelligence Approach <i>Cigdem Coskun Dilcar, and Merih Aydinalp Koksal</i>	392
Evaluation of the Water-Energy-Food Nexus in the Context of Precision Agriculture <i>Ezgi Özdemir, Emre Alp</i>	398
The WEF Nexus Approach to Achieve the Sustainable Development Goals <i>Alexandra E. Ioannou, Chrysi S. Laspidou</i>	405
The Impact of Renewable Energy on Economic Growth in CEE Countries <i>Prof. Assoc. Dr. Doriana Matraku (Dervishi), Ph.D. student Kamela Selenica</i>	408
Soil Contamination	417
Pesticides and Chemical Elements in Brazilian Pantanal Sediments <i>Silvio César Sampaio, Kathleen Jeniffer Model, Plínio Emanuel Rodrigues Silva, Floriano Luiz Suszek, Cleuciane Tillvitz do Nascimento, Natalia Pereira, Marcelo Bevilacqua Remor</i>	418
Occurrence of Hazardous Substances in Soils and River Suspended Sediment in 7 River Catchments within the Danube River Basin <i>Zsolt Jolankai, Adrienne Clement, Mate Kardos, Steffen Kittlaus, Nikolaus Weber, Ottavia Zobboli, , Oliver Gabriel, Martina Broer, Florentina Soare Carmen Hamchevici, Radoslav Tonev, Dimitar Mihalkov, Radmila Milacsic, Katarina Markovic, Lucija Levstek, Orsolya Szomolanyi, Matthias Zessner</i>	426
Impact of the Soil Stratification and Saturation on the Performance of Infiltration Boreholes <i>Ziyad Abunada, Wafa Alijla and Osama Dawoud</i>	429
Effect of Soil Microplastics on Seed Germination of Helianthus Annuus L. And Sorghum Bicolor L. <i>Mehmet Meric TUNALI, Merve TUNALI, Başak GÜVEN, Orhan YENİGÜN</i>	430
Fate and Transport of Some Commonly Used Pesticides in the Konya Plain, Turkey <i>Yağmur Ongar, Ulaş Tezel, Burak Demirel, and Nadim K. Copty</i>	434

Assessment of Surfactant-Enhanced in Situ Chemical Oxidation of Dnopl Source Zones <i>Zeynep Demiray, Nihat Hakan Akyol and Nadim Copty</i>	438
Estimating the Contribution of Road Sweeping in the Non-Point Pollutant Load Reduction in Highways and Expressways <i>Nash Jett DG. Reyes, Heeman Kang, Minsu Jeon, and Leehyung Kim</i>	439
Extreme Hydrologic Events	442
Regional Flood Loss Modelling of the Town of Bozkurt in Kastamonu, Turkey <i>Fidence Cyizere Rukundo, Ms. Candidate; Derya Deniz, Ph.D.; Yiğit Can Altan, Ph.D.</i>	443
Investigation of Flood Mitigation in Bozkurt District <i>Hayri BAYCAN, Uğur BOYRAZ,</i>	448
Elmali Dam Failure Analysis and Flood Disaster Simulation with Different Scenarios Using HEC-RAS 2D <i>İsmail Bilal Peker⁰, Abdülbaki Hacı⁰, Yasin Paşa⁰, Sezar Gülbaz⁰</i>	455
Flood Management for İstanbul Mega-City <i>Tunay ÇARPAR, Mohsen Mahmoody VANOLYA, Bulent KOCAMAN, Ali Osman ILGAZ, H. Kürşat TÜRKMEN, Tuğba ÖLMEZ HANCI, Şafak BAŞA</i>	461
Modelling and Simulation of Floods in a River Basin: First Phase towards Flood Management Using Nbs in the Oitaven-Verdugo River Basin (NW Spain) <i>Carolina Acuña Alonso, Lucia Martínez Portabales, Enrique Valero and Xana Álvarez</i>	473
Reservoir and Surface Water Bodies	477
Modelled Nitrate Concentrations in the Leachate of Germany - Compliance Checking and Gap Analysis for Reaching WFD Targets for Groundwater - <i>Kunkel Ralf, Wolters Tim and Wendland Frank</i>	478
Investigating Diffuse Pollution Dynamics in an Urban Catchment Area Using First Flush Analysis <i>Gil Cruz, Miguel Enrico Robles, Rommel Glenn Mendova and Marla Maniquiz-Redilla</i>	482
Antalya Water and Waste Water Authority (ASAT) Action Plan for Water Scarcity Caused by Climate Change <i>Cem Çakmak</i>	486
Evaluating the Proposed Check Dams Performances on Flood Mitigation in Bozkurt District <i>Hayri BAYCAN, Uğur BOYRAZ,</i>	490
Derivation of Dam Break Empirical Equation for Darlık Dam in İstanbul, Turkey <i>Abdülbaki Hacı, Ezgi Selen Tilav, İsmail Bilal Peker, Rasim Temur, Yasin Paşa, Sezar Gülbaz</i>	493

**19th IWA International Conference on Diffuse Pollution and Eutrophication
(IWA DIPCON 2019)**



Venue: Cheju Halla University, Jeju, Korea.

PREFACE

Dear Colleagues,

We are pleased to present the Proceeding book of the 4th IWA Regional Conference on Diffuse Pollution & Eutrophication (DIPCON) that was held in Istanbul, Türkiye from October 24-28, 2022. From widespread pesticide use to heavy metal emissions from vehicular transport to microplastic release into the environment, diffuse pollution has become a major threat to the environment. Widespread soil pollution and eutrophication of water bodies across all continents and their impacts on living organisms and human health are a stark manifestation of the challenges we face. Anticipated climate change is likely to exacerbate the risk to the water resources of numerous regions of the world. Addressing these challenges requires a concerted holistic approach by stakeholders including scientists, engineers, hydrologists, policy makers, NGOs, and water regulators, and awareness and participation on the part of the general public. The purpose of this conference was to bring together these various perspectives thereby contributing to the scientific debate towards alleviating these adverse environmental effects.

DIPCON 2022 was held in Istanbul, Türkiye with more than 120 participants from more than 21 countries. The city of Istanbul, a welcoming vibrant megacity with a magnificent history and natural beauty, is the ideal place to host this meeting. Joining two continents with shores on three different seas, the city underscores the need to protect the environment we live in for the benefit of all.

The conference papers are organized into 13 sessions designed to address the latest technologies and approaches to alleviate the impacts of diffusion pollution on the Environment:

- Reservoir and Surface Water Bodies
- Soil Contamination
- Groundwater Hydrology and Quality
- Emerging Pollutants
- Urban/Industrial Water
- Ecological Protection and Restoration
- Extreme Hydrological Events
- Climate Change Adaptation and Mitigation
- Nexus Approach
- Integrated Watershed Management
- Nature-Based Solutions and Implementation
- Wetland Construction and Managements
- Monitoring and Modeling

Participants at the DIPCON 2022 conference elucidated on the threat of diffuse pollution to surface water bodies, groundwater and soil environments and the latest strategies and technologies for environmental protection and restoration to address these threats. The adverse effects of extreme hydrological effects and projected climate change and the need to develop adaptation and mitigation strategies were highlighted. Recognizing the confluence of water, food and energy needs, along with the imperative to maintain ecological services, participants underlined the necessity to implement a Nexus approach and integrated water management plans that involve the active participation of all stakeholders. It is evident that societies need to resort to nature based solutions that balance the need for economic growth and food security with ecological protection. Speakers highlighted the need to utilize the latest technologies to develop models and monitoring tools at all scales for the sustainable use of available resources and the development of informed science-based policies.

We would like to particularly thank our keynote speakers: Prof. Miguel A. Medina, Jr. who discussed the potential impacts of climate change on surface and subsurface water resources; Prof. Mustafa M. Aral whose lecture was on the concept of optimal design in the management of water resources; Prof. Gang Liu who focused on the fate of microplastics in aquatic Environments; Prof. Damiá Barceló who discussed the fate and removal of pharmaceutical and emerging threats in rivers.

The conference was realized through concerted efforts of various parties. Foremost, we would like to thank all participants for sharing their latest research findings and insight and the lively discussions throughout the duration of the conference. We are also grateful to the support of IWA, in particular the Diffuse Pollution and Eutrophication Specialist Group for granting us the chance to host this conference series in Istanbul as well as their scientific and financial support. Special thanks to Istanbul University-Cerrahpaşa, Boğaziçi University, and Middle East Technical University for their support in the organization of the Conference. We also thank Istanbul University, which hosted the conference, and BUTEK for their support in financial matters. We express our sincere gratitude and appreciation to the tireless work of the Local Organizing Committee and International Programme Committee. Special thanks to our sponsors, BAŞARSOFT, SUBOR, DASK, YÜKSEL PROJECT, THY, NFB, VEOLIA and TÜBİTAK (The Scientific and Technological Research Council of Türkiye) for their sponsorship. Finally, we would like to thank UNESCO, SKATMK, NETCAD, İstanbul Metropolitan Municipality (İBB) and İstanbul Water and Sewerage Administration (İSKİ) for their support.

Sincerely,

Prof. Dr. Nadim Copty

Conference Co-Chair

IWA DIPCON 2022

Prof. Dr. Cevza Melek Kazezyılmaz-Alhan

Conference Chair

IWA DIPCON 2022

LOCAL ORGANIZING COMMITTEE

Cevza Melek Kazezyılmaz-Alhan	İstanbul University-Cerrahpaşa	Türkiye
Nadim Copty	Boğaziçi University	Türkiye
Sezar Gülbaz	İstanbul University-Cerrahpaşa	Türkiye
Dilek Eren Akyüz	İstanbul University-Cerrahpaşa	Türkiye
Uğur Boyraz	İstanbul University-Cerrahpaşa	Türkiye
Başak Güven	Boğaziçi University	Türkiye
Emre Alp	Middle East Technical University	Türkiye
İsmail Bilal Peker	İstanbul University-Cerrahpaşa	Türkiye
Kaan İlker Demirezen	İstanbul University-Cerrahpaşa	Türkiye

INTERNATIONAL PROGRAMME COMMITTEE

Alper Elçi	Dokuz Eylül University	Türkiye
Atsushi Ichiki	Ritsumeikan University	Japan
Başak Güven	Boğaziçi University	Türkiye
Cevza Melek Kazezyılmaz-Alhan	İstanbul University-Cerrahpaşa	Türkiye
Ceyda Uyguner Demirel	Boğaziçi University	Türkiye
Ceyhun Özçelik	Muğla Sıtkı Koçman University	Türkiye
Dilek Eren Akyüz	İstanbul University-Cerrahpaşa	Türkiye
Eakalak Khan	University of Nevada	USA
Emre Alp	Middle East Technical University	Türkiye
Eva Abal	The University of Queensland	Australia
Ferdinand Hellwegger	TU Berlin	Germany
Ferhan Çeçen	Boğaziçi University	Türkiye
Filiz Dadaşer Çelik	Erciyes University	Türkiye
Fiona Napier	Scottish Environment Protection Agency	UK
Fiona Regan	Dublin City University	Ireland
Fumiyuki Nakajima	The University of Tokyo	Japan
Hafzullah Aksoy	İstanbul Technical University	Türkiye
Katerina Schilling	Vienna Doctoral Programme on Water Resource Systems	Austria
Lee-Hyung Kim	Kongju National University	Korea
Luis Alberto Bravo-Inclan	Universidad Nacional Autónoma de México	Mexico
Markus Venohr	Leibniz Institute of Freshwater Ecology & Inland Fisheries	Germany
Marla Maniquiz-Redillas	De La Salle University Manila	Philippines
Mehmet Ali Küçükler	İzmir Institute of Technology	Türkiye
Melike Gürel	İstanbul Technical University	Türkiye
Mustafa Tamer Ayvaz	Pamukkale University	Türkiye
Mi-Hyun Park	University of Massachusetts Amherst	USA
Nadim Copty	Boğaziçi University	Türkiye
Puangrat Kajitvichyanukul	Chiang Mai University	Thailand
Ralf Kunkel	Forschungszentrum Jülich (DIPCON SG Chair)	Germany
Serdar Aydın	İstanbul University-Cerrahpaşa	Türkiye
Sezar Gülbaz	İstanbul University-Cerrahpaşa	Türkiye
Sungpyo Kim	Korea University	Korea
Uğur Boyraz	İstanbul University-Cerrahpaşa	Türkiye
Xiaoyan Wang	Fudan University	China
Xuyong Li	Chinese Academy of Sciences	China
Zehra Semra Can	Marmara University	Türkiye

ORGANIZERS

This conference is organized by



**the international
water association**

Diffuse Pollution Specialist Group



ODTÜ METU

SPONSORS



This conference is supported by Scientific and Technological Research Council of Türkiye (TÜBİTAK).

TÜBİTAK is the leading agency for management, funding and conduct of research in Türkiye. It was established in 1963 with a mission to advance science and technology, conduct research and support Turkish researchers. The Council is an autonomous institution and is governed by a Scientific Board whose members are selected from prominent scholars from universities, industry and research institutions.

GOLD SPONSORS



Başarsoft, has been producing Geographical Information Systems (GIS) and infrastructure solutions since 1997. Başarsoft and MapInfo products are used in many important geographic information systems projects that are ongoing today. In addition, since 2007, it is Turkey's navigation data provider for map services such as Google, iGO and Yandex.



Yüksel Proje which was formed in 1978 is providing engineering, design and construction management services in 30 countries. According to the data of ENR News Record Yüksel Proje is steadily rising in the list of the largest 225 design companies in the world, and maintains its place as one of the companies at the top of Türkiye's largest exporters list.



Subor Boru San. ve Tic. A.Ş. was founded via the partnership of "Yapı Merkezi Holding" ve "Amiantit Group of Companies" in 1996 to manufacture Fiberglass-Reinforced Polyester (CRP) pipes and sell those in domestic and overseas markets.



Established in 2000, the Turkish Catastrophe Insurance Pool (the TCIP) is a public institution with a legal identity responsible for the acquisition of Compulsory Earthquake Insurance by the public, its implementation and its management in Türkiye.

OTHER SPONSORS



Turkish Airlines is the official airline of “4th Regional Conference on Diffuse Pollution Eutrophication (DIPCON 2022)”, special discounts are offered for all delegates. To proceed with the online booking tool, please visit Turkish Airlines promocode website and use the event code “052TKM22” under the Promotion code section.



NFB is committed to providing high quality services to public and private sector organizations and institutions in the field of engineering and consulting. NFB Engineering and Consulting offers comprehensive solutions on Energy, Irrigation and Drainage, Flood Control and Protection, and Drinking - Potable Water Supply and Urban Infrastructure consultancy, feasibility, planning and design services with its trained personnel.



Around the globe, Veolia helps cities and industries to manage, optimize and make the most of their resources. The company provides an array of solutions related to water, energy and materials – with a focus on waste recovery – to promote the transition toward a circular economy.

Supporters



UNESCO is the United Nations Educational, Scientific and Cultural Organization. It seeks to build peace through international cooperation in education, sciences and culture.

UNESCO Turkey National Commission started its activities on August 25, 1949 as the only and legal representative of the General Directorate of UNESCO in Turkey.



Netcad, founded in Ankara in 1989, is the first domestic company pioneering to the digitalization of spatial data. Having been developed by the common contribution of Turkish engineers, academicians, and the users, Netcad is located at the core of spatial data ecosystem.



Turkish National Committee on Water Pollution Research and Control (TNC) is a non-profit organization founded in 1990. In addition to supporting research on water pollution, TNC also represents Turkey within IWA, creating connections with member committees from other countries and working collaboratively with them in vision of its goals and within the scope of its resources.

KEYNOTE SPEAKERS



Dr. Miguel A. Medina, Jr.

Professor Emeritus, Civil and Environmental Engineering,
Pratt School of Engineering, Duke University

Lecture Topic: Potential Impacts of Climate Change on Surface and Subsurface Hydrology and Contaminant Transport

Miguel Medina earned a Ph.D. degree in water resources and environmental engineering sciences from the University of Florida in 1976 and joined the Duke University engineering faculty thereafter. He has been a registered Professional Hydrologist since 1983. In 1984 he was selected a Fulbright Scholar, and spent 8 months at Monash University in Melbourne, Australia. Dr. Medina is a Past-President of the American Institute of Hydrology, a Fellow of the American Society of Civil Engineers (ASCE), past Associate Editor of the Journal of Hydrologic Engineering, member of the Executive Committee of the ASCE Committee on Adaptation to a Changing Climate (CACC), and member of the CACC Subcommittee on Hydroclimatology and Engineering Adaptation (HYDEA). He was named External Evaluator of the UNESCO International Hydrological Programme from 2002 to 2004, and the Lead Evaluator (2007) of the UNESCO World Water Assessment Programme. Professor Medina has conducted funded research in hydrologic and water quality mathematical modeling for the U.S. Environmental Protection Agency, the National Science Foundation, the Office of Water Research and Technology, the U.S. Air Force, the U.S. Army Waterways Experiment Station, the Naval Oceanographic Office, DuPont Engineering, the U.S. Geological Survey, the North Carolina Water Resources Research Institute, and the State of North Carolina. The results of his research are reported in such journals as *Advances in Water Resources*, *Water Resources Research*, *Journal of Hydrology*, *Journal of Contaminant Hydrology*, *Journal of Hydrologic Engineering*, *Journal of Hydraulic Engineering*, *Ground Water*, *Desalination*, *Environmental Modeling and Software*, *Applied Mathematics and Computation*, *Journal of the American Water Resources Association*, *Computing in Civil Engineering*, *Journal of Water Resources Planning and Management*, *Journal of Environmental Engineering*, *Hydrological Science and Technology*, and *Environmental Health Perspectives*.



Dr. Gang Liu

Professor and Team leader at Research center for eco-environmental sciences, Chinese Academy of Sciences

Lecture Topic: Characteristics and Fate of Nanoplastics in Water Environments

Prof. Dr. Gang Liu, finished his PhD at Delft University of Technology in 2013, and afterward worked as senior researcher at Oasen drinking water in the Netherlands. He was promoted to be assistant professor at Delft University of Technology in 2016. Since late 2018, he took the position of Professor and Team leader at Research center for eco-environmental sciences, Chinese Academy of Sciences. Now, he is visiting professor at Delft University of Technology. He has established green water processes lab and become the deputy director of CAS key lab on drinking water science and technology in 2020. His research focuses on nature-based water solutions, carbon neutral water systems and water environment biosafety, including viral safety. He is especially interested in simply, short and chemical free drinking water solutions based on riverbank filtration. More specifically, he developed new methodologies for measuring nanoplastics and viruses in aquatic environments, new concepts for assessing drinking water microbes and microbial ecology, and new models for constructing carbon neutral water systems combining water, carbon, material and resources flows. Currently, he is co-editor in chief for IWA flagship journal Water Science and Technology, managing editor for Blue Green Systems, and editors for Engineering, National Science Review, and Environmental Research. He is vice-president of Young Committee of Chinese Water Professional Association, and member of management committee of IWA specialist group Water Safety Planning, member of scientific committee for Health-Related Water Microbiology conference.



Dr. Damià Barceló

Professor, Catalan Institute for Water Research (ICRA)

Lecture Topic: Fate and Removal of Pharmaceuticals and new Threats in European Rivers under Water Scarcity and Global Change: The EU Globaqua project.

Full Professor IDAEA-CSIC, Spain. Since 2008 Director. Catalan Institute for Water Research (ICRA-CERCA). Girona, Spain. 2016 – 2020 Full Professor Chair in Biology. College of Science, King Saud University, Riyadh, Saudi Arabia. Distinguished Scientist Fellowship Program (DSFP). Doctor Honoris Causa by the Universities of Ioannina, Greece, in 2014 and by the University of Lleida, June 2021 and Almeria, Spain in May 2022, Honorary and Guest Professor at Zhejiang A & F University (ZAFU), Hangzhou, China in 2019 till March 2022. , Foreign Expert of East China University of Science & Technology, Shanghai, China, since January to December 2021 , Adjunct Professor in Sustainability Cluster, School of Engineering at the University of Petroleum and Energy Studies (UPES), Dehradun, Uttarakhand, India from January 2022-December 2026., .Recipharm Environmental Award, Sweden in 2012 , Prince Sultan Bin Abdulaziz International Prize for Water (PSIPW), 5th Award on Water Management & Protection, Saudi Arabia in 2012 and Prize King Jaime I on the Protection of Nature from Generalitat of Valencia, Spain in 2007 .

SUPERVISION OF STUDENTS: 1992 – to date > 67 PhD thesis supervised, mainly in Spain except two in Lisbon and in Amsterdam and one in Riyadh., 1992 – 2021.

EXPERTISE: Analysis, fate, risk and removal of emerging contaminants and microplastics from water, Sewage epidemiology of drugs and proteins. Since 2010 I am listed as highly cited scientists , ISI Highly Cited, , with a Hirsch-Index of 170 (130) and total number of citations over 128.000 thousand (> 83 k) and more than 1600 publications (source Google Scholar on July 11, 2022, Web of Science in parenthesis).

EDITORIAL ACTIVITIES:

1990-2022, Editor of Trends in Analytical Chemistry (TrAC), Elsevier

Since 2012 Co-Editor-in-chief of the Science of the Total Environment, Elsevier

Since 2017 Editor in chief of Current Opinion in Environmental Science and Health, Elsevier

Since 2020 Co-Editor in Chief of Case Studies of Chemical and Environmental Engineering, Elsevier.

Since 2022. Co-editor in Chief of Methods X, Elsevier

Since 2017 Editor of Process Safety and Environmental Protection, Elsevier

Since 2021, Senior Editor of Green Analytical Chemistry, Elsevier

Editor of three book series:

Comprehensive Analytical Chemistry, Elsevier,

Advances in Chemical Pollution and Environmental Management and Protection, Academic Press- Elsevier and The Handbook of Environmental Chemistry from Springer-Nature



Dr. Mustafa M. Aral

Professor Emeritus, School of Civil and Environmental Engineering,
College of Engineering, Georgia Institute of Technology, USA

***Lecture Topic: Optimal Design Concepts in Water Resources
Management***

Dr. Aral received his BS degree in 1967 from Civil Eng. Dept. at Middle East Tech. Univ. (METU), Ankara, Türkiye, His MS (1969) and PhD. degrees (1971) are from Civil and Env. Eng. Dept. at Georgia Institute of Technology, Atlanta, Georgia, USA. Upon completion of his graduate studies, he joined the faculty of Mathematics Dept. at METU as an Assistant Professor. During his tenure at METU he established the Applied Mathematics and Numerical Analysis division at the department; he was the Assistant Chairman of the Department for four years and served as Adjunct faculty at Marine Sciences (Mersin, METU) and Computer Sciences Departments. In 1977 he received his Doçent appointment from the Central University System of Türkiye in the field of Applied Mathematics and was appointed as Associate Professor at the Mathematics Department. In 1979 he was invited back to Georgia Institute of Technology where he served until 2018 as Professor and the Director of MESL Research Center which he established in 1993. In 2018 he was appointed as Professor Emeritus at Georgia Tech. During his career Dr. Aral has published over 200 technical publications in peer reviewed journals, five books, ten book chapters, over 300 hundred conference papers and numerous technical reports. He served as the Chair of several International Conferences. Among these the most noteworthy activities are the NATO Advanced Study Institute that he organized in Antalya, Türkiye in 1995; Env. Exposure and Health Conf. that was held in Atlanta, GA, USA in 2005; and he was the Tech. Chair of the ASCE/EWRI IPWE 2013 Int. Conf. that was held in Izmir, Türkiye in January 7-9, 2013. During 2009 he established the International Journal on “Water Quality, Exposure and Health” published by Springer Publishers. He was the Editor-in- Chief of this journal during 2009 - 2014. He is also on the Editorial Board of several technical journals and serves as a consultant and reviewer to European Framework programs. During his career he received twenty-eight honor citations from scientific organizations. Among these the most noteworthy national (USA) and international recognitions are Cuming Medal (2000); American Academy of Environmental Engineers Best Env. Health Research Awards (2003 and 2006); CDC Excellence in Applied Env. Health Research (2006); ASCE/EWRI James R. Croes Medal (2011); Dr. Aral is a Past-President of the American Institute of Hydrology, a Fellow of the American Society of Civil Engineers (ASCE). Dr. Aral served as the PhD advisor to 25 students who are now in academic and consulting fields in several countries around the world including Türkiye.

DETAILED PROGRAM

MONDAY, OCTOBER 24	
<i>09:30-11:00</i>	
<i>11:00-12:30</i>	
<i>12:30-13:30</i>	<i>Registration Opens</i>
<i>13:30-13:50</i>	<i>WORKSHOP: Emerging Contaminants in the Diffuse Pollution World</i> Eakalak Khan, University of Nevada
<i>13:50-14:15</i>	<i>WORKSHOP: Emerging Pollutants from Various Land Use Types</i> Lee-Hyung Kim, Kongju National University
<i>14:15-15:00</i>	<i>WORKSHOP: Land Use and Water Quality - The Impacts of Diffuse Pollution</i> Puangrat Kajitvichyanukul, Chiang Mai University
<i>15:00-15:15</i>	<i>Coffee Break</i>
<i>15:15-16:45</i>	<div style="display: flex; justify-content: space-between;"> <div style="width: 60%;"> <i>WORKSHOP: Hydrological and Flood Analyzes with Netcad Nethydro</i> <i>Umut Yegül, Civil Engineer M.Sc., Netcad Training & Technical Support</i> <i>Tuğber Küçük, International Business Development Specialist</i> </div> <div style="width: 35%; text-align: center;"> <i>DPSG Board Meeting</i> </div> </div>

TUESDAY, OCTOBER 25					
09:00-09:30	Registration				
09:30-10:15	Opening Ceremony				
10:15-11:15	<p align="center">POTENTIAL IMPACTS OF CLIMATE CHANGE ON SURFACE AND SUBSURFACE HYDROLOGY AND CONTAMINANT TRANSPORT Miguel A. Medina, Jr. (Duke University, USA)</p>				
11:15-11:45	Group Photo and Coffee Break				
11:45-12:00	RESERVOIR AND SURFACE WATER MANAGEMENT (ROOM A) CHAIR: OSAMA DAWOUD	MODELLED NITRATE CONCENTRATIONS IN THE LEACHATE OF GERMANY - COMPLIANCE CHECKING AND GAP ANALYSIS FOR REACHING WFD TARGETS FOR GROUNDWATER Ralf Kunkel, Tim Wolters and Frank Wendland	NEXUS APPROACH (ROOM B) CHAIR: EAKALAK KHAN	THE IMPACT OF RENEWABLE ENERGY ON ECONOMIC GROWTH IN CEE COUNTRIES Doriana Matraku and Kamela Selenica	
12:00-12:15		INVESTIGATING DIFFUSE POLLUTION DYNAMICS IN AN URBAN CATCHMENT AREA USING FIRST FLUSH ANALYSIS Gil Cruz, Marla Maniquiz-Redillas, Miguel Enrico Robles and Rommel Glenn Mendova		FORECASTING THE WATER CONSUMPTION OF HYDROELECTRICITY POWER PLANTS IN THE CONTEXT OF THE WATER-ENERGY NEXUS BASED ON AN ARTIFICIAL INTELLIGENCE APPROACH Çiğdem Dikcan and Merih Aydınalp Köksal	
12:15-12:30		ANTALYA WATER AND WASTE WATER AUTHORITY ACTION PLAN FOR WATER SCARCITY CAUSED BY CLIMATE CHANGE Cem Çakmak		EVALUATION OF THE WATER-ENERGY-FOOD NEXUS IN THE CONTEXT OF PRECISION AGRICULTURE Enre Alp and Ergi Özdemir	
12:30-12:45		HYDROCARBON WATER CONTAMINATION IN SOUTHERN TUNISIA: SUSTAINABILITY AND REHABILITATION CHALLENGES Houda Besser and Khansa Bisr		PROLONGED DROUGHTS EFFECTS ON STREAM NITROGEN DYNAMICS IN CENTRAL GERMANY Seifeddine Jomaa, Xiangqian Zhou, Xiaoqiang Yang and Michael Rode	
12:45-13:45	Lunch				
13:45-14:00	GROUNDWATER HYDROLOGY AND QUALITY (ROOM A) CHAIR: ALPER ELÇİ	A LABORATORY SCALE EXAMINATION OF SALINITY INTRUSION USING UNDERGROUND DAM Akif Epcin, Ayşe Nur Karayel, Babak Vaheddoust and Egemen Aras	CLIMATE CHANGE ADAPTATION AND MITIGATION (ROOM B) CHAIR: RALF KUNKEL	MODIFYING THE RUSLE FACTORS TO DEVELOP SITE-SPECIFIC LAND MANAGEMENT PRACTICES AGAINST RAINFALL-INDUCED EROSION Denzel Keith Urieta, Kirk Dominick Bautista, Adrian Vaughn Noriega, Michael Irvin So and Marla Maniquiz-Redillas	
14:00-14:15		ASSESSING THE SPATIOTEMPORAL VARIABILITY OF GROUNDWATER LEVEL AND QUALITY USING HYBRID VMD-DSE-K-MEANS TECHNIQUE Roghayeh Ghasempour, V.S. Ozgur Kirca and Seyed Mahdi Saghebani		ANALYSIS OF COOLING AND HEATING EFFECTS DURING HEAT WAVES AND COLD WAVES USING BLUE-GREEN ROOF TECHNOLOGY Munsoo Na, Sungrin Cha, Seungwon Lee, Jungmin Lee and Sangrae Kim	
14:15-14:30		INVESTIGATION OF LAKE-AQUIFER INTERACTIONS WITH EXPERIMENTAL METHODS İnci Yalçın and Cevza Melek Kazzeyilmaz-Alhan		RESILIENCE IN WATER SUPPLY SYSTEMS: TOWARDS A WATER-WISE CITY Tuğba Akdeniz and İbrahim Ethem Karadirek	
14:30-14:45		ON NUMERICAL MODELING OF GROUNDWATER FLOW IN STREAM-WETLAND-AQUIFER SYSTEMS Uğur Boyraz and Cevza Melek Kazzeyilmaz-Alhan		CLIMATE CHANGE INDUCED WATER SCARCITY RISK ASSESSMENT: COUPLING OF MCDA-AHP METHODS WITH QGIS Sena Ödensoy and Başak Güven	
14:45-15:00		ENGAGEMENT OF WASH ENTREPRENEUR TO ADDRESS GROUNDWATER CONTAMINATION Shah Riazar Rahman		MITIGATION OF DIFFUSION POLLUTION THROUGH CIRCULAR ECONOMY Enre Alp and Ece Demir	
15:00-15:30	Coffee Break				
15:30-15:45	SOIL CONTAMINATION (ROOM A) CHAIR: NADIM COPTY	IMPACT OF THE SOIL STRATIFICATION AND SATURATION ON THE PERFORMANCE OF INFILTRATION BOREHOLES Ziyad Abunada, Wafa Aljla and Osama Dawoud	NATURE-BASED SOLUTIONS AND IMPLEMENTATIONS (ROOM B) CHAIR: LEE-HYUNG KIM	HYDRAULIC BEHAVIOR AND PERFORMANCE OF SOIL WITH VARYING INFILTRATION RATES FOR GREEN STORMWATER INFRASTRUCTURES Heidi Guerra, Nash Jett Reyes, Franz Kevin Geronimo, Minsu Jeon and Lee-Hyung Kim	
15:45-16:00		GEOCHEMICAL BACKGROUND IN PARNAIBA RIVER BASIN: THE NEW BRAZILIAN AGRICULTURAL FRONTIER Jefferson Nunes dos Santos, Silvio César Sampaio, Marcelo Bevilacqua Remor, Kathleen Jenifer Model, Erivelto Mercante, Ralpo Rinaldo dos Reis, Marcio Antonio Vilas Boas, Cleuciane Tillyz Do Nascimento and Natalia Pereira		COMPARISON OF URBAN STORMWATER FLOW REDUCTION USING LID UNDER A CENTRALIZED AND DECENTRALIZED SCHEME Marla Maniquiz-Redillas and Sergi Garbanzos	
16:00-16:15		OCCURRENCE OF HAZARDOUS SUBSTANCES IN SOILS AND RIVERS SUSPENDED SEDIMENT IN 7 RIVER CATCHMENTS WITHIN THE DANUBE RIVER BASIN Zsolt Jolankai, Adrienne Clement, Mate Kardos, Steffen Kirtlaus, Nikolaus Weber, Ottavia Zoboli, Oliver Gabriel, Marcianne Bertine Broer, Florentina Soare, Carmen Hamchevici, Radoslav Tonev, Dimitar Mihalkov, Radmila Milacic, Katarina Markovic, Laciya Levstek, Orsolya Szomolanyi and Matthias Zessner		DETERMINING THE OPTIMAL LID COMBINATION THROUGH HYDROLOGICAL PERFORMANCE MODELING AND COST-EFFECTIVENESS ANALYSIS Sergi Garbanzos and Marla Maniquiz-Redillas	
16:15-16:30		EFFECT OF SOIL MICROPLASTICS ON SEED GERMINATION OF HELIANTHUS ANNUUS L. AND SORGHUM BICOLOR L. Mehmet Meric Tunali, Merve Tunali, Basak Guven and Orhan Yenigun		DEVELOPMENT OF REMEDIATION DESIGN FOR THE IN-SITU TREATMENT OF HIGHWAY RUNOFF: SELF CLEANSING DITCHES Ayush Pokharel	
16:30-16:45		ESTIMATING THE CONTRIBUTION OF ROAD SWEEPING IN THE NON-POINT POLLUTANT LOAD REDUCTION IN HIGHWAYS AND EXPRESSWAYS Nash Jett Reyes, Heeman Kang, Minsu Jeon and Lee-Hyung Kim		EVALUATION OF THE UNIT POLLUTANT LOADS AND URBAN HEAT ISLAND MITIGATION FUNCTION OF LOW IMPACT DEVELOPMENT (LID) TECHNOLOGIES Md Tashdeddul Haque, Heidi Guerra, Minsu Jeon, Nash Jett Reyes and Lee-Hyung Kim	
16:45-17:00		MODELING OF THE RAINFALL-WATERSHED-SWALE EXPERIMENTAL SYSTEM BY EPA SWMM Kebir Enre Saraçoğlu and Cevza Melek Kazzeyilmaz-Alhan			
18:30-21:30	Welcome Cocktail				

WEDNESDAY, OCTOBER 26

09:00-09:30		Registration			
09:30-09:45	FLASH ORAL PRESENTATIONS (ROOM A) CHAIR: DERYA DENİZ	FLASH ORAL PRESENTATIONS WILL START AT 10:00 A.M. EACH PRESENTER WILL HAVE 5 MINUTES TO PRESENT THEIR STUDY.	INTEGRATED WATERSHED MANAGEMENT (ROOM B) CHAIR: OTTAVIA ZOBOLI	COUPLED MODELLING APPLICATION FOR CLIMATE CHANGE IMPACT ASSESSMENT IN THE NEMUNAS RIVER WATERSHED – CURONIAN LAGOON – BALTIC SEA CONTINUUM <i>Natalja Čerkasova, Georg Umgiesser, Ali Ertürk, Rasa Idzelytė and Jovita Mėžinė</i>	
09:45-10:00				COMPLIANCE CHECKING FOR MODELLED N AND P LOADS IN SURFACE WATERS AND GAP ANALYSIS FOR REACHING MSFD AND WFD TARGETS <i>Markus Venohr, Hong Hahn Nguyen, Ralf Kunkel and Björn Tetzlaff</i>	
10:00-10:15				ESTIMATING DIFFUSE NUTRIENT LOADS OF MELEN WATERSHED BY USING SOIL AND WATER ASSESMENT TOOL (SWAT) <i>Gokhan Cuceoglu, Alpaskan Ekdal, Melike Gurel and Nusret Karakaya</i>	
10:15-10:30				INVESTIGATING APPLICABILITY OF GRASSED WATERWAY PRACTICE WITH GEOGRAPHIC INFORMATION SYSTEM <i>Mehmet Kalfazade and Alpaskan Ekdal</i>	
10:30-10:45				DECISION SUPPORT SYSTEM FOR SELECTIVE WITHDRAWAL IN WATER SUPPLY RESERVOIRS: AN APPROACH BASED ON THERMAL STRATIFICATION <i>Elif Soyer, Hakk Bayram, Nakan Cangeniş and Onur Eren</i>	
10:45-11:00				INTEGRATING PROTECTED AREA MANAGEMENT WITH RIVER BASIN MANAGEMENT PLANS AS A MEASURE TO ADDRESS DIFFUSE POLLUTION <i>Lisa Cronin, Prof. Fiona Regan and Prof. Frances Lucy</i>	
11:00-11:30		Coffee Break			
11:30-12:30		OPTIMAL DESIGN CONCEPTS IN WATER RESOURCES MANAGEMENT <i>Mustafa M. Aral (Georgia Institute of Technology, USA)</i>			
12:30-13:30		Lunch			
13:30-13:45	URBAN INDUSTRIAL WATER (ROOM A) CHAIR: MARKUS VENOHR	EVALUATION OF HEAVY METAL SORPTION CAPACITIES OF CELLULOSE BASED ADSORBENTS WITH IONIC FUNCTIONAL GROUPS – AQUEOUS COBALT (II) ION REMOVAL <i>Abdifatih A. Hashi, Buket Erdoğan, Yağmur Kuzucu, Serdar Şam, Gül Gülenay Hacısmanoğlu, Abdelhadi F. M. Deghles, Othman A. Hamed and Zehra Semra Can</i>	EXTREME HYDROLOGIC EVENTS (ROOM B) CHAIR: ŞEVKET ÇOKGÖR	FLOOD MANAGEMENT FOR ISTANBUL MEGA-CITY <i>Tunay Çarpar, Mohsen Mahmoodi Vanolya, Bülent Kocaman, Rouhollah Nasirzadehdizaji, Ali Osman Ilgaz, H. Kürşat Türkmen, Tuğba Ölmöz Hancı and Şafak Başa</i>	
13:45-14:00		RAINWATER REUSE EVALUATION BY DESIGN CAPACITY OF RAINWATER UTILIZATION FACILITIES <i>Changyeong Won, Inkyeong Sim and Jeongyeong Lee</i>		REGIONAL FLOOD LOSS MODELLING OF THE TOWN OF BOZKURT IN KASTAMONU, TURKEY <i>Filence Cyizere Rukundo, Derya Deniz and Yiğit Can Altan</i>	
14:00-14:15		A GRAPH-BASED MONITORING FRAMEWORK OF SLUDGE BULKING IN INDUSTRIAL WASTEWATER TREATMENT PLANTS VIA DYNAMIC GRAPH EMBEDDING AND BAYESIAN NETWORKS <i>Jorge Loy-Benitez, Shahzeb Tariq, Sungku Heo, Taeyong Woo, Sangyoun Kim and Changkyoo Yoo</i>		MODELLING AND SIMULATION OF FLOODS IN A RIVER BASIN: FIRST PHASE TOWARDS FLOOD MANAGEMENT USING NBS IN THE OITAVEN-VERDUGO RIVER BASIN (NW SPAIN) <i>Carolina Acuña-Alonso, Lucia Martinez, Enrique Valero and Xana Alvarez</i>	
14:15-14:30		SUSTAINABLE CITIES FOR THE FUTURE WITH THE SUSTAINABLE URBAN WATER MANAGEMENT <i>Rouhollah Nasirzadehdizaji</i>		ELMALI DAM FAILURE ANALYSIS AND FLOOD DISASTER SIMULATION WITH DIFFERENT SCENARIOS USING HEC-RAS 2D <i>İsmail Bilal Peker, Abdülbaki Hacı, Yasin Paşa and Sezar Gülbaz</i>	
14:30-14:45		NOVEL POROUS GEOPOLYMER GRANULES TO CONTROL DIFFUSE POLLUTION AND EUTROPHICATION RELATED TO AMMONIUM NITROGEN <i>Yangmei Yu and Tero Luukkonen</i>		INVESTIGATION OF FLOOD MITIGATION IN BOZKURT DISTRICT <i>Hayri Baycan and Uğur Boyraz</i>	
14:45-15:00		Coffee Break			
15:00-16:00		Poster Session			
16:00-17:00		CHARACTERISITICS AND FATE OF NANOPLASTICS IN WATER ENVIRONMENTS <i>Gang Liu (Chinese Academy of Sciences, China)</i>			
17:00-18:00		Diffuse Pollution and Eutrophication Specialist Group Open Meeting			
19:00-22:00		Gala Dinner			

THURSDAY, OCTOBER 27				
09:30-09:45	MONITORING AND MODELING 1 (ROOM A) CHAIR: AYŞEGÜL AKSOY	MODEL BASED EUTROPHICATION ASSESSMENT OF KOYCEGİZ LAKE Elif Atasoy Ayts, Elif Soyer and Ali Ertürk	EMERGING POLLUTANTS (ROOM B) CHAIR: FERDI HELLWEGER	KINETICS OF THE PHOTOLYTIC AND PHOTOCATALYTIC DEGRADATION OF VETERINARY ANTIBIOTICS Johanna Zambrano, Pedro García, Rubén Irusta-Mata, Juan José Jimenez and Rebeca López
09:45-10:00		SYSTEMIC HYDRAULIC FRACTURING CHEMICAL RISK INDICATORS FOR ASSESSING RELATIVE HAZARD LEVELS TO WATER SUPPLY Christopher Hill, Om Prakash Yadav and Eakalak Khan		ESTIMATION OF BIODEGRADATION POTENTIAL OF PHARMACEUTICALS BY BIOWIN MODELS AND COMPARISON WITH EXPERIMENTAL DATA Başak Kılıç and Ferhan Çeçen
10:00-10:15		REAL-TIME BACTERIA DETECTION USING IMAGE PROCESSING & MACHINE LEARNING BY SMARTPHONE Maryam Arain, Sheeraz Ahmed Memon, Attiya Baqai and Mohsin Memon		MODELING OF REGIONALIZED PFOA AND PFOS EMISSIONS IN AUSTRIA Steffen Kittlaus, Matthias Zessner and Ottavia Zoboli
10:15-10:30		REAL TIME MONITORING OF TEMPERATURE STRATIFICATION TO RESPOND TO EUTROPHICATION Özge Yücel Bilen, Emrehan Berkay Çelebi, Utku Berkalp Ünalan, Emine Betül Şanlı, Serbay Şişir, Sükyman Kazım Sömek, Aydoğuş Kallım, Reza Ahmadian, Şiřşek Demir and Aysegül Aksoy		RESISTANCE TO BENZALKONIUM CHLORIDES FAVORS ANTIBIOTIC RESISTANCE Gökçin Gül and Ulaş Tezel
10:30-10:45		DIFFUSE N- AND P-INPUTS INTO SURFACE WATERS OF GERMANY Ralf Kunkel, Peter Kreins, Hong Hanh Nguyen, Björn Tetzlaff, Markus Venohr, Frank Wendland, Tim Wolters and Maximilian Zimbauer		PHARMACEUTICALS RESIDUES AND BIOCIDES FROM BIOSOLIDS AND MANURE SPREAD AS FERTILIZERS: FIRST RESULTS AFTER ONE YEAR FIELD STUDY Noémie Perrin, Pierre Benoît, Dominique Patureau, Laure Wiest and Jean-Luc Bertrand-Krajewski
10:45-11:00		APPLICATION OF MACHINE LEARNING CLASSIFICATION AND REGRESSION ALGORITHMS FOR QUANTIFYING NUTRIENT TRANSPORT CONSIDERING GROUNDWATER-SURFACE WATER INTERACTIONS IN AN AGRICULTURAL WATERSHED IN CANADA Ahmed Ekayed, Sarah Rixon, Jann Levison, Andrew Birns and Pradeep Goel		VUV INDUCED PHOTO-OXIDATION OF IMIDACLOPRID IN AQUEOUS SOLUTION Selim L. Sanin and Halil Derin
11:00-11:30	Coffee Break			
11:30-12:30	FATE AND REMOVAL OF PHARMACEUTICALS AND NEW THREATS IN EUROPEAN RIVERS UNDER WATER SCARCITY AND GLOBAL CHANGE: THE EU GLOBAQUA PROJECT Damià Barceló (Catalan Institute for Water Research, Spain)			
12:30-13:30	Lunch			
13:30-15:00	WORKSHOP: Young Water Professional Workshop and Networking Marla Redillas, De La Salle University-Manila		WORKSHOP: UNESCO and Water Resources Koray K. Yılmaz, METU	
15:00-15:30	Coffee Break			
15:30-15:45	MONITORING AND MODELING 2 (ROOM A) CHAIR: V.Ş. ÖZGÜR KIRCA	OPTIMIZING THE ANNULAR PHOTOCATALYTIC REACTOR CONFIGURATION FOR THE DEGRADATION OF PERFLUOROOCTANOIC ACID (PFOA) USING AN IMMOBILIZED TITANIUM DIOXIDE: A COMPUTATIONAL FLUID DYNAMICS (CFD) ANALYSIS Mikaili Denise Loazon and Joseph Albert Mendoza	ECOLOGICAL PROTECTION AND RESTORATION (ROOM B) CHAIR: SEİPİDDİNE JOMAA	DEVELOPMENT OF AN ALGORITHM FOR THE DETECTION OF FOREST FIRE SPREAD IN AREAS WITHOUT INTERNET CONNECTION Çağdaş Tari, Elçin Tan and Sevinç Asilhan Srdaş
15:45-16:00		INVESTIGATION OF THERMAL DISCHARGE DILUTION AT RIVER MOUTH USING HYDRODYNAMIC TOOLS Fath Yorgun, Mehmet Erbişim, Murat Aksel, Oral Yağcı and Şevket Çökçör		MODELS PREDICT PLANNED PHOSPHORUS LOAD REDUCTION WILL MAKE LAKE ERIE MORE TOXIC Ferdi Hellweger
16:00-16:15		DEVELOPMENT OF A MICROFLUIDIC SYSTEM FOR THE COLORIMETRIC DETECTION OF THE DIFFUSE POLLUTION OF PHOSPHATE IN FRESH WATER SYSTEMS Rachel Bracker, Harry Beggy, Louis Free, Joyce O'Grady, Sean Power, Karen Daly, Nigel Kent, Fiona Regan and Blánaid White		USING SYSTEM DYNAMICS MODELLING TO VISUALIZE THE EFFECTS OF RESOURCE MANAGEMENT AND POLICY INTERVENTIONS ON BIODIVERSITY AT A REGIONAL SCALE Chrysi Laspidou and Konstantinos Ziliaskopoulos
16:15-16:30		LONG-TERM SPATIAL-TEMPORAL MONITORING OF EUTROPHICATION IN LAKE BURDUR USING REMOTE SENSING DATA Serra Salgat, Gizem Tuna Tuğgun and Alper Elçi		ESTIMATION OF THE SOIL ERODIBILITY FACTOR (K) FOR THE MARMARA REGION OF TURKEY WITH THE RUSLE MODEL USING GIS TECHNIQUES Alkor Ezer and Başak Güven
16:30-16:45		EXAMINING THE USE OF GEMSTAT GLOBAL DATA SOURCE FOR A WATER QUALITY MODEL İsmail Bilal Peker and Sezar Gülbaz		GREEN TRANSITION IN EUROPE: POLICY PATHWAYS TOWARDS A LOW-CARBON ECONOMY UNDER A WEF NEXUS APPROACH - THE NEXUSNET COST ACTION Giannis Adamos and Konstantinos Ziliaskopoulos
16:45-17:00		APPLICATION OF REMOTE SENSING AND IN-SITU MEASUREMENTS FOR DISCHARGE MONITORING IN LARGE RIVERS: (CASE OF POOL MALEBO IN THE CONGO RIVER BASIN) Djamel Kechnit, Raphael Tshimanga Muamba and Ammar Abdelhadi		EVALUATION OF EPA SWMM MODELING PERFORMANCE OF INFILTRATION TRENCH Kaan İlker Demirezen and Cevza Melek Kazeyirli-Ahan
17:00-17:30	Closing Ceremony			

FRIDAY, OCTOBER 28	
09:00-10:30	<i>Field Trip</i>
10:30-11:30	
11:30-12:30	
12:30-13:30	
13:30-14:30	
14:30-15:30	
15:30-16:30	
16:30-17:30	

Flash Presentations

WEDNESDAY, OCTOBER 26		POSTER NUMBER (FLASH ORAL)	TOPIC
10:00-10:05	<i>PARTICULATE PHOZZYLOGIC INDEX: TOWARDS A MORE ACCURATE AND TRANSPARENT IDENTIFICATION OF CRITICAL SOURCE AREAS</i> <i>Gerold Hepp, Ottavia Zoboli, Eva Strenge and Matthias Zessner</i>	46	Monitoring and Modelling
10:05-10:10	<i>MODELLING POTENTIAL IMPACTS OF CLIMATE CHANGE ON HEAVY METAL TRANSPORT IN DRAINAGE BASINS</i> <i>Kamil Çöllü, Muhammed Aslan, Zeynep Akdoğan and Başak Güven</i>	70	
10:10-10:15	<i>DESIGNING THE SIZING CRITERIA FOR FREE WATER SURFACE FLOW CONSTRUCTED WETLAND BASED ON RIVER FLOW INTERPOLATION</i> <i>Miguel Antonio Campos, Nicanor Chan, John Kristoffer Chua, Sophia Claudette Gaudia, Sergi Garbanzos and Marla Maniquiz-Redillas</i>	29	Wetland Management and Modeling
10:15-10:20	<i>INVESTIGATING THE EFFICIENCY OF INFILTRATION TRENCHES FOR STORMWATER PEAK FLOW AND OUTFLOW REDUCTION USING SWMM</i> <i>Sergi Garbanzos, Johaimin Panalondong, Karlo Bryan Ng Cha and Marla Maniquiz-Redillas</i>	28	Nature-Based Solutions and Implementations
10:20-10:25	<i>AN EVALUATION OF GREEN ROOF MODELING PERFORMANCE OF EPA SWMM</i> <i>Kavsar Bako and Cevza Melek Kazeyilmaz-Alhan</i>	101	
10:25-10:30	<i>EVALUATING THE PROPOSED CHECK DAMS PERFORMANCES ON FLOOD MITIGATION IN BOZKURT DISTRICT</i> <i>Hayri Baycan and Uğur Boyraz</i>	125	Reservoir and Water Bodies
10:30-10:35	<i>ASSESSMENT OF SURFACTANT-ENHANCED IN SITU CHEMICAL OXIDATION OF DNAPL SOURCE ZONES</i> <i>Zeynep Demiray, Nihat Hakan Akyol and Nadim Coptay</i>	126	Soil Contamination
10:35-10:40	<i>FATE AND TRANSPORT OF SOME COMMONLY USED PESTICIDES IN THE KONYA PLAIN, TURKEY</i> <i>Yağmur Ongar, Ulaş Tezel, Burak Demirel and Nadim Kamel Coptay</i>	108	

Poster Presentations

WEDNESDAY, OCTOBER 26		POSTER NUMBER	TOPIC
15:00-16:00	PARTICULATE PHOZZYLOGIC INDEX: TOWARDS A MORE ACCURATE AND TRANSPARENT IDENTIFICATION OF CRITICAL SOURCE AREAS TO MITIGATE PHOSPHORUS EMISSIONS <i>Gerold Hepp, Otavia Zoboh, Eva Strenge and Matthias Zessner</i>	46	Monitoring and Modelling
	MODELLING POTENTIAL IMPACTS OF CLIMATE CHANGE ON HEAVY METAL TRANSPORT IN DRAINAGE BASINS <i>Kamil Cöllü, Muhammed Aslan, Zeynep Akdoğan and Başak Güven</i>	70	
	META-RESEARCH ON NUTRIENT TRANSPORT IN SURFACE WATER AND GROUNDWATER USING A TEXT MINING ALGORITHM <i>Ahmed Elsayed, Sarah Rixon, Christina Zeuner, Jana Levison, Andrew Binns and Pradeep Goel</i>	81	
	ASSESSMENT OF RUSLE'S COVER MANAGEMENT SUB-FACTORS FOR UNIDENTIFIED URBAN LAND-USE CLASSES <i>Osama Dawoud, Aladdin Eljamassi and Muhammed Dawad</i>	85	
	THE APPLICATION OF ATMOSPHERIC AND SOIL SENSORS FOR MONITORING NATURE-BASED STORMWATER TREATMENT FACILITIES <i>Minu Jeon, Nash Jett Reyes, Hyeeseon Choi and Lee-Hyung Kim</i>	37	
	CORRELATION ANALYSIS BETWEEN WETLAND WATER LEVEL AND RAINFALL IN JANGGUN WETLAND <i>Junhyeong Lee, Jong-Gu Hwang Bo, Kisung Lee and Soojun Kim</i>	118	
	A CASE STUDY OF SOUTH KOREA: CURRENT STATUS AND PERFORMANCE ASSESSMENT <i>Hyeeseon Choi, Boram Kim, Nash Jett Reyes, Minu Jeon and Lee-Hyung Kim</i>	6	Wetland Management and Modeling
	LITERATURE ANALYSIS ABOUT CHANGING AND INFLUENCE FACTORS IN WETLAND <i>Younghoon Yoo, Jong-Gu Hwang Bo, Kisung Lee and Soojun Kim</i>	119	
	DESIGNING THE SIZING CRITERIA FOR FREE WATER SURFACE FLOW CONSTRUCTED WETLAND BASED ON RIVER FLOW INTERPOLATION <i>Miguel Antonio Campos, Nicamor Chan, John Kristoffer Chua, Sophia Claudette Gaudin, Sergi Garbanzos and Marla Maniquiz-Redillas</i>	29	
	AN OVERVIEW OF DIFFUSE POLLUTION MANAGEMENT THROUGH STORMWATER TREATMENT WETLANDS <i>Nash Jett Reyes, Franz, Kevin Geronimo, Heidi Guerra, Minu Jeon and Lee-Hyung Kim</i>	18	Climate Change Adaptation and Mitigation
	DEVELOPMENT OF A STEADY STATE-ANALYTICAL WATEROBODY NETWORK MODELING TOOL TO IDENTIFY THE INDIVIDUAL IMPACTS OF MULTIPLE POINT AND DIFFUSE NUTRIENT EMISSIONS <i>Ali Erturk, Cenk Gürevin and Natalja Cerkasova</i>	90	
	WATER FOOTPRINT CONCEPT AND FORESTS <i>Gafura A Özlemir and Batın Mehmet Yer</i>	77	
	ESTIMATION OF INFILTRATED RUNOFF COEFFICIENT FOR PREDICTING INFILTRATED WATER OF THE PERMEABLE PAVEMENT LID SYSTEM CONSIDERING THE CROSS SECTION <i>Jaerock Park, Kyungmo Im, Youngjue Seo and Hyunsuk Shin</i>	19	Integrated Watershed Management
	A STUDY ON THE SELECTION METHOD OF WATER CYCLE PRIORITY MANAGEMENT BASIN BASED ON HSPF <i>Jaemoon Kim, Jongseok Baek, Hyo Jeong Lee, Jihyun Moon and Hyunsuk Shin</i>	16	
	A NOVEL DESIGN FOR SEDIMENTS FILTRATION/ENTRAPMENT SYSTEM AT DECENTRALIZED INFILTRATION FACILITIES <i>Osama Dawoud</i>	56	
	THE CHARACTERISTICS OF DISTRIBUTION AND ENVIRONMENTAL FACTOR OF VEGETATION IN WESTERN AND SOUTHERN COAST IN KOREA <i>Ji-Won Park, Eui-Joo Kim, Jung-Min Lee, Yoon-Seo Kim, Jae-Hoon Park, Se-Hee Kim and Young-Han You</i>	59	Nature-Based Solutions and Implementations
	INTRODUCTION AND REVIEW OF PRELIMINARY CONSULTATION SYSTEM FOR LOW IMPACT DEVELOPMENT TO REDUCE OUTFLOWS AND NON-POINT SOURCE POLLUTIONS <i>Hyejeong Lee, Hyunseok Shin, Jihyun Moon, Jaemoon Kim and Youngsu Jang</i>	10	
	EVALUATION OF WATER BALANCE FOR GREEN ROOF BASED ON K-LIDM <i>Jihyun Moon, Jaemoon Kim, Hyejeong Lee, Jaerock Park and Hyunsuk Shin</i>	17	
	INVESTIGATING THE EFFICIENCY OF INFILTRATION TRENCHES FOR STORMWATER PEAK FLOW AND OUTFLOW REDUCTION USING SWMM <i>Sergi Garbanzos, Johannah Panalondong, Karlo Bryan Ng Cha and Marla Maniquiz-Redillas</i>	28	
	AN EVALUATION OF GREEN ROOF MODELING PERFORMANCE OF EPA SWMM <i>Kavsar Bako and Cevza Melek Kazeyilmaz-Alhan</i>	101	
	A LAND-SUITABILITY ANALYSIS FOR LOW IMPACT DEVELOPMENT APPLICATIONS IN ANKARA, TURKEY <i>Emre Alp, İlksen Şenocak, Hayrettin Onur Bektaş, Yasin Erkan, Gül Şimşek, Aysun Tuna, Sermin Çakıcı Alp and Mehdi H. Afşar</i>	114	
	THE IMPACT OF LID IMPLEMENTATION ON SURFACE RUNOFF BY USING EPA SWMM <i>Merve Diñcer and Secar Gülbaç</i>	123	Nexus Approach
	THE WEF NEXUS APPROACH TO ACHIEVE THE SUSTAINABLE DEVELOPMENT GOALS <i>Alexandra Isomou and Chrysi Laopidou</i>	22	
	THE IMPACT OF RENEWABLE ENERGY ON ECONOMIC GROWTH IN CEE COUNTRIES <i>Doriana Matraku and Kamela Selencia</i>	76	
	EFFECT OF LAND USE AND LAND COVER CHANGE DYNAMICS ON N'DJILI RIVER WATER QUALITY VARIATION <i>Sani Zouera, Raphael M. Tshimanga, Haddy Katshiatshia M. and Nelson Odume</i>	69	Reservoir and Water Bodies
	EVALUATING THE PROPOSED CHECK DAMS PERFORMANCES ON FLOOD MITIGATION IN BOZKURT DISTRICT <i>Hayri Boycan and Uğur Boyraz</i>	125	
	DERIVATION OF DAM BREAK EMPIRICAL EQUATION FOR DARLIK DAM IN ISTANBUL, TURKEY <i>Abdülbaki Hacı, Ezgi Selen Tlav, İsmail Bilal Peker, Rasim Temur, Yasin Paşa and Secar Gülbaç</i>	127	Soil Contamination
	FATE AND TRANSPORT OF SOME COMMONLY USED PESTICIDES IN THE KONYA PLAIN, TURKEY <i>Yağmur Ongar, Ulaş Tezel, Burak Demirel and Nadim Kamel Coptı</i>	108	
	ASSESSMENT OF SURFACTANT-ENHANCED IN SITU CHEMICAL OXIDATION OF DNAPL SOURCE ZONES <i>Zeynep Demiryaz, Nihat Hakan Akyol and Nadim Coptı</i>	126	
	PESTICIDES AND CHEMICAL ELEMENTS IN BRAZILIAN PANTANAL SEDIMENTS <i>Silvio César Sampaio, Kathleen Jennifer Model, Píllio Emanuel Rodrigues Silva, Floriano Luiz Suszek, Cleuciane Tillyz Do Nascimento, Natalia Pereira and Marcelo Bevilacqua Remor</i>	12	Ecological Restoration and Production
	CHARACTERISTICS OF HABITAT ENVIRONMENT AND POPULATION OF MANKYUA CHEJUENSE, WHICH IS RARE AND ENDANGERED PLANT IN WORLDWIDE AND GROWS ONLY IN REPUBLIC OF KOREA <i>Kim Euijoo, Jiwon Park, Jungmin Lee, Jaehoon Park, Yoonseo Kim, Sehee Kim and Younghan You</i>	63	
	THE STUDY ON THE EXOTIC PLANT MANAGEMENT CONSIDERING ON THE PLANT LIFE FORM AND BIRD POPULATION CHARACTERISTICS AT THE EXPOSED FLOODPLAIN BY DRAWDOWN IN SOUTH KOREA <i>Jae-Hoon Park, Young-Han You, Ji-Won Park, Eui-Joo Kim, Jung-Min Lee, Yoon-Seo Kim and Ho-Joon Kim</i>	62	
	ECOLOGICAL ASSESSMENT OF WATERFOUNT SPACE USING PLANTS OF WEIRS IN THE NAKDONG RIVER BASIN, REPUBLIC OF KOREA <i>Kim Euijoo, Youngsub Han, Jaehoon Park, Jiwon Park, Jungmin Lee, Yoonseo Kim, Sehee Kim and Younghan You</i>	61	
PLANT COMMUNITY, NET PRIMARY PRODUCTION AND SOIL ENVIRONMENT FACTORS IN ESTUARY, KOREA <i>Ji-Won Park, Eui-Joo Kim, Jung-Min Lee, Yoon-Seo Kim, Jae-Hoon Park, Se-Hee Kim and Young-Han You</i>	60		
CHARACTERISTICS OF VEGETATION SUCCESSION IN THE EXPOSED LAND CAUSED BY THE OPENING OF THE FLOODGATE IN SEJONG WEIR, GEUMGANG RIVER, SOUTH KOREA <i>YoonSeo Kim, Kim Euijoo, Jiwon Park, Jung-Min Lee, Se-Hee Kim, Jae-Hoon Park and Young-Han You</i>	64		
VEGETATION AND FLORA OF GONGJU AND BAEKJE WEIR IN GEUMGANG RIVER, KOREA <i>Jung-min Lee, Jae-young No, Eui-Joo Kim, Ji-won Park, Yoon-seo Kim, Se-hee Kim, Jae-hoon Park and Young-han You</i>	66		

CLIMATE CHANGE ADAPTION AND MITIGATION

MODIFYING THE RUSLE FACTORS TO DEVELOP SITE-SPECIFIC LAND MANAGEMENT PRACTICES AGAINST RAINFALL-INDUCED EROSION

Denzel Keith G. Urieta, Kirk Dominick P. Bautista, Adrian Vaughn L. Noriega, Michael Irvin H. So, and Marla Maniquiz-Redillas*

Department of Civil Engineering, De La Salle University, Manila, Philippines

*Corresponding author (marla.redillas@dlsu.edu.ph)

ABSTRACT

The global threats of soil erosion entail the development of land management practices as an adaptive approach. The established empirical model, Revised Universal Soil Loss Equation (RUSLE), is best used for estimating the soil loss rates and for identifying vulnerable areas. However, there is a knowledge gap on the individual effects of varying RUSLE factors (rainfall erosivity, soil erodibility, slope length and steepness, cover management, support practice) on soil erosion. The objective of this study was to identify which RUSLE factor had the most significant impact on soil loss rates. By increasing each factor by 5%, 10%, 20%, 40%, 80%, and 160% and holding the other factors as constant from baseline, it was determined that the rainfall erosivity (R -factor) is the most critical variable that enhances soil erosion in the area. The correlation between the modified R -factor and its corresponding average soil loss rates ranged from 0.81-0.90. This strong positive relationship was supported by holding the highest percent land area for the worst soil erosion classification and consistently having higher average soil loss rates. The results of this study can be used as a baseline data for soil erosion, and developing conservation practices should be prudent about rainfall erosivity.

Keywords: *soil erosion, Revised Universal Soil Loss Equation (RUSLE), soil loss, correlation analysis.*

1. INTRODUCTION

Soil erosion is a naturally occurring process that persists to have a global threat to agricultural production, water quality, and ecosystems. Therefore, estimating the soil loss rate of a landscape to serve as a baseline scenario is essential in developing land management practices. The Revised Universal Soil Loss Equation (RUSLE) is an empirical model that best exemplifies at identifying areas susceptible to erosion (Benavidez et al., 2018), with its five factors — rainfall erosivity, R ; soil erodibility, K ; slope length and steepness, LS ; cover management, C ; and support practice, P — determining the quantified amount. The simplicity of the RUSLE model allowed for its widescale applications across varying climatic conditions (Ghosal and Bhattacharya, 2020); however, there is a limited knowledge in evaluating the individual effects of RUSLE factors and their influence on the annual soil loss rate (Kumar et al., 2022). The objective of this study was to identify which RUSLE factor had the most significant impact on soil loss rates.

2. MATERIAL AND METHODS

The study area is located in Dolores, Quezon, Philippines ($14^{\circ}1'17.128''\text{N}$, $121^{\circ}26'21.323''\text{E}$) with predevelopment site conditions covering approximately $780,000 \text{ m}^2$. The annual soil loss rate was estimated using Wischmeier and Smith (1978), while the R -factor following El-Swaify et al. (1987); the K -factor following Williams (1995); the LS -factor following Moore and Burch (1986); the C -factor adapting the values from Hurni (1985); and the P -factor set to 1.0. The ArcGIS software aided in mapping the various outputs. Each factor was increased by 5%, 10%, 20%, 40%, 80%, and 160%, while holding the other factors as constant from baseline, to determine the correlation between the modified RUSLE factors and their corresponding average annual soil loss rates.

3. RESULTS AND DISCUSSIONS

The outputs of the RUSLE model are shown in Figure 1 wherein an average annual soil loss rate of $44 \text{ t ha}^{-1} \text{ yr}^{-1}$ was determined for the study area from an annual minimum and maximum of $2 \text{ t ha}^{-1} \text{ yr}^{-1}$ and $97 \text{ t ha}^{-1} \text{ yr}^{-1}$, respectively. Moreover, using a confidence level of 95% resulted in a margin of error of ± 0.31 , which yielded a true value ranging from $43.68 \text{ t ha}^{-1} \text{ yr}^{-1}$ to $44.32 \text{ t ha}^{-1} \text{ yr}^{-1}$ for the annual soil loss rate. In terms of soil erosion risk classification, majority of the area is under the very high category at 42%, which would necessitate a deployment of land management practices. To determine which RUSLE factor significantly stimulated soil erosion in the area, a correlation analysis was conducted between modified factors and their corresponding average annual soil loss rates. By increasing each factor by 5%, 10%, 20%, 40%, 80%, and 160%, the correlation coefficients of R -factor, LS -factor, and C -factor were between 0.81-0.90, 0.56-0.86, and 0.79-0.87, respectively. No correlation for the K -factor was determined due to soil homogeneity of the area. Figure 2 summarizes the results of modifying each RUSLE factor and the subsequent soil loss rates of the area. It can be observed that all factor modifications follow an increasing trend, although not linearly. The R -factor consistently generated higher averages except for the 40% and 160% in which the K -factor and LS -factor was the highest, respectively. This can be attributed to the distinct response of grid areas with higher erosion potential. Overall, the results suggested that R -factor has the most significant impact on soil erosion by having a strong correlation with the average soil loss rates and holding the highest percent land area for worst classification (very high or severe).

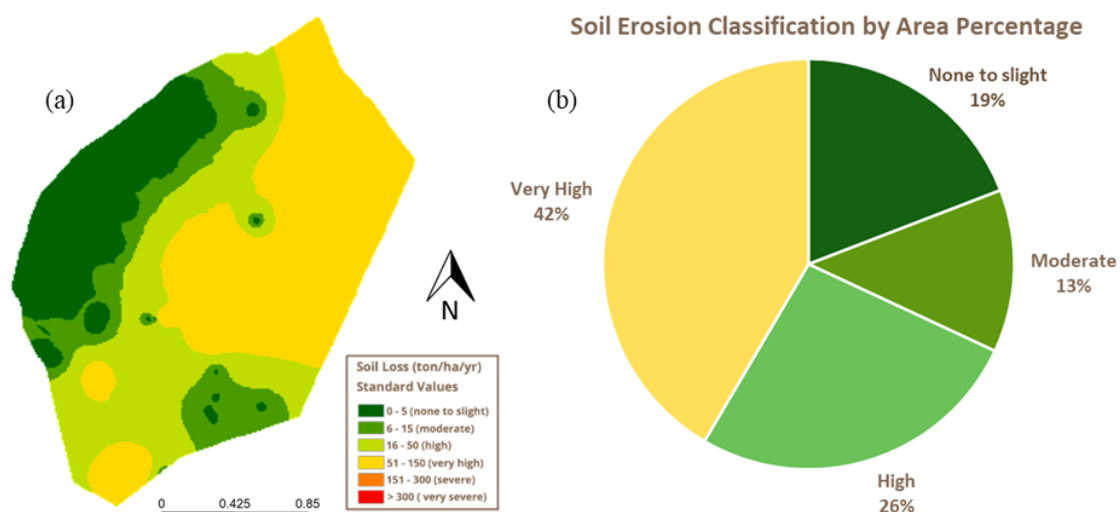


Figure 1. Soil loss rate map (a) and distribution of soil erosion classification by area percentage (b).

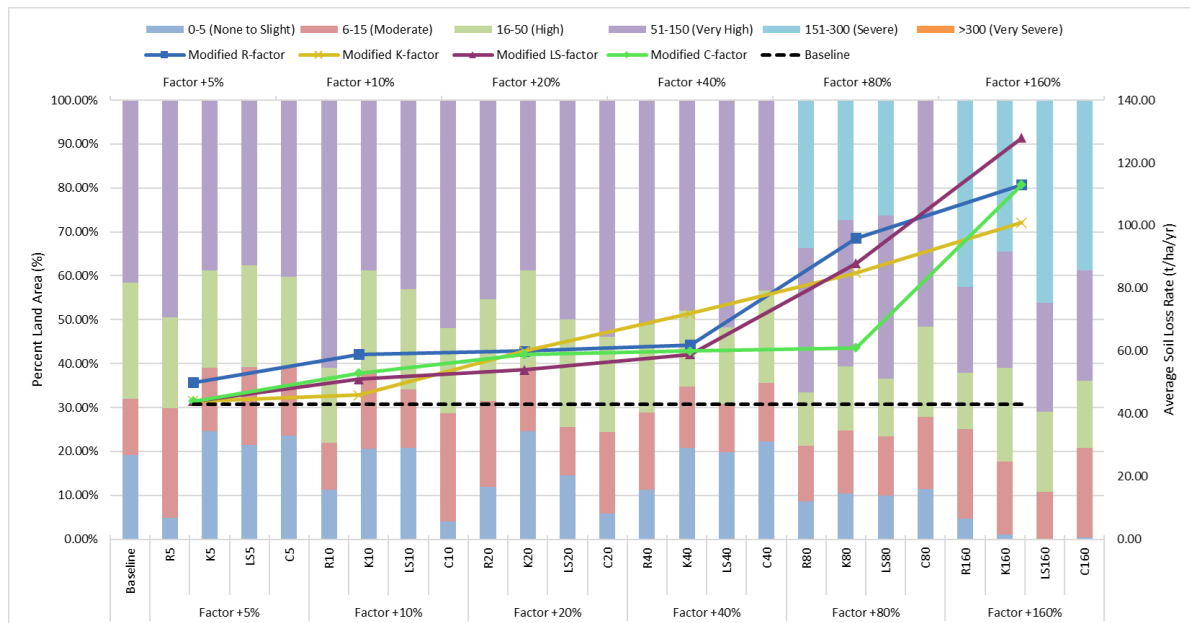


Figure 2. Modified RUSLE factors and their corresponding soil erosion classification and average soil loss rates.

4. CONCLUSIONS

The results determined that the *R*-factor is the most important variable for assessing soil erosion in the study area. Further, development of soil conservation practices should adhere critically to rainfall erosivity. An improvement of the study can be attained by incorporating field data. Finally, there is a high possibility that similar findings will be produced in a different study area from the country because of the tropical climate.

Acknowledgements: The authors acknowledge the Department of Science and Technology, Philippines - Engineering Research and Development for Technology (DOST-ERDT) for supporting and funding this research.

REFERENCES

- Benavidez, R., Jackson, B., Maxwell, D., & Norton, K. (2018). A review of the (Revised) Universal Soil Loss Equation ((R)USLE): with a view to increasing its global applicability and improving soil loss estimates. *Hydrology and Earth System Sciences*, 22(11), 6059–6086.
- El-Swaify, S. A., Gramier, C. L., & Lo, A. (1987). Recent Advances in Soil Conservation in Steepland in Humid Tropics. *Proceedings of the International Conference on Steepland Agriculture in the Humid Tropics*, 87–100.
- Ghosal, K., & das Bhattacharya, S. (2020). A Review of RUSLE Model. *Journal of the Indian Society of Remote Sensing*, 48(4), 689–707.
- Hurni, H. (1985) Erosion-Productivity Conservation Systems in Ethiopia. 4th ISCO Conference, Venezuela, 654-674.
- Kumar, M., Sahu, A. P., Sahoo, N., Dash, S. S., Raul, S. K., & Panigrahi, B. (2022). Global-scale application of the RUSLE model: a comprehensive review. *Hydrological Sciences Journal*, 67(5), 806–830.
- Moore, I.D. and Burch, G.J. (1986) Physical Basis of the Length Slope Factor in the Universal Soil Loss Equation. *Soil Science Society of America*, 50, 1294-1298.
- Williams, J. R. (1995). The EPIC model. *Computer models of watershed hydrology*, 909-1000.
- Wischmeier, W. H., & Smith, D. D. (1978). *Predicting rainfall erosion losses: a guide to conservation planning* (No. 537). Department of Agriculture, Science and Education Administration.

ANALYSIS OF COOLING AND HEATING EFFECTS DURING HEAT WAVES AND COLD WAVES USING BLUE-GREEN ROOF TECHNOLOGY

Mun Soo Na¹, Sung Min Cha^{2*}, Seung Won Lee³, Jung Min Lee⁴ and Sang Rae Kim⁵

¹. Korea Conformity Laboratories, Center for Climatic Environment Real-scale Testing, Jincheon-gun, Republic of Korea

^{2*}. JEIPI, Team of Green Infrastructure Research, Gangjin-gun, Republic of Korea (ichamini21@gmail.com)

³. JEIPI, Team of Green Infrastructure Research, Gangjin-gun, Republic of Korea

⁴. Land and Housing Institute, Department of safety Research, Yuseong-gu, Republic of Korea

⁵. Korea Conformity Laboratories, Center for Climatic Environment Real-scale Testing, Jincheon-gun, Republic of Korea

ABSTRACT

Urbanization and climate change are increasing the frequency of the urban heat island phenomenon and increasing the occurrence of various heat-related diseases. Green infrastructure technology can be used to mitigate the damage caused by these climate disasters. In this study, the damage reduction using blue-green roof technology was analyzed. As a result, at the temperature inside the building, there was a cooling effect of about 4.5 degrees during a heat wave and a heating effect of about 3.0 degrees during a cold wave. This could potentially contribute to carbon neutrality by reducing energy consumption.

Keywords: *blue-green roof, climate change, heat wave, energy saving, cooling effect.*

1. INTRODUCTION

The increase of the impervious area of the surface due to urbanization and the increase in the number of heatwave days due to climate change are causing an increase in the frequency of climate disasters such as floods and heatwaves in cities and a decrease in the quality of life of citizens. Green infrastructure facilities can help to secure the city's climate resilience from such climate disasters, and several studies have reported the effect of improving climate disasters such as heat waves and cold waves (Choi and Smith, 2021, Marando *et al*, 2019, Saaroni *et al*, 2018, Na *et al*, 2021).

In particular, in the case of a green-roof facility, it is known that it not only lowers the temperature of the roof surface, but also controls the temperature inside the building. This can be expected to reduce the possibility of heat-related diseases in the event of climate disasters such as heat waves, and by reducing energy consumption, it can also help reduce damage from indirect climate disasters such as power outages.

In this study, by installing a blue-green roof in two buildings with the same roof area, it was evaluated through long-term monitoring to identify how much influence on the indoor temperature of the building during heat waves and cold waves. Through this, we intend to estimate the contribution to carbon reduction by calculating the energy cost saved when a blue-green roof is installed among green infrastructure.

2. MATERIAL AND METHODS

Temperature monitoring system

To evaluate the cooling and heating effects of the blue-green roof, temperature sensors were installed in two buildings with the same roof area of 145.3m^2 . The temperature sensor was installed on the roof surface and inside the building. The system was built so that data is generated every minute and automatically stored on the server. One of the two buildings was operated as a control group, with a normal roof with nothing on the roof, and the other building was operated as an experimental group with a blue-green roof installed.

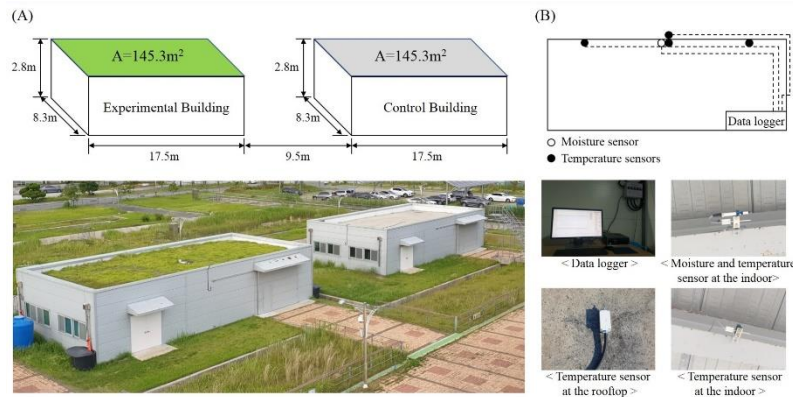


Figure 1. Experimental and control building and location of temperature sensors.

Energy cost estimation

In order to evaluate how much energy consumption can be reduced when a blue-green roof is installed, monthly electricity consumption and electricity rates were calculated to reduce the indoor temperature compared to the outside temperature. The assumptions for this are as follows.

- 1) Operating the air conditioner for 4 hours every day based on the time the maximum temperature is reached
- 2) The roof area is 145.3 m^2
- 3) Thermal energy conductivity of control $0.963\text{ m}^2\cdot^\circ\text{C}\cdot\text{hr}/\text{MJ}$, experimental group: $1.792\text{ m}^2\cdot^\circ\text{C}\cdot\text{hr}/\text{MJ}$

3. RESULTS AND DISCUSSIONS

Cooling and Heating effect

Monitoring data shows that when a blue-green roof is installed, a cooling effect of about 4.5 degrees occurs during a heat wave and a heating effect of about 3.0 degrees during a cold wave. It is believed that cooling and heating effects can be obtained only by installing a blue-green roof without using additional energy, which can lead to a reduction in energy consumption.

In order to confirm the timing of the occurrence of cooling and heating effects, winter and summer data were separated and analyzed. As a result, the surface temperature of the roof where the heating effect occurred was 3 degrees below zero, and the surface temperature of the roof where the cooling effect occurred was 25 degrees above zero.

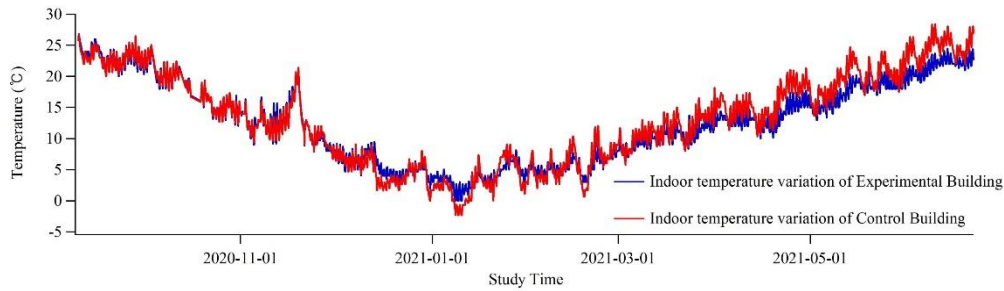


Figure 2. Room temperature variation in experimental and control building.

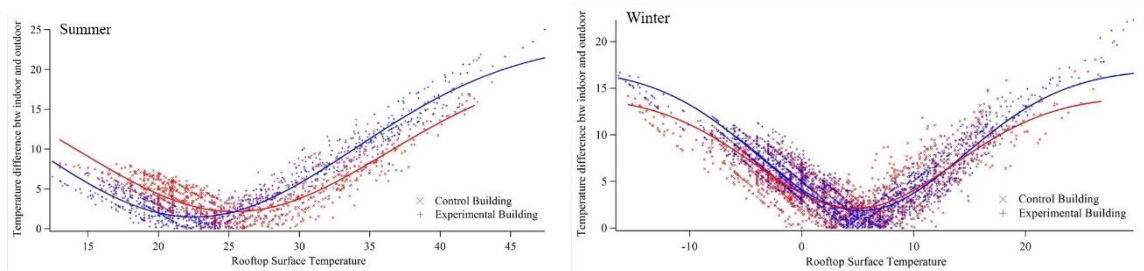


Figure 3. Temperature at which the optimal cooling and heating effect occurs according to the roof surface temperature

Energy cost estimation

The average monthly electricity consumption and electricity rates were calculated to maintain the indoor temperature at 25 degrees. It was 1990.51 kWh in the control group and 1069.78 kWh in the test group. The electricity rates was \$372.83 in the control group and \$149.81 in the experimental group. This values may be different depending on the thermal insulation properties of the building.

4. CONCLUSIONS

As a result of temperature monitoring by installing a blue-green roof, it was found that damage can be mitigated in the event of climate disasters such as heat waves and cold waves. It has been shown that the indoor temperature variations can be reduced without using additional energy, which leads to a reduction in energy consumption, and thus a potential carbon reduction effect can be obtained.

Acknowledgements: This work was supported by Korea Environment Industry & Technology Institute(KEITI) through Intelligent Management Program for Urban Water Resources Project, funded by Korea Ministry of Environment(MOE) (2019002950003)

REFERENCES

Choi, C., & Smith, P. B. (2021). The climate benefits, co-benefits, and trade-offs of green infrastructure: A systematic literature review. *Journal of Environmental Management*, 291, 112583

Marando, F., Salvatori, E., Sebastiani, A., Manes, F., (2019). Regulating Ecosystem Services and Green Infrastructure: assessment of Urban Heat Island effect mitigation in the municipality of Rome, Italy, *Ecological Modeling*, 392, 92-102

- Saaroni, H., Amorim, J. H., Hiemstra, J. A., Pearlmutter, D. (2018). Urban Green Infrastructure as a tool for urban heat mitigation: Survey of research methodologies and findings across different climatic regions. *Urban Climate*, 24, 94-110
- Na, M. S., Bae, W. B., Kang, H. M., Kim, Y. G., Kim, S. R. (2021). Quantitative evaluation of the mitigation effect of low-impact development pavement materials on urban heat island and tropical night phenomena. *Water Science and Technology*, 83(10), 2452-2462

RESILIENCE IN WATER SUPPLY SYSTEMS: TOWARDS A WATER-WISE CITY

Tuğba Akdeniz^{1*}, I. Ethem Karadirek²

¹. Antalya Water and Wastewater Administration (ASAT), Antalya, Turkey

². Akdeniz University, Faculty of Engineering, Dept. of Environmental. Eng., Antalya, Turkey

*Corresponding author (tugbaakdeniz78@gmail.com)

ABSTRACT

Sustainable management of water resources is more crucial than any ever, as water resources are under pressure due to population growth, urbanization, and climate change. Water supply systems should be planned and operated to provide safe and adequate amount of water to the consumers. On the other hand, water supply systems are vulnerable to internal and external disturbances, which might weaken the resilience of such systems. Technical and economical challenges such as pipe failures, water quality issues are internal problems whereas changes in environment and governance such as climate change are defined as external problems. Enhancing the resilience of water supply systems to ensure continuity and efficiency is crucial. IWA developed the concept of water-wise city including 17 principles under four-levels of action namely regenerative water services, water sensitive urban design, basin connected cities, water-wise communities. Enhancing the resilience of water supply systems is not only the step towards a water-wise city, but it is also a vital part of the concept. In this study, efforts to enhance water supply system of Antalya city towards a water-wise city are presented.

Keywords: *Resilience, sustainable management, water safety, water supply, water-wise city.*

1. INTRODUCTION

Water resources are under pressure due to many factors such as urbanization, population growth, climate change (Misra, 2014). Access to safe and adequate amount of water is essential for welfare. Supplying safe and adequate amount of water, which is recognized as drinking water security, supports public health, environment, and economy (Hope and Rouse, 2013). Water resources are vulnerable to a wide variety of hazards including climate change, natural disasters etc. Resilience to the disasters is defined as “*the ability of a human system to prepare and plan for, absorb, recover from, and successfully adapt to adverse events*” (NAS, 2012).

Water supply systems, which are complex and dynamic systems consisting of more than one subsystem (Karadirek et al., 2012), are impacted by natural disasters and hazardous releases (EPA, 2015). Potential hazards to water supply systems are natural disasters (drought, floods, earthquakes, storms, climate change) whereas pipe breaks, change in water quality and environmental effects are defined as potential impacts to the water supply systems (EPA, 2015).

Urban water system covers cycle of extracting raw water, water supply, wastewater collecting and discharge of treated wastewater to the receiving environment (Wang and Luo, 2021). Conventional management methods of water supply systems including continuous construction

and/or expansion of infrastructure result in overexploitation of water resources and deterioration of water quality. As a result of existing impacts on water resources, sustainable management of water systems has become more crucial. According to the International Water Association (IWA), “*water-wise’ behaviour means that leadership culture, governance arrangements, professional capacity and innovative technology are all aligned with the objective of maximising sustainable urban water outcomes*” (IWA, 2016). The water-wise city concept developed by IWA consists of 17 principles under four-levels of action namely regenerative water services, water sensitive urban design, basin connected cities, water-wise communities (IWA, 2016).

In this study, an evaluation of water supply system of Antalya city in terms of water quality and quantity is presented. Building resilience of water supply systems requires a wide range of actions against hazards and potential impacts. Actions and efforts to provide safe and adequate amount of water to the consumers are discussed in detail.

2. MATERIAL AND METHODS

Study Area

Antalya province consists of 19 districts and Antalya Water and Wastewater Administration of Antalya Metropolitan Municipality (ASAT) provides water services to the whole province. In this study, only five central districts of the province are chosen as the study area (Figure 1). Groundwater is the only source of water supplied to the system after disinfection using sodium hypochlorite as there is no need for any other treatment due to high quality of raw water (Kitis et al., 2010). The study area has an efficient SCADA system, which was established in 2006, that enables on-line monitoring of water quantity and quality along water mains and at water production facilities.

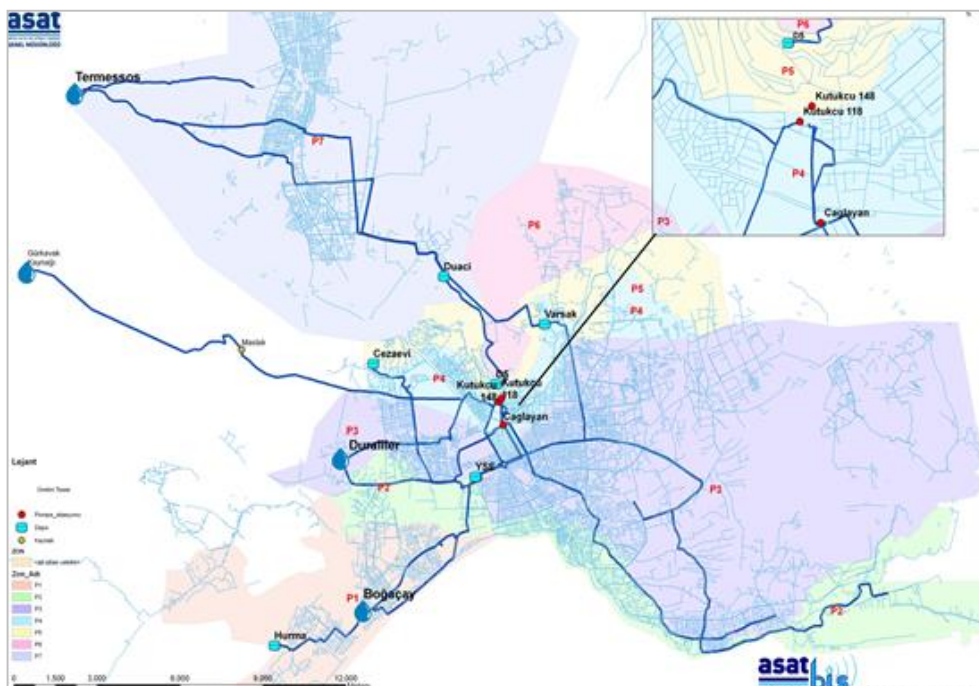


Figure1. Map showing water supply system of Antalya city

Study approach

Water supply systems are generally designed to provide continuous service to the consumers in an efficient manner (Park et al., 2013). Therefore, the resilience of the system is to ensure continuity and efficiency (Butler et al., 2014). Enhancing resilience in water supply systems is generally based on controlling and ensuring water quality and quantity. In this study, efforts and strategies related to enhancing resilience in urban water supply system of Antalya city using real time monitoring and modeling are presented.

3. RESULTS AND DISCUSSIONS

On-line Monitoring of Water Quality and Quantity

Existing SCADA system is very helpful to control water quality and quantity in the study area. Anomalies on flow rates and water pressure levels are used to ensure continuity and efficiency. The volume of water losses resulting from pipe failures is a function of awareness time (A), location time (L) and repair time (Karadirek and Aydin, 2022). Pipe failures, which weaken the reliability of water supply system, can be detected in an efficient way by SCADA system, which helps in reducing awareness time. Furthermore, real time monitoring of flow rates and water pressure levels allows detect anomalies in the distribution system. Each water distribution system has a period at which the system has the lowest water demand. The flow supplied to the system at this period is called as Minimum Night Flow (MNF). The great amount of water during the period of MNF results from the physical losses (Thornton et al. 2008). In Figure, flow rates and water pressure levels at the entrance of a subsystem, which is hydraulically isolated part of the network with a single input (usually called as District Metered Area (DMA)), are given as an example. Relatively high MNF rates, which indicate the higher leakage, were determined by the help of SCADA system. Then, a study was planned and implemented to reduce physical losses from around 87 m³/h to around 65 m³/h (Akdeniz 2022).

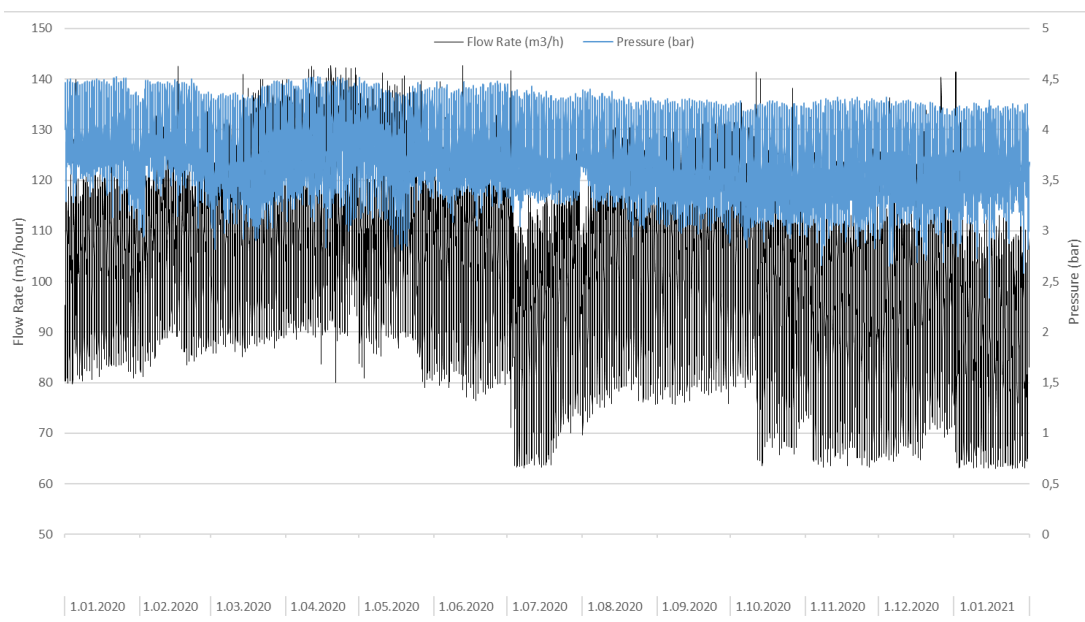
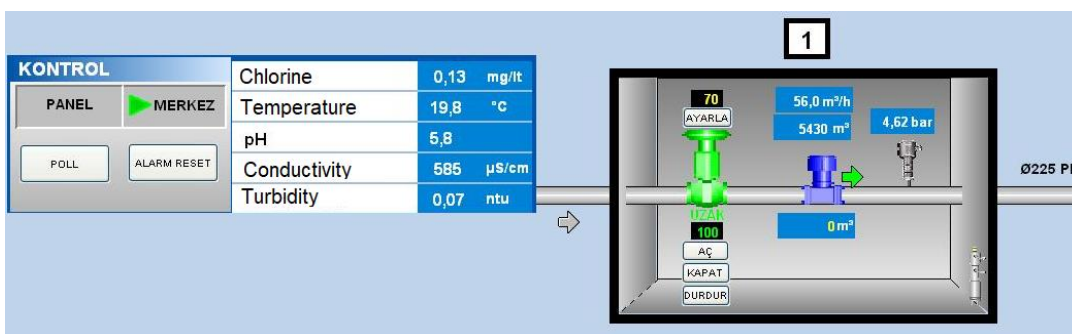


Figure 2. Flow rates and water pressure levels recorded in a monitoring station located at the entrance of a subsystem

On the other hand, status of water storage tanks is continuously monitored to provide water on a continuous basis (Figure). Continuous and real time monitoring of water quality enhance the resilience of the system. Water quality parameters (pH, residual chlorine concentration, turbidity, electrical conductivity, and water temperature) at water production facilities and along the water mains are on-line monitored and stored (Figure). Deterioration of water quality parameters can be determined by the SCADA system and necessary precautions are taken. For instance, turbidity of *Gurkavak* spring water, which is the only spring water source of the PSA, might be relatively high on rainy seasons. If the turbidity value at Gurkavak spring exceeds the value allowed by the regulations, SCADA system gives a warning and then closes the valve automatically to protect public health. The SCADA system is not only efficient to manage water quantity, but it is also helpful to provide safe water.



a)



b)

Figure 3. Status of water storage tanks (a) and water quality parameters along the water mains

Modeling Studies

Hydraulic and water quality modeling of urban water supply systems is a helpful tool to develop management strategies against potential hazards and impacts. For this purpose, hydraulic modeling of water distribution system of the study area is carried out to ensure hydraulic reliability, pressure management and to develop water demand strategies. A great effort has

been made for hydraulic modeling studies in the study area. Water supply system simulated for the study area, as an example, is given in Figure. The results of hydraulic modeling of the study area are used to take actions to ensure resilience of the system. The main aim of implementing hydraulic modeling is to develop management scenarios to improve efficiency and reliability. Conventional operation techniques include controlling parameters at certain points. However, water supply systems are dynamic systems of which main hydraulic parameters such as flow rate, water pressure and velocity show temporal and spatial changes. Hydraulic modeling is helpful to calculate the main hydraulic parameters at each point of water supply system. In the PSA, hydraulic modeling is used to enhance reliability of the system by management scenarios such as extension of water supply system, determination of critical regions requiring rehabilitation, evaluation of physical losses and pressure management. Before each action is taken in the PSA, hydraulic modeling is used as a decision support tool.

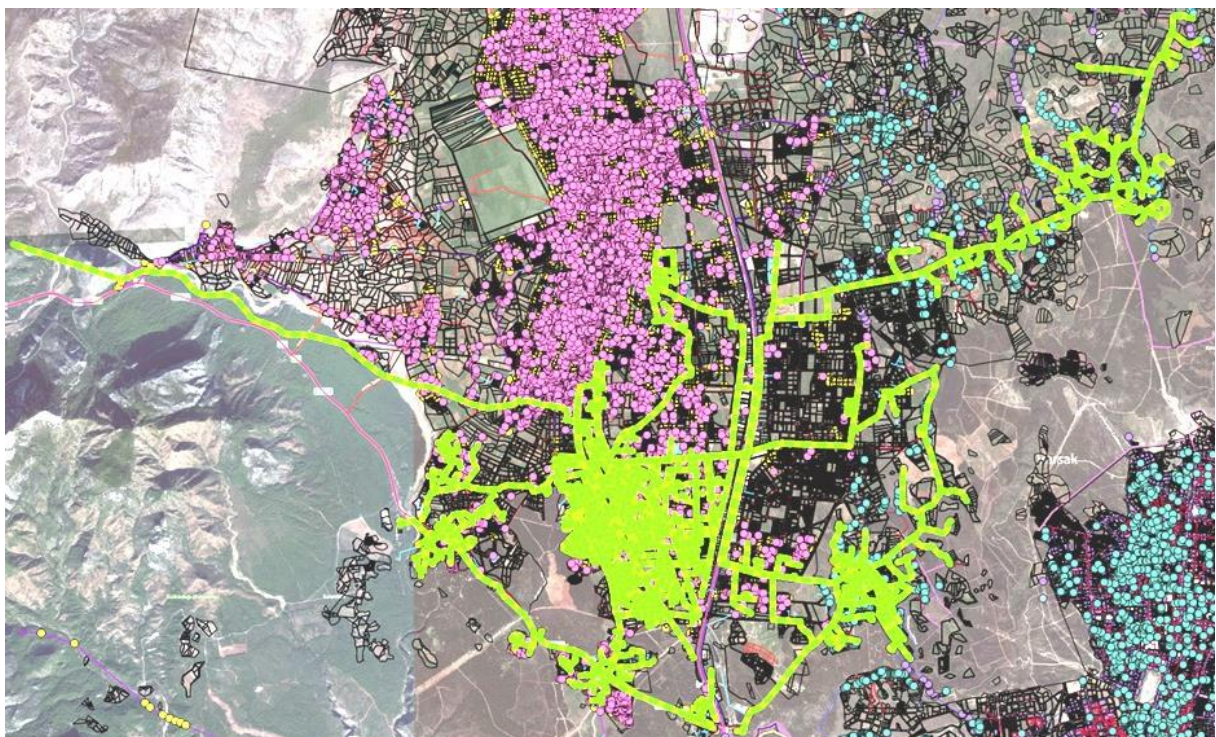


Figure4. Detailed water supply system simulated for the study area (Akdeniz 2017)

4. CONCLUSIONS

Enhancing resilience of water supply systems to provide continuous and efficient service to the consumers is essential to develop a water-wise city. On-line monitoring and modeling are helpful to ensure resilience of water supply systems towards a water-wise city. For sure, enhancing water supply systems is not only the step towards a water-wise city, but it is one of the vital parts of the concept. Further studies for other parts of urban water systems (wastewater collection systems, urban drainage systems etc.) should be carried out to develop a water-wise city, which is a requirement for sustainable management of water resources.

Acknowledgements: Authors would like to thank Antalya Water and Wastewater Administration (ASAT) of Antalya Metropolitan Municipality and Akdeniz University, Antalya, Turkey.

REFERENCES

- Akdeniz, T. (2017). Determination of Number of Booster Stations Considered by Quality Constraints in Drinking Water Networks and Evaluation in view of Costs. PhD Thesis. Akdeniz University, Turkey.
- Akdeniz, T. (2022). A Case Study on Integrated Management of Water Losses in Antalya, Turkey. *Water Practice and Technology, IWA* (in press).
- Butler, D., Farmani, R., Fu, G., Ward, S., Diao, K., Astaraie-Imani, M. (2014). A new approach to urban water management: safe and SuRe. *Procedia Engineering* 89, 347–354.
- Hope, R., Rouse, M. (2013). Risks and responses to universal drinking water security. *Philosophical Transactions of The Royal Society A-Mathematical Physical and Engineering Sciences*, 371(2002), 1-22.
- Karadirek, I. E., Kara, S., Yilmaz, G., Muhammetoglu, A., Muhammetoglu, H. (2012). Implementation of Hydraulic Modelling for Water-Loss Reduction Through Pressure Management. *Water Resources Management*, 26(9), 2555-2568.
- Karadirek, I.E., Aydin, M.E. (2022). Water Losses Management in Urban Water Distribution Systems. In: Bahadir, M., Haarstrick, A. (eds) *Water and Wastewater Management. Water and Wastewater Management*. Springer, Cham.
- Kitiş, M., Yigit N. O., Harmana B. I., Muhammetoğlu H., Muhammetoğlu A., Karadirek İ. E., Demirel İ., Ozden T., Palanci I. (2010). Occurrence of Trihalomethanes in Chlorinated Groundwaters with Very Low Natural Organic Matter and Bromide Concentrations. *Environmental Forensics*, 11(3), 264-274.
- Misra, A.K. (2014). Climate change and challenges of water and food security. *International Journal of Sustainable Built Environment*, 3, 153-165.
- National Academy of Sciences (NAS). (2012). Disaster Resilience: A National Imperative, prepared by the NAS Committee on Science, Engineering, and Public Policy. *Washington, DC: The National Academies Press*.
- Park, J., Seager, T. P., Rao, P. S. C., Convertino, M., Linkov, I. (2013). Integrating risk and resilience approaches to catastrophe management in engineering systems. *Risk Analysis* 33 (3), 356–367..
- The International Water Association (IWA). (2016). The IWA Principles Water Wise Cities, https://iwa-network.org/wp-content/uploads/2016/10/IWA_Brochure_Water_Wise_Communities_SCREEN-1.pdf (Accessed on July 2022).
- The United States Environmental Protection Agency (EPA). (2015). Systems Measures of Water Distribution System Resilience. https://cfpub.epa.gov/si/si_public_record_report.cfm?Lab=NHSRC&dirEntryId=305772 (Accessed on July 2022).
- Thornton J, Sturm R, Kunkel GA. *Water loss control*. New York: McGraw-Hill; 2008
- Wang, X. C., Luo, L. (2021). Water-wise cities and sustainable water systems: Current problems and challenges. In *Water-Wise Cities and Sustainable Water Systems*, Eds. Wang, X. C., Fu, G. IWA Publishing, 2021.

CLIMATE CHANGE INDUCED WATER SCARCITY RISK ASSESSMENT: COUPLING OF MCDA-AHP METHODS WITH QGIS

Sena Ödensoy¹ and Başak Güven^{2}*

¹ *Boğaziçi University, Environmental Sciences Institute, Istanbul, Turkey*

² *Boğaziçi University, Environmental Sciences Institute, Istanbul, Turkey*

**Corresponding author (basak.guven@boun.edu.tr)*

ABSTRACT

Water resources have a vital importance for all living beings, ecosystems and ecological cycles. However, only less than 1% of water available on Earth is available for human consumption. That is the reason why water resources are very critical resources which requires conscious and sustainable use measures. The impacts of human activities on water resources, both in quantitative and qualitative aspects, have been widely discussed and studied by many researchers for years. In the meantime, global climate crisis was emerged due to the cumulative impacts of anthropogenic activities. Impacts of climate change have been widely observed in different regions as severe precipitations causing flood events, heatwaves causing drought events and wildfires. Researches also demonstrate high confidence about the future climate change impacts on water resources. Especially Mediterranean region has been pointed out as one of the regions that will be facing with severe drought risk. This study aims to perform climate change induced water scarcity risk assessment by coupling climatic, geographical, socio-economic and infrastructural parameters. Büyük Menderes Basin was selected as the case study area considering that it is located in the Mediterranean region and it is an important basin with high agricultural activities. MCDA-AHP method was used with the coupling of QGIS and Fuzzy membership methods. Publicly available data was used to identify spatial water scarcity risks in the Basin. SSP1-1.9, SSP3-2.6 and SSP5-8.5 scenarios were used to identify subbasins with the highest water scarcity risk for 2050. Comparison of parameters causing water scarcity risk is seen as the main output of the study. On the other hand, results and discussions focus to provide insights and guide policy makers to invest in the correct and most efficient way for a sustainable water management strategy in Büyük Menderes River Basin.

Keywords: *climate change, socio-economic, risk mapping, MCDA, QGIS.*

1. INTRODUCTION

Water resources have a vital importance for all living beings, ecosystems and ecological cycles. However, only less than 1% of water available on Earth is available for human consumption. The rest is either salty water found in oceans, fresh water frozen in the polar ice caps, or too inaccessible for practical usage. Despite the limited amount of water available for human, we continuously damage these limited water resources both in terms of quality and quantity. Direct pollution sources of humans to water bodies are domestic waste water and industrial waste

water disposals. In a quantity basis, overexploitation of water resources with uncontrolled water withdrawals can be stated as the main stress on water resources. Latest due diligence studies performed in Turkey also underline the magnitude of water withdrawals from unauthorized wells for agricultural activities (T.C. Tarım ve Orman Bakanlığı, 2022).

Climate change is one of the factors that affects water resources. 'Climate change' is the term used for overall impacts of changes resulted by greenhouse gas emission increases due to human activities. Researches show a certainty of 95% that humans are the main reason of climate change and impacts are increasing day by day. In many regions, changes in precipitation and temperature trends resulted in increase of flood and drought events or melting of glaciers. These events induce alterations in hydrological systems and affecting water resources (IPCC, 2014). Researches show that Mediterranean region is one of the regions that will be highly affected by climate change impacts (IPCC, 2019). Therefore, climate change and its impact on water resources has been one of the hot topics in the latest century both globally and nationally.

Due to the multidisciplinary nature of sustainable water management issues, multi-criteria decision analysis (MCDA) has become a common tool to assess water scarcity risks (Abdullah et al., 2021). Different water scarcity definitions are available in literature according to the deriving parameters, such as climate, socio-economic and geographical characteristics (Wilhite & Glantz, 2019). In this research, we are focusing of assessing the climate induced water scarcity risk by considering climatic, geographical, socio-economic and infrastructural conditions. Buyuk Menderes Basin was selected as the study area due to the high level of agricultural, industrial and tourism activities.

2. MATERIAL AND METHODS

Different factors that are affecting our decision are connected with each other and each factor has a different priority for the specific problem. Human mind is processing this prioritization process for a simple problem immediately in their mind. However, when the problem gets complicated and factors affecting the decision increases, it is becoming impossible to do it instantly. Analytical Hierarchy Process (AHP) is a MCDA method developed with the same logic of prioritizing the forcing factors. Pairwise comparison method (PCM) is the main process used in AHP to compare each parameters impact level on the problem. In other words, it is a weighted where each parameter is compared with each other parameters. Please see Table for method used for pairwise comparison.

Table1. Pairwise comparison metrics (Saaty, 1998)

Assigned Value	Definition
1	Parameters are of equal importance
3	Parameter x is of weak importance compared with parameter y
5	Essential or strong importance of parameter x compared with y
7	Demonstrated importance
9	Absolute importance
2, 4, 6, 8	Intermediate valued between two adjacent judgments

In addition to MCDA-AHP method, fuzzy membership method was used to transform each parameter (Zadeh, 1996). This step is required to be able to compare and integrate number of datasets in different units. Fuzzy membership method transforms data in a range between 0 to 1, where 0 shows the lowest score.

Table2. Data used in the study with resources and data transformation methods

Data name	Source	Transformation method
Precipitation projections, CMIP6	EU Climate Data Store Portal (Copernicus) of EU Commissions (EC-Earth Consortium, 2020).	- Intersection of data grid and subbasins, - Weighted mean considering area
Temperature projections, CMIP6		- Intersection of data grid and subbasins, - Weighted mean considering area
Evaporation projections, CMIP6		- Intersection of data grid and subbasins, - Weighted mean considering area
Soil types	FAO Digital Soil Map of World	Weighted mean, considering area
Land Cover	CORINE Land Cover Map 2018 (EEA, 2018)	
Population	TÜİK	Urbanization land cover rates
Daily water consumption (L/day-person)	TÜİK	Weighted mean considering area
Population % receiving waste water treatment service	Province based environmental due diligence reports issued by Ministry of Environment Urbanization (T.C Çevre ve Şehircilik Bakanlığı, 2020a, 2020b, 2020c, 2020e, 2020d)	
Population % receiving water supply service		
Livestock	TÜİK	Green area land cover rates
Agricultural water usage	TÜİK, Water to Food (CWASI)	Agricultural land cover rates

Data name	Source	Transformation method
Tourism, number of beds	TÜİK	Urbanization land cover rates
Industry, % of industries	Provincial Industrial Due Diligence Report (T.C. Sanayi Genel Müdürlüğü, 2013)	Weighted mean considering area

QGIS was used as the main tool to manage, transform and visualize data. On the other hand, QGIS was also used to perform geographical analyses of the study area, including catchment delineation processes and slope determination. Please see Table for data used within the scope of the water scarcity risk assessment analysis. Different data transformation methods were implemented because of the fact that each publicly available data was obtained in a different resolution. The main data transformation methodology developed was for the transformation of all data to the subbasin level. Land cover data obtained from Climate Data Store Portal (Copernicus) of EU Commissions was used to convert socio-economic parameters. Data transformation methods used for each parameter can be also seen in Table. Taking into account the data resolution and data transformation methods, a semi-distributed model was generated as a water scarcity risk assessment tool.

Equations and Units

As a result of assignment of importance values for each parameter by performing pairwise comparison method, an importance weight is calculated for each parameter. Eigenvalue method is used to calculate the parameter weights, which is demonstrated in Equation 1 (Vahidnia et al., 2008)

$$(A - \lambda I) = 0 \quad (1)$$

where λ represents the biggest eigenvalue of the pairwise matrix, and I is the unit matrix.

In this study, pairwise matrix and parameter weight calculations were performed with 'EasyAHP' plugin tool developed in python specific for GIS.

Pairwise comparison matrix should be consistent, otherwise the MCDA analysis do not generate meaningful outputs. That's why consistency ratio (CR) calculation is a critical step in AHP-MCDA analysis. CR is calculated with equations shown in Equation 2 (Saaty, 1988).

$$Consistency\ Index\ (CI) = \frac{(\lambda - n)}{(n - 1)} \quad (2)$$

where n is the number of criteria and λ is the largest eigenvalue given in the pairwise matrix.

$$CR = CI/RI \quad (2)$$

where RI indicates an index and in this case RI = 1.24 (Saaty, 1988).

CR values lower than 0.10 shows a reasonable consistency in the pairwise comparison. However, if CR is higher or equal then 0.10, then it shows inconsistent judgment in the pairwise comparison. In this case, pairwise comparison matrix should be regenerated with different evaluation.

Weighted linear combination method was applied to create water scarcity risk maps. As a first step each parameter group (climate, geography, socio-economic, infrastructure) was assessed internally to obtain climatic water scarcity risk map, socio-economic water scarcity risk map, geographical water scarcity risk map and infrastructural water scarcity risk map. For climatic and socio-economic water scarcity risk assessment studies, SSP1-1.9, SSP3-2.6 and SSP5-8.5 climate scenarios and socio-economic assumptions were considered. Finally, generated four different water scarcity risk maps were put into MCDA-AHP analysis by using pairwise comparison metrics used in previous studies (Boultif & Benmessaud, 2017).

3. RESULTS AND DISCUSSIONS

Water scarcity risk map was obtained as a result of MCDA-AHP coupled with fuzzy membership and QGIS tool which takes into consideration climate, geography, socio-economic and infrastructure conditions of each subbasin. Assessment was performed for three different climate scenarios: SSP1-1.9, SSP3-2.6 and SSP5-8.5. Different water scarcity risk levels in subbasin level are demonstrated by QGIS based risk maps. According to the results, climatic water scarcity risk level increase can be easily observed going from SSP1-1.9 towards SSP5-8.5 scenario. The importance of immediate climate change mitigation actions in dealing with water scarcity risks is undeniable.

On the other hand, socio-economic stress is observed in subbasins located near the sea side of the Basin, including provinces of Aydın, Denizli, Mugla due to the high level of agricultural and tourism activities which all are directly correlated with high water consumption rates. On the other hand, mining industry also creates a stress on water resources in subbasins adjacent to Aydın, Denizli and Mugla.

4. CONCLUSIONS

As conclusion, the importance of sustainable water management practices in Büyük Menderes Basin can be clearly seen from the water scarcity risk maps generated within the scope of this study. Water efficient irrigation systems and stringent implication on unauthorized water consumption habits in the region should be considered as the primary action to minimize socio-economic water scarcity risks. On the other hand, improving and extending the water infrastructure system would also avoid unauthorized groundwater withdrawals. Rain water harvesting designs and projects should be considered as an improvement area for the Basin, since no clear information could be found about the rainwater management practices.

REFERENCES

- Abdullah, M. F., Siraj, S., & Hodgett, R. E. (2021). An overview of multi-criteria decision analysis (Mcd) application in managing water-related disaster events: Analyzing 20 years of literature for flood and drought events. *Water (Switzerland)*, 13(10). <https://doi.org/10.3390/w13101358>
- Boultif, M., & Benmessaud, H. (2017). *Using Climate-Soil-Socioeconomic Parameters For a Drought Vulnerability Assessment in a Semi-Arid Region : Application at the Region of El Hodna , (M ' sila , Algeria)*. October 2019. <https://doi.org/10.5937/GeoPan1703142B>
- EC-Earth Consortium (EC-Earth) (2020). EC-Earth-Consortium EC-Earth3-AerChem model output prepared for CMIP6 AerChemMIP. Earth System Grid Federation. doi:<https://doi.org/10.22033/ESGF/CMIP6.699> .
- IPCC. (2014). Climate Change 2014: Synthesis Report. Contribution. In *Contribution of Working Groups I, II and III to the Fifth Assessment Report of the Intergovernmental Panel on Climate Change*.
- IPCC. (2019). 6th Assessment Report: Technical Summary. In *Climate Change and Land: an IPCC special report on climate change, desertification, land degradation, sustainable land management, food security, and greenhouse gas fluxes in terrestrial ecosystems*.
- Saaty, T. L. (1988). *WHAT IS THE ANALYTIC HIERARCHY PROCESS ? Introduction In our everyday life , we must constantly make choices concerning what tasks to do or not to do , when to do them , and whether to do them at all . Many problems such as buying the most cost effective*. 109–121.
- T.C. Sanayi Genel Müdürlüğü. (2013). *81 İl Sanayi Durum Raporu*. 23.
- T.C. Tarım ve Orman Bakanlığı. (2022). *İklim Değişikliği ve Tarım Değerlendirme Raporu*. 114. www.tarimorman.gov.tr
- T.C Çevre ve Şehircilik Bakanlığı. (2020a). *AFYONKARAHİSAR İLİ 2019 YILI ÇEVRE DURUM RAPORU*.
- T.C Çevre ve Şehircilik Bakanlığı. (2020b). *Aydın İli 2019 Yılı Çevre Durum Raporu*.
- T.C Çevre ve Şehircilik Bakanlığı. (2020c). *Denizli İli 2019 Çevre Durum Raporu*.
- T.C Çevre ve Şehircilik Bakanlığı. (2020d). *Muğla İli 2019 Yılı Çevre Durum Raporu*.
- T.C Çevre ve Şehircilik Bakanlığı. (2020e). *Uşak İli 2019 Yılı Çevre Durum Raporu*. 4(1), 1–9. <https://pesquisa.bvsalud.org/portal/resource/en/mdl-20203177951%0Ahttp://dx.doi.org/10.1038/s41562-020-0887-9%0Ahttp://dx.doi.org/10.1038/s41562-020-0884-z%0Ahttps://doi.org/10.1080/13669877.2020.1758193%0Ahttp://sersc.org/journals/index.php/IJAST/article>
- Vahidnia, M. H., Alesheikh, a, Alimohammadi, a, & Bassiri, a. (2008). Fuzzy analytical hierarchy process in GIS application. *The International Archives of the Photogrammetry, Remote Sensing and Spatial Information Sciences*, 37(B2), 593–596.
- Wilhite, D. A., & Glantz, M. H. (2019). Understanding the drought phenomenon: The role of definitions. *Planning for Drought: Toward A Reduction of Societal Vulnerability*, 11–27. <https://doi.org/10.4324/9780429301735-2>
- Zadeh, L. A. (1996). *Fuzzy Sets*. 394–432. https://doi.org/10.1142/9789814261302_0021

MITIGATION OF DIFFUSION POLLUTION THROUGH CIRCULAR ECONOMY

Ece Demir¹, Emre Alp^{1}*

¹ Department of Environmental Engineering, Middle East Technical University, Ankara, Turkey

**Corresponding author (emrealp@metu.edu.tr)*

ABSTRACT

Agricultural water demand and diffuse pollution threatens water resources and the ecosystem. Circular economy aims to reduce unnecessary consumption and the need for excessive extraction of resources from nature. Advancements required to achieve sustainable agriculture and reach the goals set by the Green Deal can be reached by circular economy and circular agricultural practices. Water resources can be preserved while reducing pollution by using treated wastewater more often and avoiding pollutant discharges. This study aims to assess the potential of circularity in Turkey's agriculture by using treated wastewater for the irrigation of crops. The outcomes of the study is aimed to aid decision makers to develop sustainable water management as well as mitigate the sources of the diffuse pollution.

Keywords: *Circular economy, circular agriculture, wastewater reuse, diffuse pollution*

1. INTRODUCTION

Diffuse pollution sources can have a detrimental effect on the ecology and water quality of watersheds. Agricultural production, forestry, urban and rural land use, atmospheric deposition, and rural dwellings without a clear point of discharge are just a few examples of the many activities that can result in diffuse pollution. Diffuse water pollution from agriculture is a significant environmental problem that affects water bodies globally and contributes to eutrophication, health issues for humans, rising cost of water treatment, and reduced recreational opportunities.

The linear agriculture model followed to meet the food demand and huge increase in global food production in the recent decades has come at a high cost for the environment. 50% of the habitable land is now used for agriculture. 60–70% of total biodiversity loss experienced is due to the conversion of natural habitats to agricultural land. Agriculture accounts for about 70% of global freshwater withdrawals. The intensive use of chemical fertilizers and synthetic pesticides has eroded the quality of land for cultivation.

Extraction of water resources for agricultural and diffuse pollution resulting from agriculture threatens water resources and the ecosystem. The farming industry is among the Green Deal's priority sectors, owing to its central role in the production and the human-nature relationship. Advancements required to achieve sustainable agriculture and reach the goals set by the Green Deal can be reached by circular economy and circular agricultural practices. The Green Deal both, directly and indirectly, mentions circular economy to keep the integrity of the ecosystem.

According to the Porto Protocol (2020), the fundamental principle of a circular economy is to keep resources acquired from the environment in the economic circuit. A circular economy

implies reducing waste to a minimum. Doing this extends a product's life cycle and prevents formation waste. The circular economy aims to reduce unnecessary consumption and the need for excessive extraction of resources from nature. A circular economy stimulates the search for effective usage of resources rather than the ownership of new resources. Life cycles of materials are extended with practices involving refusing, rethinking, reducing, reusing, repairing, refurbishing, remanufacturing, repurposing, recycling, and recovering existing materials as long as possible.

United Nations (2021) states that circular agriculture's aim is minimal external inputs, closing nutrient loops, reducing negative impacts on the environment, guaranteeing the regeneration of biodiversity in systems, and valorizing agricultural and agro-food wastes. Circular agriculture involves an examination of the entire agro-food system to detect opportunities at all stages, from the extraction of materials to water reuse, and the utilization of agro-food wastes in the bioeconomy.

Considering irrigation accounts for the majority of overall water withdrawals, the use of nonconventional sources of water for irrigation is crucial to ensuring the long-term sustainable use of natural resources. Wastewater reuse is the treatment of domestic or municipal wastewater, tail water, etc. for specified purposes before reentering the natural water cycle; is an important part of circular agricultural practices. Wastewater generated by cities, municipalities, and farmland can be safely disposed of or reused as a resource, and it may contain nutrients that improve agricultural development when properly treated and utilized. United Nations, (2021) states that in agriculture the use of wastewater may irrigate an additional 15% of all irrigated areas. Several benefits are associated with water reuse and recycling when compared to traditional irrigation methods. Water recycling has the potential to be less costly in the long run, as groundwater becomes scarcer, the costs and energy required for pumping rise. Water collection, treatment, and distribution all demand energy. According to WateReuse Association, (2021) reusing water conserves resources, decreases pollution in vulnerable water bodies, and aids in the development of riparian zones. Water recycling ensures a consistent, steady supply of fresh water that is unaffected by environmental conditions or pumping constraints. Communities in dry locations no longer need to import water when water is recycled. Conserve, (n.d.) states that Israel, Spain, Australia, China, Greece, Italy, Kuwait, Mexico, Singapore, numerous African countries, and others employ recycled water safely and effectively in agricultural and drinking water management. It is important to note that to avoid harming plants and soils, ensure food safety, and safeguard farm workers' health, recycled water for irrigating crops would have to be of good enough quality.

More wastewater and water pollution will result from increased urban water use. The full value of water is acknowledged and captured in a circular economy. According to the World Bank Group (2022), a circular economy restores watersheds and other natural systems while minimizing negative externalities and their effects on natural resources. Increasing treated wastewater utilization and avoiding pollutant discharges help conserve water resources while reducing pollution. This study aims to assess the potential of circularity in Turkey's agriculture by using treated wastewater to irrigate crops.

2. MATERIAL AND METHODS

This study consists of 2 stages: i) determination of agricultural water demand and ii) potential wastewater to be reused for irrigation purposes as a part of a circular agricultural economy model to provide sustainable agricultural water management and mitigate diffuse pollution.

Agricultural Water Demand

Agricultural water demand is the net irrigation needs of crops considering evapotranspiration, rainfall, groundwater, and water stored in the topsoil layer. Net irrigation water needs for the crops have been calculated empirically;

$$IN = ET_c - (P_e - G_w - S_m)$$

Where:

ET_c = average monthly crop evapotranspiration (mm)

P_e = average monthly effective precipitation (mm), which may be used by the crops

G_w = is the contribution of the groundwater, and

S_m = is the water stored in the topsoil layer at the beginning of the germination period which can be used for crops.

Treated municipal wastewater reuse planning is based on soil properties, climatic variables, and the crops' irrigation water needs (FAO, n.d.). Factors that affect evapotranspiration (ET_c) include the plant's growth stage or level of maturity, percentage of soil cover, solar radiation, humidity, temperature, and wind. Irrigation needs of crops chosen for this study were strategic agricultural products which were supported by the government, and distinct geographic products in cities. The list of crops selected in this study includes barley, wheat, sunflower, apple, bean, hazelnut, peanut, rose, fig, watermelon, apricot, corn, cotton, potato, eggplant, garlic, greenhouse, citrus, tobacco, fresh tea, olive oil, grape, peach, and sugar beet. Evapotranspiration values for crops in specific areas were determined from DSI and TAGEM (2017). The term " G_w " was considered equal to zero, since the underground water table in Turkey is very low as a result of excessive pumping, according to (NASA, 2021). Additionally, it was believed that the amount of soil moisture at the time of sowing and the time of harvest was equal, due to the low moisture found in Turkish soil top layer (Bulut et al., 2013), the term " S_m " was taken to mean zero. Effective rainfall has been calculated empirically using the USDA Method (Ali & Mubarak, 2017);

$$P_e = f(SF)[1.25P_t^{0.82416} - 2.93] * 10^{0.000955ET_c}$$

Where:

P_t monthly mean precipitation,

$f(SF)$ = soil water storage factor.

The soil water storage factor was defined by the following (Ali & Mubarak, 2017):

$$f(SF) = 0.531747 + 0.295164 * D + 0.057697 * D^2 + 0.003804 * D^3$$

SF: usable soil water storage (mm).

Usable water storage of soils in Turkey were defined with respect to texture classes determined by FAO; each soil class contains a various usable water storage.

Potential of Wastewater in Turkey

According to the results of the 2018 Municipal Wastewater Statistics Survey applied by TÜİK, (2018) to all municipalities, 4.2 billion m³ of 4.8 billion m³ of wastewater discharged from the sewerage network was treated in wastewater treatment plants. Advanced treatment was applied to 47.9%, biological treatment to 27.6%, physical treatment to 24.2%, and natural treatment to 0.3% of the treated wastewater.

3. RESULTS AND DISCUSSIONS

According to Özkan & Bağcı, (2019) in our country, whose annual water consumption is 54 billion cubic meters, 40 billion cubic meters (74%) of this water is used for irrigation. The results showed that strategic agricultural products specific to a given area can be irrigated using treated wastewaters to preserve the available water resources and mitigate diffuse pollution.

4. CONCLUSIONS

The possibility of reusing treated municipal from Turkey's wastewater treatment plants is discussed in the current paper. The irrigated crops to be considered, types of agricultural soils were established, and crop water needs were calculated. Additionally, the TMWW's chemical properties were identified for safe reuse in crop production and to safeguard soils against potential pollution. One of the root causes of pollution is the unsustainable use of natural resources in our production and consumption models. Circular economy may decrease the extraction of raw materials from nature and reduce diffuse pollution. Circular economy has been discussed in the context of of the treated municipal wastewater reuse in agriculture in this article. Efficient use of resources and closing nutrient loops is another very important aspect of circular agriculture which will be discussed in future works. Turkey's potential circular agricultural resources in this context are treated wastewater, livestock manure, and crops residues.

REFERENCES

- Ali, M., & Mubarak, S. (2017). Effective Rainfall Calculation Methods for Field Crops: An Overview, Analysis and New Formulation. *Asian Research Journal of Agriculture*, 7(1), 1–12. <https://doi.org/10.9734/arja/2017/36812>
- Bulut, B., Yılmaz, M. T., Sönmez, I., & Şorman, A. Ü. (2013). *Analysis of Soil Moisture in Turkey by NOAA Land Surface Model*. METU Blog. https://blog.metu.edu.tr/tuyilmaz/files/2013/09/Bulut-Kuraklik-Toprak_nemi.pdf
- Conserve. (n.d.). *Water Reuse in Agriculture*. <http://conservewaterforfood.org/water-reuse-in-agriculture#:~:text=Water%20reuse%20is%20the%20process,reenters%20the%20natural%20water%20cycle>
- FAO. (n.d.). *Irrigation Water Needs*. <https://www.fao.org/3/s2022e/s2022e08.htm>
- NASA. (2021). *Turkey Experiences Intense Drought*. <https://earthobservatory.nasa.gov/images/147811/turkey-experiences-intense-drought>
- Özkan, M., & Bağcı, İ. (2019). *Türk Tarım Orman Dergisi*. Türk Tarım. <http://www.turktarim.gov.tr/Haber/223/kaynaktan-kullaniciya-ulasana-kadar-suyun-yarisindan-fazlasi-kaybediliyor>
- The Porto Protocol. (2022, May 13). *Circular Economy as a way of increasing efficiency in organizations*. <https://www.portoprotocol.com/circular-economy-as-a-way-of-increasing-efficiency-in-organizations/>

TÜİK. (2019). *Municipal Wastewater Statistics, 2018*. <https://data.tuik.gov.tr/Bulten/Index?p=Belediye-Atiksu-Istatistikleri-2018-30667>

United Nations. (n.d.). *Pollution and Circular Economy – United Nations Environment – Finance Initiative*. United Nations Environment Programme - Finance Initiative. <https://www.unepfi.org/pollution-and-circular-economy/pollution-and-circular-economy/>

United Nations. (2021). *UN/DESA Policy Brief #105: Circular agriculture for sustainable rural development | Department of Economic and Social Affairs*. <https://www.un.org/development/desa/dpad/publication/un-des-policy-brief-105-circular-agriculture-for-sustainable-rural-development/>

WateReuse Association. (2022, May 5). *Agricultural Reuse | WateReuse Association*. WateReuse Association | Engage. Educate. Advocate. <https://watereuse.org/educate/water-reuse-101/agricultural-reuse/>

World Bank Group. (2022, July 28). *Water in Circular Economy and Resilience (WICER)*. World Bank. <https://www.worldbank.org/en/topic/water/publication/wicer>

ESTIMATION OF INFILTRATED RUNOFF COEFFICIENT FOR PREDICTING INFILTRATED WATER OF THE PERMEABLE PAVEMENT LID SYSTEM CONSIDERING THE CROSS SECTION

Jaerock Park¹, Kyungmo Im^{2*}, Youngjae Seo¹ and Hyunsuk Shin^{3*}

¹. Ph.D Student, Department of Civil Engineering, Pusan National University, Busan, Republic of Korea

². Director General, Urban Planning Bureau, Busan Metropolitan City, Busan, Republic of Korea

³. Professor, Department of Civil Engineering, Pusan National University, Busan, Republic of Korea

*Corresponding author (hsshin@pusan.ac.kr)

ABSTRACT

The increase in flash floods in urban watersheds due to climate change and urbanization causes human life and property damage. Low impact development (LID) technology has been developed for rainwater control, and permeable pavement has been selected as a factor technology with high applicability in urban watersheds. However, the performance of the permeable pavement was evaluated only by the permeability coefficient, and the storage and infiltration runoff for the entire section were not evaluated. In this study, in order to predict the infiltrated runoff drained through the permeable pavement, the retention and drainage volume were measured through an experiment, and the infiltrated runoff coefficient CN_i was calculated through this experiment. The average CN_i for the three scenarios was 97.43, indicating that most of the rainwater is drained rather than stored. In addition, CN_i decreased to 53.24 according to the change of the underlying ground, confirming that a lot of rainwater can join groundwater through ground infiltration.

Keywords: *Low impact development, Permeable pavement, Infiltrated runoff, NRCS-CN, Runoff coefficient.*

1. INTRODUCTION

An increase in extreme rainfall due to climate change and an increase in impervious area due to urbanization cause flash floods. Low-impact development and permeable pavement were developed to prevent flooding in the city, and rainwater infiltrating through the permeable pavement is discharged into an underground storage tank at the end of the system and a rainwater conduit. CN_i was calculated by modifying the existing NRCS(Natural Resources Conservation Service)-SCS method in order to predict the amount of infiltrated water considering the entire cross-section of the permeable pavement LID system and the penetration capability of the ground. The infiltration amount prediction can be used to estimate the scale of element technology connected with the permeable pavement system. CN_i depends on the cross-section of each permeable pavement system and is affected by the original soil of the site. Therefore, it is necessary to calculate CN_i through an experiment depending on the manufacturer's product, and the experiment was conducted at the Korea Green Infrastructure Impact Development Center, Yangsan Campus, Pusan National University, Korea.

2. MATERIAL AND METHODS

NRCS-SCS

The CN value of NRCS-SCS is an index indicating the surface runoff of impervious areas with respect to rainfall. Potential holding water is calculated through type classification according to land conditions and land composition for preceding rainfall, and CN is calculated according to the equation below.

$$Q = \frac{(P - 0.2S)^2}{P + 0.8S} \quad (1)$$

$$CN = \frac{25400}{S + 254} \text{ or } S = \frac{25400}{CN} - 254 \quad (2)$$

Where, Q is the amount of runoff (mm);

S is the maximum potential retention (after runoff begins);

P is rainfall amount (mm)

CN_i can be calculated by substituting the infiltration runoff Q_i of the permeable pavement in place of the surface runoff Q.

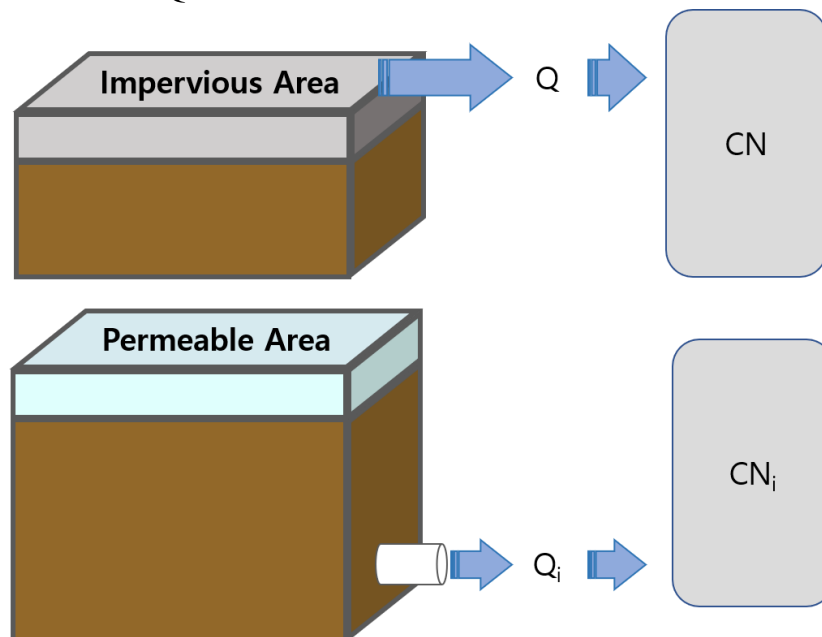


Figure1. Concept of CN and CN_i.

Korea green infrastructure and low impact development center

The Korea Green Infrastructure Center for Low Impact Development (Korea GI&LID Center) built a demonstration complex to establish the efficiency verification technology required in the development and evaluation process of low impact development element technology, and was established for the advancement of low impact development technology and education and research. The location of the Korea GI&LID Center is located within the Yangsan Campus of Pusan National University, and the parking lot-type LID facility is an external verification facility for the permeable LID of this study. It consists of permeable asphalt, permeable asphalt, impervious concrete, permeable concrete, and block pavement. It is divided into a total of 8 zones, and each zone can be individually packaged.



Figure 2. Permeable pavement verification facility in Pusan National University.

For the permeable LID verification facility, facilities such as permeable concrete, permeable asphalt, and block pavement are installed in eight $10.85 \times 2.3 \times 0.9$ (m) areas.

Infiltration water and surface water in each area are monitored through a tipping bucket flow meter in the monitoring box.



Figure 3. Tipping bucket flow meter.

Rainfall Simulator

The mobile-assembled rainfall simulator is composed of a plurality of frame assemblies, rainfall spray pipes, oscillators, and water supply devices. It can be assembled according to the site conditions, and it is easy to move by mounting wheels. Also, as a number of assembled structures (rainfall simulators) can be connected in series or in parallel, efficient rainfall simulation is possible in a wide range of site conditions as well as the oscillator. can be used to induce free fall of rainfall particles.

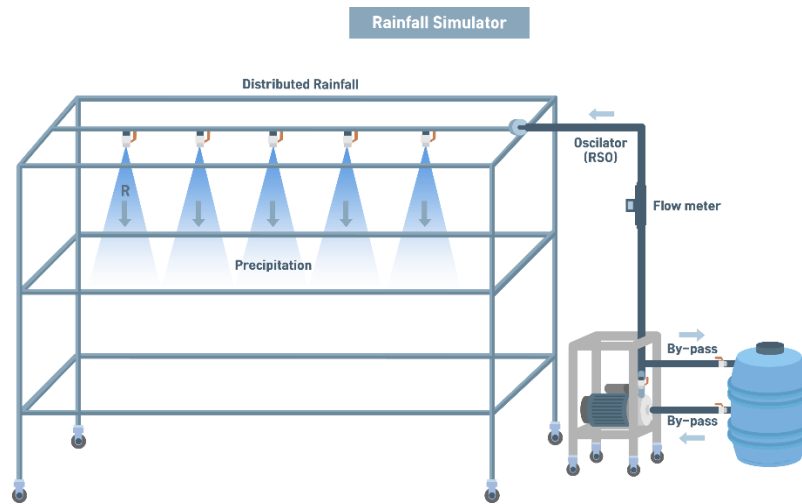


Figure 4. Mobile-assembled rainfall simulator.

Pavement and Rainfall Scenario

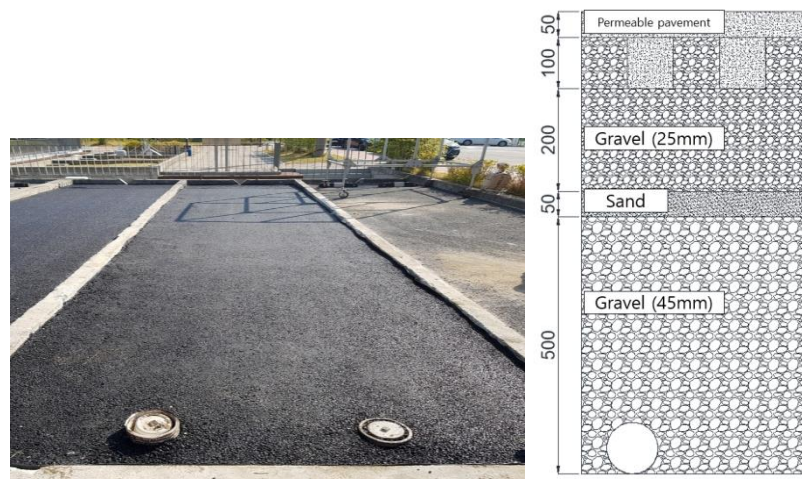


Figure 5. Permeable pavement and cross-section.

Table 1. Rainfall simulating scenario.

Time	Precipitation	Rainfall intensity
1hour	105mm	105.0 mm/hr
2hours	145mm	72.5 mm/hr
3hours	175mm	58.3mm/hr

3. RESULTS AND DISCUSSIONS

Runoff

The total runoff volume of the permeable asphalt pavement was 82.74 ~ 99.00% of the rainfall, and it was measured that an average of 93.36% of the total rainfall was infiltrated and then drained.

Due to the structural characteristics of drainage through the installed perforated pipe, it is judged that the amount of runoff occurred in excess of the water permeability of the drainage perforated pipe in the case of rainfall intensity of 105 mm/hr. The conversion time for rainfall

that passed through the permeable asphalt pavement to runoff was about 4 to 7 minutes by rainfall intensity.

Table 2. Result runoff for simulated precipitation.

	Precipitation (mm)	Drainage		Maximum Drainage		Depth of runoff (mm)
		Volume (L)	Occur time (min)	Volume (L)	Occur time (min)	
Permeable Pavement	105 mm/hr	2,167.81 82.74%	4	30.78	20	86.9
	145 mm/2hrs	3,558.57 98.33%	4	29.51	36	142.6
	175 mm/3hrs	4,323.26 99.0%	7	24.50	48	173.2

CNi

In the analysis, the maximum potential water retention and values were calculated as the total runoff for each rainfall, and this was taken as an average value and expressed as a representative value of the pitched LID system.

Table 3. CNi for permeable pavement.

	Precipitation (mm)	Area(m ²)	Total Runoff (L)	Maximum potential retention	CNi	Average CNi
Permeable Pavement	105 mm/hr		2,167.81	17.181	93.66	
	145 mm/2hrs	24.955	3558.57	2.023	99.209	97.43
	175 mm/3hrs		4323.26	1.475	99.422	

It is shown by calculating the change in the value according to the final permeability of the installed ground of the permeable LID system. It was found that the value of 97 was shown in the section from coarse sand to silt, and it was found that the section from ultrafine sand to fine sand gradually decreased at the age of 90. After neutral sand, the value will drop sharply, and a large amount of infiltrated runoff is expected to infiltrate into the ground. Therefore, it is judged that the purpose of the urban permeable LID system can be sufficiently achieved even without the connection of the storage tank depending on the system installation environment depending on the ground conditions.

Table 4. Changes in CNi due to ground infiltration

D20(mm)	k(cm/s)	CNi	(mm)	(cm/s)	CNi
0.005	3.00×10^{-8}	97.36	0.18	6.85×10^{-3}	-
0.01	1.05×10^{-5}	97.18	0.20	8.90×10^{-3}	-
0.02	4.00×10^{-5}	96.46	0.25	1.40×10^{-2}	-
0.03	8.50×10^{-5}	95.35	0.3	2.20×10^{-2}	-
0.04	1.75×10^{-4}	93.12	0.35	3.20×10^{-2}	-
0.05	2.80×10^{-4}	90.45	0.4	4.50×10^{-2}	-
0.06	4.60×10^{-4}	85.74	0.45	5.80×10^{-2}	-
0.07	6.50×10^{-4}	80.55	0.5	7.50×10^{-2}	-
0.08	9.00×10^{-4}	73.32	0.6	1.10×10^{-1}	-
0.09	1.40×10^{-3}	56.68	0.7	1.60×10^{-1}	-
0.10	1.75×10^{-3}	53.24	0.8	2.15×10^{-1}	-
0.12	2.60×10^{-3}	-	0.9	2.80×10^{-1}	-
0.14	3.80×10^{-3}	-	1.0	3.60×10^{-1}	-
0.16	5.10×10^{-3}	-	2.0	1.80	-

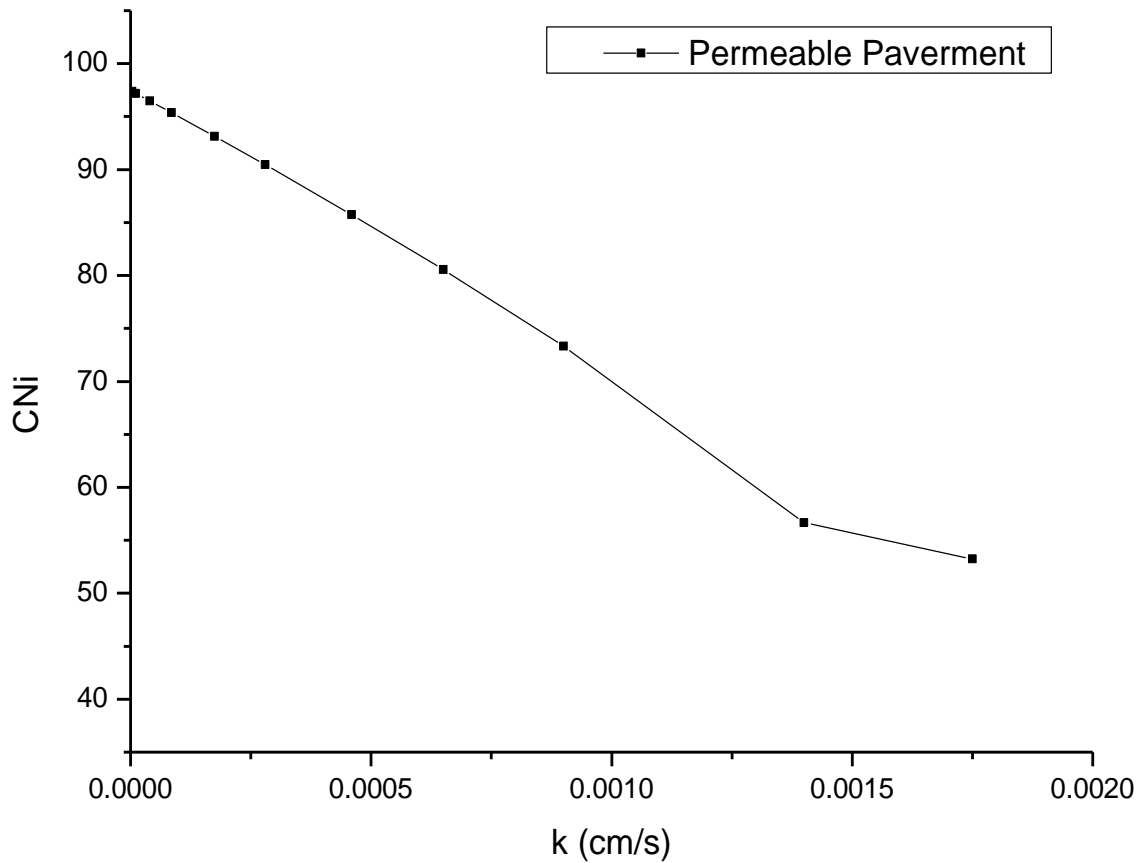


Figure 6. Changes in CNi due to ground infiltration.

4. CONCLUSIONS

In this study, the amount of runoff of the permeable pavement was calculated through rainfall simulation. Through this, the infiltrated runoff coefficient CNi for a specific permeable pavement was calculated so that the infiltrated runoff amount could be predicted during on-site construction. As a result of the calculation, the average CNi was 97.43, indicating that most of the rainwater was drained rather than stored. In addition, the CNi according to the ground infiltration capacity was calculated to predict the change in infiltrated runoff due to the infiltration of the site ground, and it was found that the CNi decreased to 53.24.

Acknowledgements: This work was supported by the " Graduate school of Green Restoration specialization " of Korea Environmental Industry & Technology Institute grant funded by the Ministry of Environment, Republic of Korea.

REFERENCES

- Navas, F. Alberto, J. Machin, A. Galan. 1990. DESIGN AND OPERATION OF A RAINFALL SIMULATOR FOR FIELD STUDIES OF RUNOFF AND SOIL EROSION, Soil Technology, 3, 385-397 French, R. H., & French, R. H. (1985). Open-channel hydraulics (pp. 598-619). New York: McGraw-Hill.
- Cahill, T. 1994. Technical Note 21: A Second Look at Porous Pavement/Underground Recharge. Technical Notes-Urban Best Management Practices. Watershed Protection Techniques. 1(2). pp 76-78.
- Chow, V.T., Maidment, D.R., and Mays, L.W., 1988. Applied hydrology., McGraw-hill International Editions
- Elizabeth A. Fassman and Samuel Blackbourn J., 2010. Urban Runoff Mitigation by a Permeable Pavement System over Impermeable Soils, Hydrologic Eng., Vol.15, No.475
- J.H. Park, 2019. A Study on Hydrological Performance for PNU Parking Lot LID Facility Based on Field Experiments and K-LIDM Modeling, Master Degree. Pusan National University.
- J.R. Park, J.H. Park, J.H. Cheon, J.H. Lee, H.S. Shin, 2020. analysis of Infiltrating Water Characteristics of Permeable Pavements in a Parking Lot at Full Scale, Water, MDPI, 12(8), 2021
- Kim, B.H. 2001. Experimental and Numerical Study on Effects of Runoff Reduction in the Permeable Pavement. M.S. dissertation, Myongji University, pp. 32-4
- Lee, J.M., Jun, S.M., Park, J.H., and Lee, S.H. 2006. A study for Hydrological Infiltration Properties of Permeable Pavement. Journal of Korea Water Resource Association, pp. 1711-1715.

DEVELOPMENT OF A STEADY STATE-ANALYTICAL WATERBODY NETWORK MODELING TOOL TO IDENTIFY THE INDIVIDUAL IMPACTS OF MULTIPLE POINT AND DIFFUSE NUTRIENT EMISSIONS

Ali Ertürk^{1*}, Cenk Gürevin¹, Natalja Čerkasova^{2,3}

¹ Department of Inland Water Resources and Management, Faculty of Aquatic Sciences, Istanbul University, Istanbul, Turkey

² Marine Research Institute, Klaipėda University, Klaipėda, Lithuania

³ Texas A&M AgriLife Research, Blackland Research and Extension Center, Temple, Texas, USA

*Corresponding author (erturkal@gmail.com, erturkali@istanbul.edu.tr)

ABSTRACT

In this study, a mathematical modeling tool that can not only estimate the water quality in terms of diffuse nutrient emissions but also can track the individual impacts of each pressure (such as the boundary conditions, point sources on different locations and emissions of diffuse nutrient that reach the system at different locations and from different land use practices) is developed. The tool is based on the analytical solution of mass balance equations, so when applying the tool solutions are obtained as mathematical functions that can represent any sub-result separately from the others rather than table solutions that only give the total impact of all impacted discharges providing a spatial differentiation within the system only. The modelling tool developed and described in this study can be used to assess the eutrophication at any location in a river basin that consists of many flowing and standing waterbodies without losing the information related to each individual impact of different pressures.

Keywords: *Diffuse nutrient loads, impact of individual pressures, water quality, eutrophication, modelling*

1. INTRODUCTION

It is known that the riverbasins are under the direct (such as the environmental pollution) or indirect (such as the climate change) anthropogenic pressure. Even though the anthropogenic pressures have many reasons; these can be grouped into two main branches, the continuous increase of the world's population and the urge of the society to increase its life standards as a result of enhanced opportunities. Considering the nowadays conditions, it is clear that these pressures will not completely disappear and probably be on an increasing trend due to the population increase. On the other hand, continuously enhancing technology also made a better raw materials/natural resources management and tools and engineering structures (such as the urban infrastructures and wastewater treatment plants) aiming to decrease anthropogenic pressures on ecosystems were developed. The efforts to decrease the anthropogenic pressures on river basins require high-cost investments. The existence of ecosystems that also provide important ecosystem services together with high costs of environmental protection-oriented investments resulted in the emergence of the concept of “ecosystem management”.

With the ecosystem management; it is possible to decrease the anthropogenic pressures on inland aquatic ecosystems, however realization of investments with high costs will be necessary. A considerable number of human pressures may occur on these watersheds each requiring measures with high-cost investments. There will be difficulties to cover the financial requirement individual infrastructure investments have high costs and financing all of them simultaneously is not possible and since any individual investment will only solve a small part of the total pressure on aquatic ecosystems the determination of the benefit of an individual infrastructure investment is not easy. This is a difficult problem especially for the counties with a relatively low GDP per capita. Under such conditions; decision support systems that should help to optimize the planning process

2. MATERIAL AND METHODS

Any watershed incorporates several components but basically some terrain and a waterbody network that consists of river and standing waterbodies. The river waterbodies can further be segmented into river reaches through which the nutrients are routed without the impact of any additional forcing from upstream to downstream. According to the land-use in the watershed, point nutrient loads may exist, however any watershed even the ones with totally natural terrain and without any human impacts will emit diffuse nutrient loads at least natural background nutrient loads that can be found in any terrestrial ecosystem. Diffuse nutrient loads are usually compositions of different emissions such as fertilizer use, livestock breeding, background loads from different land uses etc. and each of the individual load is routed through all of the downstream waterbodies until the target waterbody making very hard to distinguish the contribution of each individual nutrient load to the total load reaching the target waterbody through the watershed outlet. A computational system that is capable of routing the individual loads separately and independently required if such an information is of concern for various management questions is illustrated in Figure 1.

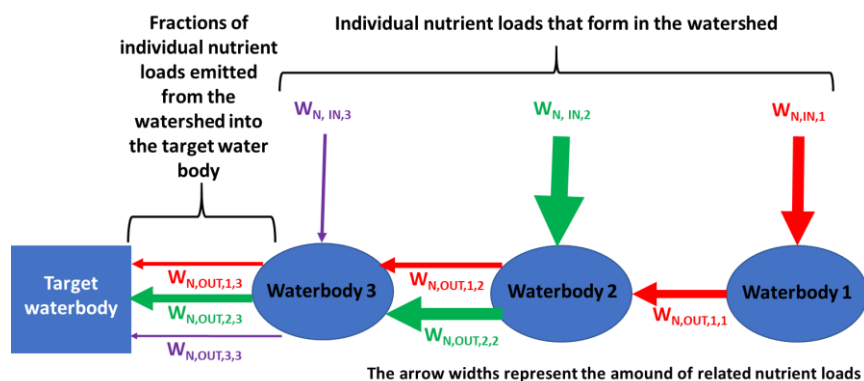


Figure 1. The modelling approach

The standing waterbodies are represented as two layered lakes of reservoirs using simplified kinetics (Figure 3) and could be classified as a simple eutrophication model. The mass balance equation as schematized in Figure 3 are constructed using the response matrix approach described by basic water quality modelling texts such as Thomann and Mueller (1987) and Chapra (1997) and solved for steady state analytically using the matrix inverse method where the multiplication with inverse matrix provides the solution in a form that the effect of any state variable related load can be observed as sum-product notation in the solution.

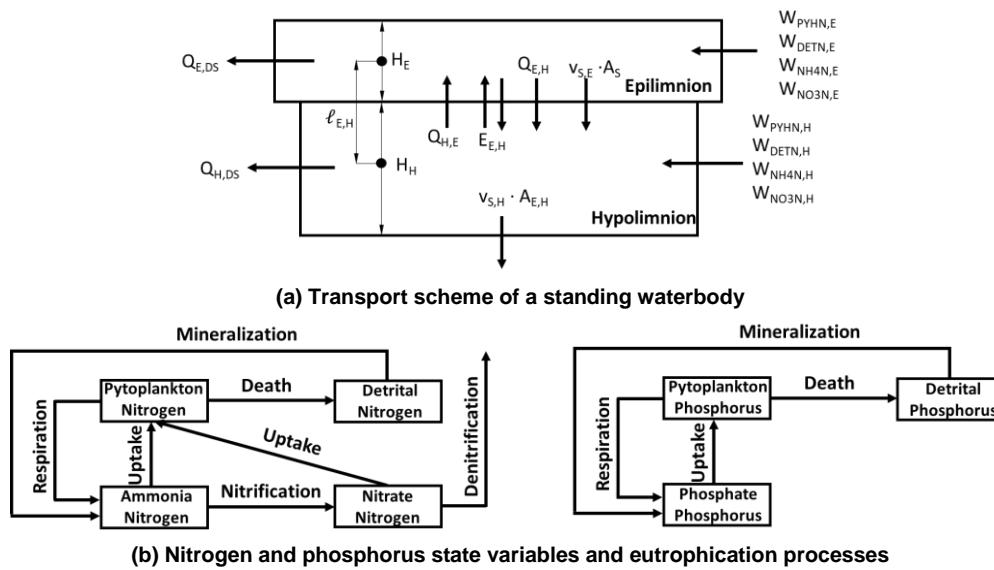


Figure 3. Representation of standing waterbodies

The river waterbodies are modelled as plug flow reactors with similar kinetics to standing waterbodies except that it is assumed that the primary production can be neglected so there is no nutrient uptake in the rivers but only death and respiration process of primary producers providing the freely available nutrient recycle. Unlike the standing waterbodies, the mass balance for river waterbodies is in the form of differential equations in a sequencing order, but still analytically solvable. The related solutions are conducted.

3. RESULTS AND DISCUSSIONS

In this study, the solutions for standing and river waterbodies mentioned in the materials and methods section are successfully implemented as high performance software that could be considered as a far more enhanced version of the SISMOD model (Erturk, 2010) and applied to a fairly complex watershed to identify the relative importance of different nutrient emissions on a target waterbody, which is a hypertrophic shallow lake.

4. CONCLUSIONS

A new modelling software is developed and applied to a real system to identify the relative importance of different point and diffuse nutrient sources from a real watershed into a lake ecosystem. More details will be given during the presentation and the full paper version of this extended abstract.

REFERENCES

- Chapra, S.C., (1997). Surface Water Quality Modeling, McGraw-Hill
- Erturk, A. (2010) A Simple Stream Water Quality Modelling Software for Educational and Training Purposes, Turkish Journal of Fisheries and Aquatic Sciences 10: 61-70, DOI: 10.4194/trjfas.2010.0109
- Thomann, R.V, Mueller, J.A., (1987). Principles of Surface Water Quality Modeling and Control, Harper Collins Publishers

WATER FOOTPRINT CONCEPT AND FORESTS

Gafura A.Özdemir¹ and Batın Mehmet Yer¹*

¹ İstanbul University - Cerrahpasa Faculty of Forestry, Turkey

**Corresponding author (gafura@iuc.edu.tr)*

ABSTRACT

Water footprint is a remarkably crucial concept in terms of sustainable water management. The concept of water footprint was first introduced by UNESCO-IHE Water Education Institute in 2014. Water footprint explains people's need for fresh water in terms of volume. The components of the water footprint are the green, blue and gray water footprint. After oxygen, the substance necessary for life is water. Types of water are surface water, groundwater, seawater, mineral water and fossil water. The total amount of water in the world is about 1.5 billion km³. The amount of fresh water is 350,000,000 km³. Plants take nutrients from the soil with water and are carried in their organs from there. Technical features, time, growing areas as well as the amount of water in the soil of the trees in the growth, development and shaping of forests. Water scarcity is measured with the Falkenmark index which is calculated by dividing the available water resources by the population. If the Falkenmark index value is 1700 m³/person/year and more, there is no water problem. Turkey is a country with water stress due to its Falkenmark index value is 1519 m³/person/year according to the 2014 WFF (World Wide Fund for Nature) report. Plants need heat, light and water for photosynthesis. The effect of climate features on life and production of living things cannot be calculated mathematically. However, statistically average values can be given. Annual rings are the place where the effects of climatic features such as temperature, precipitation, humidity, wind, light and frost are observed on forest trees. Stand density acts an important role in the production of materials and services in the forest. With the stand basal area increase in the forest the water production decreases. Forests are important in terms of water productivity. Hydrological function of the forest functions includes water production, increasing the quantity and quality of water, ensuring the continuity of water and protecting water resources. This study was aimed to raise water footprint awareness. The concept of water footprint will be explained in order to draw attention to the purpose of clean water and sanitation which are among the goals of sustainable development. Forest role of water production will be emphasized. In addition, forests have great importance in climate action, one of the goals of sustainable development. Growth and development in forest trees are shaped by climatic conditions. Water is important in terms of the growth and development of forest. Forests are much more in regions with heavy precipitation. Decrease in precipitation depending on climate change will result in water shortage. The protection of forests and the concept of water footprint are important in terms of sustainable water management. When water resources are polluted, they cannot be used. Water footprint can be reduced by reducing the amount of water used in daily life and taking precautions against water waste. Waste that is separated and recycled must be ensured.

ECOLOGICAL PROTECTION AND RESTORATION

USING SYSTEM DYNAMICS MODELLING TO VISUALIZE THE EFFECTS OF RESOURCE MANAGEMENT AND POLICY INTERVENTIONS ON BIODIVERSITY AT A REGIONAL SCALE

Chrysi Laspidou^{1*}, Konstantinos Ziliaskopoulos²

¹. University of Thessaly, Department of Civil Engineering, Volos, Greece

². University of Thessaly, Department of Environmental Sciences, Larissa, Greece

*Corresponding author (laspidou@uth.gr)

ABSTRACT

A methodology and a System Dynamics Model is constructed using published data from the IUCN Red List Index database that can be used for any region to quantify the biodiversity status. The methodology is implemented for the Nestos River catchment in Greece, showcasing how the authorities could run scenarios of different interventions, addressing the specific problems and threats to the local ecosystem that each community might be facing and how they could receive estimates of biodiversity improvements as a result of these interventions. The methodology compares and contrasts four specific threats to the ecosystem, identified from stakeholder consultation workshops, namely solid waste, agriculture, domestic wastewater and dams and water management/use. The effects of each one of the interventions to the species in the region and to the modified Red List Index overall are presented and compared, showcasing the dams as the most deleterious threat to the local ecosystem. Finally, an easy to use interface is developed and introduced in order to better connect the stakeholders with the scientific analysis and facilitate informed decision-making that could lead to smarter policy implementation and better pathways to SDG compliance.

Keywords: *Biodiversity, Red List Index, System Dynamics Model, Policy Co-creation, SDG15*

1. INTRODUCTION

Global biodiversity is declining rapidly, largely due to climate and land use change. According to the Global Assessment Report on Biodiversity and Ecosystem Services by IPBES (<https://ipbes.net/>), there is overwhelming evidence that presents an ominous picture, since the health of ecosystems is deteriorating at an alarming rate. The effects of these changes on biodiversity responses differ among ecosystems and transnational regions, especially when they have important differences in species composition. Newbold et al. (2020) have identified the Mediterranean region as one that has sustained the strongest negative responses to both land-use and climate pressures. A critical step in taking action for halting biodiversity loss is understanding how biodiversity is changing and quantifying how much it is changing. Furthermore, since biodiversity loss is directly linked to human activities, it is the decision- and policymakers that need to regulate how people relate to their natural environment, through prioritizing their regulations, interventions, infrastructure, and resource use.

In this analysis, we develop a methodology for calculating a modified Red List Index (RLI) for a scale that is smaller than national—regional or local, customized to the specific needs,

conditions, pressures, and/or threats of the region. Specifically, we demonstrate the methodology for the Nestos River basin in Greece, even though it could be applicable to any region. We then define specific pressures that are applicable to the region under study, and we include them in the model. New RLI values are obtained for a range of interventions that will mitigate the effects of the specific pressures that the ecosystem under study withstands. A visual interface is also constructed that allows stakeholders to experiment with different interventions and observe the effects they have on biodiversity through the RLI.

2. MATERIALS AND METHODS

The work presented in this analysis takes stock of stakeholder consultations during a workshop on the transboundary case study of the Greece-Bulgaria Nestos River catchment under a nexus framework to identify key interventions available for the region. Representatives of local government, businesses and the private sector, energy and water resource operators and managers, environmental organizations, NGOs, and academic/research institutes were among the workshop participants. The overarching aim of this series of workshops was the co-creation and co-design of policies targeting the effective management of water resources through the integrated management of the Water-Energy-Food-Ecosystems (WEFE) nexus. With the conclusion of the first workshop, it was possible to conclude on the major pressures that the Nestos river basin ecosystem sustains. These can be grouped in four categories: (i) agriculture with the increased use of fertilizers, pesticides and herbicides; (ii) solid waste, since some of the upstream villages on the Bulgarian side do not have a solid waste management plan and large quantities of garbage end up in the river downstream; (iii) domestic wastewater, since some of the settlements do not have a wastewater network; (iv) hydropower dams that alter and degrade the ecosystem and the availability and/or fluctuation of adequate ecological flow.

We then obtained data from the IUCN Red List Index database (<https://iucnredlist.org/>) for mainland Greece. Each species is listed in the data base with its Red List Category with the following scores (Butchart et al., 2004): 5—Extinct (EX), 4—Critically Endangered (CE), 3—Endangered (EN), 2—Vulnerable (VU), 1—Near Threatened (NT), and 0—Least Concern (LC). The list of relevant species was identified on the basis of the habitat of interest. In the case of the Nestos catchment, relevant habitats were “5.1-Wetlands (inland) - Permanent Rivers/Streams/Creeks (includes waterfalls)” and “5.13-Wetlands (inland) - Permanent Inland Deltas”. We then proceeded to further refine the list, by cross-mapping the species on our initial list with the four types of threats that we identified as important from the stakeholder workshop. In the IUCN database, the species are listed along with the corresponding threats that could potentially pressure them, and we identified the threats from the database that correspond to the ones pinpointed by the stakeholders.

We then developed an algorithm to calculate a simulated Red List Category (SRLC) for each species, depending on the level of each individual intervention previously identified, and simulated the SRLC for each species in a System Dynamics Model with STELLA software (<https://www.iseesystems.com/>).

$$SRLC_i = RLC_i \times \left(1 - \frac{WWV_i \times WWI + SWV_i \times SWI + AgrV_i \times AgrI + DV_i \times DI}{WWV_i + SWV_i + AgrV_i + DV_i + Other_i} \right)$$

Where, (S)RLC is the (Simulated) Red List Category Score of species i , WWV_i , SWV_i , $AgrV_i$, and DV_i stand for the vulnerability of species i to each of the four threats analyzed (wastewater, solid waste, agriculture and dams, respectively), while $Other_i$ is the number of threats of species i to other threats beyond these four. Vulnerability, as explained before is a binary parameter and takes values of either 0 or 1. Finally, WWI , SWI , $AgrI$ and DI denote the level of intervention in each of the four threat categories; as explained before, these exogenous variables range from 0 to 1. Having calculated $SRLC_i$ for all species, we can then calculate a new simulated RLI for the region using the same RLI equation (Butchart et al., 2007). To show the results of the model, we ran the simulation five times, once with each intervention equaling 1 and the other three interventions equaling 0 and once with all interventions equaling 1. In the former case, we explore the full potential of each intervention separately to the biodiversity of the region. In the latter case, we show the ideal scenario, when all four important pressures in the region are eliminated.

In order to be able to better visualize the improvements of the RLI as a result of interventions to the stakeholders, we normalize both the current and the simulated modified RLI scores. This is only done for visualization purposes and does not alter the value of the simulated RLI score. An overview of the methodology in a step by step fashion is shown in Figure 1a, while the model as it was done in STELLA software is shown in Figure 1b.

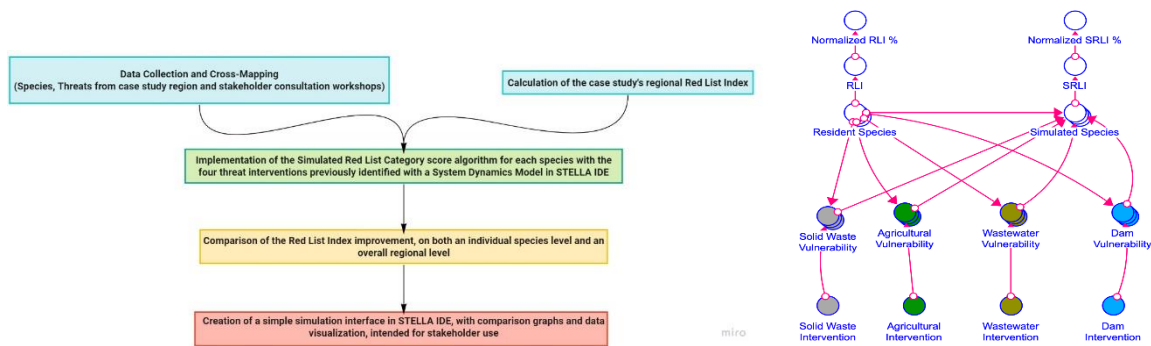


Figure 1. An overview of the (a) step by step methodology and (b) System Dynamics Model.

3. RESULTS AND DISCUSSIONS

The results of these simulations to the RLC per species are shown in Figure 2. Please note that only the species with an RLC of 1 and up (NT to EN, since no EX or CE species were identified in the case study region) are included in Figure 2, since no further RLC improvement is possible with species with an RLC score of 0.

The interface developed has been uploaded to the iseessystems website and can be accessed publicly through the following link. The interface allows the user to vary the level of each intervention in a scale of 0 to 1 and then to run the model and see the corresponding % normalized SRLI each time for the entire case study region:

<https://exchange.iseesystems.com/public/chrysi-lapidou/red-list-index-calculation-for-nestos-rbd-greece>

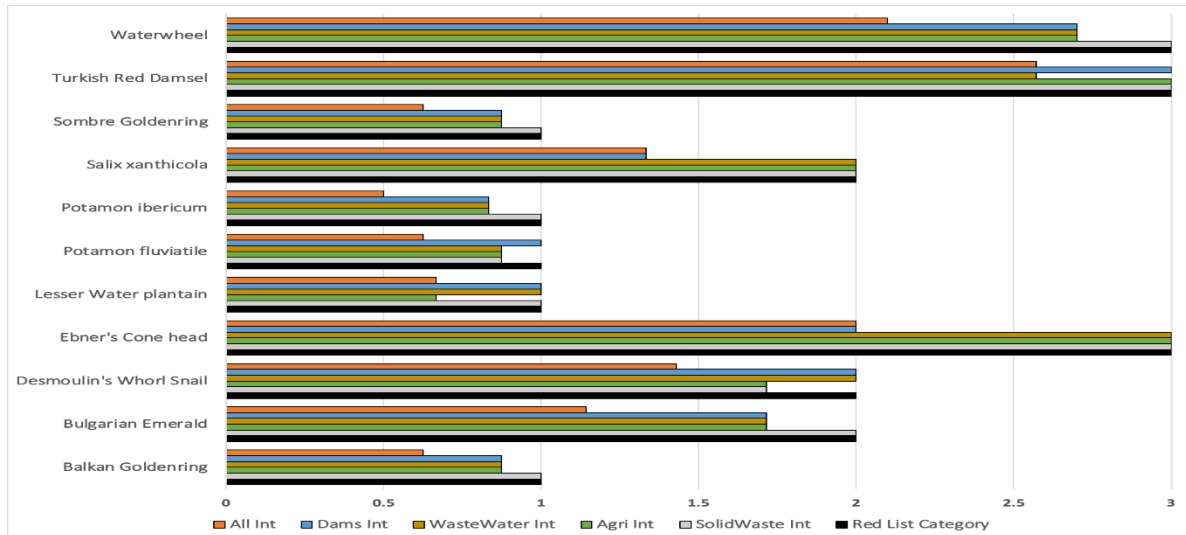


Figure 2. Results of five simulation runs analyzing the impact of all modeled interventions to the RLC per species. In the legend, the different interventions are shortened as “Int”, so “WasteWater Int” stands for Wastewater Intervention equal to 1, etc. The term “All Int” signifies that all intervention variables equal to 1, while “Red List Category” denotes the current situation with all intervention variables equal to 0 (no intervention).

REFERENCES

- Butchart, S.H.M., Stattersfield, A.J., Bennun, L.A., Shutes, S.M., Akçakaya, H.R., Baillie, J.E.M., Stuart, S.N., Hilton-Taylor, C., Mace, G.M. and Reid, W.V., 2004. Measuring global trends in the status of biodiversity: Red List Indices for birds. *PLoS biology*, 2(12), p.e383, <https://doi.org/10.1371/journal.pbio.0020383>
- Butchart, S.H., Resit Akçakaya, H., Chanson, J., Baillie, J.E., Collen, B., Quader, S., Turner, W.R., Amin, R., Stuart, S.N. and Hilton-Taylor, C., 2007. Improvements to the red list index. *PloS one*, 2(1), p.e140, <https://doi.org/10.1371/journal.pone.0000140>
- Newbold, T., Oppenheimer, P., Etard, A. and Williams, J.J., 2020. Tropical and Mediterranean biodiversity is disproportionately sensitive to land-use and climate change. *Nature Ecology & Evolution*, 4(12), 1630-1638. <https://doi.org/10.1038/s41559-020-01303-0>

CHARACTERISTICS OF VEGETATION SUCCESSION IN THE EXPOSED LAND CAUSED BY THE OPENING OF THE FLOODGATE IN SEJONG WEIR, GEUMGANG RIVER, SOUTH KOREA

Kim YoonSeo¹, Park Jae-Hoon¹, Kim Eui-Joo¹, Lee Jung-Min¹, Park Ji-Won¹, Kim Se-Hee¹, and You Young-Han^{1*}

¹ Department of biological science, Kongju National University, Gongju 32588, Republic of Korea

*Corresponding author (youeco21@kongju.ac.kr)

ABSTRACT

In order to predict plant successional series of mid-channel bar in Sejong Weir, South Korea, we investigated the vegetation and flora in the exposed areas with the floodgates open from 2019 to 2021 and Multivariate statistical analysis was conducted by linking the characteristics of topographical factors and soil environmental factors. As a result, a total of 26 communities appeared in floodplain and a total of 6 communities appeared in mid-channel bar. As a result of classifying the communities by cluster analysis, they were divided into 5 groups at 25% binding distance, each group was classified according to life form of dominant species and vegetation altitude. As a result of CCA analysis, the main environmental factors affecting the distribution of plant colonies in the exposed areas of the Geumgang river water system were altitude, distance from the waterway, soil organic content, substitution Ca, and substitution Mg. Floodplain has a lot of soil sedimentation, high soil nutrient content, and the number of plant communities is more than the mid-channel bar. pioneer plants in the floodplain were *Ambrosia trifida*, *Humulus japonicus*, *Miscanthus sacchariflorus*, *Phalaris arundinacea*, *Phragmites australis*, and *Scirpus radicans*. They will be replaced mainly by perennial plants over time.

In mid-channel bar, *Salix chaenomeloids* and *Phragmites japonica* are pioneering plants, and over time, *Salix chaenomeloids* is expected to continue to be maintained, and *Phragmites japonica* is expected to be maintained at low flow rates, But transition to *Salix chaenomeloides* community is expected in places where flow rates are high and erosion occurs. It could be seen that the vegetation of the floodplain and mid-channel bar were different, and succession of vegetation proceeded differently.

Keywords: Exposed land, Mid-channel bar, Floodplain, CCA, Cluster analysis.

1. INTRODUCTION

A river is a complex ecosystem where several organisms live, and the cross section of the river is largely divided into an aquatic area, a water purification area, and a flood site (Kim, 2005). Unlike natural forests in mountainous areas, the river ecosystem is a dynamic ecosystem that fluctuates at short intervals (e.g., 2003). The functions of the river are summarized into three categories: dimension, water supply, and environment. The dimensional function is a function of preventing flooding and drought disasters, and the drainage function is a function of taking economic benefits from rivers. In addition to the river's dimensional and drainage functions, the environmental functions are natural functions such as the habitat function of river animals and plants, the self-purification function of the water quality, and the aesthetic function (Ministry of Environment, 2002).

In 2009, the Korea government promoted the four major river restoration projects to improve water quality, restore the health of the river ecosystem, increase flood communication ability through active river management, actively cope with climate change, actively utilize river spaces in harmony with nature and humans, and diversify water resources through dredging and installing reservoirs (Audit, 2018). Since the completion of Sejongbo in 2011, the BOD, Chongin, and Chl-a of the Geumgang River have generally decreased, but the floodgates have been opened to solve these problems due to weather factors, lack of nutritional salt reduction measures, and increased stay time. The large beam of the Geumgang River water system has been partially or completely opened since June 2017, and the water level of Sejongbo has decreased from 11.8m to 8.4m (Ministry of Environment, 2021). As the water level decreased, the soil deposited from the riverbed was exposed to the atmosphere, and a new sand bar with an area of 0.293 km² was generated. Due to the expansion of various ecological habitats, wetland-grown herbs such as reeds, grasses, and mulberry trees, and native deciduous broadleaf trees such as willow trees and mulberry trees dominated the exposed areas, recovering the epidermis rate to 60% of Sejongbo. In addition, the habitat environment of land animals such as water birds and mammals, including endangered species, has diversified.(Ministry of Environment, 2021).

In this study, we investigated the vegetation distribution status in exposed areas exposed to the opening and water level of the four major rivers, and investigated which environmental factors affect the distribution of vegetation through multivariate statistical analysis. In addition, the predictable vegetation stream model of Hajungdo Island, which serves as an important habitat for endangered animals, water birds, and land animals, was developed.

2. MATERIAL AND METHODS

The area subject to this study is the section where the Hinduri Bridge, located in Sejong-ri, Yeongi-myeon, Sejong-si, passes for Sejongbo(36°28'33.65"N, 127°15'57.92"E).

The investigation point is 1km upstream based on the reservoir, and the left bank, right bank, and mid-channel bar of the exposed area caused by the lower water level due to the flood and the opening of the reservoir were investigated. In 2019, a total of 32 points were surveyed on the left bank, right bank, and mid-channel bar, and 7 points were surveyed on the mid-channel bar in 2020 and 9 points were surveyed on the mid-channel bar in 2021(Fig. 1).



Figure1. The location of studied area in Sejong weir (A: right floodplain, B: mid-channel bar, C: left floodplain).

Data Sampling

To analyze the environmental factors of the survey area, soil moisture content, soil pH, distance from the waterway, depth of the deciduous layer, soil electrical conductivity, and soil were measured. In order to analyze the chemical composition of the soil, the organic content, the substituted cation (Ca, Mg, K, Na), and the total phosphorus and total nitrogen content were analyzed.

Data Analysis

This survey was conducted from September 2019 to 2021, and field surveys were conducted once or twice at each survey point. In 2020, a field survey was conducted once in October after the flood. In 2021, a field survey was conducted once in September. In the vegetation survey, for each colony, the herbaceous layer colony was set to 1m×1m or the shrub layer colony to 2m×2m, and the sub-tree and tree layer colonies were set to be 10m×10m square. A phytosocial survey was conducted by Braun-blauquet's dominant viscosity (Braun-blauquet, 1964) for each constituent species.

Statistical analysis

Through cluster analysis, we checked which plant communities the survey sites were gathered, and a canonical response analysis (CCA) was conducted to find out which environmental

factors affected the plant community distribution. Cluster analysis and canonical response analysis used the analysis package PC-ORD 6 (MiM Software Co.) program.

3. RESULTS AND DISCUSSIONS

Cluster Analysis

As a result of classifying the communities by cluster analysis, they were divided into 5 groups at 25% binding distance, each group was classified according to life form of dominant species and vegetation altitude.

Group 1 was divided into *Phragmites australis* community (4 locations), *Scirpus radicans* community, *Cyperus glomeratus* community, and *Typha angustifolia* community (2 locations), Group 2 was divided into *Phragmites japonica* community (3 locations), *Persicaria hydropiper* community (2 locations), *Salix chaenomeloides* community, *Persicaria hydropiper-Phragmites japonica* community, and group 3 was divided into *Miscanthus sacchariflorus* community (4 locations), *Humulus japonicus* community (3 locations), *Pueraria lobata* community, *Atermisia princeps* community, *Sicyos angulatus* community (3 locations), *Salix Koreaensis* community (3 locations), group 4 was divided into *Ambrosia trifida* community (2 locations), *Conyza canadensis* community, and group 5 was divided into *Robinia pseudoacacia* community (Fig. 2).

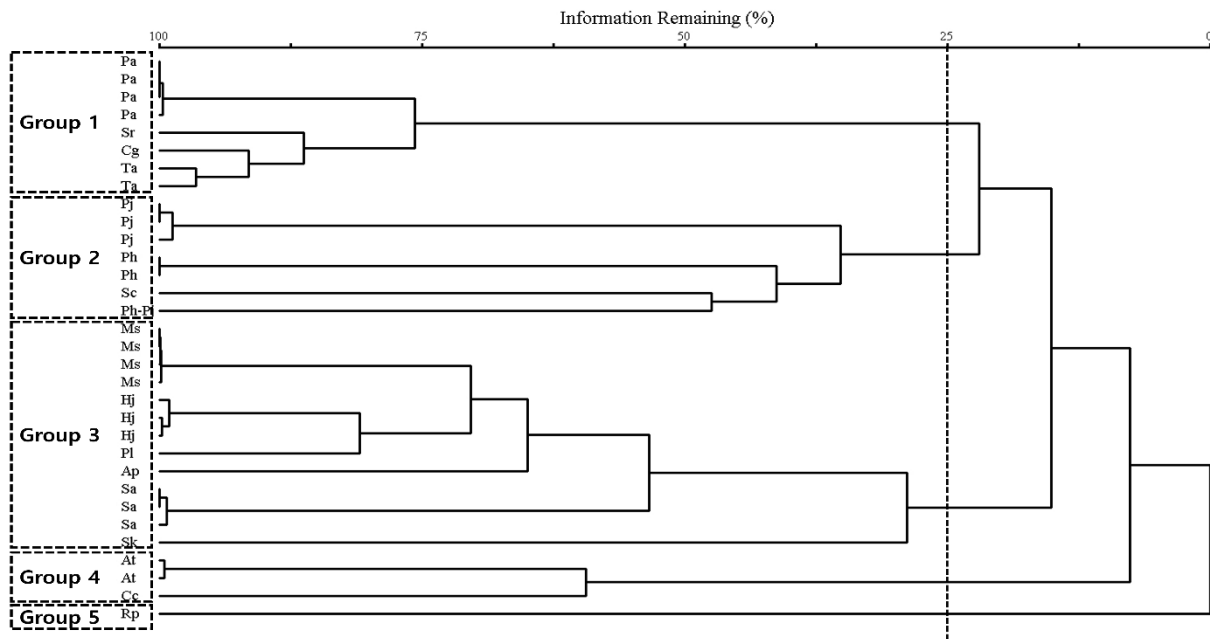


Figure 2. Dendrogram of plant communities using the plant coverage in Sejong weir.

The life types of the dominant species in the plant colony constituting Group 1 were all wet and aquatic plants (HH), and the average altitude was 0.8m. Among the plant communities constituting Group 2, all living types of dominant species except for the Willow colony (MM) were ecological and aquatic plants (HH), and the average altitude was 0.7m. The life types of the dominant species in the plant colony constituting Group 3 were surface plants (Ch), semi-intermediate plants (H), and annual plants (Th), and the average altitude was 2.6m. The life type of the dominant species in the plant colony constituting Group 4 was all annual plants (Th), and the average altitude was 2.2m. The living type of the *Robinia pseudoacacia* community that constitutes Group 5 was large terrestrial plants (MM) and had an altitude of 4.5m.

CCA

When the first and second axes were viewed as X and Y axes, respectively, altitude, distance from the waterway, and soil organic content showed positive correlations with points located in the third quadrant and negative correlations with points located in the first quadrant. In the first quadrant, vegetation that appears in areas susceptible to flooding or close to waterways was arranged. In the arranged plant colony, aquatic plants such as moonroot grass, reeds, baby birds, and pilasters were arranged (Fig. 3). These were the main species that made up river vegetation. Meanwhile, in the third quadrant, vegetation that appears in dry areas or areas where people frequently enter was arranged (Fig. 3). These vegetation were mainly arrowroot, mugwort, and Hwansam vine, which were mainly distributed on embankment slopes or high topography. Plant colonies in the first quadrant close to the waterway seem to have a low soil organic content because they are washed away by flooding, and the organic content and the plant colonies in the third quadrant, which are far from the waterway, are relatively less affected by flooding, so they are considered to have a positive correlation with organic content (Kim et al., 2014).

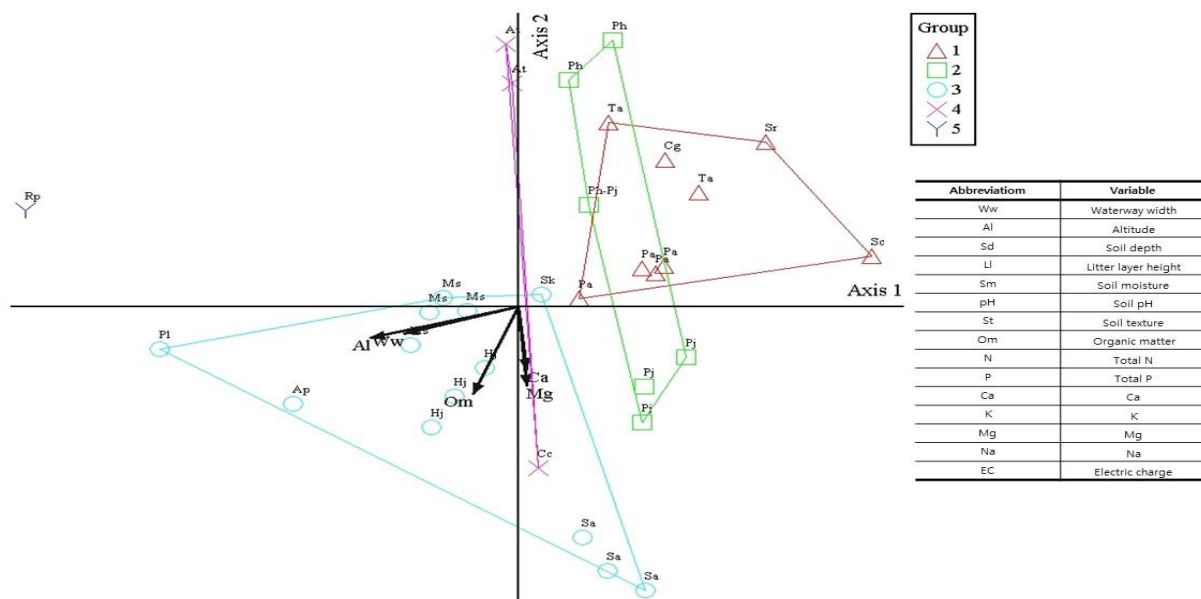


Figure 3. CCA ordination biplot of plant communities and environmental variables in 32 stands which are classified by clustering. The arrows on graph mean significant environmental variables influencing on stands.

4. CONCLUSIONS

The riverbed material in the section with a high flow rate in the mid-channel bar of the exposed area had a high ratio of sand gravel, and the riverbed material in the section with a slow flow rate and deposition was high. Most of the vegetation that had been settled on Hajungdo Island was lost due to the massive flood in 2020, but the colony of *Salix chaenomeloides* community and *Phragmites japonica* community remained.

Figure 4 shows the transition series of the load map, which has simplified vegetation due to flooding.

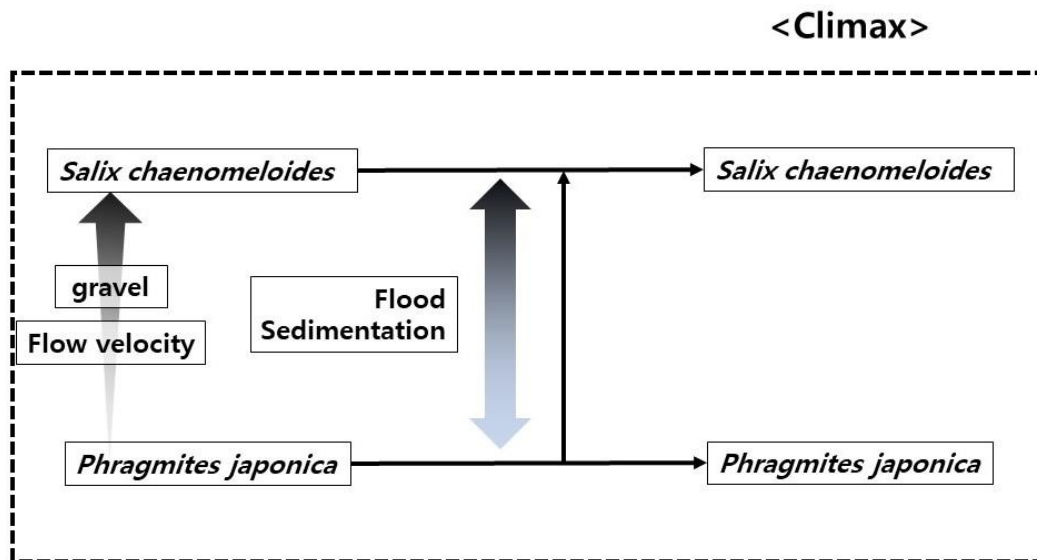


Figure 4. Prediction of plant successional series of mid-channel bar in Sejung weir.

It is believed that the transition series of the mid-channel bar caused by the water level drop in the Geumgang River water system will dominate the section with high flow rates in the same situation as the flooding of rivers. It is believed that the *Phragmites japonica* community will prevail in the section with slow flow and active sedimentation. The willow species have the adaptability to regenerate lost tissue in the event of a flood (Craig et al., 1988), especially the productivity and growth rate of root systems that can quickly stabilize deposits (Cho et al., 2021). *Phragmites japonica* has a large characteristic of physical force due to its flexible anchorage habit and stem shape, which occurs and spreads through the epiglottis, and extends radially along the ground.

Through this, it is believed that the colony of king willow settled in mid-channel bar will become a willow forest over time, and the colony of *Phragmites japonica* community will be maintained over time, or some settled *Salix chaenomeloides* community individuals will develop into king willow colonies over time.

Acknowledgements: This work was supported by Korea Environment Industry & Technology Institute (KEITI) through Wetland ecosystem valuation and carbon absorption value enhancement technology development project, funded by Korea Ministry of Environment (MOE) (2022003630003)

REFERENCES

- Audit. (2018). Audit Report – Inspection and Performance Analysis of the Four Major Rivers Restoration Project.- . pp 2.
- Craig, T.P., Price, P.W., Clancy, K.M., Waring, G.L. & Sacchi, C.F. 1988. Forces preventing coevolution in the three-trophic-level system: willow, a gall-forming herbivore, and parasitoid. *Chemical Mediation of Coevolution* (ed. K. Spencer), pp. 57–80. Academic Press, New York.

Donghwapub. Pp 150-151.

Kim. (2005). Natural River Planning and Design. Seoul. Taerim.

Kwang-Jin Cho, Jeoncheol Lim, Changsu Lee, Yeonsu Chu. (2021). Characteristics of Plant Community of Willow Forest in the Wetland Protection Areas of Inland Wetlands. Korean Wetlands Society, 23(3), 201-212.

Lee. Et al. (2003). River Environment and Waterside Plants -Conservation and Management of Vegetation-.

Ministry of Environment. (2002). River Restoration Guidelines. Pp 1-2.

Ministry of Environment. (2017). Dam-bo-Reservoir Development Service for Optimal Operation.

Ministry of Environment. (2021). Comprehensive analysis report on the opening and monitoring of four major river beams ('17.6 to 20.12).

Ronald D McLaurin, Man Woo Lee, Chang Hwan Kim. (2014). Mid-channel Island Change Analysis. JOURNAL OF THE GEOMORPHOLOGICAL ASSOCIATION OF KOREA, 21(2), 1-10.

VEGETATION AND FLORA OF GONGJU AND BAEKJE WEIR IN GEUMGANG RIVER, KOREA

Jung-Min Lee¹, Jae-young No², Eui-joo Kim¹, Ji-won Park¹, Yoon-seo Kim¹, Se-hee Kim¹, Jae-hoon Park¹ and Young-han You^{1}*

¹. Department of biological science, Kongju National University, Gongju 32588, Republic of Korea

². Doohee Institute of Ecological Research, Korea Ecosystem Service Inc., Ansan 15426, Republic of Korea

*Corresponding author (youeco21@kongju.ac.kr)

ABSTRACT

The Geumgang River is one of Korea's four major rivers with a basin area of 9,810 km², and four major river project that begins in 2010, and a total of three artificial beams were installed: Gongju Weir, Baekje Weir, and Sejong Weir. Gongju and Baekje Weir, which are Geumgang water systems, were selected as survey points, and the survey was conducted twice in total for the first and second rounds. This study was conducted to determine the characteristics of the changes of vegetation and flora in Gongju and Baekje weir of Geumgang River, before and after the opening of the floodgate of the weirs. Flora was a total of 241 taxa including 65 families, 173 genera, 217 species, 2 subspecies, 21 varieties, and 1 forma in Gongju weir, and a total of 279 taxa including 69 families, 187 genera, 252 species, 2 subspecies, 24 varieties, 1 forma in Baekje weir, respectively. In survey, a total of 22 plant communities appeared in Gongju weir and 21 community in Baekje weir. In survey in Gongju weir, there were 1 community of annual herbaceous and vine plants, 7 communities of perennial herbaceous and vine plants, and 2 communities of shrubs, 2 communities tree and subtree plants, 5 communities of exotic species, and 5 communities in artificial planting areas appeared. No endangered species were found in Gongju weir and Baekje weir. In survey in Baekje weir, there were 3 community of annual herbaceous and vine plants, 5 communities of perennial herbaceous and vine plants, and 3 communities of shrubs, 2 communities tree and subtree plants, 2 communities of exotic species, and 6 communities in artificial planting areas appeared.

Keywords: *vegetation, artificial beams, water system.*

1. INTRODUCTION

The natural river has a diverse living environment. The role of vegetation in the river ecosystem is so important that it can be said that most of the conditions are created by the shape and vegetation of the river. Therefore, the diversity of river forms and the recovery of original vegetation can be said to be the origin of the restoration of the river ecosystem (Lee et al., 1999). River ecosystems are becoming increasingly threatened as they face a variety of artificial interference. Comprehensive management strategies are needed to cope with or prevent long-term impacts on habitat and biodiversity as well as ecological functions and services (Lim et

al, 2021). In order to recover the damaged natural stream, it is necessary to create suitable vegetation and know what vegetation is suitable for the specific area. To do so, it is necessary to know the natural and humanities and social environment of the area and to properly understand the current vegetation status of the area (Kim, 2006). This study aims to investigate the number of vegetation species, populations, naturalized plants, and naturalization rates existing along the rivers of Gongju Weir and Baekje Weir, which were constructed as four major river projects, and provide basic data for the management and recovery of the river ecosystem in the Geumgang River Basin.

2. MATERIAL AND METHODS

1) Timing and Scope of Investigation

The survey period of this study was conducted in spring and autumn when river vegetation appeared in order to clearly identify plant species. In order to conduct a plant ecological evaluation of the Geumgang River's waterfront space, a total of 2km of vegetation and vegetation surveys were conducted based on the reservoir, 1km upstream and downstream.

2) Plant survey

The survey identified species appearing around the selected survey area and recorded the species name according to the Botanical Survey Table, and the observation location of special plants, endangered species, protected species, and rare species were recorded by GPS and photographed. Major emerging species were photographed and stored as a file, and the file name included the species name, shipping point, investigation tool, and date.

3) Create Existing Vegetation Diagram

The investigation was conducted in consideration of the maximum growth period of the plant, and a field survey was conducted to investigate the preparation of the existing vegetation after drawing up the vegetation sketch for the section to be investigated. In principle, clusters were classified according to the river plant cluster classification table, based on the landscape and dominant species. Existing vegetation cadet information prepared through field surveys was worked in the form of a shape file using the Geographic Information System (QGIS 2.1.0).

4) River cross-sectional view

It was conducted at the same time as the botanical survey, and the river cross-sectional survey was prepared by sketching transverse vegetation cross-sections from the waterfront (including water areas if there are aquatic plants) to the embankment, and recorded plant species and blood at regular intervals in the River Cross-sectional Vegetation Survey Table. It was always marked from left to right, and the fixed square sphere was installed in an appropriate location after fully grasping the type of colony of the entire survey site. In the river cross-sectional view, the topography, the boundary of plant clusters, representative plants, and rivers were plotted, and the size of the square sphere was set to 5x5m for herbs and shrubs, and 10x10m for subtree and tree layers.

3. RESULTS AND DISCUSSIONS

Plant statuses in the Geumgang River water system area were surveyed in a total of 312 categories, including a total of 74 families, 206 genera, 283 species, 2 subspecies, 26 strains, and 1 variety (Table 1). As for the number of species appearing at each survey point, 279 classification groups appeared in Baekjebo, and 241 classification groups appeared in Gongjubo (Table 1).

The number of families of vascular plants distributed in the area was classified in the following order: Graminae 45 (14.4%), Compositae 34 (10.9%), Leguminosae 27 (8.7%), Gramineae 22 (7.1%), Polygonaceae 16 (5.5%) and Rose (5.4%).

Table 1. Flora of vascular plants in Gongju weir and Baekje weir.

Weir	Family	Genus	Species	Subspecies	Variety	Cultivar	Total
Gongju	65	173	217	2	21	1	241
Baekje	69	187	252	2	24	1	279
Total	74	206	283	2	26	1	312

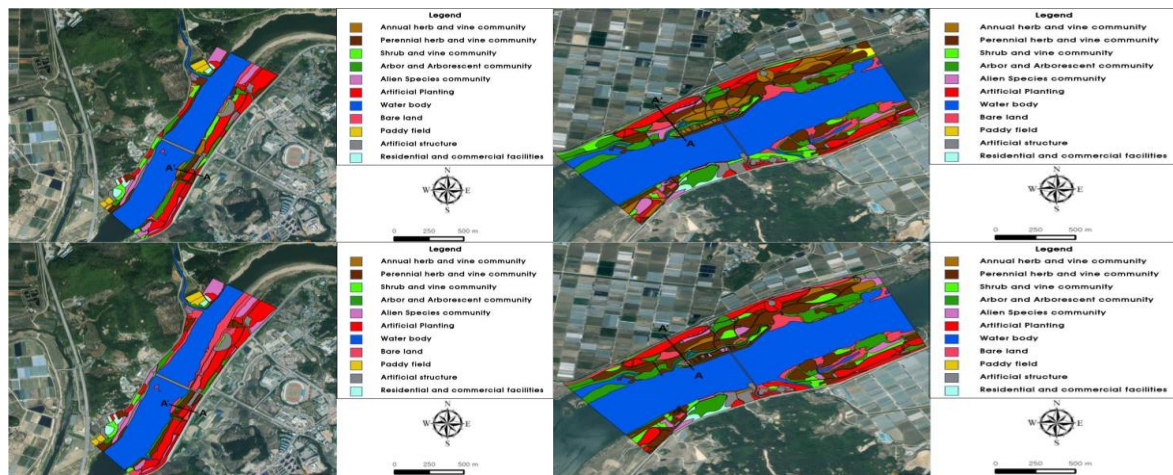


Figure 1. Actual vegetation map between 1st (top) and 2nd survey (bottom) in Gongju Weir and Baekje Weir. A-A' is a crossing vertical section of the river.

4. CONCLUSIONS

Flora was a total of 241 taxa including 65 families, 173 genera, 217 species, 2 subspecies, 21 varieties, and 1 forma in Gongju weir, and a total of 279 taxa including 69 families, 187 genera, 252 species, 2 subspecies, 24 varieties, 1 forma in Baekje weir, respectively. In survey, a total of 22 plant communities appeared in Gongju weir and 21 community in Baekje weir. In survey in Gongju weir, there were 1 community of annual herbaceous and vine plants, 7 communities of perennial herbaceous and vine plants, and 2 communities of shrubs, 2 communities of tree and subtree plants, 5 communities of exotic species, and 5 communities in artificial planting areas appeared.

Acknowledgements: * This work was supported by Korea Environment Industry & Technology Institute (KEITI) through Wetland ecosystem valuation and carbon absorption value enhancement technology development project, funded by Korea Ministry of Environment (MOE) (2022003630003)

REFERENCES

KIM D.J.(2006) " STUDY ON RESTORATION TECHNIQUE OF RIPARIAN VEGETATION ON URBAN RIVER." MASTER THESIS, UNIV. OF YEUNGNAM, GYEONGSAN, P.1-67.

LEE C.H., HONG S.K., CHO H.J., AND OH J.M. (1999). TECHNOLOGY OF NATURAL ENVIRONMENT RESTORATION. PAJU:DONGWHAPUB

LIM CH, PI JH, KIM AR, CHO HJ, LEE KS, YOU YH, LEE KH, KIM KD, MOON JS, LEE CS. 2021. DIAGNOSTIC EVALUATION AND PREPARATION OF THE REFERENCE INFORMATION FOR RIVER RESTORATION IN SOUTH KOREA. INT J ENVIRON RES PUBLIC HEALTH, 10;18(4): 1724.

DEVELOPMENT OF AN ALGORITHM FOR THE DETECTION OF FOREST FIRE SPREAD IN AREAS WITHOUT INTERNET CONNECTION

Çağdaş Tarı, Elçin Tan, and Sevinç Asilhan Sırdaş

Istanbul Technical University, Department of Meteorological Engineering

ABSTRACT

Accessing information, finding a way, or reaching our relatives can be vital when there is no any internet connection. Alternative methods may help to solve internet connection problems that may arise in natural disasters that require an emergency response, such as forest fires. Therefore, this study aims to develop solutions without the internet for storing the necessary data in the stages of detecting forest fire, determining the direction of the spread of the fire, and making the essential response to the fire. Map data (picture) is obtained via satellites and gridded so the location can be seen without an internet connection. In the following stages, we write the algorithms to process these data for determining the possible fire area. The algorithm is also reducing the data size and finding the fastest ways to reach the site will be drawn. Moreover, depending on the climate change model scenarios, local meteorological variables (wind, temperature gradient) will be stored. As a result, possible the spread directions of forest fire will be found in the areas without the internet connection.

Keywords: *Internet of things, navigation, natural disasters, image processing, satellite, forest fires.*

ESTIMATION OF THE SOIL ERODIBILITY FACTOR (K) FOR THE MARMARA REGION OF TURKEY WITH THE RUSLE MODEL USING GIS TECHNIQUES

Ezer A.¹, Guven B.²

1,2 Department of Environmental Sciences, Institute of Environmental Sciences,

Bogazici University, Istanbul, Turkey

e-mail: alkor.ezer@gmail.com

ABSTRACT

The K factor demonstrates soil erodibility among all the factors of RUSLE Model. The K factor is related to organic matter content, soil texture, soil permeability class, and other various factors, and it is mostly determined by the soil type (Renard et al., 1997). In this study, the open source of the FAO Digital Soil Map of the World (DSMW) was used. The FAO Digital Soil Map of the World is the digitized version of the FAO-UNESCO Soil Map of the World. In the data the soil units estimates are provided of physical (% sand, % silt, % clay, bulk density) and chemical properties in the topsoil and subsoil. For the calculation of K Factor defined by RUSLE Model, the soil data of the Marmara Region was taken in a shape file format. In ArcGIS10.4 software, the shape file of the soil data of Marmara Region was open in attribute table, and then exported to Excel file to compute. The symbols used for describing soil content were investigated and the sand, clay, silt and organic content were analyzed. There are many soil types in Marmara Region such as pellic vertisols, chromic luvisols, rendzinas etc. and the soil types are written and classified. These soil types have different soil contents in percentage. After organic soil content, sand, silt and clay percentages were separated, A, B, C, and D factors to calculate K factor which are defined in RUSLE Model methodology were calculated in an Excel file by using the formulas expressed in methodology part of the study. The K Factor values range from 0.049204 to 0.171464 Mg/Mj.mm. The higher K factor values are representative of the higher potential of the soil to erode the top soil. The soil type chromic vertisol have the highest K factor value, and it mostly contains clay content. In addition, the pellic vertisol, and the planasols have the second and third highest K factor value respectively.

1. RESEARCH QUESTION

How can the estimation of the soil erodibility factor (K) be done for the Marmara Region by using Revised Universal Soil Loss Equation (RUSLE) Model?

2. INTRODUCTION

The majority of the landscapes of the earth is made up of soil. Soil plays a significant role in the natural ecosystem (Singer and Warkentin, 1996), and is a major natural resource to support life on Earth. Moreover, being one of the most important cornerstones of the life processes in nature, together with water and air, has been seen as an indispensable source of life for securing basic food production. Therefore, the soil is considered to be the most important element in

meeting the basic needs of food, feed and fuel, and in the continuation of all terrestrial life (Blanco and Lal, 2008).

Soil erosion is an important social and economic problem and an essential factor in assessing ecosystem health and function. Soil erosion is the most common form of soil degradation world-wide (Bridges and Oldeman, 1999). Soil erosion can lead many adverse influences on water quality, hydrological systems, agricultural activities, and these environmental problems caused by soil erosion have long been recognized as severe problems for human sustainability (Lal, 1998). Soil erosion is a diffusion process occurring and varying from spatial characteristics over a typical landscape (Khare et al., 2016). The present form of the Earth's surface is being shaped with the effect of naturally occurring physical phenomenon (Das, 2002). Indeed, we as humanity are situated on a landscape which is mostly product of erosion. For example, the Quaternary landscapes of Iowa were formed over the period of the last 10,000 and 20,000 years (Ruhe, 1969), which might be accepted as relatively young, whereas the topsoil surfaces of the Appalachian Mountain were formed more than millions of years ago (Thornbury, 1965).

Even one single drop of water reaching the soil surface in microseconds have importance to observe the mechanism of nature, and how the natural events are interrelated. In a former research on soil erosion, the impact pressures of raindrops on a soil surface were recorded at a rate of one data point per 500 ns (5×10^{-7} second) in order to experiment those few microseconds of peak impact pressures (Nearing et al., 1987). In a more recent study, Nearing et al. (2017), also investigated the soil erosion on various spatial scales ranging from millimeters for raindrops to megameters for continents.

The factors controlling the soil erosion rate and magnitude include vegetation, fraction cover, rainfall intensity, run-off, land-use and land cover. Thus, the amount of soil loss is dependent upon intensity, duration and frequency of precipitation events, and these factors are likely to be affected by climate change, slope gradient, vegetation fraction cover, etc. Therefore, it is obvious that the risk of soil erosion can be assessed based on the inter-related processes of the slope, vegetation cover, and land-use type for rill and sheet erosion of the study area (Zhang et al., 2010). It is difficult to estimate the amount of soil erosion due to complicated interplay of many factors, such as land cover, soil structure, topography, climatic conditions, as well as human induced activities. Indeed, besides biophysical factors, socio-economic and political factors may also affect soil erosion (Ananda and Herath, 2003). Recently, especially with the help of Geographical Information Systems (GIS) and Remote Sensing (RS) techniques, analytical models such as Universal Soil Loss Equation (USLE) and Revised Universal Soil Loss Equation (RUSLE) have successfully been applied on national, regional, and watershed scales for the analysis of soil loss (Kinnell, 2000; Erdoğan et al., 2005).

In this article, the focus is the estimation of the soil erodibility factor of the RUSLE Model which is abbreviated as the K factor for the Marmara Region. K factor is an empirical measure for the soil erodibility depending upon intrinsic soil properties (Fu et al. 2006). It is one of the five factors used in RUSLE Model. This factor will be estimated by using GIS techniques for the Marmara Region of Turkey.

3. BACKGROUND INFORMATION

3.1. Description of the Study Area

Marmara region is located in the northwest part of Turkey, covering 8.6% of the total area of Turkey, with an approximate area of 72.845 km² occupying, and having more than 23 million people (Doğan et al., 2007). Marmara region gets its name from a landlocked sea belonging to the region, which is neighbouring to the Black Sea and the Aegean Sea through the straits. It is the smallest but the most densely populated region among the seven geographical regions of Turkey. The region includes 11 cities, namely İstanbul, Bursa, Edirne, Kocaeli, Balıkesir, Kırklareli, Tekirdağ, Çanakkale, Bilecik, Sakarya and Yalova. regarded as the center of main industrial sites in production of food, textile, cement, paper, house furniture, leather, petrochemical, automotive and ship construction products.



Figure 1. The Map of the Marmara Region with its 11 Districts

The region is the most industrialized region among the other regions in Turkey, and the one third of the Turkish national industry has been situated in the region. Turkey has a rapidly growing population, especially in the last few decades. The population of Turkey was approximately 13.6 million in 1927, and it has increased approximately five fold in 73 years reaching approximately to 67.8 million, in 2000. Moreover, according to the projections of the U.S. Census Bureau, the population of Turkey can reach up to 82 205 000, by 2025. Being a major city in the Marmara Region, İstanbul is the most populated city in Turkey, also the economic potential of the city is the highest among other cities of the country. Thus, the Marmara Region has densest population among the other seven regions of Turkey (DIE, 2007; U.S. Census Bureau, 2007). In the basis of the 2000 Census data, human population of the

Marmara Region was 17.3 million with an increase rate of 27%, yet the increase rate was 18.34% for Turkey, between the years 1990 and 2000. The location map of the Marmara Region is illustrated in Figure 1.

The Marmara Sea is the smallest inland sea of Turkey, connected with other two largest seas by the straits, the Bosphorus from the Black Sea side, and the Dardanelles from the Mediterranean side. Marmara Region is situated between $39^{\circ} 00' 00''$ - $42^{\circ} 00' 00''$ north latitude, and $26^{\circ} 00' 00''$ - $31^{\circ} 00' 00''$ east longitude. Thanks to the geostrategic position as a consequence of being very close to Europe, having the Bosphorus and Dardanelles Straits as a passage from the Black Sea and the Aegean Sea, the region has significant importance in industry, commerce, tourism and transportation. Rapid increase in economic developments, industrialization and urbanization arose in the Marmara Region after 1980s, because of migration from other regions and countries. This huge amount of human population density has resulted in various ecological changes especially in agricultural, forest areas. Majority of the forests and agricultural lands within the region have been transformed into urbanized areas. Istanbul as a capital has been affected from huge immigration, the city population was 3 million in 1970s, it became 7.4 million in 1990s, rising up to 12 million in 2007 (Kaya et al., 2007). The current population of the city is 15.07 million. Bursa, another important city of the Marmara region had a population of 275 953 in 1970 and reached to 1 194 687 in 2000.

3.2. Climate and Vegetation of The Study Area

Turkey is located between mid-latitude temperate climate zone and subtropical climate zone. Due to the diverse topographical structure, Turkey has various climatic regimes. Simply, the climate of Turkey is a Mediterranean-type macro climate (Iyigün et al., 2013). Turkey belongs to the risky group in terms of the potential effects of climate change and global warming. The climatic studies indicated that there is a tendency to increase in the average annual and seasonal surface temperatures, as well as the temperature at night for the last twenty years, when there is a decrease in the number of days with frost (Altınsoy et al., 2011; Sen et al., 2012; Türkeş 2011).

Turkey as a country belongs to a region described as having a warm and moderate climate (Erinc, 1984). Turkey has 7 sub-regions, which are Aegean, Black Sea, Central Anatolia, Eastern Anatolia, Marmara, Mediterranean, and Southeast Anatolia. These sub-regions are very diverse in terms of climatic conditions. Among the coastal regions of Turkey, the Aegean and Mediterranean have cool, rainy winters, having also moderately hot and dry summers. However, the Black Sea Region receives the highest amount of precipitation among other regions in the country. When it comes to average temperature values, the highest temperature is observed in the south-east part of Turkey, particularly in summer times. Towards the north-west and north-east parts of the country the temperature values decrease gradually, however the decrease in temperature values are smoother during summer with the continental effects of the inner regions. In the low altitudes, the coastal regions are warmer than the inner regions, which are generally separated by mountains with high altitudes. In general, the coastal parts of the Mediterranean Region have the highest average temperatures, followed by the Aegean, the eastern parts of the Black Sea, and the coastal parts of the Marmara Region. In addition, in the Eastern Anatolia due to continental effects and high altitudes, decrease in temperatures are observed (Tayanç et al., 1998). As an interference, the distribution of temperature variability is dependent upon the extension of the continental and topographical impacts. The Mediterranean Region are affected by subtropical air masses, this situation leads to observation of highest temperatures during winter, when compared to the other regions in Turkey. On the other hand, the lowest temperature values are recorded in the Northeastern Anatolian Plateau.

The climatic structure of the Marmara Region acts as a bridge between the Black Sea Climate and Mediterranean Climate. The region is divided into four sub-regions, which are namely: Yıldız, Ergene, Çatalca-Kocaeli, and South Marmara. The sub-region Yıldız is the part of the Marmara Region having the highest slope due to the Mountains. The Yıldız Mountains are located towards to the Black Sea and have a Black Sea Climate. Some parts of the mountains towards the inner catchments have drier climate that represents the Mediterranean Climate. When the Black Sea and the Mediterranean Climates are compared, the Black Sea Climate has lower temperatures in both winter and summer, and generally experiences rainfall events more frequently than the Mediterranean Climate of the coastal parts of Turkey. In the Black Sea Region, forests dominate along the coastal parts of the region, however, in the inner catchments of the region vegetation cover spreads sparsely. Another sub-region of the Marmara Region is Ergene, the Ergene Plains covers the most part of this sub-region. The vegetation type of the Ergene is sparsely vegetated due to dry climate. This part of the region is favorable for agricultural activities, and the farm products of the Ergene are mostly potato, rice, grape, wheat, sunflower, and tobacco. When it comes to the sub-region Çatalca-Kocaeli, this part of the region have two peninsulas situated at the eastern and western parts of the Bosphorus. In this section of the Marmara Region there are low plateaus, and also forests are located in the Black Sea coast of the sub-section. However, the forests are sparsely distributed in the southern parts of the sub-region Çatalca-Kocaeli and the climate is drier. The Adapazarı Plain is one of the most important agricultural land of this section, and it is mainly representative of the farm products such as beet, sunflower, potato, and linen. Lastly, the Southern Marmara, which is situated in the southern part of the region, also including the Gallipoli Peninsula, has medium height mountains, and also many plains, which are favorable for agricultural activities. The Uludağ Mountain is the highest mountain of the region.

3.3. RUSLE Model

Revised Universal Soil Loss Equation (RUSLE) (Renald et al., 1997) is an empirical erosion model, which is revised based on the Universal Soil Loss Equation, USLE (Wischmeier and Smith, 1978). The model USLE is developed by the United States Department of Agriculture (USDA) in 1978. The most remarkable difference between the models USLE and RUSLE is the model RUSLE includes a computer program to make calculations easier, and it also includes the data analysis component. The model RUSLE investigates how land use, soil and topography may affect the soil erosion that originates from rainfall and surface runoff (Renard et al., 1997). The USLE model was originally designed for soil loss prediction in croplands on gently sloping topography (Wischmeier and Smith, 1978). However, RUSLE has been widely applied to estimate soil erosion loss, and the model has applications in different land use conditions, such as rangelands, forests, and disturbed areas (Renard et al., 1997). Moreover, in order to predict soil erosion loss, and its spatial distribution, GIS and remote sensing technologies are commonly used to provide better accuracy in larger geographical areas (Millward and Mersey, 1999; Wang et al., 2003).

Five major factors; i. rainfall pattern (R), ii. type of soil (K), iii. topography (LS), iv. crop system (C), and v. management practices (P) are included in the USLE/RUSLE to compute approximate annual average soil erosion, through the equation below (Renard et al., 1997):

$$A = R \times K \times LS \times C \times P \quad (1)$$

where A is the the mean annual loss in ($\text{Mg}\cdot\text{ha}^{-1}\cdot\text{year}^{-1}$), R is the rainfall and runoff erosivity factor (in $\text{MJ}\cdot\text{mm}\cdot\text{ha}^{-1}\cdot\text{year}^{-1}$), K is the soil erodibility factor (in $\text{Mg}\cdot\text{h}\cdot\text{MJ}^{-1}\cdot\text{mm}^{-1}$), LS is the slope and length (in m) of slope factor, C is the cropping management factor (dimensionless), and P is the erosion control and practice factor (dimensionless).

In this study, following the derivation of these factors, which will be discussed further below, all five parameters are mapped in GIS raster format; so, the estimates of average annual soil is acquired at the pixel grid level ($30\text{ m} \times 30\text{ m}$ grid cell size). The overlay of the RUSLE model and the schematic approach to the workflow of the RUSLE model utilized in this study are illustrated in Figure 2 below.

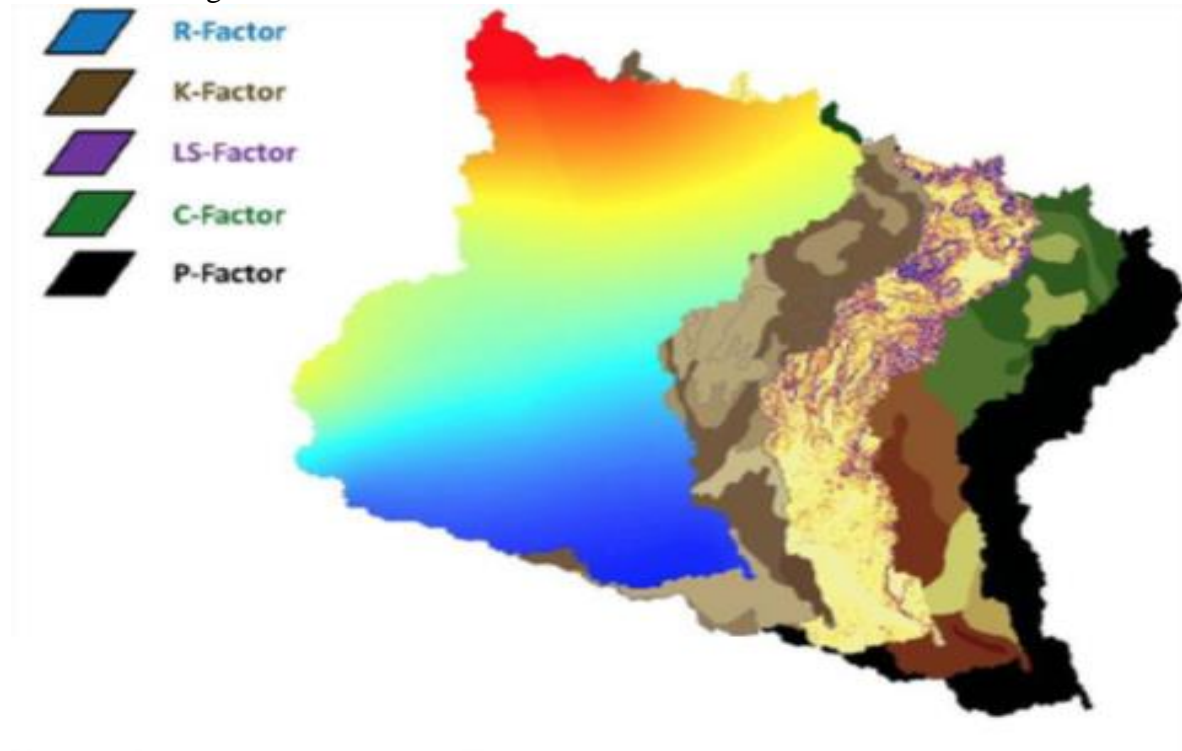


Figure 2. Overlay of the RUSLE model.

Table 1. Soil erosion risk classification based on average erosion rate estimated by RUSLE (Li et al., 2014; Tang et al., 2015).

Soil Loss (A) ($\text{t ha}^{-1}\text{ year}^{-1}$)	Erosion Risk
< 5	Very low
5 - 25	Low
25 - 50	Moderate
50 - 80	Severe
80 - 150	Very severe
> 150	Extremely severe

3.4. Soil Erodibility

Erodibility is a measure of the inherent resistance of geologic materials which are soils and rocks to erosion. High erodibility is mostly observed in geologic materials that readily displaced and transported by water. The erodibility of a soil as a material with a greater or less degree of coherence is defined by its resistance to two energy sources which are caused by the impact of raindrops on the soil surface, and the shearing action of runoff between clods in grooves or rills.

In order to examine the soil erodibility of a land there are many soil erosion models. However, the greatest obstacle in the modelling of soil erosion especially at larger spatial scales is the lack of data on soil characteristics. One of the most well-used parameter to express soil erodibility is K factor in widely used soil erosion model which is RUSLE Model.

2.5. Description and Mathematical Application of the Soil Erodibility Factor (K) of the RUSLE Model

The K-factor is connected to soil qualities such as organic matter concentration, soil texture, soil structure, and permeability, and represents a soil's sensitivity to erodibility. The K-factor is a summed annual value of the soil profile reaction to soil detachment and transport by raindrops and surface flow (Renard et al., 1997). As a result, the best way to determine soil erodibility is to take actual measurements on field plots (Kinnell, 2010). Researchers looked at the relationship between "traditional" soil parameters and soil erodibility because field measurements are expensive and often difficult to transmit in space.

K factor is an empirical measure of soil erodibility depends on intrinsic soil properties (Fu et al. 2006). The K factor values are predicted with the help of information about soil properties, such as soil texture, content of organic matter, soil structure and permeability (Renard et al., 1997; Ferreira and Panagopoulos, 2014). Wisheier and Smith (1978) were developed a monogram to obtain the K factor (Equation 2) on the basis of the percentages of silt, very fine sand, and organic matter, soil structure and permeability.

$$K = \frac{(2.1 M^{1.14} (10^{-4})^{(12-a)} + 3.25 (b-2) + 2.5 (c-3)) \times (0.1317)}{100} \quad (2)$$

where a = % of organic matter

b = non-dimensional code related to soil structure class

c = non-dimensional code related to soil permeability class

M = (% silt + % very fine sand) or (100 - %clay)

And also, unit of K factor is t. h. MJ⁻¹ mm⁻¹.

$$K = 0.0034 + 0.0405 \times \exp\left(-0.5 \left[\frac{\log D_g + 1.659}{0.7101} \right]^2\right) \quad (3)$$

Where,

D_g is the geometrical particle diameter, based on the fractions of the texture classes and arithmetic means of the particle diameter of each texture class.

$$K = \frac{SAN + SIL}{CLA} \times \frac{1}{100} \quad (4)$$

Where,

SAN, SIL and CLA are sand, silt and clay percentage, respectively.

$$K = 0.00000748(M) + 0.00448059(b) - 0.0631175(DMP) + 0.010396(REL) \quad (5)$$

Where,

M: the sum of percentage silt and very fine sand multiplied by 100 minus percent clay

b: the non-dimensional code related to the soil structure

DMP: the weighted mean of the particles smaller than 2mm

REL: the ratio between organic matter content and the content of particles between 0.1mm and 0.2mm

$$K = A \times B \times C \times D \times 0.1317 \quad (6)$$

Where,

$$A = \left[0.2 + 0.3 \exp(-0.0256 \text{ SAN} (1 - \frac{SIL}{100})) \right] \quad (6.1)$$

$$B = \left[\frac{SIL}{CLA + SIL} \right]^{0.3} \quad (6.2)$$

$$C = \left[1.0 - \frac{0.25 C}{C + \exp[(3.72 - 2.95C)]} \right] \quad (6.3)$$

$$D = \left[1.0 - \frac{0.70 \text{ SNI}}{\text{SNI} + \exp[(-5.41 + 22.9 \text{ SNI})]} \right] \quad (6.4)$$

SAN, SIL and CLA represent percent sand, silt and clay respectively. In addition, C and SNI represent organic carbon content, sand content subtracted from 1 and divided by 100 respectively.

4. RESULTS AND DISCUSSION

First of all K factor demonstrates soil erodibility among all the factors of RUSLE Model. The K factor is related to organic matter content, soil texture, soil permeability class, and other various factors, and it is mostly determined by the soil type (Renard et al., 1997). In this study, the open source of the FAO Digital Soil Map of the World (DSMW) was used. The FAO Digital Soil Map of the World is the digitized version of the FAO-UNESCO Soil Map of the World. In the data the soil units estimates are provided of physical (% sand, % silt, % clay, bulk density) and chemical properties in the topsoil and subsoil. For the calculation of K Factor

defined by RUSLE Model, the soil data of the Marmara Region was taken in shape file format. In ArcGIS10.4 software, the shape file of the soil data of Marmara Region was open in attribute table, and then exported to Excel file. The symbols used for describing soil content were investigated and the sand, clay, silt and organic content were analyzed. There are many soil types in Marmara Region such as pellic vertisols, chromic luvisols, rendzinas etc. and the soil types are written and classified in the Table 4.1. These soil types have different soil contents in percentage. After organic soil content, sand, silt and clay percentages were separated, A, B, C, and D factors to calculate K factor which are defined in RUSLE Model methodology were calculated in Excel file by using the formulas expressed in methodology part with the Equation 3.10, 3.11, 3.12, and 3.13. The K Factor values range from 0.049204 to 0.171464 Mg/Mj.mm. The higher K factor values are representative of the higher potential of the soil to erode the top soil. The soil type chromic vertisol have the highest K factor value, and it mostly contains clay content. In addition, the pellic vertisol, and the planasols have the second and third highest K factor value respectively.

In the study of Özşahin et al. (2014), the authors investigate the effects of land use and land cover changes in Kuseyr plateau of Turkey on erosion, and the study area is a part of Mediterranean basin of Turkey. According to the study based on Kuseyr plateau of Mediterranean, the soil groups are alluvial, colluvial, brown forest, non-calcic brown forest, red mediterranean, red brown, and rocky areas. Also, the K factor ranges from 0.001 to 0.065 in the study of Özşahin et al. (2014). In addition to the K factor findings of the other studies, Ozsoy et al. (2012) provides information about the soil types of the Mustafakemalpaşa River Basin in the Marmara Region, and the main soil types in the basin are non-calcic brown forest soils, and brown forest soils. According to the study of Ozsoy et al. (2012) these two great soil groups constitute 85.7% of the basin, but 9.3% is composed of rendzinas, alluvial, colluvial, and brown soils. The 5% part of the Mustafakemalpaşa River Basin is composed of water and bare rocks (Ozsoy et al., 2012). Besides all the soil information given in the study of Ozsoy et al. (2012), the study claim that it is not possible to estimate the K factor for the Mustafakemalpaşa River Basin due to the lack of information, insufficient and old soil maps for the basin.

Finally, the datum of the maps were chosen as D_WGS 1984, and also spatial reference system were chosen as UTM Zone 35 N. Also, the standard deviation of the K Factor results is $0.033508 \text{ Mg.ha.h.ha}^{-1}.\text{MJ}^{-1}.\text{mm}^{-1}$.

Table 2. K Factor Table for Marmara Region (Soil Type Classification & RUSLE Model Calculation Result for K Factor).

FID	SOIL TYPE	Sand %	Silt %	Clay %	Organic Content %	A	B	C	D	K_Factor
0	PELLIC VERTISOLS	25.1	12.2	62.7	0.68	0.37065002	3.47729735	0.99720628	0.99999539	0.169267997
1	CHROMIC LUVISOLS	64.3	12.2	23.5	0.63	0.270705562	2.610657056	0.997716674	0.983033772	0.091286898
2	CHROMIC LUVISOLS	64.3	12.2	23.5	0.63	0.270705562	2.610657056	0.997716674	0.983033772	0.091286898
3	CHROMIC LUVISOLS	64.3	12.2	23.5	0.63	0.270705562	2.610657056	0.997716674	0.983033772	0.091286898
4	CHROMIC LUVISOLS	64.3	12.2	23.5	0.63	0.270705562	2.610657056	0.997716674	0.983033772	0.091286898
5	CHROMIC LUVISOLS	64.3	12.2	23.5	0.63	0.270705562	2.610657056	0.997716674	0.983033772	0.091286898
6	CHROMIC LUVISOLS	64.3	12.2	23.5	0.63	0.270705562	2.610657056	0.997716674	0.983033772	0.091286898
7	PELLIC VERTISOLS	25.1	12.2	62.7	0.68	0.37065002	3.47729735	0.99720628	0.99999539	0.169267997
8	CHROMIC LUVISOLS	64.3	12.2	23.5	0.63	0.270705562	2.610657056	0.997716674	0.983033772	0.091286898
9	CALCIC CAMBISOLS	81.6	6.8	11.7	0.44	0.242814283	2.143587009	0.999037953	0.718478976	0.049203601
10	CHROMIC LUVISOLS	64.3	12.2	23.5	0.63	0.270705562	2.610657056	0.997716674	0.983033772	0.091286898
11	PELLIC VERTISOLS	25.1	12.2	62.7	0.68	0.37065002	3.47729735	0.99720628	0.99999539	0.169267997
12	PELLIC VERTISOLS	25.1	12.2	62.7	0.68	0.37065002	3.47729735	0.99720628	0.99999539	0.169267997
13	CALCARIC FLUVISOLS	39.6	39.9	20.6	0.65	0.363124337	2.513831277	0.997521888	0.999897187	0.119910002
14	CALCARIC FLUVISOLS	39.6	39.9	20.6	0.65	0.363124337	2.513831277	0.997521888	0.999897187	0.119910002
15	RENDZINAS	48.5	30.8	20.7	1.74	0.32705185	2.517317066	0.977541731	0.999327645	0.105921

16	ORTHIC LUVISOLS	76	9.9	14.1	0.41	0.251976769	2.257839592	0.999174913	0.862979907	0.0646073
17	CHROMIC LUVISOLS	64.3	12.2	23.5	0.63	0.270705562	2.610657056	0.997716674	0.983033772	0.091286898
18	ORTHIC LUVISOLS	76	9.9	14.1	0.41	0.251976769	2.257839592	0.999174913	0.862979907	0.0646073
19	CHROMIC LUVISOLS	64.3	12.2	23.5	0.63	0.270705562	2.610657056	0.997716674	0.983033772	0.091286898
20	CALCARIC REGOSOLS	63.5	19.2	17.3	0.76	0.280664427	2.391857637	0.996217853	0.985505084	0.086800396
21	CALCARIC FLUVISOLS	39.6	39.9	20.6	0.65	0.363124337	2.513831277	0.997521888	0.999897187	0.119910002
22	ORTHIC LUVISOLS	76	9.9	14.1	0.41	0.251976769	2.257839592	0.999174913	0.862979907	0.0646073
23	ORTHIC LUVISOLS	76	9.9	14.1	0.41	0.251976769	2.257839592	0.999174913	0.862979907	0.0646073
24	ORTHIC LUVISOLS	76	9.9	14.1	0.41	0.251976769	2.257839592	0.999174913	0.862979907	0.0646073
25	PLANOSOLS	19.8	55.2	24.8	4.27	0.439056574	2.65146508	0.974400837	0.999998534	0.149393007
26	EUTRIC CAMBISOLS	36.4	37.2	26.4	1.07	0.367099084	2.699760064	0.990309927	0.999947971	0.129253998
27	CALCIC CAMBISOLS	81.6	6.8	11.7	0.44	0.242814283	2.143587009	0.999037953	0.718478976	0.049203601
28	CALCIC CAMBISOLS	81.6	6.8	11.7	0.44	0.242814283	2.143587009	0.999037953	0.718478976	0.049203601
29	EUTRIC CAMBISOLS	36.4	37.2	26.4	1.07	0.367099084	2.699760064	0.990309927	0.999947971	0.129253998
30	CHROMIC VERTISOLS	24.1	12.2	63.7	0.68	0.37065002	3.47729735	0.99720628	0.99999539	0.171463996
31	CALCARIC FLUVISOLS	39.6	39.9	20.6	0.65	0.363124337	2.513831277	0.997521888	0.999897187	0.119910002
32	ORTHIC LUVISOLS	76	9.9	14.1	0.41	0.251976769	2.257839592	0.999174913	0.862979907	0.0646073
33	CALCARIC FLUVISOLS	39.6	39.9	20.6	0.65	0.363124337	2.513831277	0.997521888	0.999897187	0.119910002
34	ORTHIC LUVISOLS	76	9.9	14.1	0.41	0.251976769	2.257839592	0.999174913	0.862979907	0.0646073
35	PLANOSOLS	19.8	55.2	24.8	4.27	0.439056574	2.65146508	0.974400837	0.999998534	0.149393007
36	LITHOSOLS	58.9	16.2	24.9	0.97	0.284792963	2.654544006	0.992542089	0.994235324	0.098252401

37	PLANOSOLS	19.8	55.2	24.8	4.27	0.439056574	2.65146508	0.974400837	0.999998534	0.149393007
38	LITHOSOLS	58.9	16.2	24.9	0.97	0.284792963	2.654544006	0.992542089	0.994235324	0.098252401
39	CALCIC CAMBISOLS	81.6	6.8	11.7	0.44	0.242814283	2.143587009	0.999037953	0.718478976	0.049203601
40	EUTRIC CAMBISOLS	36.4	37.2	26.4	1.07	0.367099084	2.699760064	0.990309927	0.999947971	0.129253998
41	ORTHIC LUVISOLS	76	9.9	14.1	0.41	0.251976769	2.257839592	0.999174913	0,862979907	0,0646073
42	CALCIC CAMBISOLS	81.6	6.8	11.7	0.44	0.242814283	2.143587009	0.999037953	0.718478976	0.049203601
43	EUTRIC CAMBISOLS	36.4	37.2	26.4	1,07	0.367099084	2.699760064	0.990309927	0.999947971	0.129253998
44	LITHOSOLS	58.9	16.2	24.9	0.97	0.284792963	2.654544006	0.992542089	0.994235324	0.098252401
45	CALCARIC FLUVISOLS	39.6	39.9	20.6	0.65	0.363124337	2.513831277	0.997521888	0.999897187	0.119910002
46	LITHOSOLS	58.9	16.2	24.9	0.97	0.284792963	2.654544006	0.992542089	0.994235324	0.098252401

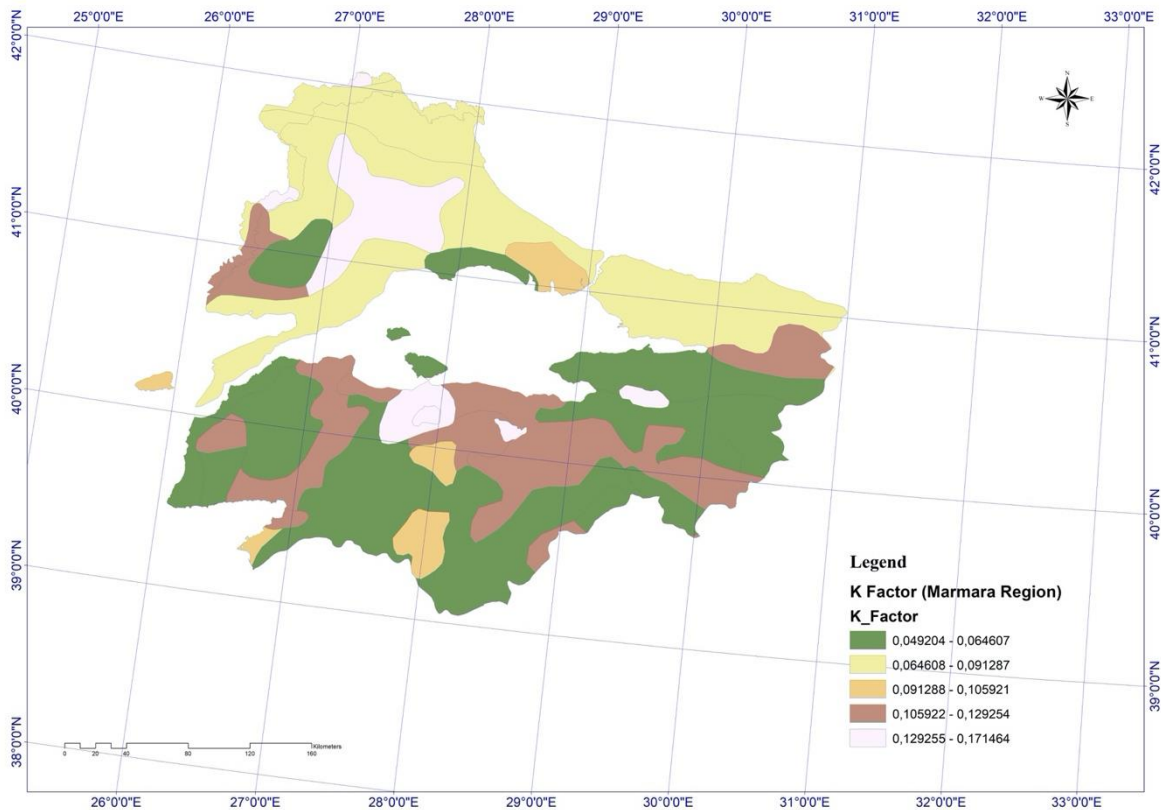


Figure 3. RUSLE Model K Factor Map created in ArcGIS for Marmara Region

5. CONCLUSION

As final words, the majority of the terrestrial areas are made up of soil. Soil plays a crucial role in the natural ecosystem (Singer and Warkentin, 1996), and is a major natural resource to support life on Earth. Also, it has significant role in life processes in nature, especially when it is combined with water and air, has been seen as an indispensable source of life for securing basic food production for most of the living organisms. With these significant characteristics of soil it is considered to be the most important element in meeting the basic needs of food, feed and fuel, and in the continuation of all terrestrial life (Blanco and Lal, 2008).

Although the soil itself is important, the loss of soil due to soil erosion is also important, and soil erosion should be assessed to investigate especially for the future image of a region in terms of soil characteristics to sustain the demands of the living organisms in a region. Soil erosion is the most common form of soil degradation world-wide (Bridges and Oldeman, 1999). Soil erosion can lead many adverse influences on water quality, hydrological systems, agricultural activities, and these environmental problems caused by soil erosion have long been recognized as severe problems for human sustainability (Lal, 1998). Soil erosion is a diffusion process occurring and varying from spatial characteristics over a typical landscape (Khare et. al., 2016). The present form of the Earth's surface is being shaped with the effect of naturally occurring physical phenomenon (Das, 2002). Indeed, we as humanity are situated on a landscape which

is mostly product of erosion. For example, the Quaternary landscapes of Iowa were formed over the period of the last 10,000 and 20,000 years (Ruhe, 1969), which might be accepted as relatively young, whereas the topsoil surfaces of the Appalachian Mountain were formed more than millions of years ago (Thornbury, 1965).

In this study RUSLE Model is used to assess the soil erosion for the Marmara Region of Turkey, and the most important factor for the impact of soil characteristics on the soil erosion which is the K factor is estimated for the region within this study. The K factor demonstrates soil erodibility among all the factors of RUSLE Model. The K factor is related to organic matter content, soil texture, soil permeability class, and other various factors, and it is mostly determined by the soil type (Renard et al., 1997). In this study, the open source of the FAO Digital Soil Map of the World (DSMW) was used. The FAO Digital Soil Map of the World is the digitized version of the FAO-UNESCO Soil Map of the World. In the data the soil units estimates are provided of physical (% sand, % silt, % clay, bulk density) and chemical properties in the topsoil and subsoil. For the calculation of K Factor defined by RUSLE Model, the soil data of the Marmara Region was taken in a shape file format. In ArcGIS10.4 software, the shape file of the soil data of Marmara Region was open in attribute table, and then exported to Excel file to compute. The symbols used for describing soil content were investigated and the sand, clay, silt and organic content were analyzed. There are many soil types in Marmara Region such as pellic vertisols, chromic luvisols, rendzinas etc. and the soil types are written and classified. These soil types have different soil contents in percentage. After organic soil content, sand, silt and clay percentages were separated, A, B, C, and D factors to calculate K factor which are defined in RUSLE Model methodology were calculated in an Excel file by using the formulas expressed in methodology part of the study. The K Factor values range from 0.049204 to 0.171464 Mg/Mj.mm. The higher K factor values are representative of the higher potential of the soil to erode the top soil. The soil type chromic vertisol have the highest K factor value, and it mostly contains clay content. In addition, the pellic vertisol, and the planasols have the second and third highest K factor value respectively.

BIBLIOGRAPHY

- Albaladejo, M.J., Stocking, M.A., 1989. Comparative evaluation of two models in predicting storm soil loss from erosion plots in semi-arid Spain. *Catena* 16, 227-236.
- Altınsoy, H., Öztürk, T., Türkeş, M., Kurnaz, M.L., 2011. Projections of Future Air Temperature and Changes in the Mediterranean Basin by Using the Global Climate Model, Proceedings of the National Geographical Congress with International Participation (CD-R), ISBN 978-975-6686-04-1, 7–10 September 2011, Türk Coğrafya Kurumu, İstanbul University
- Ananda, J., Herath, G., 2003. Soil erosion in developing countries: a socio-economic appraisal. *Journal of Environmental Management*, 68, 343-353.
- Arnold, J.G., Srinivasan, R., Mutiah, R.S., Williams, J.R., 1998. Large area hydrologic modeling and assessment part I: Model development. *Water Research Association*, 34, 73-89.
- Arnoldous, H.M.J., 1977. Methodology used to determine the maximum potential average annual soil loss due to sheet and rill erosion in Morocco. *FAO Soils Bulletin* 34, 39-51.
- Beasley, D.B., Huggins, L.F., 1981. ANSWERS Users' Manual EPA-905/9-82-001, US EPA, Chicago, Illinois, USA.
- Beskow, S., Mello, C.R., Norton, L.D., Curi, N., Viola, M.R., Avanzi, J.C., 2009. Soil erosion prediction in the Grande River Basin, Brasil using distributed modeling. *Catena*, 79, 49-59, USA.
- Berrisford, P., Dee, D.P., Fielding, K., Fuentes, M., Kallberg, P., Kobayashi, S., Uppala, S.M., 2009. The ERA-Interim Archive, ERA Report Series, 1, European Centre for Medium Range Weather Forecasts, UK.
- Bridges, E.M., Oldeman, L.R., 1999. Global assessment of human-induced soil degradation. *Arid Soil Research Rehabilitation* 13, 319-25.
- Blanco, H., Lal, R., 2008. *Principles of Soil Conservation and Management*. Springer, USA.
- Bogdanova, C., 1969. Seasonal Fluctuations in the Inflow and Distribution of the Mediterranean Waters in the Black Sea. *Academy of Sciences*, 131-139, Moscow, USSR.
- Büyükkay, M., 1989. The Surface and Internal Oscillations in the Bosphorus Related to Meteorological Forces. M Sc. Thesis, Middle East Technical University, Turkey.
- Chen, T., Niu, R., Li, P., Zhang, L., Du, B., 2010. Regional soil erosion risk mapping using RUSLE, GIS, and remote sensing: a case study in Miyun Watershed, North China. *Environmental Earth Sciences*, 63, 533-541.
- CORINE, 1992. Soil erosion risk and important land resources in the Southeastern Regions of the European Community, EUR 13233.
- Correa, S.W., Mello, C.R., Chou, S.C., Curi, N., Norton, L.D., 2016. Soil erosion risk associated with climate change at Mantaro River basin. *Peruvian Andes*, 110-124.
- Das, G., 2002. *Hydrology and Soil Conservation Engineering Including Watershed Management*, PHI Publishers, India.
- De Roo A.P.J., Jetten V.G., 1999. Calibrating and validating the LISEM model for two data sets from the Netherlands and South Africa. *Catena*, 37, 477-493.
- De Roo A.P.J., 1996. The LISEM project: an introduction. *Hydrological Processes*, 10, 1021-1025.
- De Roo A.P.J., Offermans R.J.E., Cremers N., 1996. LISEM: a single-event, physically based hydrological and soil erosion model for drainage basins' sensitivity analysis, validation and application. *Hydrological Processes*, 10, 1119-1126.
- Evans, R., 1980. Mechanics of Water Erosion and Their Spatial and Temporal Controls: an Empirical Viewpoint. In Kirkby. M.J., Morgan, R.P.C. (Eds), *Soil Erosion*, Wiley Incorporation, 109.
- Gassman, P.W., Reyes M.R., Green C.H., Arnold J.G., 2007. The soil and water assessment tool: historical development, applications, and future research directions. *Transactions of the ASABE*, 50: 1211-1250.
- Gürkan, H., Arabacı, H., Demircan, M., Eskioğlu, O., Şensoy, S., Yazıcı, B., 2016. Temperature and precipitation projections based on GFDL-ESM2M using RCP4.5 and RCP8.5 scenarios for Turkey. *Coğrafi Bilimler Dergisi*, 14, 77-88.
- Ferreira, V., Panagopoulos, T., 2014. Seasonality of soil erosion under Mediterranean conditions at the Alqueva dam watershed. *Environmental Management*, 54, 67–83.
- Figueiredo, T., Poesen, J., 1998. Effect of surface rock fragment characteristics on interrill and erosion of the a silty loam soil. *Soil and Tillage Research*, 46, 81- 95.
- Flanagan, D.C., Gilley, J.G., Franti, T.G., 2007. Water erosion prediction project (WEPP): development history,

model capabilities, and future enhancements. *Transactions of the Asabe*, 50, 1603-1612.

Foster, G. R., 1990. Process-based modelling of soil erosion by water on agricultural land. In, J. Boardman, I.D.L., Foster J.A. (Eds.), *Dearings*, 429-445, New York, John Wiley and Sons Ltd.

Fournier, F., 1960. *Climat Et Erosion*, Ph.D. Thesis, Presses University, France.

Fu, B., Chen, L., Ma, K., Zhou, H., Wang, J., 2000. The relationships between land use and soil condition in the hilly area of the Loess Plateau in Northern Shaanxi, China. *Catena*, 39, 69-78.

Fu G., Chen S., McCool K.D., 2006. Modeling the impacts of no-till practice on soil erosion and sediment yield using RUSLE, SEDD and ArcView GIS. *Soil Tillage Research*, 85, 38-49.

Gaubi, I., Chaabani, A., Mammou, A., Hamza, M.H., 2016. A GIS-based soil erosion prediction using the revised universal soil loss equation (RUSLE) (Lebna watershed, Cap Bon, Tunisia). *Natural Hazards*, 219-239.

Ganasri B.P., Ramesh H., 2016. Assessment of soil erosion by RUSLE model using remote sensing and GIS: A case study of Nethravathi Basin. *Geoscience Frontiers*, 7, 953-961.

Grunwald, S., Frede, H.G., 1999. Using the modified agricultural non-point source pollution model in German watersheds. *Catena*, 37, 319-328.

Hirschi, M.C., Barfield B.J., 1988. KYEMO- A physically based research erosion model Part I: Model development. *American Society of Agricultural Engineers*, 31, 804-813.

Irvem, A., Topaloglu, F., Uygur, V., 2007. Estimating spatial distribution of soil loss over Seyhan River Basin in Turkey. *Journal of Hydrology*, 336, 30-37.

Iyigun, C., Türkes, M., Batmaz, I., Yozgatligil, C., Purutçuoğlu, V., Koç, E., Öztürk, M., 2013. Clustering current climate regions of Turkey by using a multivariate statistical method. *Theoretical and Applied Climatology*, 114, 95-116.

Jinghu, P., Yan, W., 2014. Estimation of soil erosion using RUSLE in Caijiamiao watershed, China. *Natural Hazards*, 71, 2187-2205.

Kaya S., 2007. Multitemporal analysis of rapid urban growth in Istanbul using remotely sensing data. *Environmental Engineering Science*, 24, 228-233.

Kaya, S., Curran, P.J., 2006. Monitoring urban growth on the European side of the İstanbul metropolitan area: a case study. *International Journal of Applied Earth Observation and Geoinformation*, 8, 18-25.

Karamage, F., Zhang, C., Liu, T., Maganda, A., Isabwe, A., 2017. Soil Erosion Risk Assessment in Uganda. *Forests*, 8, 52.

Khare, D., Mondal, A., Kundu, S., Mishra, P.K., 2016. Climate change impact on soil erosion in the Mandakini River Basin, North India. *Applied Water Sciences*. 7, 2373-2383.

Kim, H.S., Julien, P.Y., 2006. Soil erosion modeling using RUSLE and GIS on the IMHA watershed. *Water Engineering Research*, 7, 1, 29-41.

Kirkby, M.J., Abrahart R., McMahon M.D., Shoa J., 1988. MEDALUS soil erosion models for global change. *Geomorphology*, 24, 35-39.

Knisel, W.G., 1980. *CREAMS: A Fieldscale Model for Chemical, Runoff, and Erosion from Agricultural Management Systems Conservation Report 26*, Science and Education Administration, USDA, Washington DC, USA.

Latocha, A., Szymanowski, M., Jeziorska, J., Stec, M., Roszczewska, M., 2016. Effects of land abandonment and climate change on soil erosion – an example from depopulated agricultural lands in the Sudetes Mts., SW Poland. *Catena*, 145, 128-141.

Leonard, R.A., Knisel, W.G., Still, D.A., 1987. GLEAMS: Groundwater loading effects of agricultural management systems. *American Society of Agricultural Engineers*, 30, 1403-1418.

Li, X., Zhang, X., Zhang, L., Wu, B., 2014. Rainfall and vegetation coupling index for soil erosion risk mapping. *Soil Water Conservation*, 69, 213-220.

Millward, A.A., Mersey J.E., 1999. Adapting the RUSLE to model soil erosion potential in a mountainous tropical watershed. *Catena*, 38, 109-129.

Morgan, R.P.C., 1991. *Soil Erosion and Conservation*, Longman Scientific and Technical, John Wiley and Sons Inc., New York, 255.

Nearing, M.A., Foster, G.R., Lane, L.J., Finkner, S.C., 1989. A process-based soil-erosion model for USDA-water erosion prediction project technology. *American Society of Agricultural*, 32, 1587-1593.

Nearing, M.A., Xie, Y., Liu, B., Ye, Y., 2017. Natural and antropogenic rates of soil erosion. *International Soil and Water Conservation Research*, 5, 77-84.

- Oliveira, A.H., Aparecida, M., Silva, M.L.N., Curi, N., Neta, G.K., França, D.A., 2013. Development of topographic factor modeling for application in soil erosion models in soil processes and current trends in quality assessment. In Soriano, M.C.H. (Eds), InTech, 111-138, New York, U.S.A.
- Ozsoy, G., Aksoy, E., Dirim, M.S., Tumsavas, Z., 2012. Determination of soil erosion risk in the Mustafakemalpaşa River Basin, Turkey, using the Revised Universal Soil Loss equation, geographical information system, and remote sensing. *Environmental Management*, 50, 679-694.
- Özşahin, E., Uygur, V., 2014. The effects of land use and land cover changes (LULCC) in Kuseyr plateau of Turkey on erosion. *Turk Journal of Agriculture Forestry*, 38, 478-487.
- United States Department of Agriculture, Agricultural Research Service, 1997. Predicting Soil Erosion by Water. A Guide to Conservation Planning with the Revised Universal Soil Loss Equation (RUSLE), Agricultural Handbook 703, U.S.A.
- Pruski, E.E., Nearing, M.A., 2002a. Climate-induced changes in erosion during the 21st century for eight U.S. locations. *Water Resources Research*, 38, 12-25.
- Rango, A., Arnoldus, H.M.J., 1987. Amenagement des bassins versants, Cahiers techniques de la FAO.
- Renard, K.G., Foster, G.A., Weesies, G.A., McCool, D.K., 1997. Predicting soil erosion by water: a guide to conservation planning with RUSLE, USDA, Agriculture Handbook No.703, Washington, DC.
- Renard, K.G., Freimund, J.R., 1994. Using monthly precipitation data to estimate the R factor in the revised USLE. *Journal of Hydrology*, 157, 287-306.
- Richter, G., Negendank, J.F.W., 1977. Soil Erosion Processes and Their Measurement in the German Area of the Moselle River. *Earth Surface Process*, 2, 261-278.
- Rozos, D., Skilodimou, H.D., Loupasakis, C., Bathrellos, G.D., 2013. Application of the revised universal soil loss equation model on landslide prevention: an example from Euboea (Evia) Island, Greece. *Environmental Earth Sciences*, 70, 3255-3266.
- Rudra, R., Dickinson, W., Clark, D., Wall, G., 1986. GAMES-A screening model of soil erosion and fluvial sedimentation on agricultural watershed. *Canadian Water Resources Journal*, 11, 58-71.
- Ruhe, R.V., 1969. Quarternary landscapes in Iowa, Iowa State University Press, Ames, Iowa.
- Ruhe, R.V., Daniels, R.B., 1965. Landscapes erosion: geologic and historic. *Journal of Soil and Water Conservation*, 20, 52-57.
- Sen, Z., Habib, Z., 2001a. Monthly spatial rainfall correlation functions and interpretations for Turkey. *Hydrology Science Journal*, 46, 525-535.
- Sen, Z., Habib, Z., 2001b. Spatial rainfall pattern identification by optimum interpolation technique and application for Turkey. *Hydrological Sciences*, 32, 85-98.
- Sheikh, A., Palria H.S., Alam, A., 2011. Integration of GIS and universal soil loss equation (USLE) for soil loss estimation in a Himalayan watershed. *Recent Research Science and Technology*, 3, 51-57.
- Singer M.J., Warkentin B. P., 1996. Soils in an environmental context: an American perspective. *Catena*, 27, 179-189.
- Stocking, M.A., Elwell H.A., 1973. Soil erosion hazard in Rhodesia. *Rhodesia Agricultural Journal* 70, 93-101.
- Stocking, M.A., Elwell, H.A., 1976. Rainfall erosivity over Rhodesia. *The Institute of British Geographers*, 1, 231-245.
- Tağıl, Ş., 2007. Tuzla Çayı havzasında (Biga Yarımadası) CBS-Tabanlı RUSLE modeli kullanarak arazi degradasyonu risk değerlendirmesi. *Ekoloji*, 17, 65, 11-20
- Tayanç, M., Dalfes, N., Karaca, M., Yenigün, O., 1998. A comparative assessment of different methods for detecting inhomogeneities in Turkish temperature data set. *International Journal of Climatology*, 18, 561-578.
- Tang, Q., Xu, Y., Bennett, S.J., Li, Y., 2015. Assessment of soil erosion using RUSLE and GIS: a case study of the Yangou watershed in the Loess Plateau, China. *Environmental Earth Sciences*, 73, 1715 - 1724.
- Thornbury, W.D., 1965. Regional geomorphology of the United States. *Soil Sciences*, 100, 148.
- Turp T., Öztürk T., Türkes M., Kurnaz L., 2014. Investigation of projected changes for near future air temperature and precipitation climatology of Turkey and surrounding regions by using the regional climate model RegCM4.3.5.
- Türkes, M., Tatli, H., 2011. Use of the spectral clustering to determine coherent precipitation regions in Turkey for the period 1929- 2007. *International Journal of Climatology*, 31, 2055-2067.
- Vitousek, P., Mooney, H., Lubchenco, J., Melillo, J., 1997. Human domination of Earth's ecosystems. *Science*, New Series, 277, 494-499.

- Voroney, R.P., van Venn, J.A., Paul, E.A., 1981. Organic carbon dynamics in crassland soil II. model validation and simulation of the long-terms effects of cultivation and rainfall erosion. *Canada Journal of Soil Science*, 61, 24, 211.
- Yang, D., Kanae, S., Oki, T., Koike, T., Musiake, K., 2003. Global potential soil erosion with reference to land use and climate changes. *Hydrology Process*, 17, 2913- 2928.
- Young, R.A., 1986. Agricultural nonpoint source pollution model: A watershed analysis tool, Conservation Report 35, Agricultural Research Service, USDA, Morris, Minnesota, USA.
- Zhang, X., Zeng, Y., Yan, N., Yuan, C., 2010. Identification of priority areas for controlling soil erosion. *Catena*, 83, 76-86.
- Wang, G., Gertner, G., Fang, S., Anderson, A.B., 2003. Mapping multiple variables for predicting soil loss by geostatistical methods with TM images and a slope map. *Photogrammetric Engineering and Remote Sensing*, 69, 889–898.
- Williams, J.R., Renard, K.G., Dyke, P.T., 1983. Epic - a New Method for Assessing Erosions Effect on Soil Productivity. *Soil and Water Conservation*, 38, 381-383.
- Wischmeier, W.H., Smith D.D., 1978. Predicting rainfall erosion losses-a guide to conservation planning, Agriculture Handbook, No 537. US Department of Agriculture Science and Education Administration, Washington, 163.
- Witinok, P.M., 1988. A critical examination of the universal soil loss equation (USLE). *Geographical Perspectives*, 62, 25-54.
- Woodward, D.E., 1999. Method to predict cropland ephemeral gully erosion. *Catena*, 37, 393-399
- Woolhiser, D.A., Smith, R.E., Goodrich, D.C., 1990. KINEROS, a kinematic runoff and erosion model: documentation and user manual, report ARS77, Agricultural Research Service, USDA, Minnesota, US.

APPENDIX A: FAO SOIL UNITS (DSMW)

J	FLUVISOLS	Q	ARENOSOLS	Z	SOLONCHAKS	K	KASTANOZEMS
Je	Eutric Fluvisols	Qe	Cambic Arenosols	Zo	Orthic Solonchaks	Kh	Haplic Kastanozems
Jc	Calcaric Fluvisols	Ql	Luvic Arenosols	Zm	Mollic Solonchaks	Kk	Calcic Kastanozems
Jd	Dystric Fluvisols	Qf	Ferralic Arenosols	Zt	Takyrlic Solonchaks	Kl	Luvic Kastanozems
Jt	Thionic Fluvisols	Qa	Albic Arenosols	Zg	Gleyic Solonchaks		
G	GLEYSOLS	E	RENDZINAS	S	SOLONETZ	C	CHERNOZEMS
Ge	Eutric Gleysols			So	Orthic Solonetz	Ch	Haplic Chernozems
Gc	Calcaric Gleysols			Sm	Mollic Solonetz	Ck	Calcic Chernozems
Gd	Dystric Gleysols	U	RANKERS	Sg	Gleyic Solonetz	Cl	Luvic Chernozems
Gm	Mollic Gleysols					Cg	Glossic Chernozems
Gh	Humic Gleysols						
Gp	Plinthic Gleysols	T	ANDOSOLS	Y	YERMOSOLS	H	PHAEZEMS
Gx	Gelic Gleysols	To	Ochric Andosols	Yh	Haplic Yermosols	Hh	Haplic Phaeozems
		Tm	Mollic Andosols	Yk	Calcic Yermosols	Hc	Calcaric Phaeozems
R	REGOSOLS	Th	Humic Andosols	Yy	Gypsic Yermosols	Hi	Luvic Phaeozems
Re	Eutric Regosols	Tv	Vitric Andosols	Yl	Luvic Yermosols	Hg	Gleyic Phaeozems
Rc	Calcaric Regosols			Yt	Takyrlic Yermosols		
Rd	Dystric Regosols	V	VERTISOLS			M	GREYZEMS
Rx	Gelic Regosols	Vp	Pellic Vertisols	X	XEROSOLS	Mo	Orthic Greyzems
		Ve	Chromic Vertisols	Xh	Haplic Xerosols	Mg	Gleyic Greyzems
I	LITHOSOLS			Xk	Calcic Xerosols		
				Xy	Gypsic Xerosols		
				Xl	Luvic Xerosols		

Figure A.1. The abbreviations of FAO Soil Units (DSMW), Part 1.

B	CAMBISOLS	D	PODZOLUVISOLS	A	ACRISOLS	O	HISTOSOLS
Be	Eutric Cambisols	De	Eutric Podzoluvisols	Ao	Orthic Acrisols	Oe	Eutric Histosols
Bd	Dystric Cambisols	Dd	Dystric Podzoluvisols	Af	Ferric Acrisols	Od	Dystric Histosols
Bh	Humic Cambisols	Dg	Gleyic Podzoluvisols	Ah	Humic Acrisols	Ox	Gelic Histosols
Bg	Gleyic Cambisols			Ap	Plinthic Acrisols		
Bx	Gelic Cambisols			Ag	Gleyic Acrisols		
Bk	Calcic Cambisols	P	PODZOLS				
Bc	Chromic Cambisols						
Bv	Vertic Cambisols	Po	Orthic Podzols	N	NITOSOLS		
Bf	Ferralic Cambisols	Pl	Leptic Podzols				
		Pf	Ferric Podzols	Ne	Eutric Nitosols		
		Ph	Humic Podzols	Nd	Dystric Nitosols		
		Pp	Placic Podzols	Nh	Humic Nitosols		
L	LUVISOLS	Pg	Gleyic Podzols				
				F	FERRALSOLS		
Lo	Orthic Luvisols	W	PLANOSOLS				
Lc	Chromic Luvisols			Fo	Orthic Ferralsols		
Lk	Calcic Luvisols	We	Eutric Planosols	Fx	Xanthic Ferralsols		
Lv	Vertic Luvisols	Wd	Dystric Planosols	Fr	Rhodic Ferralsols		
Lf	Ferric Luvisols	Wm	Mollic Planosols	Fh	Humic Ferralsols		
La	Albic Luvisols	Wh	Humic Planosols	Fa	Acric Ferralsols		
Lp	Plinthic Luvisols	Ws	Solodic Planosols	Fp	Plinthic Ferralsols		
Lg	Gleyic Luvisols	Wx	Gelic Planosols				

Figure A.2. The abbreviations of FAO Soil Units (DSMW), Part 2.

APPENDIX B: THE FAO SOIL UNITS FOR TURKEY (DSMW)

Table B.1. The Soil Unit List for Turkey of FAO Soil (DSMW).

FID	SNUM	FAOSOIL	DOMSOI	CNTCODE	CNTNAME	SQKM	COUNTRY	X	Y
7922	3185	Lc104-2/3bc	Lc	223	TU	3293	TURKEY	27	42
7927	3027	Bk49-2c	Bk	223	TU	20057	TURKEY	37	41
7939	3003	Ao111-2bc	Ao	223	TU	14013	TURKEY	33	41
7947	3188	Lc105-2/3ab	Lc	223	TU	11	TURKEY	28	42
7975	6660	Lc105-2/3ab	Lc	223	TU	7221	TURKEY	27	41
8002	3283	Vp72-3a	Vp	223	TU	4423	TURKEY	27	41
8012	3168	Kh35-2ab	Kh	223	TU	2365	TURKEY	34	42
8031	3026	Bk45-2bc	Bk	223	TU	1021	TURKEY	32	41
8038	3090	I-Be-2c	I	223	TU	227	TURKEY	43	42
8044	3016	Be122-2bc	Be	223	TU	8659	TURKEY	34	41
8053	3120	I-Rc-Xk-2c	I	223	TU	12	TURKEY	42	42
8055	3089	I-Bd-2c	I	223	TU	973	TURKEY	42	41
8056	3090	I-Be-2c	I	223	TU	20	TURKEY	43	41

8059	3004	Ao112-2bc	Ao	223	TU	18945	TURKEY	39	41
8060	3096	I-Bh-U-2c	I	223	TU	1505	TURKEY	43	41
8062	3026	Bk45-2bc	Bk	223	TU	14713	TURKEY	32	41
8065	3090	I-Be-2c	I	223	TU	202	TURKEY	42	41
8079	3028	Bk49-2c	Bk	223	TU	1675	TURKEY	42	41
8084	3093	I-Be-c	I	223	TU	20317	TURKEY	42	40
8101	3090	I-Be-2c	I	223	TU	81	TURKEY	43	41
8107	3282	Vp68-3a	Vp	223	TU	28	TURKEY	26	41
8126	3157	Kh1-2ab	Kh	223	TU	983	TURKEY	43	41
8129	3140	Jc49-1/3a	Jc	223	TU	1096	TURKEY	26	41
8133	6494	E23-2bc	E	223	TU	1119	TURKEY	29	41
8139	3206	Lo85-2b	Lo	223	TU	1525	TURKEY	27	41
8144	3188	Lc105-2/3ab	Lc	223	TU	6815	TURKEY	30	41
8151	3098	I-Bh-U-c	I	223	TU	6772	TURKEY	40	41
8157	3168	Kh35-2ab	Kh	223	TU	2500	TURKEY	36	41
8158	3206	Lo85-2b	Lo	223	TU	1003	TURKEY	28	41
8162	3185	Lc104-2/3bc	Lc	223	TU	4197	TURKEY	27	41
8174	3026	Bk45-2bc	Bk	223	TU	4298	TURKEY	35	41
8185	6997	WAT	WR	223	TU	116	TURKEY	43	41
8207	3157	Kh1-2ab	Kh	223	TU	1789	TURKEY	42	41
8217	3157	Kh1-2ab	Kh	223	TU	2768	TURKEY	43	41
8220	3098	I-Bh-U-c	I	223	TU	508	TURKEY	42	41
8227	3139	Jc49-1/3a	Jc	223	TU	1500	TURKEY	30	41
8232	3121	I-Rc-Xk-2c	I	223	TU	5229	TURKEY	34	40
8240	3026	Bk45-2bc	Bk	223	TU	858	TURKEY	36	41
8244	3310	Xk56-2/3ab	Xk	223	TU	86183	TURKEY	34	39
8249	3208	Lo91-2bc	Lo	223	TU	8151	TURKEY	32	41
8266	3157	Kh1-2ab	Kh	223	TU	3691	TURKEY	41	40
8272	3208	Lo91-2bc	Lo	223	TU	4338	TURKEY	30	41
8277	3121	I-Rc-Xk-2c	I	223	TU	950	TURKEY	35	40
8286	3016	Be122-2bc	Be	223	TU	6303	TURKEY	36	40
8287	3208	Lo91-2bc	Lo	223	TU	108	TURKEY	28	41
8318	3208	Lo91-2bc	Lo	223	TU	294	TURKEY	28	40
8326	6997	WAT	WR	223	TU	272	TURKEY	30	40
8330	3121	I-Rc-Xk-2c	I	223	TU	8975	TURKEY	36	40
8340	3016	Be122-2bc	Be	223	TU	2632	TURKEY	27	40
8342	3027	Bk49-2c	Bk	223	TU	2315	TURKEY	30	40
8353	3027	Bk49-2c	Bk	223	TU	601	TURKEY	27	40
8354	3016	Be122-2bc	Be	223	TU	9074	TURKEY	30	40
8357	3281	Vc62-3a	Vc	223	TU	1111	TURKEY	28	40
8359	3139	Jc49-1/3a	Jc	223	TU	356	TURKEY	27	40
8362	3157	Kh1-2ab	Kh	223	TU	9875	TURKEY	42	40
8364	3100	I-Bk-Kk-2bc	I	223	TU	2106	TURKEY	39	40
8367	3208	Lo91-2bc	Lo	223	TU	2669	TURKEY	27	40
8372	3173	Kk19-2/3b	Kk	223	TU	1466	TURKEY	39	40
8385	3139	Jc49-1/3a	Jc	223	TU	1040	TURKEY	28	40
8388	3208	Lo91-2bc	Lo	223	TU	15597	TURKEY	28	40
8392	6997	WAT	WR	223	TU	154	TURKEY	28	40
8395	3089	I-Bd-2c	I	223	TU	261	TURKEY	26	40
8399	6997	WAT	WR	223	TU	140	TURKEY	29	40
8417	3093	I-Be-c	I	223	TU	7789	TURKEY	43	40
8418	3114	I-Lc-E-2bc	I	223	TU	488	TURKEY	28	40
8420	3026	Bk45-2bc	Bk	223	TU	28438	TURKEY	30	39

8422	3016	Be122-2bc	Be	223	TU	529	TURKEY	26	40
8427	3208	Lo91-2bc	Lo	223	TU	1058	TURKEY	26	40
8436	3307	Xk53-2/3bc	Xk	223	TU	23619	TURKEY	37	39
8437	3288	Xh31-3a	Xh	223	TU	151	TURKEY	45	40
8440	3129	I-Re-Yh-c	I	223	TU	566	TURKEY	44	40
8442	3157	Kh1-2ab	Kh	223	TU	5898	TURKEY	43	40
8446	3306	Xk52-2/3b	Xk	223	TU	3861	TURKEY	37	40
8460	3026	Bk45-2bc	Bk	223	TU	3604	TURKEY	36	40
8461	3027	Bk49-2c	Bk	223	TU	776	TURKEY	26	40
8470	3319	Xl24-2bc	Xl	223	TU	911	TURKEY	34	40
8474	3122	I-Rc-Xk-c	I	223	TU	27347	TURKEY	43	38
8478	3311	Xk59-2/3a	Xk	223	TU	551	TURKEY	31	40
8479	3200	Lo64-3c	Lo	223	TU	18061	TURKEY	39	39
8480	3013	Be115-2/3c	Be	223	TU	10669	TURKEY	41	39
8490	3016	Be122-2bc	Be	223	TU	3526	TURKEY	30	40
8500	3320	Xl24-2bc	Xl	223	TU	1209	TURKEY	35	40
8506	3129	I-Re-Yh-c	I	223	TU	13	TURKEY	45	40
8514	3114	I-Lc-E-2bc	I	223	TU	894	TURKEY	28	40
8520	3121	I-Rc-Xk-2c	I	223	TU	333	TURKEY	34	40
8530	3139	Jc49-1/3a	Jc	223	TU	278	TURKEY	27	40
8533	3093	I-Be-c	I	223	TU	2172	TURKEY	39	39
8538	3093	I-Be-c	I	223	TU	2090	TURKEY	41	39
8558	3288	Xh31-3a	Xh	223	TU	124	TURKEY	44	39
8561	3169	Kk16-2b	Kk	223	TU	15943	TURKEY	43	39
8562	3319	Xl24-2bc	Xl	223	TU	330	TURKEY	34	39
8564	3114	I-Lc-E-2bc	I	223	TU	447	TURKEY	27	39
8577	3114	I-Lc-E-2bc	I	223	TU	6287	TURKEY	28	39
8598	3093	I-Be-c	I	223	TU	1508	TURKEY	38	39
8605	3208	Lo91-2bc	Lo	223	TU	737	TURKEY	31	39
8633	3139	Jc49-1/3a	Jc	223	TU	676	TURKEY	27	39
8647	6997	WAT	WR	223	TU	1664	TURKEY	33	39
8649	3208	Lo91-2bc	Lo	223	TU	1774	TURKEY	27	39
8659	3016	Be122-2bc	Be	223	TU	832	TURKEY	30	39
8666	3311	Xk59-2/3a	Xk	223	TU	3638	TURKEY	33	39
8668	3319	Xl24-2bc	Xl	223	TU	898	TURKEY	34	39
8674	3122	I-Rc-Xk-c	I	223	TU	1018	TURKEY	43	39
8675	3311	Xk59-2/3a	Xk	223	TU	2087	TURKEY	31	39
8680	3139	Jc49-1/3a	Jc	223	TU	3592	TURKEY	28	39
8681	3310	Xk56-2/3ab	Xk	223	TU	969	TURKEY	31	39
8684	3093	I-Be-c	I	223	TU	657	TURKEY	36	39
8688	3121	I-Rc-Xk-2c	I	223	TU	2358	TURKEY	32	39
8694	3288	Xh31-3a	Xh	223	TU	2372	TURKEY	42	39
8701	6997	WAT	WR	223	TU	3699	TURKEY	43	39
8704	3308	Xk54-3ab	Xk	223	TU	3372	TURKEY	38	38
8705	3295	Xh47-2ab	Xh	223	TU	3379	TURKEY	36	38
8708	3016	Be122-2bc	Be	223	TU	8256	TURKEY	28	38
8727	3320	Xl24-2bc	Xl	223	TU	1326	TURKEY	30	39
8735	3261	Re87-1bc	Re	223	TU	1972	TURKEY	35	39
8737	3093	I-Be-c	I	223	TU	29412	TURKEY	39	38
8740	3122	I-Rc-Xk-c	I	223	TU	377	TURKEY	42	39
8750	6997	WAT	WR	223	TU	139	TURKEY	38	39
8752	3093	I-Be-c	I	223	TU	4323	TURKEY	36	38
8755	3308	Xk54-3ab	Xk	223	TU	922	TURKEY	40	39

8757	6997	WAT	WR	223	TU	101	TURKEY	31	39
8758	6997	WAT	WR	223	TU	92	TURKEY	44	39
8761	3310	Xk56-2/3ab	Xk	223	TU	756	TURKEY	31	39
8762	3114	I-Lc-E-2bc	I	223	TU	4114	TURKEY	27	38
8766	3093	I-Be-c	I	223	TU	380	TURKEY	35	39
8768	3308	Xk54-3ab	Xk	223	TU	3436	TURKEY	37	38
8774	3319	Xl24-2bc	Xl	223	TU	1128	TURKEY	34	38
8777	6997	WAT	WR	223	TU	91	TURKEY	31	39
8778	3016	Be122-2bc	Be	223	TU	1392	TURKEY	31	38
8786	3114	I-Lc-E-2bc	I	223	TU	1547	TURKEY	31	38
8787	6997	WAT	WR	223	TU	63	TURKEY	39	38
8794	3026	Bk45-2bc	Bk	223	TU	5681	TURKEY	32	38
8797	3325	Zg15-3a	Zg	223	TU	673	TURKEY	35	38
8813	3191	Lc63-3bc	Lc	223	TU	26043	TURKEY	40	38
8815	3139	Jc49-1/3a	Jc	223	TU	1191	TURKEY	30	38
8829	3139	Jc49-1/3a	Jc	223	TU	1512	TURKEY	28	38
8832	6997	WAT	WR	223	TU	467	TURKEY	31	38
8835	3121	I-Rc-Xk-2c	I	223	TU	1082	TURKEY	33	38
8837	3013	Be115-2/3c	Be	223	TU	5110	TURKEY	36	38
8838	3114	I-Lc-E-2bc	I	223	TU	2654	TURKEY	29	38
8844	3309	Xk55-3ab	Xk	223	TU	21970	TURKEY	39	37
8854	3310	Xk56-2/3ab	Xk	223	TU	1104	TURKEY	30	38
8860	3114	I-Lc-E-2bc	I	223	TU	956	TURKEY	27	38
8861	3311	Xk59-2/3a	Xk	223	TU	3882	TURKEY	33	38
8862	3114	I-Lc-E-2bc	I	223	TU	5733	TURKEY	31	37
8863	3504	I-Be-E-c	I	223	TU	24951	TURKEY	34	37
8875	3139	Jc49-1/3a	Jc	223	TU	2876	TURKEY	28	38
8887	3114	I-Lc-E-2bc	I	223	TU	822	TURKEY	30	38
8898	3280	Vc56-3a	Vc	223	TU	2868	TURKEY	37	38
8904	6997	WAT	WR	223	TU	688	TURKEY	32	38
8916	3016	Be122-2bc	Be	223	TU	11220	TURKEY	28	37
8918	6997	WAT	WR	223	TU	151	TURKEY	30	38
8919	3208	Lo91-2bc	Lo	223	TU	1386	TURKEY	32	38
8928	3139	Jc49-1/3a	Jc	223	TU	770	TURKEY	30	38
8932	3122	I-Rc-Xk-c	I	223	TU	580	TURKEY	40	38
8935	6997	WAT	WR	223	TU	215	TURKEY	30	38
8938	6659	Bk49-2c	Bk	223	TU	3473	TURKEY	31	37
8945	3289	Xh33-3a	Xh	223	TU	14	TURKEY	45	38
8946	3139	Jc49-1/3a	Jc	223	TU	751	TURKEY	32	37
8949	3016	Be122-2bc	Be	223	TU	1479	TURKEY	30	37
8952	3114	I-Lc-E-2bc	I	223	TU	1746	TURKEY	31	37
8958	3325	Zg15-3a	Zg	223	TU	678	TURKEY	34	38
8959	3016	Be122-2bc	Be	223	TU	1029	TURKEY	32	37
8961	3114	I-Lc-E-2bc	I	223	TU	5262	TURKEY	28	37
8969	3193	Lc76-3b	Lc	223	TU	2558	TURKEY	35	37
8978	3276	Vc1-3a	Vc	223	TU	1231	TURKEY	42	37
8982	3504	I-Be-E-c	I	223	TU	344	TURKEY	33	37
8983	3280	Vc56-3a	Vc	223	TU	7096	TURKEY	35	37
8984	6997	WAT	WR	223	TU	63	TURKEY	27	38
8996	3122	I-Rc-Xk-c	I	223	TU	2662	TURKEY	41	37
9020	6997	WAT	WR	223	TU	112	TURKEY	32	37
9027	3279	Vc50-3ab	Vc	223	TU	155	TURKEY	43	37
9030	3289	Xh33-3a	Xh	223	TU	68	TURKEY	45	37

9033	3093	I-Be-c	I	223	TU	0	TURKEY	43	37
9047	6997	WAT	WR	223	TU	200	TURKEY	35	37
9049	3298	Xk26-2/3a	Xk	223	TU	2992	TURKEY	40	37
9051	3114	I-Lc-E-2bc	I	223	TU	8347	TURKEY	30	37
9070	3277	Vc47-3b	Vc	223	TU	189	TURKEY	42	37
9074	3016	Be122-2bc	Be	223	TU	2465	TURKEY	31	37
9075	3108	I-E-Xk-bc	I	223	TU	35	TURKEY	42	37
9079	3137	Jc36-2/3a	Jc	223	TU	453	TURKEY	38	37
9088	3139	Jc49-1/3a	Jc	223	TU	752	TURKEY	31	37
	3093	I-Be-c	I	223	TU	4951	TURKEY	32	37
9107	6997	WAT	WR	223	TU	61	TURKEY	30	37
9109	3192	Lc69-3a	Lc	223	TU	1611	TURKEY	37	37
9116	3280	Vc56-3a	Vc	223	TU	2401	TURKEY	36	36
9123	3312	Xk9-2/3a	Xk	223	TU	1209	TURKEY	39	37
9133	3322	Xy4-2/3a	Xy	223	TU	324	TURKEY	40	37
9137	3133	I-Xk-2c	I	223	TU	132	TURKEY	38	37
9140	3280	Vc56-3a	Vc	223	TU	870	TURKEY	32	37
9146	6997	WAT	WR	223	TU	68	TURKEY	29	37
9151	3139	Jc49-1/3a	Jc	223	TU	719	TURKEY	30	37
9159	3299	Xk27-2ab	Xk	223	TU	414	TURKEY	39	37
9171	3299	Xk27-2ab	Xk	223	TU	7	TURKEY	38	37
9188	3299	Xk27-2ab	Xk	223	TU	230	TURKEY	38	37
9193	3114	I-Lc-E-2bc	I	223	TU	782	TURKEY	30	37
9212	3191	Lc63-3bc	Lc	223	TU	116	TURKEY	37	37
9275	3001	Ao102-2c	Ao	223	TU	2860	TURKEY	33	36
9283	6997	WAT	WR	223	TU	83	TURKEY	36	36
9298	3191	Lc63-3bc	Lc	223	TU	58	TURKEY	37	36
9320	3191	Lc63-3bc	Lc	223	TU	777	TURKEY	36	36
9384	3563	Vp39-3b	Vp	223	TU	74	TURKEY	36	36

APPENDIX C: THE SOIL CONTENT PROPERTIES OF FAO SOIL (DSMW)

Table C.1. The Soil Content Properties of FAO Soil (DSMW).

Soil unit symbol	sand % topsoil	sand % subsoil	silt% topsoil	silt% subsoil	clay % topsoil	clay % subsoil	pH water topsoil	pH water subsoil	OC % topsoil	OC % subsoil
A	53,3	44,3	17,2	17,1	29,5	38,6	5,2	5,2	1,74	0,63
AF	61,7	52,5	14,4	12,9	23,9	34,6	5,4	5,3	0,91	0,34
AF 1	81,1	75,5	8,7	8,9	10,2	15,6	5,7	5,5	0,35	0,2
AF 2	61,7	44,5	14,3	10,8	24	44,7	5,1	5,2	1,05	0,37
AF 3	21,3	13,1	25,7	24,4	52,9	62,3	5	4,9	1,85	0,58
AG	40,9	36,8	27,2	29,7	32,1	33,4	5,1	4,9	2,26	0,34
AG 1	89,3	72,5	7,2	9,5	3,5	17,9	5,5	5,1	0,5	0,16
AG 2	9,6	15,8	75,2	64,7	15,3	19,6	4,4	4,2	3,07	0,25
AG 3	35,2	32	17,9	24,8	47,2	43,2	5,2	5,1	1,99	0,38
AH	31,3	27,1	24,8	25,1	43,8	47,8	5	5,4	3,34	1,49
AH 1	72,8	71,9	14,6	10,6	12,6	17,4	5	5	1,58	0,9

AH 2	52,4	45,4	27,9	33	19,6	21,5	5,1	5,7	4,46	1,95
AH 3	9,2	7,4	26,1	22,2	64,8	70,4	5	5,3	2,88	1,25
AO	53,6	43,4	15,8	16	30,6	40,6	5,1	5,2	2,25	0,75
AO 1	82,3	68,1	8,6	11,4	9,2	20,5	5	5,1	0,3	0,21
AO 2	51	41,3	21,6	17,2	27,4	41,5	5,3	5	1,73	0,73
AO 3	33	28,9	14,2	15,5	52,9	55,6	5,2	5,4	1,84	0,89
AP	57	46,2	15,6	17,1	27,1	36,8	5,3	5	1,09	0,26
AP 1	80	65,1	12	14,6	7,8	20,3	5,6	5	0,69	0,2
AP 2	58,7	45,4	16,3	17,4	25	37,1	5,8	5,6	0,87	0,29
AP 3	10,4	8,8	22,7	22	66,7	69,6	4,5	4,6	2,91	0,49
B	60,4	60	17	16,6	22,5	23,4	6,9	7,2	1,17	0,57
BC	40,1	41,8	21,5	22,7	38,4	35,5	5,7	5,8	1,44	0,74
BC 1	80	60	10	25	10	15	5,6	5,7	1	0,5
BC 2	56,7	56,8	23,6	20,6	19,8	22,5	5,8	5,9	1,22	0,61
BC 3	15,3	19,3	18,5	25,7	66,3	55	5,6	5,6	1,77	0,93
BD	32,7	29,8	30,3	37,6	37,1	32,3	4,9	5,3	3,28	0,87
BD 1	70	65	20	20	10	15	4,8	5,2	3	1
BD 2	39,9	38,2	34,1	38,4	26	22,7	5,4	5,8	4,26	1,33
BD 3	27,8	24,2	27,8	37	44,4	38,8	4,6	5	2,62	0,57
BE	36,4	41,7	37,2	32,1	26,4	26,3	6,9	7,1	1,07	0,51
BE 1	84,5	78,3	6,1	7,6	10,4	15,4	6,7	6,6	0,2	0,2
BE 2	36,4	40,4	41,1	35,2	22,5	24,4	6,9	7	1,26	0,56
BE 3	18,8	22,7	35,7	35,5	45,4	41,6	7,1	7,4	0,68	0,25
BF	34,2	31,5	15,5	18,7	50,2	50	5	5,2	2,76	0,72
BF 1	82,2	89,5	10	8,3	8	3,2	4,6	4,8	2	0,75
BF 2	60	50	12	14	28	36	4,9	5	2,5	0,75
BF 3	22,3	17	16,9	21,3	60,7	61,7	5,1	5,2	3,22	0,75
BG	34,2	35,3	20,4	16,1	45,4	48,4	5,9	5,8	1,82	1,31
BG 1	78,9	76,4	8,2	7,2	12,4	15,6	4,9	4,9	0,9	0,21
BG 2	71,3	75,5	3,7	2,3	25	22,2	7,4	7,6	0,18	0,1
BG 3	6,9	8,3	30	23,7	63,1	68,1	5,8	5,5	2,68	2,09
BH	55,2	60,4	21	16,5	23,8	23,2	5,3	5,8	3,86	1,78
BH 1	82,5	81,1	6,1	2,9	11,6	16,1	5,7	7	0,95	0,25
BH 2	54,2	53,4	25,7	21,1	20,1	25,6	5,2	5,5	5,11	2,52
BH 3	35	34	35	30	30	36	5,7	5,6	3,45	1,12
BK	81,6	81,6	6,8	6,7	11,7	11,8	7,6	8,2	0,44	0,22
BK 1	88,2	86,2	4,2	4,4	7,7	9,4	7,7	8,2	0,26	0,18
BK 2	59,5	66,1	15,1	13,6	25,5	20,3	7,5	8,2	0,77	0,29
BK 3	10,3	13,8	40	41,9	49,7	43,4	8,6	8,7	0,84	0,49
BV	23,3	20	26	26,1	50,7	53,9	7,4	7,4	1,1	0,53
BV 1	35	33	25	25	40	42	7	7	1	0,4
BV 2	25	22	30	30	45	48	7,2	7,2	1,5	0,5
BV 3	23,3	20	26	26,1	50,7	53,9	7,4	7,4	1,1	0,53
BX	42,4	43,2	31,2	29,9	26,4	27	5,3	6,3	1,48	1,26
BX 1	75	71	20,6	24	4,5	5	5,2	5,3	1	0,7
BX 2	50	52	30	28	20	20	5,3	6,3	1,2	0,8
BX 3	26,2	29,3	36,5	32,8	37,4	38	5,3	7,2	1,48	1,26
C	42,9	38,8	27,6	27,1	29,5	34,2	7,3	8,1	1,52	0,56
CG	32	30	45	45	23	25	7	8	3,6	1,8
CG 1	80	70	10	10	10	20	6,5	7,6	3	1
CG 2	30	23	50	55	20	22	7	7,8	3,6	1,5
CG 3	42	38	22	22	36	40	7,2	8	3,6	1,5
CH	32,2	30,8	44,1	45,7	23,7	24	7,1	8	3,04	0,97

CH 1	80	75	10	10	10	15	7	8	2	0,7
CH 2	27,3	24,9	55,1	57,2	17,6	18	7,1	8,1	2,44	0,81
CH 3	42	42,5	22	22,8	36	36,1	7,6	7,7	2,89	0,96
CK	41,6	39,3	26,6	25,4	31,8	35,3	7,5	8,3	1,32	0,51
CK 1	80,5	41,5	8,6	14,7	11	43,9	6,7	8,8	1,01	0,32
CK 2	41,4	47,9	31,7	28,4	26,8	23,8	7,6	8,1	1,47	0,67
CK 3	16,1	17,9	26,8	25,7	57,1	56,3	7,7	8,4	1,17	0,25
CL	46,3	40,2	24,9	24,5	28,8	35,4	7,1	7,9	1,27	0,49
CL 1	79,7	68,7	4,4	3,5	16	27,8	7,2	7,6	0,72	0,35
CL 2	41,2	33,3	33,8	32	25	34,8	7,1	8	1,47	0,56
CL 3	39,9	39,7	17,3	19,9	42,9	40,5	7,1	8	1,22	0,49
D	40,2	35	50,3	47,2	9,6	17,8	5,3	5,2	1,09	0,24
DD	3	2,4	87,8	84,3	9,2	13,3	4,4	4,8	1,14	0,4
DD 1	70	65	18	15	12	20	4,5	4,9	1	0,3
DD 2	3	2,4	87,8	84,3	9,2	13,3	4,4	4,8	1,14	0,4
DD 3	45	40	15	10	40	50	4,6	5	1,5	0,5
DE	71,1	65,5	17,8	15	11,1	19,5	5,3	5,1	1,47	0,2
DE 1	71,1	65,5	17,8	15	11,1	19,5	5,3	5,1	1,47	0,2
DE 2	50	40	40	40	10	20	5,5	5,8	2	0,6
DE 3	45	40	15	10	40	50	5,5	6	2,2	0,7
DG	46,4	37,2	45,2	42,2	8,4	20,6	5,8	5,4	0,65	0,13
DG 1	70	60	20	20	10	20	5,6	5,8	2	0,6
DG 2	46,4	37,2	45,2	42,2	8,4	20,6	5,9	5,4	0,65	0,13
DG 3	50	40	15	10	35	50	5,8	6,2	2	0,6
E	48,5	45	30,8	32	20,7	23	7,6	7,5	1,74	0,9
E 1	70	67	10	11	20	22	7,5	7,8	0,9	0,5
E 2	50	47	25	26	25	27	7,6	8	1,96	0,9
E 3	30	27	35	36	30	32	7,5	8,2	2	1
F	35,7	31,1	16,3	15,8	48	53	5	5,2	1,93	0,75
FA	23,5	22,1	27,4	25,8	49,1	52	5,2	5,4	2,63	0,98
FA 1	83	70,3	5,3	9,4	11,7	20	5,8	5,4	0,62	0,33
FA 2	55	48	9	10	36	42	5,2	5,4	2	0,7
FA 3	13,6	14,1	31,1	28,6	55,3	57,4	5,1	5,4	3,03	1,11
FH	12,8	9,1	21,6	23	65,5	67,8	4,8	5,1	3,49	1,44
FH 1	80	69	6	6	14	25	4,6	5	3	1
FH 2	45	40	25	20	30	40	4,8	5,1	3,5	1,3
FH 3	13	9,1	20,9	23	66	67,8	4,9	5,1	3,64	1,48
FO	28,7	25,8	18,4	17,3	52,9	56,9	5,1	5,3	1,92	0,67
FO 1	79,1	65,5	7	5,6	13,9	29	4,6	4,8	0,65	0,36
FO 2	45,7	44,5	30,1	29	24,2	26,5	5,4	5,5	1,53	0,23
FO 3	15,7	13,9	16,5	15,5	67,8	70,6	5,1	5,3	2,21	0,81
FP	44,7	33,6	20,6	27,4	34,8	38,8	4,8	4,7	1,36	0,55
FP 1	80	63	6	7	14	30	4,8	4,6	1	0,3
FP 2	42	34,5	42	39,4	16	26,1	4,8	4,6	1,04	0,32
FP 3	57,7	32,6	5,8	15,4	36,5	51,5	4,7	4,7	1,69	0,78
FR	40,4	36,8	14,8	13,3	44,6	49,8	5,3	5,4	1,52	0,63
FR 1	80,7	76,2	4,1	4,3	14,6	19,4	5,3	5,1	0,65	0,29
FR 2	69,8	60,3	7,7	7,9	22,5	31,5	5,3	5,4	0,81	0,36
FR 3	23,9	21	18,9	16,9	57,2	61,9	5,2	5,3	1,84	0,83
FX	52,6	47,2	7,8	6,8	39,5	45,9	4,8	4,9	1,23	0,41
FX 1	79	68,6	5,8	6,3	14,8	24,7	5,3	5	0,81	0,3
FX 2	72,9	62,3	5,9	6,7	21,3	31	5	4,9	0,91	0,34
FX 3	8,6	7,5	8,9	7,4	82,4	85	4,4	4,8	1,73	0,58

G	32,9	44,3	23,7	19,7	43,4	37	6,1	6,4	2,02	0,72
GD	18,9	33,9	21,8	18	59,3	48,2	4,7	4,7	2,92	1,63
GD 1	80	80	5	5	15	15	5	5,3	2,3	1,2
GD 2	51,3	53,6	28,1	28,1	20,7	18,3	5,3	6,2	2,59	0,55
GD 3	11,8	30,5	20,5	14,4	67,7	55,1	4,5	4,3	2,96	1,93
GE	42,8	50,3	20,4	18,4	36,8	32,9	6,4	6,8	1,3	0,52
GE 1	82,1	83,2	6,5	4,5	11,4	12,3	6,8	6,9	0,81	0,23
GE 2	51	49,9	24,2	22	28,2	31,5	6,6	7,1	1,41	0,4
GE 3	25,5	38,1	23,1	19,7	51,3	42,3	6,1	6,4	1,35	0,78
GH	40,5	32,6	30,3	27,9	29,2	39,5	5	5,3	6,56	1,91
GH 1	80	80	5	5	15	15	4,6	5,3	5	1,5
GH 2	55,8	46,7	31,7	31,4	12,6	22	4,6	5,5	7,2	2,4
GH 3	25,2	18,6	29	24,5	45,9	57,1	5,4	5,2	5,27	1,42
GK	31,8	46,3	18	14,9	50,2	38,7	7	7,9	0,98	0,21
GK 1	80	80	5	5	15	15	7	7,5	1	0,3
GK 2	63,6	65,6	7,7	3,2	28,7	31,2	7	7,6	0,72	0,26
GK 3	25,6	41,8	21	17,6	53,4	40,5	7	8	1,04	0,2
GM	26,4	50,2	25,9	16,2	47,7	35,7	6	6,4	2,44	0,78
GM 1	81,5	89,4	8,2	5,8	10,4	4,8	7,1	6,5	0,77	0,3
GM 2	41,4	57,4	38,4	20	26,6	33,8	7,4	7,9	2,57	1,08
GM 3	20,5	45,6	25	16,1	54,5	38,4	5,6	6,1	2,54	0,7
GP	17,9	22,9	51,9	40,4	30,1	36,8	5,2	5,2	2,73	0,42
GP 1	40	40	50	45	10	15	5	5,2	2	0,4
GP 2	24,1	24,1	57,1	49,9	18,8	25,9	5,1	5,2	1,3	0,31
GP 3	8,6	21	44,1	26	47	53,1	5,5	5,1	4,88	0,59
GX	50	40	30	30	20	30	6	5,8	4,23	1,18
GX 1	80	80	5	5	15	15	6	5,8	2	1
GX 2	55	45	30	30	15	25	6	5,8	4	2
GX 3	25	20	30	25	45	55	6	5,8	4	2
H	37,3	52	25,7	20,5	37	27,5	6,5	6,8	1,57	0,53
HC	40,8	40,8	22,5	25,7	36,8	33,4	7,9	8,4	2,17	0,8
HC 1	75	70	15	15	10	15	7,2	8,2	2	0,8
HC 2	56,9	56,8	23	21,2	20,2	22	7,8	8,3	1,59	0,59
HC 3	8,5	8,8	21,5	34,9	70	56,3	8,2	8,6	3,33	1,23
HG	34,6	65,2	22,2	13,8	43,3	21	6	6,3	1,82	0,38
HG 1	83	90,8	6,6	3,3	10,3	5,9	5,9	6,9	0,7	0,11
HG 2	64,1	74,8	11,7	5,5	24,2	19,7	6,6	6,4	0,52	0,16
HG 3	13	56,2	29,5	19,3	57,6	24,6	5,6	6	2,72	0,53
HH	37,2	46	31,2	26,7	31,6	27,4	6,7	6,9	1,09	0,5
HH 1	75	70	20	20	5	10	6,5	6,7	1,5	0,5
HH 2	45,5	55,7	30,9	24,7	23,6	19,7	6,6	6,7	1,02	0,3
HH 3	20,7	26,5	31,9	30,8	47,5	42,8	7,3	7,6	1,28	0,92
HL	39,1	46,9	26,5	20,7	34,6	32,4	6,4	6,6	1,46	0,63
HL 1	75	70	15	10	10	20	6,4	6,6	1,5	0,5
HL 2	43,5	53,4	31,2	27,8	25,5	18,8	6,6	6,8	1,23	0,52
HL 3	33,2	38,3	20,2	11,2	46,6	50,5	6,4	6,6	1,8	0,75
I	58,9	56	16,2	17	24,9	27	7,1	7,2	0,97	0,4
I 1	75	72	15	16	10	12	8,3	8,3	0,31	0,2
I 2	65	62	15	16	20	22	7	7,2	1	0,4
I 3	55	52	15	16	30	32	4,8	5,5	2,3	0,8
J	55,8	52,7	22,2	23,5	22	23,8	6,3	6,3	1,32	0,81
JC	39,6	41,7	39,9	39,8	20,6	18,5	8	8,1	0,65	0,24
JC 1	68,9	62,9	16,7	20,1	14,4	17	8	8,2	0,28	0,11

JC 2	20,9	36,4	54	44,8	25,2	18,9	8	8,1	0,84	0,27
JC 3	10	10	50	50	40	40	8	8,2	0,9	0,3
JD	35,9	33,9	39,4	37,2	24,8	28,9	4,5	4,4	2,16	1,3
JD 1	79,5	85,9	13,5	9,3	7	4,8	5,6	5,5	1,31	0,77
JD 2	32,5	25,7	44,1	42,9	23,5	31,5	4,3	4,3	1,68	1,66
JD 3	2,3	6,8	51,3	48,2	46,5	45,1	4,1	3,6	4,47	0,74
JE	70,8	67	12,8	14,1	16,5	18,9	6,6	6,9	1,15	0,67
JE 1	80,1	79,5	8,6	7,6	11,4	12,9	6,4	6,5	0,76	0,25
JE 2	56,2	55,1	19,1	19,6	24,7	25,4	6,8	7,2	0,93	0,29
JE 3	21	21,1	36,9	40,1	42,2	38,9	7,2	7,4	2,61	0,83
JT	11,7	7,8	36,8	40,3	51,5	52	4,1	3,6	2,57	1,67
JT 1	50	50	30	30	20	20	3,5	2,8	2	1
JT 2	30	9,1	36,7	48,6	33,3	42,3	3,6	2,8	3	1,5
JT 3	5,8	7,4	34	37,5	60,2	55,2	4,3	3,8	2,57	1,67
K	39,1	42,6	37	33,9	23,9	23,4	7,6	7,9	1,93	0,89
KH	54,5	60,4	27,3	22,9	18,2	16,7	7,7	8,2	2,16	0,8
KH 1	80	65	10	10	10	25	7,2	8	1,2	0,5
KH 2	54,5	60,4	27,3	22,9	18,2	16,7	7,7	8,2	2,16	0,8
KH 3	40	40	20	20	40	40	7,7	8,5	2	0,8
KK	16,5	20,7	48,9	48	34,4	31,3	8	8,2	1,5	1,01
KK 1	80	70	15	15	5	15	8	8,2	1,5	1
KK 2	18,5	26,9	54,9	47,7	26,7	25,5	8	8,2	1,48	1,11
KK 3	12,5	11,8	37	39,3	50	48,9	7,9	7,9	1,55	0,81
KL	36,7	42,4	40,3	33,8	23,1	23,9	7,1	7,5	2	0,87
KL 1	80	70	5	5	15	25	7,1	7,5	1,6	0,8
KL 2	35,1	50,1	45,8	31,7	19	18,2	7,3	7,7	1,83	0,87
KL 3	41,4	39	23,5	22,8	35,2	38,2	7,3	7,4	1,73	1,01
L	70,4	64,5	10,3	9,9	19,3	25,7	6,7	7,2	0,51	0,27
LA	87,5	81,8	6,2	5,9	6,4	12,3	6,7	7,3	0,47	0,21
LA 1	90,1	84,5	4,5	4,6	5,3	10,9	6,8	7,4	0,28	0,16
LA 2	47,8	40,3	30,3	25,1	21,9	34,6	5,5	4,7	3,2	0,94
LA 3	50	30	25	20	25	50	6	6,5	1,5	0,5
LC	64,3	59	12,2	11,2	23,5	29,8	6,4	6,5	0,63	0,35
LC 1	80,2	73,3	7,7	6,9	12,1	19,8	6,4	6,6	0,3	0,22
LC 2	57,6	51	16,4	15,9	26,1	33,1	6,2	6,3	0,64	0,41
LC 3	29,2	31,4	13,6	12,3	57,3	56,6	6,5	6,8	1,51	0,48
LF	74,6	67,7	9,6	8,9	15,9	23,4	6,4	7	0,39	0,25
LF 1	82,2	75,1	7,3	6,7	10,5	18,3	6,1	6	0,37	0,22
LF 2	64,4	55,8	13,5	12,9	22,1	31,3	6,3	8,9	0,39	0,28
LF 3	26,9	26,1	19,1	18,2	54,1	55,6	5,7	5,6	0,54	0,5
LG	59,9	53,4	13,4	12,6	26,7	34	6,5	6,9	0,73	0,31
LG 1	81,7	71,9	6	5,8	12,3	22,3	6,3	6,7	0,45	0,2
LG 2	55,4	48,5	18,3	17,5	26,3	34,1	6,5	7,1	0,83	0,23
LG 3	42,4	41,3	12,7	10,6	44,9	48,2	6,8	7,2	0,85	0,52
LK	75,4	69,5	7,4	8,2	17,2	22,4	7,7	8,2	0,34	0,23
LK 1	84,3	79,7	5,1	5	10,6	15,4	7,5	8,1	0,26	0,17
LK 2	64	55,3	10,9	12,5	25,2	32,2	7,9	8,3	0,44	0,33
LK 3	46,7	39,1	14,8	17,7	38,6	43,3	8,4	8,9	0,49	0,36
LO	76	71,9	9,9	8,9	14,1	19,2	6,4	6,7	0,41	0,21
LO 1	87,1	81,6	4,2	4,2	8,7	14,3	6,3	6,6	0,33	0,17
LO 2	53,7	49,6	23,3	22,1	23	28,3	6,7	7	0,57	0,28
LO 3	43,5	43,1	13,4	12,3	43,1	44,6	6,3	6,2	0,66	0,4
LP	69,9	57,5	10,5	10,9	19,5	31,6	5,9	5,6	0,73	0,35

LP 1	74,8	65,1	11	11,6	14,2	23,3	5,7	5,5	0,55	0,32
LP 2	65,1	49,9	10,1	10,2	24,9	39,9	6,1	5,7	0,92	0,42
LP 3	45	35	10	10	45	55	6,3	5,6	1	0,4
LV	26,1	26,8	27,3	22,5	46,7	50,9	6,6	7,1	1,86	0,84
LV 1	55	50	20	15	25	35	6,6	7	1	0,4
LV 2	48,4	36,3	28,3	25,1	23,3	38,7	6,6	8,4	0,49	0,19
LV 3	23,8	17,2	28	19,8	48,4	63	6,6	6,5	2,55	1,16
M	37,9	47,9	35	30,4	27,1	21,6	6,6	6,6	3,23	0,78
MG	30	25	50	45	20	30	6,3	6,5	4	1,4
MG 1	75	70	15	10	10	20	6,1	6,3	3	1
MG 2	30	25	50	45	20	30	6,3	6,5	4	1,4
MG 3	40	35	20	15	40	50	6,3	6,8	4,5	1,3
MO	33,3	29,2	46,4	44,2	20,4	26,7	6,1	5,8	3,65	1,11
MO 1	75	70	15	10	10	20	6,1	5,8	3	1
MO 2	33,3	29,2	46,4	44,2	20,4	26,7	6,1	5,8	3,65	1,11
MO 3	40	35	20	15	40	50	6,3	7	4	1,4
N	57,9	46,6	13,3	12	28,9	41,4	6	6,1	1,12	0,46
ND	38,9	31,9	17,6	13,8	43,6	54,4	5,2	5,2	1,57	0,44
ND 1	85,1	78,2	7,3	8,5	7,7	13,3	4,6	4,8	1,04	0,39
ND 2	55	45	20	20	25	35	5,2	5,2	1,5	0,5
ND 3	15,8	13	22,7	15,8	61,6	71,3	5,5	5,4	1,64	0,52
NE	68,4	57,8	10,5	10	21,2	32,2	6,3	6,5	0,6	0,32
NE 1	81,8	72,7	5,9	6,2	12,3	21,1	6,3	6,3	0,34	0,21
NE 2	57,1	46,9	18,1	15,6	24,8	37,3	6,3	6,9	0,89	0,47
NE 3	22,8	13,1	21,2	15,9	55,9	70,7	6,7	6,9	1,33	0,48
NH	6,4	5,4	29,8	21,5	63,9	73,3	5,5	5,4	4,04	1,47
NH 1	80	70	8	5	12	25	5,2	5,4	2	0,8
NH 2	55	45	20	15	25	40	5,3	5,4	3	1
NH 3	6,4	6,3	29,8	24,6	63,9	69,2	5,3	5,2	4,01	1,65
O	35	35	40	40	25	25	4,9	4,6	46,33	49,37
OD	35	35	40	40	25	25	4,2	4,1	47,3	49,76
OD 1	70	70	20	20	10	10	4,2	4,1	50	60
OD 2	35	35	40	40	25	25	4,2	4,1	50	60
OD 3	10	10	45	45	45	45	4,2	4,1	50	60
OE	35	35	40	40	25	25	6,3	5,3	41,46	46,78
OE 1	70	70	20	20	10	10	6,3	5,3	40	45
OE 2	35	35	40	40	25	25	6,3	5,3	40	45
OE 3	10	10	45	45	45	45	6,3	5,3	40	45
OX	35	35	40	40	25	25	4,2	4,1	56,1	55,58
OX 1	70	70	20	20	10	10	4,2	4,1	55	55
OX 2	35	35	40	40	25	25	4,2	4,1	55	55
OX 3	10	10	45	45	45	45	4,2	4,1	55	55
P	69,5	72	23,9	22,2	6,7	7	4,6	4,8	3,86	1,24
PF	64,9	66,9	26,3	23	8,5	10	5	5,4	1,25	0,28
PF 1	94	94,4	3,3	3,6	2	2	5,3	5,6	0,6	0,31
PF 2	35,7	39,4	49,3	42,4	15	17,9	4,7	5,2	1,9	0,25
PF 3	43	40	40	40	17	20	4,8	5,4	2	0,5
PG	87,3	79,9	9,6	15,5	3,2	8,5	4,2	4,6	3,36	1,37
PG 1	87,3	79,9	12,3	15,5	3,2	8,5	4,2	4,6	3,36	1,37
PG 2	60	58	30	27	10	15	4,4	5	3,4	1
PG 3	43	40	40	40	17	20	4,4	5	3,4	1
PH	80,8	84,8	16,5	13,7	2,8	1,6	4,3	4,5	3,18	0,88
PH 1	96	93,9	3	4,9	1,1	1,3	4,3	4,5	1,11	1,2

PH 2	50,4	66,5	43,4	31,4	6,3	2,2	4,4	4,7	7,33	0,24
PH 3	43	40	40	40	17	20	4,5	4,9	5	0,5
PL	51,3	51,3	40,1	41	8,7	7,7	4,1	4,5	4,52	1,41
PL 1	90	90	9	8	1	2	4	4,4	3	1
PL 2	51,3	51,3	40,1	41	8,7	7,7	4,1	4,5	4,52	1,41
PL 3	43	40	40	40	17	20	4,2	4,6	3	1
PO	67,9	74,4	28,7	21,9	3,6	3,7	5	5,2	1,65	0,72
PO 1	91,4	90,9	8,2	7,2	0,8	2	4,7	5,4	0,44	0,28
PO 2	49	58	44	36,6	7	5,4	5,3	4,9	2,47	1,16
PO 3	43	40	40	40	17	20	4,7	5,5	2,5	1
PP	56,5	62,9	28,3	24,8	15,2	12,4	4,7	4,8	8,62	2,68
PP 1	98,6	96	1,1	2	0,3	2	4,9	4,3	0,94	1,75
PP 2	56,7	62,6	32,5	31,3	10,8	6,1	4,7	5,2	15,82	3,15
PP 3	22	30	38	41	40	29	4,6	4,8	1,88	0,9
Q	91,9	91,8	3,2	3	5	5,4	6,2	6,3	0,23	0,13
QA	92,6	92,4	3,6	3,7	3,7	5,8	5,9	5,8	0,87	0,1
QA 1	92,6	92,4	3,6	3,7	5,5	5,8	5,9	5,8	0,87	0,1
QA 2	93	84	3	3	4	8	5,5	5,9	1	0,2
QA 3	89	85	5	5	6	10	5,7	6	1,2	0,3
QB	92	92,4	3,1	2,8	4,9	5	6,4	6,4	0,21	0,12
QB 1	92	92,3	3,2	2,9	4,8	5	6,4	6,4	0,21	0,12
QB 2	89	83	3	5	8	12	6,4	6,6	1	0,25
QB 3	48,5	92,9	16	3	35,6	4,2	6,4	6,9	0,4	0,16
QF	91,7	91,2	3,3	3,1	5,1	5,8	5,9	6,4	0,27	0,15
QF 1	92	91,6	3	3	5	5,5	5,9	6,4	0,27	0,15
QF 2	90	86	3	4	7	10	6	5,5	0,5	0,15
QF 3	85	81	5	7	10	12	5,9	5,4	0,8	0,2
QL	92,8	91,7	2,7	2,9	4,7	5,5	6,3	6,1	0,2	0,12
QL 1	92,6	91,7	2,7	2,9	4,8	5,5	6,3	6	0,2	0,12
QL 2	87	80	3	5	10	15	6,3	6,1	0,8	0,2
QL 3	83	75	5	7	12	18	6,3	6,1	0,8	0,2
R	70,6	71,9	14,1	13,7	15,4	14,3	6,7	7	0,57	0,43
RC	63,5	62,8	19,2	18,4	17,3	18,7	7,6	7,6	0,76	0,41
RC 1	82,2	82,1	6,9	6,9	10,9	11,1	7,5	7,6	0,33	0,33
RC 2	38,7	37,1	35,5	33,8	25,8	28,8	7,5	7,6	0,58	0,52
RC 3	30	35	40	33	30	32	7,5	7,6	0,8	0,6
RD	82,1	79,2	6,7	5,7	11,3	15,1	7	6,8	0,27	0,15
RD 1	83	79,2	6,5	5,7	10,5	15,1	7	6,8	0,27	0,15
RD 2	40	44	37	38	23	18	6,2	5,6	0,5	0,16
RD 3	30	35	40	33	30	32	6	5,8	0,7	0,23
RE	68,3	71,6	15,1	15,2	16,6	13,2	6,4	6,8	0,5	0,45
RE 1	82,8	79,9	7,5	8,2	9,7	11,7	6,4	6,6	0,29	0,23
RE 2	38,7	43,8	36,9	38,2	24,6	17,9	6,9	7,1	0,82	1,04
RE 3	30	35	40	33	30	32	6,1	6,5	0,99	0,3
RX	82,5	87,5	9,9	6,3	7,7	6,3	5,4	5,5	1,7	0,77
RX 1	82,5	87,5	9,9	6,3	7,7	6,3	5,2	5	1,7	0,77
RX 2	40	44	37	38	23	18	5,4	5,5	2	0,8
RX 3	30	35	40	33	30	32	5,4	5,6	2,2	0,8
S	55,4	47,3	20,4	19,8	24,2	32,8	8,2	8,6	0,65	0,48
SG	53,9	37,7	25,5	26,2	20,6	36,1	8	8,7	0,67	0,45
SG 1	79,7	58	8,9	10,9	11,5	31,2	7,9	9,5	0,26	0,1
SG 2	35,4	21,5	44,9	40,3	19,5	38,1	7,1	7,7	0,5	0,2
SG 3	39,3	29,5	19,7	28,5	41	42	9,9	9,2	1,82	1,31

SM	51,7	59,7	31,9	21	16,4	19,2	7,6	8,5	1,14	0,46
SM 1	80	60	10	15	10	25	7,5	8,5	1,2	0,4
SM 2	55,4	59,7	25	21	19,6	19,2	7,6	8,5	1,14	0,46
SM 3	40	35	20	15	40	50	7,8	9	1,5	0,5
SO	57,6	47,2	13,5	16,8	29	35,9	8,5	8,7	0,39	0,51
SO 1	86,6	69,4	9,6	13,2	3,7	17,5	6,6	7,1	0,44	3,06
SO 2	59,5	47,7	16,4	20,5	24,4	31,6	8,8	9,4	0,4	0,19
SO 3	40,4	35,4	11,2	13	48,5	51,6	9,2	8,2	0,37	0,19
T	42,1	43,1	38,1	38,3	19,8	18,7	5,8	6,1	5,23	2,63
TH	41	42,6	41,3	41	17,7	16,4	5,4	5,7	7,03	3,66
TH 1	72,8	74,4	19,3	18,2	8	7,3	5,4	5,9	9,57	2,32
TH 2	34,3	36,2	49,5	49,9	16,2	13,9	5,3	5,7	6,97	4,42
TH 3	7,6	8,1	40,8	35	51,7	57	4,9	5	9,65	5,16
TM	31,2	27,5	39,6	42,8	29,2	30	6,3	6,5	3,95	1,93
TM 1	70	75	20	20	10	5	6,3	6,5	3,5	1,5
TM 2	38,5	34	44,5	49	17	17,3	6,5	6,9	4,35	2,37
TM 3	9,3	7,7	24,9	24,2	66	68,1	5,5	5,2	2,36	0,72
TO	38,2	41,6	36,6	35	25,2	23,5	6	6,4	3,02	1,08
TO 1	45	50	50	45	5	5	6	6,4	2,5	1
TO 2	43,5	48,1	41,1	39	15,5	12,9	6,4	6,8	3,31	1,15
TO 3	12	9,1	14	14,7	74	76,1	4,3	4,5	1,57	0,74
TV	64,5	67	26,2	26,3	9,3	6,7	6,3	6,5	1,4	0,84
TV 1	75,5	69	19,5	25,5	5	5,6	6,5	6,5	0,87	0,38
TV 2	42,5	63	39,7	27,9	18	9,1	5,8	6,3	2,3	0,74
TV 3	40	50	35	30	25	20	5,8	6,3	3	1
U	50,8	47	16,8	18	32,3	35	4,1	4,2	2,38	2
U 1	70	67	10	11	20	22	4,1	4,2	2	1,5
U 2	50,8	47	16,8	18	32,3	35	4,2	4,2	2,38	2
U 3	30	27	30	31	40	42	4,2	4,3	3	2
V	24,6	22,4	14,4	13,4	61	64,2	7,3	7,7	0,68	0,51
VC	22,4	20,8	24,5	23,5	53	55,7	7,8	8	0,69	0,46
VC 1	44	40	30	34	26	26	7	7,5	1	0,5
VC 2	43,7	39,4	28,6	33	27,3	27,6	7,8	7,9	1,43	0,76
VC 3	20,2	18,8	23,9	22,5	55,8	58,6	7,8	8	0,61	0,43
VP	25,1	22,8	12,2	11	62,7	66,1	7,2	7,6	0,68	0,52
VP 1	55	45	15	17	30	38	7	7,5	1	0,5
VP 2	53,2	44,2	15,9	16,5	31,1	39,4	7,8	7,8	0,76	0,57
VP 3	24,4	22,4	11,5	10,9	64,2	66,7	7,2	7,6	0,67	0,52
W	61,4	51,3	21,9	18,1	16,7	30,6	6,3	6,8	1,25	0,41
WD	19,8	15,2	55,2	47,5	24,8	37,3	4,7	5,1	4,27	0,53
WD 1	90	75	5	5	5	20	4,5	5	1,2	0,2
WD 2	28,5	23,5	61,5	55,5	9,8	21	4,5	4,5	1,5	0,13
WD 3	11,1	6,2	49	45,1	39,9	48,8	4,9	5,7	4,63	0,81
WE	76,6	68,9	10,3	7,5	13,1	23,4	6,2	6,4	0,46	0,24
WE 1	88,9	77,8	4,6	3,7	6,6	18,3	6,3	6,4	0,23	0,15
WE 2	52,1	47,4	24,4	16,3	23,5	36,3	5,7	6,5	1,06	0,59
WE 3	40,2	53,4	19,7	15,6	40,2	31	6,6	6,7	0,53	0,13
WH	60	50	10	10	30	40	4,8	5,4	2	0,5
WH 1	85	70	5	5	10	25	4,5	5,2	1,5	0,3
WH 2	65	50	10	10	25	40	4,8	5,4	2	0,5
WH 3	40	35	15	15	40	50	5,2	5,6	2,2	0,55
WM	21,1	16,6	56,8	41,6	22,2	41,8	5,9	6,6	2,02	0,65

WM 1	85	70	5	5	10	25	5,6	6,4	1,5	0,5
WM 2	21,1	16,6	56,8	41,6	22,2	41,8	5,9	6,6	2,02	0,65
WM 3	40	35	15	15	40	50	6	6,8	2,2	0,7
WS	69,1	57,6	16,7	14,1	14,3	28,3	6,9	7,8	0,72	0,34
WS 1	78,2	65,3	13	11,6	8,9	23,1	7,1	8,4	0,65	0,3
WS 2	50,3	42,1	25,3	19,3	24,4	38,7	6,7	7,4	0,87	0,46
WS 3	40	30	20	20	40	50	7	8,5	0,9	0,4
WX	65	50	10	10	25	40	5	5,6	2	0,5
WX 1	85	70	5	5	10	25	4,8	5,4	2	0,5
WX 2	65	50	10	10	25	40	5	5,6	2	0,5
WX 3	40	35	15	15	40	50	5,2	5,8	2	0,5
X	72,8	67,7	10,5	11	16,8	21,4	7,2	7,4	0,36	0,25
XH	54,8	52,4	20,6	21,5	24,9	26,3	7,7	8,2	0,53	0,24
XH 1	75,9	75,8	12,5	12,1	11,7	12,3	7,8	8,7	0,65	0,23
XH 2	55	52	21	21	24	27	7,7	8,2	0,5	0,25
XH 3	33,8	28,9	28,8	31	38,2	40,3	7,9	8,1	0,44	0,27
XK	48,7	37,4	29,9	36,4	21,6	26,1	8,2	8,4	0,64	0,36
XK 1	85,8	77,9	3,8	7,8	10,3	14,3	8,4	9,2	0,5	0,25
XK 2	20,5	18,2	57,9	54,6	21,8	27	8,3	8,3	0,67	0,34
XK 3	47,5	54,2	12,9	10,5	39,6	35,3	7,6	8,1	0,83	0,37
XL	76	70,8	8	8,4	16,1	20,9	7,1	7,3	0,32	0,24
XL 1	83,3	79,3	6,5	6,2	10,3	14,5	7,1	7,2	0,22	0,17
XL 2	66,7	62,3	10,8	10,8	22,7	27,1	7	7,3	0,39	0,3
XL 3	38,2	27	12,7	16,2	49,2	56,9	7,9	8,2	0,58	0,45
XY	64,6	56,3	21,1	23,5	14,4	20,2	8,4	8,1	0,38	0,22
XY 1	96,7	86,6	1,3	5,3	2	8,1	8,8	8,4	0,23	0,12
XY 2	32,4	26	40,9	41,7	26,7	32,3	7,9	7,8	0,52	0,31
XY 3	40	35	22	23	38	42	8,5	8,2	0,5	0,25
Y	49,2	42,4	26	27,9	24,8	29,3	7,7	7,8	0,33	0,23
YH	50,4	40,8	29	38,9	20,6	20,3	6,6	6,8	0,3	0,2
YH 1	75	75	12	12	13	13	6,4	6,8	0,3	0,2
YH 2	50,4	40,8	29	38,9	20,6	20,3	6,6	6,8	0,4	0,25
YH 3	35	30	27	30	38	40	6,8	7	0,4	0,25
YK	63,5	51	17,9	21,1	18,7	27,5	8	8,2	0,26	0,2
YK 1	82,4	76,7	10,4	15	7,6	8,4	7,7	7,9	0,12	0,13
YK 2	57,7	47,3	25,7	30,3	16,6	21,9	8,2	8,2	0,3	0,24
YK 3	31,4	3,3	25	24	43	71,3	8,4	8,6	0,5	0,29
YL	69,8	53	5,7	8,3	24,4	38,7	6,3	7	0,4	0,2
YL 1	80	75	6	6	14	19	6,3	6,8	0,35	0,2
YL 2	69,8	53	5,7	8,3	24,4	38,7	6,3	7	0,4	0,25
YL 3	35	30	12	16	53	54	6,5	7,2	0,4	0,3
YT	10	5	40	40	50	55	8	7,4	0,41	0,4
YT 1	50	45	25	25	25	30	7,8	7,2	0,3	0,3
YT 2	45	40	28	33	27	27	8,2	7,6	0,4	0,3
YT 3	9	2	35	40	56	58	8,2	8	0,4	0,3
YY	49	48,5	10,7	9,4	40,3	41,8	8,3	8	0,13	0,16
YY 1	96	94,7	3	4,1	1	1,2	8	7,7	0,13	0,16
YY 2	35	30	40	40	25	30	8,3	8	0,15	0,15
YY 3	2	2,3	18,3	14,7	79,5	82,4	8,5	8,3	0,12	0,12
Z	39,5	36,7	23,4	24,8	37,2	38,6	9	9,2	0,49	0,36

ZG	47,8	41,7	8,5	11	43,8	47,4	9,2	9,2	0,38	0,35
ZG 1	78,1	62,1	8,2	13,9	13,7	23,9	10,6	10,2	0,2	0,2
ZG 2	65,9	66,5	3,6	5,1	30,5	28,8	10,4	10,4	0,11	0,23
ZG 3	23,6	19,2	11	12,4	65,5	68,5	8,7	8,7	0,41	0,35
ZM	48,4	48,9	34,1	36,9	17,5	15,3	8,5	8,7	1,83	0,97
ZM 1	85	75	5	5	10	20	8,2	8,5	1,5	0,7
ZM 2	48,4	48,9	34,1	36,9	17,5	15,3	8,5	8,7	1,83	0,97
ZM 3	30	20	30	25	40	55	8,7	8,7	1,8	0,9
ZO	43,2	37,2	24,6	24,5	32,4	38,2	9,3	9,5	0,4	0,28
ZO 1	95,6	75,9	0,8	2,5	4,2	21,3	8,9	10,1	0,18	0,07
ZO 2	37,9	34,7	45,6	46,2	16,6	19,2	9,5	9,4	0,49	0,24
ZO 3	22,2	20,5	15,7	13,7	62,2	65,7	9,3	9,4	0,42	0,42
ZT	19,2	25,2	37,6	39,6	43,1	35,2	8,4	8,7	0,39	0,31
ZT 1	50	45	35	45	15	10	8,2	8,5	0,3	0,25
ZT 2	46,9	63,9	30,7	24,6	22,1	11,5	8,3	8,6	0,25	0,23
ZT 3	5,4	5,8	41,1	47,2	53,6	47,1	8,4	8,7	0,46	0,36

PLANT COMMUNITY, NET PRIMARY PRODUCTION AND SOIL ENVIRONMENT FACTORS IN ESTUARY, KOREA

Ji-won Park¹, Eui-joo Kim¹, Jung-Min Lee¹, Yoon-seo Kim¹, Jae-Hoon Park¹, Se-hee Kim¹ and Young-han You^{1*}

¹ Department of biological science, Kongju National University, Gongju 32588, Republic of Korea

*Corresponding author (youeco21@kongju.ac.kr)

ABSTRACT

Estuary brackish wetlands are ecosystems formed in ecotone where freshwater and seawater are periodically affected. Plant communities are composed of special species with a range of tolerance to environmental stress and periodicity of salinity and humidity gradients in estuary. Plants adapted in this way have a lower diversity of plant species than other ecosystems on Earth, and the Net Primary Production (NPP) of plant communities is very high. In this study, from the past to the present in Korea, brackish wetland vegetation was analyzed in terms of Net Primary Production (NPP) and organic carbon stock, and the relationship between biomass production and soil physicochemical environmental factors was explained to find the cause of the change in CO₂ absorption conducted on plant communities for vegetation restoration in estuary wetlands. As a result, the accumulation of organic carbon present in major plant communities per unit area was decreased in order of; *Salix pierotii* community (6.305 ton/ha) > *Phacelurus latifolius* community (3.049 ton/ha) > *Phragmites australis* community (2.596 ton/ha) > *Bolboschoenus planiculmis* community (0.369 ton/ha) > *Schoenoplectus triqueter* community (0.189 ton/ha) > *Carex scabrifolia* community (0.1 ton/ha) > *Suaeda glauca* community (0.099 ton/ha) > *Suaeda japonica* community (0.098 ton/ha). These communities were mainly distributed in the high tide, and the accumulation of organic carbon increased as the content of soil phosphorus (Ava-P) among environmental factors of the soil increased.

Keywords: littoral, halophyte, coastal, salt marsh, sand dune.

5. INTRODUCTION

Globally, due to climate change, the trend of warming has accelerated as the average temperature has risen by 1.4°C over the past 30 years, and abnormal climate phenomena have been reported due to frequent heat waves, heavy snowfall, typhoons, and wildfires. The international community recognized the seriousness of climate change and adopted the Kyoto Protocol in 1997, which imposed obligations on developed countries, and in 2016, the Paris Agreement, in which both developed and developing countries participated, took effect to reduce the increase in global average temperature compared to pre-industrial times. Efforts are being made to keep it below 2.0°C and to keep it below 1.5°C. Among the types of wetlands, brackish wetlands are known as excellent Critical Transition Zones (CTZs) with various ecosystem services such as ecological functions and biodiversity functions based on material circulation and production (Levin et al., 2001). As a result of studying the material dynamics

of brackish wetlands with a focus on carbon rather than nitrogen through a recent study on blue carbon, brackish wetlands produce organic matter more than agricultural land or land waters of the same area, so it was classified as a place with the highest productivity on earth. (Correl, 1978). Accordingly, overseas research on brackish wetlands is increasing day by day, and research related to carbon balance and biodiversity such as blue carbon are being conducted. Therefore, the purpose of this study is to find the cause of changes in organic carbon absorption by linking the vegetation and soil environmental factors of brackish wetlands in Korea.

6. MATERIAL AND METHODS

Study site overview

In this study, from the past to the present in Korea, research on the vegetation of brackish wetlands, the amount of existing plant communities, the NPP (organic carbon content) of the plant communities, and the physicochemical environmental factors of the soil are related to plants suitable for vegetation restoration in brackish wetlands. The purpose of this study was to analyze the causes of changes in NPP (organic carbon uptake) according to community and environmental factors.

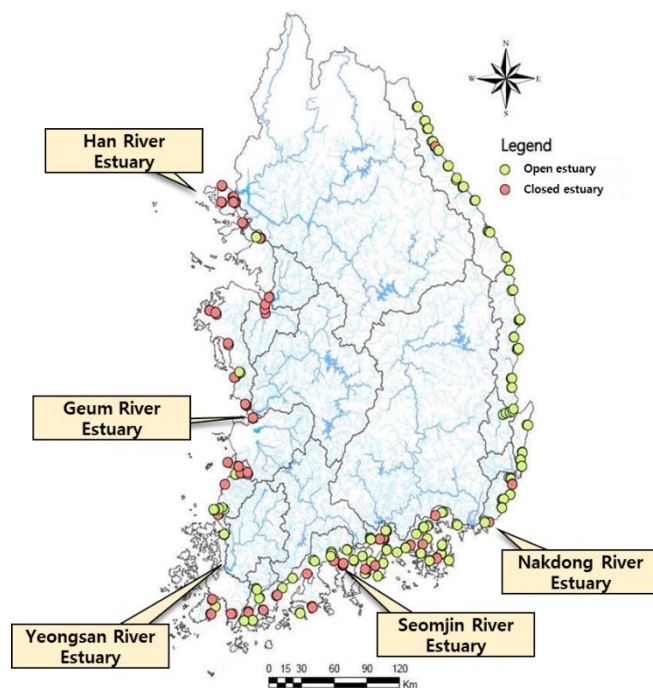


Figure 1. Distribution of brackish wetlands in Korea.

Table1. Number of vegetation by water system

Division	Number of Brackish wetland	Number of community				
		Total	Average	Max	Min	
Total	325	326	3.8	12	0	
Water system	Han River	59	87	3.3	10	0
	Nakdon River	125	199	3.9	11	0
	Yeongsan River-Seomjin River	115	180	3.7	12	0
	Geum River	26	69	5.0	9	1

7. RESULTS AND DISCUSSIONS

Table 2. Net primary productivity and related characteristics of major terrestrial biome.

Ecosystem type	Area (10 ⁶ km ²)	Net primary productivity(gm ⁻² yr ⁻¹)				Biomass (kg m ⁻²)			
		Range	Average	sum	Underground(ratio)	Range	Average	Sum (10 ⁹ t)	
Rain forest	17.0	1000-3500	2200	37.4	0.095	6-80	45	765	
Tropical forest	7.5	1000-2500	1600	12.0		6-60	35	260	
Temperate forest	Evergreen forest	5.0	600-2500	1300	6.5		6-800	35	175
	Deciduous forest	7.0	600-2500	1200	8.4	0.19-0.91	6-60	30	210
Northern coniferous forest	12.0	400-2000	800	9.6	0.28-0.38	6-40	20	240	
Bushland	8.5	250-1200	700	6.0	0.39-6.23	2-20	6	50	
Savanna	15.0	200-2000	900	13.5		0.2-15	4	60	
Temperature grassland	9.0	200-1500	600	5.4	0.22-4.8	0.2-5	1.6	14	
Tundra, Alpine	8.0	10-400	140	1.1		0.1-3	0.6	5	
Desert and semi-desert scrub	18.0	10-250	90	1.6	0.45-5.7	0.1-4	0.7	13	
Rocks, Sand, Ice	24.0	0-10	3	0.07		0-0.2	0.02	0.5	
Plow	14.0	100-4000	65	9.1		0.4-12	1	14	
Swamp, Marsh, Estuary	2.0	800-6000	3000	6.0		3-50	15	30	
Lake and River	2.0	100-1500	400	0.8		0-0.1	0.02	0.05	
Sum	149		782	117.5			12.2	1837	

Table 3. Average dry weight and soil environmental values of major plant species in brackish wetlands.

Main species	<i>Suaeda maritima</i>	<i>Phragmites australis</i>	<i>Suaeda japonica</i>	<i>Suaeda glauca</i>	<i>Carex scabrifolia</i>	
Dry weight(g/m ²)	289.7 (25.2-1,371)	1281.7 (10.9-4,654)	48.4 (23.9-116.1)	48.6 (12.3-139.6)	49.4 (11.2-118.4)	
Soil environment	pH	7.6(±0.5)	7.3(±0.6)	7.8(±0.6)	7.7(±0.4)	6.8(±1.0)
	Organic matter(%)	3.5(±2.0)	4.1(±1.8)	4.7(±0.8)	4.5(±1.2)	3.8(±2.4)
	Cl content(%)	7.1(±3.6)	10.4(±13.2)	3.2(±2.7)	3.3(±2.1)	2.4(±2.1)

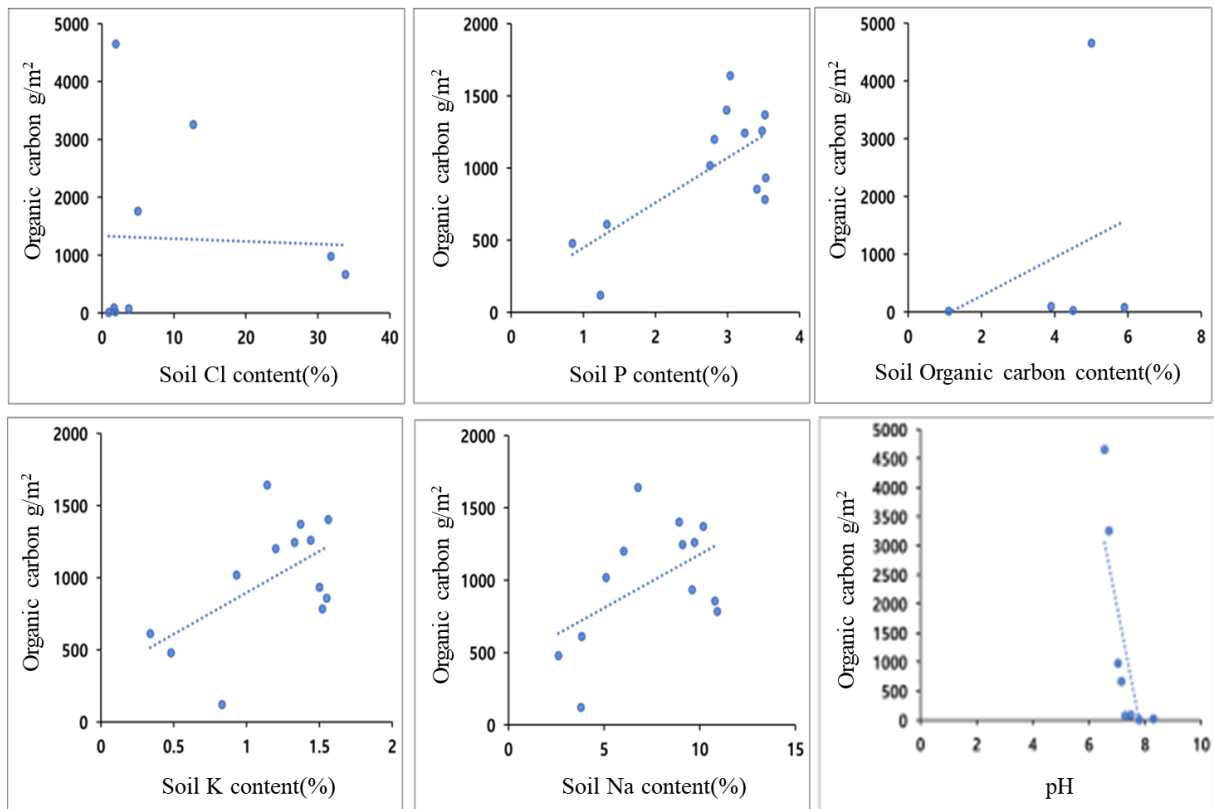


Figure 2. Correlation graph between brackish wetland plant communities and environmental factors.

Acknowledgements: This work was supported by Korea Environmental Industry & Technology Institute (KEITI) through Wetland Ecosystem Value Evaluation and Carbon Absorption Value Promotion Technology Development Project, funded by Korea Ministry of Environment (MOE)(2022003630003)

REFERENCES

- Correll, D. L., (1978). Estuarine productivity. *Bioscience*, 28(10), 646-650.
- Levin, L. A., Boesch, D. F., Covich, A., Dahm, C., Erséus, C., Ewel, K. C., Kneib, R. T., Moldenke, A., Palmer, M. A., Snelgrove, P., Strayer, D., and Weslawski, M. (2001). The function of marine critical transition zones and the importance of sediment biodiversity. *Ecosystems*, 4(5), 430-451.

ECOLOGICAL ASSESSMENT OF WATERFORNT SPACE USING PLANTS OF WEIRS IN THE NAKDONG RIVER BASIN, REPUBLIC OF KOREA

Eui-Joo Kim¹, Young-Sub Han², Jae-Hoon Park¹, Ji-Won Park¹, Jung-Min Lee¹, Yoon-Seo Kim¹, Se-Hee Kim¹ and Young-Han Youl^{1*},

¹. Department of Life science, Kongju National University, Gongju-si, Chungcheongnam-do, Republic of Korea

². Forest ecology & Restoration Center, Korea Forest Conservation Association, Daejeon Metropolitan city, Republic of Korea

*Corresponding author (youeco21@kongju.ac.kr)

ABSTRACT

The vegetation composition and environmental factors of the Nakdong River, one of the representative rivers of Korea, were investigated and three river ecological evaluation methods were applied. As a result, the vegetation grade of the Stream Wetland Vegetation Evaluation used by the National Institute of Ecology was evaluated as 2.0% for Grade I (8,566 m²), 4.7% for Grade II (20,689 m²), and 48.3% for Grade III. (211,187 m²) and 45.0% of class IV (196,372 m²). According to the results of using the National Institute of Biological Resources Stream Habitat Conformity Type method, 11.3% of Grade I (60,154 m²), 42.3% of Grade II (225,578 m²), and 4.9% of Class III are evaluated. Grade (26,100 m²), 18.3% of grade IV (97,365 m²), and 23.3% of grade V (124,017 m²). As a result of the evaluation of the Riparian Vegetation Index used by the National Institute of Environmental Research, the vegetation standard RVI was 46.6 in grade C (normal). It was confirmed that different results were derived depending on the evaluation method even in the same space, and the advantages and disadvantages of each were confirmed. It is believed that reliability can be increased by using an appropriate evaluation method according to the location, environment, and purpose of Korea, and the unity and objectivity of river evaluation results can be improved by establishing and utilizing an integrated evaluation system that combines and improves evaluation methods.

Keywords: river vegetation, vegetation assessment, vegetation grade, river evaluation method, river habitat suitability.

1. INTRODUCTION

Cases of physical deformation such as dams and weirs that control the flow of rivers for freshwater use are increasing nationwide, and accordingly, ecological problems are continuously emphasized along with water quality and environmental problems such as eutrophication (Large and Petts, 1994). In river ecosystems, there are many changes in species diversity according to topographical characteristics and environmental variables, and the physical properties such as water depth and water velocity are directly related to chemistry such as salinity and eutrophication, and running water also affects vegetation and species diversity (Lee et al., 2003). In the case of Korea, because of the large seasonal variation in precipitation,

the fluctuation of river flow is very large, so it has natural conditions and structural characteristics that are unfavorable to water resource management (Kim, 2008). Reflecting these characteristics of rivers, it contributed to the preparation of integrated national countermeasures in order to stably prepare for climate change and increased uncertainty in water resources (Ministry, 2013). In the case of Korea, most studies have simply evaluated rivers using vegetation or studied river vegetation. Quantitative evaluation of the health of river vegetation or multi-angle analysis research through diversification of evaluation is insufficient. Therefore, in this study, first, an aquatic ecosystem survey was conducted in the waterfront area of the Nakdong River. Second, changes in the aquatic ecosystem according to time and river flow were identified. Third, the riverside space was evaluated and analyzed in various ways. Through this, we intend to provide basic data and methods for the evaluation of waterfront space.

2. MATERIAL AND METHODS

2.1 Study area

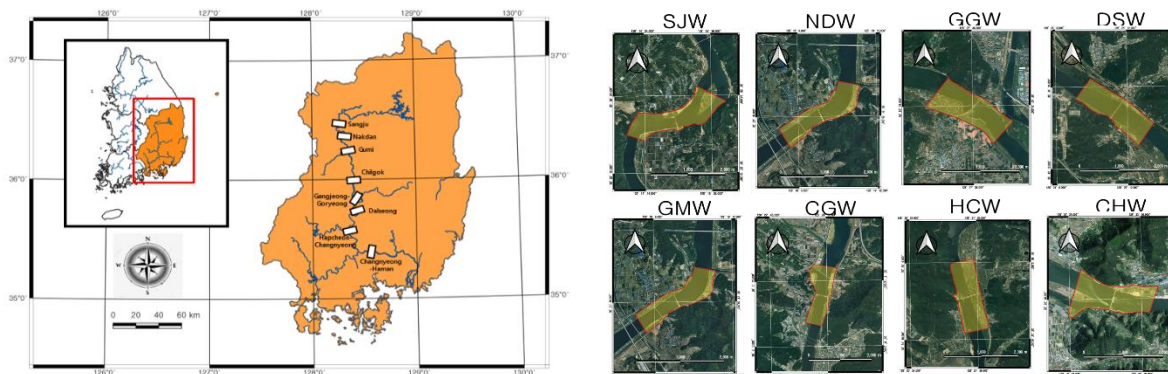


Figure1. Location of study sites in 8 weirs in Nakdong river basin.

2.2 Flow chart

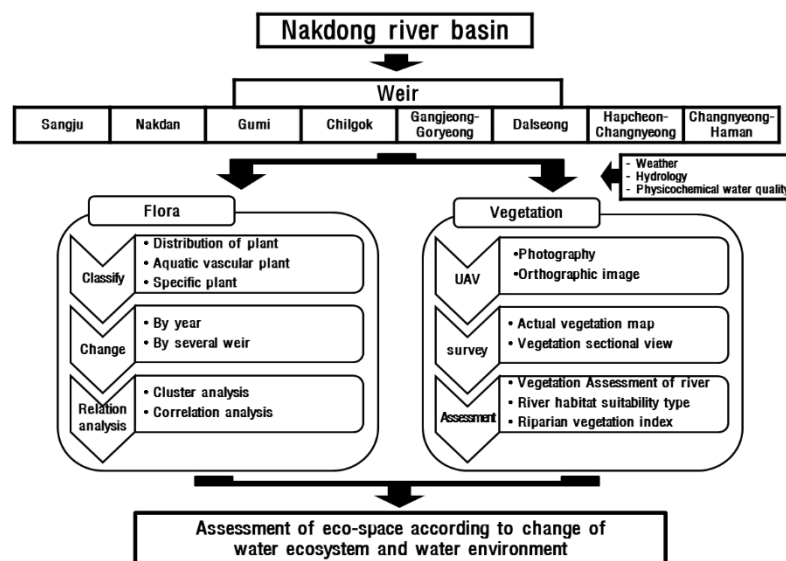


Figure2. Research flow chart.

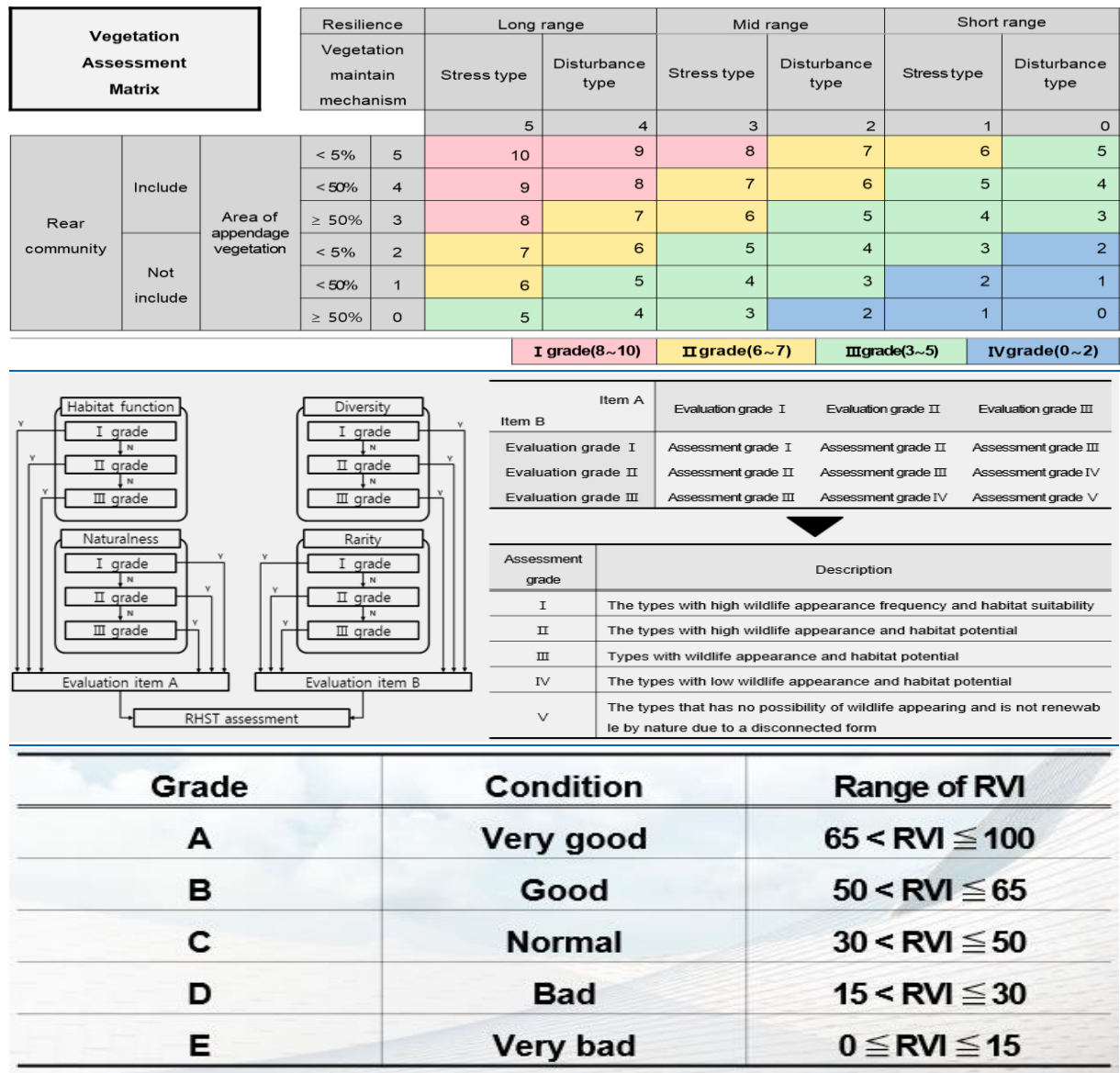


Figure3. River ecological evaluation methods (Vegetation assessment of river wetland (var)(upper), River habitat suitability type (RHST)(middle) and Riparian Vegetation Index(RVI)(below)).

3. RESULTS AND DISCUSSIONS

3.1 Vegetation Assessment of River Wetland (VAR)

Table1. Grade of Var from before the flood season (BF) and after the flood season (AF) in the weirs

Grade	SJW		NDW		GMW		CGW		
	Area	Ratio	Area	Ratio	Area	Ratio	Area	Ratio	
BF	I	3,486.5	1.1	3,515.2	1.3	0	0.0	11,273.6	4.2
	II	5,351.8	1.7	24,396.8	8.8	18,565.2	3.0	52,160.5	19.6
	III	193,129.9	60.6	95,353.3	34.3	312,249.0	50.0	67,339.7	25.3
	IV	116,744.1	36.6	154,533.5	55.6	293,844.9	47.0	135,345.8	50.9
	Total	318,712.3	100.0	277,798.8	100.0	624,659.1	100.0	266,119.6	100.0
AF	I	6,061.9	2.0	9,948.2	4.0	6,252.8	1.0	25,994.0	9.3
	II	3,087.1	1.0	13,113.2	5.3	46,274.3	7.6	1,603.8	0.6
	III	188,241.1	62.8	86,612.2	35.0	256,657.4	42.0	57,642.0	20.6
	IV	102,403.5	34.2	137,467.0	55.6	301,475.2	49.4	194,998.8	69.6
	Total	299,793.6	100.0	247,140.6	100.0	610,659.7	100.0	280,238.6	100.0
Grade	GGW		DSW		HCW		CHW		
	Area	Ratio	Area	Ratio	Area	Ratio	Area	Ratio	
BF	I	5,649.1	1.0	2,611.0	0.6	3,878.5	0.6	15,781.0	3.7
	II	32,095.3	5.5	17,602.5	4.2	5,828.0	1.0	17,095.4	4.0
	III	203,289.0	34.6	152,475.4	36.1	384,012.3	63.4	268,401.9	63.4
	IV	345,989.9	58.9	250,022.4	59.1	211,814.6	35.0	121,799.8	28.8
	Total	587,023.3	100.0	422,711.3	100.0	605,533.4	100.0	423,078.1	100.0
AF	I	9,897.3	1.7	8,865.5	2.1	5,937.3	1.0	17,908.6	4.1
	II	33,496.1	5.7	20,149.1	4.8	16,746.7	2.9	23,462.2	5.4
	III	266,023.8	45.5	181,364.3	43.0	391,536.3	67.2	274,669.1	62.9
	IV	274,709.8	47.0	211,426.9	50.1	168,780.4	29.0	120,601.6	27.6
	Total	584,127.0	100.0	421,805.8	100.0	583,000.7	100.0	436,641.5	100.0

3.2 River Habitat Suitability Type (RHST)

Table2. Grade of RHST from before the flood season (BF) and after the flood season (AF) in the weirs

Grade	SJW		NDW		GMW		CGW		
	Area(m ²)	Ratio	Area(m ²)	Ratio	Area(m ²)	Ratio	Area(m ²)	Ratio	
BF	I	11,227.0	2.7	44,729.8	12.1	99,959.6	13.4	65,037.8	15.9
	II	142,014.2	34.5	96,704.0	26.2	331,654.9	44.4	56,377.7	13.7
	III	49,570.7	12.0	30,652.0	8.3	19,066.7	2.6	5,832.5	1.4
	IV	115,900.5	28.1	80,784.6	21.9	145,101.4	19.4	69,772.9	17.0
	V	93,419.6	22.7	116,756.2	31.6	151,168.5	20.2	213,198.1	52.0
	Total	412,131.9	100.0	369,626.7	100.0	746,951.1	100.0	410,219.0	100.0
AF	I	8,445.9	2.0	38,756.4	10.5	95,588.3	12.8	27,597.8	6.7
	II	138,243.0	33.5	94,382.3	25.5	315,467.9	42.3	45,740.1	11.2

	III	54,979.6	13.3	27,027.8	7.3	19,066.7	2.6	5,832.5	1.4
	IV	98,337.2	23.9	66,547.6	18.0	153,159.2	20.5	131,646.2	32.1
	V	112,338.21	27.3	142,912.6	33.7	163,373.2	21.9	199,319.8	48.6
	Total	412,131.9	100.0	369,626.7	100.0	746,655.3	100.0	410,136.4	100.0
	Grade	GGW		DSW		HCW		CHW	
BF		Area(m ²)	Ratio	Area(m ²)	Ratio	Area(m ²)	Ratio	Area(m ²)	Ratio
	I	51,586.5	7.5	45,113.6	10.0	128,522.7	18.9	50,535.4	9.9
	II	282,299.3	41.0	285,543.6	63.2	304,882.1	44.8	300,875.0	59.0
	III	22,747.3	3.3	6,626.4	1.5	84,449.9	12.4	1,066.5	0.2
	IV	203,996.5	29.6	67,141.0	14.9	57,379.3	8.4	42,428.8	8.3
	V	127,456	18.5	47,354.5	10.5	105,757.0	15.5	115,265.9	22.6
	Total	688,086.2	100.0	451,779.2	100.0	680,991.0	100.0	510,171.7	100.0
AF	I	55,639.6	8.1	34,681.5	7.7	147,004.8	21.7	58,044.0	11.4
	II	323,316.6	47.2	295,414.9	65.4	299,792.1	44.3	296,539.0	58.2
	III	43,874.1	6.4	3,750.3	0.8	42,198.2	6.2	1,066.5	0.2
	IV	132,883.4	19.4	69,672.3	15.4	70,106.4	10.4	52,988.6	10.4
	V	129,475.8	18.4	48,260.1	10.7	116,945.2	17.3	101,276.6	19.9
	Total	685,189.5	100.0	451,779.2	100.0	676,046.6	100.0	509,914.7	100.0

3.3 Riparian Vegetation Index (RVI)

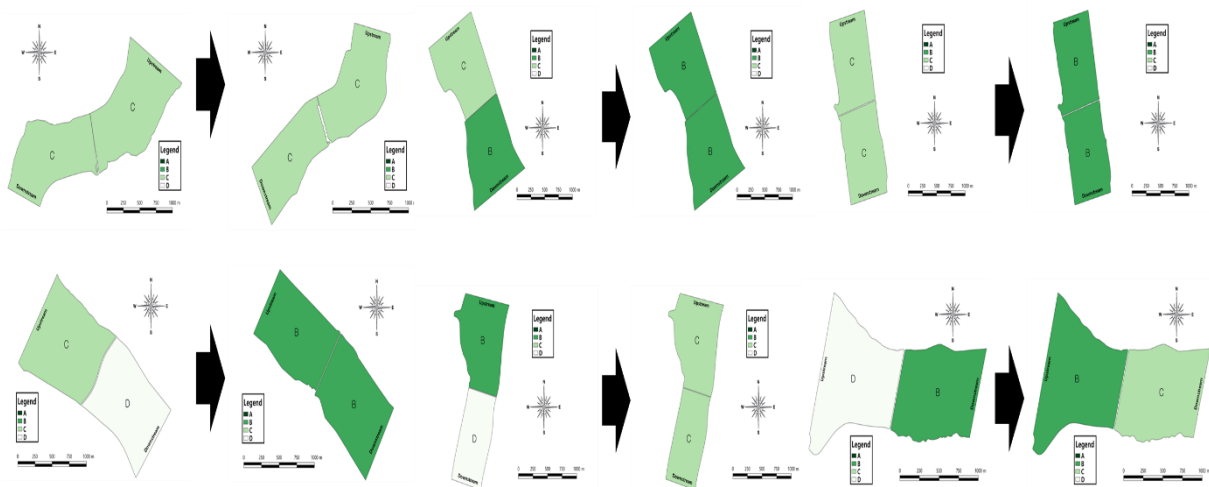


Figure4. The RVI was no different from before the flood season (BF) and after the flood season (AF) in the weirs.

4. CONCLUSIONS

It was confirmed that different results were derived depending on the evaluation method even in the same space, and the advantages and disadvantages of each were confirmed. It is believed that reliability can be increased by using an appropriate evaluation method according to the location, environment, and purpose of Korea, and the unity and objectivity of river evaluation results can be improved by establishing and utilizing an integrated evaluation system that combines and improves evaluation methods.

Acknowledgements: Acknowledgements: This research has performed as Project Open Innovation R&D(21-DW-001) and supported by K-water

REFERENCES

- Large, A. R. G., & Petts, G. E. (2009). 21: Rehabilitation of River Margins. The rivers handbook: hydrological and ecological principles, 401.
- Lee, K. B., Kim, C. H., Lee, D. B., Kim, J. G., Park, C. W., & Na, S. Y. (2003). Species diversity of riparian vegetation by soil chemical properties and water quality in the upper stream of Mankyong River. Korean Journal of Environmental Agriculture, 22(2), 100-110.
- Kim, S. B. (2008). Wetland and Environment Resources. Worin Publishing Co. 61-83.
- Ministry of Environment. (2013). River riparian vegetation health condition investigation and assessment (I). pp. 172.

THE STUDY ON THE EXOTIC PLANT MANAGEMENT CONSIDERING ON THE PLANT LIFE FORM AND BIRD POPULATION CHARACTERISTICS AT THE EXPOSED FLOODPLAIN BY DRAWDOWN IN SOUTH KOREA

Jae-Hoon Park¹, Ho-Joon Kim², Ji-Won Park¹, Jung-Min Lee¹, Eui-Joo Kim¹, Yoon-Seo Kim¹ and Young-Han You^{1*}

1. Kongju National University, Dep. of Life Science, Gongju, South Korea

2. K-water, Water Resources & Environmental Research Center, Daejeon, South Korea

*Corresponding author (youeco21@kongju.ac.kr)

ABSTRACT

This study was conducted to determine the effect of plant dispersal and growth characteristics, and bird population characteristics on an exotic plant development. For this, we monthly monitored the vegetations for two years (2018-2019) in floodplains rapidly exposed by drawdown in Gongju, Sejong, and Seungchon weirs in South Korea. As a result, exotic plants were introduced more easily when the number of vine plants increases, and vine plants have introduced competitively with runner plants. The number of vine plants increased as the number of animal-dispersed plants increased. The introduction of animal-dispersed plants failed due to a decrease in the number of vine plants, an increase in the total number of bird species observed, the number and length of terrestrial bird species. In addition, the introduction of them succeeded due to an increase in the number of vine plants, the total number of bird species and individuals observed and the number of waterbird individuals. In summary, the early development of exotic plants in floodplains rapidly formed due to drawdown in temperate seasonal forest is affected by the vine plant through runner plant and bird characteristics, and the effects of these factors should be considered for the exotic plant management aimed at the floodplains rapidly formed.

Keywords: *Aquatic ecosystem, Avifauna, Flora, Sand bar, Wetland.*

1. INTRODUCTION

Rivers act as important channels for seed distribution and migration of river plants (Esper-Reyes et al., 2018). Thus, succession of vegetation occurring in rivers can be affected by the dispersal of plants introducing the river. Seeds of wetland plants have been adapted to reach and be accumulated by water in areas most ideal for germination and development (Soons et al., 2017). Seed dispersal is important for gene flow in plant populations (Nazareno et al., 2021). In particular, seeds dispersed by animals have stronger genetic connectivity than those dispersed by water or wind (Nazareno et al., 2021). However, the success of development of dispersed plants depends heavily on the dispersed capacity of each species and the regional stability (Howe & Miritti, 2004). In addition, plant dispersal can be affected by the growth forms of surrounding vegetation. *Siclos angulatus* L., known as South Korea and Japan's representative invasive alien species, uses vines to cover river areas to form colonies. In the Tama River in Japan, after *S. angulatus* dominated by disturbance, the development of many native plants that had previously grown naturally was not observed in understory vegetation,

except for *Miscanthus sacchariflorus* (Maxim.) Hack. (Uchida et al., 2012). Thus, disturbances occurring in rivers may threaten the unique ecosystem by increasing the possibility of inflow of invasive alien species that compete with endemic species. Therefore, this study was conducted to obtain basic data on the management plan of exotic plants flowing into the river by researching the early successional development of exotic plants related to a bird population in a floodplain rapidly formed due to the drawdown within a weir.

2. MATERIAL AND METHODS

Study area

This study was conducted in floodplains within Gongju, Sejong and Seungchon weirs, which are installed in the rivers of South Korea, a temperate region (Figure 1). The sediments of these floodplains were exposed to atmosphere for the first time since drawdown of the weirs in 2018. The temperature and precipitation of three weirs were analyzed through the daily average values distributed through the ‘Open MET Data Portal’ website of Korea Meteorological Administration (KMA, 2015). Daily precipitation corresponding to average temperature was the highest at about 23°C, and heavy rains more than 100 mm occurred in the range of 18°C-25.6°C. This air temperature range appeared between June and September in time (Figure 1).

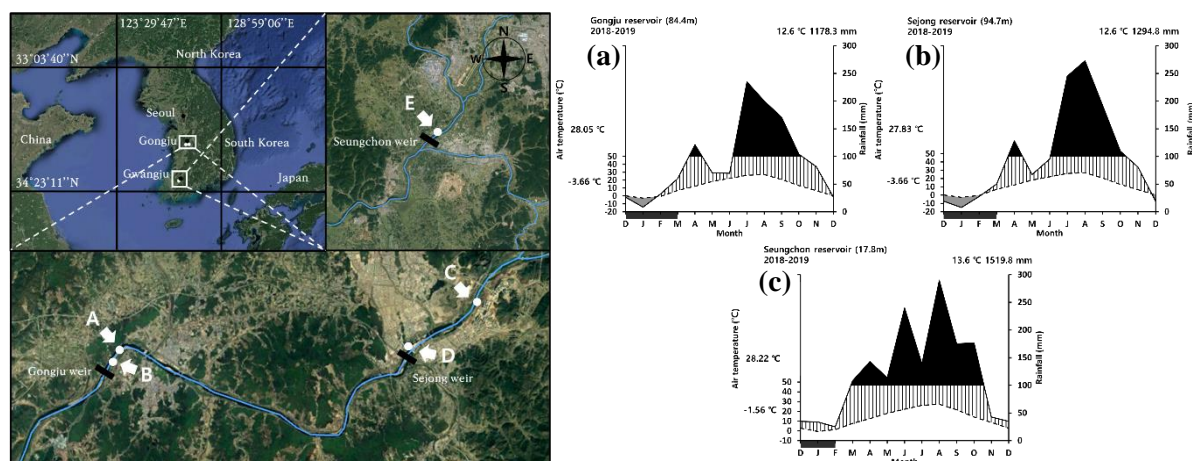


Figure 1. The key map of researched upper site (A) and lower site (B) of Gongju weir, upper site (C) and lower site (D) of Sejong weir and the researched site of Seungchon weir (E) to observe flora on the floodplain in South Korea and the climate diagrams of Gongju (a), Sejong(b), Seungchon (c) weirs during studied two years. In the key map, the blue line means the river line. In the climate diagrams, the spotted and bold lines mean a monthly average air temperature (°C) and rainfall (mm) respectively. The black colored and slash lined area mean the period of rainfall (mm) over and under 100 mm respectively. The grey colored area means a dry period. The darkish area within the x-axis means the period of an average daily air temperature (°C) under 0 °C. Upper and below temperatures on the Y-axis mean monthly maximum and minimum temperatures.

Vegetation study

From April 2018 to November 2019, the flora of three weirs were investigated to observe vegetation changes occurring in floodplains located in Gongju, Sejong, and Seungchon weirs. The plant species was identified using the line transect method, and by drawing a line from land to river, all the species that appeared along the line were recorded. In addition, an on-site monitoring survey was conducted once a month to observe species appeared over time. The

line transect researched were set up in 5 sites on Gongju, 7 sites on Sejong and 4 sites on Seungchon weirs.

Life form for each species were analyzed using the data collected using line transect. In order to organize the data, the classification of exotic species was prepared according to the scientific name list listed in the 'Nature', the website of Korea National Arboretum (KNA, 2021) and the life form was classified according to the method of Lee (1996). He largely classified plant life forms using seed dispersal, growth form, and rhizome development (Lee, 1996). In this study, wind- or water-dispersed, animal-dispersed, mechanically dispersed, gravitationally dispersed plants, vine plants, runner (stolon) plants, rosette plants, plants with rhizome were used.

Avifauna

The relationship between bird and vegetation was investigated to understand the effect of bird characteristics on the development of exotic plants. The data of avifauna was used by the National Institute of Biological Resources of the Ministry of Environment, which was investigated in Gongju, Sejong, and Seungchon weirs from July to September 2018 and 2019. Birds that live mainly around rivers are classified as waterbirds, and birds that live inland are classified as terrestrial birds. In order to analyze avifauna, the data of body length between head to tail of each bird species according to the method of Lee et al. (2014) were used as well as the data of the number of bird species and individuals.

Statistical analysis

The collected phytosanitary data were organized by time for the observed weirs. Path analysis was performed using the JASP statistical program (JASP team, 2017). For bird data, factor analysis was performed with vegetation data observed in the floodplains using the Statistica software program (Statsoft inc. 2004). In the case of South Korea, which is a temperate region, plants have died due to seasonal changes after September. Thus, vegetation development can be affected not only by the characteristics of birds flowing into the area but also by the seasonal changes. Therefore, data after September were excluded from factor analysis. Before conducting path analysis and factor analysis on plant and bird data, all data were standardized to eliminate errors by units of each variable (No and Jeong, 2002).

3. RESULTS AND DISCUSSIONS

As a result of this study, there was a negative correlation between the vine plants and the runner plants (Figure 2). Vine plants generally adapt strategically to light in their habitat through various forms such as tendril climber, petiole climber, stem twiner, and root climber (Klimeš and Klimešová 1994; Llorens 2008). They also grow vertically as well as horizontally (Klimeš and Klimešová 1994; Llorens 2008). Similar to vines, the stolons grow horizontally and can be used for exploring environments with abundant resources suitable for growth and for vegetative propagation (Klimeš and Klimešová 1994). Therefore, even within the early pioneers, vine and runner plants can have a competition for light between each other. However, in the case of *Calystegia sepium* (L.) R.Br., the investment in vine stems in total biomass can depend on the amount of soil nutrients (Klimeš and Klimešová 1994). Thus, this competition may be affected by soil nutrients as well as light.

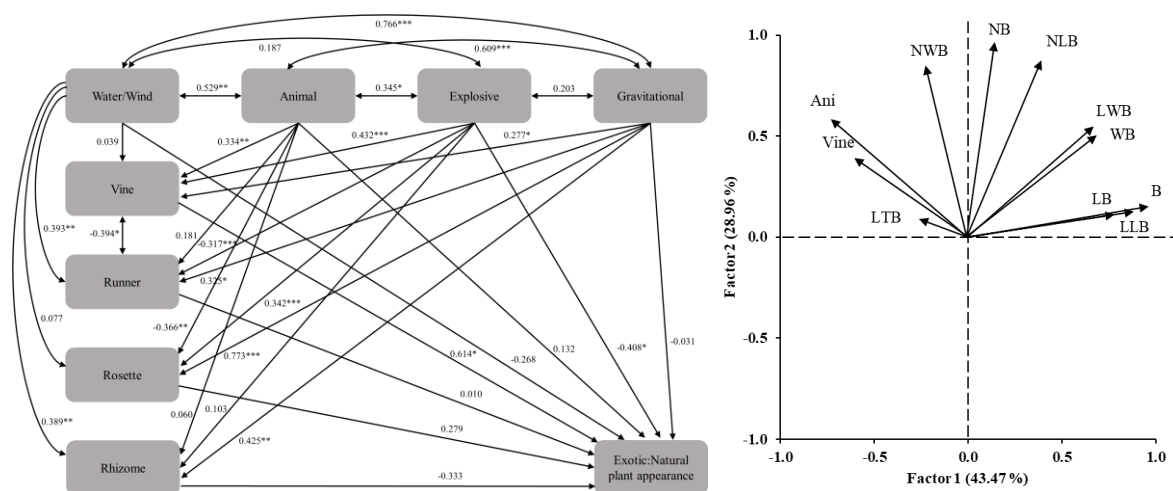


Figure 2. The results of path analysis (left) on the exotic:natural plant appearance rates by the appearance rate of the seed dispersal and the plant growth types and factor loadings (right) of factor analysis on the number of total bird species (B) and total bird individuals (NB), the number of waterbird species (WB) and waterbird individuals (NWB), the number of terrestrial bird species (LB) and terrestrial bird individuals (NLB), the length of total bird (LTB), waterbird (LWB) and terrestrial bird (LLB) individuals on the number of animal dispersal (Ani) and vine (Vine) species. In the path analysis, the double arrows mean the correlation and single directed arrows mean regression. the numbers on the arrows mean standardized coefficients and the *, **, *** mean the significance probability $p < 0.05$, $p < 0.01$ and $p < 0.001$ respectively.

Most of the results of the regression relationship of the dispersal and growth form on the certain plant did not match the appearance ratios (Figure 2).

It indicates the certain plant development may be directly or indirectly affected by dispersal and growth characteristics whether they have those or not. As the number of wind- or water-dispersed plants increased, the number of plants with runner and rhizome increased. Dispersal by wind or water helps seeds reach areas with stable germination and development relatively easily (Soons et al., 2017). Considering this, the dispersal by water greatly contributes to the formation of early pioneer plant community in floodplains by transporting not only seeds but also various propagule to places stable for germination and development (Corenblit et al., 2015; Soons et al., 2017).

As the number of animal-dispersed plants increased, the number of vine plants increased although the plants that share the characteristics of vine and dispersal by animal have not appeared. However, the increase in the number of plants dispersed mechanically and gravitationally, which are positively correlated with animal-dispersed plants, increased the number of vine plants. Among them, the appearance ratios of plants with vine characteristic were 56% (mechanical) and 10% (gravitational), respectively. This result shows that some vine plants dispersed mechanically and gravitationally can be directly dispersed by animal.

The number of vine and animal-dispersed plants increased when the number of terrestrial bird species entering into the floodplains increased and the body length of birds decreased regardless of their habitat (Table 1). In the study of *Hemiphaga novaeseelandiae*, the body mass of birds moved farther as the body mass was relatively large (Wotton and Kelly, 2012). In addition, the longer the time for seeds to pass through the bird's stomach, the longer the spread of plant seeds (Wotton and Kelly, 2012).

Table 1. The factor loadings of the number of observed total bird species and individuals, the number of waterbird species and individuals, the number of terrestrial bird species and individuals, the length of waterbird and terrestrial bird species on the number of animal dispersal and vine species.

Items	Abb.	Factor loadings	
		Factor 1	Factor 2
No. of animal dispersed plant species	Ani	-0.7	0.6
No. of vine species	Vine	-0.6	0.4
No. of bird species	B	1.0	< 0.3
No. of bird individuals	NB	< 0.3	1.0
No. of waterbird species	WB	0.7	0.5
No. of terrestrial bird species	LB	0.8	< 0.3
No. of waterbird individuals	NWB	> -0.3	0.9
No. of terrestrial bird individuals	NLB	0.4	0.9
Length of birds	LTB	> -0.3	< 0.3
Length of waterbirds	LWB	0.7	0.5
Length of terrestrial birds	LLB	0.9	< 0.3

Therefore, in this study, small birds can play a role in introducing plant seeds in nearby areas into the floodplain without spreading them far by staying longer in the area around the floodplain for longer than large birds. In this study, the major small terrestrial birds were *Passer montanus* (Linnaeus) and *Paradoxornis webbianus* (Gould). These two species accounted for about 52% of the total bird population observed. Therefore, these two bird species can play a key role in seed dispersal into the floodplain in East Asia.

Vine and animal-dispersed plants were more observed as the number of waterbird individuals increased. This means that unlike terrestrial birds, seed dispersal is not caused by specific bird species, but by various bird species that share same habitats. According to population survey of waterbirds between protected and unprotected wetlands designated as Ramsar wetlands in Morocco, the number of waterbird individuals was greater in protected wetlands than in unprotected wetlands (Kleijn et al., 2014). In addition, protected wetlands had a smaller water body area than non-protected wetlands and a larger area of bare and short-grass land (Kleijn et al., 2014). This means that the number of waterbird individuals can vary depending on the habitat environments including vegetation characteristics in the aquatic ecosystem. Therefore, vegetation development in exposed alluvial areas in the floodplains adjacent to waterbird habitats can occur better with the larger waterbird population, regardless of bird species.

The number of vine and animal-dispersed plants was higher as the body length of the observed birds was smaller (Figure 2) because the small birds can enter the vines more easily than the large birds.

4. CONCLUSIONS

The appearance ratio of exotic plants to native plants increased when the number of vine plants increased. However, the vine plants appeared only 11% per total plants in the floodplains, and the appearance ratio of them was relatively low compared to the plants with rosette leaves and rhizomes. This means that the vine plant development in the floodplain can induce the introduction of non-vine exotic plants.

The introduction of these vine plants was affected by the terrestrial bird species and waterbird individual numbers. However, vine plants were in competition with runner plants for resources in the floodplains. The runner plants had a strategy of being dispersed by the transport of the propagule by water. In these moist areas, the introduction of the mechanically dispersed plants was not well achieved because the fruits are not well dried.

Overall, it was found that the early exotic vegetation development in the floodplains rapidly exposed by drawdown in temperate climate was affected by the vine plants which are related to the runner plants and bird characteristics. Therefore, in order to manage exotic plants for the floodplains rapidly exposed, the effects of these factors should be considered.

Acknowledgements: This work was supported by Korea Environment Industry & Technology Institute(KEITI) through Wetland Ecosystem Value Evaluation and Carbon Absorption Value Promotion Technology Development Project, funded by Korea Ministry of Environment(MOE)(2022003630003)

REFERENCES

- Corenblit, D., Baas, A., Balke, T., Bouma, T., Fromard, F., Garófano-Gómez, V., González, E., Gurnell, A. M., Hortobágyi, B., Julien, F. & Kim, D. (2015). Engineer pioneer plants respond to and affect geomorphic constraints similarly along water–terrestrial interfaces world-wide. *Global Ecology and Biogeography*. 24(12), 1363-1376.
- Esper-Reyes, K. A., Mariano, N. A., Alcalá, R. E., Bonilla-Barbosa, J. R., Flores-Franco, G., Wehncke, E. V. (2018). Seed dispersal by rivers in tropical dry forests: An overlooked process in tropical central Mexico. *Journal of Vegetation Science*. 29(1), 62-73.
- Howe, H. F. & Miritti, M. N. (2004). When seed dispersal matters. *BioScience*, 54, 651-660.
- JASP team (2017). JASP computer software (Version 0.14.1).
- Klimeš L. & Klimešová J. (1994). Biomass allocation in a clonal vine: effects of intraspecific competition and nutrient availability. *Folia Geobotanica*. 29(2), 237-244.
- Kleijn, D., Cherkaoui, I., Goedhart, P.W., van der Hout, J. & Lammertsma, D. (2014) Waterbirds increase more rapidly in Ramsar-designated wetlands than in unprotected wetlands. *Journal of Applied Ecology*. 51(2), 289-298.
- KMA (2015). National Climate Data Center. <https://data.kma.go.kr>.
- KNA (2021). Checklist of Vascular Plants in Korea. <http://www.nature.go.kr>.
- Lee, W. T. (1996). *Lineamenta Florae Koreae*. Seoul: Academybook.
- Llorens, A. M. & Leishman, M. R. (2008). Climbing strategies determine light availability for both vines and associated structural hosts. *Australian Journal of Botany* 56, 527-534.
- Lee, W. S., Koo, T. H., Park, J. Y. & Taniguchi, T. (2014). *A field guide to the birds of Korea*. Seoul: LG Evergreen Foundation.
- Nazareno, A. G., Knowles, L. L., Dick, C. W., Lohmann, L. G. (2021). By Animal, Water, or Wind: Can Dispersal Mode Predict Genetic Connectivity in Riverine Plant Species?. *Frontiers in plant science*. 12, 626405.
- No, H. J. & Jeong, H. Y. (2002) *Well-defined statistical analysis according to statistica*. Seoul: Hyeongseol Publisher.
- Soons, M. B., de Groot, G. A., Cuesta Ramirez, M. T., Fraaije, R. G., Verhoeven, J. T. & de Jager, M. (2017). Directed dispersal by an abiotic vector: wetland plants disperse their seeds selectively to suitable sites along the hydrological gradient via water. *Functional Ecology*. 31(2), 499-508.
- StatSoft, Inc. (2004). STATISTICA (data analysis software system), version 7. www.statsoft.com.
- Uchida, T., Nomura, R., Asaeda, T. & Rashid, M. H. (2012) Co-existence of *Sicyos angulatus* and native plant species in the floodplain of Tama River, Japan. *International Journal of Biodiversity and Conservation*. 4(9), 336-347.

Wotton, D. M. & Kelly, D. (2012) Do larger frugivores move seeds further? Body size, seed dispersal distance, and a case study of a large, sedentary pigeon. *Journal of Biogeography*. 39(11), 1973-1983.

CHARACTERISTICS OF HABITAT ENVIRONMENT AND POPULATION OF MANKYUA CHEJUENSE, ENDANGERED ENDEMIC FERN IN KOREA

Eui-Joo Kim¹, Ji-Won Park¹, Jung-Min Lee¹, Jae-Hoon Park¹, Yoon-Seo Kim¹, Se-Hee Kim¹ and Young-Han You^{1*},

¹. Department of Life science, Kongju National University, Gongju-si, Chungcheongnam-do, Republic of Korea

*Corresponding author (youeco21@kongju.ac.kr)

ABSTRACT

Mankyua chejuense is a rare and endangered plant that grows only in the Gotjawal wetland in Jeju Island, Republic of Korea, and is a small and wintergreen fern with a height of about 10 cm. In order to prepare a conservation and restoration plan for these community, we targeted a 15 population and investigated their habitat topography, soil characteristics, vegetation, and density in winter season. The habitat environment was a temporal swamp, which was submerged for a while and then drained during the rainy season. They lived in the lower layer of deciduous trees, and the density of the above-ground part was 1-373 ind./m², and the ratio of sexual reproduction individuals was clumped distributed as 0-85%. As for the relationship between environmental factors and density had a positive correlation with wetland area, altitude, rock exposure rate, organic matter content, and negative correlation with litter depth and soil electrical conductivity. The population density was abundant as the wetland area was wide, the sea level, rock exposure rate and organic matter content were higher, the litter depth was shallower, and the value of soil electrical conductivity was lower. Therefore, to stably preserve the habitat and density, the priority is not to damage the Gotjawal wetland. During restoration, it is necessary to form a deciduous broad-leaved tree with a high rock rate, an upper layer that receives sufficient light during the growing season, and a wide temporal swamp area. In addition, constant management is required to prevent fallen leaves from accumulating in winter.

Keywords: Korea's endemic plants, ferns, soil environment, population density, wetland area.

1. INTRODUCTION

The definition of Gotjawal is a lava forest where trees and thorn vines are formed where large and small rock mass-shaped sub-lava flows and Pahoi Hoi lava are distributed. This occupies 6.1% of the island's area, and about 46% of the total area of Jeju is inhabited by plants. There are a total of four Gotjawal in Jeju Island, and among them, *Mankyua chejuense*, an endangered plant in the world and a special plant in Korea, lives in the Jocheon-Hamdeok Gotjawal. Jeju fern ginseng is a fern plant belonging to the genus *Mankyua*. Most recently, it has been reported as a fast and new species, and is an evergreen plant that reproduces asexually mainly by rhizomes. They are in danger of extinction due to their very small, narrow population and an

island-like distribution. However, until recently, the natural habitat of Gotjawal has been severely damaged due to the reckless development of Gotjawal, and the area and number of the population have drastically decreased, and the population is being affected by the decline. Nevertheless, quantitative studies related to the ecological characteristics of this species as well as studies on specific genome analysis are insufficient. Moreover, there is no comprehensive study. Therefore, conservation and restoration will inevitably be difficult due to the lack of ecological information. Therefore, there is an urgent need for research on population biology information that identifies the integrated relationship between the population characteristics-genetic diversity-environmental factors of the research subject.

2. MATERIAL AND METHODS

2.1 Statue of Study area

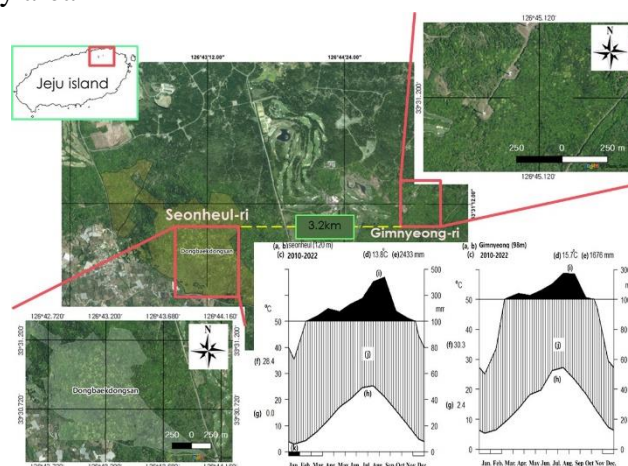


Figure 1. Communities of *M. chejuense* in Seonheul-ri and Gimnyeong-ri, Jeju Island and Climate diagram in seonheul-ri and Gimnyeong-ri (a): location name, (b): altitude, (c): the period of observation, (d): mean temperature, (e): mean annual precipitation, (f): maximum temperature of warmest month, (g): minimum temperature of coldest month, (h): mean daily monthly temperature, (i): mean daily monthly precipitation, (j): humid period, (k): a month in which the average daily minimum temperature is 0°C or lower.

Table 1. Description of study site and population of *M. chejuense*.

Population ID	Site	GPS Coordinate		Physiognomy type	Canopy tree speices
		N	E		
a		33°30'	126°43'	Evergreen borad-leaved	<i>Quercus salicina</i>
b	Seonheul-ri, Jocheon-eup,	33°30'	126°43'	Deciduous broad-leaved	<i>Ulmus parvifolia</i>
c	Jeju-si	33°30'	126°43'	D-b-1	<i>U. parvifolia</i>
d		33°30'	126°43'	E-b-1	<i>Castanopsis sieboldii</i>
e		33°31'	126°44'	D-b-1	<i>U. parvifolia</i>
f		33°31'	126°44'	D-b-1	<i>U. parvifolia</i>
g	Gimnyeong-ri, Jocheon-eup,	33°31'	126°44'	D-b-1	<i>U. parvifolia</i>
h	Jeju-si	33°30'	126°44'	E-b-1	<i>Camillia japonica</i>
I		33°31'	126°44'	D-b-1	<i>U. parvifolia</i>
j		33°31'	126°44'	E-b-1	<i>Eurya japonica</i>

k		33°31'	126°44'	D-b-l	<i>Cudrania tricuspidata</i>
l		33°31'	126°44'	D-b-l	<i>U. parvifolia</i>
m		33°31'	126°44'	D-b-l	<i>U. parvifolia</i>
n		33°31'	126°45'	D-b-l	<i>U. parvifolia</i>

2.2 Measurement items

- Habitat environment: Wetland area, Altitude, Slope degree, Rock exposure, Crown projection
- Soil characteristics: Depth of soil and litter, Organic matter, Electrical conductivity
- Population dynamic: Population size, Number of individuals with sporophyll leaf, Spatial distribution
- Statistical Analysis: Factor analysis

3. RESULTS AND DISCUSSIONS

3.1 Habitats of *M. chejuense*

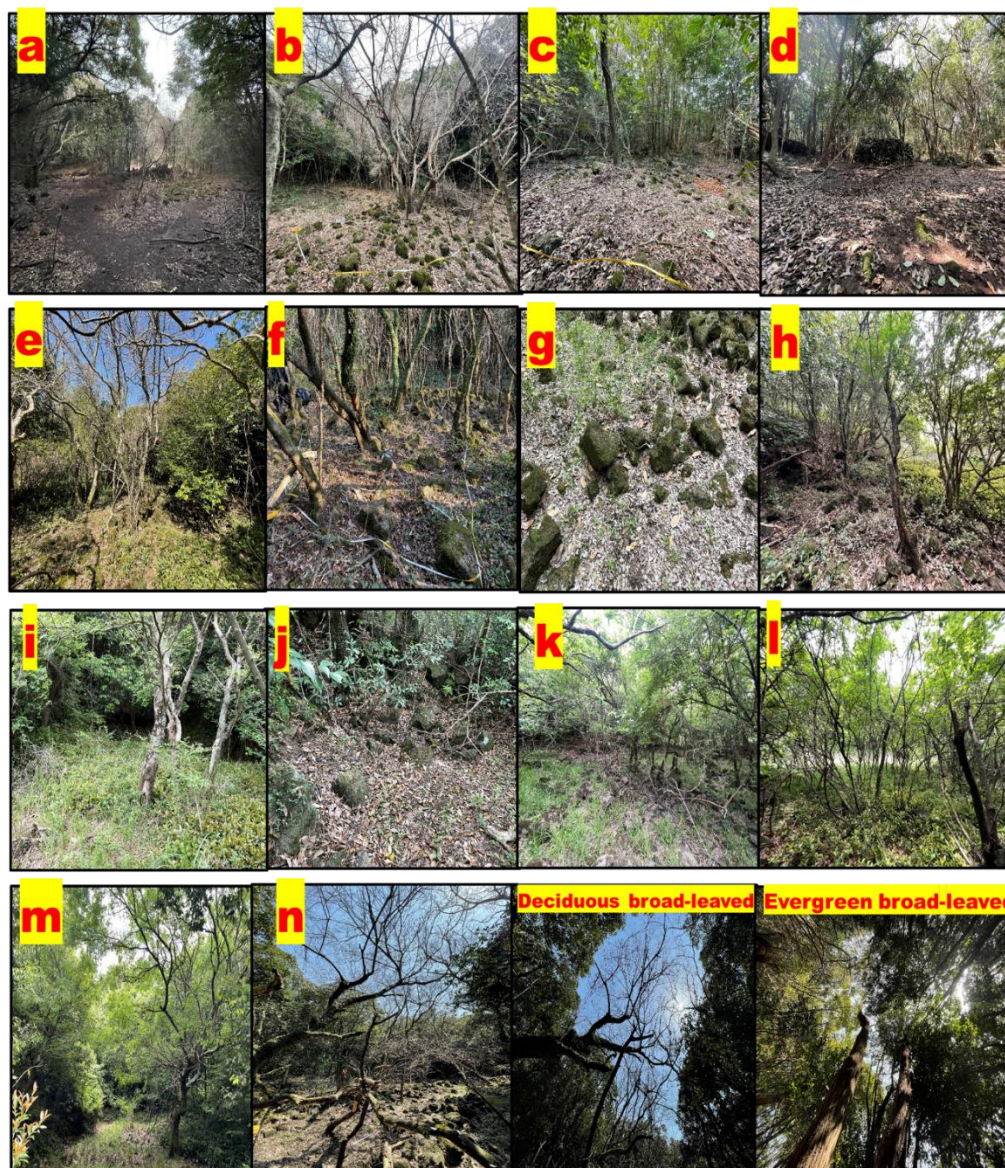


Figure 1. Status and crown in habitat of each *M. chejuense*.

3.2 Characteristics of habitats physicochemical and population density

Table 2. Habitat physicochemical characteristics

Population ID	Wetland area (m)	Altitude (m)	Slope degree (°)	Rock exposure (%)	Topographic wetness index	Soil depth (cm)	Litter layer (cm)	Organic matter (%)	Electrical conductivity (µS/cm)
a	56.7	136.0	96.4	20.0	10.0	5.7	0.9	0.7	0.8
b	34.2	136.0	89.3	80.0	8.0	4.8	2.8	4.3	0.5
c	47.8	144.0	138.9	70.0	7.0	6.2	2.4	0.6	0.4
d	30.0	129.0	26.7	10.0	8.0	7.9	15.2	4.2	1.1
e	22.1	94.0	125.7	50.0	6.0	8.9	0.9	1.3	0.3
f	31.2	103.5	300.0	40.0	12.0	5.9	3.0	2.6	0.6
g	6.2	104.5	130.0	25.0	12.0	6.7	1.8	2.6	0.5
h	17.3	116.5	26.7	70.0	9.0	3.9	0.4	1.2	0.4
I	4.9	92.0	40.0	40.0	10.0	6.9	2.0	1.1	0.2
j	4.5	92.0	148.6	10.0	6.0	10.0	0.6	1.0	0.7
k	27.3	93.0	278.3	60.0	7.0	7.1	1.2	1.2	0.5
l	51.5	94.5	90.0	30.0	7.0	5.4	4.3	1.3	0.5
m	60.5	84.0	85.0	30.0	20.0	7.0	3.0	1.1	0.4
n	490.6	105.5	116.3	60.0	11.0	5.8	1.1	1.4	0.3

Table 3. Population density of *M. chejuense*

Population ID	Trophophyll leaf (no./m ²)	Sporophyll leaf (number of ind. with reproductive part / total ind.)
a	270.0	85
b	80.0	85
c	206.0	75
d	1.0	0
e	26.0	60
f	21.0	30
g	8.0	20
h	9.0	15
I	17.0	35
j	18.0	60
k	14.0	0
l	117.0	60
m	88.0	80
n	373.0	60

3.3 Crown projection and spatial distribution

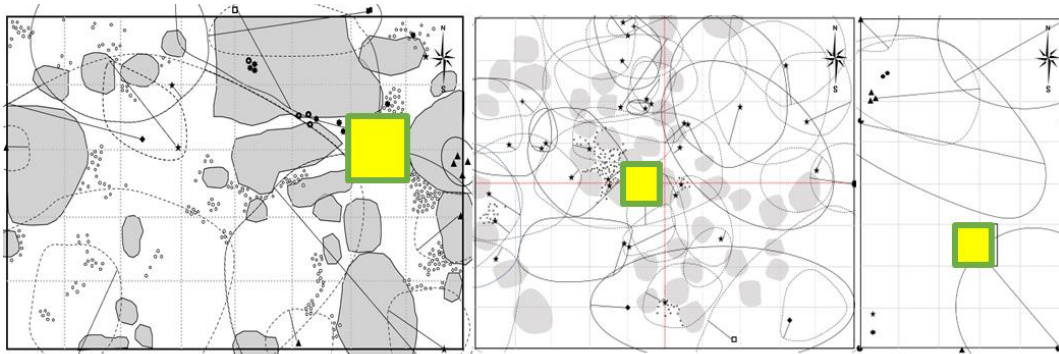


Figure 2. Crown projection in habitat of *M. chejuense* by population size (right: large, middle: medium, left: small).

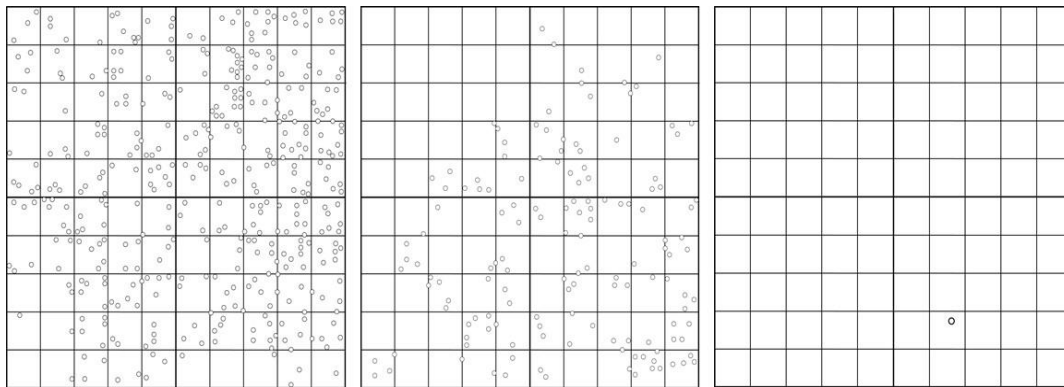


Figure 3. Crown projection in habitat of *M. chejuense* by population size (right: large, middle: medium, left: small).

3.4 Relationship between population size and environmental factors

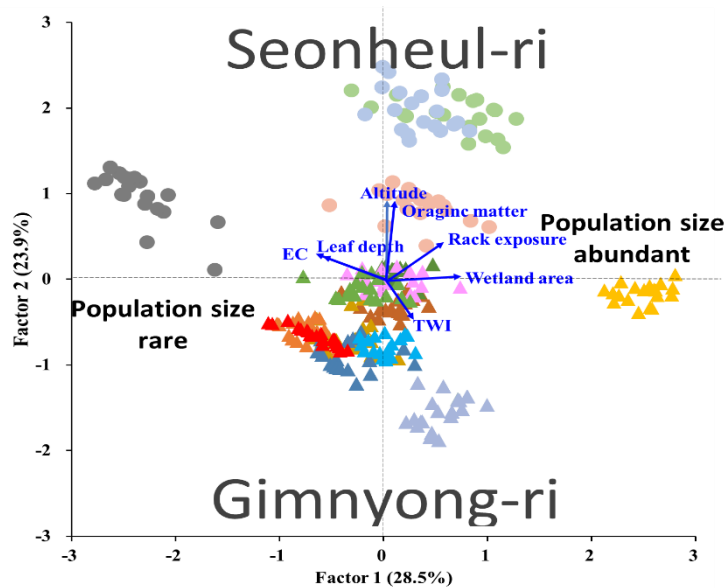


Figure 4. Factor analysis on physicochemical characteristic of *M. chejuense*.

Table 3. Factor loading values for physicochemical characteristics of *M. chejuense*.

Item	Factor 1	Factor 2
Wetland area	270.0	85
Altitude	80.0	85
Rock exposure	206.0	75
Leaf depth	1.0	0
Electrical conductivity	26.0	60
Organic matter	21.0	30
Topographic wetness index	8.0	20
Expl.Var	9.0	15
Prp. total	17.0	35

4. CONCLUSIONS

To stably preserve the habitat and density of *M. chejuense* the priority is not to damage the Gotjawal wetland. During restoration, it is necessary to form a deciduous broad-leaved tree with a high rock rate, an upper layer that receives sufficient light during the growing season, and a wide temporal swamp area. In addition, constant management is required to prevent fallen leaves from accumulating in winter.

Acknowledgements: 1. This work was supported by Korea Environmental Industry & Technology Institute (KEITI) through Wetland Ecosystem Value Evaluation and Carbon Absorption Value Promotion Technology Development Project, funded by Korea Ministry of Environment (MOE)(2022003630003). 2. This research was supported by Basic Science Research Program through the National Research Foundation of Korea(NRF) funded by the Ministry of Education(NRF-2018R1D1A1B07050269)

5. REFERENCE

- Sun, B. Y., Kim, M. H., Kim, C. H., & Park, C. W. (2001). *Mankyua* (Ophioglossaceae): a new fern genus from Cheju Island, Korea. *Taxon*, 1019-1024.
- Kim, H. R., Shin, J. H., Jeong, H. M., & You, Y. H. (2014). Effects of environmental factors on the growth response of above-and below-ground parts of *Mankyua chejuense*, endangered endemic plant to Jeju province, in Korea. *Journal of Ecology and Environment*, 37(2), 61-67.
- Lee, K.M., Shin, J. H., Jeong, H. M., Kim, H. R., Kim J. H., Shin, D. H. & You, Y. H. (2012). Characteristics of vegetation structure and habitat of *Mankyua chejuense*(Ophioglossaceae), endangered plant in Korea. *Journal of Korean Wetlands Society*, 14(1), 35-45.

EVALUATION OF EPA SWMM MODELING PERFORMANCE OF INFILTRATION TRENCH

Kaan İlker Demirezen¹ and Cevza Melek Kazezyılmaz-Alhan^{1}*

¹ Istanbul University-Cerrahpaşa, Civil Engineering Department, İstanbul, Türkiye

**Corresponding Author (meleka@iuc.edu.tr)*

ABSTRACT

Water scarcity is one of the biggest problems in the world. Besides water scarcity, reaching clean water is also a serious issue for some countries. To be able to fight against these difficulties, engineers have been working on significant improvements on implemented projects. Among these, low impact development (LID) best management practices (BMPs) are one of the most popular implementations recently. LIDs are referred to as nature-based solutions that can control the quality and the quantity of stormwater runoff. LIDs consist of different practices such as rain barrels, green roofs, permeable pavement, vegetative swale, and bioretention. The infiltration trench, which is the focus of this study, is among these practices. The infiltration trench consists of a rectangular ditch, filled with gravel, and has permeable soil around. In this study, the modeling performance of EPA SWMM of infiltration trenches is evaluated by comparing the modeling results with the experimental data. Results show that the experimental measurements are in good agreement with the EPA SWMM output.

Keywords: *infiltration trench, low impact development (LID), EPA SWMM, green infrastructure.*

1. INTRODUCTION

Low Impact Development (LID) practices help to reduce the adverse effects of a dense population, and they provide stormwater management. By means of their nature-based structures, LIDs provide peak flow control and groundwater recharge by increasing the infiltration capacity of the zone. Infiltration trench, bioretention, vegetative swale, rain barrel, and green roofs are among the LIDs (EPA 2020). LIDs have become popular implementations in recent years due to providing a sustainable environment. For this reason, many studies have been performed about LIDs recently. Some of the studies focus on the performance of LID's by observing their site implementations (Loperfidio et al., 2014; Jia et al., 2015;). On the other hand, some studies focus on the modeling of LIDs to see their effects and performances under different scenarios (Chahar et al., 2012; Lee et al., 2010; Ahmed et al., 2017). There are few software programs that have the capability to model LID applications. U.S. Environmental Protection Agency Storm Water Management Model (EPA SWMM) is among these few programs.

This study investigates the hydrological modeling performance of EPA SWMM of LIDs, in particular infiltration trenches. The model results are generated with different rainfall intensities, gravel diameters,

and berm heights. The calculated overflow on the infiltration trench, and the drainage out of the infiltration trench are compared with the experimental data obtained in a former study by Demirezen and Kazezyilmaz-Alhan (2022).

2. MATERIAL AND METHODS

EPA SWMM is a stormwater management computer program that calculates water quality and quantity on a watershed, aquifer, open channel, reservoir, and pipe by using hydrological and hydraulic tools. As well as these instruments, the hydrological model of green infrastructures, such as infiltration trench, vegetative swale, permeable pavement, green roof, and bioretention can also be performed.

For infiltration trench modeling, 3 layers, i.e., surface, storage, and drain layers should be defined in EPA SWMM. The parameters of the surface layer consist of the berm height, which is the water depth over the gravel layer until the overflow starting point, the vegetation volume fraction, which is the volume that is kept by the plants over the infiltration trench, S-surface roughness, which is Manning's roughness coefficient for the gravel layer on the infiltration trench, and the surface slope, which is the slope of the infiltration trench. The parameters of storage layer, which represents the gravel layer, consist of the thickness, the void ratio, the seepage rate, and the clogging factor, which is a factor that describes the clogging on infiltration trench. The parameters of drain layer consist of the drain exponent and the drain coefficient, which are the parameters to calculate the drainage rate as a function of drain offset height and the stored water depth until overflow begins, and the offset height, which is the height of drainage pipes from bottom of the infiltration trench in the storage layer.

The data collected from Rainfall-Watershed-Infiltration trench (RWI) experimental system by Demirezen and Kazezyilmaz-Alhan (2022) is employed to test the modeling capability of EPA SWMM. The RWI system consists of 40-m² of steel surface representing the watershed, 40 nozzles over the steel surface representing rainfall system and a textile tank made of polyethylene representing the infiltration trench. EPA SWMM model of RWI system is given in Figure 1. The experimental data was obtained for 3 different rainfall intensities (41.6 mm/h, 55.5 mm/h, and 66.6 mm/h), 2 different berm heights (3.5 cm and 18.5 cm), and 2 different gravel diameters (0.5 cm-1.2 cm and 3.2 cm-7.0 cm).

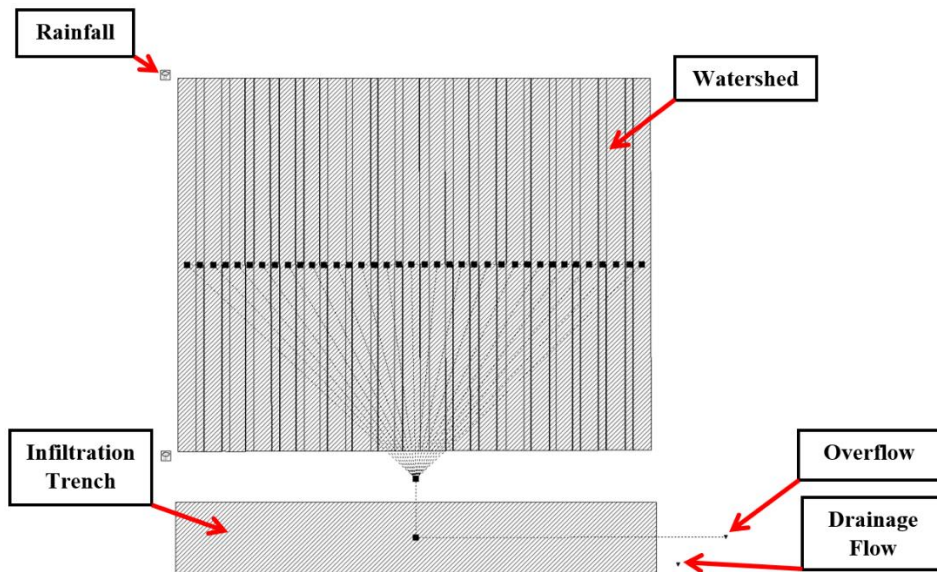


Figure 1. Modeling of the RWI experimental setup with EPA SWMM.

3. RESULTS AND DISCUSSIONS

Figure 2 shows the comparisons of the measured overflow and drainage flow values with the ones that are acquired as output from the EPA SWMM model. In Figure 2 (a) and (b), the rising limbs, falling limbs, and the maximum values of the overflow hydrographs of EPA SWMM outputs and experiment measurements are in good agreement obtained for 41.6 mm/h rainfall intensity, 18.5 cm berm height, 0.5 cm-1.2 cm gravel diameter and for 66.6 mm/h rainfall intensity, 3.5 cm berm height, 3.2 cm-7.0 cm gravel diameter, respectively. Similar argument can be made for drainage flow.

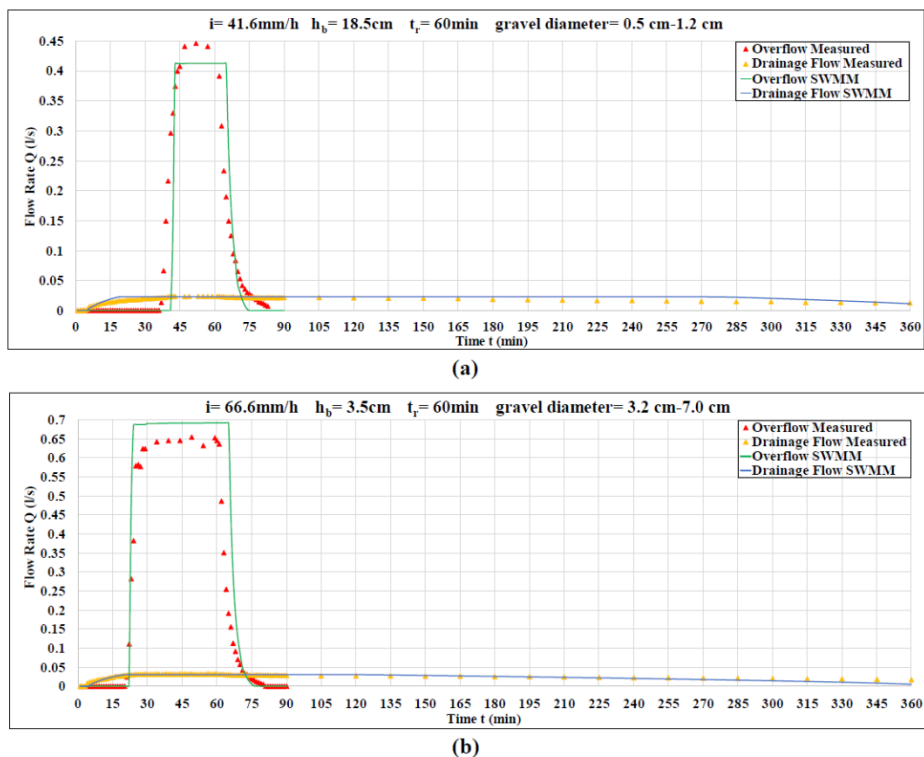


Figure 2. Overflow and drainage flow results comparison between EPA SWMM outputs and experimental data.

4. CONCLUSIONS

In this study, the hydrological modeling capability of EPA SWMM for infiltration trench is investigated. The results of the EPA SWMM outputs are compared with the experimental data obtained from the large-scale RWI experimental setup by Demirezen and Kazezyılmaz-Alhan (2022). In conclusion, the overall overflow and drainage flow results of the EPA SWMM model are in good agreement with experimental measurements.

Acknowledgements: This work was supported by the Scientific Research Projects Coordination Unit of Istanbul University-Cerrahpaşa, Project No. 30063.

REFERENCES

- Ahmed, K., Chung, E.S., Song, J.Y., Shahid, S. (2017). Effective design and planning specification of low impact development practices using Water Management Analysis Module (WMAM): Case of Malaysia, *Water*, 9(3).
- Chahar, B. R., Grailot, D., Gaur, S. (2012). Storm-water management through infiltration trenches, *Journal of Irrigation and Drainage Engineering*, 138(3).
- Demirezen, K. İ., & Kazezyılmaz-Alhan, C. M. (2022). Evaluation of the Hydrological Performance of Infiltration Trench with Rainfall-Watershed-Infiltration Trench Experimental Setup. *Journal of Hydrologic Engineering*, 27(3), 04021050.
- Environmental Protection Agency, United States. (2020). *Saving the Rain: Green Stormwater Solutions for Congregations*, EPA 841-R-20-001.
- Jia, H., Wang, X., Ti, C., Zhai, Y., Field, R., Tafuri, A. N., Cai, H., & Yu, S. L. (2015). Field monitoring of a LID-BMP treatment train system in China. *Environmental monitoring and assessment*, 187(6), 1-18.
- Lee, J. G., Heaney, J. P., & Pack, C. A. (2010). Frequency methodology for evaluating urban and highway storm-water quality control infiltration BMPs. *Journal of Water Resources Planning and Management*, 136(2), 237-247.
- Loperfido, J. V., Noe, G. B., Jarnagin, S. T., & Hogan, D. M. (2014). Effects of distributed and centralized stormwater best management practices and land cover on urban stream hydrology at the catchment scale. *Journal of Hydrology*, 519, 2584-259

WETLAND CONSTRUCTION AND MANAGEMENT

A CASE STUDY OF SOUTH KOREA: CURRENT STATUS AND PERFORMANCE ASSESSMENT OF TREATMENT WETLANDS

Hyeseon Choi¹, Boram Kim², Nash Jett Reyes³, Minsu Jeon⁴ and Leehyung Kim^{5*}

¹ Univ Lyon, INSA Lyon, DEEP, EA7429, 11 rue de la Physique, F-69621, Villeurbanne cedex, France

² Univ Lyon, INSA Lyon, DEEP, EA7429, 11 rue de la Physique, F-69621, Villeurbanne cedex, France

³ Department of Civil and Environmental Engineering, Kongju National University, 1223-24 Budaedong, Seobukgu, Cheonan city, Chungnamdo, 31080, Republic of Korea

⁴ Department of Civil and Environmental Engineering, Kongju National University, 1223-24 Budaedong, Seobukgu, Cheonan city, Chungnamdo, 31080, Republic of Korea

⁵ Department of Civil and Environmental Engineering, Kongju National University, 1223-24 Budaedong, Seobukgu, Cheonan city, Chungnamdo, 31080, Republic of Korea

ABSTRACT

The efficiency of nature-based facilities is mostly evaluated in terms of their pollutant removal capabilities. A total of 54 treatment wetlands (TW) installed across South Korea were monitored to evaluate their pollutant removal performance. Among the different types of wetlands studied, hybrid systems were found to be the most effective in terms of pollutant removal due to their complex configurations and functions. Newly constructed treatment wetlands have unstable performance and thus, a stabilization period ranging from two to five years is required to assess the facility's pollutant removal capabilities. A comparison between the conventional pollutant removal-based evaluation and a developed multi-criteria index was also performed to determine the key changes in the results of evaluation when different methods are employed.

Keywords: *Treatment wetland; Land use; Nature-based solution; Non-point source*

1. INTRODUCTION

Since the year 2000, environmental preservation has become an important component of government policies in South Korea (Lim and Park, 2010). Recent policies for managing non-point source (NPS) pollution were also formulated to address the environmental impacts of diffuse pollution. The four major rivers restoration project was a part of the Green New Deal Policy in the year 2009 which mainly focused on water resources management, flood control, and ecosystem rehabilitation (Cha et al., 2011). Among the different types of nature-based solutions (NBS) utilized in South Korea, treatment wetland (TW) is one of the most commonly used facilities for treating stormwater runoff and wastewater from various land uses (i.e. urban, agricultural, livestock, and industrial areas). TW aim to mimic the functions of natural wetlands. These engineered systems can be classified as free water surface wetlands (FWS), horizontal or vertical subsurface flow wetlands (H,V-SSF) and hybrid wetland systems. Although the analysis of the effect on nonpoint pollution reduction facilities is carried out through continuous monitoring projects, only the evaluation is performed at each individual facility, and the overall effect analysis and efficiency evaluation of total TW applied in Korea is not performed.

Therefore, this study intends to conduct an efficiency study of domestic nonpoint pollution reduction facilities through the overall monitoring results of TW applied in Korea.

2. MATERIAL AND METHODS

The Korean ministry of environment has been installing various Low Impact Development (LID) and Green Infrastructures (GI) facilities throughout the country since 2008 in accordance with the second phase of the comprehensive NPS management plan. A total of 54 TWs were installed at 35 locations across South Korea from 2011 to 2018. Among them, 13, 25, 3 and 10 were installed in urban, agricultural, industrial, commercial and livestock areas, respectively. Four types of TW evaluated in this study are illustrated in Figure 1. Cell-type free water surface (Cell-FWS) TW were composed of a series of cell like compartments that perform specific functions. The first cell serves as a sedimentation tank, whereas succeeding cells were designed to perform biological treatment processes. Cell-type facilities were configured to efficiently treat shock loads. Flow-type FWS (Flow-FWS) TW are characterized by a series of meanders designed to maximize the hydraulic retention time of the facilities. Like Cell-FWS TW, Flow-FWS systems have specified areas for sedimentation and biological treatment processes despite the lack of distinct boundaries that separate each treatment unit. The combination of Cell-FWS and Flow-FWS was referred to as Hybrid-FWS, whereas the facilities configured as the combination of horizontal and vertical subsurface flow-types were designated as Hybrid-SS

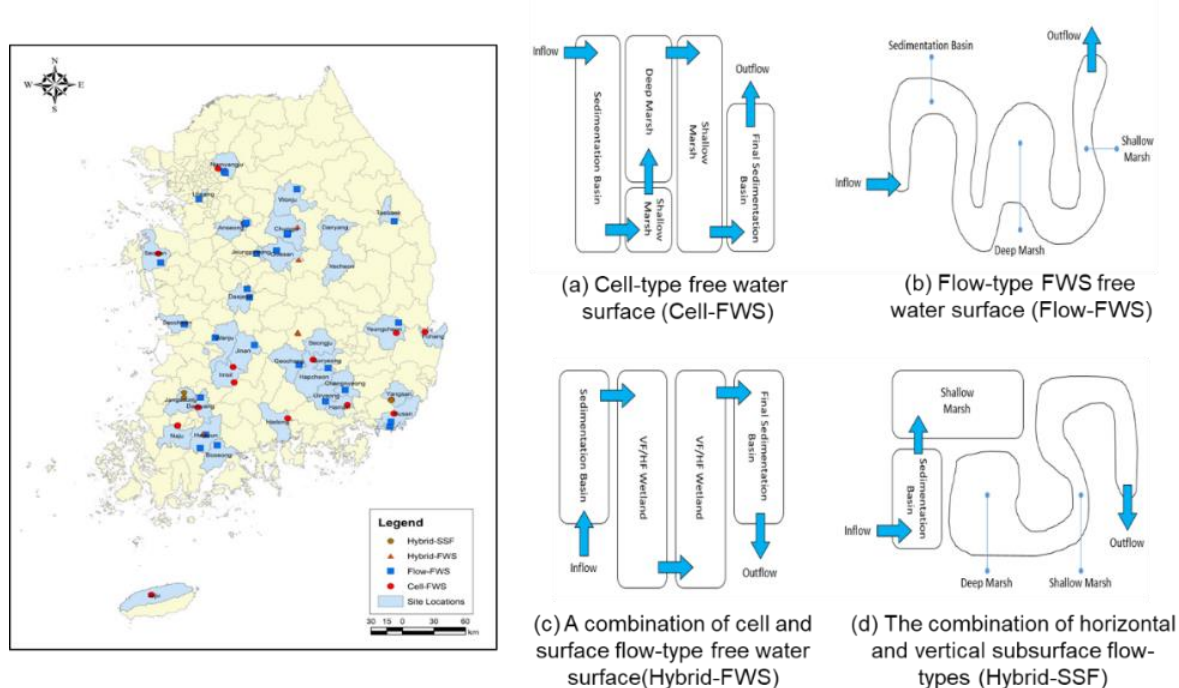


Figure 1. Locations of monitored TW and schematic diagram of the TW type

3. RESULTS AND DISCUSSIONS

The changes in the pollutant removal efficiency of the TW with respect to the period of operation were shown in Figure 2. The efficiency of the facilities may vary greatly due to the influence of influent pollutant concentrations, hydraulic and hydrologic characteristics of monitored events, degree of wetlands stability, and the effect of maintenance activities. Based

on the mean removal efficiency, the TW stabilization period for the steady removal of BOD and COD was four to five years. In the case of particulate matter (SS) and nutrients (TN and TP), consistent patterns of removal were observed after two to three years of operation. A closer examination (not shown) of the individual removal efficiencies indicated that a five-year stabilization period is required to achieve stable nutrients and organic matter removal, whereas particulates removal did not show notable differences with respect to the year of operation. TW usually have low plant density during the early stages of operation. The soil layers in artificial systems may also have significantly different characteristics as compared with natural wetlands. Due to the abovementioned reasons, TW may not exhibit adequate pollutant removal capabilities during the early stages of operation due to the unstable formation of microbial colonies and vegetative covers. While the components for biological remediation are developing in newly TW, sedimentation, filtration, and adsorption can be considered as the dominant treatment mechanisms for stabilizing wetland systems. Unlike natural wetlands where peat layers are well-formed, some TW use engineered soil layers with highly variable characteristics. TW soils have low organic matter and nutrient contents at the beginning of operation, making them reliable sinks for the adsorption, deposition, and decomposition of pollutants. Sparsely vegetated systems may also show low potentials of pollutant removal by means of phytoremediation.

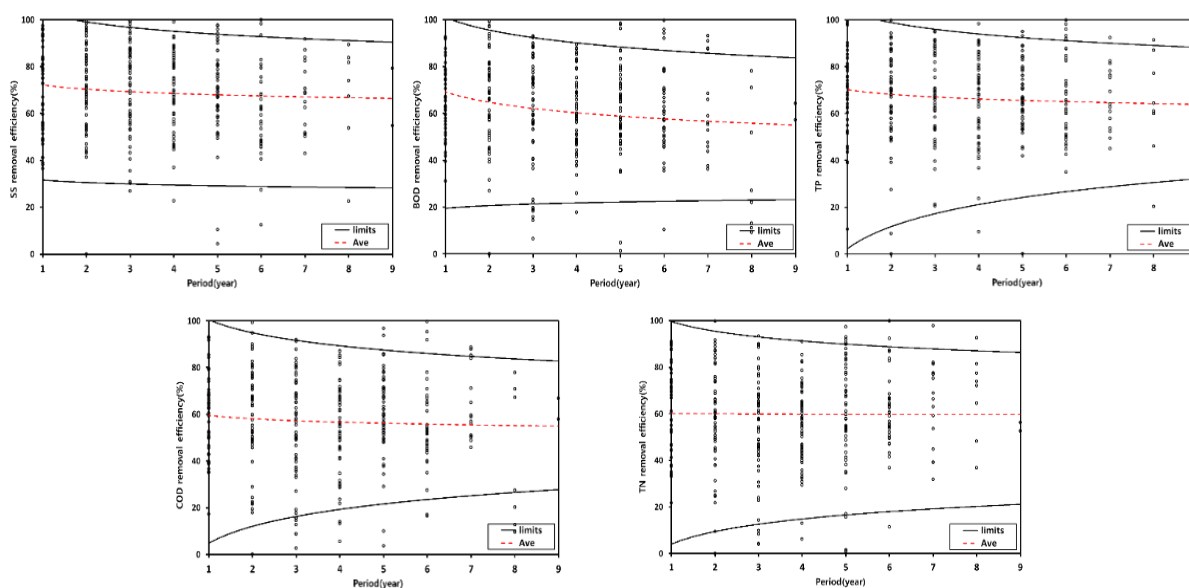


Figure 2. Pollutant removal performance of TW with respect to the period of operation

4. CONCLUSIONS

TW serve as important NBS that assist in environmental restoration and sustainable development. This study evaluated the current status of various TW installed across South Korea to determine the sustainability of these facilities in performing various ecosystem services. TW installed in agricultural and urban areas receive highly polluted runoff that can potentially degrade receiving water bodies. Since the runoff from forested catchments contains relatively low pollutant concentrations, it is recommended to install the facilities in locations close to the point or non-point source pollution sources. The stabilization period of TW usually takes four to five years to effectively treat organics and approximately two to three years to

achieve adequate removal of particulates and nutrients in water. This on-going project still collects monitoring data of all 54 TW for further time-scale, statistical analyses.

Acknowledgements: This work was supported by Korea Environmental Industry & Technology Institute (KEITI) through Wetland Ecosystem Value Evaluation and Carbon Absorption Value Promotion Technology Development Project, funded by Korea Ministry of Environment (MOE) (2022003630005).

REFERENCES

- Lim, T., and Park, J. 2010. Korea's Experiences with Development: Revisiting MDGs from a Time Perspective. *Korean Journal of Policy Studies*, 25.
- Cha, Y.J., Shim, M., Kim, S.K., River, N., 2011. The Four Major Rivers Restoration Project. *Water Green Econ. Pract. Towar. Rio +20*.

DESIGNING THE SIZING CRITERIA FOR FREE WATER SURFACE FLOW CONSTRUCTED WETLAND BASED ON RIVER FLOW INTERPOLATION

*Miguel Antonio Campos, Nicanor Chan, John Kristoffer Chua, Sophia Claudette Gaudia, Sergi Garbanzos, and
Marla Maniquiz-Redillas**

Department of Civil Engineering, De La Salle University, 2401 Taft Avenue, Malate, Manila 1004, Philippines

**Corresponding author (marla.redillas@dlsu.edu.ph)*

ABSTRACT

Free Water Surface Flow Constructed Wetlands (FWS CW) are a type of low impact development (LID) structure that can help in flow attenuation, thereby mitigating the impacts of unprecedented runoff accumulation from urbanization and the rapidly changing climate conditions. The objective of this paper is to assess the sizing of FWS CW structures through river flow interpolation methods. The river discharge was interpolated using the Drainage-Area Ratio (AR) method and the Geographically Weighted Flow Distribution Curve (GWFDC), which was used in conjunction with the hydraulic retention time (HRT) to estimate the size of the proposed wetland. For both methods, a linear relationship was observed for the HRT and surface area, while an inverse relationship was observed for the depth and surface area. Smaller FWS CW sizes have been recommended to accommodate the limited space for construction. The use of FWS CW can solve the excess runoff issues experienced by the study area.

Keywords: *free water surface flow constructed wetland, low impact development, river flow interpolation.*

1. INTRODUCTION

The growing trend of urbanization has also promoted the expansion of impervious surfaces, disrupting the natural hydrological regime in urbanized areas, and increasing the impacts of runoff accumulation. Low impact development structures (LID) have recently been adopted in many locations for runoff attenuation. Constructed wetlands, particularly Free Water Surface Flow Constructed Wetlands (FWS CW), are a type of LID structure that can provide surface runoff flow detention, given that its main capabilities include the capture, slowing down, and treating the runoff (CH2M Hill Canada, 2014). Given its potential for mitigating the impacts of flooding, this paper aims to assess the sizing of FWS CW structures through river flow interpolation methods. Research about the area, depth, and hydraulic retention time (HRT) of wetlands can promote LID, especially in areas where LID research is not yet extensive while adding insight for designing constructed wetlands for future implementations.

2. MATERIAL AND METHODS

The study area is the Binahaan River in Leyte, Philippines (11°7'0" N, 125°1'59" E). Two methods were used to estimate the streamflow data in Binahaan River, namely the Drainage-Area Ratio (AR) Method and the Geographically Weighted Flow Distribution Curve (GWFDC)

Method. The AR method, as shown in Equation 1, is commonly used to statistically transfer streamflow from a gauged location to an ungauged location based on the drainage areas of both sites (Asquith et al., 2006), while the GWFDC method, as shown in Equations 2 and 3, maximizes regional information and weighting streamflow at gauged stations by their distance to the ungauged station (Shu & Ouarda, 2012). The hydraulic retention time (HRT) was also assessed to obtain the proposed area of the wetland. The discharge in Binahaan River was estimated based on its corresponding exceedance probabilities using the Python software.

$$Q_1 = Q_2 \left(\frac{A_1}{A_2} \right)^\phi \quad (1)$$

Where Q_1 is the estimated streamflow for the ungauged site, Q_2 is the streamflow at the gauged site, A_1 is the drainage area of the ungauged site, A_2 is the drainage area of the gauged site, and $\phi = 1$.

$$Q_d = \frac{\sum_{j=1}^n w_j Q_{dj}}{\sum_{j=1}^n w_j} \quad (2)$$

$$w_j = \frac{1/d_j}{\sum_{j=1}^n 1/d_j} \quad (3)$$

Where Q_d is the combined estimate of streamflow at the ungauged site, n is the number of gauged sites, Q_{dj} is the estimation from gauged site j , w_j is the weight corresponding to that gauged site, and d_j is the distance between the ungauged site and the gauged site.

$$t = \frac{Ad\varepsilon}{Q} \quad (4)$$

Where t is the hydraulic retention time in days, A is the area of the constructed wetland in square meters, d is the water depth in m, ε is the wetland porosity, and Q is the flow rate of the river in cubic meters per day.

3. RESULTS AND DISCUSSIONS

The GWFDC method tended to predict higher flows for low exceedances and lower flows for high exceedances, as compared with the AR method. In the estimation of CW size, Figures 1a-d and 2a-d show the possible areas for the different flowrate methods under varying exceedances for the AR and GWFDC methods, respectively. Results from this assessment indicate that there is an apparent trend between HRT, depth, and the wetland area. A direct relationship was observed between the HRT and the area of constructed wetland, due to the wetland requiring more space for the storage of water. Conversely, an indirect relationship was seen between water depth and area, where an increasing the water depth will cause the area to decrease in value. This was due to the constructed wetland being deeper which requires lesser area for construction.

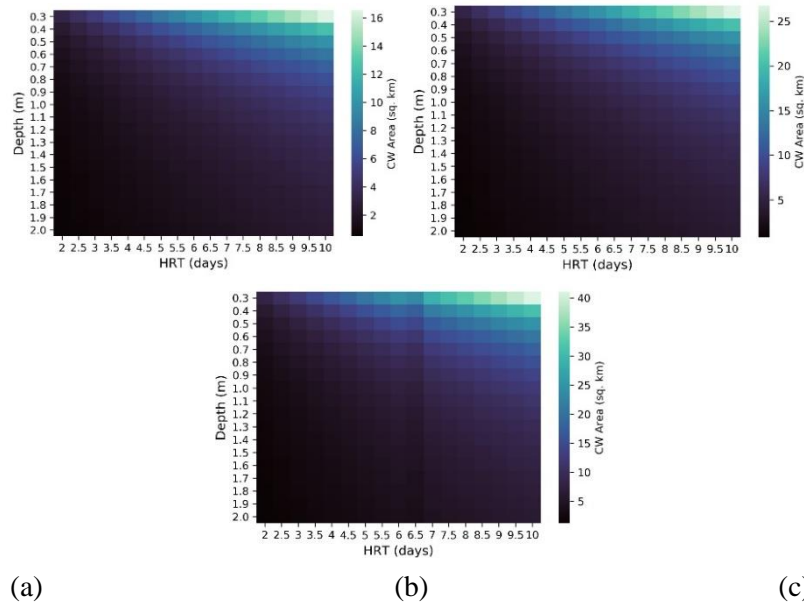


Figure1. Possible sizing criteria based on drainage-area ratio (AR) method estimated flows in the (a) 90%, (b) 60%, and (c) 30% exceedance

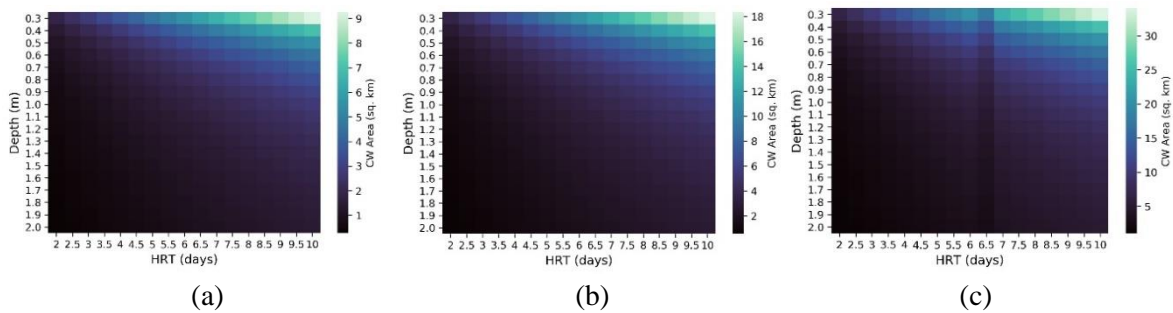


Figure2. Possible sizing criteria based on Geographically Weighted Flow Distribution Curve (GWFDC) method estimated flows in the (a) 90%, (b) 60%, and (c) 30% exceedance

4. CONCLUSIONS

Results have shown that there is a notable difference between the AR and GWFDC methods, with the GWFDC attaining higher flows for low exceedances and lower flows for high exceedances. Relationships were observed between the HRT, water depth, and surface area, which can support in CW design. In the selected site, HRTs tended to range from 2 days to 14 days and depths ranged from 0.3 m to 2.0 m under varying flow rates. It is recommended that a larger depth should be utilized on the site as FWS CW construction can be constrained by the available vacant area on the site.

Acknowledgements: This research was supported by the Department of Science and Technology (DOST) in the Philippines under the ‘DOST’s Grants to Outstanding Achievement in Science and Technology’ Program.

REFERENCES

Asquith, W. H., Roussel, M. C., & Vrabel, J. (2006). Statewide analysis of the drainage-area ratio method for 34 streamflow percentile ranges in Texas. *Scientific Investigations Report*. <https://doi.org/10.3133/sir20065286>

- CH2M Hill Canada. (2014). Wetland Design Guidelines City of Saskatoon. https://www.saskatoon.ca/sites/default/files/documents/transportation-utilities/construction-design/new-neighbourhood-design/wetlands_design_guidelines.pdf
- Shu, C., & Ouarda, T. B. M. J. (2012). Improved methods for daily streamflow estimates at ungauged sites. *Water Resources Research*, 48(2). <https://doi.org/10.1029/2011wr011501>

LITERATURE ANALYSIS ABOUT CHANGING AND INFLUENCE FACTORS IN WETLAND

Younghoon Yoo¹, Jong-Gu Hwang Bo², Kisung Lee², and Soojun Kim^{2}*

¹ *INHA University, Program in Smart City Engineering, Incheon, Republic of Korea*

² *INHA University, Department of Civil Engineering, Incheon, Republic of Korea*

**Corresponding author (sk325@inha.ac.kr)*

ABSTRACT

In East Asia, where 15% of Ramsar wetlands are located, has a high preservation value due to various wetland types and biodiversity. But, There are being raised many problems, such as decreased in wetland area and damage to biodiversity. In order to manage and preserve wetlands, it is necessary to identify the changing and influence factors in wetlands and analyze how each factor affects them. In this study, the changing and influence factors were derived through literature analysis in East Asia. By analyzing the relationship each factor, Further research direction was presented considering the factors of change in wetlands.

Keywords: *Wetland, Literature Analysis, Changing and Influence Factors*

1. INTRODUCTION

In this Study, the changing and influence factors that affect wetland in East Asia were derived and Literature analysis was conducted to analyze the effect of direct and indirect changes in wetlands for each country. we used scientific literature related in wetland and, through keyword analysis derived changing and influence factors and performed the connectivity analysis between each factor by country.

2. MATERIAL AND METHODS

According to the Global Wetland Outlook (2018), there are three factors of wetland change: direct factors that cause biological and physical changes, indirect factors due to social base, and Global megatrend. Direct change factors were classified as physical regime, extraction, introduction, structural change, and indirect change factors were classified as water-energy infrastructure, food and fibre, infrastructure, tourism & recreation, local climate change impacts.

Global megatrend affects both direct and indirect factors, and it is suggested for reasons such as rapid population growth, changes in consumption patterns, urbanization, lack of importance of climate change and wetlands.

Seifollahi-Aghmiuni et al. (2019) conducted a literature case analysis related to promote strategies for securing biodiversity, managing plans, and building resilience of wetland ecosystems in the Arctic wetland landscapes according to climate and land use changes. They

used The Web of Science Core Collection (WoS) bibliographic database directing the search to identify scientific Arctic wetland literature.

3. RESULTS AND DISCUSSIONS

The influence of changing factors in wetlands

In order to analyze the influence of changing factors in wetlands, keywords selected for each detailed changing factors, and we classified the scientific literature according to detailed changing factors by country.

Country Name	Direct Drivers											
	PHYSICAL				EXTRACTION			INTRODUCTION		STRUCTURAL MODIFICATION		
	Water quantity and frequency	Sediment	Salinity	Thermal	Water	Biota	Soil and Peat	Nutrients, chemicals and solid wastes	Invasive Species	Drainage	Conversion	Burning
Brunei	20.00	12.50	7.50	2.50				10.00	40.00	5.00		2.50
Cambodia	32.86	18.57	8.57	1.43	2.86	1.43		15.71	10.00	4.29		4.29
China	21.80	14.42	5.82	11.39	0.98	0.46	0.05	26.57	6.34	1.98	0.07	10.13
Indonesia	24.68	15.85	5.89	8.56	0.70	0.42	0.14	19.07	10.24	4.07	0.28	10.10
Japan	24.38	16.03	4.35	11.51	0.34	0.26		21.23	10.91	3.07	0.09	7.84
Korea	19.88	19.48	3.98	8.55	0.99	0.60		22.86	15.71	2.19		5.77
Laos	25.00	10.42	2.08					18.75	22.92	10.42		10.42
Malaysia	17.55	17.31	9.07	7.18	0.82	1.06		23.32	12.37	3.06		8.24
Myanmar	29.41	14.71	1.47	10.29			1.47	16.18	16.18	2.94	1.47	5.88
Philippines	19.25	13.58	6.42	9.43	0.38	0.38		15.09	18.49	3.77		13.21
Singapore	17.89	15.60	3.67	7.34	2.29	2.75		17.43	25.69	2.29	0.92	4.13
Thailand	20.26	18.52	5.35	6.95	0.72	0.43		23.30	15.92	1.74		6.80
Vietnam	26.07	22.06	5.51	3.51	0.75			18.30	14.54	2.01		7.27
Average	51.26				1.56			35.93		11.25		
	23.00	16.08	5.36	6.82	0.83	0.71	0.01	19.06	16.87	3.60	0.22	7.43

Country Name	Indirect Drivers											
	Water-energy Infrastructure	Food and fibre				Infrastructure			Tourism and Recreation	Localized climate change impacts	Governance /Legislation	Natural Processes & components
		Agriculture	Forestry	Aquaculture	Fisheries	Industry and Mining	Transport	Construction				
Brunei	4.00	2.00	54.00			2.00	4.00		2.00	6.00	18.00	8.00
Cambodia	2.54	11.02	25.42	3.39	13.56	3.39	3.39		2.54	11.86	19.49	3.39
China	2.52	10.43	15.76	2.84	1.25	5.08	6.03	0.33	2.19	11.45	24.09	18.02
Indonesia	0.90	9.00	33.12	5.40	5.40	5.31	1.80	0.18	2.88	7.47	21.42	7.11
Japan	2.48	10.17	33.45	1.18	3.43	3.31	6.86	0.12	1.06	7.57	18.32	12.06
Korea	3.10	14.08	13.80	0.56	2.25	5.35	5.07		1.97	6.48	30.14	17.18
Laos		20.83	29.17	2.08	8.33	2.08	4.17			4.17	20.83	8.33
Malaysia	1.38	7.01	37.81	4.74	4.44	6.12	2.96	0.20	4.34	4.24	19.55	7.21
Myanmar		14.84	34.38	3.13	7.03	2.34	2.34		3.13	10.16	18.75	3.91
Philippines	0.48	8.79	24.70	9.03	9.98	5.94	1.66		1.66	4.99	24.94	7.84
Singapore	1.89	5.03	33.33	5.03	5.66	5.03	5.03		3.14	6.29	25.79	3.77
Thailand	1.33	10.80	35.07	7.16	7.77	4.49	2.06	0.24	2.43	2.31	18.57	7.77
Vietnam	1.79	12.54	30.62	10.10	4.07	3.42	3.75		0.98	7.00	16.94	8.79
Average	1.72	51.31				7.85			2.18	6.92	21.29	8.72
	1.72	10.50	30.82	4.20	5.78	4.30	3.47	0.08	2.18	6.92	21.29	8.72

Figure1. Heat map between East Asia countries and drivers regarding wetland changes

Analysis of Connectivity and Relationship between Changing factors

In order to analyze the connectivity and relationship by country, we performed relationship analysis based on direct and indirect factors. The relationship analysis presented in a graph and connectivity was expressed based on the weight of research papers derived from keywords by each direct and indirect factor.

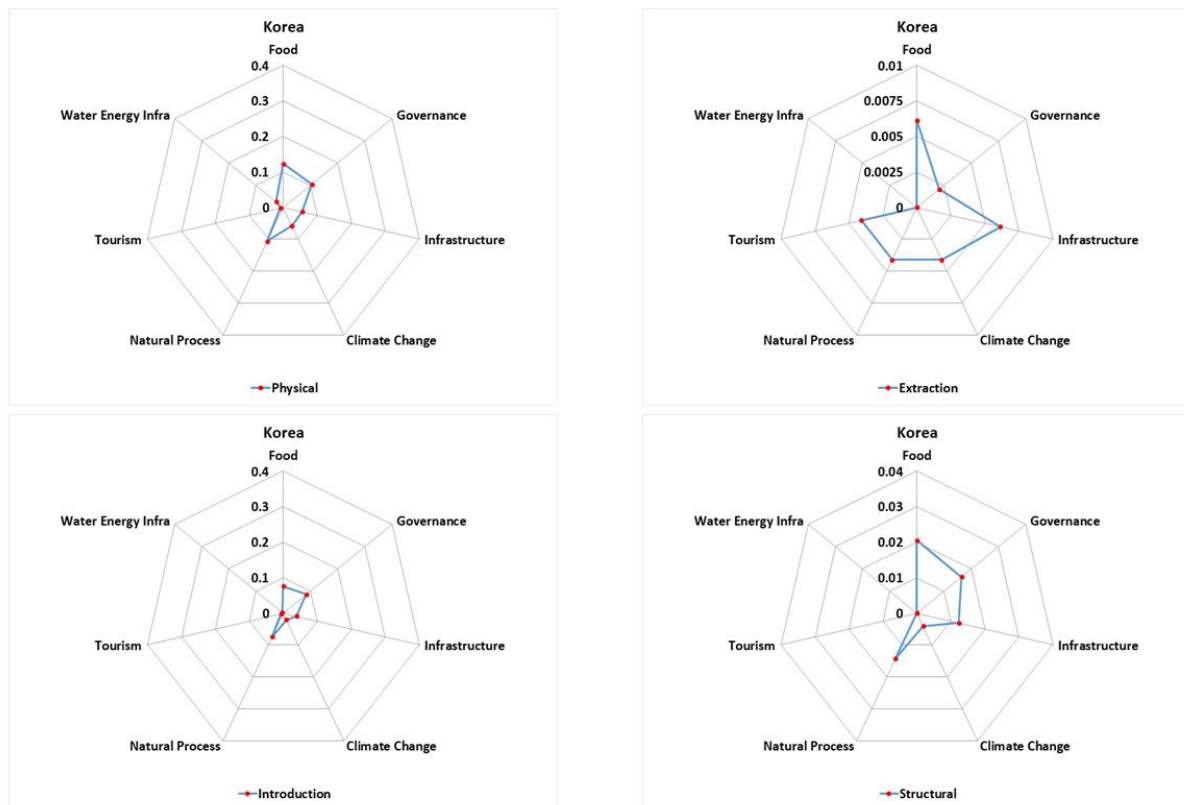


Figure 2. Connectivity & relationship analysis between direct and indirect drivers (Korea)

4. CONCLUSIONS

In this study, in order to derived the changing and influence factors in wetland and analyzed the effects of wetland due to factors, conducted literature analysis using scientific wetland literature published in 13 countries in East Asia. The scientific wetland literature collected for the past 50 years, and extract the keyword in order to identify the effect of factor by country. Relationship analysis was conducted based on the frequency of keyword appearance of direct and indirect factors in order to identify the connection of research by country, and finally, further research direction was proposed in consideration of factors.

Acknowledgements: This work was supported by Korea Environmental Industry & Technology Institute (KEITI) through Wetland Ecosystem Value Evaluation and Carbon Absorption Value Promotion Technology Development Project (2022003630001).

REFERENCES

- Ramsar Convention on Wetlands. (2018). Global Wetland Outlook: State of the world's wetlands and their services to people, Gland, Switzerland: *Ramsar Convention Secretariat*.
- Seifollahi-Aghmiuni S, Kalantari Z, Land M and Destouni G. (2019). Change Drivers and Impact in Arctic Wetland and Landscape-Literature and Gap Analysis. *Water*, 11(4): 722.

AN OVERVIEW OF DIFFUSE POLLUTION MANAGEMENT THROUGH STORMWATER TREATMENT WETLANDS

Nash Jett DG. Reyes¹, Franz Kevin F. Geronimo¹, Heidi B. Guerra¹, Minsu Jeon¹, Lee-Hyung Kim^{1*}
¹. Kongju National University, Civil and Environmental Engineering Department, Cheonan City, South Korea
*Corresponding author (leehyung@kongju.ac.kr)

ABSTRACT

Stormwater treatment wetlands are nature-based systems that are commonly used for diffuse pollution management. Despite the growing number of publications concerning these technologies, there are still no studies that performed in-depth analyses of the publications based on an extensive collection of bibliographic information. The terms ("constructed wetland*" OR "treatment wetland*" OR "engineered wetland*" OR "artificial wetland*") AND ("stormwater*" or "storm water*") were used to retrieve the publications, from January 1990 to December 2020, in the Web of Science database. Analyses revealed that the number of publications continued to increase over the years, with USA, Australia, and China having the highest scientific productivity in terms of the number of publications. Most of the studies focused on the water quality remediation capabilities of stormwater treatment wetlands. Specifically, the removal of nutrients (i.e. nitrogen and phosphorus) in stormwater was widely explored. Further studies on the treatment of micropollutants and carbon capture capabilities of stormwater wetlands are still recommended since it was identified that inquiries on these fields of research were relatively scarce.

Keywords: *Bibliometrics, diffuse pollution, stormwater, treatment wetland*

1. INTRODUCTION

Diffuse pollution increases the risk of water quality degradation and aquatic ecosystem deterioration. Stormwater runoff serves as the most common diffuse pollution in various land uses. In urban and industrial areas, stormwater runoff may contain considerable amounts of particulates, heavy metals, organic and inorganic compounds, and other substances that are generated from anthropogenic-related activities. Agricultural runoff also contains high nutrients concentration due to the extensive application agricultural enrichments on farmlands. Generally, the stormwater runoff from various land uses greatly contributes to the influx of pollutant loads in receiving water bodies. Nature-based solutions are increasingly being utilized to manage stormwater runoff quality and quantity. This approach primarily relies on employing natural processes to effectively manage or restore damaged ecosystems. Constructed wetlands are one of the most commonly used and socially-accepted nature-based systems in stormwater management (Sharley et al., 2017). A great number of studies regarding the functions, design, and factors affecting the treatment performance of stormwater treatment wetlands have already been published, but in-depth analyses of the publications based on an extensive collection of bibliographic information have not been performed yet. This study was conducted to determine

the status and trends of scientific publications focused of stormwater treatment wetlands. The major research hotspots, knowledge gaps, and future research directions were also identified through metadata analysis.

2. MATERIALS AND METHODS

Bibliographic information were obtained from the Web of Science (WoS) database. The terms ("constructed wetland*" OR "treatment wetland*" OR "engineered wetland*" OR "artificial wetland*") AND ("stormwater*" or "storm water*") were used to retrieve the publications, from January 1990 to December 2020, relevant to stormwater treatment wetlands. Initial results were filtered to limit the list to articles published in English. Terms were also standardized to remove duplicate entries or erroneous items in the database. The bibliographic information were visualized through science mapping softwares. Contingency matrices were generated through the cortex platform (cortex.net) and network maps were created through the VOSViewer software.

Table 1. Data and input parameters used in the science mapping software

Software	Parameter	Inputs/Method of analysis
VOSviewer (Network map)	Bibliographic database file	WoS plaintext file
	Type of analysis	Co-occurrence
	Unit of analysis	Author keywords
	Counting method	Full counting (terms have the same weight)
	Minimum number of co-occurrence	5
Cortex (Contingency matrix)	Bibliographic database file	WOS plaintext file
	Field values	Author keywords – Country
	Contingency analysis measure	Author keywords – Year of publication
	Number of nodes	Chi ² 10 (Default software value)

3. RESULTS AND DISCUSSIONS

The first publication about stormwater treatment wetlands registered in the WoS database was in the year 2012. From 2012 up to the year 2021, a total of 413 scientific publications focused on stormwater treatment wetlands were recorded. The countries with the most number of publications concerning stormwater treatment wetlands were shown in Figure 1a. USA had the greatest contribution (32%, 165 articles), followed by Australia (14%, 71 articles), and China (12%, 62 articles). The major subject areas related to stormwater treatment wetlands were Environmental Sciences Ecology, Engineering, and Water Resources. Further analyses revealed that most of the publications were categorized in multiple subject areas, indicating that the field of stormwater treatment wetlands research is multidisciplinary in nature. Keywords represent the actual contents of scientific publications (Zhao et al., 2021). There were 1120 unique keywords identified from the 413 retrieved articles, but only 127 terms had a frequency of at least five times. Excluding the terms used in the query, the most frequently used keywords in the related publications were phosphorus (n=37), water quality (n=26), best management practice (n=24), nutrient (n=23), and nitrogen (n=22). This indicated that most studies on stormwater treatment wetlands were focused on water quality improvement and treatment of nutrients (i.e. nitrogen and phosphorus) in stormwater runoff. Based on the analysis of keywords, it was noted that studies regarding the capability of stormwater wetlands for treating contaminants of emerging concern, such as microplastics, pharmaceutical compounds, and per- and polyfluoroalkyl substances, among others, were not widely explored yet. There were also studies that report the carbon sequestration potential of constructed

NATURE BASED SOLUTIONS AND IMPLEMENTATIONS

DETERMINING THE OPTIMAL LID COMBINATION THROUGH HYDROLOGICAL PERFORMANCE MODELING AND COST-EFFECTIVENESS ANALYSIS

*Sergi Garbanzos and Marla Maniquiz-Redillas**

Department of Civil Engineering, De La Salle University, 2401 Taft Avenue, Malate, Manila 1004, Philippines

**Corresponding author (marla.redillas@dlsu.edu.ph)*

ABSTRACT

Low impact development (LID) structures have been extensively studied for their hydrological benefits and economic performance in varying sites. The lack of research on its optimization, however, makes it difficult to further improve its performance. The objective of this study is to determine the optimal LID combinations using hydrological performance modeling and cost-effectiveness analysis. Four rainfall percentiles (80th, 90th, 95th, 99th) and three LID controls, namely the bioretention (BR), infiltration trench (IT), and permeable pavement (PP), and their combinations were selected for application in a residential park area. By getting the flow reduction of each LID control under varying surface areas and their respective life cycle costs, the cost-effectiveness (C/E) ratio was then computed. Results from this assessment have shown that the IT and IT+PP scenarios were the most cost-effective ones regardless of LID size. The C/E ratios of the 99th percentile also tended to be distant from the other percentiles, indicating that it is an unsustainable choice. From the selected rainfall amounts, the 90th and 95th percentiles appear to be the ideal choice for capture. The use of C/E analysis can be an effective tool in determining cost-effective LID combinations within a site.

Keywords: *cost-effectiveness analysis, flow reduction, life cycle cost, low impact development, stormwater management model.*

1. INTRODUCTION

The hydrologic and economic performance of LID controls in comparison with traditional drainage infrastructure have been recognized in recent years, leading to its widespread application in various places around the world. Identifying both the costs and benefits of these structures can help in optimizing their design and preparing the budget for projects (Jiang, et al, 2018), but optimization to improve LID performance remains an issue due to a limited number of studies, particularly in developing countries (Pour, et al., 2020). The objective of this study is to determine the optimal LID combinations using hydrological simulations and cost-effectiveness analysis. The results of this study can provide insight on which LID type and combination are practical in each site considering its hydrological performance and life cycle cost together with changing rainfall amounts.

2. MATERIAL AND METHODS

The selected study site is a residential park located in Bacoor, Cavite, Philippines (14°27'6.3432", 120°56'48.264"). Rainfall data used for simulation included the 80th, 90th, 95th, and 99th rainfall percentiles of historical rainfall from the nearest rain gauge in the vicinity. To obtain the flow reduction of the BR, IT, and PP controls and their different combinations in the site, the Stormwater Management Model (SWMM) was used. Varying LID surface areas were applied in each scenario created for comparison. Cost data of the LID controls were gathered from previous studies (Mei, et al., 2018; Leimgruber, et al., 2019) to compute the life cycle cost (LCC), as shown in Equation 1. Using the simulated flow reduction, which was deemed as the present value benefit (PVB), and the computed LCC, which was deemed as the present value cost (PVC), the C/E ratio was then computed as shown in Equation 2. A lower value of this index would indicate that it is the more cost-effective choice.

$$LCC = C + A \frac{(1 + d)^n - 1}{d(1 + d)^n} \quad (1)$$

Where LCC represents the life cycle cost or present value cost, C for the initial construction cost (\$), A for the annual maintenance cost (\$), d for the real discount rate, and n for the design life (years).

$$C/E = \frac{PVC}{PVB} \quad (2)$$

Where PVC is the present value cost and PVB is the present value benefit.

3. RESULTS AND DISCUSSIONS

A total of 2,112 simulations were performed in SWMM in consideration of the seven LID scenarios, four rainfall percentiles, and varying surface areas of each LID control. The C/E ratio values were then compared as shown in Figures 1a-d, which show the mean, median, minimum, and maximum C/E ratios of each scenario, respectively. Results have shown that the scenarios with the lowest average C/E ratios include the IT and IT+PP scenarios in all rainfall percentiles, while the BR and BR+PP scenarios generated the largest values in all percentiles as well. A similar relationship was observed in the median, where most of the low C/E scenarios have been found in the IT, PP, and IT+PP scenarios, indicating that they mostly consist of low indices. The lowest or minimum C/E value for all percentiles was seen in the IT scenario, as it was characterized by its low costs and the large area of capture in the selected site. The BR scenario, on the other hand, had the greatest values using the same index. In comparing the rainfall percentiles, it was observed that the 99th percentile was very distant from all other percentiles, which implies that attaining this amount would be less ideal. The optimal rainfall amount for capture given these choices would then be around the 90th to 95th percentile, as it maximizes the amount of rainfall treated while remaining cost-effective.

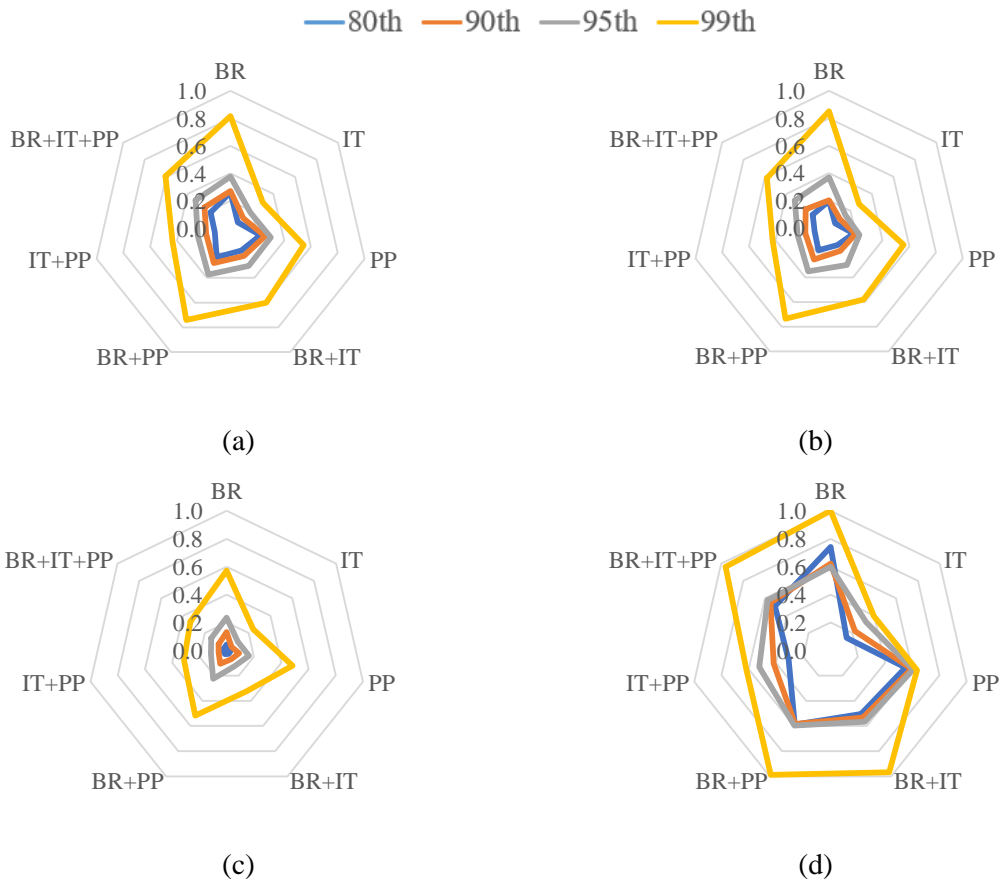


Figure 1. The (a) mean (b) median, (c) minimum, and (d) maximum of the calculated cost-effectiveness ratios

4. CONCLUSIONS

The cost-effectiveness analysis performed in this study has shown that the IT and IT+PP scenarios generated the lowest C/E ratio values in most rainfall values, showing that the two are the optimal LID combinations in the selected site. Conversely, the BR and BR+PP scenarios generated the highest C/E values. Attaining the 90th to 95th rainfall percentile was ideal for maximizing the rainfall captured without heavily increasing its cost.

Acknowledgements: The authors would like to thank and acknowledge the Department of Science and Technology - Engineering Research and Development for Technology (DOST-ERDT) in the Philippines for the funding of this research.

REFERENCES

- Jiang, Y., Zevenbergen, C., & Ma, Y. (2018). Urban pluvial flooding and stormwater management: A contemporary review of China's challenges and "sponge cities" strategy. *Environmental Science & Policy*, 80, 132–143. <https://doi.org/10.1016/j.envsci.2017.11.016>
- Leimgruber, J., Krebs, G., Camhy, D., & Muschalla, D. (2019). Model-Based Selection of Cost-Effective Low Impact Development Strategies to Control Water Balance. *Sustainability*, 11(8), 2440. <https://doi.org/10.3390/su11082440>
- Mei, C., Liu, J., Wang, H., Yang, Z., Ding, X., & Shao, W. (2018). Integrated assessments of green infrastructure for flood mitigation to support robust decision-making for sponge city construction in an urbanized watershed. *Science of The Total Environment*, 639, 1394–1407. <https://doi.org/10.1016/j.scitotenv.2018.05.199>

Pour, S. H., Wahab, A. K. A., Shahid, S., Asaduzzaman, M., & Dewan, A. (2020). Low impact development techniques to mitigate the impacts of climate-change-induced urban floods: Current trends, issues and challenges. *Sustainable Cities and Society*, 62, 102373. <https://doi.org/10.1016/j.scs.2020.102373>

COMPARISON OF URBAN STORMWATER FLOW REDUCTION USING LID UNDER A CENTRALIZED AND DECENTRALIZED SCHEME

Marla Maniquiz-Redillas and Sergi Garbanzos*

Department of Civil Engineering, De La Salle University, 2401 Taft Avenue, Malate, Manila 1004, Philippines

**Corresponding author (marla.redillas@dlsu.edu.ph)*

ABSTRACT

In recent years, the use of sustainable drainage practices called low impact development (LID) has become a trend in many countries due to its ability to alleviate urban flooding and improve natural infiltration. One of the major challenges in the application of LID structures includes its optimal set up within an area to maximize its efficiency. The objective of this study is to evaluate the outflow reduction of varying LID arrangements using Stormwater Management Model (SWMM). Infiltration trenches (IT) and permeable pavements (PP) were distributed over the site under an 80th, 90th, 95th, and 99th rainfall percentile. Three models were arranged for comparison: the single centralized model (SCM), integrated decentralized model (IDM), and land-use separated decentralized model (LUSDM). Results have shown that the IDM model generally produced the best results for most of the simulations, attaining an average outflow reduction that is 16.6% better in the IT scenarios and 1.48% better in the PP scenarios for both the SCM and LUSDM distributions in all rainfall percentiles. The decentralization of LID sub-catchments and structures is recommended to optimize its use within an area.

Keywords: *decentralization, flow reduction, low impact development, stormwater management model, urban runoff*

1. INTRODUCTION

The widespread urbanization has advanced the development of impervious surfaces, thereby prompting the modification of traditional drainage infrastructures to more sustainable, environmentally friendly alternatives. Low impact development (LID) is one of the stormwater practices aiming to follow a “design with nature approach” (Fletcher, et al., 2015) to intercept runoff, slowing and soaking it in the soil thereby improving natural infiltration and reducing downstream flows (York & Jacob, 2020). One of the major challenges in the strategic planning cycle of LID controls is its distribution pattern (Zhang & Chiu, 2018) as the goal is to maximize the efficiency of these stormwater controls. The objective of this study is to evaluate the outflow reduction of varying LID arrangements using Stormwater Management Model (SWMM). The findings of this study can help in determining which model arrangements are more effective in stormwater simulation studies to further optimize results.

2. MATERIAL AND METHODS

A residential park area located in Bacoor, Cavite, Philippines (14°27'6.3432", 120°56'48.264") with an approximate area of 1,151 m² was selected as the site for this study. Four rainfall

percentiles (80th, 90th, 95th, and 99th percentiles) were set for simulation based on the collected 40-year rainfall data. Using Stormwater Management Model (SWMM), three (3) models were created to assess the outflow reduction in different model arrangements. This included the single centralized model (SCM), which is composed of only one sub-catchment, the integrated decentralized model (IDM), which is composed of six (6) sub-catchments based on the observed flow direction of runoff, and land use separated decentralized model (LUSDM), which is composed of nine (9) sub-catchments to disconnect all land uses in the site. These models were simulated under infiltration trench (IT) and permeable pavement (PP) practices, whose surface area depended on the available spaces on the site.

3. RESULTS AND DISCUSSIONS

Figures 1a and 1b present the outflow reduction comparison between the three models under IT and PP structures, respectively. In the IT scenarios, it was observed that the IDM had the best reductions on average in the 80th (78.95%) and 90th (34.57%) percentiles, while the SCM had the best results in the 95th (25.02%) and 99th (19.11%) percentiles. The LUSDM simulations poorly performed on these scenarios because the pervious areas were separated from the impervious areas in the model, thereby underestimating the amount of rainfall that can be treated by the proposed infiltration trenches. On the other hand, the PP scenarios had the best results on average in the LUSDM, in terms of the 80th (24.10%), 95th (16.93%), and 99th (8.29%) rainfall percentiles. The IDM had the best reductions in the 90th (19.53%) percentile, and generally had the second-best results from this assessment, having reductions 1% higher than the LUSDM model. Despite having the least values in almost all percentiles, the SCM still had close values compared to the other decentralized models, especially in the higher percentiles. Results have also shown that decentralized models are generally more effective in lower rainfall amounts (80th and 90th), as opposed to the higher rainfall amounts due to the overestimation of centralized models in the capture of high-intensity rainfall. In the selected site, the IDM generally performed well in all given scenarios, making it the most appropriate arrangement for simulations.

4. CONCLUSIONS

Results have concluded that the IDM has better results than the SCM and the LUSDM, attaining a reduction that is 16.6% larger on average in the IT scenarios and 1.48% larger on average in the PP scenarios. The IDM also appeared to perform better in lower rainfall amounts (80th and 90th) than in higher rainfall intensities (95th and 99th). Having a decentralized model and LID arrangement is recommended to optimize the LID's flow reduction capability.

Acknowledgements: The authors would like to thank and acknowledge the Department of Science and Technology - Engineering Research and Development for Technology (DOST-ERDT) in the Philippines for the funding of this research.

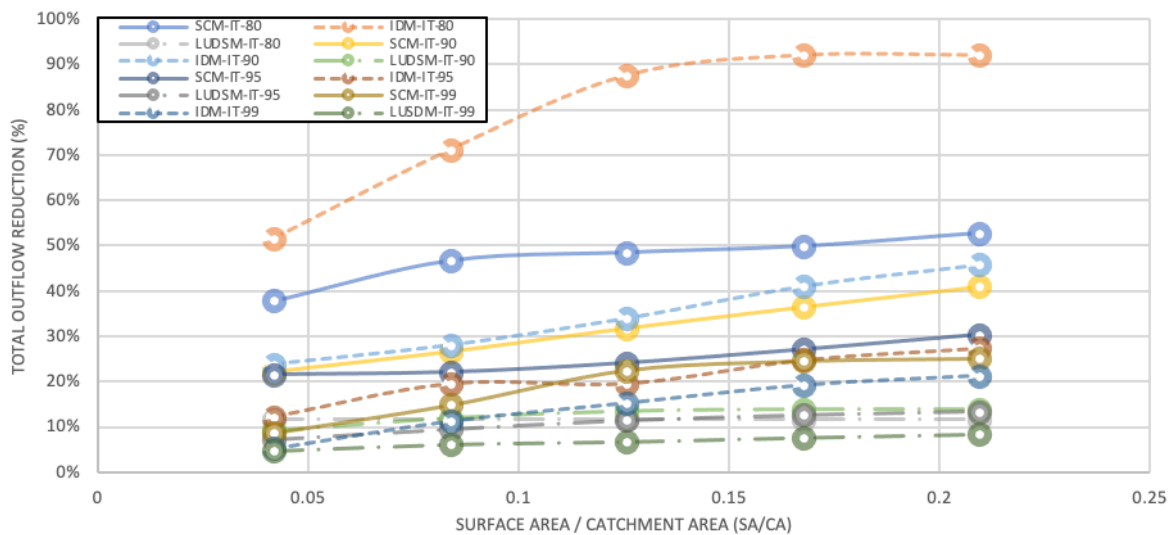
REFERENCES

Fletcher, T. D., Shuster, W., Hunt, W. F., Ashley, R., Butler, D., Arthur, S., Trowsdale, S., Barraud, S., Semadeni-Davies, A., Bertrand-Krajewski, J.-L., Mikkelsen, P. S., Rivard, G., Uhl, M., Dagenais, D., & Viklander, M. (2015). SUDS, LID, BMPs, WSUD and more – The evolution and application of terminology

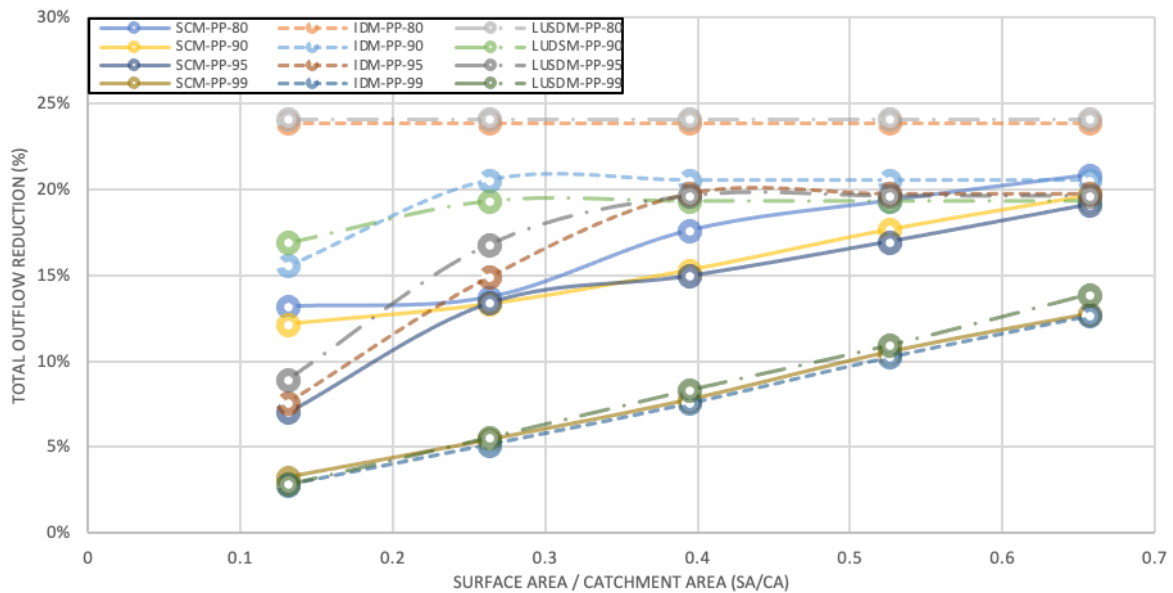
surrounding urban drainage. *Urban Water Journal*, 12(7), 525–542.
<https://doi.org/10.1080/1573062X.2014.916314>

York, C. R. H., & Jacob, J. S. (2020). Chapter 8—Harnessing Green Infrastructure for Resilient, Natural Solutions. In R. Colker (Ed.), *Optimizing Community Infrastructure* (pp. 147–164). Butterworth-Heinemann.
<https://doi.org/10.1016/B978-0-12-816240-8.00008-2>

Zhang, K., & Chui, T. F. M. (2018). A comprehensive review of spatial allocation of LID-BMP-GI practices: Strategies and optimization tools. *Science of The Total Environment*, 621, 915–929.
<https://doi.org/10.1016/j.scitotenv.2017.11.281>



(a)



(b)

Figure 1. Comparison of single centralized model (SCM), integrated decentralized model (IDM), and land use separated decentralized model (LUSDM) in (a) infiltration trenches (IT) and (b) permeable pavements (PP) concerning total outflow reduction and surface area/catchment area (SA/CA)

HYDRAULIC BEHAVIOR AND PERFORMANCE OF SOIL WITH VARYING INFILTRATION RATES FOR GREEN STORMWATER INFRASTRUCTURES

Heidi Guerra, Nash Jett Reyes, Franz Kevin Geronimo, Minsu Jeon, Lee-Hyung Kim*
Department of Civil and Environmental Engineering, Kongju National University
*Corresponding author (leehyung@kongju.ac.kr)

ABSTRACT

A lab-scale infiltration system was used to compare the applicability of a low infiltration soil as a base layer in gravel-filled infiltration systems with emphasis on runoff capture and suspended solids removal. Clayey soil used for a low infiltration system was compared to sandy soil representing a high infiltration system. Findings showed that infiltration rates increased with the water depth above the gravel-soil interface indicating that the available depth for water storage affects this parameter. Runoff capture in low infiltration systems was also found to be less affected by rainfall characteristics as compared to high infiltration systems. Based on runoff capture and pollutant removal analysis, a media depth of at least 1 m for low infiltration systems is required to capture and treat a 10-mm rainfall in Korea. A maximum infiltration rate of 200 mm/h was also found to be ideal to provide enough retention time for pollutant removal. Moreover, low infiltration systems are more susceptible to horizontal flows and that the length of the structure may be more critical than the depth in this condition.

Keywords: *green infrastructure, infiltration systems, hydraulic behavior, soil infiltration*

1. INTRODUCTION

The rapid shift from pervious to impervious surfaces due to urbanization has become apparent through frequent flooding, declining base flows, and water quality impairment in streams, rivers, and shallow groundwater (Shuster, 2005). As a result, stormwater management solutions leaned towards low impact development (LID) strategies that mimic pre-urbanization hydrology through retention, infiltration, evapotranspiration and filtration (USEPA, 2000). In areas that are experiencing periods of drought, like South Korea, or where the in-situ soil infiltration capacity is low, the treated stormwater may be stored for reuse. Therefore, the application of stormwater infiltration LID systems may be broadened instead of being limited by in-situ soil or rainfall characteristics (Begum et al., 2008; Akram et al., 2014).

In this study, an infiltration system utilizing gravel and soil media was investigated. The runoff capture capacity between low infiltration and high infiltration media were compared and their corresponding effect on pollutant removal with emphasis on suspended solids were analysed. The study aims to develop basic design provisions for LID applications under different rainfall and soil characteristics.

2. MATERIAL AND METHODS

A lab-scale infiltration device as shown in Figure 1 (a) was constructed and assembled for the experiments. It is composed of a 0.7x0.2x0.6 m (LxWxH) acrylic tank and polyvinyl chloride

(PVC) pipes for the inlet and outlet. The media were arranged inside the tank as depicted in Figure 1 (b) and has a storage volume of 0.028 m³. Two setups were studied; one employs a well-graded clay soil representing a low infiltration system (LIS) while the other one employs a uniformly-graded sandy soil representing a high infiltration system (HIS).

A semi-synthetic stormwater was used as inflow with a turbidity of 100 NTU (equivalent to 1600 mg/L) and was fed to the infiltration device at inflow rates of 250, 500, and 1000 mm/h. The water level in the tank as well as the outflow and overflow rates were monitored while inflow, outflow, and overflow samples were collected for turbidity measurement and PSD analysis.

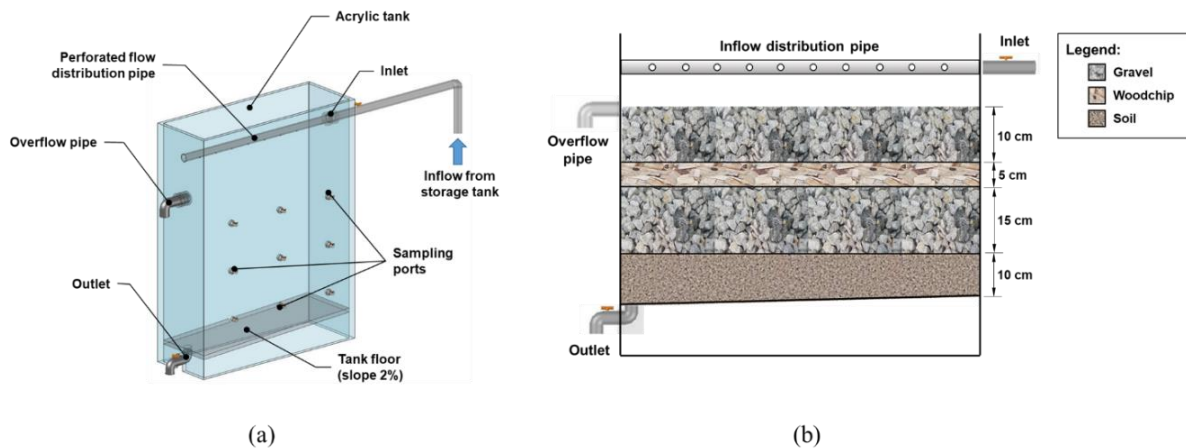


Figure 1. Infiltration device indicating parts and arrangement of the media

3. RESULTS AND DISCUSSIONS

In all the experiments conducted, it was observed that as the water level rose, the infiltration rates increased. The water level above the soil created a positive hydraulic head which pushed the water unto the soil and induced an increase in infiltration rate. Thus, it can be inferred that the available depth for water storage within and above the soil media can influence the infiltration rates in stormwater treatment systems.

In terms of runoff reduction, findings show that as the inflow rate increased, the amount of captured runoff also increased in HIS but remained constant in LIS. This signifies that the rainfall depth and intensity influences the amount of runoff capture more significantly in HIS than in LIS due to the limited infiltration capacity in LIS. Moreover, it was estimated that to achieve 100% capture of the runoff generated by a 10-mm rainfall in Korea, at least 1 m of gravel media depth is required over a low infiltration soil. On the other hand, HIS requires only 0.4 m to achieve the same runoff capture. However, in terms of water quality, a minimum depth 0.9 m is suggested. Moreover, a drawdown time of 9 h corresponding to an infiltration rate of 200 mm/h was estimated to be the optimum condition for pollutant removal.

As the inflow rate increased, the vertical flow in LIS remained constant while the horizontal flow rapidly increased (Figure 2(a)) indicating that systems with silty or clay soils are more susceptible to horizontal flow especially during heavy rainfall. This also induced an increase in the amount of solids escaping the treatment system thereby decreasing the captured TSS as shown in Figure 2(b). Avoiding this phenomenon would require increasing the depth of the facility. However, in areas with site-specific constraints the available depth is limited, the length of the system should be increased to encourage treatment through horizontal flow. Therefore,

the variation of flow and its corresponding effect on the removal of suspended solids should be considered in the design of infiltration systems.

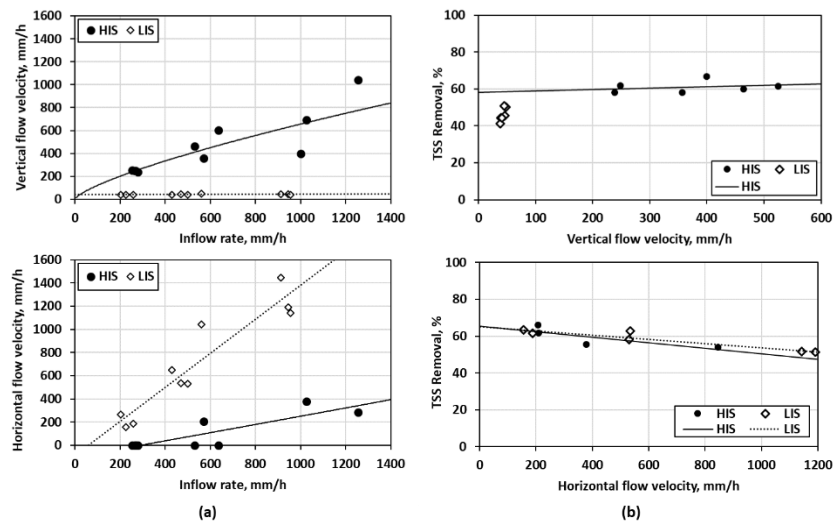


Figure 2. (a) Variation in vertical and horizontal flow with respect to inflow rate and (b) TSS removal

4. CONCLUSIONS AND FUTURE WORK

The major findings in this study as well as recommendations for future work are as follows:

- Aside from the rainfall depth and inflow rates, the water depth can influence the infiltration rates in stormwater treatment system. Infiltration rates are found to increase with water levels until either the infiltration capacity or overflow level is reached.
- High infiltration systems can capture and treat larger volumes of runoff as compared to low infiltration systems but low infiltration systems can capture and treat a consistent amount of runoff that can be infiltrated or released to the storm drains.
- For optimum runoff capture and pollutant removal, a minimum depth of 0.9 m and maximum infiltration rate of 200 mm/h was found to be ideal to provide enough retention time.
- Infiltration systems with or built above silty or clay soils are found to be more susceptible to horizontal flow. Therefore, the length of the media bed is more critical than the depth in this condition and should be considered in the design process.

Acknowledgements: This work was supported by Korea Environmental Industry & Technology Institute (KEITI) through Wetland Ecosystem Value Evaluation and Carbon Absorption Value Promotion Technology Development Project, funded by Korea Ministry of Environment (MOE) (2022003630005).

REFERENCES

- Akram, F., Rasul, M.G., Khan, M.M.K., and Amir, M.S.I.I. (2014), A review on Stormwater Harvesting and Reuse. *Int. J. Environ. Ecol. Geol. Min. Eng.*, 8(3), 188-197.
- Begum, S., Rasul, M.G., and Brown, R.J. (2008). Stormwater treatment and reuse techniques: A review. *Proceedings of 2nd International Conference on Waste Management, Water Pollution, Air Pollution, Indoor Climate*, October 26-28, Corfu, Greece.
- Shuster W.D., Bonta, J., Thurston, H., Warnemuende, E., and Smith, D.R. (2005). Impacts of impervious surface on watershed hydrology: A review. *Urban Water J.*, 2(4), 263-275.
- USEPA (US Environmental Protection Agency) (2000). *Low impact development (LID): A literature review*. Report EPA-841-B-00-005, USEPA Office of Water, Washington DC, USA.

DEVELOPMENT OF REMEDIATION DESIGN FOR THE *IN-SITU* TREATMENT OF HIGHWAY RUNOFF: SELF CLEANSING DITCHES

Ayush Pokharel

SILT, Civil Engineering, Kathmandu, Nepal

1. Abstract

Highway contamination is one of the main sources of pollution of water bodies through transfer of pollutants via drainage. The main causes of highway pollution are oil spills, accidents, contamination by tyre grips, road salt and numerous other waste materials. All these pollutants are washed away into drainage ditches by rain and find their way into the receiving water bodies. The water in these drainage ditches, however, carries innumerable pollutants and harmful substances from the highways into the receiving water bodies. These substances have not only been polluting the receiving water bodies for decades, but have also been disturbing their ecosystems and hampering the reproduction processes of aquatic life forms. In many parts of the world where people use water from rivers, lakes and oceans for their daily needs, they are either being forced to drink polluted water, or being charged hefty amounts of money for its purification. Further, as a result of carrying polluted water for years, the ditches themselves have become highly polluted. This study is focused on identification and *In-Situ* remediation of the different pollutants present in highway runoff. The Highway Department of United Kingdom (UK) is also a concerned party in the studies and remediation of these pollutants.

Keywords: *Highway contamination, Drainage ditches, In-Situ remediation*

2. Introduction

There are a large number of potential pollutants (suspended solids, fine particles, heavy metals, nutrients, organic chemicals including herbicides and pesticides and faecal indicator bacteria) on highways and routine cleaning is a must, especially in the case of gully pots, entrapment structures and carriage ways (Kayhanian, et al., 2017). Accumulation of leaves, plastic and other waste materials in gully pots can cause damage due to spillage. In this context, proper management of plants and regular use of herbicides for weeds on the motorways and around drains is a must.

Highway runoff carrying pollutants has been affecting the receiving water bodies for a very long time illustrated by Urban development and its impact on water quality (Arnold, et al., 1996). Previous studies show that the quality of both, the water and the sediments, is affected by the highway runoff. Further, the aquatic ecosystems, i.e., living organisms and communities, are adversely affected by the metals, hydrocarbon and anions in the runoff (Moy, et al., 2003).

In UK the Highway Agency has been tasked with ensuring the clean-up of the discharge from roadways and motorways into the receiving stream or river. The Highway Agency has fixed treatments plants for predicted pollutants concentration for example in M40 motorways depth and velocity monitors are installed. The Highway Agency has installed treatment plants to deal with the predicted levels and concentration of pollutants, and simultaneously coordinates with the Environment Agency to coordinate with the Environmental Quality standard (EA, 2003).

Highways England is interested in re-designing the ditches to make them self-cleaning and this study is also focused on research and provision of new ideas for improvement of English motorways, primarily with regard to drainage ditches.

The main objectives of this studies are as follows.

1. To better understand the relations between pollutant concentrations in highway run off and traffic flows, frequency of rainfall, rainfall intensity and rainfall durations.
2. To evaluate the various impacts of highway runoff on receiving water.
3. To develop a model to evaluate the potential for implementation of a ‘SUDs’ approach for the remediation of highway run off.

3. Research Gap

Transportation and mobility are one of the main standards for development in the modern society. However, the portion of road covers the land and that landscape will have a physical chemical and biological impact on the health as well as on the environment.

There are many studies done for the identification and classification of the highway pollutants (Kayhanian et al., 2011, German et al., 2002, Ngabe et al., 2000, Davis et al., 2001, Huang et al., 2004, Zhao et al., 2010). This study however is based on the remediation of the highway runoff by *In-Situ* treatment. This study has tried to replace the old ditches by new self-cleansing ditches and has also work on the *In-Situ* remediation of highway runoff. *In-Situ* remediation is based on the classification of biologically compositable pollutants and chemical pollutants which needs to be treated. Enhancement of new technology such as smart ditches has also been focused.

This study has tried to work on the remediation of long-time highway runoff scales. Identification of the key contaminants in the different layer of the soil has also been covered in the literature which includes the soil overlaying the system and the water aquifer as well as the receiving water bodies. All of this process is performed by the construction of different contours of equal elevation at the site of the study, identification of major pollutants, rainfall characteristics of that area. Correct calculation of the flow based on this study has helped in the design of the retention pound which will accumulate the pollutants.

4. Methodology

4.1 Theory

When the road is levelled or nearly levelled the drainage as well as the velocity required for self cleaning is difficult. The solution for this problem is to vary the gradient of the cross fall of the carriage ways so that the ditches do not over float. The spacing between the drainage ditches and the gullies can be calculated by the formula

$$\frac{0.235b_{13}^{12}h_{13}^{16}}{m} = (IW)_{13}^{16} \quad (1)$$

Where b is the width of the rectangular gutter (mm)

h is the maximum depth of the water or the depth of the gutter (mm)

I is the rainfall intensity (mm/h)

W is the width of the carriage way.

m is the outlet spacing (mm)

From the point of views of safety, it is very necessary to make the Gutter trapezoidal in cross section. There are replacements in formula for making it into a rectangular portion where b is replaced by

$$b = w + 0.5k \quad (2)$$

where w is the width of the bottom of the trapezoidal channel,

k is the sum of the contingents of the angle of the inclination of the two sides of the trapezium.

In area where there is discharge being done by surface water runoff directly to ditches, care should be taken to ensure that the water table beneath the highway should not be affected by the water in the ditches. There is a need of surface water swear to discharge the extra sewage. However, in the UK French drains are constructed which can serve in both lowering the ground water table as well as well as surface water swear.

Ditches have been used for many years to solve the problems of drainage on cut or fill slope. To mintage the risk of erosion rills and gullies a special type of ditch called Drainage interceptor ditches are been used.

4.2 Procedure

This portion of the road has existing drainage system as well as space for making a sediment transportation pound. The rainfall data were collected from the metrological station of oxford. With the help of the collected perimeter the area calculation of the road sections where done in auto cad. The Total area of the road portion was found out to be 55193.6089 sq. m and the total area covered by the entire study area was found out to be 102960 sq.m. A path was created in google earth with as many points as possible so as to create a contour of that area. With the help of TCX converter the different coordinates of the drawing then where levelled into its altitude longitude and latitude. After the coordinate system was fixed in excel quick grid was used to draw the contour between same altitudes. It was then exported to auto cad to find out the contours between the different planes.



Figure-1 Google earth Image of Project location (source: Google earth 2019)

4.2 Design of self-cleansing Retention pond Pond

The design of the retention along the junction 10-11 in M40 motorways at oxford was done using MDSuDS (Micro Drainage for Sustainable Drainage Design) software. (MDSuDS 2017, Version 2.1) From the measurement done in Auto Cad, (Auto cad 2019, student Version) the areas of the pond were purposed.

Table -1 Input parameters for the Design of Self cleansing Pond

Pounding Area		Filter Area	
Exceedance level (m)	113.00	Base Level (m)	109.15
Base Level (m)	110.00	Depth above Base(m)	0.10
Free board (mm)	100	Diameter (mm)	150
Base area	200	No of Barrels	4
Length (m)	20	Manning's n	0.016
Slope	0.10		
Side slope	0.00		
Top Area (m ²)	200		
Base perimeter (m)	60		
Top Perimeter (m)	60		
Filter rate (m/hr)	28.7		

Exceedance level, Base level and Free board is the actual measurement of the field. Top area of 200 sq. meter is taken by comparing

5. Result

The final results were obtained after the water collected in the drainage ditches at junction 10-11 on M40 motorways was passed on to the designed retention pond. The Pond was designed in such a way that it could collect all the sewage water from the motorways and a design period of the pond was considered as 100 years. Rainfall and flood prediction were also done for the designed years. Different pollutants present in the sewage was designed to be treated in the retention pond before the water goes out to the Souldern Brook. There are two types and class of pollutants which are classified as metals and organic pollutants.

Different concentration of the pollutants was obtained and compared with the Environmental quality standard (EQS). The following table estimates the different pollutants concentration at input and output and also evaluation of the volume reduced in the self-cleansing pond.

Table -2 Pollution Concentration (source: EQS 2004)

Pollution Concentration (mg/L)										
Pollutant name	Input (mg/L)				Output (mg/L)			Reduction (%)		
	EQS	Mean	Minimum	Maximum	Mean	Minimum	Maximum	Mean	Minimum	Maximum
Copper	0.001 - 0.028	0.0403	0.0403	0.0403	0.0403	0.0403	0.0403	0	0	0
Filter Copper	0.03	0.01747	0.01747	0.01747	0.01747	0.01747	0.01747	0	0	0
Zinc	0.008	0.0006	0.0006	0.0006	0.0006	0.069899	0.069899	0	0	0
Benzobfluoranthene	1.7*10 ⁻⁵	0.00014	0.00014	0.00014	0.00014	0.00014	0.00014	0	0	0
Benzokfluoranthene	0.00027	0	0	0	0	0	0	0	0	0
Benzopyrene	0.0082	0.00014	0.00014	0.00014	0.00014	0.00014	0.00014	0	0	0
Indeno123cdypyrene	0.0082	0.001	0.001	0.001	0.001	0.00046	0.00046	54	54	54
Benzoghiperylene	0.008	0	0	0	0	0	0	0	0	0

There were a lot of pollutants that were found out whose concentration was above Drinking Water and Freshwater Environmental Quality Standards (EQS). These pollutants are considered as significant determinants and need for the remediation before they are drained to the Cherwell Valley. The main significant pollutants are listed in the table.

The study identified high concentrations of Copper and zinc in the site. These pollutants are observed to maximum level due to storm water falling on the road surface interacts human activities (e.g. accidents and dispersion of chemicals), wearing of road materials and vehicles (e.g. brakes, tires).

6. Conclusion

Having identified the main pollutants that are transported in the highway runoff, it is now possible to design retaining structures to store the highway runoff for a suitable period of time so as to remediate the pollutants on the site itself. This is a big step forward in addressing the

gap between pollution control and remediation of highway runoff, as well as a new practice toward sustainability in the UK.

The process of contamination transfer and *In-Situ* treatment before it reaches the receiving water body is described below.

Storm water falling on the road surface interacts with residual materials from human activities such as accidents and dispersion of chemicals, wearing of road materials and vehicles e.g. brakes, tires, and leaching from construction materials (corrosion of metallic roof, leaching of biocides from plastic, etc.).

This storm water then passes on to the smart ditches and full retention oil traps which carry the storm water to the retention pond.

In the retention pond the pollutants are treated to cause there to biodegradation and plants like *Pistia Stratiotes* absorb the harmful pollutants which are non-bio degrade.

The water from the retention pond goes to the receiving water, which in our case, is Shouldern Brook.

The above steps illustrate the process of pollutant transfer and treatment on the site. The capacity of the receiving pond is designed in accordance with the projections of the rainfall data for the area. Further, these retention ponds are designed to accommodate runoff of upto a kilometre and need to be constructed at 1km interval.



Figure-2 Designed pond (source: *Suds software*)

The designed retention pond as in figure is designed in such a way that it can filtrate most of the water leaving the impurities on the ground which will be taken by the plants through the roots. This type of detention pond design will also facilitate a long-term remediation process. This practice of the remediation can also be termed as natural remediation on site. In a hundred years period this site can be cleaned and new plantation can be thought off.

This process of creating a self-cleansing ditch is new and is thought to solve the problems of drainage disposal from highway. This kind of technology can also be employed in another feeder, primary or tertiary road network as well.

6.2 The way forward for further studies

The process of transfer of contamination is a very slow process. It is highly recommended that experimental design should be done on a long-term basis to identify the characteristics and true relation between transfer of the contaminants and their decay process.

Table -3 Not significant and Key Determinants

Determinants	
Not significant	Significant
Platinum	Copper
Palladium	Filter Copper
Simazine	Zinc
Amitrole	Benzobfluoranthene
Diuron	Benzokfluoranthene
Bromacil	Benzopyrene
Atrazine	Indeno123cdypyrene
Acenaphthylene	Benzoghiperylene
Acenaphthene	
Fluorene	
Fluorene	
Anthracene	
Dibenzo(ah)anthracene	

A number of possible relationships associated with highway runoff quality can be proposed:

- There is a correspondence between seasonal variation in climate and the highway runoff. The pollutants concentration is found highly in winter as there is a use of salt which combines with these metals. This way the mobility of the metals increases as well as the pollutants from the salt, particularly Aluminium Silicate (Clay) also combines and moves with the flow.
- A link may exist between runoff concentration and the rainfall. There has been seen that the concentration of the pollutants increases with rainfall duration. A 60 min study was undertaken to find out the level of concentration and the runoff and is found that the concentration increases. This result has been kept in the appendix.

To solve the problems of metals and other pollutants a phytoremediation technology can be used. Metals translocation and accumulation in the plants can solve to reduce the access metals in the runoff.

Table-4 Examples of hyperaccumulators and their accumulation characteristics (source: Odjegba2004)

Plant species	Pollutants	Results	Reference
Pistia stratiotes	Ag, Cd, Cr, Cu, Hg, Ni, Pb and Zn	All elements accumulated mainly in the root system.	Odjegba and Fasidi 2004
H. annuus	Pb	Pb concentrated in the leaf and stem indicating the prerequisites Of a hyperaccumulator plant	Boonyapookana et al. 2005
Arabis gemmifera	Cd and Zn	Hyperaccumulator of Cd and Zn, with phytoextraction capacities almost equal to T. caerulescens	Kubota and Takenaka 2003
Sunflower	Benzobfluoranthene	Synthetic Chelating agents did not increase the uptake of heavy metals for equal soluble concentrations in the presence and absence of chelates. Proper use of soil amendments increased the phytoextraction of Benzobfluoranthene	Tandy et al. 2006; Clemente et al. 2006; Chen et al. 2006
A. bisulcatus and B. juncea	Benzokfluoranthene and Benzopyrene	There was a substantial improvement in B. juncea accumulation	LeDuc et al. 2006
B. napus and B. juncea	Indeno123cdypyrene	Lipid changes in B. juncea, the well-	Quartacci et al. 2006; Belimov et al. 2005;

		known B. napus hyperaccumulator Species.	Nouairi et al. 2006; Sheng and Xia 2006
--	--	--	---

Phytoremediation at the contaminated side can be thus used to solve the high contamination. The root biomass is able to immobilize the bio mass and uptake, precipitate and finally gets stored in the branches and other parts of the plant.

Copper and filter copper can be reduced in volume from the highway runoff by the use of Pistia Stratiotes. Pistia stratiotes need a sandy and silty clay soil for its growth. Motorways in UK are made up with sandy and silty soil hence are beneficial for the growth and developments of this plants. All the plants species that are specified in the table above can be planted along the motorways of United Kingdom.

Acknowledgements: I would also like to give special thanks to my family as a whole for their continuous support and understanding when undertaking my research and writing my project. Your prayer for me was what sustained me this far.

8. Refrances

Davis et al., A.P. Davis, M. Shokouhian, S.B. Ni. 2001. *Loading estimates of lead, copper, cadmium, and zinc inurban runoff from specific sources*. 44., 997-1009

EQS, 2004. Environmental Quality Standards, Annex G

Eriksson, E., Baun, A., Scholes, L., Ledin, A., Ahlman, S., Revitt, M., Noutsopoulos, C. and Mikkelsen, P.S. 2007. *Selected stormwater priority pollutants – A European perspective. Science of the Total Environment* 383: 41-51.

F Moy, R W Crabtree, T Simms., 2003. **THE LONG TERM MONITORING OF POLLUTION FROM HIGHWAY RUNOFF: FINAL REPORT**, R&D Technical Report P2-038/TR1.

German, J., Svensson, G., 2002. **Metal content and particle size distribution of street sediments and street sweeping waste**. Water Science and Technology 46, 191e198.

Huang et al., X.J. Huang, T. Pedersen, M. Fischer, R. White, T.M. Young. 2004. **Herbicide runoff along highways. 1. Field observations**. Environ. Sci. Technol. 38., 3263-3271

Kayhanian, M., Givens, B., 2011. **Processing and analysis of roadway runoff micro (<20 mm) particles**. Journal of Environmental Monitoring 13 (10), 2720e2727.

Masoud Kayhanian., Hui Li., John T.Harvey., XiaoLiangc. 2019. **Application of permeable pavements in highways for stormwater runoff management and pollution prevention: California research experiences. International Journal of Transportation Science and Technology**

MDSuDS 2017, **Version 2.1 A complete SuDS design and analysis solution, from conceptual design to hydraulic flow analysis**

Ngabe et al., B. Ngabe, T.F. Bidleman, G.I. Scott. 2000. *Polycyclic aromatic hydrocarbons in storm runoff from urban and coastal South Carolina.*, Sci. Total Environ. 255 (2000) 1-9

Ngabe et al., B. Ngabe, T.F. Bidleman, G.I. Scott. 2000. **Polycyclic aromatic hydrocarbons in storm runoff from urban and coastal South Carolina.**, Sci. Total Environ. 255 (2000) 1-9

Nouairi, I., Ben Ammar, W., Ben Youssef, N., Daoud, D. B., Ghorbal, M. H., & Zarrouk, M. (2006). **Comparative study of cadmium effects on membrane lipid composition of Brassica juncea and Brassica napus leaves.** Plant Science, 170(3), 511–519.

Odjegba, V. J., & Fasidi, I. O. (2004). **Accumulation of trace elements by Pistia stratiotes: Implications for phytoremediation.** Ecotoxicology, 13, 637–646.

Penda Corp. Manufacturing today. 2011. Business media publications., east Randolph., Chicago. Penda crop, 2011. <https://www.penda.com>

Quartacci, M. F., Argilla, A., Baker, A. J. M., & Navari-Izzo, F. (2006). **Phytoextraction of metals from a multiple contaminated soil by Indian mustard.** Chemosphere, 63(6), 918–925.

Queensland case study. Journal of Environmental Engineering 126: 313-320
Smartditch uk., 2019, <https://smartditch.co.uk/>

Zhao, H., Li, X., Wang, X., Tian, D., 2010. **Grain size distribution of road-deposited sediment and its contribution to heavy metal pollution in urban runoff in Beijing, China.** Journal of Hazardous Materials 183 (1e3), 203e210.

EVALUATION OF THE UNIT POLLUTANT LOADS AND URBAN HEAT ISLAND MITIGATION FUNCTION OF LOW IMPACT DEVELOPMENT (LID) TECHNOLOGIES

*Md Tashdedul Haque, Nash Jett DG. Reyes, Heidi B. Guerra, Minsu Jeon, Lee-Hyung Kim**
Kongju National University, Civil and Environmental Engineering Department, Cheonan City, South Korea
*Corresponding author (leehyung@kongju.ac.kr)

ABSTRACT

LID technologies were previously used solely for stormwater runoff treatment, but further advancements in the design of these systems also expanded their functions and benefits. This study assessed the unit pollutant loads generated in various urban features (i.e. roads and parking lots) and the effectiveness of LID facilities in treating NPS pollutant loads. Moreover, the contribution of LID technologies in alleviating UHI conditions was also investigated in this inquiry. As compared to the typical unit pollutant loads in South Korea, it was found that the stormwater unit pollutant loads in the study area were relatively low due to the limited anthropogenic activities and pollutant generation opportunities in the catchment area. It was also noted that the mean surface temperature in LID facilities are up to 7.5°C lower than the surrounding paved environment, indicating that nature-based systems are beneficial for mitigating the UHI effect.

Keywords: LID facilities, unit pollutants load, UHI

INTRODUCTION

Several countries around the world have implemented low-impact development (LID) strategies for a variety of application scenarios (Hilliges et al., 2017). Apart from the increase in point and non-point pollutant generation, highly developed and paved areas generally affect microclimate conditions. The urban heat island (UHI) effect, which is described as the phenomenon wherein the observed ambient temperature in urban areas are greater than those in the surrounding rural areas, is also considered one of the major effects of land use changes (Balany et al., 2020).. Increasing the green space coverage can provide a multitude of benefits to urban areas, including stormwater management, temperature, control of increased biodiversity, and improved air quality (Shafique et al., 2017). This study assessed the unit pollutant loads generated in various urban features (i.e. roads and parking lots) and the effectiveness of LID facilities in treating NPS pollutant loads. Moreover, the contribution of LID technologies in alleviating UHI conditions was also investigated in this inquiry

MATERIAL AND METHODS

The schematic diagrams of LID facilities, Infiltration, Trench (IT) and rain garden (RG), located at the Kongju National University (KNU), Chungnam Province, South Korea were

illustrated in Figure 1. The IT and RG have dimensions (L:W: H) of 5:1.2:1.3 and 6:1.2:1.2, respectively and were constructed to treat stormwater runoff from 100% impervious road and parking lot. A total of 65 rainfall events were monitored for the IT from 2009 to 2021, whereas 27 events, from 2014 to 2021, were monitored for RG.. Standard laboratory procedure were conducted to determine total suspended solids (TSS), biochemical oxygen demand (BOD), and chemical oxygen demand (COD) concentrations in stormwater. The concentrations of nutrients, such as total nitrogen (TN) and total phosphorus (TP), in, stormwater were also investigated in the study. In order to evaluate the effects of LID technologies in UHI effect mitigation, the Testo-875 thermal infrared camera was utilized to record temperatures inperaturesin the facility and the surrounding area.

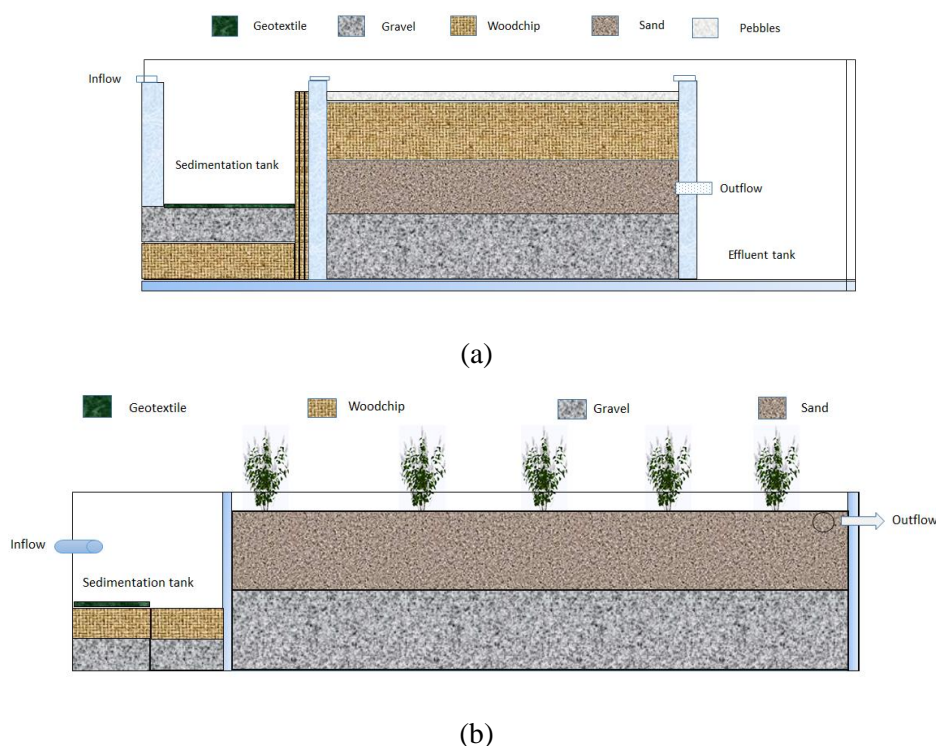


Figure 1. Schematic diagrams of the (a) IT and (b) RG

RESULTS AND DISCUSSIONS

The annual influent and effluent unit pollutant loads in the facilities were shown in Figures 2a and 2b. The annual influent TSS, BOD, COD, TN, and TP unit pollutant loads in the IT were 0.46 kg/ha/yr, 0.51 kg/ha/yr, 0.45 kg/ha/yr, 0.15 kg/ha/yr, and 0.02 kg/ha/yr, respectively. As compared to the observed influent pollutant loads in IT, the influent stormwater samples collected from RG exhibited 7% to 28% lower pollutant loads. Moreover, the deposition of pollutants in the catchment area of RG are relatively lower since parking lots are seldom used during academic breaks. Among the analyzed water quality parameters, mean BOD loads were found the highest due to the accumulation of plant detritus within the vicinity of the facilities. The effluent pollutant loads were considerably reduced after undergoing treatment from the LID facilities. The sedimentation tank primarily contributed in the removal of particulates and particulate-bound pollutants, whereas the filter media greatly enhanced the removal of finer

particles that cannot be removed through sedimentation. In the case of RG, the presence of plants further enhanced the removal of pollutants through uptake and assimilation.

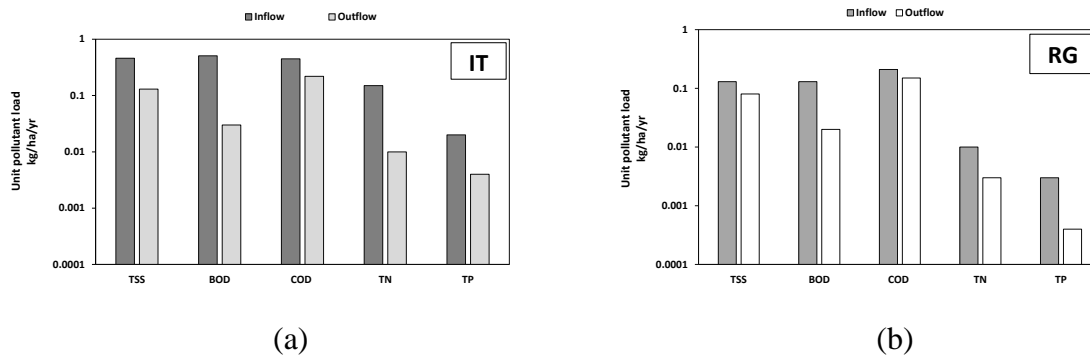


Fig 2 Average annual pollutant loads in the a) IT and b) RG

The report published by KEI indicated that the typical BOD, TP, and TN unit pollutant loads in the runoff from a 100% impermeable catchment were approximately 44 kg/ha/yr, 2 kg/ha/yr, and 17 kg/ha/yr. As shown in Figure 3, the pollutant loads in the stormwater collected from Kongju National University’s parking lots and roads were relatively lower than the typical unit pollutant loads in South Korea, implying that minimum intervention is required to treat the runoff from the study area. Since anthropogenic-related activities in the university’s compound are limited, especially during the academic breaks, the potential sources of pollutants are also reduced

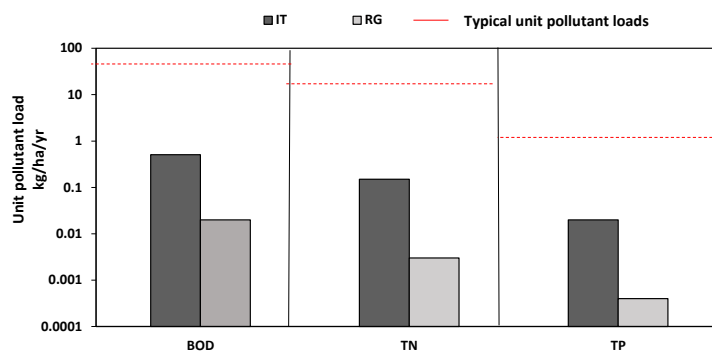


Figure 3. Comparison of the studied stormwater runoff and the typical unit pollutant load values in South Korea

The effect of LID facilities in the urban surface temperature was exhibited in Figure 4. It can be noted that the mean surface temperature in LID facilities are up to 7.5°C lower than the surrounding paved environment. As compared to the recorded surface temperature in IT (13.56°C), the mean surface temperature in RG (16.52 °C) was relatively higher. Despite the presence of plants inside RG, this facility was directly exposed to sunlight which caused elevated surface temperatures. Overall, the thermal images revealed a positive impact of LID technologies in mitigating UHI effect.

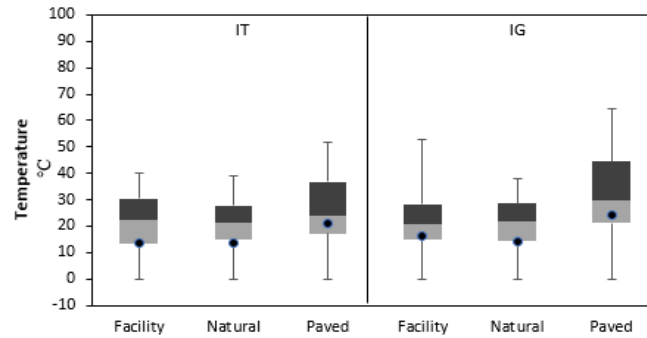


Fig 4 Box plot of highest average temperature for IT and RG

CONCLUSION

The application of LID technologies are one of the vital options for NPS pollution control and UHI effect mitigation in urban areas. The assessment of the unit pollutant loads in stormwater revealed that considerable amounts of particulates, organics, and nutrients can be washed-off in urban areas during storm events. Nature-based treatment facilities, such as the RG and IT, were capable of removing pollutants in stormwater runoff. Specifically, the sedimentation in filtration mechanisms considerably reduced the pollutant fractions in the influent. Apart from NPS pollutant removal, the facilities also exhibited an environmental cooling effect, implying that nature-based systems are capable of alleviating UHI conditions in an urban area.

ACKNOWLEDGMENT

This work was supported by Korea Environmental Industry & Technology Institute (KEITI) through Wetland Ecosystem Value Evaluation and Carbon Absorption Value Promotion Technology Development Project, funded by Korea Ministry of Environment (MOE) (2022003630005).

References

- Balany, F., Ng, A. W., Muttill, N., Muthukumaran, S., & Wong, M. S. (2020). Green infrastructure as an urban heat island mitigation strategy—a review. *Water*, 12(12), 3577.
- Hilliges, R., Endres, M., Tiffert, A., Brenner, E., & Marks, T. (2017). Characterization of road runoff with regard to seasonal variations, particle size distribution, and the correlation of fine particles and pollutants. *Water Science and Technology*, 75(5), 1169-1176.
- Shafique, M., & Kim, R. (2017). Application of green blue roof to mitigate heat island phenomena and resilient to climate change in urban areas: A case study from Seoul, Korea. *Journal of Water and Land Development*, 33(1), 165

MODELING OF THE RAINFALL-WATERSHED-SWALE EXPERIMENTAL SYSTEM BY EPA SWMM

Kebir Emre Saraçoğlu¹ and Cevza Melek Kazezyılmaz-Alhan^{2,}*

¹ *Istanbul University-Cerrahpaşa, Civil Engineering Department, Istanbul, Turkey*

² *Istanbul University-Cerrahpaşa, Civil Engineering Department, Istanbul, Turkey*

**Corresponding author (meleka@iuc.edu.tr)*

ABSTRACT

Urbanization and global climate change cause flooding to be experienced with more destructive effects in living areas. In order to mitigate these effects, various engineering solutions are being introduced. Low Impact Development (LID) is one of these solutions which are both environmentally friendly and low-cost methods and therefore, widely used. The most common types of LIDs are vegetative swale, bioretention, green roof, rain barrel, and rain garden. The Environmental Protection Agency Storm Water Management Model (EPA SWMM) is one of the few programs which can model many types of LIDs. In this study, the modeling performance of EPA SWMM for vegetative swale was investigated by comparing the modeling results with the experimental data. Results show that the experimental measurements are in good agreement with the EPA SWMM outputs, but there is room for improvement.

Keywords: Vegetative Swale, Low Impact Development, EPA SWMM, Hydrological Modeling.

1. INTRODUCTION

Urbanization leads to significant changes in the hydrological behavior of watersheds. In addition, catastrophic events such as floods occur more frequently and severely. Some engineering methods have been put forward to mitigate the devastating effects of disasters. Low Impact Development (LID) is also one of these methods. Vegetative swales are one of the preferred types of LIDs to delay the surface flow and increase infiltration and storage volume. Vegetative swale is a vegetated open channel structure with side slopes. Nowadays, numerical models are widely used to design vegetative swales. These models help us to characterize the hydrological performance of vegetative swale by simplifying their behavior. However, there are limited number of models that can be used to simulate the hydrological behavior of vegetative swales. One of these models is the Environmental Protection Agency Storm Water Management Model (EPA SWMM).

In the literature, there are very limited studies that have focused on the modeling of vegetative swale. Abida et al. (2007) developed a model for the design and analysis of a grass swale-

perforated pipe system. Imteaz et al. (2013) tested the accuracy of the MUSIC (Model for Urban Stormwater Improvement Conceptualisation) for different stormwater treatment methods. Liu et al. (2015) used the Long-Term Hydrologic Impact Assessment-LID 2.1 (L-THIA-LID 2.1) for 16 different scenarios to determine the effects of BMPs on water quantity and water quality. Rujner et al. (2018) modeled the behavior of a vegetative swale using the Mike SHE. Mei et al. (2018) carried out an analysis of the effects of LIDs on flood mitigation with the SWMM and Life Cycle Cost (LCC). Gao et al. (2019) investigated the effects of a LID Layout Plan for a highway service area in China on hydrological behavior with the EPA SWMM. Li et al. (2020) investigated the optimum LID design and hydrological performance using the SWMM 5.

In this study, modeling capability of EPA SWMM for vegetative swale was investigated. For this purpose, the experimental data obtained from Rainfall-Watershed-Swale (RWS) experimental system by Saraçoğlu and Kazezyılmaz-Alhan (Saraçoğlu, 2022) was employed. RWS system was modeled using the EPA SWMM and the model outputs were compared with the measurements.

2. MATERIAL AND METHODS

The EPA SWMM is a widely used rainfall-runoff model. The feature that makes this model superior to other models, is its modeling ability of various types of LIDs. EPA SWMM allows for modeling LID types of bioretention, rain garden, green roof, permeable pavement, infiltration trench, and rain barrel. In EPA SWMM, different layers need to be defined, such as the surface, soil, storage, drain, and pavement for different LID types. In these layers, various numbers of design parameters are used. Vegetative swale has the least number of design parameters with only one layer, which is the surface layer, among the types of LIDs. Its design parameters are the berm height, vegetation volume fraction, surface roughness, surface slope, and swale side slope.

The data obtained from the RWS experimental system by Saraçoğlu (2022) was used to test the EPA SWMM results. Therefore, RWS system was modeled in EPA SWMM. RWS consists of 3 main components which are the sprinkler system, watershed area, and swale module. It was designed to test different parameters of a vegetative swale. The parameters taken into account in the experiments are rainfall intensity, rainfall duration, areal rainfall, surface roughness, and soil hydraulic conductivity. The EPA SWMM model of RWS is presented in Figure 1.

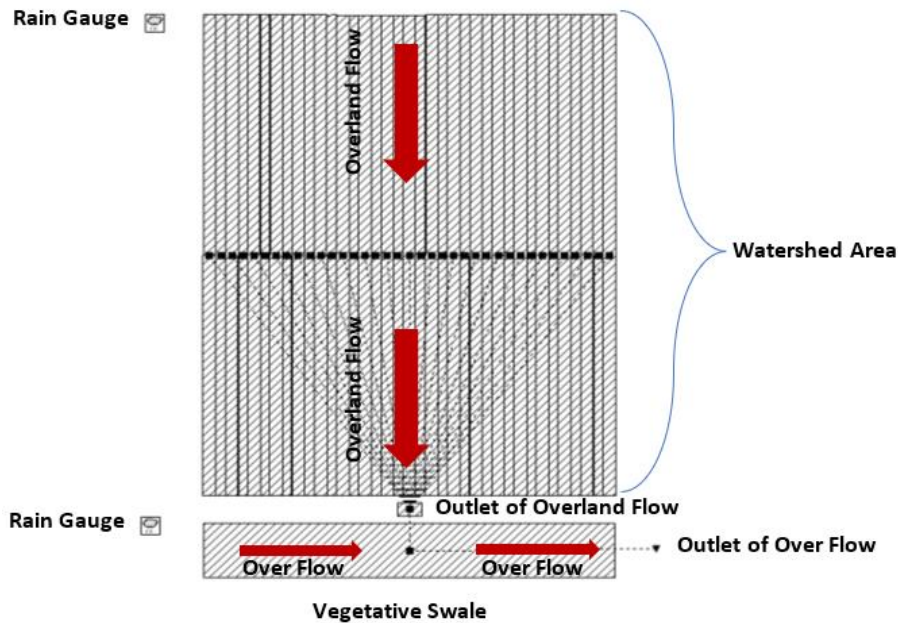


Figure 1. EPA SWMM model of RWS experimental system.

3. RESULTS AND DISCUSSION

In the modeling study of the vegetative swale by EPA SWMM, rainfall intensities of 20 and 30 mm/h, rainfall durations of 15 and 25 min, grass heights of 7 and 11 cm, and 4 different areal rainfall scenarios were used. A total number of 14 simulations were carried out for the vegetative swale. Figure 2 (a) and (b) show the results obtained for 20 mm/h rainfall intensity and 15 min of rainfall duration and 30 mm/h rainfall intensity and 25 min of rainfall duration, respectively. Both graphs are obtained with the same grass height of 7 cm and under the same rainfall scenario R-A (which represents the areal rainfall over the whole watershed). The model results are in general in good agreement with measurements. However, improvements can be made, in particular for the falling limb part of the hydrograph.

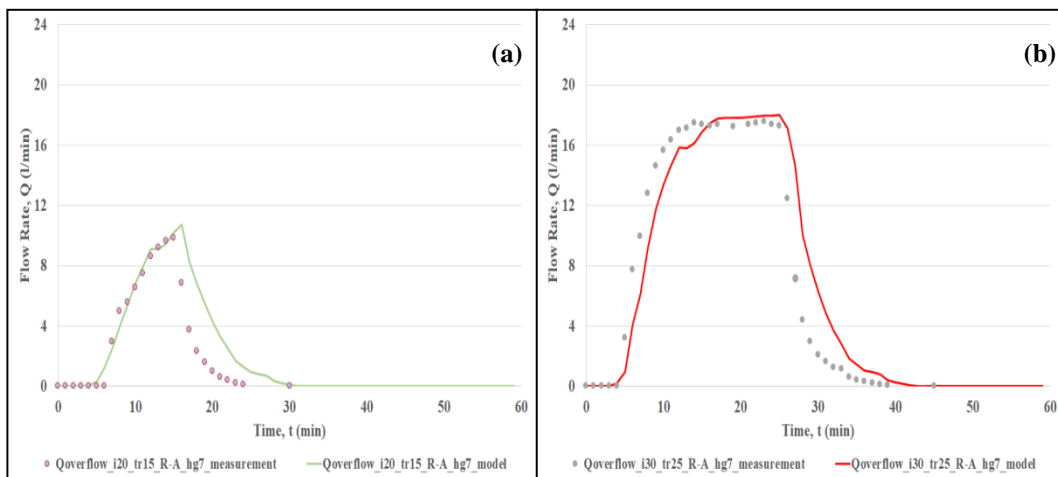


Figure 2. The measured and calculated over flow comparisons.

4. CONCLUSIONS

In this study, the capability of the EPA SWMM to model a vegetative swale was evaluated. For this purpose, the hydrological model of the RWS experimental system was generated using the EPA SWMM and model outputs were compared with experimental data. Results show that the calculated over flow values are in acceptable range but there is room for improvement. Moreover, EPA SWMM does not contain any design parameters for defining soil, storage, and drain properties. With the inclusion of these layers and related parameters in the EPA SWMM for vegetative swale, the design and modeling of vegetative swale can be carried out more effectively and accurately.

Acknowledgements: The authors acknowledge the funding provided by Istanbul University-Cerrahpaşa Scientific Research Projects Unit.

REFERENCES

- Abida, H., Sabourin, J.F. and Ellouze, M., 2007, ANSWAPPS: Model for the analysis of grass swale-perforated pipe systems, *Journal of irrigation and drainage engineering*, 211–221.
- Gao, J., Pan, J., Tang, R., Guo, S. and Liu, Y., 2019, LID facility layout and hydrologic impact simulation in an expressway service area, *Polish journal of environmental studies*, HARD Publishing Company, 28(6), 4153–4162.
- Imteaz, M.A., Ahsan, A., Rahman, A. and Mekanik, F., 2013, Modelling stormwater treatment systems using MUSIC: Accuracy, resources conservation and recycling, 71, 15–21.
- Li, Y., Huang, J.J., Hu, M., Yang, H. and Tanaka, K., 2020, Design of low impact development in the urban context considering hydrological performance and life-cycle cost, *Journal of flood risk management*, Blackwell Publishing Inc., 13(3).
- Liu, Y., Bralts, V.F. and Engel, B.A., 2015, Evaluating the effectiveness of management practices on hydrology and water quality at watershed scale with a rainfall-runoff model, *Science of the total environment*, Elsevier, 511, 298–308.
- Mei, C., Liu, J., Wang, H., Yang, Z., Ding, X. and Shao, W., 2018, Integrated assessments of green infrastructure for flood mitigation to support robust decision-making for sponge city construction in an urbanized watershed, *Science of the total environment*, Elsevier B.V., 639, 1394–1407.
- Rujner, H., Leonhardt, G., Marsalek, J., Perttu, A.M. and Viklander, M., 2018, High-resolution modelling of the grass swale response to runoff inflows with Mike SHE, *Journal of hydrology*, 562, 411–422.
- Saraçoğlu, K.E., Kazezyılmaz-Alhan, C.M., 2022, Evaluation of vegetative swale performance via experimental and mathematical modeling, Ph.D. Thesis, Istanbul University-Cerrahpaşa, Istanbul.

INTRODUCTION AND REVIEW OF PRELIMINARY CONSULTATION SYSTEM FOR LOW IMPACT DEVELOPMENT TO REDUCE OUTFLOWS AND NON- POINT SOURCE POLLUTIONS

Hyojeong Lee¹, Hyunsuk Shin^{1*}, Jihyun Moon¹, Jaemoon Kim², Youngsu Jang²

¹. Pusan National University, Civil and Environmental Engineering, Busan, Republic of Korea

². Pusan National University, Green Land & Water Management Research Institute, Busan, Republic of Korea

*Corresponding author (hsshin@pusan.ac.kr)

ABSTRACT

In this study, the aim and implementation procedures of the “Pre-consultation system for LID”, the type and preference of facilities mainly applied in Republic of Korea, and the direction in the future. In addition, it discussed about green area, necessary countermeasures, and installation countermeasures through the development project report that completed the Seoul “Pre-consultation system for LID” from 2014 to 2021.

Keywords: *low impact development(LID), pre-consultation system, stormwater, installation countermeasure*

1. INTRODUCTION

In Republic of Korea, the impermeable layer has increased rapidly due to urbanization since the 1960s, causing many urban problems due to distortion of natural hydrological cycle, such as an increase in water surface outflow, evapotranspiration, and a decrease in infiltration rate. In 2014, the Seoul Metropolitan Government amended and promulgated the Seoul Metropolitan Government Framework Ordinance on “Water Cycle Recovery and LID”, and at the same time enforcing to the “Pre-consultation system for LID” that keep to green space and hydrological cycle and water environment.

The consultation period of the “Pre-consultation system for LID” should be considered from the initial stage of establishing various development plans (authorization of development projects) to minimize water surface outflow and NSPs outflow.

In this study, the aim and implementation procedures of the “Pre-consultation system for LID”, the type and preference of facilities mainly applied in Republic of Korea, and the direction in the future.

2. MATERIAL AND METHODS

The “Pre-consultation system for LID” is applied to projects subject to installation of stormwater storage and infiltration facilities, which are stormwater management stipulated in the Seoul Metropolitan Government Ordinance, for the purpose of circulating and eco-friendly management of stormwater.

The developer or admitter of the development project shall plan and consult on the introduction of stormwater management facilities to minimize the water surface outflow from the project site before the approval of various development projects. The Seoul Metropolitan Government sets the amount of stormwater for each classification of reference facilities to reduce and the amount of runoff, applies the amount of stormwater for each land use in the project area, and calculates the amount of installation measures for infiltration facilities, use, storage, and other facilities. If the calculated necessary countermeasures and installation countermeasures are compared and the installation countermeasures are larger than the necessary countermeasures, the consultation is completed by reasonable that it has been properly reviewed.

In fact, this study compared the area of the project, green area, necessary countermeasures, and installation countermeasures through the development project report that completed the Seoul “Pre-consultation system for Low Impact Development” from 2014 to 2021.

3. RESULTS AND DISCUSSIONS

A total of 34 reports of prior consultations on LID completed between 2014 and 2021 in Seoul, Republic of Korea were investigated. As a result, the Seoul Metropolitan Government approved development projects with a total area of 5,000 m² to 460,000 m², and some projects have a green space area of 140 m² to 150,000 m², with a minimum of 1.6% and a maximum of 36.4%. Generally LID facilities applied were penetration facilities such as permeable pavement, Dry well, infiltration trench, infiltration channel, stormwater storage tank, and green roof of which the most frequently introduced facilities were permeable pavement (over 85%), infiltration trench (5%) and green roof (3%).

According to the result of how much the installation countermeasures are over-designed compared to the necessary countermeasures, 4 projects are over-designed and 10 projects are under-designed less than 0.1%, so it is necessary to present the standard scope range when applying facilities.

4. CONCLUSIONS

This study investigated the introduction and status of the “Pre-consultation system for LID” in Seoul Republic of Korea, and compared the calculation results of necessary countermeasures and using the types and sharing of stormwater storage.

There are 4 development projects with an installation countermeasure of more than 25%, which are considered to be over-designed compared to the necessary countermeasures, and six under-designed projects need to be recommended to install additional facilities to solve water problems in preparation for climate change.

As such, in Korea, the “Pre-consultation system for LID” has been in effect since 2014, and the number of consultations has increased every year. However, there is a lack of data on the actual application of facilities proposed in the preliminary consultation and the verification of the efficiency of each facility.

In addition, more than 85% of permeable pavements are applied, then excellent infiltration system is induced by equipment-type facilities such as Dry wells and infiltration trenches, but natural type facilities need to be spread considering multifunctional aspects such as continuous improvement of urban stormwater environment and response to climate change.

To this end, during prior consultation on low-impact development, appropriate standards should be presented through facility monitoring and verification of application effects, not only considering whether simple installation measures exceed necessary measures.

Acknowledgements: This work was supported by the "Graduate school of Green Restoration specialization " of Korea Environmental Industry & Technology Institute grant funded by the Ministry of Environment, Republic of Korea.

REFERENCES

- Woo-seok Han (2011). A Case Study on the Application of Low Impact Development in the U.S. to Improve Urban Rainwater Management, *Journal of Korea Research Institute for Human Settlements Brief*, (344), 1-6.
- Jung-Hee Choi (2014). The Characteristics and the Meaning of the Entire Revision of Seoul Metropolitan Ordinance on Rainwater Management, *Journal of clean technology*, 15(4), 21-32.
- Min-Kyu Ji, Hee Sagong & Yong-Joon Joo (2020). A Study on The Introduction of LID Prior Consultation for Small-Scale Development projects, *Journal of clean technology*, 26(2), 151-157.
- Seoul, Republic of Korea (2016). Pre-consultation system for Low Impact Development Guideline

EVALUATION OF WATER BALANCE FOR GREEN ROOF BASED ON K-LIDM

Jihyun Moon¹, Jaemoon Kim², Hyojeong Lee³, Jaerock Park⁴ and Hyunsuk Shin^{5*}

¹ Department of Civil and Environmental Engineering, Pusan national University, Busan, Republic of Korea

² Green Land and Water Management Research Institute, Busan, Republic of Korea

³ Department of Civil and Environmental Engineering, Pusan national University, Busan, Republic of Korea

⁴ Green Land and Water Management Research Institute, Busan, Republic of Korea

⁵ Department of Civil and Environmental Engineering, Pusan national University, Busan, Republic of Korea

*Corresponding author (hsshin@pusan.ac.kr)

ABSTRACT

Due to rapid climate change and increased impervious surface by urbanization, Low Impact Development is emerging as a solution to this problem. This study analyzed the green roof system based on water balance using K-LIDM. Korea GI&LID center was utilized as study area and short-term rainfall was applied. As a result of the simulation, the rate of runoff reduction was 5.25~36.48%. As Green roof system depends on many environmental factors, more experiment with various specification is necessary to evaluate the quantitative water balance. This study result can be utilized as basis for establishing the general guidelines of green roof design.

Keywords: LID, green roof, K-LIDM, water balance

1. INTRODUCTION

Recently, urban flooding and drought has increasing due to climate change and urbanization. LID techniques referring to systems that use or mimic natural processes that result in the infiltration, evaporation and use stormwater to protect and control water quality is considered as new way to treat the damages in an environmental way. Green roof, the system that control the runoff by filtering, absorbing or detaining rainfall, has been studied and tested enough in USA, but those experiments are insufficient in Korea. This study researched the water balance according to various rooftop's parameters using Korea K-LIDM that is modeling program for Korea.

2. MATERIAL AND METHODS

Low Impact Development(LID)

LID minimizes the effect of development on nature and maintains the natural environment. LID techniques provide temporary retention area, increase infiltration, allow for pollutant removal and control the stormwater. This is very cost-effective as it reduces the cost of treating and managing rainfall. In this study, the target LID technique is green roof system.

K-LIDM

K-LIDM is a LID modeling program developed in Korea and analyze stormwater outflow reduction based on HSPF model. There are many applicable LID facilities including Porous

pavement, Bio-retention, Green roof, Rain tank, Planter box, Infiltration basin, Infiltration trench, Vegetated swale, Sand filter and Vegetable filter strip. All facilities are hydrologically linked and analyzed channel routing to each facility.

Study area and modeling

The study area is the rooftop of the Korea Green Infrastructure and Low Impact Development Center(Korea GI&LID Center) located at Pusan National University Yangsan Campus in Mulgeum-eup, Yangsan-si, Gyeongsangnam-do. Green roof consists of green roof, sidewalks, wooden boards, and impermeable concrete. Green roof, shown in Figure 1, area is 6m(B)×8m(L) and is covered with 150mm of soil and plants. Table 1 shows the parameters entered in K-LIDM.



Figure1. Korea GI & LID Center and green roof zone

Table1. Green Roof Facility Dimensions

Green Roof Facility Dimension	
Green Area(ha)	0.0048
Depth of Material(mm)	150
Slope of Roof top	0.001
Vegetative Cover	Ground Cover
Length of Roof top	8

3. RESULTS AND DISCUSSIONS

Short-term rainfall scenarios were used for the 2, 5, 10, 20, 30-year return period, the duration for 60, 120, 180 minutes, and the time distribution 5-minute intervals using the Huff's third quartile storm. The results are shown in Table 2.

Table 2. Green roof flood reduction rate in short –term rainfall.

Return Period	Peak Discharge Reduction(%)			Runoff Volume Reduction(%)			Time to Peak Reduction(min)		
	60	120	180	60	120	180	60	120	180
Duration(mm)									
2 year	36.48	16.21	12.66	41.71	32.29	30.32	5	5	0
5 year	21.48	10.49	7.59	29.83	23.78	21.79	0	5	0
10 year	14.14	8.41	6.29	25.05	19.97	18.36	0	0	5
20 year	10.19	6.81	5.57	21.79	17.37	15.98	0	0	5
30 year	8.93	6.17	5.25	20.28	16.15	14.87	0	0	5

As a result of the modeling, the shorter the reproduction period and the longer the duration in the same reproduction period, the lower the effect of runoff volume reduction rate. The maximum flood reduction rate was 36.48% for 43mm rainfall, and reduction rate was under 20% for 60.50mm.

4. CONCLUSIONS

In this study, the water balance according to the various specifications of green roof was analyzed by K-LIDM modeling. The short-term rainfall event was simulated and the rate of peak discharge reduction, runoff volume reduction, time to peak reduction was compared to before LID installation.

1. In the short-term rainfall scenario of 2, 5, 10, 20, 30-year return period, the duration for 60, 120, 180 minutes, green roof showed 5.25~36.48% runoff volume reduction rate compared to general concrete rooftop.

2. The shorter the reproduction period and the longer the duration in the same reproduction period, the lower the effect of runoff volume reduction rate.

3. As the green roof is affected by many environmental factors, it can be used as a data for establishing the standardization of the design guidelines of green roof.

Acknowledgements: This work was supported by the "Graduate school of Green Restoration specialization " of Korea Environmental Industry & Technology Institute grant funded by the Ministry of Environment, Republic of Korea.

REFERENCES

- Kim, S. B. (2020). Hydrological Performance Evaluation Method for Green Roof System Based on K-LIDM Modeling, Master's thesis, Pusan National University.
- Kim, B. S. (2019). A Study on Hydrological Performance for PNU Planter Box LID Facility Based on Field Experiments and K-LIDM Model, Master's thesis, Pusan National University.
- Jang, Y. S., Kim, J. M., Park, J. R. & Shin, H. S. (2017). Analysis of Water Cycle Efficiency in Korea GI&LID center using K-LIDM, *KSCE Journal of civil engineering*, 10, 392-393.

INVESTIGATING THE EFFICIENCY OF INFILTRATION TRENCHES FOR STORMWATER PEAK FLOW AND OUTFLOW REDUCTION USING SWMM

*Sergi Garbanzos, Johaimin Panalondong, Karlo Bryan Ng Cha, and Marla Maniquiz-Redillas**
Department of Civil Engineering, De La Salle University, 2401 Taft Avenue, Malate, Manila 1004, Philippines
*Corresponding author (marla.redillas@dlsu.edu.ph)

ABSTRACT

The issues brought upon by climate change and urbanization intensify the extreme weather conditions experienced today. To lessen these impacts, the concept of low impact development (LID) is currently being studied to improve the hydrological situations in urbanized locations. This study aims to investigate the efficiency of infiltration trench LIDs in an urbanizing region using the Stormwater Management Model (SWMM). The site area for this study is a road network located in Palo, Leyte, Philippines, and was modeled using a 30-year historical rainfall data and SWMM to obtain the hydrograph differences between the present condition and proposed LID scenarios. Infiltration trenches with varying sizes (2000, 4000, 6000 sqm.) were simulated, which generated nearly a 50% outflow and peak flow reduction for all sub-catchments. Since the flow reduction appeared to be comparable in the 4000 and 6000 sqm. scenarios, it was deduced that increasing it further from these values was inconsequential and excessive. The use of infiltration trench LID controls can be useful tools in mitigating runoff problems in urban areas.

Keywords: *hydrograph analysis, infiltration trench, low impact development, stormwater management.*

1. INTRODUCTION

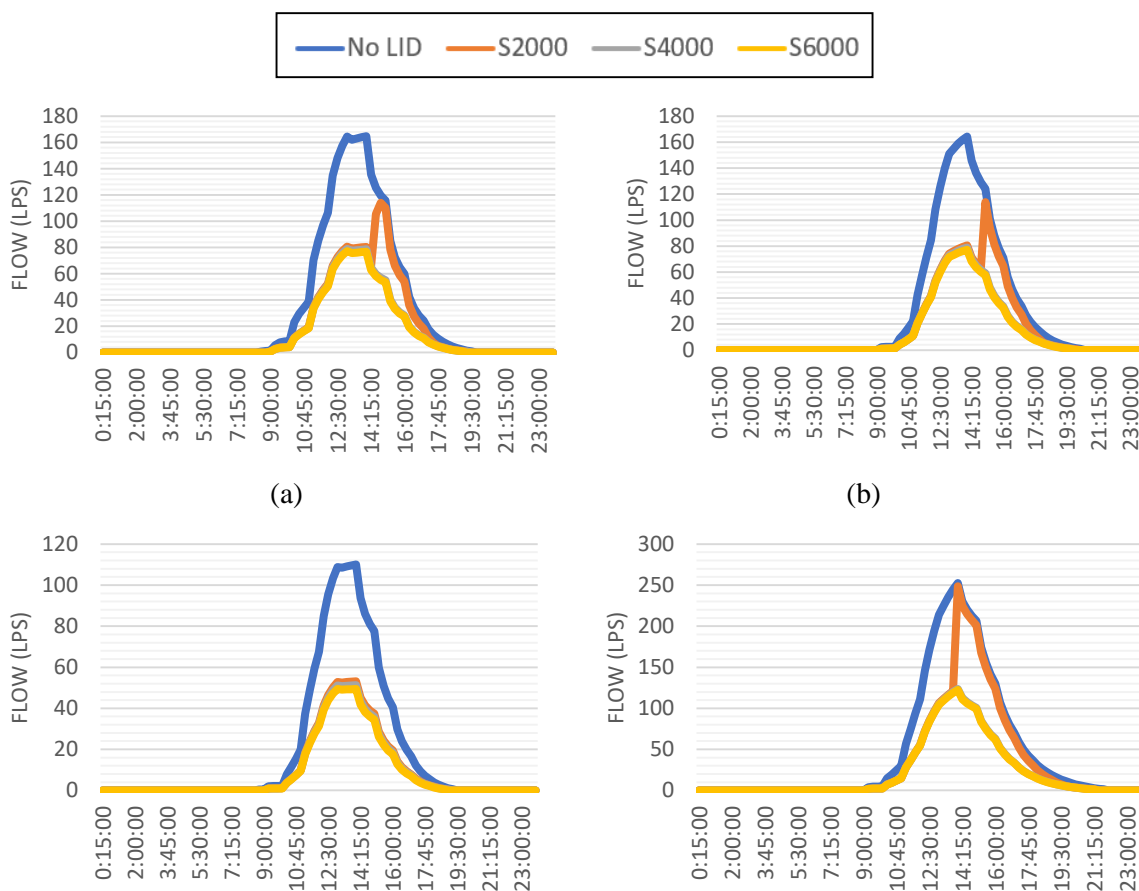
The changing climate conditions in recent years heightened the severity and duration of extreme weather events such as heavy precipitation and drastic flooding events (Wuebbles et al., 2014). The decrease in natural infiltration due to the spread of impermeable surfaces further amplifies these occurrences, significantly increasing peak discharges and total runoff yield from stronger storms in urbanized regions (Chin et al., 2013). The concept of low impact development (LID), a practical approach for managing stormwater, limiting runoff, and controlling rainfall levels (Shafique & Kim, 2016), has then been supported to alleviate the hydrological impacts of urbanization. The aim of this study is to investigate the efficiency of infiltration trench LIDs in an urbanizing region using the Stormwater Management Model (SWMM). The results of this study can present the effectiveness of LID structures, specifically infiltration trenches, in reducing the outflow and peak flow of rapidly urbanizing regions to mitigate local flooding issues and potentially decrease the size of drainage pipes.

2. MATERIAL AND METHODS

The Palo Bypass Road located in Palo, Leyte, Philippines (11°10'22"N, 124°59'23"E) was selected as the study area. Rainfall data were collected from the nearest rain gauge in the vicinity for the years 1990 to 2020 and were distributed and disaggregated over 24 hours using the Weibull Plotting Position and Triangle method. The Stormwater Management Model (SWMM) was used for modeling a no LID scenario and LID scenarios. The three simulated LID scenarios were named S2000, S4000, and S6000, which were representative of adding infiltration trenches with surface areas of 2000, 4000, and 6000 sqm. respectively. These were compared with the no LID scenario to determine the efficiency of infiltration trench structures within the applied sub-catchments.

3. RESULTS AND DISCUSSIONS

Figures 1a-e show the hydrograph comparisons for the five sub-catchments in the study site. SWMM results have shown that the total outflow of each sub-catchment underwent significant changes given the infiltration trench applications, peaking at a 70% reduction for all scenarios in sub-catchment 3. On average, outflow reductions from the S2000, S4000, and S6000 yielded around 41.55%, 50.37%, and 51.43% for all sub-catchments, respectively. Peak flow reductions, on the other hand, attained an average reduction rate of 41.45%, 49.81%, and 50.81% for the three LID scenarios as well. Both outflow and peak flow reductions within the 4000 sqm to 6000 sqm mark were observed to be similar to one another, indicating that further increasing the size at this point would be uneconomical.



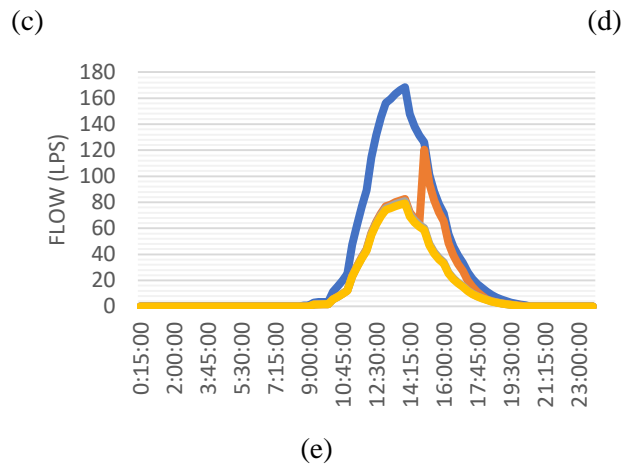


Figure1. Hydrograph comparison of the no LID and LID scenarios in (a) sub-catchment 1, (b) sub-catchment 2, (c) sub-catchment 3, (d) sub-catchment 4, and (e) sub-catchment 5

4. CONCLUSIONS

This assessment has demonstrated the infiltration trenches' peak and outflow reduction capability in large sizes. In the study site, the application of these structures managed to decrease both parameters by about 50% from their current condition. The point of diminishing returns, however, can be observed when the LID surface area was increased from 4000 to 6000 square meters due to nearly similar reductions for a large increase of surface area.

Acknowledgements: This research was supported by the Department of Science and Technology (DOST) in the Philippines under the 'DOST's Grants to Outstanding Achievement in Science and Technology' Program.

REFERENCES

- Chin, A., O'Dowd, A. P., & Gregory, K. J. (2013). 9.39 Urbanization and River Channels. In J. F. Shroder (Ed.), *Treatise on Geomorphology* (pp. 809–827). Academic Press. <https://doi.org/10.1016/B978-0-12-374739-6.00266-9>
- Shafique, M. and Kim, R. (2015). Low Impact Development studies: A review of current research and recommendations for future directions. *ECOL CHEM ENG S.*, 22(4), 543-563, <https://doi.org/10.1515/eces-2015-0032>
- Wuebbles, D. J., Kunkel, K., Wehner, M., & Zobel, Z. (2014). Severe Weather in United States Under a Changing Climate. *Eos, Transactions American Geophysical Union*, 95(18), 149–150. <https://doi.org/10.1002/2014eo180001>

AN EVALUATION OF GREEN ROOF MODELING PERFORMANCE OF EPA SWMM

Kavsar Bako¹, Cevza Melek Kazezyılmaz-Alhan^{2*}

¹ Istanbul University-Cerrahpaşa, Civil Engineering Department, Istanbul, Turkey

² Istanbul University-Cerrahpaşa, Civil Engineering Department, Istanbul, Turkey

*Corresponding author (meleka@istanbul.edu.tr)

ABSTRACT

In this work, green roof modeling capability of EPA SWMM is evaluated and the modeling methods, which need improvements, are determined. In particular, the drainage flow equation is improved and the percolation equation is further investigated. Percolation through the soil layer is taken into account with unsaturated hydraulic conductivity which is considered as an exponential function of soil moisture content. The related exponential coefficient HCO value is determined for four different types of substrates using the measured unsaturated hydraulic conductivities and soil moisture content data from steady state tests. The determined HCO values will help to more accurately model the flow through these green roof substrates in SWMM. In addition, comparison of the improved drainage flow equation results with experimental data proved that the improved equation represents the drainage flow more accurately.

Keywords: *Green Roof, Low Impact Development, EPA SWMM, Hydrologic Model.*

1. INTRODUCTION

Green roof is a common type of “Low Impact Development (LID)” practices introduced to reduce the negative impacts of urbanization and preserve the natural hydrological cycle. Green roofs consist of three main layers: Drainage layer, soil layer for growing plants and surface layer for vegetation. The “soil” used as a growth media for green roofs is very different from naturally occurring soils and there is a limited amount of information on the standard agronomic properties of such mixtures (Rossman and Huber 2016a). Therefore, the flow motion in these media will be different from that of natural soil.

The U.S. Environmental Protection Agency Stormwater Management Model (EPA SWMM) is one of the most widely used software for green roof hydrology simulations. Many studies evaluated the overall green roof modeling performance of SWMM. SWMM models the flow over and through the green roof system in three different layers, i.e., surface layer, soil layer and drainage layer. Therefore, modeling details for each layer needs further investigation. In this study, the green roof modeling capability of SWMM to model green roofs is investigated. A drainage flow equation for green roofs is developed by employing the experimental results conducted by Vesuviano (2014) for different types of drainage mat. Then, to improve the accuracy of the green roof percolation model of SWMM, accurate values for HCO coefficient were determined using experiments conducted for different green roof substrates done by Peng *et al.* 2020.

2. MATERIAL AND METHODS

In SWMM green roof module, the infiltration of surface water into the soil layer, f_1 , is modeled with the Green-Ampt equation. The rate of percolation through the soil layer into the drainage layer f_2 is modeled using Darcy's Law. The runoff rate over the soil layer surface q_1 and the drainage mat flow rate q_3 are computed using the Manning equation.

SWMM Drainage flow model

SWMM drainage flow model does not take the storage capacity of the drainage mat into account. Therefore, in this study, the storage capacity of the drainage mat is represented by introducing the drainage mat void thickness D_{s3} into the drainage flow equation. Then, the experimental data by Vesuviano (2014), which was obtained for different types of drainage mat with different drainage length and surface slope conditions, is compared with the SWMM results to further improve the drainage flow equation. The following improved equation is obtained:

$$q_3 = \frac{1}{n_3} s^{\frac{1}{2}} \frac{1}{L} \phi_3 (d_3 - D_{s3})^2 \quad (1)$$

Where q_3 is the drainage flow rate, L is the drainage length of the layers, s is surface slope (m/m), ϕ_3 is void fraction of the drainage mat, d_3 is depth of water in the drainage mat (m), n_3 is a roughness coefficient for the mat.

SWMM Percolation model

SWMM assumes that the percolation rate is equal to the unsaturated hydraulic conductivity which changes as a function of moisture content and is given as follows:

$$K(\theta) = K_s e^{-HCO(\phi-\theta)} \quad (2)$$

where K_s is the saturated hydraulic conductivity, θ is the moisture content, ϕ is the porosity and HCO is a calibration parameter which can be estimated from soil test data. Thus, the percolation rate expression is as follows:

$$f_2 = K_s e^{-HCO(\phi-\theta)} \quad (3)$$

If the moisture content θ is less than or equal to field capacity FC, then the percolation rate becomes zero. The coefficient HCO characterizes the exponential decrease in hydraulic conductivity with decreasing moisture content. The most accurate way of estimating HCO is from laboratory tests that measure hydraulic conductivity K as a function of soil moisture content θ for the particular soil under consideration (Rossman and Huber 2016b).

3. RESULTS AND DISCUSSIONS

Improved Drainage flow equation

The experiments conducted by Vesuviano (2014) were done for drainage mats types of ZinCo Floradrain FD 25, FD 40 and ZinCo Floraset FS 50, drainage mat lengths of 2 and 5 m and surface slope conditions of 2% and 18%. The experimental results are compared with the improved drainage flow equation. The results show that the drainage flow calculated with the improved equation is in better agreement with the measured data than the one calculated with the original drainage flow equation, i.e., Manning's equation (Figure 1).

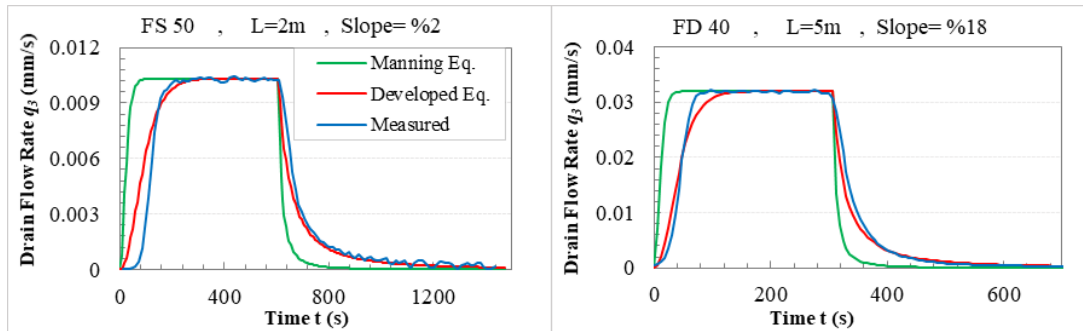


Figure1. Comparison of the measured drainage flow for different drainage mat types and the calculated drainage flows using Manning and the improved equation.

Determination of HCO values

(Peng *et al.* 2020) conducted experiments to measure unsaturated hydraulic conductivities for four representative green roof substrates using steady state and transient techniques on test column in 540 mm high and diameter of 300 mm. In addition, they determined the substrate characteristics including porosity, maximum water holding capacity (MWHC) and saturated hydraulic conductivity (Ks). The tested green roof substrates are Heather with Lavender Substrate (HLS), Sedum Carpet Substrate (SCS), Marie Curie Substrate (MCS) and New Substrate Mix (NSM) substrate. In this study, the steady state data is employed to obtain HCO values for different substrates.

HCO values are estimated by fitting a straight line to the plot of the logarithm of K versus θ obtained from equation 2. In order to determine the best fitting HCO value Microsoft Excel Solver Add-Ins function was set to minimize the sum of the squared (SSQ) deviations between the measured and calculated hydraulic conductivities. Figure 2 shows the fitted line for each substrate. Using first test data, HCO was determined for SCS, NSM, HLS and MCS substrates as 39, 35, 17 and 18. Using second test data HCO was determined as 35, 28, 19 and 21 in the same order.

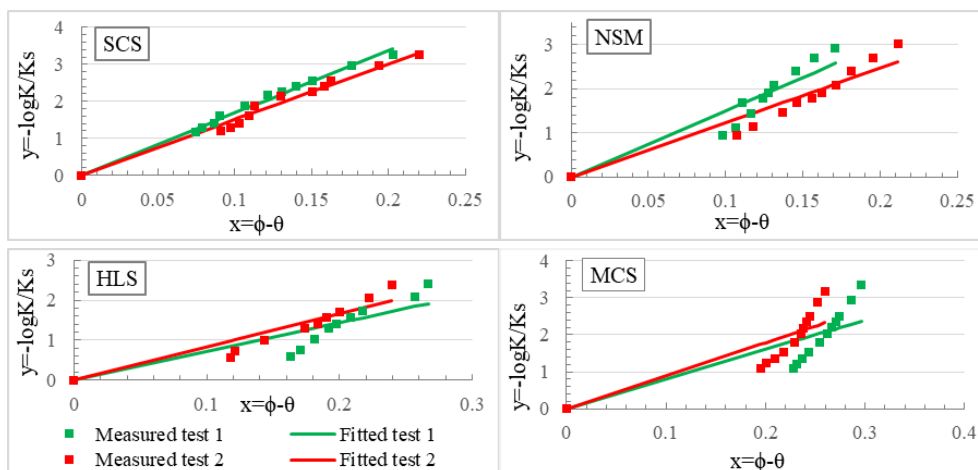


Figure 2. HCO Estimation for the four substrates.

4. CONCLUSIONS

In this study, the green roof modeling capacity of EPA SWMM is evaluated. In particular, an improved equation representing the drainage mat flow more accurately is developed. Then, green roof percolation model is examined and HCO values for four types of substrate were determined using the experimental data by Peng *et al.* 2020.

REFERENCES

- Peng, Z., Smith, C., and Stovin, V., 2020. The importance of unsaturated hydraulic conductivity measurements for green roof detention modelling. *Journal of Hydrology*, 590 (May), 125273.
- Rossman, L.A. and Huber, W.C., 2016a. *Storm Water Management Model Reference Manual Volume III – Water Quality*. United States Environmental Protection Agency.
- Rossman, L.A. and Huber, W.C., 2016b. *Storm Water Management Model Reference Manual Volume I – Hydrology (Revised)*. United States Environmental Protection Agency.
- Vesuviano, G.M., 2014. A Two-Stage Runoff Detention Model for a Green Roof. (*Doctoral dissertation, University of Sheffield*).

THE IMPACT OF LID IMPLEMENTATION ON SURFACE RUNOFF BY USING EPA SWMM

Merve Dinçer(1), Sezar Gülbaz (2)

(1) *Faculty of Engineering, Civil Engineering Department, Istanbul University – Cerrahpaşa,
Avcılar, Istanbul, Turkey*

E-mail: merveedincer@gmail.com

(2) *Faculty of Engineering, Civil Engineering Department, Istanbul University - Cerrahpaşa, Avcılar,
Avcılar, Istanbul, Turkey*

E-mail: sezarg@iuc.edu.tr

ABSTRACT

New techniques are needed to ensure environmental sustainability, to protect water resources, and to reduce the negative impact of urbanization on the environment and water resources. Low Impact Development (LID) implementation, which involves natural methods to reduce the negative impacts of urbanization, has great importance. LID is a storm water management practice to protect the hydrological cycle and mitigate the adverse effects of floods. LID can be used to describe a land planning and engineering design approach to manage storm water runoff as part of green infrastructure. Within the scope of this study, the effects of LID on storm water runoff are analyzed by using Environmental Protection Agency Storm Water Management Model (EPA SWMM). For this purpose, subcatchments which have various land use type such as high density, low density residential and forest are defined into the model. Then, different types of LID such as bio-retention cell, rain garden, green roof, permeable pavement and rain barrel are introduced into the model to investigate the effect of these applications on surface runoff. Hydrographs of these subcatchments are obtained from EPA SWMM with and without LID. Then, the hydrographs are compared to analyze the impacts of LID. The model results show that LID implementations has several benefits such as improving management of runoff and flooding, and reducing impervious surfaces and peak flow and volume of surface runoff.

Keywords: *EPA SWMM, Storm water Management, Low Impact Development (LID), Sustainable Environment.*

A LAND-SUITABILITY ANALYSIS FOR LOW IMPACT DEVELOPMENT APPLICATIONS IN ANKARA, TURKEY

İlksen Şenocak¹, Hayrettin Onur Bektaş², Yasin Erkan³, Gül Şimşek⁴, Aysun Tuna⁵,
Sermin Çakıcı Alp⁶, Mehdi H. Afşar⁷, Emre Alp^{1*}

¹ Department of Environmental Engineering, Middle East Technical University, Ankara, Turkey

² Ankara Water and Sewerage Administration, Ankara, Turkey

³ Maptech Elektronik, Ankara, Turkey

⁴ Department of City and Regional Planning, Atatürk University, Erzurum, Turkey

⁵ Department of City and Regional Planning, Bolu Abant İzzet Baysal University, Bolu, Turkey

⁶ Faculty of Architecture, Hacettepe University, Ankara

⁷ Department of Civil Engineering, Middle East Technical University, Ankara, Turkey

*Corresponding author (emrealp@metu.edu.tr)

ABSTRACT

Urbanization is increasing all over world, and it leads to increase in impervious areas, such as roads, rooftops, or parking lots. Since eliminating urbanization is not possible, new alternatives should be applied. Low Impact Development (LID) practices are appropriate alternative to handle floods and diffuse pollution. Within the scope of the study, application criteria for LID applications, such as land slope, soil characteristics, climate characteristics, land use, etc. and technical details about design are compiled by literature research and Multi-Criteria-Decision Making method was applied along with GIS and Remote Sensing to determine the suitable locations for LID applications in Ankara. The outcomes of the study can aid decision makers to control flood and urban diffuse pollution at the location where impervious areas are dominant.

Keywords: *water-centric ecocity, sustainable stormwater management, low impact development (LID), remote sensing, geographic information systems (GIS)*

1. INTRODUCTION

Urbanization is increasing all over world, and it leads to increase in impervious areas, such as roads, rooftops, or parking lots. Impervious lands pose an obstacle for water for its transfer processes. Rainwater in urban areas with conventional stormwater management systems cause excessive runoffs, increase in peak flows, decrease in infiltration rates, and water quality, as well as urban flooding and nonpoint source pollution (Eckart, McPhee, & Bolisetti, 2017). Therefore, there is direct impact on the ecosystem, and the hydrological cycle. Decreasing urbanization to prevent impervious lands is not possible; however, while making progress in urban development, changing urban conception can be solution. In 1987, Eco-City approach was proposed for sustainable urban development. Eco-City is a city which provide sustainable

development by balancing social, economic, and environmental factors. An Eco-City uses renewable energy sources, generates ecological footprint and pollution as low as possible. Moreover, in Eco-Cities, land use is effective, wastes are composted, recycled, or converted to energy (Novotny & Brown, 2014). Within this approach, Eco-City will not contribute climate change, or its effect will be negligible. For Eco-Cities, one of the concerns is water management. Especially for stormwater management Low Impact Development (LID) can be suggested. LID aims at reducing hydrological effects of urbanization. LID facilitates flood management, increasing infiltration, decreasing temperatures, removing air and water pollution (Jensen, Quinn, & Davis, 2010). LID can be exemplified with bioretention cells, rain gardens, green roofs.

Within the scope of this study, land suitability of LID in a location in Ankara, Turkey is assessed with Multi Criteria Decision Making using GIS and Remote Sensing. Study area has been experiencing significant flood events due to unplanned urbanization and insufficient infrastructure. For example, on 11 June 2020, rainfall coming down during the evening hours causes flooding in Keçiören, and Yenimahalle districts. Some shop owner has died due to electrical shock while evacuating of floodwater (Milliyet, 2020). In this period, 250 houses and workplaces have flooded (Hürriyet, 2020). Furthermore, on 5 April 2018, Mamak receive heavy rain at noon hours. Especially Boğaziçi district was more affected by flood, 6 people were injured, almost 164 vehicles and more than 20 workplaces were damaged (NTV, 2018).

2. MATERIAL AND METHODS

This study aims to assess the suitability of Low Impact Development (LID) applications in Ankara by employing Remote Sensing Methods and Geographic Information System (GIS). Remote Sensing (RS) provides an effective tool to identify sites in detail and to cover both public and private areas (Jensen, Quinn, & Davis, 2010). Remote Sensing offers thematic map based on image classification; for instance, land cover visualization in spatial and temporal range (Foody, 2002). There exist different types of remote sensing methods. Jensen et al. (2010) use Light Detection and Ranging (LiDAR) for suitability estimation of LID in their research. Kang et al. (2014) use Landsat-5 Thematic Mapper (TM) satellite sensor to analyze stormwater management practices. The other method for obtaining remotely sensed data is Unmanned Aerial Vehicle (UAV). Kamnik et al. (2017) practice on UAV for potential site selection of rainwater harvesting and green area retention.

Within the scope of the study, LID strategies, application criteria, such as land slope, soil characteristics, climate characteristics, land use, etc. and technical details about design are compiled by literature research to determine LID applications which are feasible for Ankara. Considering previously flash floods, 2 different study area are selected in Ankara. Stormwater and sewage network maps, land cover maps as well as land use, previous floods, socio-economical status are collected from the archives of Ankara Water and Sewerage Administration. Subsequently, field studies were conducted and collected data are validated by in-situ examination.

In this study, satellite images were obtained for 2 different districted 5 km² area in Ankara. Stormwater networks, stream routes, locations of manhole cover, and their physical conditions are determined by satellite images due to the fact that UAV flights are banned intracity, and after 30 m above the ground, jammers block the signals of UAV which cause to lose control of the drone. Simultaneously, field studies are carried, and in-situ observations are conducted. Digital Elevation Model (DEM) and Digital Surface Model (DSM) are generated from processed images and DEM and DSM data is converted SHP format by 1x1 m grid with determined X, Y, Z coordinates. Similarly, land use and land cover data are obtained by satellite images.

Collected data is transferred to GIS environment, design criteria are evaluated with respect to LID criteria, and their severity is designated. Multi-Criteria Decision-Making method is used to determine suitable site selection in study area. In this extent, city, district, and neighborhood scale to building scale is detailed. Related indicators are used for efficiency and locational performance of LID applications. Watershed characteristics, such as drainage area, land use, slope, runoff direction, permeability rate, soil texture, and hydraulic conductivity is significant for LID location selection. Due to the complexity of the decision and impossibility of trial-error methods, during LID site selection optimization, criteria are limited by existing literature and expert opinion. By using Multi-Criteria Decision Tools, different system data are combined, and cost-benefit analysis and alternatives are prioritized before representing the project to policymakers and stakeholders.

3. RESULTS AND DISCUSSIONS

The location of LID strategies and the application type were evaluated by holistic approach and are planned for the study area. As consequent of suitability analysis, obtained data is used to identify green spaces that are suitable for LID applications which are component of green infrastructure system as a part of stormwater management. Within this framework, on the upper scale, water centric conceptual suggestions are developed for cities, on the mesoscale, suitable LID locations and types are detected for districts. In addition, in selected areas, for public and private areas landscape design project and its cost analysis are prepared. In suggested projects, for plant species selection and water management efficiency, alternatives of firm soil covering, landscape components and other architectural components are developed. LID implementations can be applied on front-sides of the buildings, green spaces of public buildings. Available roofs can be used for LID practices as well as for infiltration strips on roadsides. Rain barrels can be impellent on catchments, and permeable pavements can be placed.

4. CONCLUSIONS

Unplanned urbanization leads to rise in impervious areas and unbalancing hydrological cycle. By virtue of reduction in infiltration flood occurrence increases, and bring along decrease in water quality, ecological damage, economic loss, injuries, and death for humans. Since

eliminating urbanization is not possible, new alternatives should be applied. LID practices are appropriate alternative to handle aforementioned floods and diffuse pollution. In addition, LID is favorable approach to allow sustainable stormwater planning where flood occurrence is frequent. It is expected that the outcomes of this study will aid the decision makers in Ankara to mitigate the effects of floods in the locations where impervious areas are dominant.

REFERENCES

- Eckart, K., McPhee, Z., & Bolisetti, T. (2017, December 31). Performance and implementation of low impact development – A review. (D. Barcelo, Ed.) *Science of The Total Environment*, 607-608, 413-432. doi:<https://doi.org/10.1016/j.scitotenv.2017.06.254>
- Foody, G. M. (2002). Status of land cover classification accuracy assessment. *Remote Sensing of Environment*, 80(1), 185-201. doi:10.1016/s0034-4257(01)00295-4
- Hürriyet*. (2020). Retrieved August 16, 2022, from <https://www.hurriyet.com.tr/gundem/ankaradaki-saganakta-250-ev-ve-is-yerini-su-basti-41539920>
- Jensen, C. A., Quinn, R. J., & Davis, T. H. (2010, November). Urban watershed management: Using remote sensing to implement Low Impact Development. *Next generation infrastructure systems for eco-cities*. doi:10.1109/INFRA.2010.5679206
- Kamnik, R., Grajfoner, B., Butyrin, A., & Perc, M. N. (2017). Rainwater harvesting and green area retention potential detection using commercial unmanned aerial vehicles. *IOP Conf. Series: Earth and Environmental Science*, 90. doi:10.1088/1755-1315/90/1/012113
- Kang, M., Mesev, V., & Myint, S. W. (2014). Urbanization and Quality of Stormwater Runoff: Remote Sensing Measurements of Land Cover in an Arid City. *Korean Journal of Remote Sensing*, 30(3), 399-415. doi:<https://doi.org/10.7780/kjrs.2014.30.3.6>
- Milliyet*. (2020). Retrieved August 16, 2022, from <https://www.milliyet.com.tr/galeri/meteoroloji-uyarmisti-ankarada-saganak-hayati-felc-etti-6233107/14>
- Novotny, V., & Brown, P. (2014, April). Cities of the Future - Towards integrated sustainable water and landscape management. *IWA Publishing*, 13. doi:<https://doi.org/10.2166/9781780405308>
- NTV*. (2018). Retrieved August 16, 2022, from https://www.ntv.com.tr/galeri/turkiye/ankarada-sel-felaketi-6-yarali,FUacrbMh4E2Hfxu_btslFA/8l3YOnkpXEuFVWnvGSm4zw

URBAN/INDUSTRIAL WATER

A GRAPH-BASED MONITORING FRAMEWORK OF SLUDGE BULKING IN INDUSTRIAL WASTEWATER TREATMENT PLANTS VIA DYNAMIC GRAPH EMBEDDING AND BAYESIAN NETWORKS

*Jorge Loy-Benitez, Shahzeb Tariq, SungKu Heo, Taeyong Woo, Sangyoun Kim, ChangKyo Yoo**

Integrated Engineering, Dept. of Environmental Science and Engineering, College of Engineering, Kyung Hee University, 1732 Deogyong-daero, Giheung-gu, Yongin-si, Gyeonggi-do, 17104, Republic of Korea

**Corresponding author (ckyo@khu.ac.kr)*

ABSTRACT

Sludge bulking affects wastewater treatment plants (WWTPs), lowering effluent quality and spreading pollution on discharge areas. The current study proposed a graph-based monitoring framework for sludge bulking events. The proposed outline replaces background knowledge on mechanical-chemical-physical reactions with feature extraction from historical datasets under normal operating conditions and causal relationships between process variables. The dynamic graph embedding (DGE) method extracts similarities among process variables in temporal and neighborhood dependencies, and the dynamic Bayesian network (DBN) computes the prior and posterior probabilities of a belief, which are updated for each timestep; changes in these probabilities mark the possible root cause of the sludge bulking event. The DGE outperformed linear and non-linear feature extraction methods with a 98% detection rate, zero false alarms, and 1% misdetections. The DBN-based diagnostic method identified most of the root causes of sludge bulking, governed by sudden COD drops, with 98% accuracy, outperforming state-of-the-art methods by 11%.

Keywords: *Sludge bulking monitoring, Diffuse pollution, Dynamic graph embedding, Dynamic Bayesian networks, Industrial wastewater, Activated sludge process.*

1. INTRODUCTION

Water pollution has been a hot topic for years, with various wastewater treatment plants (WWTPs) architectures and practices suggested. These facilities protect people and the environment from hazardous effluent concentrations. The activated sludge process (ASP) is the most widely used method for extracting nutrients and organic matter from WWTPs (Forouzanmehr et al., 2021).

Due to ASP's physical and chemical interactions, efficient biomaterial conversion is difficult. High effluent concentration from ASP is often caused by incorrect gravity separation of biomass flocs (sludge bulking). Sludge bulking is ASP's most important task. It causes sludge settling depletion, sludge loss, and effluents that consistently violate quality limits. Sludge bulking degrades treatment performance, releasing low-quality treated water and supporting

industrial pollution. Proper monitoring of sludge bulking to take proactive countermeasures is crucial for WWTP sustainability.

Deep learning frameworks for process monitoring often place a greater emphasis on non-linear internal interactions than on the causal linkages between conforming variables. Graph models and causality analysis have been combined for data modeling via inspection of likelihood changes in several engineering fields. From a diagnostic point of view, probable failures and causes can be identified as the root causes (Wang et al., 2018). Zhao H. (2018) presented the dynamic graph embedding (DGE) approach for fault detection tasks in the context of event detection; this method encodes sequence knowledge by integrating temporal and neighborhood information to calculate similarity metrics for process variables (Zhao, 2018).

Along with process monitoring, determining abnormal event causes is crucial to a plant's performance. This study explores the potential of graph models for data-intensive monitoring of sludge bulking. BN models fit non-linear and uncertain characteristics of complex processes using directed acyclic graphs (DAG). Moreover, the dynamic Bayesian networks (DBN) extend BN to treat time-varying process data attributes through a recursive algorithm (Mamdikar et al., 2021). The presented framework has two stages: 1) detecting sludge bulking occurrences using DGE to inspect variable node changes, and 2) locating sludge bulking root causes using dynamic Bayesian networks (DBN). The proposed data-intensive monitoring framework is trained and validated in a WWTP to treat the wastewater of a steel and iron-making plant in South Korea.

2. MATERIALS AND METHODS

Industrial wastewater plant data description

The measured dataset was from a South Korean coke and steel-making WWTP using ASP. Fig. 1 shows the plant layout with five 900-m³ aeration basins and a secondary settler (1200 m³). Degradation in water treatment allows effluent to be a source of hazardous pollutants that support diffuse pollution. BET-3 wastewater comes directly from a coke-making plant, while BET-2 wastewater is pretreated upstream wastewater. Coke effluent is polluted with inhibitory chemicals and coal liquors such as thiocyanate, phenolics, cyanides, ammonium, and polyhydrocarbons (COD).

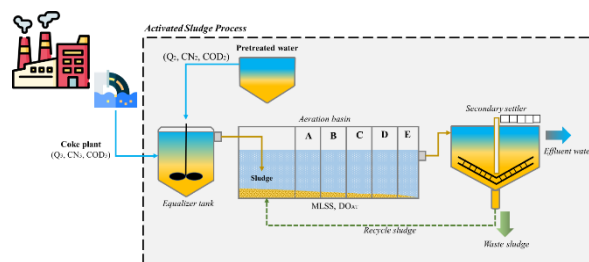


Figure 1. The layout of the ASP-WWTP for the treatment of steel-making plant wastewater.

The dataset comprises a two-year dataset measured by the daily average. It is composed of eight process variables: influent flowrates for BET units 2 and 3, COD of units 2 and 3, dissolved oxygen (DO_{AT}), cyanide of BET-2 (CN_2), cyanide of BET-3 (CN_3), and mixed liquor suspended solids (MLSS).

Dynamic Graph Embedding-Based Bulking Event Detection

Modeling the DGE-based event detection of sludge bulking states is conducted with the training dataset, including process variables measured under normal conditions. Then, these measurements are formed into augmented matrices, where feature extraction is performed. From this step, the Hotelling (T^2) statistic is utilized for the detection task, computed by **Eqs. (1-2)** (Zhao, 2018).

$$T^2 = \left\| U_2^T X_i V_2 \Omega_V^{-1} V_2^T X_i^T U_2 \right\|_F^2 \quad (1)$$

Where $\Omega_V \in \mathbb{R}^{l \times l}$ is the covariance matrix.

$$\Omega_V = \frac{1}{n-l+1} \sum_j \left(V_2^T X_i^T U_2 - K_V \right) \left(V_2^T X_i^T U_2 - K_V \right)^T \quad (2)$$

Considering $K_V = \frac{1}{n-l+1} \sum_j V_2^T X_i^T U_2 \in \mathbb{R}^{l \times m_1}$.

The discrimination between faulty or non-faulty conditions in a measurement set should be defined by a confidence limit computed through a non-parametric Kernel density estimator (*KDE*) to estimate the probability density function of a random variable with a certain confidence level, which in this study is 95%, $\alpha = 0.05$ (Yan et al., 2016). This way, the limit T_α^2 is the threshold for which, when their respective statistics surpass the limit, it is considered as faulty or, in this case, in a sludge bulking state.

Dynamic Bayesian Networks Root-Cause Diagnosis for Sludge Bulking States

A root-cause diagnostic task enables the user to determine the propagation route of the sludge bulking condition. This work identifies and characterizes three major sludge bulking mechanisms, as summarized in **Table 1**. These pathways are validated by earlier research (Han et al., 2021). The graph constructed by Granger analysis is utilized as the network for the DBN, for which the conditional probabilities for each node are estimated by maximum likelihood estimation (*MLE*). These probabilities estimate a parent node's influence over the child node.

Table 1. Description of the scenarios for sludge bulking state pathways with their respective root cause.

Scenario	Sludge bulking state pathway	Root cause
1	Low DO	Low DO
2	Low F/M - BET ₂	Low COD ₂
3	Low F/M - BET ₃	Low COD ₃

The DBN network's parameters are estimated using a dataset of sludge bulking events divided into the above pathways. Second, each step draws a conclusion from updated child node evidence. The backward analysis estimates any set of variables' posterior probability from available evidence. This posterior probability is the fault or sludge bulking likelihood. As this probability grows, abnormal events are more likely. The transition mechanism of belief update in the children's nodes is described in **Eq. (3)**.

$$P(Z_t | Z_{t-1}) = \prod_{i=i}^n P(Z_{i,t} | Pa(Z_{i,t})) \quad (3)$$

where $Z_{i,t}$ is the evidence for the i^{th} node at time t , n is the number of nodes, and $Pa(Z_{i,t})$ represents the parent nodes of Z_i from the same and previous time slices.

T^2 for each variable maps a contribution at each timestamp. Considering a contribution threshold of $\omega = 50\%$, the root cause variable is the root node with the highest contribution. When root nodes do not contribute the most, they are used to update beliefs. As the belief spreads, a comparison of sludge bulking probability at time t and $t-1$ generates a percentage change. The variable that changes sludge bulking probability the most is the root cause.

3. RESULTS AND DISCUSSIONS

Sludge Bulking Event Detection

Table 2 shows the detection task performance results divided by the dataset. The test dataset contains sludge bulking events starting from the 51st sample, so the detection rate, false alarm rate, and misdetection rate can be calculated. **Figure 2** shows DGE-based sludge bulking detection. First, the probe dataset's T^2 statistic and \hat{I}^2 computed from ICA should be below the confidence limit because there is no sludge bulking. The PCA, DPCA, and KPCA methods yielded false alarms with a FAR of 1.97%, 1.72%, and 1.47%, respectively; the ICA method showed a FAR of 5.65% and had the most erratic behavior for differentiating states in the dataset; while the DGE method had 0% FAR. A low FAR prevents unnecessary alarm activations when the process is in normal operating conditions. Due to the DPCA and KPCA's dynamism and non-linearity, the FAR was slightly lower than the PCA.

The PCA, DPCA, KPCA, and ICA methods yielded 12%, 10%, 6%, and 16% unnecessary alarm triggers in the test dataset. Due to the dynamic nature of DPCA, temporal information helps recognize patterns to generate an accurate process representation under normal conditions. False alarms can cause economic losses by assigning resources to an inexistent conflict, misleading WWTP sustainable management. The DGE avoided false alarms and achieved a 0% FAR.

A near-zero MDR is crucial for monitoring quality. Misdetection (Type II error) occurs when a problematic sample fails to detect sludge bulking. Misdetecting an abnormal event can lead to failure because the necessary actions are not taken. DGE had the lowest MDR (0.67%), indicating near-zero behavior. PCA, DPCA, KPCA, and ICA account for large MDR values of 50.67%, 51.3%, 47.3%, and 13.33%, respectively.

Table 2. Performance of the sludge bulking event detection using different methods.

	Probe dataset	Test dataset		
	False alarm (%)	Detection rate (%)	False alarm rate (%)	Missdetection rate (%)
PCA	1.97	49.33	12	50.67
DPCA	1.72	48.67	10	51.33
KPCA	1.47	79	6	47.33
ICA	5.65	86.67	16	13.33
DGE	0	99.33	0	0.67

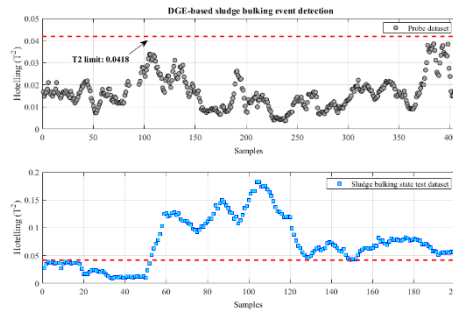


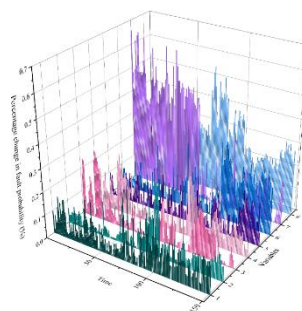
Figure 2. The sludge bulking detection performance via Dynamic Graph Embedding.

Dynamic Bayesian Networks Root-Cause Diagnosis.

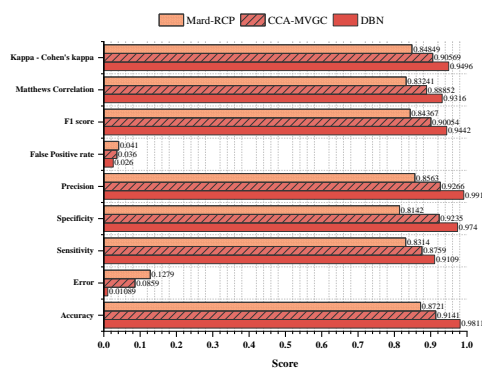
Test dataset with sludge bulking events is used for diagnostics. **Fig. 3(a)** shows the percentage change in fault probability for each variable with the previous timestamp. According to the three root causes, variables 7 and 8, COD₂ and COD₃, have dominant behavior. DO has a lower impact on sludge bulking.

Most extreme changes in belief about previous timestamps are attributed to low COD₂ and low COD₃, attributing abnormalities to low F/M. It affects granule formation and stability. The highest percentage change in the sludge bulking state, 45.38%, was attributed to COD₂ during the detected abnormal event, indicating low COD₂ as the potential root cause. The COD₃ node reports the second-highest change percentage, 26.40%, within an abnormal alarm. Change percentages of COD₂ and COD₃ peaked in samples 51st – 150th and 90th – 201st, respectively, consistent with sludge bulking causes. The 150th sample showed sporadic DO depletion, indicating this was the root cause of sludge bulking.

To analyze the consistency of the diagnostic process, a multilabel confusion matrix was computed for Mard-RCP, CCA-MVGC, and DBN, comparing computed and actual sludge bulking root causes. Low COD₂, low COD₃, and low DO cause sludge bulking. **Figure 3(b)** shows that the proposed diagnostic process outperformed the other methods in classifying the existing sludge bulking process to its root cause. The proposed method achieved 98.1% accuracy, outperforming Mard-RCP and CCA-MVGC by 11.1% and 6.8%, respectively. The proposed method has the lowest error rate at 0.01%, making it the second-best diagnostic method.



(a)



(b)

Figure 3. Diagnostic process results via (a) percentage change in fault probability and (b) performance metrics for sludge bulking root cause classification in the ASP-WWTP.

4. CONCLUSIONS

This study used graph-driven methods to monitor sludge bulking in a steel-making ASP-WWTP. First, DGE detects sludge bulking by comparing process variables and extracting temporal and neighborhood dependencies. Offline modeling is done with normal process data without sludge bulking. The method was validated using probe and test datasets to determine the DGE's ability to detect abnormal events. It was also compared to state-of-the-art PCA and KPCA methods. The DGE method yielded zero FAR for the probe and test datasets and 99% and 0.67% DR and MDR. Second, DBN is used to diagnose sludge bulking. Variation in abnormality probability reports the node causing the event, determining the root cause of sludge bulking. Granger causality determines the WWTP process's parent and child nodes. Children nodes use evidence to compute conditional probabilities, updating the network at each timestamp.

Acknowledgments: This work was supported by the National Research Foundation of Korea (NRF) grant funded by the Korean government (MSIT) (No.2021R1A2C2007838), the Korea Ministry of Environment (MOE) as a Graduate School specializing in Climate Change, and the Ministry of Environment “Promising Green Enterprise Technology Innovation Project” (No. 2020003160009).

REFERENCES

- Forouzanmehr, F., Le, Q.H., Solon, K., Maisonnave, V., Daniel, O., Buffiere, P., Gillot, S., Volcke, E.I.P., 2021. Plant-wide investigation of sulfur flows in a water resource recovery facility (WRRF). *Sci. Total Environ.* 801, 149530. <https://doi.org/10.1016/j.scitotenv.2021.149530>
- Han, H.G., Dong, L.X., Qiao, J.F., 2021. Data-knowledge-driven diagnosis method for sludge bulking of wastewater treatment process. *J. Process Control* 98, 106–115. <https://doi.org/10.1016/j.jprocont.2021.01.001>
- Wang, T., Lu, G., Liu, J., Yan, P., 2018. Graph-Based Change Detection for Condition Monitoring of Rotating Machines: Techniques for Graph Similarity. *IEEE Trans. Reliab.* 68, 1034–1049. <https://doi.org/10.1109/TR.2018.2866152>
- Yan, W., Guo, P., Gong, L., Li, Z., 2016. Nonlinear and robust statistical process monitoring based on variant autoencoders. *Chemom. Intell. Lab. Syst.* 158, 31–40. <https://doi.org/10.1016/J.CHEMOLAB.2016.08.007>
- Zhao, H., 2018. Dynamic graph embedding for fault detection. *Comput. Chem. Eng.* 117, 359–371. <https://doi.org/10.1016/j.compchemeng.2018.05.018>

NOVEL POROUS GEOPOLYMER GRANULES TO CONTROL DIFFUSE POLLUTION AND EUTROPHICATION RELATED TO AMMONIUM NITROGEN

Yangmei Yu ^{a*}, Tero Luukkonen ^a,

^a Fibre and Particle Engineering Research Unit, University of Oulu, Finland.

* Corresponding author: yangmei.yu@oulu.fi

Abstract

Ammonium nitrogen (NH_4^+) is one of the major nitrogen species causing eutrophication. In this study, a novel and simple method to produce cation-exchange material based on porous geopolymer granules is presented and the suitability of the granules is demonstrated for NH_4^+ removal/recovery. The granules were characterized for their pore structure and adsorption performance in packed-bed column experiments. The porous geopolymeric granules showed clearly a higher adsorption capacity in comparison to non-porous granules with a similar composition. The results indicated that porous geopolymeric granules could be potentially used for the removal NH_4^+ ions in a continuous process, and thus they would be potentially suited for diffusion pollution and eutrophication control.

Keywords: *eutrophication, adsorption, porosity, geopolymer*

Introduction

Ammonium nitrogen (NH_4^+) is one of the major nitrogen species, which leads to eutrophication and deterioration of aquatic ecosystems. Possible NH_4^+ removal techniques include biological processes, adsorption, or stripping at high pH. Of these techniques, adsorption-based processes would be best suited for diffusion pollution control due to their low energy demand, simple operation, and easy replaceability after exhaustion.

Geopolymers are novel cation-exchanger materials with amorphous aluminosilicate structure. They can be prepared with a low-energy process at ambient temperature and pressure via mixing of solid aluminosilicate precursor with alkali activator solution. The present study aimed to boost the adsorption performance by introducing a high level of porosity into the geopolymer granules while keeping the preparation method simple and up scalable. Dynamic adsorption-desorption experiments were performed to assess the impact of the porosity of novel geopolymer granules for the NH_4^+ removal and recovery.

Materials and methods

Metakaolin (MetaMax from BASF, USA) and solid anhydrous sodium metasilicate (VWR Alfa Aesar, Germany) were employed as an aluminosilicate precursor and alkali activator, respectively, for the granule preparation. Hydrogen peroxide (H_2O_2) was used as a granulation fluid and to generate pores to the granules. The granules were prepared by first milling metakaolin with sodium metasilicate at Al/Na molar ratio of 1.0. The milled mixture was then placed in a high-shear granulator (Eirich EL1). H_2O_2 solution (concentration 10 weight-%) or

only water as a reference (to prepare non-porous granules) was dosed dropwise to the granulator during ~20 min while the mixer speed was 1200 rpm. Before use, the granules were pre-treated with 0.1 M acetic acid (Merck, Germany), to bring their pH value to close to neutral, and then rinsed with deionized water. Particles between 2-4 mm were used for column adsorption experiments.

The pore structure morphology and chemical composition of the granules were characterized with field energy dispersive X-ray spectrometer (FE-SEM-EDS) using a Zeiss Ultra plus instrument.

The NH_4^+ adsorption-desorption experiments (Fig. 1) were carried out in a plastic column (inner diameter of 4.3 cm, height of 9.9 cm, packed bed height of 5 cm that was 20 g of geopolymer granules with particle size 2-4 mm. A NH_4^+ solution (200 mg/L NH_4^+) was pumped through the column (flow rate of 0.5 L/h, ~ 9 min empty bed contact time).

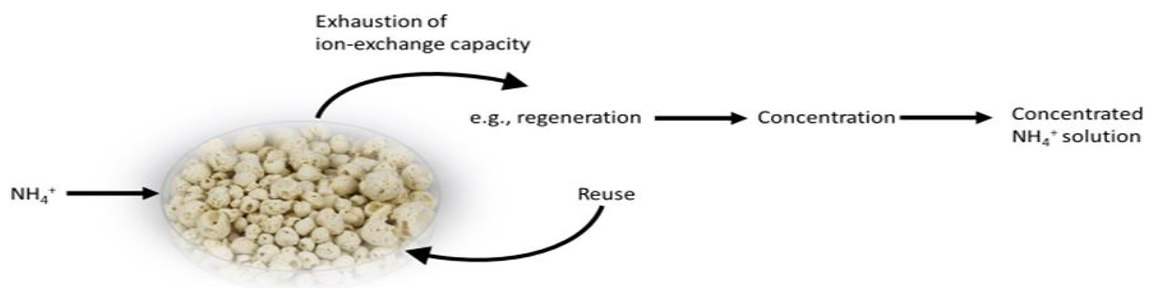


Fig.1. Concept of porous granules for adsorption-desorption experiment

Results and discussions

The pore structure plays a crucial role in adsorption, as it could enhance the diffusion of the adsorbate into the adsorbent and allow more sites for adsorption to function (Novais et al., 2016). **Fig. 2** presents surface morphology and the cross-sections of porous and non-porous geopolymer granules. Granules treated with H_2O_2 exhibit clearly higher porosity compared with non-porous granules. The pores of porous granules were formed by the decomposition of H_2O_2 used in the granulation process at the high pH present in the freshly prepared granules.

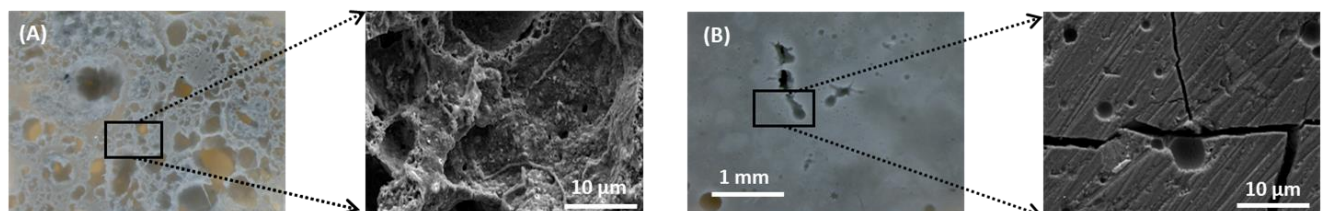


Fig. 2. Porous (A) and non-porous (B) geopolymer granules imaged with optical microscopy and scanning electron microscopy (SEM).

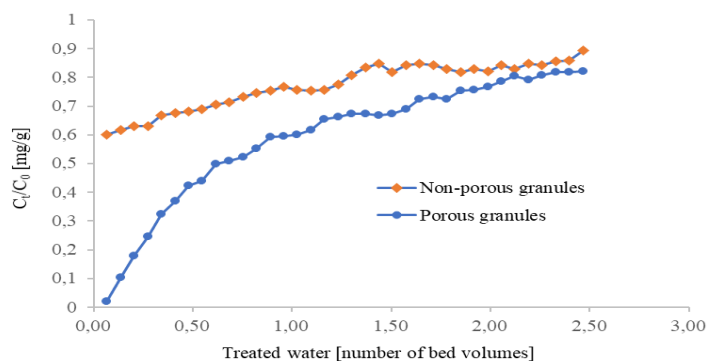


Fig. 3. NH_4^+ adsorption by porous and non-porous granules. (Experimental condition; granule dosage = 20 g; initial NH_4^+ = 200 mg/ L. pH = 6 ± 0.2 . Flow rate = 0.5 L/ hour. Temp. = 22 °C; Time = 6 hour)

The cumulative removal amounts up to 6 h are shown in **Fig. 3**. The adsorption experiments showed that the porous granules had more than two times the cumulative uptake of NH_4^+ (15.07 mg/g) when compared to non-porous granules (6.68 mg/g). Thus, it was shown that the internally porous structure led to a significant improvement in the adsorption capacity. The porous granule preparation method presented here could be a useful tool for further development of geopolymer-based adsorbents.

Conclusions

The present work reported a promising new method to obtain highly porous metakaolin-based geopolymer granules. The granules could be utilized to control diffuse NH_4^+ pollution in portable and easily replaceable cartridges. The next stage in the work will be to study the desorption and recovery of NH_4^+ over extended number of cycles.

Acknowledgments

This work was financially supported by the Business Finland (project TYPKI, 43643/31/2020) and Academy of Finland (InStreams profiling, 326291). Part of the work was carried out with the support of the Centre for Material Analysis, University of Oulu, Finland.

References

- Meng, J., Shi, L., Hu, Z., Hu, Y., Lens, P., Wang, S., Zhan, X. (2021). Novel electro-ion substitution strategy in electrodialysis for ammonium recovery from digested sludge centrate in coastal regions. *Journal of Membrane Science*, 120001.
- Novais, R. M., Buruberry, L. H., Seabra, M. P., Labrincha, J. A. (2016). Novel porous fly-ash containing geopolymer monoliths for lead adsorption from wastewaters. *Journal of hazardous materials*, 318, 631-640.
- Ward, A. J., Arola, K., Brewster, E. T., Mehta, C. M., Batstone, D. J. (2018). Nutrient recovery from wastewater through pilot scale electrodialysis. *Water research*, 135, 57-65.

RAINWATER REUSE EVALUATION BY DESIGN CAPACITY OF RAINWATER UTILIZATION FACILITIES

Changyeon Won¹, Inkyeong Sim¹, Jeongyong Lee^{2*}, Heeman Kang^{3*}

¹ Department of Water Resources and Environmental Engineering, HECOREA. Inc, Seoul, Korea (Republic of)

² Environmental Engineering, WOOWON. Inc, Ansan, Korea (Republic of)

³ Korea Expressway Corporation, Environment Research Division, Gyeonggi-do, Korea (Republic of)

*Corresponding author (jjangaw1@daum.net)

ABSTRACT

Due to the increase of impervious area and frequent occurrence of localized heavy rain in urban areas, the amount of runoff increases compared to pervious spaces thereby resulting in urban flooding occurrence. In addition, although the demand for water is increasing due to the improvement of living standards, urbanization and industrialization, the development and conservation of water resources is still necessary. As such, rainwater utilization facilities are being installed in consideration of the size and flow in highly urbanized land uses. Rainwater utilization facilities collect and reuse rainwater for living, landscaping, and industrial purposes. Since the 「Act on Enforcement Decree Of The Act On Promotion And Support Of Water Reuse」 is amended in 2014, rainwater utilization facilities have been increasing every year. In this study, the satisfaction rate and guarantee rate, utilization rate for rainwater utilization facilities in Korea were evaluated. Also, the appropriateness of the scale of the rainwater utilization facilities was evaluated. As a result of the adequacy analysis, it was observed that the sizing coefficient applied to the facility capacity design expands the most from 0.03 to 0.05.

Keywords: *Rainwater capacity, rainwater guarantee rate, rainwater utilization rate, rainwater satisfaction rate*

1. INTRODUCTION

In relation to the evaluation of rainwater utilization facilities, studies such as feasibility analysis of rainwater management application in housing maintenance projects (Kim and Joo, 2013) and a study on rational sizing of rainwater utilization facilities in apartment houses (Lee and Jeong, 2017) were conducted. The enforcement decree of the act on promotion and support of water reuse suggests that the storage capacity that can store rainwater for a certain period is at least the size of the roof multiplied by 0.05 m by the rainwater catchment area. Therefore, most of the installed rainwater utilization facilities have a corresponding sizing and capacity scale. 0.05 m means 50 mm of rainfall received from the roof surface. In this study, in order to evaluate the water consumption by design capacity of rainwater facilities, the scale calculation coefficient of 0.01 to 0.07 for calculating the storage tank capacity was applied to determine the possible water consumption. In addition, the difference resulting from each coefficient was compared and analyzed by analyzing the supply overflow rate, rainwater guarantee rate and utilization rate by type of target facility installed.

2. MATERIAL AND METHODS

Material

The target facilities were classified into business facilities, educational facilities, sports parks, and apartments based on the land use of the target facilities by utilizing all of rainwater facilities installed and operated in Korea. Research was conducted on the Yesan government office for business facilities, the Geochang Middle School for educational facilities, Hoengseong Sports Park for sports parks, and Yeongjongdo Apartments for apartment houses. Figure 1 shows the summary of the different facilities employed in this study.

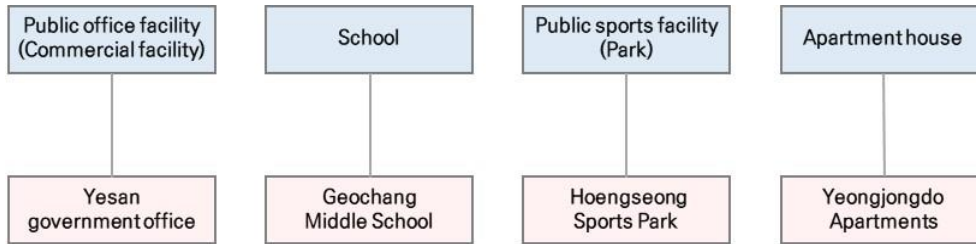


Figure1. Target research facilities

Methods

For the evaluation method of rainwater utilization facilities, the amount of rainwater inflow for the catchment area was calculated using daily rainfall data for the last 10 years (2011~2020). And rainwater satisfaction, rainwater guarantee, and rainwater utilization were calculated using the storage tank capacity and usage data for each case area. The calculation formula for each item is as follows.

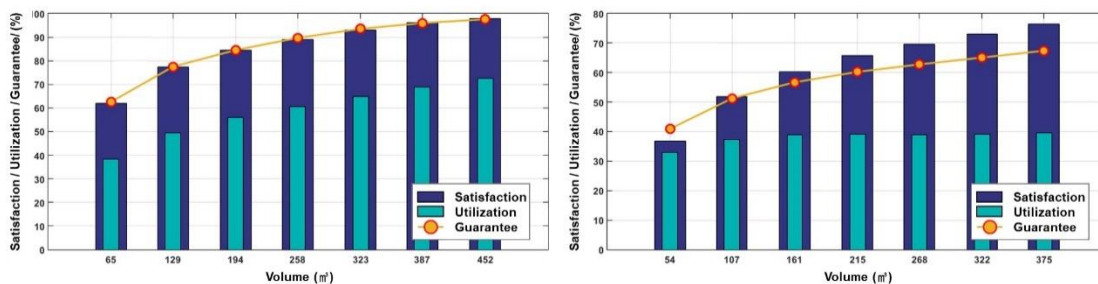
$$\text{Usable amount of rainwater (m}^3\text{)} = \text{Catchment area (m}^2\text{)} \times \text{Rainfall (m)} \quad (1)$$

$$\text{Rainwater satisfaction (\%)} = \frac{\text{Usable amount of rainwater (m}^3\text{)}}{\text{Rainwater demand (m}^3\text{)}} \times 100 \quad (2)$$

$$\text{Rainwater guarantee (\%)} = \frac{\text{Days of rainwater use (day)}}{\text{Total number of days (day)}} \times 100 \quad (3)$$

$$\text{Rainwater utilization (\%)} = \frac{\text{Usable amount of rainwater (m}^3\text{)}}{\text{Storage capacity (m}^3\text{)}} \times 100 \quad (4)$$

3. RESULTS AND DISCUSSIONS



a.

b.

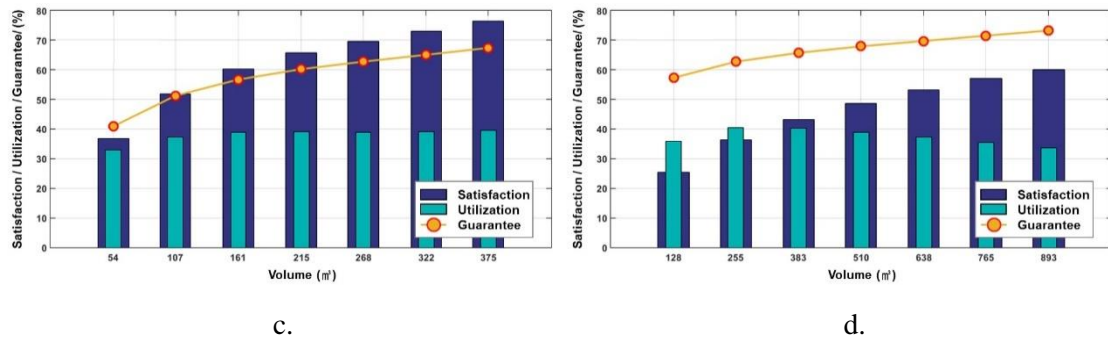


Figure 2. Comparison of rainwater satisfaction at varying rainfall volume in a. Yesan government office, b. Geochang middle school, c. Hoengseong sports park and d. Yeongjongdo apartments

As a result of analyzing the supply satisfaction rate - rainwater guarantee rate - utilization rate by capacity of rainwater utilization facilities by facility type, it was observed that the rainwater guarantee rate increased as the capacity of rainwater utilization facilities increased, regardless of the facility (Figure 2). The supply sufficiency rate also increased as the capacity of the rainwater utilization facility increased, regardless of the facility. On the other hand, in both cases of sports facilities (parks), it was analyzed that the utilization rate decreased as the facility capacity increased. In addition, in Geochang Middle School and Yeongjongdo Apartments, as the scale factor increased, the rate of rainwater transfer showed an increasing trend and then decreased. The representative facilities by type were Yesan government office for business facilities, Geochang Middle School for educational facilities, Hoengseong Sports Park for sports parks, and Yeongjongdo Apartments for apartment houses.

4. CONCLUSIONS

This study revealed that appropriate sizing is needed for rainwater utilization technology. Large facilities tend to be oversized, while small facilities tend to overflow. Therefore, when comparing the supply satisfaction rate, rainwater guarantee rate, and rainwater utilization facility utilization rate, it would be reasonable to design the reservoir by applying a scale calculation coefficient of 0.03 to 0.05. The calculation coefficient in this study may be used to design similar rainwater utilization technology.

REFERENCES

Ministry of Environment of Korea (2008). Guidebook for Installation and Management of Rainwater Utilization Facilities.

EVALUATION OF HEAVY METAL SORPTION CAPACITIES OF CELLULOSE BASED ADSORBENTS WITH IONIC FUNCTIONAL GROUPS – AQUEOUS COBALT (II) ION REMOVAL –

Abdifatah A. Hashi¹, Buket Erdoğan², Yağmur Kuzucu³, Serdar Şam⁴, Gül G. Hacıosmanoğlu⁵, Abdelhadi F. M. Deghles⁶, Othman A. Hamed⁷, and Zehra S. Can^{8*}

^{1,2,3,4,5,8} Marmara University, Environmental Engineering Department, Istanbul, Turkey

⁶ Al-Istiqlal University, Palestine

⁷ An-Najah National University, Palestine

*Corresponding author (zehra.can@marmara.edu.tr)

ABSTRACT

This study focuses on developing a novel foam material with ionic functional groups using the most abundant natural resource, cellulose, for the removal of heavy metals. Ionic functionalities were introduced to cellulose-based foam for increased affinity towards heavy metals. Based on the type of cellulose polymer used in the synthesis, four different cellulose based foam material batches were obtained, these are, activated cellulose, cellulose acetate, carboxymethyl cellulose, and acetylated carboxymethyl cellulose based foam materials. Heavy metal removal capacity of each foam material was tested using cobalt as the model heavy metal. At pH of 6.5, foam dose of 10 g/L, and initial Co²⁺ concentration of 100 mg/L, heavy metal removal capacities of the foam samples varied between 2% to 36 %, while foam material produced by cellulose acetate revealed the highest removal efficiency, 36%. Co²⁺ removal efficiency of cellulose acetate based foam increased to 50% when 15 g/L of foam sample was used under otherwise the same experimental conditions. Adsorption behavior of the cellulose acetate based foam material was also studied, which suggested Sips isotherm model as the most suitable adsorption mechanism.

Keywords: heavy metal removal, cellulose, adsorption, cobalt, isotherm

1. INTRODUCTION

Various industries such as battery production, tanneries, metal plating, mining, etc. employ heavy metals in production chemistry and as a result produce wastewaters including heavy metals in remarkable concentrations, which pose a vital threat to the environment. Heavy metals are toxic to humans either by direct exposure or via bioaccumulation in fresh water and marine biota, and in vegetation as a result of soil pollution (Bailey et al., 1999; Doris et al., 2000).

Electrodeposition and chemical precipitation are generally used to remove dissolved heavy metal species despite their disadvantages; the former is costly due to high electric energy consumption and the latter requires large settling tanks and produces high volumes of chemical sludge which is subject to further treatment. Therefore, numerous studies have sought low cost methods; among those, scavenging metals via adsorption has been the most abundantly investigated. If an adsorbent requires little or no pre-treatment and/or is a waste or a by-product of some process, it is usually considered as a low-cost material. For this cause, many “unusual” materials, majority of which are wastes or by-products of agriculture, even tree barks and wood

dusts, ground husks of grains and shells of nuts, and brewed herbs have been employed as adsorbents (Gloaguen and Morvan, 1997; Ajmal et al., 1998; Low and Lee, 2000; Bulut and Tez, 2007; Chen et al., 2022). Separation of heavy metals from aqueous media also necessitates a further step of metal recovery and using combustible materials with low ash content as adsorbents presents a great advantage in this manner. Cellulose is a natural, and abundant polymer. Therefore, researchers within the last few decades have focused on developing cheap, eco-friendly, cellulose-based sorbents with high sorption capacity (Aniagor et al., 2021). Cellulosic adsorbent materials propose a great deal in terms of small particle size, high combustibility and low ash content. This study aims to develop a novel foam like adsorbent material with ionic functional groups using cellulose, for the removal of heavy metals.

2. MATERIAL AND METHODS

Synthesis of foam samples

2.1.1. *Synthesis of activated cellulose foam sample (AC)*

1,4-phenylene diisocyanate (1g) was added to the gel produced from activated cellulose, followed by the addition of THF (0.5 mL) and catalytic amount of diisopropyl amine (2 drops). The mixture was stirred at room temperature for an hour, then few drops of water were added. The resulting foam was washed with distilled water (100.0 mL) several times, filtered and dried at 60°C for an hr.

2.1.2. *Synthesis of carboxymethyl cellulose (CMC)*

CMC was produced from cellulose by the addition the of 50% NaOH dropwise, and a suspension of sodium chloroacetate. 1 g of produced CMC and 1 mL distilled water were stirred in a beaker until a clear gel was obtained. 10 mL N, N-dimethyl acetamide (DMAc) were added to the gel followed by addition of catalytic amount of diisopropyl amine (2 drops). Excess amount of 1,6-hexamethylene diisocyanate was then added. The mixture was stirred at room temperature for an hour. The resulting foam was washed with distilled water several times, filtered and dried at 60°C for an hour.

2.1.3. *Synthesis of acetylated carboxymethyl cellulose based foam (AcCMC)*

CMC was firstly acetylated by the addition of acetic acid, and H₂SO₄ under nitrogen. Then, in a 200 mL beaker, acetylated CMC (0.2 g) was mixed with 1,6-hexamethylene diisocyanate (3.0mL), followed by the addition of THF (0.5 mL) and catalytic amount of diisopropyl amine (6 drops). The mixture was stirred at room temperature for an hour. The resulting foam was washed with distilled water several times, filtered and dried at 60°C for an hour.

2.1.4. *Synthesis of cellulose acetate based foam (CAc)*

A clear gel was obtained from cellulose acetate by dissolving in DMAc. 1,4-phenylene diisocyanate (1g) was added to the produced gel, followed by the addition of THF (0.5 mL) and catalytic amount of diisopropyl amine (6 drops). The mixture was stirred at room temperature for an hour. The resulting foam was washed with distilled water several times, filtered and dried at 60°C for an hour.

Determination of Heavy Metal Removal Capacities

Aqueous solutions of cobalt were prepared at 100 mg/L initial concentration. 0.1 g of each adsorbent material, was added into a flask containing 10 ml aqueous Co solution. The pH of all test solutions were 6.5. Adsorption experiments were carried out in a temperature controlled shaker (IKA, Germany) in batch mode at 25 °C for 24 hours with a mixing speed of 200 rpm. After the adsorption process, the samples were filtered with 0.2 µm PTFE filter. Then, the remaining cobalt concentrations were measured by atomic absorption spectroscopy using a Perkin Elmer AAnalyst 400 spectrometer. In order to assess the adsorption capacity, mass of Co adsorbed per unit mass of foam material was calculated using Equation 1.

$$q_e = \frac{(C_0 - C_e)V}{m} \quad (1)$$

In Equation 1, C_0 and C_e are the initial and equilibrium concentrations of heavy metals (mg/L), q_e is the mass of pollutant adsorbed per unit mass of adsorbent (mg/g), V is the solution volume (L) and m is the adsorbent mass (g).

The percent (%) removal efficiency was calculated using Equation 2

$$Re\% = \frac{(C_0 - C_e)}{C_0} \times 100\% \quad (2)$$

where $Re\%$ is the percent removal efficiency.

Isotherm studies

10 mL of aqueous solutions at 20, 40, 60, 80, and 100 mg/L initial concentrations were transferred into flasks. 0.15 g of cellulose acetate based foam material, was added into each flask containing 10 ml aqueous Co solution. The pH of all test solutions were 6.5. Adsorption experiments were carried out in a temperature controlled shaker (IKA, Germany) in batch mode at 25 °C for 24 hours with a mixing speed of 200 rpm. After the adsorption process, the samples were filtered with 0.2 μ m PTFE filter. Then, the remaining heavy metal concentrations were measured by atomic absorption spectroscopy using a Perkin Elmer Analyst 400 spectrometer.

Isotherm models

The isotherm models Langmuir, Freundlich, Sips and Dubinin-Astakhov were tested since they are the most commonly used isotherms in the aqueous phase adsorption studies. The parameters of the isotherm models were determined by nonlinear optimization technique using Microsoft Office Excel software (Microsoft Corp., USA) as described by a Tran et al., 2017. The obtained models were evaluated according to Chi square (χ^2), correlation coefficient (R^2) and normalized root mean square error (NRMSE).

3. RESULTS AND DISCUSSIONS

Heavy Metal Removal Capacities of Cellulose Based Adsorbents

As can be seen in Figure 1, Co removal capacities of the foam samples varied between 2% to 36 %. While the foam produced by activated cellulose had the lowest Co removal efficiency (<1%), foam material produced by cellulose acetate revealed the highest removal efficiency, 36%. Solid phase concentrations of Co , as represented by the q values, varied between 0.05 and 3.84 mg/g.

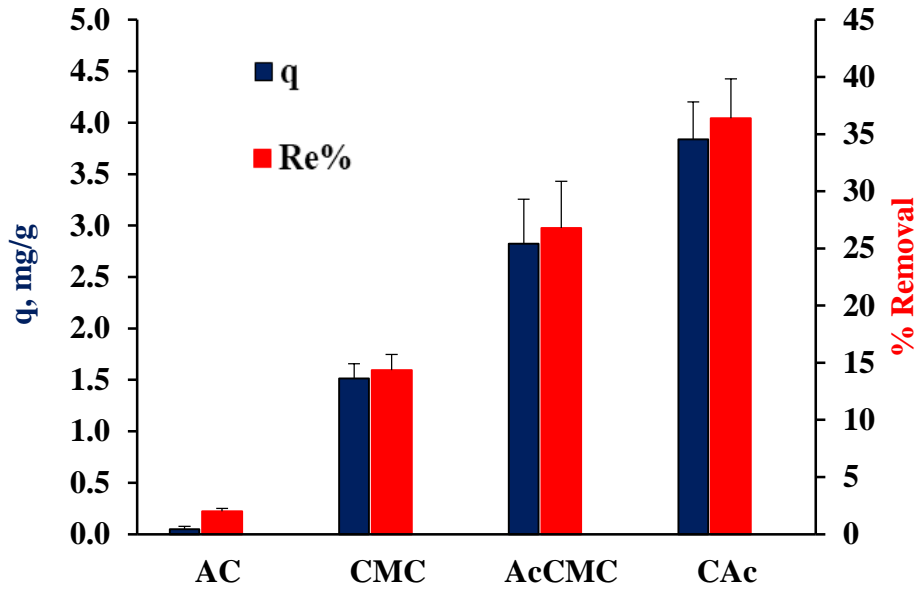


Figure 1. Co^{2+} adsorption capacities of cellulose based foam samples (Initial Co^{2+} concentration 100 mg/L, contact time 24 h, adsorbent dosage 10 g/L, pH 6.5)

Equilibrium Study of Co^{2+} Adsorption onto CAC

24-hour equilibrium studies were conducted at 25 °C, and pH 6.5, using 15 g/L CAC, and varying the initial concentration of Co^{2+} between 20–100 mg/L. The results are given in Figure 2. As can be seen in Figure 2, q values vary between 1–3.23 mg/g. The highest removal efficiency, 96.7%, was obtained for initial Co^{2+} concentration of 20 mg/L. Percent removal efficiencies gradually decreased when the initial Co^{2+} concentration in solution increased. For 100 mg/L initial Co^{2+} concentration, percent removal was as low as 49.6%.

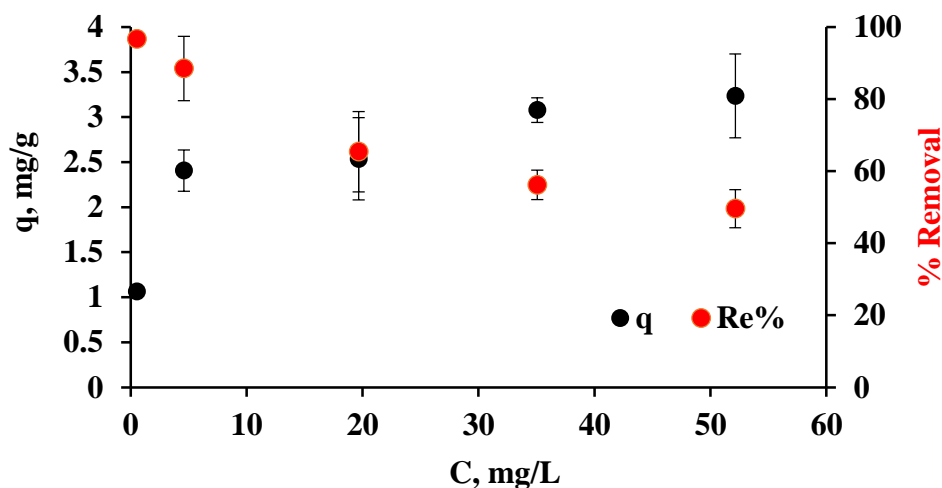


Figure 2. Equilibrium data for Co^{2+} adsorption onto CAC

Adsorption equilibrium data for the removal of Co^{2+} ions from aqueous solutions by cellulose acetate based foam were analyzed using the two-parameter models, Langmuir, and Freundlich, and three-parameter models, and Dubinin-Astakhov, and Sips.

Figure 3 shows the fit of the isotherm models to the experimental data for the adsorption of Co^{2+} ions from aqueous solutions by CAC. Calculated parameters of the tested isotherm models, and their goodness of fit measures are presented in Table 1. In Table 1, R^2 is the correlation coefficient, χ^2 represents Chi square, and NRMSE is the normalized root mean square error. NRMSE and χ^2 values close to zero, and R^2 value close to unity demonstrate that the model is effective at estimating the experimental results. Among the applied models, Langmuir, Freundlich, Sips and Dubinin-Astakhov showed good performances with high R^2 values, but Sips isotherm had a slightly better fit to the experimental data with the smallest NRMSE value, and the highest R^2 value. The maximum adsorption capacity calculated by Sips model was found to be 84.5 mg/g (at 298 K). Sips isotherm is a combination of both Langmuir and Freundlich isotherm models (Sips, 1948). As such, it is a hybrid model. This three-parametric isotherm is highly valid for predicting monolayer adsorption in homogenous and heterogeneous systems (Wang and Guo, 2020). Metal adsorbents generally fit Sips model (Chen et al., 2022).

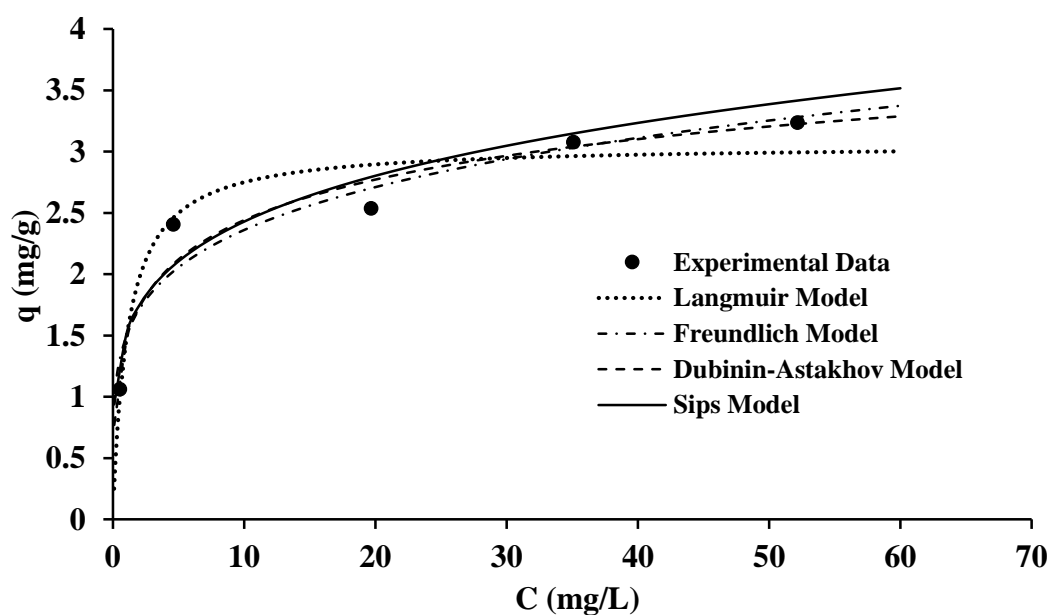


Figure 3. Model fit of adsorption isotherm of Co^{2+} adsorption onto CAC (Initial Co^{2+} concentration 20–100 mg/L, contact time 24 h, CAC dosage 15 g/L, pH 6.5)

Table 1. Isotherm model parameters and goodness of fit measures

Model	Equation	Model Parameters	Goodness of fit measures
Langmuir	$q_e = \frac{Q_{max}^o K_L C_e}{1 + K_L C_e}$	Q_{max} (mg/g) = 3.1 K_L (L/mg) = 0.893	$R^2 = 0.929$ $\chi^2 = 0.076$ NRMSE = 0.094
Freundlich	$q_e = K_F C_e^n$	K_F ((mg/g)/(mg/L) ⁿ) = 1.491 n = 0.1994	$R^2 = 0.918$ $\chi^2 = 0.132$ NRMSE = 0.101
Sips	$q_e = \frac{q_m^s K_S C_e^{1/n_S}}{1 + K_S C_e^{1/n_S}}$	q_m^s (mg/g) = 84.5 K_S (mg/L) ^{-1/n_S} = 0.018 1/n _S = 0.207	$R^2 = 0.936$ $\chi^2 = 0.094$ NRMSE = 0.089
Dubinin-Astakhov	$q_e = q_{DA(max)} \cdot \exp \left\{ -K_{DA} \left[RT \ln \left(\frac{C_S}{C_e} \right) \right]^{n_{DA}} \right\}$	$q_{DA(max)}$ (mg/g) = 3.95 K_{DA} ((mol/kJ) ^{n_{DA}}) = 0.0004 n _{DA} = 1.569	$R^2 = 0.919$ $\chi^2 = 0.130$ NRMSE = 0.101

4. CONCLUSIONS

This study investigated the synthesis and use of novel cellulose based adsorbents for the removal of heavy metals from aqueous solutions. Co²⁺ was selected as the target heavy metal and different cellulose based materials (i.e., activated cellulose, carboxymethyl cellulose, acetylated carboxymethyl cellulose and cellulose acetate based foams) were synthesized. The comparative adsorption studies showed that among the synthesized materials, cellulose acetate based foam exhibited the highest adsorption capacity and percent removal efficiency for Co²⁺ ions. Using this adsorbent material, equilibrium adsorption studies were conducted. Isotherm models including Langmuir, Freundlich, Sips and Dubinin-Astakhov models were used to describe the experimental data, where Sips isotherm model provided the best fit. The maximum adsorption capacity by Sips model was calculated as 84.5 mg/g and the highest percent removal efficiency (experimental) was 96.7%. The results of this study are expected to contribute to developing insights on the design and synthesis of novel adsorbent materials for the removal of heavy metals from aqueous solutions.

Acknowledgements: This study was supported by The Scientific and Technological Research Council of Turkey (TUBITAK) and The Higher Council for Innovation and Excellence of Palestine (HCIE), 2521 International Bilateral Research Project (Grant Number: 120N633), and the authors gratefully acknowledge TUBITAK and HCIE.

REFERENCES

- Ajmal, M., Khan, A.H., Ahmad, S. (1998). Role of sawdust in the removal of copper(II) from industrial wastes. *Water Research*, 32 (10), 3085-3091.
- Aniagor, C.O., Abdel-Halim, E.S., Hashem, A. (2021). Evaluation of the aqueous Fe (II) ion sorption capacity of functionalized microcrystalline cellulose. *J. Environ. Chem. Eng.* 9(4), 105703
- Bailey, S.E., Olin, T.J., Bricka, R.M. (1999). A review of potentially low-cost sorbents for heavy metals. *Water Research*, 33(11), 2469-2479.
- Bulut, Y., & Tez, Z. (2007). Removal of heavy metals from aqueous solution by sawdust adsorption. *Journal of Environmental Sciences*, 19(2), 160-166.
- Chen, X., Hossain, M. F., Duan, C., Lu, J., Tsang, Y. F., Islam, M. S., Zhou, Y. (2022). Isotherm models for adsorption of heavy metals from water - A review. *Chemosphere*, 307(1), 135545.
- Dorris, K.L., Zhang, Y., A Shukla, A. (2000). The removal of heavy metal from aqueous solutions by sawdust adsorption - removal of copper. *Journal of Hazardous Materials*, 80(1-3), 33-42.

- Gloaguen, V., & Morvan, H.J. (1997). Removal of heavy metal ions from aqueous solution by modified barks. *Environmental Sci. Health*, 32 (4), 901-912.
- Low, K.S., & CS Lee, C.S. (2000). Sorption of cadmium and lead from aqueous solutions by spent grain. *Process Biochemistry*, 36 (1-2), 59-64.
- Sips, R. (1948). On the structure of a catalys surface. *J. Chem. Phys.*, 16, 490–495.
- Tran, H.N., You, S.-J., Hosseini-Bandegharai, A., Chao, H.-P. (2017). Mistakes and inconsistencies regarding adsorption of contaminants from aqueous solutions: a critical review. *Water Research*, 120, 88–116.
- Wang, J., & Guo, X. (2020). Adsorption isotherm models: classification, physical meaning, application and solving method. *Chemosphere*, 258, 127279.

SUSTAINABLE CITIES FOR THE FUTURE WITH THE SUSTAINABLE URBAN WATER MANAGEMENT

Rouhollah Nasirzadehdizaji

Infrastructure Department, Yüksel Proje Inc., Ankara, 6610, Turkey

**Corresponding author (rnasirzadeh@yukselproje.com.tr)*

ABSTRACT

Management of water resources is becoming more complex due to the diversification of the issues encountered in terms of range and dimension on a global scale. Droughts and flash floods because of the effects of climate change are among those serious challenges for sustainable water resources management. Water scarcity and declining access to clean water are prominent and pervasive problems that are rapidly deteriorating across the globe. These problems have caused many cascading issues, both socially and economically. The most important of these issues is that the sustainability of life in ecosystems is under threat. These issues point to the need for new approaches to develop, control and manage water resources, and as such, the issue has started to be discussed in international meetings, programs, and commissions. Together, the environment and population form a living, dynamic system with a series of interrelated impacts that, if not managed properly, can lead to imbalances and even chaos. The concept of sustainable development has evolved to promote sustainable living in response to the economic and social pressures created by society's demands on natural resources. Key components of a sustainable urban environment include environmental protection and the integration of health and socioeconomic aspects into urban development. In this context, urban water infrastructure services include drinking water supply networks, wastewater, and stormwater drainage systems. Therefore, in line with the potable water and sewerage master plans, the objective of these projects is conducted to ensure adequate and efficient water, wastewater, and stormwater services are provided in an environmentally, financially, and institutionally sustainable manner.

Keywords: *urban water management, water sustainability, alternative water resources, water quality, climate change.*

1. INTRODUCTION

To answer the question of where and how much water was found in the past, it has become necessary to consider the amount and quality of the water and to assess the factors that affect both. Water resources are handled in the scope of “environment” in a wide range. The environment is a whole in terms of natural resources such as water, air, and soil; therefore, water resource management should be evaluated within the framework of the environment, as an intervention to one resource affects the others. The main purpose of integrated watershed management is not just about water volume, but to identify all aspects and resources of a watershed so that more consistent management decisions can be made (Harmancıoğlu et al., 2002).

Today, water resources are facing major problems on a global scale. Water scarcity is becoming a prominent and widespread problem, with water quality rapidly deteriorating throughout the world. Rapid urbanization in many developing countries without proper land use management and control leads to inadequate sanitation and solid waste management, as well as loss of water resources. It is estimated that by 2050, 70% of the population will live in cities (Aksu, 2011). The increase in impermeable areas (land use change) and unsustainable drainage (canals and waterways) is causing erosion, pollution, flooding, and overflows. Traditional approaches used in the management of urban water systems need to be based on the planning of a large-scale centralized infrastructure that aims to control variables such as water supply and demand and wastewater treatment plants and reduce uncertainties. The centralized infrastructure approach leads to the collection of different water services, such as drinking water, wastewater, and stormwater, in separately managed areas within the existing infrastructure. This system results in the independence of the departments responsible for the different parts of the water chain (water production, purification, distribution, wastewater collection, and treatment), which leads to acting relatively independently from each other in both internal and external works. To address today's water issues, the entire water cycle must be considered as a whole. To this end, the Integrated Urban Water Management (IUWM) framework has been developed, recognizing that water is an indispensable element of almost all urban services.

2. MATERIAL AND METHODS

Most urban master planning projects rarely consider all the infrastructure components related to urban water management. Thus, their outputs are poor and are few efficiency indicators. The urban water system performs the following tasks:

- providing the population with drinking water (water supply),
- collection and treatment of city-generated sewage before it is discharged into rivers or other receiving environments, thereby protecting the environment and water resources (protection for the future) and preventing the spread of diseases (sanitation),
- install stormwater drainage systems to reduce harmful effects on the quality of receiving waters after the urban occupation and,
- collecting and disposing of solid waste to reduce health risks from clogging and contamination of natural and designed systems with solid waste.

The main objectives of these services are related to safety (such as stormwater flood control), health, and environmental management.

Integrated Water Resources Management (IWRM) is increasingly being implemented as a tool to promote the sustainable management of water resources at the river basin level. Cities are generally located within a larger basin or may contain several smaller basins. Cities often draw water from upstream water sources, supplying and discharging wastewater into downstream water bodies in the basin. These form the external components of the city that must be managed along with the main watershed. In terms of urban water system management, IWRM refers to IUWM. Integrated Water Resources Management includes the management of water facilities and their interactions as part of Integrated Urban Management which contains the components of urban development (a driving force on the economic and social development of the city), environment, health, and institutional components. It is represented by a legal framework,

capacity building and monitoring of necessary information, service management, and development. In this context, the adapted framework of the IUWM applied to the sustainable cities programs and master plan projects is shown in **Figure 1**.

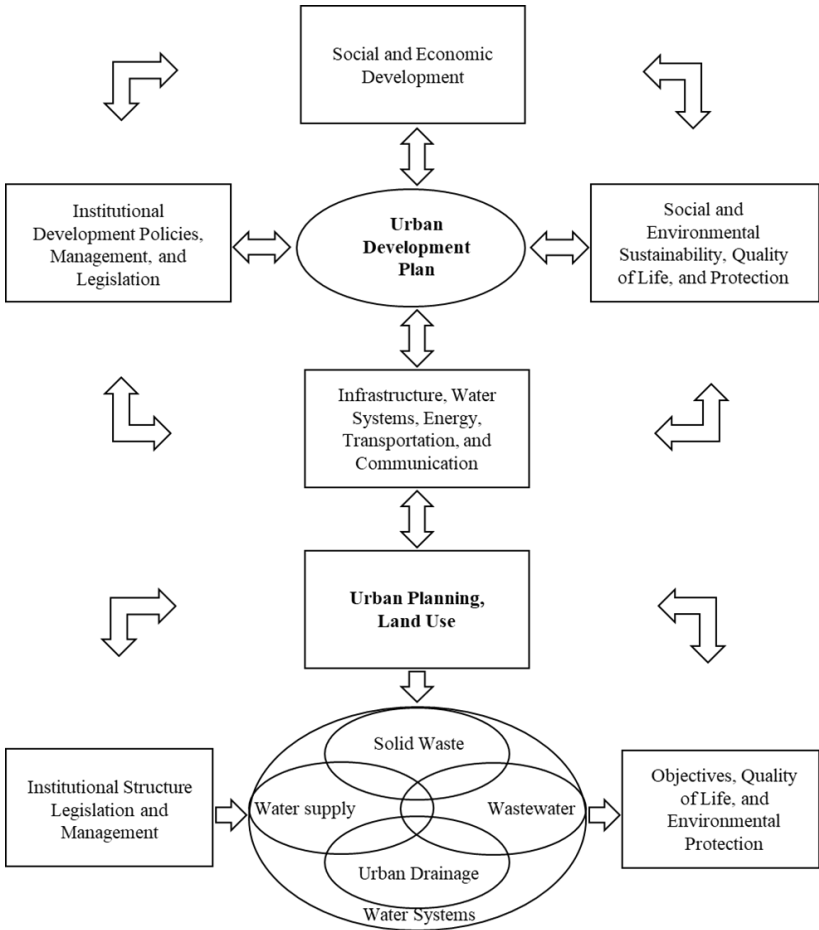


Figure 1. Integrated urban water management (IUWM) scheme (Tucci, 2009).

3. RESULTS AND DISCUSSIONS

The role of the IUWM is the improved, integrated, and effective management of water (quantity and quality) for different uses in urban areas. It covers traditional and alternative water sources involving freshwater (surface water, groundwater, and desalinated water), wastewater (e.g., reclaimed water), and the resource management structure (e.g., gray water or stormwater). In addition, the IUWM calls for the harmonization of urban development and watershed management agendas to ensure sustainable economic, social, and environmental relations across the urban-rural continuum. In other words, it is an adaptive and iterative process that enables cities to respond to changes and leads to covering the environmental, economic, social, technical, and political aspects of water management. Hence, a successful IUWM approach requires a structured process for communities to reflect their needs and knowledge of water management.

In general, integrated water management for the city is an approach that combines all elements of the water cycle and land use planning to ideally achieve social, economic, and environmental outcomes. Integrated water management, along with the city's land use planning and water

resources, identifies the challenges of population growth and the effects of climate change, and aims to improve the current quality of life in the city, which leads to improving the working environment in all aspects. Thus, making the city an ideal place for life, production, and development.

4. CONCLUSIONS

Ideal cities handle their water sustainably. This means the efficient provision of robust, reliable, and easily accessible water, as well as reliable sanitation and pollution-protected waterways. Sustainability also means being resilient and adaptable to extreme weather events that can lead to problems such as floods and famine. There are different challenges to ensuring water sustainability. Although the demand for water in cities is increasing, aquifers' water level is seriously falling or depleted from excessive groundwater withdrawal. On the other hand, water resources face difficulties across the globe due to changes in weather conditions caused by climate change. Cities are responsible for protecting their citizens from pollutants, diseases, and devastating storm surges that can be difficult to predict. Urbanization has increased impervious areas that can lead to flooding, resulting in increased demand for drinking water and increased sanitation. There is no single appealing strategy for achieving urban water sustainability. Hence, certain strategies and best practices are needed to make cities better and safer, and sustainable for the future. In this regard, modern planning practices need to be adaptive and risk-based, as well as flexible enough to account for contingencies or developments. Optimization of the water resources begins with a good knowledge of assets, system performance, and the types and levels of usage, both current and projected. Combination of this information with information about the system's vulnerabilities, risks, and stress points leads to actionable plans that can help utilities achieve greater efficiency. Demonstrating how these vulnerabilities threaten city operations and the quality of life, as well as city competitiveness, will provide important information for decision-makers in water management for appropriate planning. Cities in developed countries have historically improved their prosperity and economies particularly when water and sanitation issues are adequately addressed. Therefore, to be prosperous and sustainable cities in terms of water resources, developing countries will need to improve their water and sanitation systems, as well as water quality.

Acknowledgements: The author would like to thank all colleagues in the infrastructure department, especially Anıl OLGAÇ, manager of the infrastructure department at Yüksel Proje Inc., for their contributions and efforts.

REFERENCES

- Harmancıoğlu, N.B., Gül A. & Fıstıkoğlu O, (2002). Entegre Su Kaynakları Yönetimi. Türkiye Mühendislik Haberleri Dergisi – SUI, *Türkiye İnşaat Mühendisleri Odası*, 47/2002-3, (419, s. 29-39).
- Aksu, L, (2011). Dünya'da ve Türkiye'de Nüfus Analizleri. *Istanbul Journal of Sociological Studies*, 0 (25), 219-311.
- Tucci, C.E.M, (2009). Integrated Urban Water Management in Large Cities: A Practical Tool for Assessing Key Water Management Issues in the Large Cities 0 of the Developing World. *World Bank*.

EMERGING POLLUTANTS

KINETICS OF THE PHOTOLYTIC AND PHOTOCATALYTIC DEGRADATION OF VETERINARY ANTIBIOTICS

Johanna Zambrano^{a,b}, Pedro Antonio García-Encina^{a,b}, Juan José Jiménez^{a,c}, Rebeca López-Serna^{a,c}, Rubén Irusta-Mata^{a,b,*}

^a Institute of Sustainable Processes. University of Valladolid. Dr. Mergelina s/n, 47011 Valladolid. Spain

^b Department of Chemical Engineering and Environmental Technology, School of Industrial Engineering, University of Valladolid, Dr Mergelina s/n 47011 Valladolid, Spain.

^c Department of Analytical Chemistry, University of Valladolid, Campus Miguel Delibes, Paseo Belen 7, 47011 Valladolid, Spain

*Corresponding author (ruben.irusta@uva.es)

ABSTRACT

The removal of a mixture of four veterinary antibiotics (VA) – tetracycline (TET), ciprofloxacin (CIP), sulfadiazine (SDZ) and sulfamethoxazole (SMX) – via photo-degradation and photocatalysis with TiO₂ was investigated in a batch reactor under different initial concentrations. Ultra-high performance liquid chromatography coupled to a mass spectrometry (UHPLC-MS/MS) was used to determine the removal of these VA. The removal via photolysis was around 98 - 99% after 100 hours for TET, 122 hours for CIP, 212 hours for SDZ and 240 hours for SMX. Nevertheless, the removal via photocatalysis was around 99 - 100% after 4.2 hours for TET, 3.5 hours for CIP, 7.1 hours for SDZ and 16.5 hours for SMX. The photolysis for the VA followed a first-order irreversible kinetic model. The photocatalysis of TET, CIP and SDZ followed a Langmuir-Hinshelwood kinetic model, and adsorption was considered the limiting step. SMX followed a first-order irreversible kinetic model. The VA degradation was enhanced by the use of a catalyst. Additionally, electrical energy per order (E_{EO}) was assessed to estimate the electrical energy efficiency of each process. The energy consumption for photocatalysis was considerably lower than for photolysis. This study determined, for the first time, an overall degradation rate constant for a wide range of TET, CIP, SDZ and SMX concentrations. Furthermore, when working at pH 8 (typical pH from livestock farms wastewater) and a VA mixture whose concentrations resemble the characteristics of real water samples, this study showed that photolysis and photocatalysis are potential processes for wastewater treatment with low energy consumption.

Keywords: Photodegradation; E_{EO} ; TiO₂; UVC; antibiotics

1. INTRODUCTION

Antibiotics are one of the most important pharmaceutical groups used by humans and are also used in veterinary medicine and aquaculture. Veterinary antibiotics (VA) are widely used to increase animal production and prevent, control or treat diseases. The widespread use of antibiotics means that they are commonly found in wastewater, surface water, ground water,

and drinking water at trace concentration levels, ranging from ng/L to mg/L. The presence of VA in aquatic environments has become an increasing global concern due to their potential adverse effects to the environment and significant public health implications [1].

The growing interest in VA has led to extensive studies on environmentally friendly processes which can be cost effective. Over the last few years, advanced oxidation processes (AOPs) such as ozonation, Fenton oxidation, electrochemical degradation, photolysis and photocatalysis had been widely studied for wastewater treatment. Specially, ultraviolet (UV) irradiation has demonstrated its effectiveness for chemical oxidation and water and wastewater disinfection. Direct and natural photolytic decomposition and transformation of many organic pollutants has been proved. Moreover, photocatalysis has emerged as a promising technique for VA removal as it can mineralize a variety of recalcitrant organics through the generation of hydroxyl radical (OH^\bullet) which is highly reactive and non-selective. Titanium dioxide (TiO_2) is the most widely used catalyst due to its abundance, photo stability, good performance and non-toxic characteristics [2].

Photocatalytic processes have shown to be a suitable choice because they can obtain high mineralization percentages. However, most of the previous studies found in the literature have focused on a single contaminant which may not be representative of real water treatment conditions [3]. From this perspective, the aim of this study is to determine the photolytic and photocatalytic degradation of a mixture of TET, CIP, SDZ and SMX, as representative compounds of fluoroquinolones, sulfonamides and tetracyclines, the three antibiotic families most frequently found in piggery water samples, at small concentrations similar to those found in real samples.

To determine the influence of the initial concentration on the photolytic (UVC) and photocatalytic (UVC/ TiO_2) degradation of TET, CIP, SDZ and SMX, four different initial concentrations (20, 100, 500 and 1000 $\mu\text{g/L}$) of each compound were used. These concentrations were selected to resemble a range of VA concentrations in manure which can be found in the literature. To our knowledge, no other authors have published rate constants for TET, CIP, SDZ and SMX by fitting experimental data over a wide range of concentrations to a single general equation. In the literature is common to find studies with different initial VA concentration and a rate constant for each concentration, which is not correct, because when the other operating parameters do not change, the rate constant does not change with concentration. Removals, kinetics and energy consumption were studied and compared with the literature. Other important parameters which can influence the efficiency of the process – such as pH, light intensity, type of radiation, use of O_2 , and irradiation time – remained unchanged during the operation time. However, they were considered in the comparison with the literature.

2. MATERIAL AND METHODS

2.1. Chemicals and reagents

Individual stock solutions of 1 g/L for TET, SDZ and SMX were prepared on a weight basis in methanol (MeOH). CIP was dissolved in H₂O/MeOH (1:1) containing 0.2% v/v hydrochloric acid (HCl). MeOH of high analytical grade was acquired from Sigma-Aldrich (Stockholm, Sweden), VA of high purity grade (N95%) and HCl (37%) were obtained from Sigma-Aldrich (Tres Cantos, Madrid, Spain). CIP, SDZ and SMX were acquired as neutral non-solvated molecules and TET was purchased as a hydrochloride. P-25 titanium dioxide (Degussa AG, Germany) was supplied by Quimidroga S.A. TiO₂ specific surface was 50 ± 15 m², the particle size was 21 nm and the bandwidth energy was 3.2 eV. Ultrapure water was generated by a Milli-Q (MQ) Advantage Ultrapure Water purification system and filtered through a 0.22 µm Millipak Express membrane and an LC-Pak polishing unit by Merk Millipore (Billercia, MA, USA).

2.2. Experimental set-up

The photoreactor system consists of a methacrylate reactor formed by two concentric tubes. The outer tube has an inner diameter of 14 cm and the inner tube has an outer diameter of 6 cm. These measurements have been designed so that the wall of the inner tube to the outside does not exceed 4 cm in order to avoid loss of radiant energy. The active zone in the reactor is delimited by the two tubes and the liquid level, which has a useful volume of 5.6 L. Philips UVC lamp (TUV PL-L 36W/4P 1CT/25) with a peak emission at 257.7 nm and TiO₂ in suspension were used. A homogeneous incident flux of 13.33 mW/cm² was used. A cylindrical shape diffuser placed at the bottom of the reactor, which injected air from a diaphragm pump, was used for a continuous mixing.

2.3. Degradation analysis

Photolytic and photocatalytic degradation experiments were performed under UVC irradiation at 25 °C and a pH of 8.0. Tests were performed with a mixture of four antibiotics to a final concentration of 1000, 500, 100 and 20 µg/L per antibiotic. After filling the reactor, for the photolytic analysis, an initial sample was taken to determine the initial antibiotic concentration and the UVC lamp was immediately turned on. For the photocatalytic analysis, an initial sample was taken to determine the initial antibiotic concentration. After that, TiO₂ was added to the reactor under continuous mixing to obtain a concentration of 1 g/L. The solution was stirred under dark conditions for 30 min and two samples were taken every 15 min. After 30 min the UVC lamp was switched on and samples were taken at prefixed intervals, filtered through 0.22 mm pore-size nylon syringe filters (Fisherbrand) and stored at 4 °C before analysis. Experiments were conducted in triplicate.

2.4. Analytical method

The quantitative determination of selected antibiotics was carried out by ultra-high performance liquid chromatography (UHPLC) coupled to a MS/MS spectrometry. The chromatographic separation was carried out using an Exion LC AD instrument from AB Sciex (Framingham, MA, USA) and a reversed-phase column EVO C18 (50 × 2.1 i.d. mm, 1.7 µm

particle size) from Phenomenex (Torrance, CA, USA). MS/MS analysis was performed by a triple quadrupole 6500+ from AB Sciex in selected reaction monitoring (SRM) mode. The procedure was based on the one previously developed by López-Serna et al. [4], employing direct injection of the (diluted) samples, without any pre-concentration step.

2.5. Kinetic analysis

Four kinetic models – zero-order (Eq. 1), pseudo-first order irreversible (Eq. 2), pseudo-first order reversible (Eq. 3) and Langmuir-Hinshelwood (Eq. 4) – were used to fit the experimental data.

$$r = -\frac{dC}{dt} = k_0 \quad (1)$$

$$r = -\frac{dC}{dt} = k_1 \cdot C \quad (2)$$

$$r = -\frac{dC}{dt} = k_2 \cdot (C - C_e) \quad (3)$$

$$r = -\frac{dC}{dt} = \frac{k_r \cdot K \cdot C}{1 + K \cdot C} \quad (4)$$

where, r is the rate of antibiotics degradation ($\mu\text{g}\cdot\text{L}^{-1}\cdot\text{min}^{-1}$), C is the concentration at any time ($\mu\text{g}\cdot\text{L}^{-1}$), C_e is the concentration at equilibrium ($\mu\text{g}\cdot\text{L}^{-1}$), k_0 is the zero-order rate constant ($\mu\text{g}\cdot\text{L}^{-1}\cdot\text{min}^{-1}$), k_1 is the pseudo-first order irreversible rate constant (min^{-1}), k_2 is the pseudo-first order reversible rate constant (min^{-1}), and k_r ($\mu\text{g}\cdot\text{L}^{-1}\cdot\text{min}^{-1}$) and K ($\text{L}\cdot\mu\text{g}^{-1}$) are the rate constant and the adsorption constant, respectively.

Integrating Eq. (1), (2), (3) and (4) with respect to the limits $C = C_0$ (C_0 is the initial antibiotic concentration before irradiation and after 30 min to reach the adsorption equilibrium when TiO_2 is used) and $C = C_t$ (C_t is the antibiotic concentration at time t (min) under light irradiation), Eq. (5), (6), (7) and (8) can be obtained:

$$C_t = C_0 - k_0 \cdot t \quad (5)$$

$$C_t = C_0 \cdot e^{-k_1 \cdot t} \quad (6)$$

$$C_t = C_e + (C_0 - C_e) \cdot e^{-k_2 \cdot t} \quad (7)$$

$$-\ln\left(\frac{C_t}{C_0}\right) - K \cdot (C_t - C_0) = k_r \cdot K \cdot t \quad (8)$$

2.6. Electrical energy determination

In order to compare photocatalysis by means of energy consumption with other advanced oxidation processes (AOP), the electrical energy per order (E_{EO}) was calculated. E_{EO} is defined as the electrical energy required to reduce the concentration of a pollutant by one order of magnitude (90%) in a fixed volume of polluted water. E_{EO} is calculated as follows:

$$E_{EO} = \frac{P \cdot t}{V \cdot \log\left(\frac{C_0}{C_f}\right)} \quad (9)$$

where, P is the rated power (kW) of the AOP system, V is the volume (m³) of water treated in the time t (h), C₀ (µg/L) is the initial antibiotic concentration before irradiation (and after 30 min to reach the adsorption equilibrium when TiO₂ is used), and C_f (µg·L⁻¹) is the final antibiotic concentration.

3. RESULTS AND DISCUSSIONS

3.1. Degradation of veterinary antibiotics

To the best of our knowledge, for the first time, a mixture of four antibiotics with an initial concentration range adjusted to those that can be found in real water samples was used to analyze the degradation of VA via photolysis and photocatalysis. VA photolysis was studied in batch experiments for 180 min. For the four antibiotics, a decrease in the initial concentration over time was observed. In all the studied conditions, TET showed a higher decrease in its initial concentration because it is a very light sensitive antibiotic. In a literature review, Prakash et al., [5] compared the photolysis of tetracyclines, quinolones and sulfonamides, and showed that tetracyclines can obtain high removals, around 80%, while quinolones and sulfonamides achieve very low removals.

Moreover, photocatalysis was evaluated for 180 min. Starting with an initial VA concentration of 100 µg/L before adsorption, complete removal of TET was obtained at 180 min and at 90 min CIP was totally removed. At 20 µg/L before adsorption, complete removal of TET and CIP was obtained at 75 and 60 min, respectively. In all the studied conditions, CIP showed the highest decrease in its initial concentration. Considering the pH_{ZPC} and pH solution, CIP was dissociated – hence its cations enhanced its adsorption capacity on the negatively charged TiO₂ through electrostatic attraction [6]. Adsorption into the catalyst is crucial to obtain high removal percentages. In the following sections, we will determine the kinetics of the photolytic and photocatalytic processes as well as the removal percentages than can be obtained by these processes.

3.2. Kinetics of degradation of veterinary antibiotics

The photolysis and photocatalysis of the four veterinary antibiotics were investigated with zero-order and pseudo-first order kinetic models. A pseudo-first order kinetic model was evaluated and considered both an irreversible and a reversible reaction. It was considered that the photolytic and the photocatalytic reaction could reach an equilibrium where parental compounds and byproducts generated during the process would compete for the photons, electron holes produced on the catalyst and/or the generated oxidation species. Additionally, the Langmuir-Hinshelwood kinetic model, which considered adsorption as the limiting step, was used to study the kinetics of photocatalysis. To calculate the kinetic parameters of

photocatalysis, the experimental data was considered after adsorption when the UVC light was turned on.

The kinetic parameters were obtained by an adjustment of the experimental data to a zero-order kinetic was done as shown in Eq. (5) by drawing the concentration data versus time. If the kinetics is a zero-order, then the experimental data will fit to a straight line with the ordinate at the origin C_0 and slope $-k_0$. Analogously transforming Eq. (6), Eq. (9) is obtained:

$$-\ln\left(\frac{C_t}{C_0}\right) = k_1 \cdot t \quad (9)$$

By drawing $-\ln(C_t/C_0)$ versus t , if the kinetics is a pseudo-first order irreversible, then the experimental data will fit to a straight line with the ordinate at the origin C_0 and slope k_1 . The experimental data was also fitted to a pseudo-first order reversible kinetics by transforming Eq. (7) into:

$$-\ln\left[\frac{C_t - C_e}{C_0 - C_e}\right] = k_2 \cdot t \quad (10)$$

By drawing $-\ln[(C_t - C_e)/(C_0 - C_e)]$ versus t , if the kinetics is a pseudo-first order reversible, then the experimental data will fit to a straight line with the ordinate at the origin and slope k_2 . For this, we must find the values of parameters k_2 and C_e which would make the experimental data fit best to that straight line. Those parameters were obtained by the GRG Nonlinear Solving method. Fitting experimental data of photolysis and photocatalysis as in step 3, the C_e obtained was 0, it means that the kinetic model that best fit was the pseudo-first order irreversible model. Additionally, for photocatalysis, when the experimental data was fitted to a pseudo-first order irreversible kinetic model at small antibiotic concentrations, the experimental data started to disperse from the line. Therefore, we inferred that the photocatalysis of the antibiotic might be limited by the adsorption of the antibiotics into the catalyst and that the photocatalytic process might follow a Langmuir-Hinshelwood kinetics [7]. Once again, the best values of the constants k_r and K in Eq. (8) were obtained using the GRG Nonlinear Solving method. The coefficient of determination R^2 was used to decide whether the experimental data better fit a zero-order, pseudo-first order irreversible/ reversible, or Langmuir-Hinshelwood kinetics model.

3.2.1. Photolysis

Pseudo-first order irreversible kinetics presented R^2 values closer to unity and fit best to the experimental data for the photolysis of TET, CIP, SDZ and SMX (Fig. 1). TET and CIP were degraded faster than SDZ and SMX. TET presented the higher rate constant in the photolytic process. The pseudo-first order irreversible rate constant for the removal of antibiotics by photolysis were 0.00073 min^{-1} for TET, 0.00055 min^{-1} for CIP, 0.00031 min^{-1} for SDZ and 0.00027 min^{-1} for SMX.

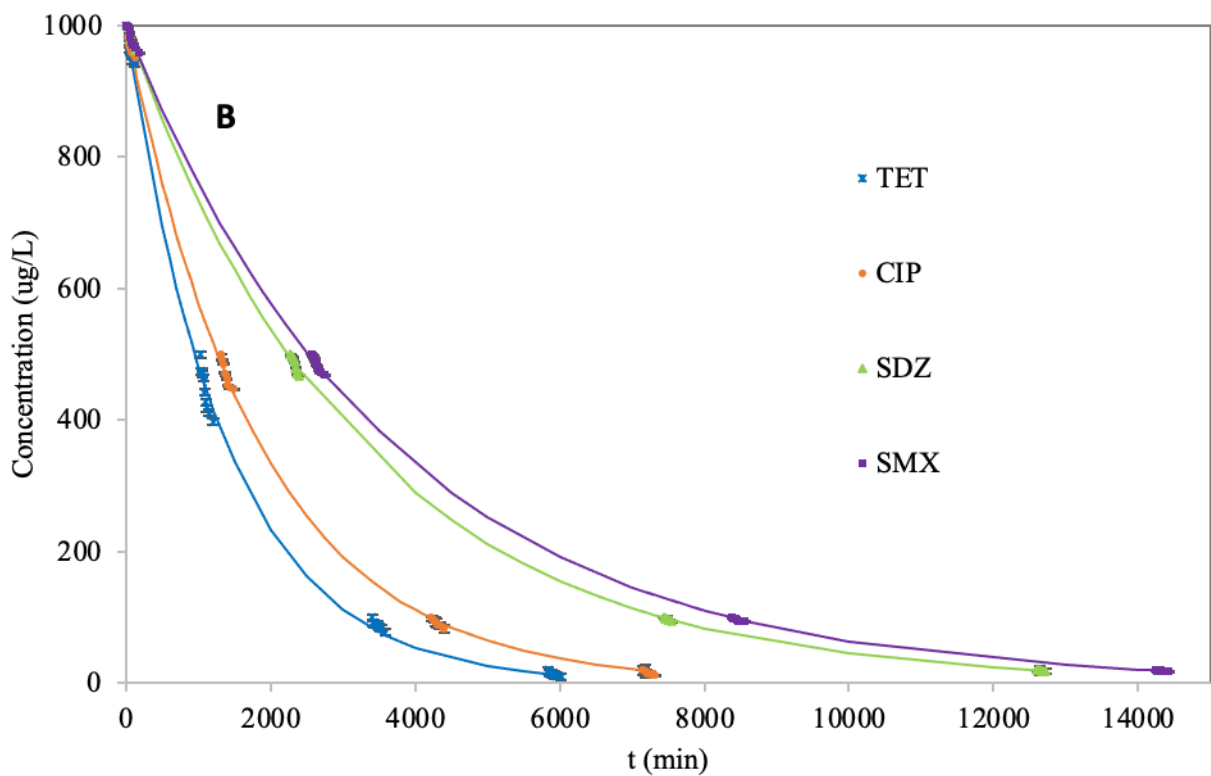
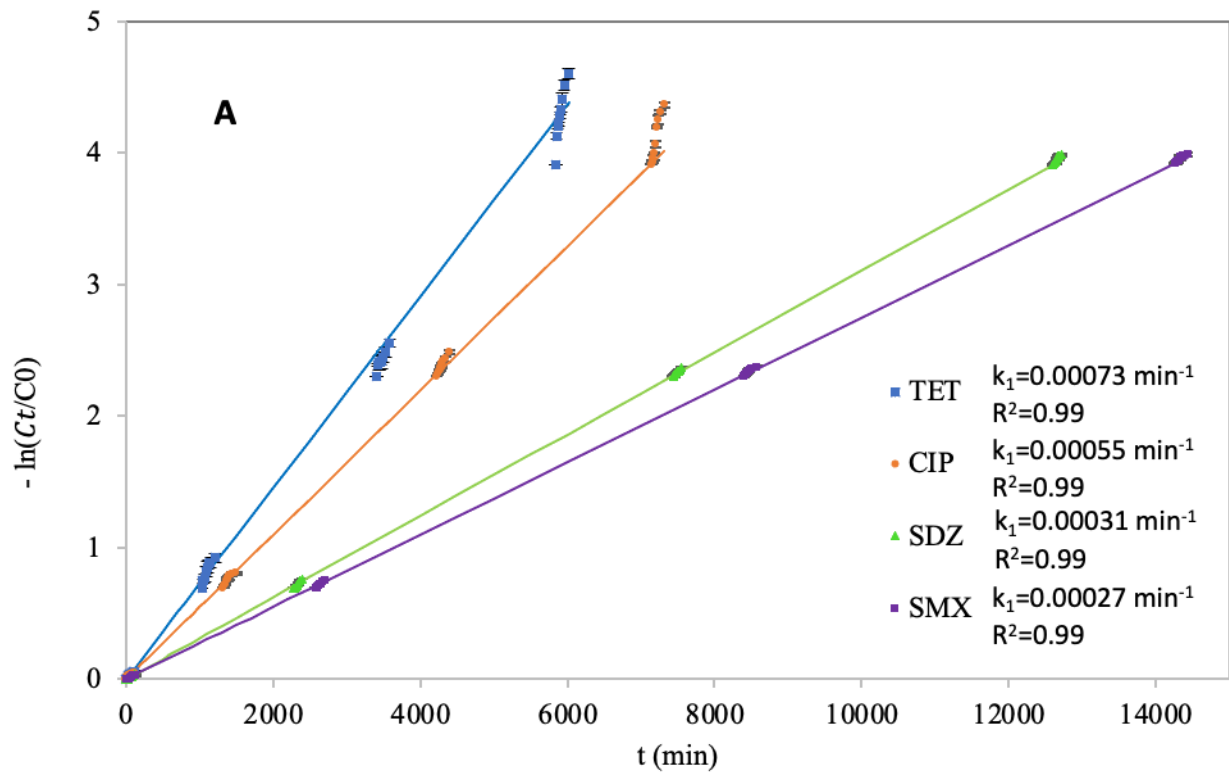


Fig. 1. (A) Linear representation of pseudo-first order kinetics for the antibiotic removal by photolysis. (B) Antibiotic concentration variation by photolysis along time. Error bars represent \pm standard error of the mean.

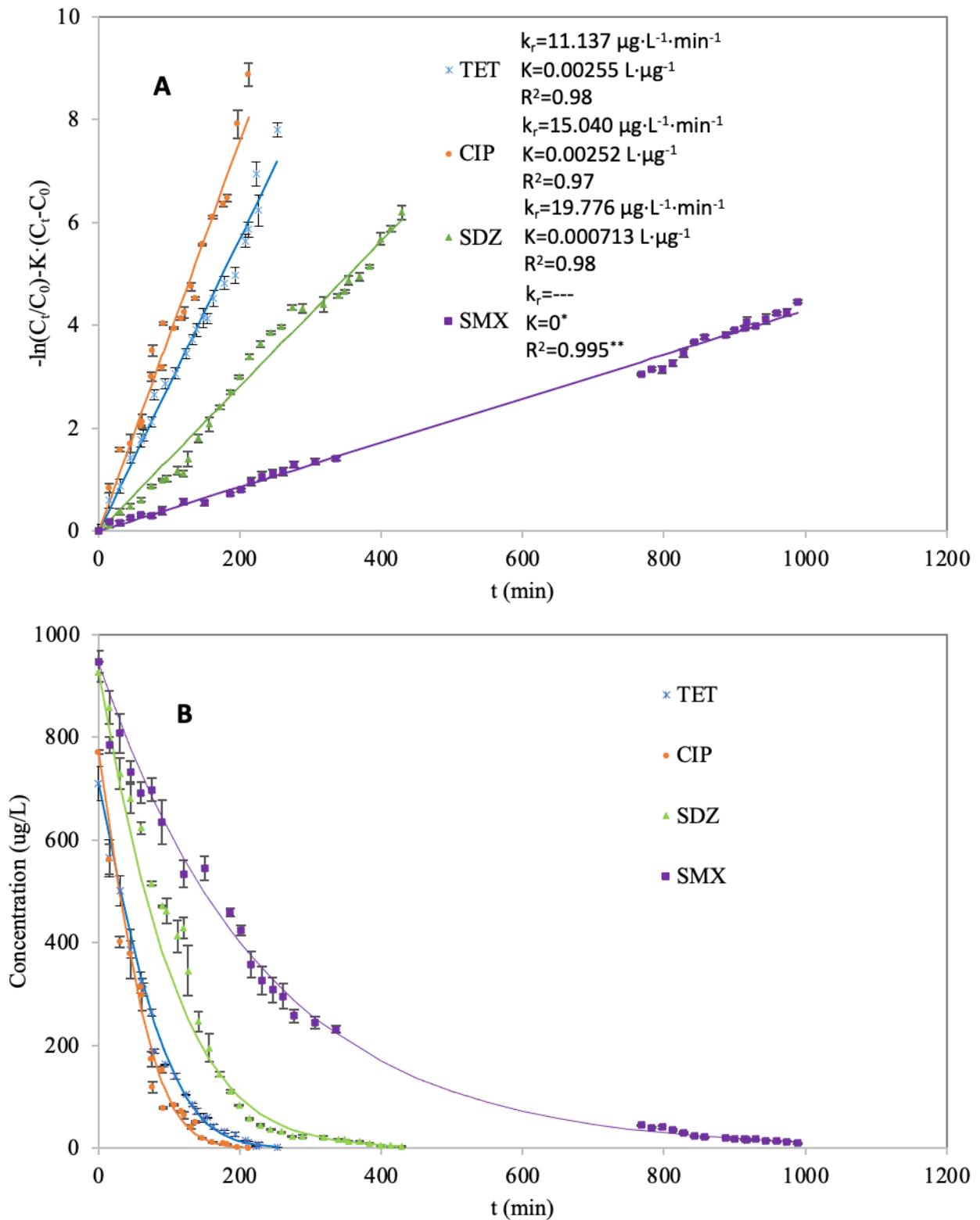


Fig. 2. Linear representation of Langmuir-Hinshelwood kinetics for the antibiotic removal by photocatalysis. (B) Antibiotic concentration variation by photocatalysis along time. Error bars represent \pm standard error of the mean.

* Photocatalysis of SMX adjusted to a pseudo-first order kinetics because $K=0$

** The linear adjust corresponds to a pseudo-first order kinetics because $K=0$

3.1.1. Photocatalysis

The Langmuir-Hinshelwood kinetics model best fit to the experimental data for the photocatalysis of TET, CIP and SDZ (Fig. 2). CIP had the highest rate constants of the four antibiotics. CIP removal was faster than the other three antibiotics in photocatalysis due to its better absorption into the catalyst; the log K_{ow} of CIP (1.32) was higher than that of TET (-1.37), SDZ (-0.09) and SMX (0.89), indicating that CIP has a better affinity to TiO_2 . When applying the Langmuir-Hinshelwood kinetics model to SMX, the K (constant for adsorption) obtained was 0, which means that SMX photocatalysis was not limited by adsorption. SMX followed a first-order irreversible kinetic model with a k_1 of 0.0044 min^{-1} .

3.2. Removal of veterinary antibiotics

The removal of the four veterinary antibiotics by photolysis is shown in Fig. 1B, while their removal by photocatalysis can be seen in Fig. 2B. TET removal by photolysis was 99% after 100 h and TET removal by photocatalysis was 99.75% after 4.2 h. Comparing the literature with the results obtained in the present study, the findings agree on the capacity of photolysis and photocatalysis to degrade TET, with enhanced degradation when using a catalyst and UV irradiation. CIP removal by photolysis was 98.7% after 122 h and CIP removal by photocatalysis was 99.90% after 3.5 h. Other studies have reported the same trend for CIP as the ones observed in the present study; photo degradation by UV irradiation and complete removal of CIP by the use of TiO_2 powder. SDZ removal by photolysis was 98.1% after 212 h and SDZ removal by photocatalysis was 99.61% after 7.1 h. SDZ is very stable and little degradation was observed in the absence of TiO_2 . However, SDZ proved to be photosensitive and further degradation can be obtained by photocatalysis [8]. The results for SDZ are consistent with previous findings in the literature. SMX removal by photolysis was 98.2% after 240 h and SMX removal by photocatalysis was 98.84% after 16.5 h. The SMX results are comparable with those from the literature; photolysis and photocatalysis demonstrated their ability to degrade SMX, with a higher removal when using TiO_2 .

3.3. Energy consumption

The electrical energy consumption for the photolytic and photocatalytic degradation of the veterinary antibiotics was calculated. The E_{EO} values for photolysis were 339.06 $\text{kWh/m}^3/\text{order}$ for TET, 449.84 $\text{kWh/m}^3/\text{order}$ for CIP, 795.31 $\text{kWh/m}^3/\text{order}$ for SDZ, and 897.71 $\text{kWh/m}^3/\text{order}$ for SMX. SMX turned out to be the antibiotic which consumed more energy for its degradation. Likewise, for the photocatalytic process, SMX presented the highest E_{EO} value. The E_{EO} values for photocatalysis were 14.96 $\text{kWh/m}^3/\text{order}$ for TET, 12.07 $\text{kWh/m}^3/\text{order}$ for CIP, 20.39 $\text{kWh/m}^3/\text{order}$ for SDZ, and 62.10 $\text{kWh/m}^3/\text{order}$ for SMX. The faster photolysis rate of TET and the higher photocatalytic rate of CIP means that they are the antibiotics with the lowest electrical energy consumption in each process. E_{EO} values for photolysis were around 15 to 37 times higher than the E_{EO} values for photocatalysis.

4. CONCLUSIONS

Removal efficiencies, kinetics and energy consumption were evaluated for the photo-degradation (UVC) and photocatalytic-degradation with TiO₂ (UVC/TiO₂) of a mixture of four antibiotics at different initial concentrations. TET, CIP, SDZ and SMX proved to be photosensitive and capable of being removed by either photolysis or photocatalysis. Photocatalysis attained the higher degradation percentages. This study has analyzed for the first time the photolytic and photocatalytic degradation kinetics of VA over a wide range of concentrations, such as those found in real water samples, using a general equation for the whole set of concentrations analyzed and not using individual equations for each initial concentration which is a misconception found in the literature. Its limitation is that it is only applicable for the pH and temperature used in this study. The photolysis for the four veterinary antibiotics followed a first-order irreversible kinetic model. The photocatalysis of TET, CIP and SDZ followed a Langmuir-Hinshelwood kinetic model, and adsorption was considered as the limiting step. SMX followed a first-order irreversible kinetic model. The calculation of the electrical energy consumed by both processes showed that photocatalysis is energy efficient compared with other systems. These results are helpful to assess the extent of degradation of VAs in water treatment processes by photolysis and photocatalysis. UVC photocatalysis with TiO₂ was found to be efficient and cost-effective in the removal of VAs. Further investigations shall be done in the influence of different parameters such as ions and oxidants present in real water samples that could enhance the photolytic and photocatalytic degradation of VAs.

Acknowledgements: This work was supported by the regional government of Castilla y León (UIC 071, CLU 2017-09 and VA080G18). The authors also thank “Ministerio de Ciencia, Innovación y Universidades” (PID2020-113544RB-I00) and the EU-FEDER (CLU 2017-09 and CTQ2017-84006-C3-1-R) for the financial support of this work. Johanna Zambrano wishes to thank the government of Castilla y León for her Doctorate Contract.

REFERENCES

- [1] D. Cheng, H.H. Ngo, W. Guo, S.W. Chang, D.D. Nguyen, Y. Liu, Q. Wei, D. Wei, A critical review on antibiotics and hormones in swine wastewater: Water pollution problems and control approaches, *J. Hazard. Mater.* 387 (2020) 121682. <https://doi.org/10.1016/j.jhazmat.2019.121682>.
- [2] R. Yuan, Y. Zhu, B. Zhou, J. Hu, Photocatalytic oxidation of sulfamethoxazole in the presence of TiO₂: Effect of matrix in aqueous solution on decomposition mechanisms, *Chem. Eng. J.* 359 (2019) 1527–1536. <https://doi.org/10.1016/j.cej.2018.11.019>.
- [3] J. Gomes, J. Lincho, E. Domingues, R.M. Quinta-Ferreira, R.C. Martins, N-TiO₂ photocatalysts: A review of their characteristics and capacity for emerging contaminants removal, *Water (Switzerland)*. 11 (2019) 373. <https://doi.org/10.3390/w11020373>.
- [4] R. López-Serna, M. Petrović, D. Barceló, Development of a fast instrumental method for the analysis of pharmaceuticals in environmental and wastewaters based on ultra high performance liquid chromatography (UHPLC)-tandem mass spectrometry (MS/MS), *Chemosphere*. 85 (2011) 1390–1399. <https://doi.org/10.1016/j.chemosphere.2011.07.071>.
- [5] A. Prakash, A. Verma, S. Goyal, P. Gauba, Remediation of Antibiotics from the Environment, *J. Basic Appl. Eng. Res.* 2 (2015) 633–636. <http://www.krishisanskriti.org/jbaer.html>.
- [6] J. Li, M. Cui, Kinetic study on the sorption and degradation of antibiotics in the estuarine water: an evaluation based on single and multiple reactions, *Environ. Sci. Pollut. Res.* (2020). <https://doi.org/10.1007/s11356-020-10194-4>.
- [7] B. Ohtani, Photocatalysis A to Z-What we know and what we do not know in a scientific sense, *J. Photochem. Photobiol. C Photochem. Rev.* 11 (2010) 157–178. <https://doi.org/10.1016/j.jphotochemrev.2011.02.001>.
- [8] X. Xiang, L. Wu, J. Zhu, J. Li, X. Liao, H. Huang, J. Fan, K. Lv, Photocatalytic degradation of sulfadiazine in suspensions of TiO₂ nanosheets with exposed (001) facets, *32 (2021) 3215–3220*.

PHARMACEUTICALS RESIDUES AND BIOCIDES FROM BIOSOLIDS AND MANURE SPREAD AS FERTILIZERS: FIRST RESULTS AFTER ONE YEAR FIELD STUDY

Pernin Noémie^{1*}, Benoit Pierre², Patureau Dominique³, Wiest Laure⁴, and Bertrand-Krajewski Jean-Luc¹

¹Univ Lyon, INSA Lyon, DEEP, EA 7429, 11 rue de la physique, F-69621 Villeurbanne cedex, France

² Université Paris-Saclay, INRAE, AgroParisTech, UMR ECOSYS, Thiverval-Grignon, France

³ INRAE, Univ Montpellier, LBE, 102 Avenue des étangs, 11100, Narbonne, France

⁴ Univ Lyon, CNRS, Université Claude Bernard Lyon 1, Institut des Sciences Analytiques, UMR 5280, 5 Rue de la Doua, F-69100, Villeurbanne, France

*Corresponding author (noemie.pernin@insa-lyon.fr)

ABSTRACT

The Telesphore project aims to identify and to quantify the transfers of pharmaceuticals residues and biocides and their related processes from biosolids and manure spread on grassland as fertilizers. Real land-spreading conditions were reproduced on six in-situ lysimeters and the pathway of pharmaceuticals and biocides was tracked by sampling infiltrated water and soil over one year. The study has focused on 32 pharmaceuticals, biocides and their transformation products, selected from their previous detection in several organic fertilizers. Six months after biosolids and manure spreading, the soil concentrations were in the range of nanograms per gram of soil and only few compounds were detected in infiltrated water. Ketoprofen was found to be the most mobile and persistent pharmaceutical compound after biosolids application whereas thiabendazole was the most frequently detected substance in infiltrated water after manure amendment.

Keywords: *land spreading, drugs, sludge, infiltration, soil contamination, lysimeters.*

1. INTRODUCTION

The Telesphore project aims to identify and quantify the transfers of selected human and veterinary pharmaceuticals and biocides after land spreading of biosolids and manure. Some studies have already been conducted in situ (Gros et al. 2019) but they focus on pharmaceuticals only. Moreover, comparison of biosolids and manure regarding the same micropollutants is rare. In this paper, we present the first results of an experiment with six in situ lysimeters after two applications of solar dried biosolids from an urban wastewater treatment plant (WWTP) and liquid manure from a dairy farm applying strict rules for PDO (Protected Designation of Origin) reblochon cheese production. Sampling of both infiltrated water and soil at different depths allow exploring the fate of these selected micropollutants within the lysimeters under real agricultural operation of a pasture according to times and rates of application.

2. MATERIAL AND METHODS

The study site is located in Scientrier, French Alps. Six 1-m deep lysimeters of 2 m x 2 m area have been built and filled with sandy loam soil excavated from the same location, by ensuring that the initial succession of layers of soils and degrees of compaction were reproduced within

the lysimeters. Lysimeters MA and MB receive manure, lysimeters SA and SB receive biosolids, and lysimeters RA and RB are used as reference without spreading. MA, SA and RA have a concrete invert and are used for monitoring micropollutants in infiltrated water samples. MB, SB and RB have no invert and are used to monitor micropollutants at different depths in soil carrots, sampled just before the next land spreading. Solar dried biosolids from the local WWTP and dairy cow manure were applied two times, on 5 Nov. 2020 and on 03 Jun. 2021, following the rates and calendar of local agricultural practices.

32 pharmaceuticals and biocides compounds have been selected for monitoring from a preliminary suspect screening approach (Guirronet, 2021) carried out on 5 urban WWTP sludge samples, 5 liquid manures and on 1 manure with bedding material, all produced in the region: antibiotic (fluoroquinolones, cyclines, macrolides, sulfonamides, diaminopyridines class), anti-parasitic (ivermectine, imidiazothiazole, benzimidazoles, triazoles, tetrahydropyrimidine class), disinfectant (bisbiguanidine, organochlorine class), herbicide/insecticide (sulfaximine, uracil, organophosphate class).

Infiltrated water was collected 16 times during the first year of experiment in lysimeters MA, SA and RA. The soil was sampled in lysimeters MB, SB and RB on 03 Jun. and 28 Oct. 2021. The carrots were sliced in four layers: 0 – 10 cm, 10 – 40 cm, 40 – 60 cm, 60 – 100 cm depth.

3. RESULTS AND DISCUSSIONS

Only 17 compounds among 32 are detected in biosolids, including 4 transformation products, and only 11 in liquid manure. The same pharmaceuticals and biocides are detected in sludge applied in Nov. 2020 and Jun. 2021, with similar concentration levels, except 3-amino-5-methylisoxazole (a sulfamethoxazole metabolite) whose concentration is below LoQ (10 ng/g DW-dry weight) in Nov. 2020 and 1.5 µg/g DW in Jun. 2021. For comparison, in dewatered municipal biosolids Gottschall et al. (2012) reported higher concentrations (in ng/g) for ofloxacin (1400 versus 377 – 474 for this study), triclosan (10900 vs. 13-42), ciprofloxacin (3260 vs. 28 - 59), tetracycline (513 vs. 17 - 30), and epitetracycline (334 vs. 19 - 31 ng/g). Concentrations in liquid manure are very low (which is consistent with the strict rules applied at the farm), ranging from 0.1 ng/g DW for thiabendazole to 14.4 ng/g DW for 3-amino-5-methylisoxazole. As an example of available local data of veterinary drug administration, tetracycline represents 22 % of prescribed antibiotics but the concentration in liquid manure was only 1.0-1.4 ng/g.

Between Nov. 2020 and Oct. 2021, eight compounds were found in infiltrated water sampled in lysimeter SA (A first assessment of the mass balance for pharmaceutical residues and biocides between organic fertilizers spread and the amount recovered in soil and infiltrated water is in progress and will be presented at the conference.

Table 1). Only two pharmaceuticals were quantified in the samples from Jun. to Oct. 2021: thiabendazole (14 – 33 ng/L) in three samples from lysimeters with manure application and trimethoprim (120 ng/L) in the last sample of SA.

The number of compounds detected in soil is higher 210 days after the first spreading (05 Nov. 2020 – 03 Jun. 2021) than 147 days after the second one (03 Jun. – 28 Oct. 2021). Anhydro-erythromycin and trimethoprim are found in all layers of all lysimeters including the reference,

which suggests their persistent presence in soil prior to the experiments. An unexpected concentration profile is found for ketoprofen at the end of the first year of experiment in both lysimeters MA and SA. This compound is detected at all depths in a range of concentration between 0.36 and 2.43 ng/g DW with the liquid manure application, and between 0.35 and 0.53 ng/g DW after the application of biosolids. The predominant mechanism for this compound is assumed to be biodegradation, with low lixiviation (Wassenaar et al. 2015).

A first assessment of the mass balance for pharmaceutical residues and biocides between organic fertilizers spread and the amount recovered in soil and infiltrated water is in progress and will be presented at the conference.

Table 1. . Detection frequency of pharmaceuticals and biocides in infiltrated water (n = 16)

Compounds	Liquid manure	Biosolids
Albendazole-2-aminosulfone	6.3%	-
Anhydroerythromycin	6.3%	-
Desmethyl-ofloxacin	-	12.5%
Flubendazole	-	12.5%
Ketoprofen	-	31.3%
Levamisole	6.3%	18.8%
Thiabendazole	50.0%	12.5%
Trimethoprim	-	6.3%

4. CONCLUSIONS

Diversity and loads of pharmaceuticals and biocides are higher in solar dried biosolids than in the liquid manure. Concentrations in soil and infiltrated water are very low and close to the LoD. Some transformation products (anhydroerythromycin, albendazole-2-aminosulfone and desmethyl-ofloxacin) were found in leachate and/or soil samples, emphasizing the importance of tracking both parent compounds and transformation products. No quantifiable accumulation is observed between the first land-spreading and the second one. Further exploration of processes under controlled conditions is needed to fully understand the processes related to and transfers of pharmaceutical residues and biocides from urban sludge and manure used as fertilizers. The *in-situ* experiments will continue for two years, along with additional tests in lab scale columns under controlled conditions.

Acknowledgements: The authors thank the Rhône-Méditerranée-Corse water agency for the financial support of the Telesphore project. This work was also realised thanks to the support of the Graduate School H2O'Lyons (ANR-17-EURE-0018) of the Université de Lyon (UdL) as part of the programme "Investissements d'Avenir " run by Agence Nationale de la Recherche (ANR).

REFERENCES

- Gottschall, N., Topp, E., Metcalfe, C., Edwards, M., Payne, M., Kleywegt, S., Russell, P., and Lapen, D.R. (2012). Pharmaceutical and Personal Care Products in Groundwater, Subsurface Drainage, Soil, and Wheat Grain, Following a High Single Application of Municipal Biosolids to a Field. *Chemosphere* 87 (2): 194-203.
- Gros, M., Mas-Pla, J., Boy-Roura, M., Geli, I., Domingo, F., and Petrović, M. (2019). Veterinary Pharmaceuticals and Antibiotics in Manure and Slurry and Their Fate in Amended Agricultural Soils: Findings from an Experimental Field Site (Baix Empordà, NE Catalonia). *Science of The Total Environment* 654 (mars): 1337-49.

- Guirronet, A. (2021). *Développements méthodologiques autour du couplage chromatographie liquide-spectrométrie de masse, pour la quantification de composés vétérinaires présents à l'état de traces dans des matrices complexes environnementales*. PhD thesis, Univ. Lyon 1, Lyon, France.
- Wassenaar, T., Bravin, M.N., Dumoulin, F., and Doelsch, E. (2015). Ex-ante fate assessment of trace organic contaminants for decision making: A post-normal estimation for sludge recycling in Reunion. *J. of Environmental Management* 147 (1): 140-51.

MODELING OF REGIONALIZED PFOA AND PFOS EMISSIONS IN AUSTRIA

Steffen Kittlaus¹, Matthias Zessner^{1*}, and Ottavia Zobolia¹

¹ TU Wien, Institute for Water Quality and Resource Management, Karlsplatz 13, 1040 Wien, Austria

*Matthias Zessner (mzessner@iwag.tuwien.ac.at)

ABSTRACT

Surface water pollution with poly- and perfluorinated compounds (PFAS) is a well-recognized problem, but knowledge about contribution of different emission pathways, especially diffuse ones, is very limited. This study investigates the potential of the pathway oriented MoRE model in shedding light on the relevance of different emission pathways on regional scale and in predicting concentrations and loads in unmonitored rivers. Modelling was supported with a tailor-made monitoring program aimed to fill gaps on concentration in different environmental compartments. The study area covers the whole Austrian territory including some additional transboundary catchments and it focuses on perfluorooctanoic acid (PFOA) and perfluorooctanesulfonic acid (PFOS). These two PFAS are regulated and therefore their production and use in Europe are currently decreasing. Nevertheless, these compounds are still emitted into the environment via legacy pollution and as transformation products from other PFAS. These two compounds were selected for this study in view of the larger information availability compared to other PFAS. Despite considerable uncertainties in the input data, model validations show that this approach performs significantly better than previous modelling frameworks based on population-specific emission factors, population density and wastewater treatment plant information. The study reveals the predominance of emissions via municipal wastewater treatment plants for PFOS and a relevant role of diffuse emission pathways for PFOA. Results suggest that unpaved areas contribute the biggest share to total diffuse emissions, but the estimation of these pathways is affected by the highest uncertainty in the input data and requires better input data from monitoring.

Keywords: *PFAS, status assessment, regionalized pathway analysis, emission model, MoRE.*

1. INTRODUCTION

Contamination of the aquatic environment with per- and polyfluoroalkyl substances (PFAS) is a well-recognized problem (Evich et al., 2022), but quantitative assessment of emission from different sources and via different pathways is scarce. Limited and fragmented data on PFAS pollution in media linked to emissions (e.g. soils or industrial discharges), confidential information on PFAS content in products and poor understanding of degradation and transformation of these substances in the environment are major challenges hindering a proper quantification of emissions (Gold and Wagner, 2020). The hypothesis behind this study is that a pathway-oriented modelling approach, fed with data obtained via a tailor-made monitoring program covering the main compartments linked with emissions, can achieve a much higher accuracy in the regionalized estimation of emissions, river loads and river concentrations of PFAS. This hypothesis was tested on the entirety of river catchments in Austria. Besides evaluating the performance of the proposed approach, this study aimed to analyze the spatial pattern of pollution of surface waters with PFOA and PFOS as well as the contribution and relative relevance of different emission pathways in different regions.

2. MATERIAL AND METHODS

The selected approach of emission modelling is based on the MoRE model presented by Fuchs et al. (2017) and implemented into the MoRE modelling framework (Fuchs et al., 2017). This pathway-oriented approach estimates the emissions for the different point and diffuse pathways (see figure 1). The timestep is annual and the spatial resolution is at sub-catchment level. The spatial model domain is the state of Austria. Transboundary river basins are partly included (small headwaters outside of Austria and the whole Inn river including sub-catchments in Italy, Switzerland and Germany), while the Danube upstream of the confluence with the Inn river is considered as a boundary condition and thus its observed PFAS load is included as external input into the model domain. From the March river (border to Slovakia and Czech Republic) only sub-catchments (e.g. Zaya) are included. The model domain (93 771 km²) is divided into 894 sub-catchments with an average size of 105 km². The temporal coverage is chosen based on the available input and validation data. The tailor-made monitoring was carried out during 2016/2017 (Zoboli et al., 2019).

3. RESULTS AND DISCUSSIONS

The calculated annual river loads were validated with loads calculated from monitoring data at 14 locations. The validation of modelled river loads against loads calculated from observation data yields a satisfactory Kling-Gupta model efficiency coefficient (KGE) (PFOA=0.58, PFOS=0.72). The components of the KGE reveal that the correlation ($r_{PFOA}=0.99$, $r_{PFOS}=0.98$) is very high, the variability ratio ($\gamma_{PFOA}=0.90$, $\gamma_{PFOS}=0.90$) is reasonable but for both substances with values of β being 1.41 for PFOA and 1.26 for PFOS the model is biased and overestimates the loads. This can be partly attributed to the overestimation of the discharge.

The relative contribution of different pathways to total emissions largely diverges in catchments of different size and characteristics, as presented by way of example for eight catchments. The Wulka catchment shows the highest contribution of municipal wwtp emissions to the total emissions for PFOA and PFOS. This is caused by a high amount of treated wastewater in a

catchment with high population density and rather low annual precipitation, thus with a low area specific runoff. In the Zaya catchment similar patterns can be seen, but the wastewater load is lower and therefore other diffuse pathways contribute to a larger degree to the total emissions. As the annual total runoff is very low in the Zaya catchment, emissions via “overland surface runoff” are negligible and emissions via “groundwater + interflow” are rather small. Other catchments like Pram, Mattig, Raba and Mura show a more balanced contribution of different pathways, with a major share coming from diffuse pathways. The Ötztaler Ache is an alpine catchment with low settlement density. Therefore, the main emission inputs in the Mean and Worst-case model variant stem from the natural runoff components (groundwater, interflow and overland surface runoff) while for the Best-case variant nearly no emissions were estimated.

4. CONCLUSIONS

We combined the MoRE model with parametrization of substance-specific data obtained from literature and a tailor-made monitoring program in different environmental compartments. With this approach we achieved a model performance for prediction of river loads and concentrations which is clearly better than the performance obtained with regionalization approaches based on population-specific emission factors, population density and wwtp information. Thus, it can be concluded that the additional effort dedicated to targeted monitoring and data processing is rewarded with significantly better results. Model results can be used for estimating environmental concentrations in unmonitored rivers, assessing the relevance of different emission pathways and the effectiveness of measures for pollution reduction. These investigations are a promising basis for an extension of the MoRE application to PFAS of emerging concern, others than PFOS and PFOA.

REFERENCES

- Evich MG, Davis MJB, McCord JP, Acrey B, Awkerman JA, Knappe DRU et al. (2022) Per- and polyfluoroalkyl substances in the environment. *Science* (New York, N.Y.) 375(6580):eabg9065.
- Fuchs S, Kaiser M, Kiemle L, Kittlaus S, Rothvoß S, Toshovski S et al. (2017) Modeling of Regionalized Emissions (MoRE) into Water Bodies: An Open-Source River Basin Management System. *Water* 2017; 9(4):239.
- Gold SC, Wagner WE. (2022) Filling gaps in science exposes gaps in chemical regulation. *Science* (New York, N.Y.) 2020; 368(6495):1066–8.
- Kittlaus S, Clara M, van Gils J, Gabriel O et al. (2022) Coupling a pathway-oriented approach with tailor-made monitoring as key to well-performing regionalized modelling of PFAS emissions and river concentrations; *Science of the Total Environment*, 894, 157764.
- Zoboli O, Clara M, Gabriel O, Scheffknecht C, Humer M, Brielmann H et al. (2019) Occurrence and levels of micropollutants across environmental and engineered compartments in Austria. *Journal of Environmental Management* 2019; 232:636–53.

ESTIMATION OF BIODEGRADATION POTENTIAL OF PHARMACEUTICALS BY BIOWIN MODELS AND COMPARISON WITH EXPERIMENTAL DATA

Başak Kılıç^{1*} and Ferhan Çeçen¹

¹ Institute of Environmental Sciences, Boğaziçi University, Istanbul, Turkey

*Corresponding author (basak.kilic@boun.edu.tr)

ABSTRACT

In this study the biodegradation potential of four pharmaceuticals, namely diazepam, lamotrigine, metformin and glibenclamide was investigated under aerobic conditions. First, BIOWIN models were used to estimate the theoretical biodegradability. Then, their outputs were compared with experimental data taken from literature. In evaluation of experimental results, biodegradation rates and sorption of pharmaceuticals were considered. A deviation was seen between theoretical estimations and experimental findings, except for lamotrigine. For diazepam, metformin and glibenclamide experimental results indicated slightly higher biodegradation than BIOWIN models.

Keywords: Activated sludge, biodegradation, BIOWIN, pharmaceuticals, sorption.

1. INTRODUCTION

Although pharmaceuticals are found at very low concentrations in WWTP influents, they can exert many effects on the aquatic environment if they are not removed. In biological treatment it is important to know about the biodegradation potential and biodegradation rate of a substance. Therefore, BIOWIN models have been suggested as a screening tool to obtain information about biodegradability. They belong to the EPI (Estimation Programs Interface) Suite (US EPA, 2012) and consist of six models that predict the rate of aerobic biodegradation of a chemical in the presence of mixed microbial populations (Balakrishnan et al., 2020; Dimitrov et al., 2007). The aim of this study is to investigate the biodegradation potential of four pharmaceuticals, namely diazepam, lamotrigine, metformin and glibenclamide.

2. MATERIAL AND METHODS

The values obtained from BIOWIN models stand either for biodegradability or indicate the time required for biodegradation. In this study BIOWIN values were compared with the experimental data taken from several laboratory-scale aerobic biological treatment units reported in literature. The k_{biol} , first-order reaction rate constant, stands for biodegradation rate. If $k_{\text{biol}} < 0.1 \text{ L.gss}^{-1}.\text{d}^{-1}$, this indicates no substantial biological degradation. If $0.1 < k_{\text{biol}} < 10 \text{ L.gss}^{-1}.\text{d}^{-1}$, partial removal takes place by biological transformation and if $k_{\text{biol}} > 10 \text{ L.gss}^{-1}.\text{d}^{-1}$, more than 95% removal can be expected (Ternes and Joss, 2006). In addition, $\log K_d$ which describes the partitioning of a compound between the sludge and liquid phases was taken into account. According to a study, pharmaceuticals having $\log K_d > 2.7$ generally tend to sorb to sludge (Ternes et al., 2004).

3. RESULTS AND DISCUSSIONS

The results of BIOWIN models are given in Table 1.

Table1. BIOWIN outputs of selected pharmaceuticals.

Name	BIOWIN 1	BIOWIN 2	BIOWIN 3	BIOWIN 4	BIOWIN 5	BIOWIN 6
	> 0.5: fast biodegradation < 0.5: not to degrade fast		5–4.75: hours 4.75–4.25: hours to days 4.25–3.75: days 3.75–3.25: days to weeks 3.25–2.75: weeks 2.75–2.25: weeks to months 2.25–1.75: months < 1.75: refractory		≥ 0.5: rapidly biodegradable < 0.5: not rapidly biodegradable	
Diazepam	0.7678	0.8085	2.3311	3.4819	0.0837	0.0217
Lamotrigine	-0.2067	0.0002	1.9501	2.9308	-0.3281	0.0006
Metformin	0.6861	0.7640	2.9137	3.6614	0.3287	0.2379
Glibenclamide	0.7267	0.3764	1.7137	3.1837	-0.2668	0.0005

Diazepam: According to some experiments diazepam did neither tend to sorb to sludge ($\log K_d < 2.7$) (Hyland et al., 2012; Ternes et al., 2004; Wick et al., 2009), nor biodegraded ($k_{\text{biol}} < 0.1 \text{ L}_{\text{gss}}^{-1} \cdot \text{d}^{-1}$) (Suarez et al., 2012; Wick et al., 2009). In an MBR, only 20% of diazepam was removed by degradation and 32% of it was sorbed onto sludge (Kim et al. 2014). But, in another case diazepam was not detected in secondary effluent due to complete removal (Verlicchi et al., 2013). Although BIOWIN values indicate low biodegradability, according to experimental results, the biodegradation potential of diazepam varies between low and high.

Lamotrigine: Lamotrigine was persistent in bench-scale activated sludge systems and no significant degradation took place in 14 days (Bollmann et al., 2016). In another case lamotrigine degraded slowly and about 95% of it still remained after 6 days (Zonja et al., 2016). BIOWIN models also indicate that lamotrigine has a very low biodegradation potential.

Metformin: Metformin exhibited fast biodegradation and 98.6% of it was removed after 10 hours. Its k_{biol} ($10.48 \text{ L}_{\text{gss}}^{-1} \cdot \text{d}^{-1}$) and $\log K_d$ (0.48) values indicate high biodegradability and low sorption potential, respectively (Blair et al., 2015). In another case 98% of metformin was degraded in an MBR, while sorption onto sludge was only 1% (Kim et al., 2014). Biodegradation is the main mechanism in metformin removal. Experiments indicate that metformin biodegrades more rapidly than predicted from BIOWIN values.

Glibenclamide: The removal efficiency of glibenclamide in a WWTP was 37% (Verlicchi et al., 2013). In a conventional activated sludge system (SRT=10 d, HRT=11.5 h) the removal was only around 46.1%. The use of two pilot-scale MBRs with HRTs of 7.2 and 15 h enhanced the removal up to 82–96% (Radjenovic et al., 2009). Moreover, in another case primary biodegradation was 100% in 19 days and ultimate biodegradation was 52% within almost three weeks (Markiewicz et al., 2017). Experimental studies show that glibenclamide is not refractory as indicated by BIOWIN models.

4. CONCLUSIONS

- Results obtained from experiments and BIOWIN models are compatible with each other for lamotrigine, while in experiments slightly higher biodegradation is observed for diazepam, metformin and glibenclamide than predicted from BIOWIN models. In experiments glibenclamide appeared to be not as refractory as predicted from BIOWIN estimations.

- BIOWIN models take only the single substance into consideration. Since in real systems the wastewater is composed of several substances, a pharmaceutical may also be removed as a secondary or cometabolic substrate.
- Predictive tools such as BIOWIN models can be very helpful for having an initial idea about biodegradability of pharmaceuticals under aerobic conditions. They can also be used for experimental design.

Acknowledgements: The authors acknowledge the grant provided by Bogazici University Research Fund Grant Number 19Y00D6.

REFERENCES

- Balakrishnan, A., Kanchinadham, S.B.K., & Kalyanaraman, C. (2020). Assessment on biodegradability prediction of tannery wastewater using EPI Suite BIOWIN model. *Environmental Monitoring and Assessment*, 192, 732.
- Blair, B., Nikolaus, A., Hedman, C., Klaper, R., & Grundl, T. (2015). Evaluating the degradation, sorption, and negative mass balances of pharmaceuticals and personal care products during wastewater treatment. *Chemosphere*, 134, 395–401.
- Bollmann, A.F., Seitz, W., Prasse, C., Lucke, T., Schulz, W., & Ternes, T. (2016). Occurrence and fate of amisulpride, sulpiride, and lamotrigine in municipal wastewater treatment plants with biological treatment and ozonation. *Journal of Hazardous Materials*, 320, 204–215.
- Dimitrov, S., Pavlov, T., Nedelcheva, D., Reuschenbach, P., Silvani, M., Bias, R., Comber, M., Low, L., Lee, C., Parkerton, T., & Mekenyan, O. (2007). A kinetic model for predicting biodegradation. *SAR QSAR in Environmental Research*, 18(5-6), 443-457.
- Hyland, K.C., Dickenson, E.R.V., Drewes, J.E., & Higgins, C.P. (2012). Sorption of ionized and neutral emerging trace organic compounds onto activated sludge from different wastewater treatment configurations. *Water Research*, 46(6), 1958–1968.
- Kim, M., Guerra, P., Shah, A., Parsa, M., Alaei, M., & Smyth, S.A. (2014). Removal of pharmaceuticals and personal care products in a membrane bioreactor wastewater treatment plant. *Water Science & Technology*, 69(11), 2221-2229.
- Markiewicz M., Jungnickel C., Stolte S., Białk-Bielińska A., Kumirska J., & Mroziak W. (2017). Ultimate biodegradability and ecotoxicity of orally administered antidiabetic drugs. *Journal of Hazardous Materials*, 333, 154-161.
- Radjenovic, J., Petrovic, M., & Barcelo, D. (2009). Fate and distribution of pharmaceuticals in wastewater and sewage sludge of the conventional activated sludge (CAS) and advanced membrane bioreactor (MBR) treatment. *Water Research*, 43, 831-841.
- Suarez, S., Reif, R., Lema, J.M., & Omil, F. (2012). Mass balance of pharmaceutical and personal care products in a pilot-scale single-sludge system: influence of T, SRT and recirculation ratio. *Chemosphere*, 89(2), 164–171.
- Ternes, T.A., Herrmann, N., Bonerz, M., Knacker, T., Siegrist, H., & Joss, A. (2004). A rapid method to measure the solid–water distribution coefficient (K_d) for pharmaceuticals and musk fragrances in sewage sludge. *Water Research*, 38, 4075–4084.
- Ternes, T., & Joss, A. (2006). Human pharmaceuticals, hormones and fragrances – The challenge of micropollutants in urban water management. IWA Publishing, London.
- US EPA. (2012). Estimation Programs Interface Suite™ for Microsoft® Windows, v 4.11. United States Environmental Protection Agency, Washington, DC, USA.
- Verlicchi, P., Galletti, A., Petrovic, M., Barcelo, D., Al Aukidy, M., & Zambello, E. (2013). Removal of selected pharmaceuticals from domestic wastewater in an activated sludge system followed by a horizontal subsurface flow bed — analysis of their respective contributions. *Science of the Total Environment*, 454–455, 411–425.
- Wick, A., Fink, G., Joss, A., Siegrist, H., & Ternes, T.A. (2009). Fate of beta blockers and psycho-active drugs in conventional wastewater treatment. *Water Research*, 43(4), 1060–1074.
- Zonja, B., Perez, S., & Barcelo, D. (2016). Human metabolite lamotrigine-N2-glucuronide is the principal source of lamotrigine-derived compounds in the WWTPs and surface water. *Environmental Science & Technology*, 50(1), 154-164.

RESISTANCE TO BENZALKONIUM CHLORIDES FAVORS ANTIBIOTIC RESISTANCE

Gökçin Gül¹, Ulaş Tezel¹

¹Boğaziçi University, Environmental Sciences Department, İstanbul, Turkey

*Gokcin Gül (gokcin.gul@gmail.com)

ABSTRACT

Antimicrobial resistance is the major health threat that human society is facing today. It is believed the main cause of antimicrobial resistance development is exposure of microorganisms to biocides such as quaternary ammonium compounds (QACs) at low concentrations in the environment. QAC-induced resistance mechanisms also confer cross- and co-resistance to many antibiotics. The aim of this study is to clarify the relationship between QACs resistance and antibiotic susceptibility by using different microorganisms having different tolerance to benzalkonium chlorides (BACs), a most extensively used QACs. Minimum inhibitory concentration (MIC) of 18 antibiotics belonging to different antibiotic groups for *E. coli* (BAC MIC: 16 µg BAC/ml), *Serratia marcescens* (>1024 µg BAC/mL) and two *Pseudomonas sp.* (1024 µg/mL, degrades BACs) were checked. The lowest MIC was reported for quinolones whereas penicillins were the least effective antibiotics on the bacteria tested. Results showed that *E. coli*, which is susceptible to BACs, is also the most susceptible bacteria to almost all antibiotics. *Serratia marcescens* is more resistant to antibiotics than *E. coli* but it showed less resistance than *Pseudomonas sp.*, which can also degrade BACs. *Pseudomonas sp.* strains (BIOMIG1-SEW and AS), which possess highest resistance to all antibiotics are not only highly resistant to BACs but also, they can biodegrade BACs. Given the fact, that many antibiotics are biodegradable by certain microorganisms; these findings suggest that catabolic enzymes that involve in BAC degradation may also facilitate resistance to antibiotics.

Keywords: antibiotic resistance, benzalkonium chlorides, biocides, biocide resistance, micropollutants.

1. INTRODUCTION

Biocides are chemicals that are used to kill microorganisms. Since the SARS-CoV-2 pandemic, the use of biocides has been increasing due to new cleaning habits of human society. Among biocides, quaternary ammonium compounds (QACs) are high product volume chemicals due to their unique physical/chemical properties such as; surface-activity, detergency and antimicrobial properties (McDonnell and Pretzer, 2001). After biocides are used, they end up in wastewater. Since wastewater treatment plants are designed to remove easily degradable organic pollutants, most of biocides pass through wastewater treatment plants and are discharged into the environment. After biocides are released into nature, they are transported through distances and accumulate in different compartments (Martinez-Carballo et al., 2007; Hughes et al., 2012). Due to dilution, the biocide concentrations are generally very low in the environment. QACs were reported to be found in water bodies in the range of µg/L (McDonnell

and Pretzer, 2001). Bacteria in the environment are exposed to biocides at their sub-inhibitory concentrations which facilitate the development and dissemination of biocide resistance in bacteria (Martinez, 2008). It was suggested that QAC-induced resistance mechanisms also confer cross- and co-resistance to many antibiotics. (Buffet-Bataillon et al., 2012; Gaze et al., 2005; Schluter et al., 2007). Loughlin et al. (2002) reported that adaptation of *Pseudomonas aeruginosa* to BACs, one of the most commonly used form of QACs, cause to increase resistance against chloramphenicol. Many biocide and antibiotic resistance mechanism are similar. Therefore, several biocide resistance mechanisms can also act against antibiotics, in other words biocide resistance favors antibiotic resistance (Scenihr, 2009; Hegstad et al., 2010; Tezel and Pavlostathis, 2012). QAC resistant *Staphylococcus aureus* and triclosan resistant *Pseudomonas aeruginosa* also show resistance to several group of antibiotics (Akimitsu et al., 1999; Chuanchuen et al., 2001). *Pseudomonas stutzeri*, which was a chlorhexidine resistant bacterium, shows resistance to QACs, several antibiotics and triclosan (Russell, 1998). Moreover, it was found that after long-term BAC exposure, microorganisms become more resistant to antibiotics (Tandukar et al., 2013). Above-mentioned resistance occurs because most of biocide resistance mechanisms like efflux pumps and biodegradation are also effective against antibiotics, so acquisition of biocide resistance may also cause antibiotic resistance. Widespread use of BACs not only lead to proliferation of BAC resistance but also development of BAC degrading enzymes in microorganisms. *Pseudomonas fluorescens*, *Bacillus niabensis* *Thalassospira sp.*, *Stenetrophomonas spp.*, *Achromobacter spp.* and *Pseudomonas putida* and *Pseudomonas aeruginosa* were reported as BAC degrading bacteria (Nishihara et al., 2000; Bassey et al., 2011). *P. putida* and *P. aeruginosa* groups are dominant BAC degraders among all.

Recently in our laboratories, a novel *Pseudomonas sp.* strain BIOMIG1 were isolated from sewage, activated sludge, soil and sea sediments (Ertekin et al., 2016). This strain was found to be resistant to benzalkonium chlorides (BACs) and degrade BACs. Given the fact that the strain BIOMIG1 is common in the environmental biological systems, the objective of this research is to clarify the relationship between BACs resistance and antibiotic susceptibility by using different microorganisms having different tolerance to benzalkonium chlorides (BACs). To find the relationship, minimum inhibitory concentration (MIC) of 18 antibiotics belonging to different antibiotic groups for above mentioned bacteria was calculated and compared by using macro dilution and E-test methods. In our study the relation between BAC degradation, BAC resistance and antibiotic susceptibility is established by using the strain BIOMIG1 and other bacteria that show different tolerance to BACs

2. MATERIAL AND METHODS

Microorganism and Antibiotic Selection

In our study, 18 antibiotics belonging to 9 different antibiotic groups were used. Antibiotics were selected according to the list of compounds that were presented within the study of the global occurrence of pharmaceuticals in river waters prepared by Hughes et al. (2012): amoxicillin, azithromycin, penicillin g, chloramphenicol, ciprofloxacin, clarithromycin, clindamycin, doxycycline, enrofloxacin, erythromycin, kanamycin, levofloxacin, norfloxacin, ofloxacin, sulfamethoxazole, tetracycline, trimethoprim and vancomycin.

In order to find that relationship between BAC resistance and antibiotic resistance, four microorganisms which show different resistance to BACs were used; a novel *Pseudomonas sp.*, strain BIOMIG1 (BIOMIG1 SEW), *Serratia marcescens* strain BIOMIG4 and *E.coli* strain BIOMIG3. *Pseudomonas sp.*, BIOMIG1 SEW and *Serratia marcescens* strain BIOMIG4 are tolerant to BACs up to 1024 mg/L, whereas *E.coli* strain BIOMIG3 is susceptible to BACs (BACs MIC: 16 mg/L). In addition, BIOMIG1 SEW can degrade BACs under aerobic condition. *Pseudomonas sp.*, strain BIOMIG1 AS isolated from activated sludge was found to be the ecotype of *Pseudomonas sp.*, strain BIOMIG1 isolated from sewage. In addition, like BIOMIG1 SEW, *Pseudomonas sp.*, strain BIOMIG1 AS shows resistance to BACs up to 1024 mg/L and it has the capability to degrade BACs.

Susceptibility Testing by Macro Dilution

The susceptibilities of each microorganism against 18 antibiotics were determined using macro dilution assay as described by Clinical and Laboratory Standards Institute (CLSI, 2012). A single colony of each microorganism was transferred into sterile falcon tube containing 5 mL Mueller-Hinton broth. Colonies were taken from CHROM®Agar Orientation plates. After microorganism were grown overnight in Mueller-Hinton broth, they were diluted in Mueller-Hinton broth to a turbidity comparable to that of a 0.5 McFarland turbidity standard (c.a. 0.5×10^8 CFU/mL). This suspension was further diluted 1:100 with Mueller-Hinton broth. A 1 mL of the diluted culture sample was transferred to culture tubes containing 1 mL broth and a range of antibiotics concentrations from 1 to 1024 mg/L (Antibiotics is diluted by factor 2). The tubes were incubated at room temperature (22°C) for 24 hours and the growth measured with a UV/Vis spectrometer at 600 nm wavelength. Tubes containing nutrient broth having the same antibiotics concentrations but without any culture were used as blanks.

Susceptibility Testing by E-test Method

The susceptibility of each microorganism against 18 antibiotics was determined using E-Test assay as described by Clinical and Laboratory Standards Institute (CLSI, 2012). A single colony of each microorganism was transferred into sterile falcon tube containing 5 mL Mueller-Hinton broth. Colonies were taken from CHROM®Agar Orientation plates. After microorganism were grown overnight in Mueller-Hinton broth, they were diluted in Mueller-Hinton broth to a turbidity comparable to that of a 0.5 McFarland turbidity standard (c.a. 0.5×10^8 CFU/mL). This suspension was further diluted 1:100 with Mueller-Hinton broth. Optimally, within 15 minutes after adjusting turbidity of inoculum suspension, a sterile cotton swab was dipped into the adjusted suspension. The dried surface of a Mueller-Hinton agar plate was inoculated by streaking the swab over the entire sterile agar surface. This procedure repeated by streaking two more times, rotating the plate approximately 60° each time to ensure an even distribution of inoculum. Once the agar plate was completely dry, the antibiotic strip (E-Test strip) was applied aseptically with the help of sterile tweezer and plates were incubated overnight at 22°C. After 24 hours of incubation, plates were photographed by using BioRad EZ-DOC imager with Image Lab program. The corresponding antibiotic concentration, at the point where no cell growth was observed on E-Test strips, has been reported as the minimum inhibitory concentration of antibiotic (MIC). Since 256 mg/L was the highest antibiotic concentration present in the E-test strips, a homogeneous growth on MH agar has been reported as greater than 256 mg/L (> 256 mg/L).

3. RESULTS AND DISCUSSIONS

Macro dilution assay and E-test method results were shown in Table 1. The susceptibility of four microorganisms which are *Pseudomonas sp.* BIOMIG1 AS, *Pseudomonas sp.* BIOMIG1 SEW, *E.coli*, *Serratia marcescens* against 18 antibiotic were reported in terms of MIC (mg/L).

Table 1. MIC values of 4 microorganisms against 18 antibiotics according to macro dilution and E-test methods.

MACRO DILUTION METHOD					E-TEST METHOD				
ANTIBIOTIC NAME	ISOLATES MIC (mg/L)				ANTIBIOTIC NAME	ISOLATES MIC (mg/L)			
	BIOMIG1 SEW	BIOMIG1 AS	<i>E.coli</i>	<i>Serratia marcescens</i>		BIOMIG 1-SEW	BIOMIG 1-AS	<i>E.coli</i>	<i>Serratia marcescens</i>
Penicillin G	361.09	602.64	44.53	>1024	Penicillin G	>256	>256	16	>256
Amoxicillin	205.08	211.44	81.58	391.27	Amoxicillin	>256	>256	2	>256
Ciprofloxacin	0.41	0.30	0.01	0.12	Ciprofloxacin	0.25	0.38	0.003	0.064
Enrofloxacin	0.90	0.94	0.01	0.25	Enrofloxacin	1	0.75	0.016	0.25
Norfloxacin	0.93	1.20	0.04	0.27	Norfloxacin	1.5	1	0.03	0.38
Ofloxacin	2.19	2.74	0.03	0.47	Ofloxacin	1	1.5	0.047	0.38
Levofloxacin	1.24	1.28	0.02	0.26	Levofloxacin	0.75	0.5	0.02	0.19
Sulfamethoxazole	58.00	97.68	15.47	12.38	Sulfamethoxazole	48	64	8	12
Trimethoprim	455.48	480.24	0.29	2.30	Trimethoprim	>32	>32	0.38	0.75
Tetracycline	8.56	5.01	1.05	5.04	Tetracycline	8	6	0.75	6
Doxycycline	5.17	5.12	0.56	2.34	Doxycycline	4	4	0.75	2
Clarithromycin	>512	>512	13.19	37.67	Clarithromycin	>256	>256	16	48
Erythromycin	218.57	237.59	19.82	56.06	Erythromycin	192	>256	8	16
Azithromycin	201.04	360.42	2.95	4.91	Azithromycin	>256	>256	3	4
Clindamycin	>1024	>1024	424.90	227.28	Clindamycin	>256	>256	>256	192
Kanamycin	3.87	3.27	1.27	2.06	Kanamycin	2	1	1.5	1.5
Vancomycin	>1024	>1024	206.29	742.37	Vancomycin	>256	>256	>256	>256
Chloramphenicol	70.02	66.43	6.47	26.58	Chloramphenicol	192	>256	6	16

Results show that *Pseudomonas sp.* BIOMIG1s was around tenfold resistant than BAC susceptible *E.coli* and more than 2 fold resistant than BAC resistant *Serratia marcescens* for penicillin g, amoxicillin, enrofloxacin, norfloxacin, ofloxacin, levofloxacin, ciprofloxacin, trimethoprim, erythromycin, azithromycin, clarithromycin and chloramphenicol. For the rest of the antibiotics; sulfamethoxazole, kanamycin, vancomycin, tetracycline, doxycycline and clindamycin, *Pseudomonas sp.* BIOMIG1s was more than two fold resistant than BAC susceptible *E.coli*. *Pseudomonas sp.* BIOMIG1s were found to be the most resistant bacteria to all of the antibiotics except from amoxicillin and penicillin g. *Serratia marcescens* was found to be the most resistant bacteria to penicillin g and amoxicillin.

When the MIC results were examined according to antibiotic groups, it can be seen that microorganisms have higher MIC values for penicillin g, amoxicillin, clindamycin and vancomycin than they have for other antibiotics. Amoxicillin, penicillin g, clindamycin and vancomycin antibiotics were group together since all microorganism have high MIC values for these antibiotics. After them, macrolides, chloramphenicol, sulfonamides, kanamycin and tetracyclines have high MIC values respectively. Whereas all microorganisms show very low MIC values for fluoroquinolone group of antibiotics; ciprofloxacin, enrofloxacin, norfloxacin, ofloxacin and levofloxacin.

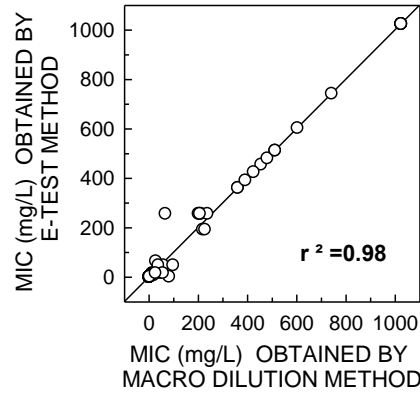


Figure 1. The comparison of MIC values obtained by macro dilution method and E-test method.

The MIC values that were obtained by E-test method were compared with the MIC values that were obtained by macro dilution method (Figure 2). The r^2 value was found to be 0.98 that indicated that MIC values obtained by E-test method and macro dilution method is very similar.

4. CONCLUSIONS

Results showed that *Pseudomonas sp.* BIOMIG1s were more resistance to 16 out of 18 tested antibiotics than the other bacteria tested. Furthermore, it was found that *Pseudomonas sp.* BIOMIG1 exhibits an approximately 10 fold resistance compared to *E.coli* and more than 2 fold resistance compared to *Serratia marcescens* against 13 out of 18 antibiotics. In addition, BAC resistant *Serratia marcescens* was more tolerant to antibiotics compared to BAC susceptible *E.coli*. These results may suggest that BAC resistance mechanisms also favor antibiotic resistance.

Acknowledgements: This project is partially supported by The Scientific and Technological Research Council of Turkey, TUBITAK,113Y528

REFERENCES

- Akimitsu, N., Hamamoto, H., Inoue, R. I., Shoji, M., Akamine, A., Takemori, K. I., ... & Sekimizu, K. (1999). Increase in resistance of methicillin-resistant *Staphylococcus aureus* to β -lactams caused by mutations conferring resistance to benzalkonium chloride, a disinfectant widely used in hospitals. *Antimicrobial Agents and Chemotherapy*, 43(12), 3042-3043.
- Bassey, D. E., & Grigson, S. J. W. (2011). Degradation of benzyldimethyl hexadecylammonium chloride by *Bacillus niabensis* and *Thalassospira sp.* isolated from marine sediments. *Toxicological & Environmental Chemistry*, 93(1), 44-56.
- Buffet-Bataillon, S., Tattevin, P., Bonnaure-Mallet, M., & Jolivet-Gougeon, A. (2012). Emergence of resistance to antibacterial agents: the role of quaternary ammonium compounds—a critical review. *International Journal of Antimicrobial Agents*, 39(5), 381-389.
- Chuanchuen, R., Beinlich, K., Hoang, T. T., Becher, A., Karkhoff-Schweizer, R. R., & Schweizer, H. P. (2001). Cross-resistance between triclosan and antibiotics in *Pseudomonas aeruginosa* is mediated by multidrug efflux pumps: exposure of a susceptible mutant strain to triclosan selects *nfxB* mutants overexpressing MexCD-OprJ. *Antimicrobial Agents and Chemotherapy*, 45(2), 428-432.
- Clinical and Laboratory Standards Institute (CLSI). M100-S22, (2012). Performance standards for antimicrobial susceptibility testing; twenty-second informational supplement.

- Ertekin, E., Hatt, J.K., Konstantinidis, K.T., Tezel, U. (2016). Similar microbial consortia and genes are involved in the biodegradation of benzalkonium chlorides in different environment. *Environmental Science and Technology*, 50, 4303-4313.
- Gaze, W. H., Abdousslam, N., Hawkey, P. M., & Wellington, E. M. H. (2005). Incidence of class 1 integrons in a quaternary ammonium compound-polluted environment. *Antimicrobial Agents and Chemotherapy*, 49(5), 1802-1807.
- Hegstad, K., Langsrud, S., Lunestad, B. T., Scheie, A. A., Sunde, M., & Yazdankhah, S. P. (2010). Does the wide use of quaternary ammonium compounds enhance the selection and spread of antimicrobial resistance and thus threaten our health? *Microbial Drug Resistance*, 16(2), 91-104.
- Hughes, D., Andersson, D.I. (2012). Selection of resistance at lethal and non-lethal antibiotic concentrations. *Current Opinion Microbiology*, 15, 555-560.
- Loughlin, M. F., Jones, M. V., & Lambert, P. A. (2002). Pseudomonas aeruginosa cells adapted to benzalkonium chloride show resistance to other membrane-active agents but not to clinically relevant antibiotics. *Journal of Antimicrobial Chemotherapy*, 49(4), 631-639.
- Martinez, J.L. (2008). Antibiotics and antibiotic resistance genes in natural environments. *Science*, 321, 365-367.
- Martinez-Carballo, E., Sitka, A., Gonzalez-Barreiro, C., Kreuzinger, N., Furhacker, M., Scharf, S., Gans, O. (2007). Determination of selected quaternary ammonium compounds by liquid chromatography with mass spectrometry. Part I. Application to surface, waste and indirect discharge water samples in Austria. *Environmental Pollution*, 145, 489-496.
- McDonnell, G., & Pretzer, D. (2001). New and Developing Chemical Antimicrobials. In: Block, S. S., (Eds), *Disinfection, Sterilization, and Preservation*, (pp.431-441). Philadelphia: Lippincott Williams & Wilkins.
- Nishihara, T., Okamoto, T., & Nishiyama, N. (2000). Biodegradation of didecyldimethylammonium chloride by Pseudomonas fluorescens TN4 isolated from activated sludge. *Journal of Applied Microbiology*, 88(4), 641-647.
- Russell, A. D. (1998). Mechanisms of bacterial resistance to antibiotics and biocides. *Progress in Medicinal Chemistry*, 35, 133-198.
- Schlüter, A., Szczepanowski, R., Pühler, A., & Top, E. M. (2007). Genomics of IncP-1 antibiotic resistance plasmids isolated from wastewater treatment plants provides evidence for a widely accessible drug resistance gene pool. *FEMS Microbiology Reviews*, 31(4), 449-477.
- Scientific Committee on Emerging and Newly Identified Health Risks (SCENIHR), 2009. Assessment of the antibiotic resistance effects of biocides. *European Commission, Directorate-General for Health & Consumers*, Brussels, Belgium.
- Tandukar, M., Oh, S., Tezel, U., Konstantinidis, K. T., & Pavlostathis, S. G. (2013). Long-term exposure to benzalkonium chloride disinfectants results in change of microbial community structure and increased antimicrobial resistance. *Environmental Science & Technology*, 47(17), 9730-9738.
- Tezel, U., Pavlostathis S.G., 2012. The Role of quaternary ammonium compounds on antimicrobial resistance in the environment. In Keen P.L., and Montforts M.H.M.M. (Eds), *Antimicrobial Resistance in the Environment*, (pp. 349-389), John Wiley & Sons.

VUV INDUCED PHOTO-OXIDATION OF IMIDACLOPRID IN AQUEOUS SOLUTION

S.L. Sanin^{1*}, H. Derin²

¹Hacettepe University Department of Environmental Engineering, Ankara Turkey,

²Hacettepe University Department of Environmental Engineering, Ankara Turkey

*sanin@hacettepe.edu.tr

Abstract: Neonicotinoids are widely used pesticides and they found in ecosystem. VUV processes are among the promising effective and economical water treatment processes for the removal of imidacloprid. Our VUV focused treatment results show that flow rate had marginal impact, pH played an important role, slowest at pH=11, for the degradation rate of imidacloprid. Presence of inorganic ions decreased the decomposition rate of imidacloprid, in the order of $\text{CO}_3^{2-} > \text{HCO}_3^- > \text{NO}_3^-$. Dissolved oxygen did not change both on the degradation and mineralization mechanisms. Kinetic analyses showed that degradation of imidacloprid by the VUV process followed a pseudo first order reaction kinetic. Reduction rate constants for 5 mg/L imidacloprid varied between 1.3877 min⁻¹ and 1.9213 min⁻¹, depending on the experimental conditions. 80% TOC reduction of imidacloprid solution (Co=10 mg/L) was successfully attained within 2 h VUV irradiation.

Keywords: *Imidacloprid; Photooxidation; VUV, Groundwater pollution, Remediation*

1. INTRODUCTION

Neonicotinoids are found in food, soil and especially in water matrices because once they were considered as relatively safe pesticides and are widely used all around the world to sustain agricultural production. Among them, imidacloprid, the first generation neonicotinoid insecticide, is the most commonly used one. Recent research challenge the early claim of safe chemical (Zhang et al, 2018; Christen et al., 2016). There have been raising concerns over the usage of imidacloprid due to its potential adverse effects on bee populations (Christen et al., 2016). Moreover, presence of imidacloprid in natural water resources causes various environmental problems due to its high water solubility and low biological and chemical degradation. Their effective removal from water is a challenging problem and require development of innovative and advance technologies. In a recent paper Rozsa (2019) listed VUV process among the alternative water treatment methods. That is why a feasible, safer and greener treatment method from water is among the current research interests for imidacloprid.

In this paper, we are reporting successful photo-degradation of imidacloprid in water using VUV lamps ($\lambda < 200$ nm), without addition of chemicals or catalysts. Kinetic parameters and optimum degradation conditions (flowrate, pH, initial concentration, D.O.) are determined. Inhibitory conditions (presence of CO_3^{2-} , HCO_3^- and NO_3^-) are also investigated.

2. MATERIAL AND METHODS

Working solutions of imidacloprid were prepared daily by diluting the stock solution with ultrapure water to predetermined concentration (2.5 – 10 mg/L). Aqueous stock solution of imidacloprid (200 mg/L) was refrigerated at 4 °C and kept in the dark where it was stable and steady for several months. 500 ml working solution is circulated between reactor and reservoir during (**Figure 1**) VUV irradiation process for photooxidation analyses.

Flow rate was set to 500 mL/min during the experiments. VUV lamp was turned on 30 minutes before pumping, to warm up the lamp and to reach optimal effectiveness. Aliquots (1 mL) of irradiated solutions were collected at different treatment times from 0 to 120 min for analysis.

Initial and final pH, conductivity, and temperature values were measured by pH and conductivity meter (Mettler-Toledo). Quantitative measurements were carried out by UV-Vis spectrophotometer (Thermo Fisher Scientific Genesys 10S). Photo-degradation speciation is also carried out by using HPLC. Methanol method is used for actinometry tests. Photo-degradation of imidacloprid followed first order degradation in all three initial concentrations (2.5, 5 and 10 mg/L), given in **Figure 2**.

3. RESULTS AND DISCUSSIONS

Imidacloprid was very stable under acidic (pH=3) and natural (pH≈6.5) conditions at least for 100 days of hydrolysis whereas, its hydrolytic degradation notably increased under alkaline (pH=11) condition by following first order kinetic pattern (**Figure 3**).

VUV process was very efficient and powerful for elimination of imidacloprid from water under all the experimental conditions investigated. VUV produced $\bullet\text{OH}$ without addition of chemicals, played the most important role and was the main oxidizing agent in the decomposition of aqueous imidacloprid. Increase in flow rate has increased the removal rate of imidacloprid but it was not statistically significant. pH of the solution was the most influencing factor in the degradation of imidacloprid by the VUV process. The slowest degradation rate was observed at pH=11. Reduction in $\bullet\text{OH}$:imidacloprid ratio at higher initial imidacloprid concentration decreased the removal rate of imidacloprid. Inorganic ions noticeably inhibited the decomposition of imidacloprid, in the order of $\text{CO}_3^{2-} > \text{HCO}_3^- > \text{NO}_3^-$ (**Figure 4**). Dissolved oxygen had negligible impact on the reduction rate of imidacloprid. Contributions of oxidative $\text{HO}_2\bullet/\text{O}_2\bullet^-$ as well as reductive $\text{H}\bullet$ and e-aq to imidacloprid degradation were insignificant due to their lower reactivity with imidacloprid compared to $\bullet\text{OH}$. Apparently, just as primary ($\text{H}\bullet$ and e-aq) and secondary ($\text{HO}_2\bullet/\text{O}_2\bullet^-$) radicals, dissolved oxygen did not have much impact on mineralization of aqueous imidacloprid either. 80% TOC reduction of imidacloprid and its intermediates was successfully achieved in 2 h of VUV irradiation.

Our results show that VUV initiated photo-oxidation of imidacloprid is an additive free, effective and sustainable water/groundwater treatment alternative.

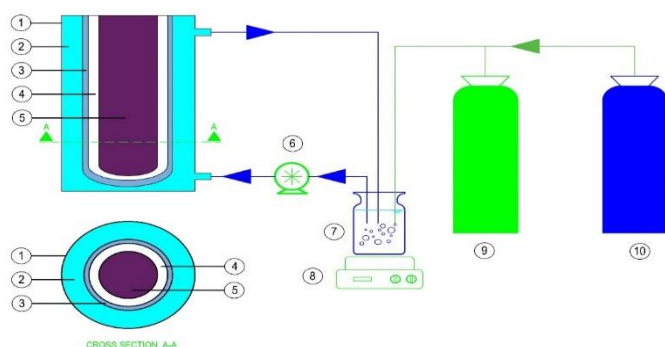


Figure 1. Schematic diagram of the VUV photooxidation system. (1: Annular photoreactor, 2: Experimental solution, 3: Quartz sleeve, 4: Space between sleeve and VUV lamp, 5: VUV lamp, 6: Peristaltic pump, 7: Reservoir, 8: Magnetic stirrer, 9: N_2 cylinder, 10: O_2 tank)

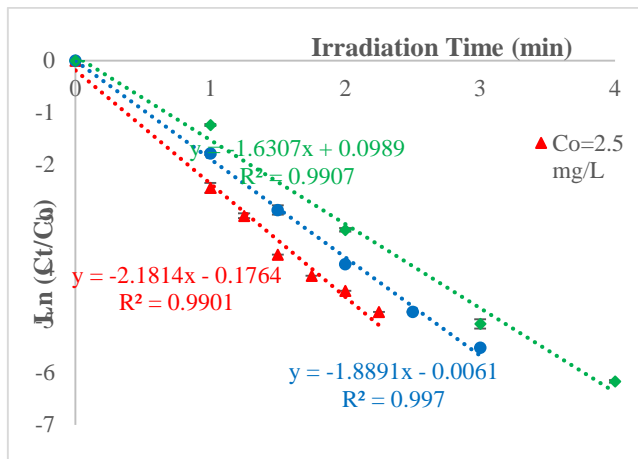


Figure 2. Photodegradation of Imidacloprid by the VUV process as a function of initial concentration and irradiation time ($Q=500$ mL/min, $pH\approx 6.5$).

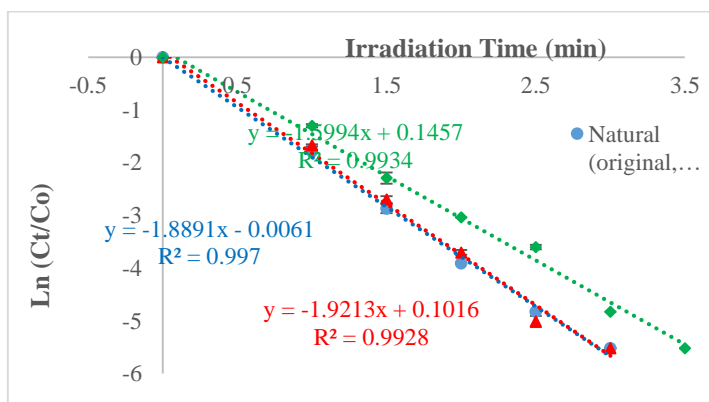


Figure 3. Effect of solution pH on the VUV initiated degradation of Imidacloprid ($C_0 = 5$ mg/L, $Q=500$ mL/min).

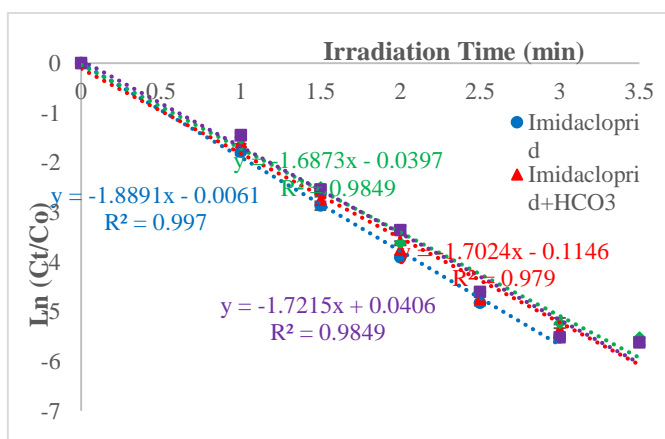


Figure 4. Effects of inorganic ions, HCO_3^- , CO_3^{2-} , NO_3^- ($C_0 = 5$ mg/L) on the VUV initiated degradation of Imidacloprid ($C_0 = 5$ mg/L, $Q=500$ mL/min, $pH\approx 6.5$).

4. CONCLUSIONS)

Our results show that VUV initiated photo-oxidation of imidacloprid is an additive free, effective and sustainable water/groundwater treatment alternative.

Water composition is the main cause for scavenging.

Acknowledgements: The author(s) acknowledge the grant, provided by Turkish Scientific Research Council (TÜBİTAK) funded this research (Project no: 119Y011).

REFERENCES

Christen, V., Mittner, F., Fent, K. (2016). Molecular effects of neonicotinoids in honey bees (*Apis mellifera*), *Environ. Sci. Technol.*, **50**, 4071–4081.

Zhang, Q., Li Z. , Chang C.H., Lou J.L., Zhao M.R., Lu C., (2018), Potential human exposures to neonicotinoid insecticides: a review *Environ. Pollut.*, **236**, 71-81.

Rozsa, G., Nafradi, M., Alapi, T., Schrantz, K., Szabo, L., Wojnarovits, L., Takacs, E., Tungler, A. (2019). Photocatalytic, photolytic and radiolytic elimination of imidacloprid from aqueous solution: Reaction mechanism, efficiency and economic considerations *Applied Catalysis B: Environmental*, **250**, 5, 429-439.

INTEGRATED WATERSHED MANAGEMENT

DECISION SUPPORT SYSTEM FOR SELECTIVE WITHDRAWAL IN WATER SUPPLY RESERVOIRS: AN APPROACH BASED ON THERMAL STRATIFICATION

Elif Soyer^{1*}, Haluk Bayram², Nalan Canigeniş³, and Onur Eren³

¹ Marmara University, Environmental Engineering Department, Istanbul, Turkey

² Istanbul Medeniyet University, Field Robotics Laboratory, BILTAM, Istanbul, Turkey

³ Izmit Water Company (ISAS), Kocaeli, Turkey

*Corresponding author (elif.soyer@marmara.edu.tr)

ABSTRACT

We consider the problem of how effectively and systematically water withdrawal depth is determined in water supply reservoirs with a multilevel intake. In the traditional way, based on the operator's own experience and the water samples taken from varying depths, he/she decides from which intake port water is withdrawn. Our goal is to help the operator in this decision-making process and provide a systematic way to this process. For this purpose, we present an algorithmic approach as a decision support system for the estimation of water withdrawal level in a stratified reservoir. We validate the approach using long-term data collected from a water supply reservoir and make a comparison between the approach and the operator's decision. The results reveal 80% of matching percentage between the decisions on the withdrawal depths made by the approach and the operator when the depth tolerance is set to 10 meters. In case of 15-meter depth tolerance, the matching percentage becomes more than 90%.

Keywords: *surface water bodies, selective withdrawal, thermal stratification, water inlet structure, reservoir operational strategy, decision support system, water quality, water supply reservoirs.*

1. INTRODUCTION

Assessments regarding water withdrawn from water supply reservoirs are crucial in delivering adequate quantities of water in the best available quality. Although water taken is treated at the plant, the location of withdrawal or selected depth determines the amount of chemicals needed and directly affects processes and operational problems. Administrative managers and water treatment operators are responsible for making decisions for the overall treatment facility. Those decisions start from the very first beginning if the treatment plant is configured with multilevel intake ports, so that selective withdrawal of high-quality water can be achieved (Dortch and Holland, 1984; Davis et al., 1987; AWWA-ASCE, 2005). Flexible operation considerations are based on reservoir stratification, physical and chemical water quality process parameters, algae counts and blooms and trihalomethane formation potential together with raw water chlorine demand (Qasim et al., 2000).

Water quality parameters can vary significantly in types and concentrations depending on the depth of water in the reservoir. Their relative importance and effects are also determined by seasonal changes, especially in thermal stratification periods. Thermal stratification seasons and turnover periods, when the reservoir is completely mixed and hence constituents are likely to be present throughout all the depths of the reservoir, strongly affect the concentrations of contaminants expected at the drinking water intake. Simulations of contaminant spills and their arrival to the plant show that different operational responses are required especially in summer spills (Jeznach et al., 2016). Thermal simulation models were studied to meet downstream water temperature objectives (Fontane et al., 1981). Some of the water quality constituents gradually increase over the stratification season since they accumulate in the lower depths (hypolimnion/stagnant zone) of the reservoir. However, when the stratification is broken in winter times, top layers are enriched in nutrients from hypolimnion, full circulation occurs, and an almost uniform distribution of chemical and biological water quality parameters is observed throughout the overall depths. Therefore, during the stratification season, it is important to implement an effective and timely withdrawal of some constituents such as Fe and Mn, algae and phytoplankton, phosphorous, and other water quality parameters (Barbiero et al, 1997; Casamitjana et al, 2003; Slavik et al, 2013; Bertone, 2015). Treatment plant operators need to consider numerous different parameters when making decisions on the selection of the depth through which water is taken into the plant. There are studies focusing on developing approaches using scenario based models to investigate the effects of abstracting raw water from varying levels (such as the deepest region or the bottom of the dam) or from varying levels of different reservoirs on water quality as well as on the problems observed during operation of the treatment plant and its processing costs (Slavik et al, 2013; Bertone et al, 2018). Identifying an optimal withdrawal strategy has also great significance on long term operational concerns of a water supply reservoir (Barbiero et al, 1997; Elçi, 2008; Çalışkan and Elçi, 2009), and on minimizing the environmental impacts when water is taken from a certain level and is released to a downstream river (Weber et al, 2017). The aim of this study is to develop an approach to be used in the decision-making process of the determination of reservoir depth through which water is supplied to the drinking water treatment plant, i.e location of inlet structure's open gate. The main contributions of the paper are as follows:

- Developing an algorithmic approach as a decision support system for recommending water withdrawal elevation,
- Validating the approach using long-term data collected from a water supply reservoir and comparing the approach with the operator's decision.

2. MATERIAL AND METHODS

In this section, an algorithmic approach used to determine the depth from which water is supplied to the treatment plant, and an application of this approach are explained.

2.1. Decision-Making in Operation: An Algorithmic Approach

The approach is outlined in Algorithm 1. The approach requires as inputs an array (*Temp_List*), which contains water temperatures measured at all consecutive depths for the reservoir and a temperature threshold (*Temp_Threshold*) for determining whether there occurs thermal

stratification. Thermal stratification is the marked layering, characterized by how far light penetrates, and it results in an abrupt temperature transition occurring between the upper warm layer and the bottom cold layer (Raven et al., 2012).

Algorithm 1: Determine_Thermal_Stratification_Depths

```

Inputs: * Temp_List // an array of temperature values for each depth
           * Temp_Threshold // temperature threshold for thermal stratification
// Initialize upper and lower levels of the stratification
Stratification_UpperLevel, Stratification_LowerLevel  $\leftarrow$   $\emptyset$ 
// Check whether a thermal stratification occurs
If  $\max(\text{Temp\_List}) - \min(\text{Temp\_List}) > \text{Temp\_Threshold}$ 
    Stratification_MidPoint_Temp  $\leftarrow$   $\text{mean}(\text{Temp\_List})$ 
    Stratification_UpperLevel_Temp  $\leftarrow$  average of the temperatures in Temp_List which are greater than Stratification_MidPoint_Temp
    Stratification_LowerLevel_Temp  $\leftarrow$  average of the temperatures in Temp_List which are less than Stratification_MidPoint_Temp
    Stratification_UpperLevel  $\leftarrow$  depth at which the temperature is closest to Stratification_UpperLevel_Temp
    Stratification_LowerLevel  $\leftarrow$  depth at which the temperature is closest to and just above Stratification_LowerLevel_Temp
End If
Return Stratification_UpperLevel, Stratification_LowerLevel

```

An example of determining the location of thermal stratification and its boundaries on the real temperature data are shown in Figure 1. Evaluating in detail all the water quality parameters measured along the depth, the treatment plant operator decided that the water intake depth should be 110 meters. The raw water was taken to the plant from this depth on the same day.

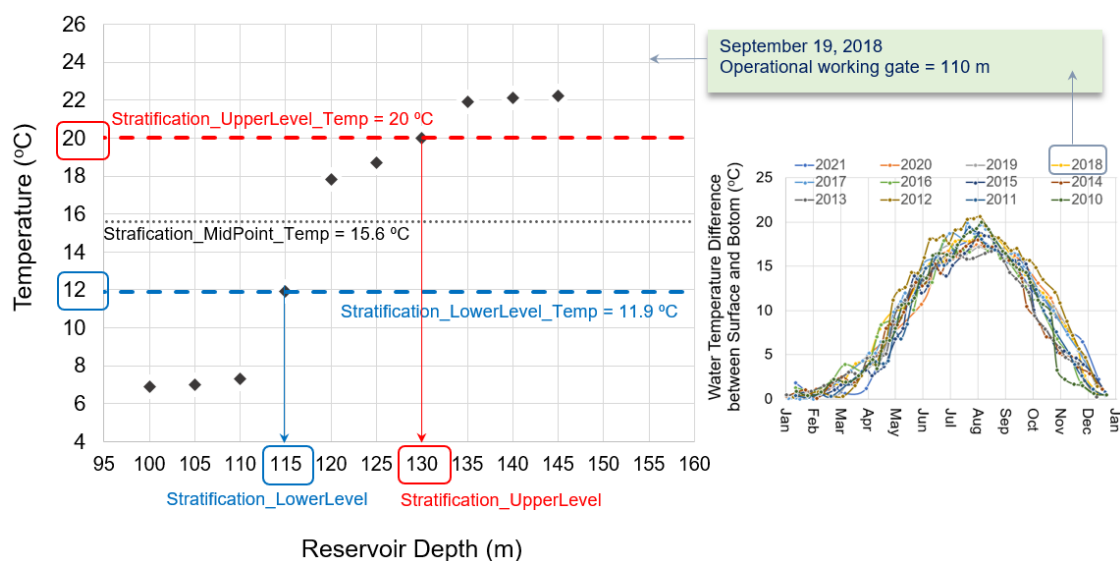


Figure 1. Left: Water temperature variation with reservoir depth, location of thermal stratification (September 19, 2018) and terminology used in Algorithm 1. The black dots denote the temperature measurements at each depth. Right: Temperature variation between 2010 and 2021 in Yuvacık Reservoir.

2.2. Case Study: Yuvacık Reservoir

Yuvacık Reservoir (40.6741 °N, 29.9694 °E) is located in Kocaeli, Turkey, and is fed by Kirazdere, Kazandere, and Serindere creeks. The minimum and maximum operational water levels of the dam are 112.5 m and 169.3 m, respectively. In order to optimize water quality parameters and ensure process efficiencies in the treatment plant, the intake structure was

configured with several withdrawal depths vertically. These are located between 110 m to 160 m relative to the sea level.

Manually sampled and laboratory analyzed data from the surface (maximum being 169.3 m) to a depth of 100 m for the period of 2000-2021 was provided by Izmit Water Company (İSAŞ). The parameters monitored include temperature, pH, turbidity, conductivity, dissolved oxygen, iron, manganese, color, chlorophyll-a, ammonium, nitrate nitrogen, phosphates, UV254 absorbance, silicates, and light penetration. These 15 water quality parameters were measured at least twice per month from 2000 to 2021 in the reservoir between the depths of 100 to 160 m at 5 m intervals. Some of them, such as pH, temperature, conductivity, turbidity, dissolved oxygen, iron, manganese, and chlorophyll-a, were monitored three times a month. In Yuvacık Reservoir, at discrete depths of 5-meter intervals through 60-meter overall depth, water temperature was monitored three times a month on average, therefore, a total of 801 temperature data were included in the analysis. In the Yuvacık Water Treatment Plant, the water quality parameters monitored throughout all the elevations in the reservoir are evaluated separately while determining the elevation of the working gate on the intake structure. Besides, based on the operator's experiences in achieving treatment objectives, variations in a certain group of parameters are examined in more detail. Among these parameters are pH, temperature, iron, manganese, algae, dissolved oxygen and turbidity. Considering operational experiences and source specific characteristics of Yuvacık Reservoir, it is understood that the recommended water intake depth (*Stratification_LowerLevel*) presented with the proposed approach coincides with the probable region of the choice made by the operator after evaluating all parameters separately by extreme care and effort. We observe from the dataset that stratifications occur mostly when the difference between the maximum and minimum temperatures is higher than 10 °C. Hence, the temperature threshold value (*Temp_Threshold*), defined in Section 2.1 where the decision-making process is explained in Algorithm 1, was chosen as 10 °C in this case study conducted for Yuvacık Reservoir. The stages defined in the decision-making process were carried out and the results obtained are given in the Results and Discussions Section below.

3. RESULTS AND DISCUSSIONS

Temperature measurements collected at 5-meter depth intervals for the last 21 years were analyzed. This historical dataset indicates that temperature stratifications exist from late April and mostly around the beginning of May through late October. It becomes more apparent during summer, especially in August, when an obvious thermocline develops. Figure 2 shows the lower and upper depths of the stratified region for the days when a thermal stratification is expected to take place in the reservoir. The operator's preferences for withdrawal depth and the recommended depth determined by the approach are also displayed in Figure 2. When the lower and upper boundaries of the stratified region are examined in terms of depth and temperature change, it is seen that this layer becomes wider and more diffused especially from July to August and the temperature difference between the upper and lower levels takes the greatest values in this period. When the reservoir is thermally stratified, the agreement between the depth suggested by the approach developed here and the depth selected by the operator is very high, either being the same or remaining within 10 meters of error.

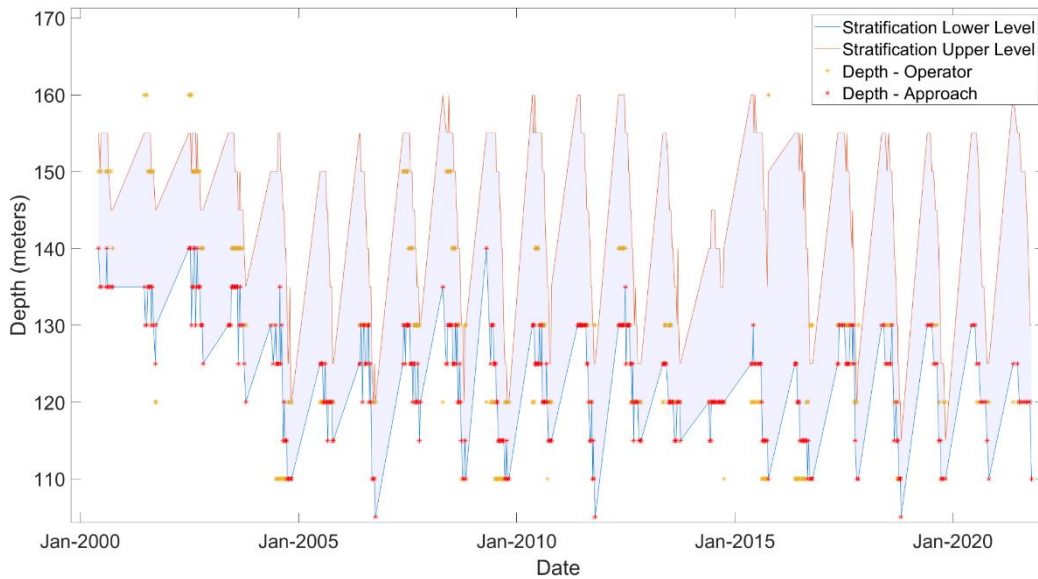


Figure 2. Location of stratified layer and withdrawal depth (depth tolerance = 10 meters)

Figure 3 clearly demonstrates that the decisions made by the approach and the operator are highly consistent. Matching percentages are also reported for 5, 10, and 15 meters of error, i.e. deviations between the approach's result and working gate.

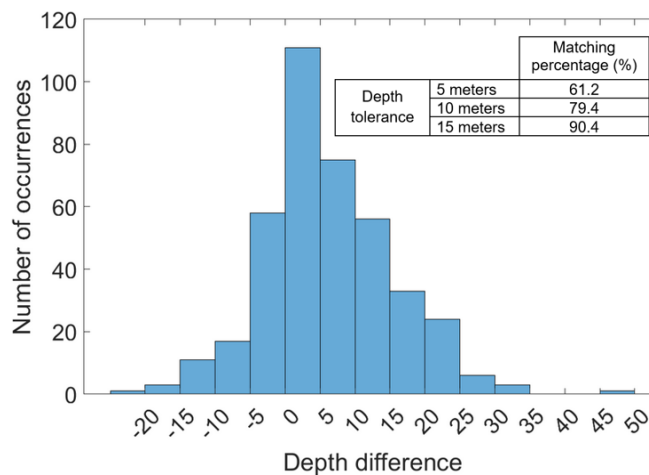


Figure 3. Histogram of depth differences between the operator's decision and the approach and the table for the percentage of the approach's decisions consistent with the operator (Top-right).

In late summer and fall, progressive mixing occurs along the depth of the reservoir due to declining air temperatures. Temperature differences between the surface and bottom of the reservoir become insignificant and hence stratification is not observed. In such cases, since Algorithm 1 does not detect thermal stratification, it will not provide any recommendation for water withdrawal depth and the treatment plant operator will base his/her decision on individual assessment of water quality parameters.

4. CONCLUSIONS

This paper considered the problem of determining the water withdrawal depth for water supply reservoirs with a multilevel intake. We presented a decision support-based approach for

estimating the location of thermal stratification and water withdrawal level in a stratified reservoir. We validated the approach using the long-term data collected from a water supply reservoir, Yuvacık Reservoir, Kocaeli, Turkey, and compared the decision made by the approach with the operator's decision. According to this comparison, the two decisions coincide with 80% of the matching percentage when the depth tolerance is 10 meters. In case of 15-meter depth tolerance, the matching percentage becomes more than 90%. We are currently working on developing machine learning based techniques for estimating the withdrawal depth. In addition to the temperature data, we plan to make use of other water quality parameters in this estimation. In our future work, we would also like to verify our approach using new datasets collected from other reservoirs.

Acknowledgements: We thank Emre Eren and Deniz Denizeri from ISAS Water Company for gathering the water quality dataset and their collaborative effort during discussions on the collected data.

REFERENCES

- AWWA ASCE (2005) *Water Treatment Plant Design*. 4th Ed. McGraw-Hill.
- Barbiero, R. P., James, W. F., Barko, J. W. (1997). The effects of a change in withdrawal operations on phytoplankton and nutrient dynamics in Eau Galle Reservoir, Wisconsin (USA). *Internationale Revue der gesamten Hydrobiologie und Hydrographie*, 82(4), 531-543.
- Bertone, E., Stewart, R. A., Zhang, H., Bartkow, M., & Hacker, C. (2015). An autonomous decision support system for manganese forecasting in subtropical water reservoirs. *Environ. Modelling & Software*, 73, 133-147.
- Bertone, E., O'Halloran, K., Bartkow, M., & Mann, K. (2018). Autonomous intake selection optimisation model for a dual source drinking water treatment plant. *Wat. Sci. and Technol.: Water Supply*, 18(1), 279-287.
- Casamitjana, X., Serra, T., Colomer, J., Baserba, C., Pérez-Losada, J. (2003). Effects of the water withdrawal in the stratification patterns of a reservoir. *Hydrobiologia*, 504(1), 21-28.
- Çalışkan, A. and Elçi, Ş. (2009) Effects of Selective Withdrawal on Hydrodynamics of a Stratified Reservoir. *Water Resources Management*. 23. 1257-1273.
- Davis, J.E, Holland, J.P., Schneider, M.L., Wilhelms, S.C. (1987). *SELECT: A Numerical one-dimensional model for selective withdrawal*. Instruction Report E-87-2, U.S. Army Engineer Waterways Experiment Station, Vicksburg, MS.
- Dortch, M.S. and Holland, J.P. (1984) *A Technique to Optimally Locate Multilevel Intakes for Selective Withdrawal Structures*. Department of the Army, Waterways Experiment Station, Corps of Engineers.
- Elçi, S. (2008) Effects on thermal stratification and mixing on reservoir water quality. *Limnology*. 9. 135-142.
- Fontane, D. G., Labadie, J. W., Loftis, B. (1981). Optimal control of reservoir discharge quality through selective withdrawal. *Water Resources Research*, 17(6), 1594-1602.
- Jeznach, L.C., Jones, C., Matthews, T., Tobiason, J.E., Ahlfeld, D.P. (2016) A framework for modeling contaminant impacts on reservoir water quality. *Journal of Hydrology*. 537, 322-333.
- Qasim, S.R., Motley, E.M., Zhu, G. (2000) *Water Works Engineering: Planning, Design, and Operation*. Prentice-Hall, Inc.
- Raven, P.H., Hassenzahl, D.M. Berg, L.R. (2012) *Environment*. John Wiley & Sons.
- Slavik, I., Uhl, W., Skibinski, B., Rolinski, S., Petzoldt, T., Benndorf, J. Scheifhacken, N., Paul, L., Funke, M., Lohr, H., Völker, J., Borchardt, D. (2013) A decision support procedure for integrative management of dammed raw water reservoirs. *Water Science and Technology: Water Supply*, 13, 2, 349.
- Weber, M., Rinke, K., Hipsey, M.R., Bohrer, B. (2017) Optimizing withdrawal from drinking reservoirs to reduce downstream temperature pollution and reservoir hypoxia. *Jour. of Environ. Management*. 197. 96-105.

ESTIMATING DIFFUSE NUTRIENT LOADS OF MELEN WATERSHED BY USING SOIL AND WATER ASSESMENT TOOL (SWAT)

Gokhan Cuceloglu¹, Alpaslan Ekdal^{2*}, Melike Gurel² and Nusret Karakaya³

1. University of Oxford, Environmental Change Institute, Oxford, UK

2. Istanbul Technical University, Environmental Engineering Department, Istanbul, Türkiye

3. Bolu Abant İzzet Baysal University, Environmental Engineering Department, Bolu, Türkiye

*Alpaslan Ekdal (ekdala@itu.edu.tr)

ABSTRACT

Achieving the objectives of water quality in water supply resources requires comprehensive understanding of processes and estimation of nutrient loads. Melen Watershed was considered as one of the main water supply sources to compensate for future water demand of İstanbul, Türkiye. Diffuse pollution is a major contributor for water quality deterioration in Melen Watershed. In this study, Soil and Water Assessment Tool (SWAT) was used to estimate temporal and spatial variation of nutrient loads in the watershed. Our results yield that the unit pollution loads for total nitrogen (TN) varies between 0.04 – 17.86 kg/ha/year whereas the total phosphorus (TP) varies between 0.006 – 4.18 kg/ha/year in Melen Watershed. The information generated by using the SWAT model will constitute an important framework for the sustainable management of the watershed.

Keywords: SWAT, Melen Watershed, İstanbul, Diffuse Pollution, Watershed Modeling.

1. INTRODUCTION

Diffuse pollution has become a challenging issue in watershed management and is a major cause of impairment of water bodies around the world (Novotny, 2003). Elevated nutrient loads may negatively impact water quality, increase costs of pollutant mitigation and water treatment especially in water resources used for water supply. Achieving the objectives of water quality requires comprehensive understanding of processes and estimation of nutrient loads. Physically-based watershed modeling has proved to be an effective tool that can identify diffuse pollution loads at different temporal–spatial scales.

Melen Watershed was considered as one of the main water supply sources to compensate for future water demand of İstanbul. The main income in the watershed is through cultivation of nuts and corn in the rural areas. Industrial activities are concentrated in urban areas of Duzce Province. As a result, several environmental problems such as domestic and industrial wastewater discharges, runoff from agricultural and residential areas, deforestation and soil erosion adversely affect the water quality of water bodies in the watershed (Erturk et al., 2010;

Karakaya and Evrendilek, 2010; Gurel et.al., 2011). Therefore, it is essential to quantify diffuse pollution within the watershed for effective planning of basin protection plans.

This study aims to estimate diffuse nutrient loads and provide basis of modeling framework for climate change impacts and eutrophication modeling in planned Melen Reservoir, which is located downstream of the watershed.

2. MATERIAL AND METHODS

Soil and Water Assessment Tool (SWAT) is a continuous-time, semi-distributed, process-based model developed to evaluate alternative management strategies on water resources and diffuse pollution in large river basins (Arnold et al., 2012). In this study, SWAT was used as watershed model to simulate both hydrology and water quality. Model calibration has been performed by using SWAT-CUP software (Abbaspour et al., 2007). Spatial data required for the model were obtained from freely available online sources whereas the temporal data sets (hydrometeorological) and other model inputs such as fertilizer applications, livestock, septic tanks etc. were provided by local institutes. Nutrient concentrations in the river were collected from the field studies. Total nitrogen (TN) and total phosphorus (TP) were used to calibrate SWAT model at nine different water quality monitoring stations for 18 months (July 2020 - December 2021) located upstream of the basin where the effect of anthropogenic activities is minimum.

3. RESULTS AND DISCUSSIONS

The unit pollution loads estimated for TN (0.04 – 17.86 kg/ha/year) and TP (0.006 – 4.18 kg/ha/year) align with the unit pollution loads given in the literature (Özcan et al. 2016). Although we present annual loads for the watershed to compare other studies, using physically based models for watersheds such as SWAT, provides both spatial (subbasin or hydrologic response unit level) and temporal variability (wet and dry seasons). Spatial distribution of the diffuse pollution loads (ton/year) in the study area is provided in Figure 1. These maps show the hotspots for diffuse pollution, which are mostly located around the planned reservoir. In addition to livestock raising, these areas are noted for intense agricultural activities, which are the primary source of diffuse pollution in the watershed.

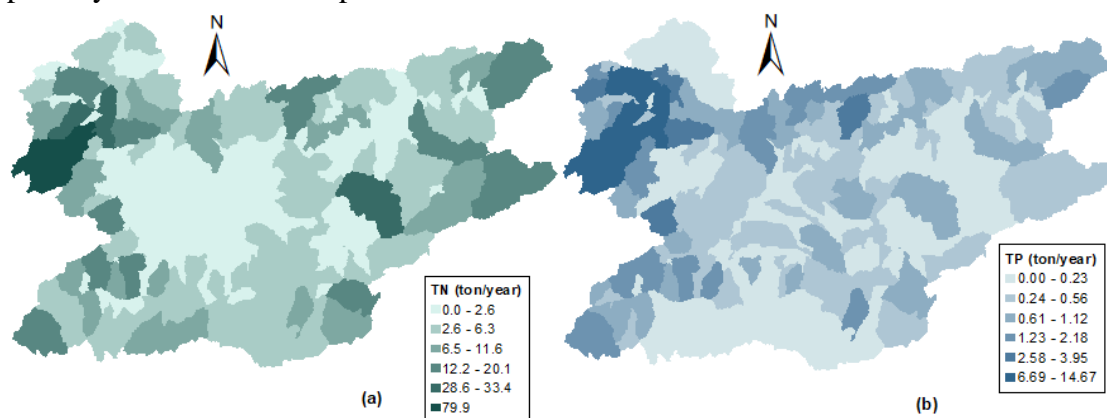


Figure1. Estimated Nutrient Loads for Melen Watershed a) Total Nitrogen, b) Total Phosphorus

4. CONCLUSIONS

SWAT model was applied successfully in order to estimate the diffuse pollutants loads in Melen Watershed, Türkiye. Hydrological process models can investigate the spatial-temporal changes of diffuse pollutant loads comprehensively. This provides the decision makers the opportunity of making a scientifically sound selection by generating the required information for the determination of pollution control strategies. The information generated by using the results obtained within this study for Melen Watershed will constitute an important framework for the sustainable management of the watershed.

Acknowledgements: Authors of the study would like to acknowledge funding by the Scientific and Technological Research Council of Türkiye (TÜBİTAK) for the project entitled “River Ecological Flow Prediction Model and Its Application”, Project number 116Y447.

REFERENCES

- Abbaspour, K.C., Yang, J., Maximov, I., Siber, R., Bogner, K., Mieleitner, J., Zobrist, J., & Srinivasan, R. (2007). Modelling hydrology and water quality in the pre-alpine/alpine Thur watershed using SWAT. *J. Hydrol.* 333, 413-430.
- Arnold, J.G., Moriasi, D.N., Gassman, P.W., Abbaspour, K.C., White, M.J., Srinivasan, R., Santhi, C., Harmel, R.D., Griensven, a. Van, VanLiew, M.W., Kannan, N., & Jha, M.K. (2012). SWAT: Model Use, Calibration, and Validation. *The American Society of Agricultural and Biological Engineers* (55), 1491–1508.
- Erturk, A., Gurel, M., Ekdal, A., Tavsan, C., Ugurluoglu, A., Seker, D.Z., Tanik, A., & Ozturk, I. (2010). Water quality assessment and meta model development in Melen watershed - Turkey. *Journal of Environmental Management.* (91), 1526–1545.
- Gurel, M., Erturk, A., Seker, D. Z., Tanik, A., Ekdal, A., Avsar, C., & Ozturk, I. (2011). Estimation of monthly diffuse nutrient loads for a watershed in Turkey, *Water and Environment Journal*, (25), 219-229.
- Karakaya, N., & Evrendilek, F. (2010). Water quality time series for Big Melen Stream (Turkey): Its decomposition analysis and comparison to upstream. *Environmental Monitoring and Assessment.* (165), 125–136.
- Novotny, V. (2003). *Water Quality, Diffuse Pollution and Watershed Management* (2nd edition), John Wiley and Sons Inc., New York, USA.
- Özcan, Z., Kentel, E., & Alp, E. (2016). Determination of unit nutrient loads for different land uses in wet periods through modelling and optimization for a semi-arid region. *Journal of Hydrology*, (540), 40-49.

INVESTIGATING APPLICABILITY OF GRASSED WATERWAY PRACTICE WITH GEOGRAPHIC INFORMATION SYSTEM

Mehmet Kalfazade, Alpaslan Ekdal*

Istanbul Technical University, Environmental Engineering Department, Istanbul, Türkiye

**kalfazade@itu.edu.tr*

ABSTRACT

Diffuse pollution caused by agricultural activities has become one of the major problems threatening surface water and groundwater quality. The aim of this study is to develop a decision support system/tool that includes scientifically based Geographic Information System (GIS) analysis that enables the determination of the physical applicability of the grassed waterway in order to prevent or reduce diffuse source pollution before it reaches water resources. Within the scope of this study, it is investigated whether the grassed waterways are suitable for the selected watershed by evaluating the design principles of grassed waterways, land use data, digital elevation models, soil maps and drainage network. As a result of the GIS analyses, it was determined that there are 4891 kilometers of ephemeral stream in the Manyas Lake Watershed, and grassed waterway application can be physically applied to 480 kilometers of it.

Keywords: *diffuse pollution, structural BMP, grassed waterway, GIS.*

1. INTRODUCTION

Diffuse pollution caused by agricultural activities has become one of the main problems threatening surface water and groundwater quality. Lands that has been deforested and converted to agricultural and urban areas cause major water quality problems around the globe (Novotny, 1999). Best management practices can be designed in line with various goals and objectives such as flood control, pollutant removal, ecological sustainability of the receiving water body. In order to achieve these goals, engineering and ecological principles are taken into consideration in the design processes. These principles include hydrology of the watershed, soil structure/percolation rate, existing state of the receiving environment, water quality. Local regulations and standards also play an important role in the design of best management practices.

Grassed waterways are ditches with suitable vegetation that convey water at low speed to a safe outlet in order to reduce the carrying capacity of the canal flow. It prevents erosion by filtering the flowing water during heavy rain, and slows down the flow of stormwater (Muthukrishnan et al., 2004; Fiener and Auerswald, 2003). It also prevents formation of gullies on the soil. Nutrients in the flowing water are adsorbed as they move along the grassed waterways (Dermisis et al., 2010).

The aim of this study is to develop a decision support system/tool that includes scientifically based Geographic Information System (GIS) analysis that enables the determination of the

physical suitability of the grassed waterway in order to prevent or reduce diffuse source pollution before it reaches water resources.

Within the scope of this study, it is investigated whether the grassed waterways are applicable for the selected watershed by evaluating the design principles of grassed waterways, land use data, digital elevation models, soil maps, drainage network. Thus, it will contribute to the protection, development and sustainable management of fresh water resources in the study area.

2. MATERIAL AND METHODS

Study Area

Manyas Lake Watershed is located in Susurluk Watershed, at the western part of Türkiye. Manyas Lake Watershed has an area of 291 km². Manyas Lake, with a surface area of 192 km², is Türkiye's 6th largest lake. Its average depth is 3 m, and its deepest point is 5 m in the southern part of the lake. The surface water bodies that discharge to the lake are Kocaçay (Manyas Stream), Dutlu Stream, Sığircı Stream, and Mürvetler Stream.

GIS Applications

The flow chart of the analysis procedure to be created in the GIS environment and the data to be used during these processes is given in Figure.

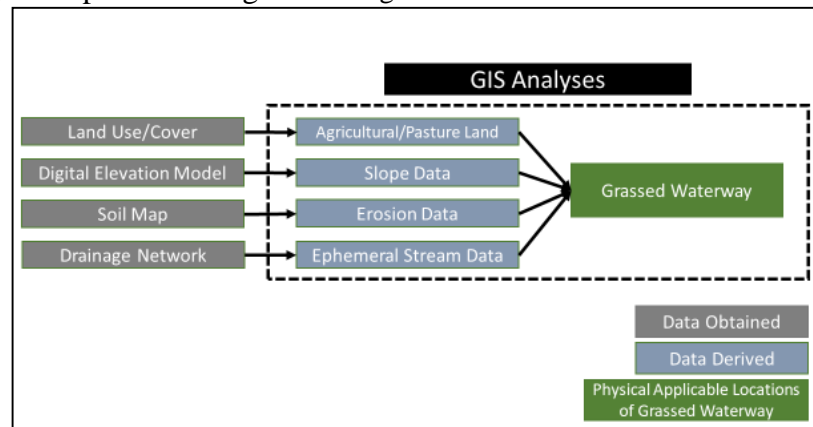


Figure1. GIS application flow chart

The Digital Elevation Model (DEM), land use data, soil erosion data, and river network data of the watershed were used to determine the regions within Manyas Lake Watershed which are physically suitable for grassed waterway application.

By using the river network data, the data with the "ephemeral stream" feature was saved as a separate layer. By using the data with "Buffer" feature, a buffer zone of 50 meters was created from the left and right banks of the ephemeral streams. With the "Select by Location" feature, these areas have been selected by overlapping with agricultural-pasture areas and locations with moderate and severe soil erosion. Ephemeral streams in the overlapping regions were saved as a separate layer. With the "Feature Vertices to Points" feature, the start and end points were obtained. Level data in meters have been assigned to these points based on the Digital Elevation Model data with 5m x 5m resolution with the "Extract Values to Points" feature. Then, these points were combined using the "Dissolve" feature, and the elevations read from the DEM using the statistics option were combined with the "MIN" and "MAX" elevations, and the ephemeral stream data overlapped with the agricultural and pasture areas. The average slope of the ephemeral streams, the length of which is calculated, was calculated with the calculation $\frac{((\text{starting level} - \text{ending level}) / \text{ephemeral stream length}) * 100}{100}$. Considering that the average channel slope for grassed waterways should not exceed 5%, ephemeral streams with a channel slope above 5% were not considered in the average slope analysis. Thus, priority areas where a

grassed waterway can be applied, namely ephemeral streams in areas with a channel slope of less than 5%, in agricultural and pasture areas with a high probability of erosion, have been obtained in the Manyas Lake Watershed.

3. RESULTS AND DISCUSSIONS

The river network prepared at 1/25000 scale and the proposed grassed waterway locations of the Manyas Lake Watershed are given in Figure. As a result of the GIS analyses, it was determined that there are 4891 kilometers of ephemeral stream in the Manyas Lake Watershed and grassed waterway application can be physically applied to 480 kilometers of them.

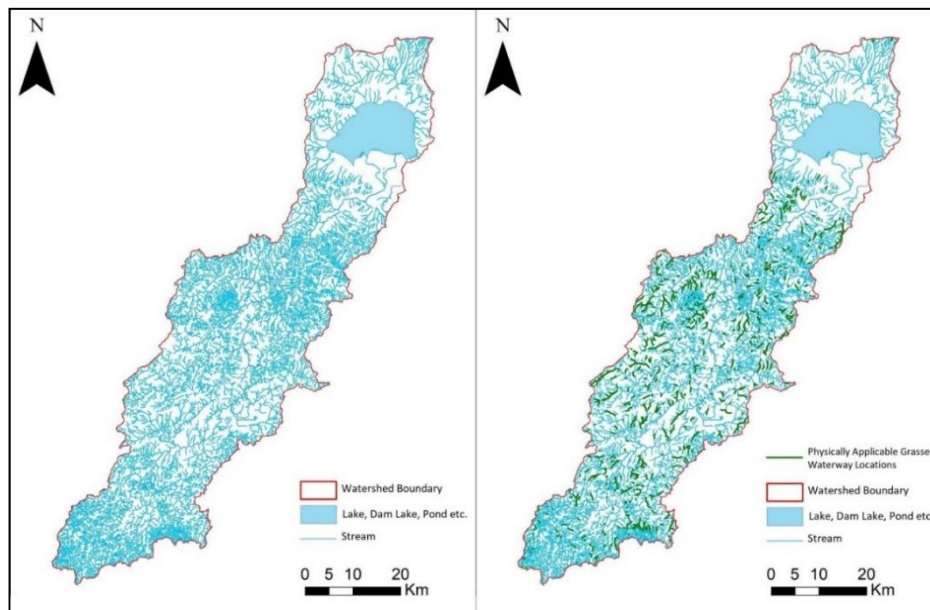


Figure2. Physically Applicable Grassed Waterway Locations

4. CONCLUSIONS

Although grassed waterways are among the most common best management practices, they are not used widely in Türkiye. Their capacity to reduce surface flow velocity and erosion may not be valued enough. GIS applications are the first step for finding suitable locations for grassed waterways and it should be further investigated on site before construction.

Acknowledgements: Authors would like to acknowledge Scientific and Technological Research Council of Türkiye (TUBITAK) (1003) for their support through project entitled “Development of an Integrated Ecosystem Modelling Based Decision Support System for Management of Manyas Lake Watershed” with project number 116Y407, and Istanbul Technical University Scientific Research Fund through project entitled “Investigating the Physical Applicability of Structural Best Management Practices with the Aid of Geographical Information System with project number 42492.

REFERENCES

- Dermisis, D., Abaci, O., Papanicolaou, A. N., & Wilson, C. G. (2010). Evaluating grassed waterway efficiency in southeastern Iowa using WEPP. *Soil Use and Management*, 26(2), 183-192.
- Field, R., & Tafuri, A. N. (Eds.). (2006). The use of best management practices (BMPs) in urban watersheds. *DEStech Publications, Inc.*
- Fiener, P., & Auerswald, K. (2003). Effectiveness of grassed waterways in reducing runoff and sediment delivery from agricultural watersheds. *Journal of Environmental Quality*, 32(3), 927-936.
- Novotny, V. (1999). Diffuse pollution from agriculture—a worldwide outlook. *Water science and technology*, 39(3), 1-13.

INTEGRATING PROTECTED AREA MANAGEMENT WITH RIVER BASIN MANAGEMENT PLANS AS A MEASURE TO ADDRESS DIFFUSE POLLUTION

Cronin Lisa^{1,2*}, Regan Fiona^{1,3}, and Lucy Frances²

¹Dublin City University Water Institute, Glasnevin, Dublin 9, Ireland

²Centre for Environmental Research Innovation and Sustainability CERIS, Atlantic Technological University,
Department of Environmental Science, Sligo, Ireland

³School of Chemical Sciences, Glasnevin, Dublin 9, Ireland

[*lisa.cronin@atu.ie](mailto:lisa.cronin@atu.ie)

ABSTRACT

More than half of the river and lake water bodies in Europe are of less than good ecological status or potential (EEA, 2021) and River Basin Management Plan (RBMP) reports across Europe highlight that the ‘wicked problem’ of diffuse agricultural pollution (Patterson, Smith and Bellamy, 2013; Thornton et al., 2013; Sharma, 2020) remains a persistent issue for water quality (Jacobsen, Anker and Baaner, 2017). Biodiversity is in crisis and the rate of loss of biodiversity is accelerating (Brondízio *et al.*, 2021). Freshwater biodiversity is most impacted and diffuse pollution was identified as one of the key contributors to biodiversity loss in the EU (EEA, 2015).

The OECD promotes ‘collaborative governance’ as one of the key policies to effectively tackle diffuse pollution (OECD, 2017) and it is integrated into the implementation of the Water Framework Directive (WFD) (Graversgaard *et al.*, 2017; Antwi *et al.*, 2021; Söderberg *et al.*, 2021) and integral to its effective implementation (Voulvoulis, Arpon and Giakoumis, 2017). Similarly, Interreg Europe Policy Learning Platform (2020) advances multi-stakeholder governance for more effective biodiversity protection and conservation.

The purpose of this article was to identify the synergies between challenges and pressures for Protected Areas (PAs) and river basins under the WFD and explore integrated management as an additional measure to address diffuse pollution whilst aiding the restoration of biodiversity. Although the benefits for integrated management for biodiversity and for water quality are frequently recognized, the author found little evidence of frameworks and initiatives for co-management of protected areas and river basins despite the many synergies and clear benefits for both, but also the further co-benefits for climate adaptation and for the delivery of the UN Sustainable Development Goals.

Keywords: challenges for protected areas, pressures on water quality, integrated management for biodiversity, diffuse pollution, non point source pollution.

1. INTRODUCTION

In the Water Framework Directive (WFD), Europe has some of the most progressive water quality legislation in the world (Carvalho *et al.*, 2019) and with Natura 2000 under the Birds

and Habitats Directives (Nature Directives), it has the largest coordinated network of protected areas (PAs) on the planet (European Commission, 2022). However, despite such legislation and protection, environmental trends in Europe have not improved since 2015 with only 2 of the 13 policy objectives for biodiversity expected to be met (EEA, 2019). Preventing diffuse pollution remains a significant challenge (Collins *et al.*, 2016; Boezeman, Wiering and Crabbé, 2020) and diffuse sources, especially those from agriculture, are one of the greatest impediments to achieving ‘good status’ under the WFD (EEA, 2018). In many PAs agriculture is the predominant land use (Caković *et al.*, 2021), with Vijay and Armsworth, (2021) highlighting that cropland overlaps with 6% of PAs and is responsible for approx. 18% of anthropogenic impacts in PAs. There are many synergies between the objectives of the WFD and the Nature Directives (Janauer, Albrecht and Stratmann, 2015) but current implementation approaches are inadequate to deliver the required outcomes for water quality or biodiversity.

2. MATERIAL AND METHODS

A web-based search of scientific literature and of grey literature was conducted with combinations of the following terms used to search for information: ‘challenges/threats to Pas, challenges for conservation, challenges for Natura 2000/biodiversity, challenges/pressures for water quality (WQ), challenges for diffuse/non point source pollution, integrated management (IM) of protected areas, IM for WFD, IM for water quality and IM for biodiversity. Where new keywords were identified, these were used to identify other relevant articles and the bibliography of articles was also scanned. Only literature in English from the last ten years was included, analyzed and collated based on relevant title and abstract. The key challenges for each of the areas (PAs, conservation, Natura 2000, WQ, diffuse pollution, biodiversity) were identified and categorized into 9 broad categories (invasive alien species, climate change, human land use, finance, stakeholder engagement, evidence, pollution, overexploitation and climate change). A figure was then constructed to highlight the drivers and challenges for water quality, freshwater biodiversity and protected areas and identify the synergies between them.

3. RESULTS AND DISCUSSIONS

Synthesis of the literature identified eight key pressures on water quality (Collins *et al.*, 2016; Teurlinx *et al.*, 2019) with seven key challenges to addressing diffuse water pollution (Harris, 2013), seven challenges for PAs (Hoffmann, 2022) and seven key global drivers of freshwater biodiversity loss (Mazor *et al.*, 2018; Williams-Subiza and Epele, 2021). Figure 1 clearly demonstrates the significant degree of overlap with these primary anthropogenic drivers - climate change, invasive species, pollution, land use and resource extraction all strongly impacting on biodiversity and water quality.

In dealing with water and land problems Harris (2013) argues that environmental systems are complex and therefore aspects cannot be successfully managed individually, but ‘managing whole systems rather than places and resources’ (Broderick, 2008) delivers benefits for multiple species (Pittock *et al.*, 2015), for biodiversity and climate change (Shin *et al.*, 2022) and aids reversal of freshwater biodiversity loss and delivers for SDGs (Tickner *et al.*, 2020).

Many authors advocate for an integrated approach involving all stakeholders to reduce diffuse

pollution (Hendry and Reeves, 2012; OECD, 2017; Graversgaard *et al.*, 2018) but most EU member states have not prioritized administrative integration to deliver for WFD and reduce diffuse pollution, and this fragmentation is hampering effective implementation of the legislation (Wiering, Boezeman and Crabbé, 2020). Adaptive management (AM) is an approach used to manage complex systems (Eberhard *et al.*, 2009) and many authors advocate for the use of AM for effective PA management (McCarthy and Possingham, 2007; Canessa *et al.*, 2016) particularly due to the increasing uncertainty associated with climate change (Hoffmann, 2022). This approach is similar to AM for water quality (Eberhard *et al.*, 2009; Bieroza, Bol and Glendell, 2021), AM to address diffuse pollution (Broderick, 2008) AM for wetlands (Ignar and Grygoruk, 2015) and AM for river flows (Summers, Holman and Grabowski, 2015). Despite their merits, all of these are siloed approaches when really what's required is an integrated adaptive management approach for whole ecosystems.



Figure 1: Synergies between challenges for PAs, drivers of biodiversity loss and pressures on water quality including addressing diffuse pollution.

CONCLUSIONS

Urgent action is required to address the drivers of biodiversity loss (Tickner *et al.*, 2020). Integrating the management of PAs and water quality in the RBMPs has significant advantages

and is a measure that can and should be adopted, to not only decrease biodiversity loss and improve water quality, but to deliver for climate adaptation and for the SDGs.

Acknowledgements: The authors acknowledge the financial support provided by the Atlantic Technological University.

REFERENCES

Antwi, S.H. *et al.* (2021) ‘River Basin Management Planning in the Republic of Ireland: Past, Present and the Future’, *Water*, 13(15), p. 2074. Available at: <https://doi.org/10.3390/w13152074>.

Bieroza, M.Z., Bol, R. and Glendell, M. (2021) ‘What is the deal with the Green Deal: Will the new strategy help to improve European freshwater quality beyond the Water Framework Directive?’, *Science of The Total Environment*, 791, p. 148080. Available at: <https://doi.org/10.1016/j.scitotenv.2021.148080>.

Boezeman, D., Wiering, M. and Crabbé, A. (2020) ‘Agricultural Diffuse Pollution and the EU Water Framework Directive: Problems and Progress in Governance’, *Water*, 12, p. 2590. Available at: <https://doi.org/10.3390/w12092590>.

Broderick, K. (2008) ‘Adaptive Management for Water Quality Improvement in the Great Barrier Reef Catchments: Learning on the Edge’, *Geographical Research*, 46(3), pp. 303–313. Available at: <https://doi.org/10.1111/j.1745-5871.2008.00525.x>.

Brondízio, E. *et al.* (2021) *Global assessment report on biodiversity and ecosystem services of the Intergovernmental Science-Policy Platform on Biodiversity and Ecosystem Services*. Available at: <https://doi.org/10.5281/zenodo.383188>.

Canessa, S. *et al.* (2016) ‘Adaptive management for improving species conservation across the captive-wild spectrum’, *Biological Conservation*, 199, pp. 123–131. Available at: <https://doi.org/10.1016/j.biocon.2016.04.026>.

Carvalho, L. *et al.* (2019) ‘Protecting and restoring Europe’s waters: An analysis of the future development needs of the Water Framework Directive’, *Science of The Total Environment*, 658, pp. 1228–1238. Available at: <https://doi.org/10.1016/j.scitotenv.2018.12.255>.

Collins, A.L. *et al.* (2016) ‘Tackling agricultural diffuse pollution: What might uptake of farmer-preferred measures deliver for emissions to water and air?’, *Science of The Total Environment*, 547, pp. 269–281. Available at: <https://doi.org/10.1016/j.scitotenv.2015.12.130>.

Eberhard, R. *et al.* (2009) ‘Adaptive management for water quality planning - From theory to practice’, *Marine and Freshwater Research - MAR FRESHWATER RES*, 60. Available at: <https://doi.org/10.1071/MF08347>.

EEA (2015) *Biodiversity Briefing*. Available at: <https://www.eea.europa.eu/soer/2015/europe/biodiversity> (Accessed: 25 June 2022).

EEA (2018) *European waters -- Assessment of status and pressures 2018* — European Environment Agency. Available at: <https://www.eea.europa.eu/publications/state-of-water> (Accessed: 13 June 2022).

EEA (2019) *The European environment — state and outlook 2020 — Knowledge for transition to a sustainable Europe*. Available at: <https://www.eea.europa.eu/soer/publications/soer-2020> (Accessed: 14 June 2022).

European Commission (2022) *Natura 2000 - Environment*. Available at: https://ec.europa.eu/environment/nature/natura2000/index_en.htm (Accessed: 28 June 2022).

Graversgaard, M. *et al.* (2017) ‘Stakeholder Engagement and Knowledge Co-Creation in Water Planning: Can Public Participation Increase Cost-Effectiveness?’, *Water*, 9, p. 191. Available at: <https://doi.org/10.3390/w9030191>.

- Graversgaard, M. *et al.* (2018) ‘Opportunities and Barriers for Water Co-Governance—A Critical Analysis of Seven Cases of Diffuse Water Pollution from Agriculture in Europe, Australia and North America’, *Sustainability*, 10(5), p. 1634. Available at: <https://doi.org/10.3390/su10051634>.
- Harris, R. (2013) ‘Addressing Diffuse Pollution’, in: *Prince of Wales Food and Farming Summer School*, Organic Research Centre, Elm Farm, Newbury.
- Hendry, S. and Reeves, A. (2012) ‘The regulation of diffuse pollution in the European Union: science, governance and water resource management’, *International Journal of Rural Law and Policy* [Preprint]. Available at: <https://doi.org/10.5130/ijrlp.i1.2012.2699>.
- Hoffmann, S. (2022) ‘Challenges and opportunities of area-based conservation in reaching biodiversity and sustainability goals’, *Biodiversity and Conservation*, 31(2), pp. 325–352. Available at: <https://doi.org/10.1007/s10531-021-02340-2>.
- Ignar, S. and Grygoruk, M. (2015) ‘Wetlands and Water Framework Directive: Protection, Management and Climate Change’, in Stefan Ignar and Mateusz Grygoruk (eds) *Wetlands and Water Framework Directive: Protection, Management and Climate Change*. Cham: Springer International Publishing (GeoPlanet: Earth and Planetary Sciences), pp. 1–7. Available at: https://doi.org/10.1007/978-3-319-13764-3_1.
- Interreg Europe Policy Learning Platform (2020) *Good governance for biodiversity | Interreg Europe - Sharing solutions for better policy*. Available at: <https://www.interregeurope.eu/find-policy-solutions/policy-briefs/good-governance-for-biodiversity> (Accessed: 29 June 2022).
- Jacobsen, B.H., Anker, H.T. and Baaner, L. (2017) ‘Implementing the water framework directive in Denmark – Lessons on agricultural measures from a legal and regulatory perspective’, *Land Use Policy*, 67, pp. 98–106. Available at: <https://doi.org/10.1016/j.landusepol.2017.05.021>.
- Janauer, G.A., Albrecht, J. and Stratmann, L. (2015) ‘Synergies and Conflicts Between Water Framework Directive and Natura 2000: Legal Requirements, Technical Guidance and Experiences from Practice’, in S. Ignar and M. Grygoruk (eds) *Wetlands and Water Framework Directive: Protection, Management and Climate Change*. Cham: Springer International Publishing (GeoPlanet: Earth and Planetary Sciences), pp. 9–29. Available at: https://doi.org/10.1007/978-3-319-13764-3_2.
- Mazor, T. *et al.* (2018) ‘Global mismatch of policy and research on drivers of biodiversity loss’, *Nature Ecology & Evolution*, 2(7), pp. 1071–1074. Available at: <https://doi.org/10.1038/s41559-018-0563-x>.
- McCarthy, M.A. and Possingham, H.P. (2007) ‘Active Adaptive Management for Conservation’, *Conservation Biology*, 21(4), pp. 956–963.
- OECD (2017) *Diffuse Pollution, Degraded Waters: Emerging Policy Solutions | READ online, oecd-ilibrary.org*. Available at: https://read.oecd-ilibrary.org/environment/diffuse-pollution-degraded-waters_9789264269064-en (Accessed: 13 June 2022).
- Patterson, J.J., Smith, C. and Bellamy, J. (2013) ‘Understanding enabling capacities for managing the “wicked problem” of nonpoint source water pollution in catchments: A conceptual framework’, *Journal of Environmental Management*, 128, pp. 441–452. Available at: <https://doi.org/10.1016/j.jenvman.2013.05.033>.
- Pittock, J. *et al.* (2015) *Managing freshwater, river, wetland and estuarine protected areas*. ANU Press. Available at: <https://www.jstor.org/stable/j.ctt1657v5d.26>.
- Sharma, A. (2020) ‘The Wicked Problem of Diffuse Nutrient Pollution from Agriculture’, *Journal of Environmental Law*, 32(3), pp. 471–502. Available at: <https://doi.org/10.1093/jel/eqaa017>.
- Shin, Y.-J. *et al.* (2022) ‘Actions to halt biodiversity loss generally benefit the climate’, *Global Change Biology*, 28(9), pp. 2846–2874. Available at: <https://doi.org/10.1111/gcb.16109>.
- Söderberg, C. *et al.* (2021) ‘The link between collaborative governance design and markers of legitimacy: Comparing Swedish water- and large carnivore management’, *Environmental Policy and Governance*, 31(6), pp. 563–579. Available at: <https://doi.org/10.1002/eet.1958>.

- Summers, M.F., Holman, I.P. and Grabowski, R.C. (2015) 'Adaptive management of river flows in Europe: A transferable framework for implementation', *Journal of Hydrology*, 531, pp. 696–705. Available at: <https://doi.org/10.1016/j.jhydrol.2015.10.057>.
- Teurlinx, S. *et al.* (2019) 'Towards restoring urban waters: understanding the main pressures', *Current Opinion in Environmental Sustainability*, 36, pp. 49–58. Available at: <https://doi.org/10.1016/j.cosust.2018.10.011>.
- Thornton, J. *et al.* (2013) 'Eutrophication as a “wicked” problem', *Lakes & Reservoirs: Research & Management*, 18. Available at: <https://doi.org/10.1111/lre.12044>.
- Tickner, D. *et al.* (2020) 'Bending the Curve of Global Freshwater Biodiversity Loss: An Emergency Recovery Plan', *BioScience*, 70(4), pp. 330–342. Available at: <https://doi.org/10.1093/biosci/biaa002>.
- Voulvoulis, N., Arpon, K.D. and Giakoumis, T. (2017) 'The EU Water Framework Directive: From great expectations to problems with implementation', *Science of The Total Environment*, 575, pp. 358–366. Available at: <https://doi.org/10.1016/j.scitotenv.2016.09.228>.
- Wiering, M., Boezeman, D. and Crabbé, A. (2020) 'The Water Framework Directive and Agricultural Diffuse Pollution: Fighting a Running Battle?', *Water*, 12(5), p. 1447. Available at: <https://doi.org/10.3390/w12051447>.
- Williams-Subiza, E.A. and Epele, L.B. (2021) 'Drivers of biodiversity loss in freshwater environments: A bibliometric analysis of the recent literature', *Aquatic Conservation: Marine and Freshwater Ecosystems*, 31(9), pp. 2469–2480. Available at: <https://doi.org/10.1002/aqc.3627>.

COMPLIANCE CHECKING FOR MODELLED N AND P LOADS IN SURFACE WATERS AND GAP ANALYSIS FOR REACHING MSFD AND WFD TARGETS

Venohr Markus^{1*}, Nguyen Hong Hanh^{1,2}, Kunkel Ralf³ and Tetzlaff Björn³

¹. Leibniz Institute of Freshwater Ecology and Inland Fisheries, Department Ecohydrology and Biogeochemistry, Berlin, Germany

². Senckenberg Research Institute and Natural History Museum Frankfurt, Germany

³. Forschungszentrum Jülich, Agrosphere Institute (FZJ), 52425 Jülich, Germany

*Corresponding author (markus.venohr@igb-berlin.de)

ABSTRACT

Based on the pathway specific spatially-differentiated modelling of Total Nitrogen (TN) and Total Phosphorus (TP) emissions via diffuse pathways as well as from urban systems and point sources, the total nutrient emissions to surface waters were quantified. Subsequent in-water retention and transport in rivers towards the sea were modelled and validate against observed loads. Under considerations of current conditions and a reduction scenario, we determined the reduction need of loads and, via reverse modelling, of nutrient emissions to meet EU legislations such as the EU Water Framework Directive and the EU Marine Strategy Framework Directive (MSFD).

Under mean current conditions nutrient emissions into German surface waters amount to 475,000 t N/yr and 19,500 t P/yr. Of these, a mean of 28 % and 21 %, respectively, is retained in surface waters. The load comparison revealed a good statistical agreement without a pronounced tendency for a systematic bias between modelled and observed loads.

For recent conditions a TN reduction requirement of 12 % was found. Under the scenario of a fully implemented EU Nitrate Directive (EU-ND), the MSFD targets were largely achieved or reduction needs significantly reduced. For phosphorus, emissions need to be reduced by 33 %, however reduction needs show a different spatial pattern than such as of TN. While the TN reduction can largely be achieved through the implementation of the EU-ND, the management approaches for P and thus the achievement of the target are much more demanding.

Keywords: *nutrient emissions, stakeholder involvement, hydro economic modeling, environmental measures.*

1. INTRODUCTION

High nutrient emissions into groundwater and surface water continue to be a Europe-wide problem. For the effective implementation of the EU Nitrates Directive, the EC Water Framework Directive (WFD) and the EU Marine Strategy Framework Directive (MSFD), it is necessary to consider both the areas that contribute significantly to the total nutrient load in river basins and the corresponding nutrient emission pathways. Furthermore, it is indispensable to assess the extent to which the various legally enshrined mitigation measures can contribute

to achieving the environmental objectives. To this end, the AGRUM-DE project was initiated and funded with the close participation of all German federal states.

In AGRUM-DE, a nationwide model was developed to quantify nitrogen and phosphorus inputs to groundwater and surface waters with input pathway-related and regional differentiation, and to determine the need for action and possible action scenarios for all German river basins. The aim was to obtain harmonized input data for the model across Germany and to develop a common, closely coordinated approach for the status analysis and the need for action.

2. MATERIAL AND METHODS

We used the model network AGRUM-DE consisting of the individual models RAUMIS - mGROWA - DENUZ - WEKU - MEPhos - MONERIS (Gömann et al., 2020, Herrmann et al., 2015, Kunkel & Wendland, 1997, Wendland et al., 2004, Tetzlaff, 2006, Venohr et al., 2011, Nguyen and Venohr 2021) as a uniform methodology to predict nutrient emissions to surface waters via 12 different pathways using an area differentiated approach throughout Germany (Schmidt et al., 2022). Considered emission pathways were water erosion, wash-off, artificial drainage, groundwater, interflow, atmospheric deposition, municipal waste water treatment plants, industry, rainwater sewers, combined sewers overflows, cesspits and exfiltration from leaky sewage pipes. In-water retention and transport were modelled at the scale of hydrological sub-catchments according to Venohr et al. (2011) and Lemm et al (2021) considering surface water area distribution, runoff conditions and water temperature.

For the model application mean long-term run off from the years 1980-2010 were used, while for all other input parameters, e.g. nitrogen balances, atmospheric deposition, waste water treatment and collection recent data, mostly for the years 2013-2018, were considered.

Model results were validated against monitored runoff, N- and P- concentrations and loads in surface waters using the statistical validation criteria mean absolute deviation (MAD), regression coefficient (r^2), Nash-Sutcliffe model efficiency (NSE) and PBIAS.

Based on the current state set-up of the models the reduction needs of nutrient emission to reach the goals of the EU Water Framework Directive (WFD, 2000/60/EC, for TP) and the EU Marine Strategy Framework Directive (MSFD, Directive 2008/56/EC, for TN) were derived. Subsequently, the effects of the implementation of the EU Fertilizer Ordinance (EU-FO, EU 2019/1009) and the EU Nitrate Directive (EU-ND, 91/676/EEC) were modelled. Based on this reduced emission scenario, the remaining emission reduction need to meet the goals of the WFD and MSFD were quantified, again.

3. RESULTS AND DISCUSSIONS

Taking into account all diffuse and urban input pathways, the total inputs for the current conditions amount to 475,000 t N/yr and 19,500 t P/yr. The diffuse input pathways contribute a total of 80 % (TN) and 59 % (TP) to the total inputs. Assuming the reduction scenario, the total N emissions are reduced to 329,000 t N/yr, whereby the share of unchanged urban and point source emissions increases only relatively slightly to 29 %.

On average, 28 % (TN) and 21 % (TP) of the emitted nutrients are retained in surface waters. Retention varies depending on the distribution of water surface areas, runoff and water temperature. Thus, the highest percentage retention values are found in the tributaries in the

east of the North German Lowlands. The accumulative TN retention from input to seas can sometimes be well over 60 %.

By applying the in-water retention to the modelled emissions the loads in surface waters were determined. The validation of modelled against observed loads for the years 2010-2016 showed no significant bias (< 5%) and, with a MAD of 19 % (TN) / 23 % (TP) and a NSE of 1.0 (TN) / 0.98 (TP), a good agreement with the observed loads.

Under current conditions, the need for emission reduction to achieve the goals of WFD and MSFD amounts to 53,000 t N/yr (11 %) and 5,500 t P/yr (28 %), and is, for TN, mainly concentrated in the North German Lowlands. For phosphorus, the pattern is less clear and concentrates to areas with increased inputs or low runoff contributions (low dilution of emissions). Assuming the scenario conditions, the reduction need for nitrogen is reduced to 2,800 t N/yr or 1 %, leaving a reduction requirement only in the German part of the Oder catchment, some Baltic Sea direct catchments in Schleswig-Holstein and the German parts of the Meuse.

4. CONCLUSIONS

Reduction goals currently targeted by the EU-FO and EU-ND can at mid-term largely lead to the achievement of the MSFD objectives. For TP, a considerable input reduction has been achieved in recent decades through improved wastewater collection and treatment. A further reduction by 28 % to meet the WFD goals, as suggested by this study, will only be possible by additional measures also addressing diffuse emissions.

Acknowledgements: The authors acknowledge the grant provided by LAWA and the provisioning of data, knowledge and feedback from the federal states of Germany.

REFERENCES

- Gömann et al. (2020): <https://www.flussgebiete.nrw.de/regional-hoch-aufgeloeste-quantifizierung-der-diffusen-stickstoff-und-phosphoreintraege-ins-4994>.
- Herrmann et al. (2015): doi.org/10.1016/j.ejrh.2015.06.018
- Kunkel and Wendland (1997): <https://link.springer.com/content/pdf/10.1007/s002540050126.pdf>.
- Lemm et al (2021): DOI: 10.1111/gcb.15504
- Nguyen and Venohr 2021: doi.org/10.1007/s11356-021-12440-9
- Schmidt et al. (2022): Bestimmung der Nährstoffbelastung und des Handlungsbedarfs in den deutschen Flussgebieten. *Wasser und Abfall*, 24(4), 22-30.
- Tetzlaff (2006) <https://core.ac.uk/download/pdf/34935893.pdf>
- Schaap et al. (2018): https://www.umweltbundesamt.de/sites/default/files/medien/1410/publikationen/2018-10-17_texte_79-2018_pineti3.pdf.
- Venohr, M. et al. (2011): doi.org/10.1002/iroh.201111331.
- Wendland et al. (2004): DOI 10.1007/s00254-004-1013-4.

COUPLED MODELLING APPLICATION FOR CLIMATE CHANGE IMPACT ASSESSMENT IN THE NEMUNAS RIVER WATERSHED – CURONIAN LAGOON – BALTIC SEA CONTINUUM

Natalja Čerkasova^{1,4,*}, Georg Umgiesser^{1,2}, Ali Ertürk³, Rasa Idzelytė¹, Jovita Mėžinė¹

¹ Marine Research Institute, Klaipėda University, Klaipėda, Lithuania

² CNR — National Research Council of Italy, ISMAR — Institute of Marine Sciences, Venice, Italy

³ Department of Inland Water Resources and Management, Faculty of Aquatic Sciences, Istanbul University, Istanbul, Turkey

⁴ Texas A&M AgriLife Research, Blackland Research and Extension Center, Temple, Texas, USA

*Corresponding author (Corresponding author's e-mail)

ABSTRACT

We set-up a coupled hydrological-hydrodynamic modeling framework using available high-resolution data to study the climate change impact for river - lagoon - marine environment continuum. We used SWAT model to predict the changes in discharge, sediment and nutrient loads according to two climate change scenarios (RCP4.5 and RCP8.5). The SWAT model output were used to run hydrodynamic model SHYFEM to predict the changes in the Curonian Lagoon and the southeastern part of the Baltic Sea under the same future conditions.

Eutrophication is one of the top issues in the Baltic Sea and inland waters of its drainage basin. Initial results of this study showed that the implemented nutrient reduction measures will not lead to improvements of the system under the projected future climate conditions. We suggest the policymakers to initiate additional actions (crop and land use management, livestock production, water resource management, etc.) for diminishing these potential negative effects due to the extensive use of the natural resources.

Keywords: SWAT, SHYFEM, modelling, climate change, Curonian Lagoon.

1. INTRODUCTION

A variety of EU legislations (Nitrates Directive (ND, 1991/696/EC), Water Framework Directive (WFD, 2000/60/EC), Marine Strategy Framework Directive (MSFD, 2008/56/EC)) obliges the member states to implement management strategies in order to achieve good ecological and chemical status for all surface waters. Climate change and the adaptation to it is one of the most important issues for the planning and implementation of measures that are focused on nutrient input reduction in the rivers and, subsequently, to the coastal and marine environment. The objective of this study that was supported within a project “ECO-NEWS” is to predict the environmental changes in the Nemunas River watershed – Curonian Lagoon – Baltic Sea - Lithuanian coastal zone continuum, and possible impacts of these changes on the biosphere, using a set of state-of-the-art coupled hydrological, hydrodynamic, and water quality numerical models to quantify these changes. In this paper we report our achieved results of this ongoing study.

2. MATERIAL AND METHODS

Study site

The study area is located in the southeastern part of the Baltic Sea, comprising of the Nemunas River watershed, Curonian Lagoon, and an exclusive economic zone of the Republic of Lithuania (Figure 1). The Curonian Lagoon is the largest coastal lagoon in Europe, with an area of 1 578 km² and a drainage area of 100 458 km² (Čerkasova et al., 2016). The Nemunas River is a largest tributary of the Curonian Lagoon, which supplies about 98% of the total inflowing water (Jakimavičius, 2012). Eutrophication significantly affects the Curonian Lagoon and the Baltic Sea due to high amounts of nutrients what are transported through the Nemunas River, as a result, eutrophication still remains the major threat to the marine environment.

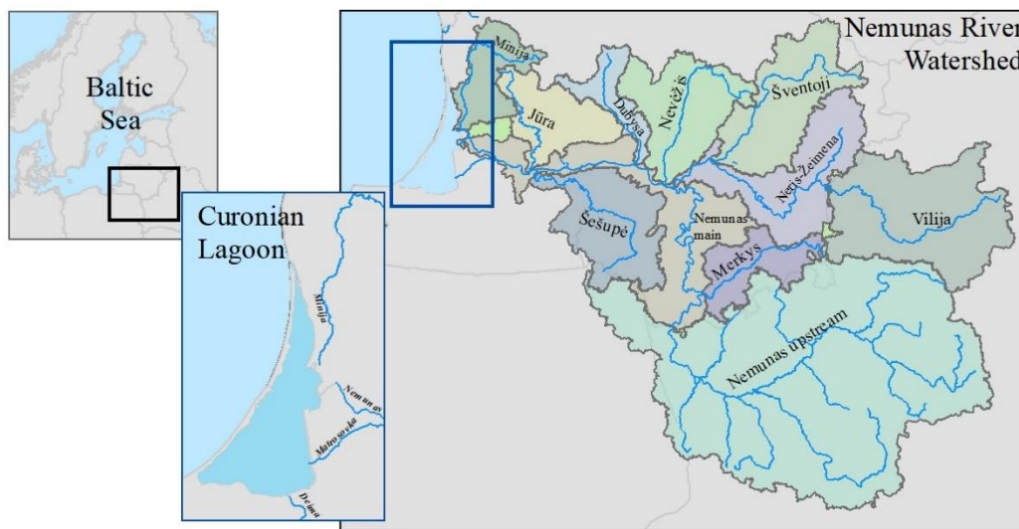


Figure1. Nemunas River watershed and Curonian Lagoon with respect to the Baltic Sea.

Model setup and Climate change scenarios

Data used for the hydrological model setup is described in our previous papers (the reader is referred to Čerkasova et al. (2021) for more details). To setup the hydrodynamic model for the Curonian Lagoon and the Baltic Sea the meteorological data from CORDEX (Coordinated Regional Downscaling Experiment) scenarios for Europe was used. The Rossby Centre regional climate model (RCA4) was chosen with the following four global climate models: EC-Earth (ICHEC), IPSL-CM5A-MR (IPSL), HadGEM2-ES (MOHC), and MPI-ESM-LR (MPI). The dataset covers historical period 1970-2005 and a period of 2006-2100 according to two Representative Concentration Pathway (RCP) scenarios: RCP4.5 and RCP8.5. Sea boundary conditions were obtained from SMHI (Swedish Meteorological and Hydrological Institute) for the same periods and the BIAS correction according to the monitoring data for the period 1993-2005 was performed.

Modelling systems coupling

A drainage basin model (SWAT – soil and water assessment tool) was used for modeling of the Nemunas River watershed. An open source hydrodynamic finite element model SHYFEM, which incorporates various options for eutrophication modelling as well, has been set up for the modeling of the Curonian Lagoon and the Baltic Sea. Models were linked through the water temperature and river discharge data. Additional outputs related to nutrient loads transported to

the Curonian Lagoon from the watershed were produced as well. The output of the SWAT model was used as boundary data in Nemunas and Minija entry points in the SHYFEM numerical grid. The linked modeling framework allows us to quantify the possible changes in flow, nutrient, and sediment delivery to the Curonian Lagoon. In addition, both models are transboundary, therefore the impact of the climate change to the lagoon and sea will be evaluated from all sources.

3. RESULTS AND DISCUSSIONS

The results of the coupled modelling system denote that during the winter season higher river water discharges in the lagoon are projected. This leads to a net nutrient load increase, which is associated with the ongoing practices of land use management, as well as increasing soil freezing-thawing cycles, having more liquid precipitation (rain) during the future winter seasons.

The increasing river discharges also lead to the modification of the water exchange regime in the study area. The changes indicate an increased exchange between the lagoon and the sea during winter, while it is lower during summer. The projected discharging river water load will impact the water residence time (WRT) in the lagoon by shortening it during winter, especially in the northern part (area above the Nemunas river, Fig.1), and increasing WRT during summer. Due to the increased water outflow from the lagoon to the Baltic Sea, the saltwater intrusions events from the sea into the lagoon is also projected to decrease, while the water temperature in the lagoon is expected to increase more steadily.

4. CONCLUSIONS

In light of the current climate change trends and projections for the southeastern Baltic Sea region, the efforts already set in motion for reducing the unfavorable impact on the biosphere might not be adequate. The policymakers must initiate actions, such as crop and land use management, livestock production management, water resource management, for diminishing these potential negative effects due to the extensive use of the natural resources, even though the implemented measures might not lead to instantaneous results. The end goal of this study is to provide the policymakers and authorities with projected scenarios of the climate change and quantify its effects on the water cycle and quality, as well as the entire biosphere in the Nemunas River - Curonian Lagoon - Baltic Sea continuum, and help to identify potential evidence-based solutions to deal with the emerging issues.

Acknowledgements: This study was conducted within a project “ECO-NEWS” that was funded by the Research Council of Lithuania (LMTLT), via. agreement No S-MIP-21-24.

REFERENCES

- Čerkasova N., Ertürk A., Zemlys P., Denisov V., & Umgiesser G. (2016). Curonian Lagoon drainage basin modelling and assessment of climate change impact, *Oceanologia*, 58, 2, 90-102.
- Čerkasova N., Ertürk A., Umgiesser G. (2021). Modelling framework for flow, sediments and nutrient loads in a large transboundary river watershed: A climate change impact assessment of the Nemunas River watershed, *Journal of Hydrology*
- Jakimavičius D. (2012). Changes of water balance elements of the Curonian lagoon and their forecast due to anthropogenic and natural factors (Ph.D. thesis), Kaunas University of Technology.

A STUDY ON THE SELECTION METHOD OF WATER CYCLE PRIORITY MANAGEMENT BASIN BASED ON HSPF

Jaemoon Kim¹, Jongseok Baek², Hyojeong Lee³, Jihyun Moon⁴ and Hyunsuk Shin^{5*}

¹. Green Land and Water Management Research Institute, Busan, Republic of Korea

². Korea Institute of Hydrological Survey, Goyang, Republic of Korea

³. Department of Civil and Environmental Engineering, Pusan national University, Busan, Republic of Korea

⁴. Department of Civil and Environmental Engineering, Pusan national University, Busan, Republic of Korea

⁵. Department of Civil and Environmental Engineering, Pusan national University, Busan, Republic of Korea

*Corresponding author (hsshin@pusan.ac.kr)

ABSTRACT

The concept of water cycle management is changing due to climate change and urbanization. Globally, water cycle management methods have been carried out by dividing urban and non-urban, but recently, research on approaching water cycle management methods at subwatershed units has emerged for integrated management. This study aims to conduct a study on the priority management method of water cycle in the concept of basin units. Based on the landuse provided by the Ministry of Environment, landuse changes by subwatershed in the watershed were analyzed, and water cycle priority management watershed was selected according to the urbanization rate. This result is believed that the priority management area extracted based on landuse will be used as basic data in performing water cycle management in the concept of the watershed.

Keywords: *Water cycle, HSPF, landuse, Priority management area*

1. INTRODUCTION

Due to the recent abnormal climate phenomenon caused by climate change, the frequency of storm and flood damage such as typhoons, torrential rains, and tsunamis is frequent, and the increase in impervious area is caused by the rapid increase of population in urban basins and continuous urbanization. In this study, A watershed water cycle priority management area was selected according to whether or not the impervious surface area increased or decreased according to the change in landuse.

2. MATERIAL AND METHODS

A study was conducted on the Nakdonggang River, South Korea. The Nakdonggang River basin is located at 127°29'~129°18' and 35°03'~37°13' South Korea, with a basin area of 23,702 km², accounting for about a quarter of the area in South Korea, with an average elevation of EL.291.2m and a basin average slope of 32.3%. An analysis was performed by subwatershed of the Nakdonggang River basin. The Nakdonggang River basin was built based on HSPF to analyze the change in water cycle according to the increase or decrease in the impervious surface area of the Nakdonggang River basin.

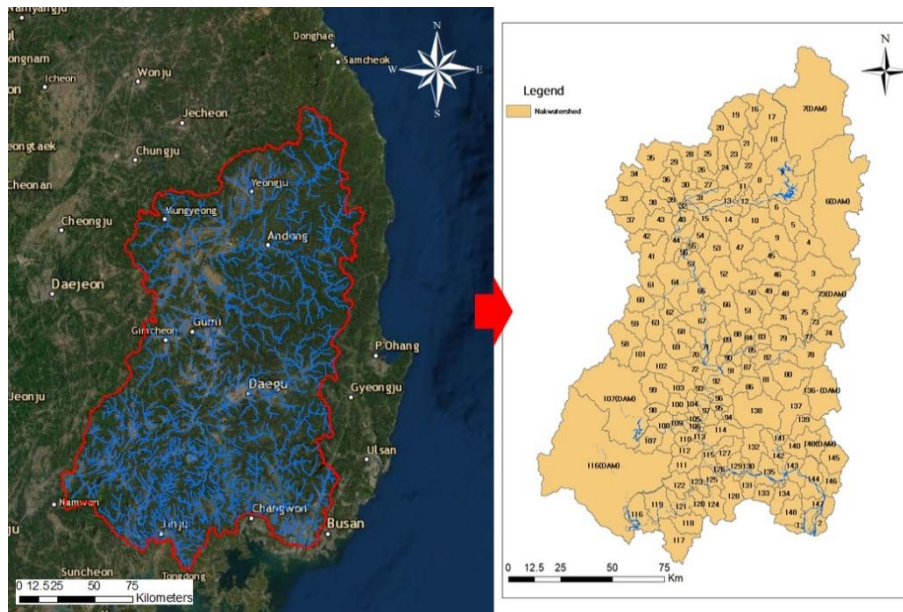


Figure1. Nakdonggang River Basin.

3. RESULTS AND DISCUSSIONS

The Nakdonggang River basin, which was built, was calibrated before analyzing the water cycle by applying the land use map in 1975 and the land use map in 2019. Major points were selected and calibration was performed. After completing the calibration, the rate of change in watershed water cycle was calculated.

Table 1. Table caption.

Observed Station	R2			
	Calibration		Verification	
Uiseong County (Pungjigyo Bridge)	0.90	Very good	0.91	Very good
.... Daegu City (Gangchanggyo Bridge)	0.91	Very good	0.92	Very good
Hapcheon County (Hwanggang Bridge)	0.91	Very good	0.92	Very good
Uiryong-gun (Jeongamgyo Bridge)	0.90	Very good	0.91	Very good
Haman-gun (Gyenae-ri)	0.92	Very good	0.91	Very good

4. CONCLUSIONS

In this study, the Nakdonggang River basin was divided subwatershed and the rate of change in water cycle according to land use was analyzed. As a result, changes were severe in the subwatershed where urbanization progressed a lot. It is believed that it will be used as basic data for selecting a water cycle priority management area according to the rate of change in water cycle.

Acknowledgements: This work was supported by the "Graduate school of Green Restoration specialization " of Korea Environmental Industry & Technology Institute grant funded by the Ministry of Environment, Republic of Korea.

REFERENCES

- Lee, K.S., Cung, E.S., Shim, M.J., Kim, Y.O. (2006). Sustainable Water Resources Planning to Prevent Streamflow Depletion in an Urban Watershed: 2. Application. *Journal of Korea Water Resources Association*, 39(11), 947-960.
- Choi, H.I., Park, S.Y., Song, J.H., Park, M.J. (2013). "Identification of Flood Risk Areas using a Multi-criteria Decision Making Method." *Journal of KOSHAM*, 13(2), 237-243.
- Kim, E.S., Sim, K.B., Jung, G.H., Nam, Y.K., Choi, H.I. (2014). Lake Environmental Risk Index using PSR Framework. *J.Korea Soc. Hazard Mitig*, 14(2), 317-326.
- Joo, H.J., Lee, M.J., Choi, C.H., Kim, S.J., Kim, H.S. (2018). A Study on the Selection of Representative Indicators of Flood Vulnerability Assessment. *J.Korean Soc. Hazard Mitig*, 18(6), 335-346.

A NOVEL DESIGN FOR SEDIMENTS' FILTRATION/ENTRAPMENT SYSTEM AT DECENTRALIZED INFILTRATION FACILITIES

*O. Dawoud*¹

¹ Istinje University, Faculty of Engineering and Natural Sciences, Istanbul, Turkey
osama.dawoud@istinje.edu.tr

ABSTRACT

The current study introduces a novel design of the filtration system that is used above the stormwater infiltration boreholes. The innovative design aims at overcoming the problems examined in conventional designs, which include the low capacity of the filtration system and the full clogging of the borehole entrance by sediments deposition. The new design employs a cylinder of porous concrete that is placed above the infiltration borehole in a single chamber. This chamber serves as a sand trap and a storage chamber at the same time. The model was tested in the lab using a down-scaled model. The system performance was observed for flow routing, sediments removal, and potential clogging. The new design was found to provide many significant advantages over the conventional one beside its high capacity. It showed a higher resiliency against shocks of high loads of sediments. It also creates a quasi-steady flow around the filtration cap which provides further opportunity for the sediments to safely settle in the retention infiltration tank. The system can be easily customized, and its performance is under high control. Results showed that the filtration efficiency was 94% of the applied influent which had a concentration 5.25 kg/m^3 for waterborne sediments. Given the wide range of amendments that can be applied to the tested model, the outcomes suggest a high potential of the novel design for enhancing capacity and durability of deep stormwater infiltration systems.

Keywords: *Waterborne sediments; sand entrapment; porous concrete; infiltration boreholes.*

Introduction

Stormwater harvesting using soak-away systems is one of the widely used stormwater harvesting techniques [1]–[3]. Such systems employ deep infiltration boreholes to facilitate stormwater percolation to deep aquifer if the upper layer has low permeability. Although these systems are widely used, clogging by sediments that are transported by runoff are often reported.

Thus, there is a need for a new system for sediments entrapment and filtration that is resilient to shock loads of high sediments and resistant to the hydrodynamic loads. Also, the system shall provide a high capacity of sediments filtration; and more importantly, the filter capacity shall be recoverable.

The current study proposed and tested a novel design for the sediments filtration system employing porous concrete as the filter media. The use of the porous concrete for stormwater infiltration applications has been well investigated by previous researchers [4]–[7]. The current study was formulated in accordance to the outcomes of these studies.

Design of the Model

The conventional sediments' entrapment system, which is currently used, is composed of two chambers, as show in *Fig. 1.* The sand-trap chamber is designed to allow for sedimentation of large waterborne particles. An overflow pipe transfer water from this chamber to the infiltration chamber where the water

percolates the infiltration borehole. The conventional design involves placing a geotextile fabric above the infiltration borehole to filter the undesired sediments. However, this system is prone to several problems. The turbulence in the sand-trap chamber reduces its effectiveness as large particles are lifted and moved to the infiltration chamber by the hydrodynamic forces. This causes the sediments to deposit above the infiltration borehole in the infiltration chamber. Given that the capacity of the geotextile filter area is very limited, the clogging of the filter is accelerated until the seepage fully stops.

The sketch on the right side of Fig. 1. shows the updated design which consists of a single chamber that is sized to serve both storage and sedimentation purposes. Cylindrical caps of porous concrete are located above the infiltration boreholes. These cylindrical caps work as filters for various types of sediments.

The proposed design was foreseen to overcome the problems associated with the conventional one by different mechanisms. The area of the active surface of the filter media is larger than its size in the conventional design which is limited to the opening cross-sectional area of the infiltration borehole. In addition, the direction of liquid flow into the filter media is perpendicular to the gravity force. This allows for sedimentation of large particles before reaching the filter media and they would not contribute the clogging of the filter. Furthermore, the capacity and performance of the filter can be easily customized by changing cylinder size and the characteristics of the porous concrete. It can be optimized according to the hydraulic characteristics of the inflow, sediments load, and the capacity of the infiltration borehole.

The system would exhibit better resiliency against high loading rates of sediments that cause sudden clogging of filter media. Such clogging would start at lower parts of the cylinder. This maintains the upper parts operating until intervention is conducted. Also, the proposed design is simpler and easier to be cleaned; and the capacity of the filtration system is recoverable by backwashing of the porous concrete.

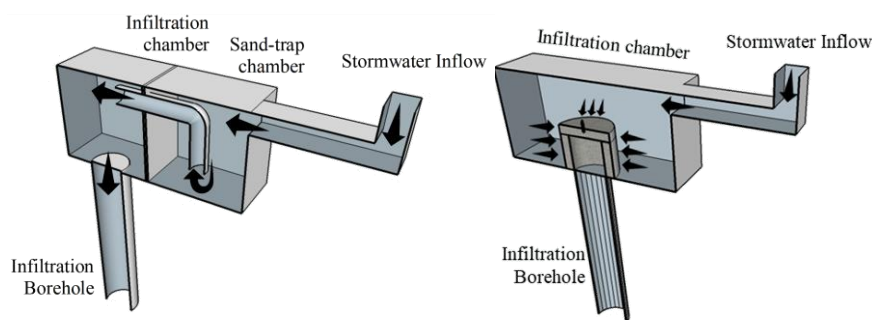


Fig. 1. The conventional sediments entrapment system above infiltration boreholes (LEFT), and the updated design of sediments entrapment/filtration system above infiltration boreholes (RIGHT).

The experimental setup used for verification of the proposed design involved two 1-m³ water tanks that are placed at different levels, as shown in Fig. 2. The upper tank is called the source tank and it contained the water that was contaminated with sediments. This tank is drained through a 4-inch pipe to the lower tank. The drainage pipe represents the stormwater inflow pipe as proposed for the new system in Fig. 2. The lower tank had a drainage pipe fitted in the center of the base of the tank. The two tanks at their original status has the same orifice characteristics.

A hollow cylinder of porous concrete that is 40 cm in outer diameter, 10 cm in thickness, and 30 cm in height was prepared of porous concrete. The hollow cylinder was covered by a 10 cm cap, making the whole height of the filter 40 cm. The porous concrete was prepared according to **Error! Reference source not found.**

The permeability of the concrete that was used for the test was tested using the Standard Test Method for Permeability of Granular Soils (Constant Head) [8]. Result showed the porous concrete had a hydraulic conductivity of 8.9 mm/s.

The setup was tested for two runs. In the first run, the upper tank was filled with 1-m³ of clean water that is free from sediments. Then it was drained into the lower tank where the filter cylinder is located. The depth in both tanks was monitored and recorded every 1 minute. This test was conducted to identify the reference behavior of the system and the original pattern of the routed outflow.

For the second run of the test, the upper tank was filled with water of a sediments content of 30 kg/m³. The sediments used for the test were acquired from the deposited soil at Asqula Infiltration Basin in

Gaza Strip, Palestine. This was conducted due to the limited information available on the waterborne sediments in Gaza Strip. The soil sample acquired from the infiltration basin is believed to represent the characteristics of the sediments transported by runoff in Gaza Strip. Size gradation was acquired by sieve analysis and hydrometer analysis as shown in Fig. 3. Analysis shows that 56.1% of the sediments were fines. Also, it was found that the organic matter in the sediments was 6% by mass. The contaminated water was drained to the lower tank while manually agitating the water the upper tank. The effluent from the upper and the lower tanks was sampled every 1 minute. These water samples were analyzed for total suspended solids (TSS). Also, the change of water depth by time was recorded every minute.

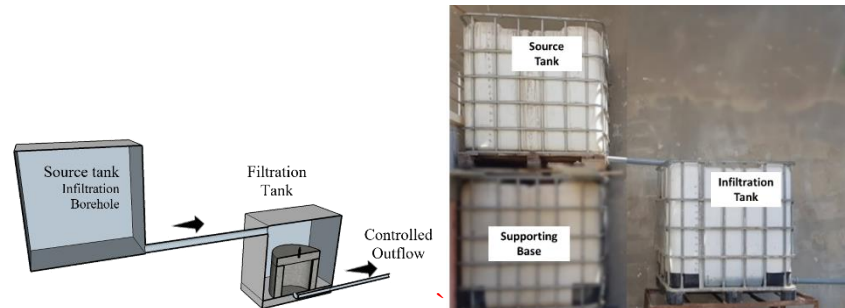


Fig. 2. Implementation of the experiment in the lab: Illustration sketch (Left); Lab setup of the experiment (Right).

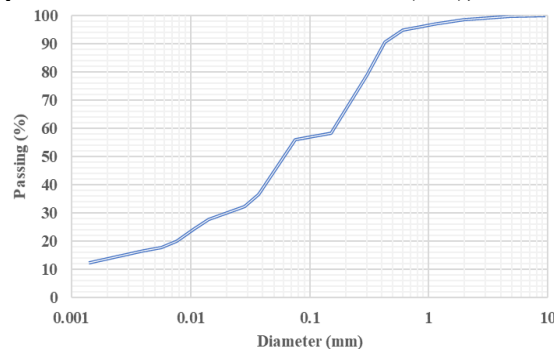


Fig. 3. Size gradation of the sediments used for the experiment

Table 1. The corresponding component weights for one cubic meter of porous concrete

Component	Content
Course Aggregates (16-20 mm)	800 kg/m ³
Course Aggregates (5-10 mm)	800 kg/m ³
Fine aggregates (Silica Sand - Class D)	320 kg/m ³
Portland Cement	400 kg/m ³
Water	160 Litre/m ³
Admixtures	2.5 Litre/m ³

Results

The first run of the test showed that using the porous concrete filter has exhibited a routing effect to the outflow pattern in the lower tank, as shown in Fig. 4. This routing of the inflow would not be a problem since the rate of water percolation into the infiltration borehole, which is considerably less than the rate of inflow that the infiltration chamber receives. This in fact is beneficial to the system performance as the water is retained around the filter cylinder which allows for sediments to settle down before they reach the filter media.

The second run showed a different behavior. As expected, the storage rate increased because the permeability of the filter media decreased by time. It peaked after the 6th minute as 46 cm compared to the 35 cm peak that was noticed when the clean water was used, as shown in **Error! Reference source not found.**

During the second run, partial clogging of the filter was noticed. After the 12th minute, the water level in the lower tank seems to constant at 20 cm. In fact, the flow continued in a rate that could not be visually distinguished. However, the water was totally drained after 6 hrs.

The sediments load in the effluent from the upper tank and the lower tank was calculated from the TSS analysis and the flow rate that was calculated for each tank. The time changes in the sediments load are shown in *Fig. 5*. The effluent from the upper tank carried a sediments load that was not constant. This can be ascribed to the manual agitation method that was applied. Also, the sediments differential settling could be another factor that caused this pattern. The total mass that was transferred from the upper tank to the lower one was calculated as 25.23 kg. This indicates that 4.77 kg settled in the upper tank and were not transported to the lower tank. The overall mass that appeared in the effluent was calculated as 1.62 kg. This indicates that the system was sufficient to remove 94% of the sediments that appeared in the influent. The maximum concentration of the sediments that was observed in the effluent was 0.523 kg/m³ compared to the maximum 5.25 kg/m³ that was recorded in the influent.

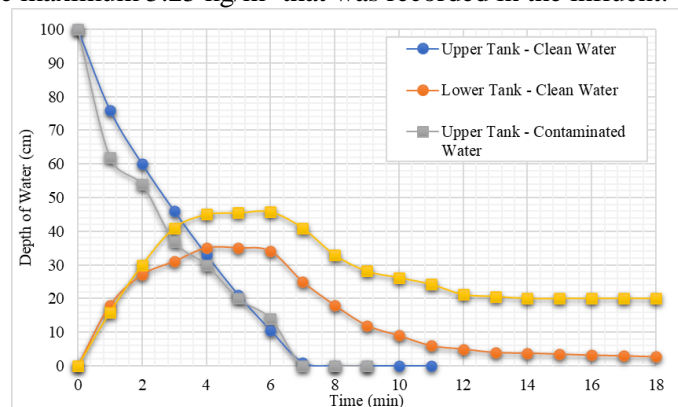


Fig. 4. Outflow rates from upper tank and lower tanks for the two runs of the test: clean water (circles), and contaminated water (squares)

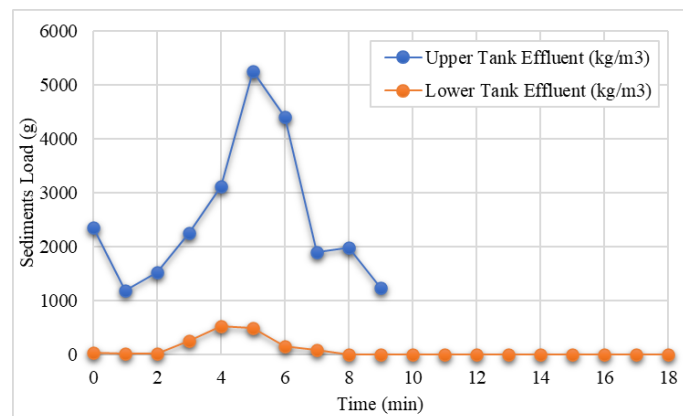


Fig. 5. The sediments load received by the infiltration chamber in comparison to the sediments load in the effluent

Discussion

The hydraulic behavior of the new design is governed by the characteristics of the porous concrete, the geometric design of the chamber, the geometric design of the filtration cylinder, and the capacity of the infiltration borehole. Thus, this hydraulic behavior can be easily adapted to the hydrological conditions of any site.

The designed system showed that clogging occurred at some point that reduced the flow rate through the cylinder. At the end of the observation period, the depth of water was 20.5 cm. This means that the clogging was concentrated at that depth. This can be ascribed to the settling of the sediments during the test, which generated a differential profile of sediments concentration that increases by depth. In fact,

this behavior of the clogging makes the design more resilient to shock loads. The same settling of sediments in conventional designs is sufficient to cause clogging.

The design was tested under an extreme condition of sediments load. However, the removal efficiency was relatively high. Sediments breakthrough was of fine sediments only. Relying on the size gradation of the sediments (See Figure 4), and the overall ratio of sediments removal (See Figure 6). It can be concluded that 90.4% of the fine sediments were removed by the system. However, this percentage can be enhanced applying some amendments to the design of the cylindrical filter and the materials used for constructing it.

Conclusions

The experiment conducted in the current study showed that the new design of the sediments filtration system has a good potential alternative for the conventional design. It offers several privileges that facilitate the control of the water quality that reaches the aquifer. It has a higher filtration capacity and offer more durability and resiliency to shock loads. Future studies could enhance the understanding and optimization of the system by investigation of the three-dimensional hydraulic behavior of water in the chamber would help optimizing the design standards of the chamber. Also, detailed design of the backwash system and assessment of the recovered capacity are required. Amendment of the porous concrete to enhance its capability for adsorption of heavy metals and other contaminants would be highly demanded. Future research might include the numerical modeling of the system hydraulics and the sediments entrapment/sedimentation.

References

- [1] C. Martin, Y. Ruperd, and M. Legret, "Urban stormwater drainage management: The development of a multicriteria decision aid approach for best management practices," *Eur. J. Oper. Res.*, vol. 181, no. 1, pp. 338–349, Aug. 2007, doi: 10.1016/j.ejor.2006.06.019.
- [2] M. Roldin, L. Locatelli, O. Mark, P. S. Mikkelsen, and P. J. Binning, "A simplified model of soakaway infiltration interaction with a shallow groundwater table," *J. Hydrol.*, vol. 497, pp. 165–175, Aug. 2013, doi: 10.1016/j.jhydrol.2013.06.005.
- [3] C. Saraswat, P. Kumar, and B. K. Mishra, "Assessment of stormwater runoff management practices and governance under climate change and urbanization: An analysis of Bangkok, Hanoi and Tokyo," *Environ. Sci. Policy*, vol. 64, pp. 101–117, Oct. 2016, doi: 10.1016/j.envsci.2016.06.018.
- [4] L. Chu and T. F. Fwa, "Evaluation of surface infiltration performance of permeable pavements," *J. Environ. Manage.*, vol. 238, pp. 136–143, May 2019, doi: 10.1016/j.jenvman.2019.02.119.
- [5] N. Xie, M. Akin, and X. Shi, "Permeable concrete pavements: A review of environmental benefits and durability," *J. Clean. Prod.*, vol. 210, pp. 1605–1621, Feb. 2019, doi: 10.1016/j.jclepro.2018.11.134.
- [6] M. B. Chopra, E. Stuart, and M. P. Wanielista, "Pervious pavement systems in Florida - Research results," in *Low Impact Development 2010: Redefining Water in the City - Proceedings of the 2010 International Low Impact Development Conference*, 2010, pp. 193–206. doi: 10.1061/41099(367)18.
- [7] Coughlin J. Patrick, Campbell Chelsea D., and Mays David C., "Infiltration and Clogging by Sand and Clay in a Pervious Concrete Pavement System," *J. Hydrol. Eng.*, vol. 17, no. 1, pp. 68–73, Jan. 2012, doi: 10.1061/(ASCE)HE.1943-5584.0000424.
- [8] ASTM D2434-68, "Test Method for Permeability of Granular Soils (Constant Head)," ASTM International, 2006. doi: 10.1520/D2434-68R06.

THE CHARACTERISTICS OF DISTRIBUTION AND ENVIRONMENTAL FACTOR OF VEGETATION IN WESTERN AND SOUTHERN COAST IN KOREA

Ji-won Park¹, Eui-joo Kim¹, Jung-Min Lee¹, Yoon-seo Kim¹, Jae-hoon Park¹, Se-hee Kim¹, and Young-han You^{1*}

¹. Department of biological science, Kongju National University, Gongju 32588, Republic of Korea

*Corresponding author (youeco21@kongju.ac.kr)

ABSTRACT

Coastal littoral is known to be strongly correlated to vegetation patterns through a complex interplay of biological and physical processes. In particular, the west and south coasts in Korea are very close to the coastline and have a gentle slope, forming a large area of coastal littoral. In order to clarify the distribution characteristics and current status of the salt marshes in coastal salt marshes on the west and south coasts of Korea, the vegetation and flora of the coastal salt marshes, environmental factors, and physical distribution were investigated. As a result of this study, The halophyte community distributed in the coastal dune is far from the coastline, Soil composition is made of sand, and tidal salt marshes are distributed in areas close to the coastline or inside the high tide line and The percentage of clay soils with poor drainage was high. Therefore, it can be seen that the inundation effect of soil composition and seawater affects the distribution of halophyte community in the western and southern coasts in Korea.

Therefore, It is judged that the coastal ecosystem needs a management strategy for elements that interfere with the natural flow of water through restoration, such as removal of estuary dams, which have a great influence on these environmental factors.

Keywords: *littoral, halophyte, coastal, salt marsh, sand dune.*

1. INTRODUCTION

Korea is a peninsula surrounded by sea on three sides and has a wide coastline, and the western and southern coasts are very difficult to enter and have a gentle slope, forming a wide coastal ecosystem (Shim et al., 2009; Lee et al., 2009). Littoral Zone is located between high tide and low tide due to tidal waves and refers to an area that is periodically affected by seawater (Olowokudejo and Oyebanji, 2016), and is an ecological Ecotone that transitions from a marine ecosystem to a terrestrial ecosystem (Zohary and Gasith, 2014) has a unique composition of plant species that is different from that of terrestrial ecosystems (Smith and Smith, 2001) and inherently high biodiversity (Wetzel, 2001)

Littoral zone ecosystems have been severely fragmented or destroyed as a result of natural factors such as environmental changes and natural disasters caused by climate change and human activities such as urbanization, commercialization and tourism (Gedan et al., 2009). As

a result, the current coastal plant ecosystem is under potential threat, and studying the effects of various environmental factors on plant species is important to determine how disturbances and environmental changes affect plant species (Fenu et al., 2013). The purpose of this study is to investigate the diversity and distribution characteristics of plant communities in the plant societies that develop in coastal ecosystems along the west and south coasts of Korea, and to use them as basic data for conservation and restoration.

2. MATERIAL AND METHODS

Study site overview

The western and southern coasts of Korea have large tidal differences and gentle slopes, forming a wide coastal ecosystem equivalent to 2.7% of the country. In addition, as an Ecotone that connects the inland and marine ecosystems, it not only serves as a buffer zone with functions such as charging surface water or groundwater, controlling soil erosion and sedimentation, and purifying pollutants, but also storing and supplying nutrients to various living organisms. It is an ecosystem inhabited by species (Han, 2008). In this study, from May 2019 to August 2019, field surveys were conducted on salt marshes along the coast with a radius of 500 m centered on 48 vertex coordinates distributed in the west and south coasts (Figure. 1).

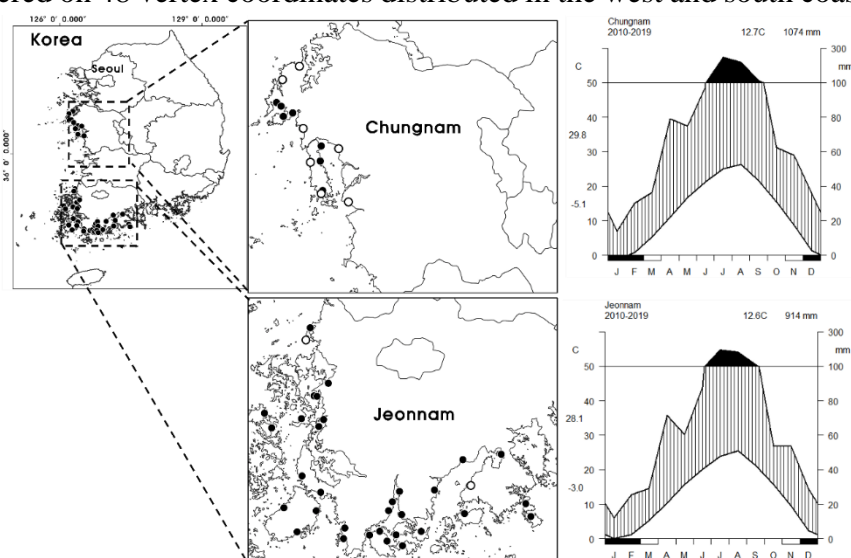


Figure1. Location of 48 investigated areas and climate diagram in west and south coasts in Korea.

Vegetation survey

This survey was conducted during the summer season, when plant growth is most prosperous, from May to August 2019, and field surveys were conducted once or twice at each survey point. For the vegetation survey of coastal salt marshes, a 1m×1m rectangle was installed for each colony in the entire survey area, and a plant sociological survey was conducted by Braun-blanquet's dominance map for each constituent species (Braun-blanquet, 1964)

Environmental factor investigation

In order to measure the soil environment of the plant community in the investigation area, electrical conductivity, soil texture, soil moisture content, and pH were measured at the center point of the square area during field investigation. Soil texture was classified into sand, clay, gravel, and bedrock, and the ratio of each soil was classified according to the soil ratio criteria

of Koo (2009) according to the type of habitat. A soil moisture meter (DEMETRA BAKELITE SOIL TESTER) was used. In order to understand the physical distribution of plant communities, the distance between the coastline and the center point of the plant community was calculated using the geographic information program using the national single coastline shape file using the coastline DEM information of the Ministry of Oceans and Fisheries.

3. RESULTS AND DISCUSSIONS

Horizontal distribution of plant communities and vegetation

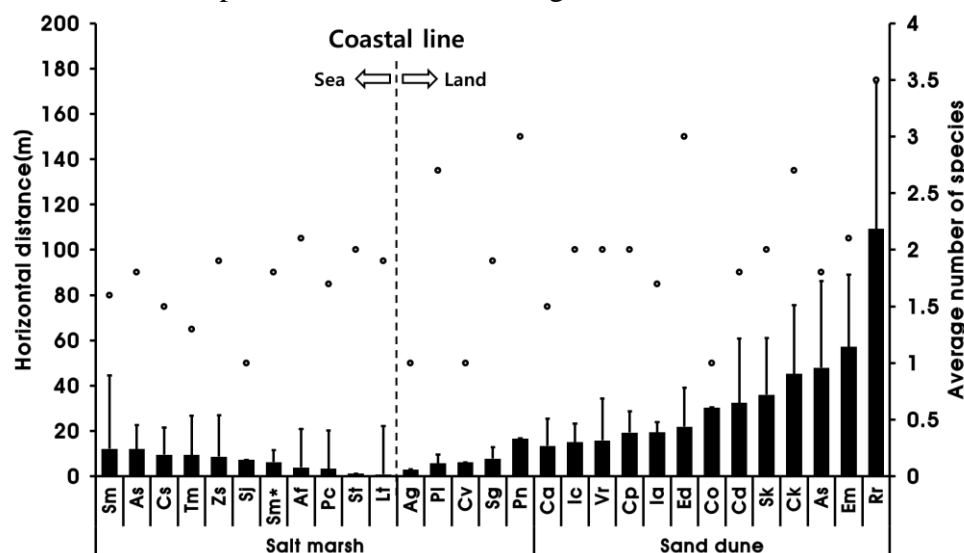


Figure2. Horizontal distance of littoral vegetation and average number of species.

*Acronyms: Sm: *Suaeda maritima* community, As: *Artemisia scoparia* community, Cs: *Corispermum stauntonii* community, Tm: *Triglochin maritimum* community, Zs: *Zoysia sinica* community, Sj: *Suaeda japonica* community, Sm*: *Suaeda malacosperma* Af: *Artemisia fukudo* community, Pc: *Phragmites communis* community, St: *Scirpus triqueter* community, Lt: *Limonium tetragonum* community, Ag: *Atriplex gmelinii* community, Pl: *Phacelurus latifolius*, : Ca: *Calystegia soldanella* community, Ic: *Imperata cylindrica* community, Vr: *Vitex rotundifolia* community, Cp: *Carex pumila* communitiy, Ia: *Ischaemum antheophoroides* community, Ed: *Elymus dahuricus* community Co: *Corispermum stauntonii* community Cd: *Cynodon dactylon* community, Sk: *Salsola komarovii* community, Ck: *Carex kobomugi* community, As: *Argusia sibirica* community, Em: *Elymus mollis* community, Rr: *Rosa rugosa* community.

Table1. Area of halophyte communities.

Habitat	Community name	Area(m ²)
Salt marsh	<i>Phragmites communis</i> community	88,064.3
	<i>Zoysia sinica</i> community	22,639.4
	<i>Suaeda maritima</i> community	21,886.9
	<i>Limonium tetragonum</i> community	5,189.3
	<i>Carex scabrifolia</i> community	3,318.5

	<i>Artemisia fukudo</i> community	3,158.1
	<i>Triglochin maritimum</i> community	1,715.6
	<i>Suaeda japonica</i> community	523.8
	<i>Suaeda malacosperma</i> community	280.4
	<i>Artemisia scoparia</i> community	198.0
	<i>Suaeda glauca</i> community	195.6
	<i>Puccinellia nipponica</i> community	140.1
	<i>Atriplex gmelinii</i> community	137.1
	<i>Phacelurus latifolius</i> community	136.9
	<i>Scirpus triqueter</i> community	58.4
	<i>Chenopodium virgatum</i> community	45.8
Sand dune	<i>Elymus mollis</i> community	18,117.2
	<i>Vitex rotundifolia</i> community	2,073.6
	<i>Rosa rugosa</i> community	1,816.1
	<i>Argusia sibirica</i> community	899.4
	<i>Ischaemum antheophoroides</i> community	761.1
	<i>Calystegia soldanella</i> community	663.1
	<i>Salsola komarovii</i> community	567.9
	<i>Carex pumila</i> community	552.1
	<i>Carex kobomugi</i> community	528.4
	<i>Elymus dahuricus</i> community	394.9
	<i>Imperata cylindrica</i> community	203.4
	<i>Cynodon dactylon</i> community	162.3
	<i>Corispermum stauntonii</i> community	34.1

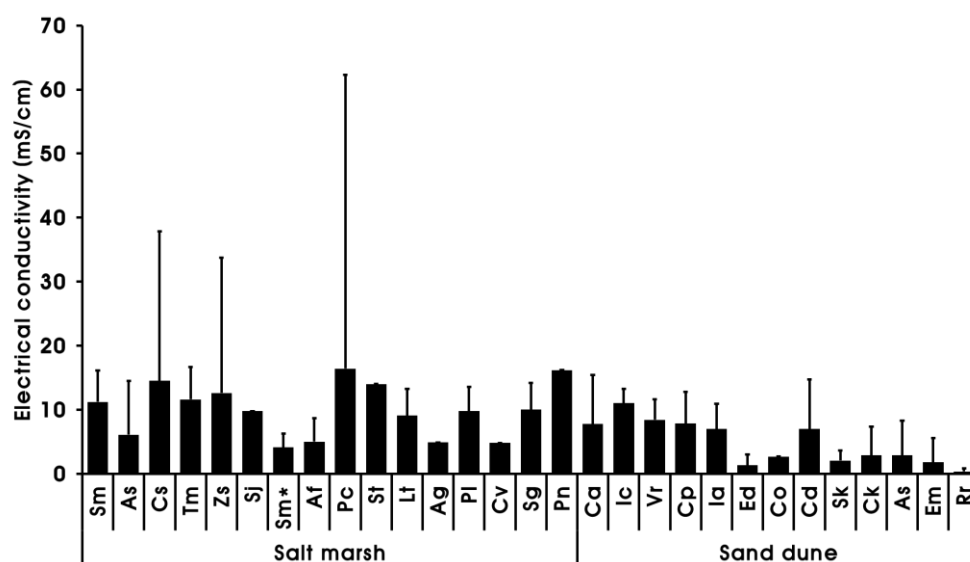


Figure3. Electrical conductivity of dominant halophyte community.

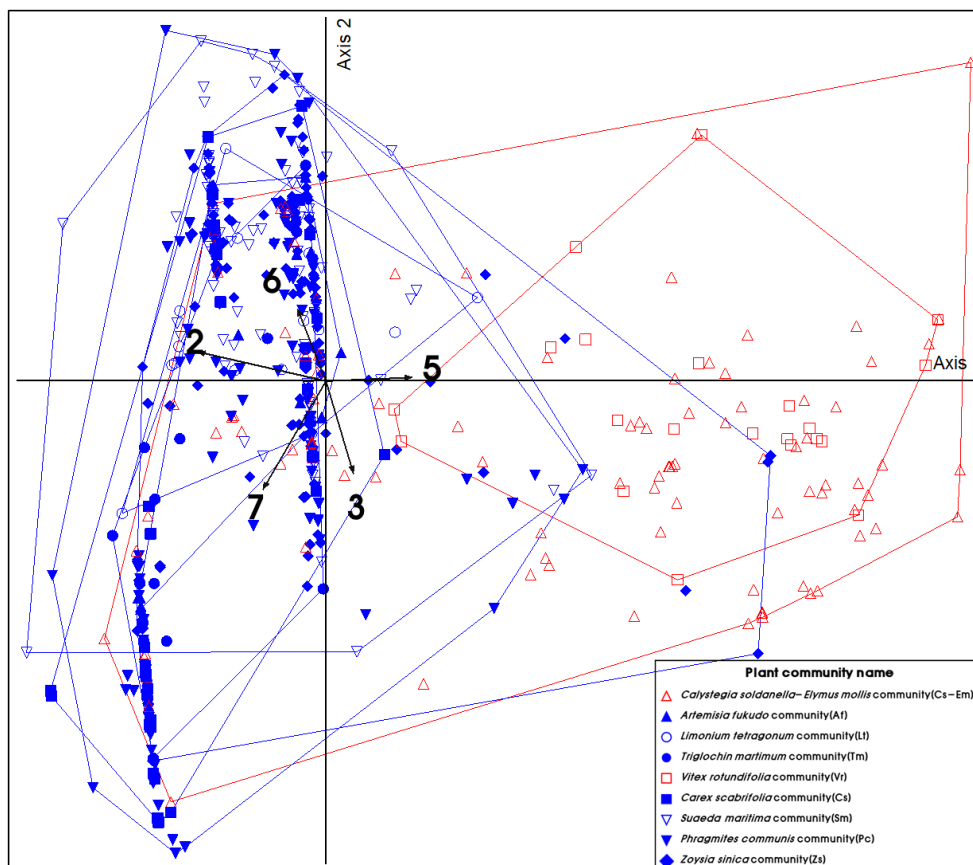


Figure 4. CCA ordination biplot of importance value and 8 environmental variables in 597 stands which are classified by plant community. The arrows on graph mean significant environmental variables which are influencing on stands

* Characteristics: 1: Electrical conductivity, 2: Soil moisture content, 3: pH, 4: Horizontal distance to the sea, 5: Sand(%), 6: Grave(%), 7: Clay(%), 8: Bedrock(%)

* Red color: Salt marsh community, Blue color: sand dune community

4. CONCLUSIONS

When examining the diversity of plant communities and species composition according to the horizontal distance from the shoreline, focusing on a single community, the average number of species appeared higher in the sand dune area as the plant communities distributed farther inland from the shoreline. On the other hand, in the case of plant communities distributed close to the ocean or flooded at high tide, it was confirmed that the average number of species was relatively lower than that of plant communities distributed inland.

It is judged that only plant species with high salinity concentration and resistance to inundation effects due to periodic tides are distributed due to the interaction with environmental factors, and as a result, a single colony with low species composition appears (Emery et al., 2001; Pennings and Moore, 2001).

In the case of the *Phragmites communis* community, the average horizontal distribution is located closer to the inland, but it has an advantage over competition with other plant species due to population expansion through asexual reproduction such as underground and a wide growing environment (Hong and Kim, 2012; 2014). In addition, when viewed from previous studies that ground and underground diameters make a high contribution to saline habitats such as salt marshes and brackish waters, the high height and population expansion of reeds inhibited

the growth and growth of other plant species, resulting in a low average number of species. is considered to have appeared (Burdick et al., 2001; Bart and Hartman, 2002).

Acknowledgements: This work was supported by Korea Environmental Industry & Technology Institute (KEITI) through Wetland Ecosystem Value Evaluation and Carbon Absorption Value Promotion Technology Development Project, funded by Korea Ministry of Environment (MOE)(2022003630003)

REFERENCES

- Bart, D., & Hartman, J. (2002). Constraints on the establishment of *Phragmites australis* in a New Jersey salt marsh. *Wetlands*, 22, 201-213.
- Braun-Blanquet, J. (1964). *Pflanzensoziologie. Grundzuge der Vegetationskunde*. Springer-Verlag, Wien. New York.
- Burdick, D.m., Buchsbaum, R., & Holt, E. (2001). Variation in soil salinity associated with expansion of *Phragmites australis* in salt marshes. *Environmental and Experimental Botany*, 46(3), 247-261.
- Emery, N.C., Ewanchuk, P.J., & Bertness, M.D. (2001). Competition and salt-marsh plant zonation: stress tolerators may be dominant competitors, *Ecology*, 82(9), 2471-2485.
- Fenu, G., Garboni, M., Acosta, A. & Bacchetta, G. (2013.) Environmental factors influencing coastal vegetation pattern: new insights from the Mediterranean basin, *Folica Geobo.* 48, 493-508.
- Gedan, K.B., Silliman, B.R., & Bertness, M.D. (2009). Centuries of human-driven change in salt marsh ecosystems, *annu, Rev, Marine Sci.* 1, 117-141.
- Han, Y.U., (2008). The characteristics of halophyte vegetation of salt marshes in the Southern and Western coasts of Korea, Master's Thesis, Mokpo National University, Muan-gun, Korea.
- Hong, M.G., & Kim J.G., (2012). Growth characteristics of cutting culms sectioned at different positions from three reed populations. *J. of Korean Environmental Restoration Technology*, 15(1), 53-62.
- Hong, M.G., & Kim, J.G., (2014). Role and effects of winter buds and rhizome morphology on the survival and growth of common reed (*Phragmites australis*), *Paddy and Water Environment*, 12(Supp. 1), S203-2009
- Koo, B.H., (2009). *Wetland Ecology. Landscape*, Seoul,
- Lee, J.S., IIm, B.S., Myeong, H.H., Park, J.W., & Kim, H.S., (2009). Soil environment analysis and habitati of halophyte ofr restoration in the salt marshes of southern and western coasts of Korea, *Korean J. Plant Res.* 22(1), 102-110.
- Olowokudejo, J., & Oyebanji, O., (2016). Floral diversity of the littoral vegetation of Southeastern Nigeria. *International Journal of Biodiversity and Conservation* 8(12), 320-333.
- Pennings, S.C., & Moore, D.J., (2001). Zonation of shrubs in wester Atlantic salt marshes, *Oecologia*, 126, pp. 587-594.
- Shim, H.B., Cho, W.B., & Choi, B.H., (2009). Distribution of halophytes in coastal salt marsh and on sand dunes in Korea, *Korean J. Pl. Taxon.* 39(4), 264-276.
- Smith, R.I., & Smith, T.M., (2001). *Ecology and Field Biology*, 6th Benjamin Cummings Inc., New York.
- Waisel, Y., (1972). *Biology of halophyte*, Academic press, INC, [United kingdom] London, LTD.
- Zohary, T., & Gasith, A., (2014). The littoral zone. pp. 517-532. *Lake Kinneret*. Springer.

MONITORING AND MODELING

SYSTEMIC HYDRAULIC FRACTURING CHEMICAL RISK INDICATORS FOR ASSESSING RELATIVE HAZARD LEVELS TO WATER SUPPLY

Christopher Hill¹, Om Prakash Yadav², and Eakalak Khan^{3}*

¹. Civil, Construction and Environmental Engineering Dept., North Dakota State University, Fargo, ND, USA

². Industrial and Systems Engineering Dept., North Carolina A&T State University, Greensboro, NC, USA

³. Civil and Environmental Engineering and Construction Dept., University of Nevada, Las Vegas, NV, USA

*Corresponding author (eakalak.khan@unlv.edu)

ABSTRACT

Hydraulic fracturing (HF) is a disruptive technology that has unlocked a vast amount of hydrocarbon resources but presents risks to drinking water supply. There are research gaps in system dynamics related to HF chemical transparency, variety, and hazard levels. The aim of the study was to develop and apply a repeatable methodology for reporting relative HF chemical hazard levels to drinking water supply. New individual parameter and aggregated risk indicators with associated approaches are provided. Chemical mobility risk levels, based on octanol-water and organic carbon-water partition coefficient metrics, appear to have decreased but change in chemical toxicity has been limited. The aggregated metric indicates a 42.6% risk reduction between 2014 and 2020. Overall, the study reveals past progress and methods for fostering future improvements related to HF chemical stewardship.

Keywords: *chemical mobility; risk; unconventional oil and gas development; water contamination.*

DEVELOPMENT OF A MICROFLUIDIC SYSTEM FOR THE COLORIMETRIC DETECTION OF THE DIFFUSE POLLUTION OF PHOSPHATE IN FRESH WATER SYSTEMS

Rachel Bracker^{1,2}, Harry Beggy^{2,3}, Louis Free^{2,3}, Joyce O'Grady^{1,2}, Sean Power^{2,4}, Karen Daly⁵, Nigel Kent^{2,4},
Fiona Regan^{1,2*}, Blánaid White^{1,2}

1. Dublin City University, School of Chemical Sciences, Dublin 9, Ireland
2. Dublin City University, DCU Water Institute, Dublin 9, Ireland
3. Dublin City University, School of Electronic Engineering, Dublin 9, Ireland
4. Dublin City University, School of Mechanical and Manufacturing Engineering, Dublin 9, Ireland
5. Teagasc Food Research Centre, Johnstown Castle, Wexford, Ireland.

* Fiona Regan (fiona.regan@dcu.ie)

EXTENDED ABSTRACT

Low cost, reliable, and robust optical analysis systems for the detection of nutrients and pollution in water systems is a major area of focus in research today. A project working to enhance a previously demonstrated lab-on-a-disc centrifugal microfluidic system for the colorimetric detection of phosphate in freshwater will be discussed. The previous system utilized a horizontally based diode/photodiode combination for colorimetric detection of the analyte at 880 nm using the molybdenum blue method (O'Grady et al., 2021). While this system has obtained good sensitivity and decent customisability, it was subject to deformities and discrepancies on the edges of the disk caused during the manufacturing process. This new system will utilize a vertically based spectrometer which will eliminate the impact of these discrepancies caused during disk production and assembly. Results from preliminary studies demonstrating its response to the analyte phosphate as KH_2PO_4 will be presented and evaluated, along with studies into the reproducibility of the system and analytical performance criteria.

Keywords: *spectroscopy; microfluidics; colorimetric detection; environmental analysis; phosphate detection*

REFERENCES:

O'Grady, J., Kent N., Regan, F. (2021). Design, build and demonstration of a fast, reliable portable phosphate field analyser. *Case Stud. Chem. Environ. Eng.*, **4**, 100168

REFERENCES

- Arcy, B. D., Kim, L., & Maniquiz-redillas, M. (2018). *Wealth Creation without Pollution*.
- He, J., Valeo, C., Chu, A., & Neumann, N. F. (2011). Prediction of event-based stormwater runoff quantity and quality by ANNs developed using PMI-based input selection. *Journal of Hydrology*, 400(1–2), 10–23. <https://doi.org/10.1016/j.jhydrol.2011.01.024>
- Li, G., Xiong, J., Zhu, J., Liu, Y., & Dzakpasu, M. (2021). Design influence and evaluation model of bioretention in rainwater treatment: A review. *Science of the Total Environment*, 787(13), 147592. <https://doi.org/10.1016/j.scitotenv.2021.147592>
- Li, S., Kazemi, H., & Rockaway, T. D. (2019). Performance assessment of stormwater GI practices using artificial neural networks. *Science of the Total Environment*, 651, 2811–2819. <https://doi.org/10.1016/j.scitotenv.2018.10.155>
- Mai, Y., & Huang, G. (2021). Hydrology and rainfall runoff pollutant removal performance of biochar-amended bioretention facilities based on field-scale experiments in lateritic red soil regions. *Science of the Total Environment*, 761, 143252. <https://doi.org/10.1016/j.scitotenv.2020.143252>
- Riad, S., Mania, J., Bouchaou, L., & Najjar, Y. (2004). Rainfall-runoff model using an artificial neural network approach. *Mathematical and Computer Modelling*, 40(7–8), 839–846. <https://doi.org/10.1016/j.mcm.2004.10.012>
- Sungji, K., Jiwon, L., & Kyungik, G. (2020). Inflow and outflow event mean concentration analysis of contaminants in bioretention facilities for non-point pollution management. *Ecological Engineering*, 147(December 2019), 105757. <https://doi.org/10.1016/j.ecoleng.2020.105757>

DIFFUSE N- AND P-INPUTS INTO SURFACE WATERS OF GERMANY

Kunkel R.^{1*}, Kreins P.², Nguyen H.³, Tetzlaff B.¹, Venohr M.³, Wendland F.¹, Wolters T.¹, Zinnbauer M.²

¹ Forschungszentrum Jülich, Agrosphere Institute (FZJ), 52425 Jülich, Germany

² Johann Heinrich von Thünen-Institute, Bundesallee 50, 38116 Braunschweig, Germany

³ Leibniz-Institute of Freshwater Ecology and Inland Fisheries (IGB), Department Ecohydrology and Biochemistry, Müggelseedamm 310, 12587 Berlin, Germany.

*Corresponding author (r.kunkel@fz-juelich.de)

ABSTRACT

In the project AGRUM-DE a nutrient model system has been applied to quantify long-term N- and P-inputs into groundwater and surface waters from diffuse and point sources in Germany. The nutrient model system consists of the models RAUMIS focusing on agricultural N balance surpluses, DENUZ-WEKU and MEPhos focusing on diffuse sources of N and P and the MONERIS model dealing with point source emissions and nutrient retention in surface waters. In total, 6 diffuse and 6 point source inputs into surface waters have been considered. Model results have been validated against monitoring data successfully. Total model results show nitrogen emissions of about 455000 tons per year, dominated by diffuse sources (77 % of the total emission). The input pathways groundwater and interflow are of highest significance regarding surface water pollution. Phosphorus emissions sum up to 20000 tons per year, while diffuse and point sources are of almost equal importance. Here, water erosion and municipal waste water treatment plants are the most important pathways at the national scale.

Keywords: *Water Framework Directive; nutrient pollution; catchment management, hydro economic modeling network, agricultural environmental measures*

1. INTRODUCTION

The fundamental objective of the Water Framework Directive is to achieve good status of all surface waters and groundwater by 2015. The current draft of the management plan for the river basins in Germany shows that this goal has not been reached in the majority of water. Nutrient inputs (N and P) from point sources and diffuse sources are of particular importance with regard to achieving the water quality goals. In order to limit the nutrient in-puts, measures must be developed and implemented. Integrated large scale agricultural-economical-hydrological models are powerful tools to analyze the actual pollution loads and “hot spot” areas and to predict the temporal and spatial effects of reduction measures.

2. MATERIAL AND METHODS

We used the model network AGRUM-DE consisting of the individual models RAUMIS – mGROWA - DENUZ - WEKU -MEPhos - MONERIS (Gömann et al., 2020, Herrmann et al., 2015, Kunkel & Wendland, 1997, Wendland et al., 2004, Tetzlaff, 2006, Venohr et al., 2011) as a uniform methodology to predict the nitrogen intakes into groundwater and the nitrogen losses to surface waters from 12 different pathways at the regional and river basin scale (water erosion, wash-off, artificial drainage, groundwater, interflow, atmospheric deposition,

municipal waste water treatment plants, industry, rainwater sewers, combined sewers overflows, cesspits and exfiltration from leaky sewage pipes) using an area differentiated approach throughout Germany (Schmidt et al., 2022).

Model results are validated on the basis of various observed values, e.g., observed nitrate concentrations in surface near groundwater, observed N₂/Ar values in groundwater, N- and P-concentrations in surface waters and runoff data from surface water gauging stations. This as-is analysis was first used to determine the different origins and levels of nutrient inputs, which made it possible to spatially identify pollution hotspots and thus priority areas for the implementation of measures. The model results can be used to develop regional P and N reduction requirements to achieve the protection goals for groundwater and surface waters to achieve the marine protection goals.

3. RESULTS AND DISCUSSIONS

Nitrogen

The diffuse N-inputs to surface waters have been calculated for Germany using the water balance for the time period 1981-2010, N-deposition data from the PINETI 3 data set (Schaap et al. 2018) and the nutrient balance from agriculture for the period 2014-2016. In total, roughly 1.5 mio. tons of nitrogen (surplus) enter the soil of Germany each year. Roughly 60 % of this amount is either immobilized or denitrified in the soil, resulting to a nitrogen output from the soil of about 600000 tons N/year, which may either enter the surface waters by direct runoff or enter the groundwater with groundwater recharge. As can be seen from the left part of figure 1, interflow is the most important direct runoff component for diffuse N-inputs into surface waters. Drainages, N-deposition on water bodies, erosion and wash-off are of minor importance for nitrogen. Roughly two third (390000 tons/year) of the N-outputs from soils are entering the groundwater and may be denitrified on its way through the aquifer up to the surface waters. Denitrification in groundwater may be very effective in unconsolidated rock areas in particular in the northern and southern parts of Germany, whereas consolidated rock areas usually does not show significant denitrification in the aquifer. In total, roughly 70 % of the N-inputs into groundwater are denitrified in the aquifers, leading to a total N-input from groundwater to

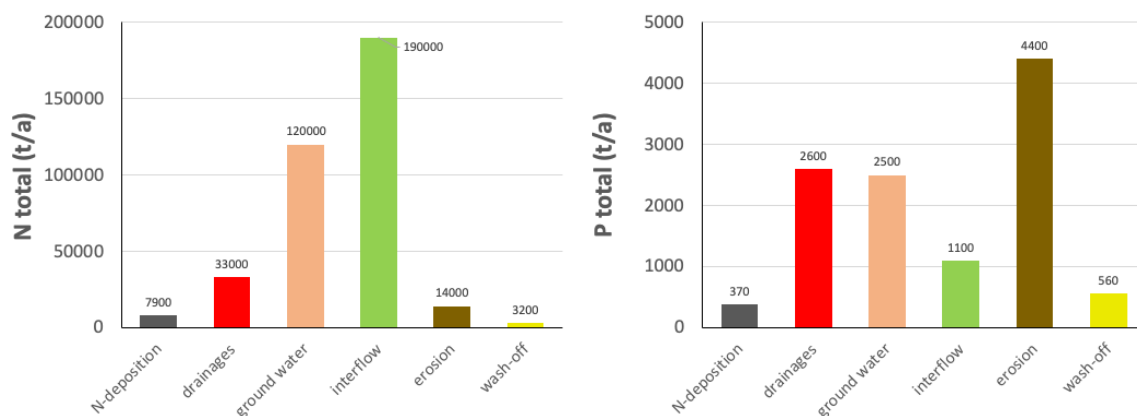


Figure 1. Total Nitrogen (left) and Phosphorous (right) inputs into surface waters in Germany from diffuse sources.

surface waters of 120000 tons N/year. In addition to the total N-inputs into surface waters from diffuse sources of 380000 t N/year, about 75000 t N/year are contributed by N-Inputs from urban systems.

Phosphorous

The total P-inputs into surface waters from diffuse sources amounts to about 11500 tons/year and is much smaller than the nitrogen inputs. In contrast to nitrogen, phosphorous adsorbs to spoil particles and enriches in the soil. Therefore, most P-inputs (40 %) into surface waters contribute from erosion (4400 tons/year), see also right part of figure 1. P-inputs from drainages and groundwater, each with about 2500 tons/year (20 %) are import input pathways for Phosphorous, too. Together with the P-inputs from urban systems of about 8000 tons/year, phosphorus emissions sum up to 20000 tons per year. Water erosion and municipal waste water treatment plants are the most important pathways at the national scale. The situation can differ greatly at sub-regional or local levels. The share of urban system inputs to the total inputs into surface waters are much higher for P (40 %) compared to N (17 %).

REFERENCES

- Gömann, H., Kreins, P., Brandes, E. and Pflingsten, T. (2020): Regionalisierte Quantifizierung der landwirtschaftlichen Flächenbilanzüberschüsse in Nordrhein-Westfalen, Teilbericht I zum Vorhaben GROWA+ NRW 2021, Köln/Braunschweig, 85 p.
- Herrmann, F.; Keller, L.; Kunkel, R.; Vereecken, H.; Wendland, F. (2015): Determination of spatially differentiated water balance components including groundwater recharge on the Federal State level—A case study using the mGROWA model in North Rhine-Westphalia (Germany). *J. Hydrol. Reg. Stud.* 2015, 4, 294–312.
- Kunkel R. and Wendland F. (1997): WEKU - A GIS-supported stochastic model of groundwater residence times in upper aquifers for the supraregional groundwater management, *Environmental Geology* Vol. 30, pp. 1-9.
- Schmidt, B., Kuhn, U., Trepel, M., Krüger, A., Kreins, P., Zinnbauer, M., Eysholdt, M., Wendland, F., Kunkel, R., Tetzlaff, B., Wolters, T., Venohr, M., Nguyen, H. (2022): Bestimmung der Nährstoffbelastung und des Handlungsbedarfs in den deutschen Flussgebieten. *Wasser und Abfall*, 24(4), 22-30.
- Tetzlaff B (2006): Die Phosphatbelastung großer Flusseinzugsgebiete aus diffusen und punktuellen Quellen. PhD thesis, Universität Hannover/Forschungszentrum Jülich GmbH, Hannover/Jülich, Germany
- Schaap, M.; Hendriks, C.; Kranenburg, R.; Kuenen, J.; Segers, A.; Schlutow, A.; Nagel, H-D; Ritter, A.; Banzhaf, S. (2018): PINETI-3: Modellierung atmosphärischer Stoffeinträge von 2000 bis 2015 zur Bewertung der ökosystem-spezifischen Gefährdung von Biodiversität durch Luftschadstoffe in Deutschland; Umweltbundesamt, Dessau, Germany; *UBA-Texte* 79/2018, 149p.
- Venohr, M., Hirt, U., Hofmann, J., Opitz, D., Gericke, A., Wetzig, A., Behrendt, H. (2011): Modelling of Nutrient Emissions in River Systems - MONERIS - Methods and Background. *International Review of Hydrobiology*, Vol. 96, pp. 435-483.
- Wendland, F., Kunkel, R. and Voigt, H.-J. (2004): Assessment of groundwater residence times in the pore aquifers of the River Elbe Basin, *Environmental Geology* Vol. 46, pp. 1-9.

INVESTIGATION OF THERMAL DISCHARGE DILUTION AT RIVER MOUTH USING HYDRODYNAMIC TOOLS

Fatih Yorgun¹, Mehmet Erbişim¹, Murat Akse², Oral Yağcı³ and Şevket Çokgör^{3}*

¹ HEC Engineering, Turkey

² Alanya Alaaddin Keykubat Üniversitesi, Turkey

³ İstanbul Teknik Üniversitesi, Turkey

**Corresponding author (Corresponding author's e-mail)*

ABSTRACT

Thermal power plants play an important key role and high percentage in the energy supply. Two different fluids are used in the cooling process of the steam boiler in thermal power plants. As a result of cooling with air and/or water, the temperature of the fluid used in cooling is discharged to the environment where the fluid is supplied. In this study, the dilution process of seawater, which is used for the cooling of a thermal power plant located on the seashore, after being discharged back into the sea via river mouth, was investigated using numerical modeling process. The open source Delft3d software and its modules were used in the dilution calculations. Measurement results of various dates and locations were used to determine the accuracy and validation of the model. The relative error value was calculated in the range of 0.7-2.5% in the results of the analysis made compared with the field measurements.

Keywords: *Thermal discharge, Dilution, Numerical model, Computational fluid dynamics*

OPTIMIZING THE ANNULAR PHOTOCATALYTIC REACTOR CONFIGURATION FOR THE DEGRADATION OF PERFLUOROCTANOIC ACID (PFOA) USING AN IMMOBILIZED TITANIUM DIOXIDE (TiO₂): A COMPUTATIONAL FLUID DYNAMICS (CFD) ANALYSIS

Mikaila Denise H. Loanzon¹, and Joseph Albert M. Mendoza^{1*}

¹ Mapua University, School of Chemical, Biological, Materials Engineering, and Sciences, Manila, Philippines

*Corresponding author: jammendoza@mapua.edu.ph

ABSTRACT

A comprehensive computational fluid dynamics (CFD) model was developed for the degradation of perfluorooctanoic acid (PFOA) in an annular reactor with TiO₂ photocatalysts immobilized at the centre, and an ultraviolet (UV) lamp in the inner tube. The chemical kinetic model for the degradation follows a pseudo-first-order reaction and considers the surface irradiance. Results revealed that at a Reynolds Number (Re) of 20 and 60 W/m², 22% of PFOA degraded within 1000 seconds, which agreed with previous studies. The effect of various process variables was also investigated. Based on the results, a low Re value is more favourable as this condition reached higher degradation efficiency. A degradation rate of 66% was reached when the PFOA concentration was 0.5 ppm. Increasing the concentration results in a lower degradation due to the decreased capacity to break down PFOA molecules. The rate of PFOA disappearance also improved when the surface irradiance increased. At 107.21 W/m², 32% of PFOA degraded. Similarly, increasing the length of the catalyst zone to 200 mm improved the degradation rate to 25%. The developed CFD model can aid in designing and scaling up immobilized photocatalytic reactors.

Keywords: *annular reactor, computational fluid dynamics (CFD), perfluorooctanoic acid (PFOA), photocatalysis, TiO₂.*

1. INTRODUCTION

Perfluoroalkyl and polyfluoroalkyl substances (PFAS) are a class of fluorinated synthetic substances that have established their importance in different commercial and industrial applications for many years because of their thermal and chemical stability, hydrophobic and lipophobic nature (Pelch et al., 2019). These are extensively used in non-stick, stain-proof, and waterproof consumer products. Because of their strong C-F bonds, these pollutants are difficult to degrade. Thus, they become persistent in the environment and can accumulate and bio-magnify in organisms (Loi et al., 2011). Drinking water has been considered one of the significant sources of PFAS exposure in humans. At present, the utilization of photocatalysis for organic pollutant degradation, including PFAS, has gained attention because it can be applied to pollutants that are complex and difficult to degrade. Titanium dioxide (TiO₂) is known for its excellent performance, low cost, and low toxicity. Studies also revealed that it

could oxidize and degrade organic pollutants, including organic dyes (Pino et al., 2020) and PFAS (Fàbrega et al., 2014). Computational fluid dynamics (CFD) is considered effective in predicting fluid flow, heat and mass transfer, and chemical reactions. It is also an inexpensive tool because it eliminates the need for more pilot-scale tests. Although there are experimental studies regarding photocatalytic reactors and degradation of pollutants, such as phenol and dyes, few computational studies consider PFOA as the model pollutant. With that in mind, this study primarily aims to: (1) set up a model for an annular photocatalytic reactor using computational fluid dynamics (CFD), (2) simulate the photocatalytic degradation of perfluorooctanoic acid (PFOA) using immobilized titanium dioxide nanoparticles (TiO_2), and (3) determine the effect of Reynolds number (Re), initial PFOA concentration, length of catalyst zone, and surface irradiance to the reaction rate and degradation efficiency.

2. MATERIAL AND METHODS

This section provides the procedures to model the photocatalytic degradation of PFOA in an annular photocatalytic reactor using CFD.

Computational Fluid Dynamics (CFD) Modeling

To simulate the photocatalytic degradation of PFOA, computational fluid dynamics was used. CFD is a mathematical modeling tool that can predict fluid-flow phenomena following the conservation laws, such as the conservation of mass, momentum, and energy governing fluid motion.

2.1.1. Radiation field modeling

Computational fluid dynamics can be utilized to calculate the radiation field throughout the reactor and on the catalyst's surface. The radiative transport equation can be used from the literature (Gravelle, 2014). It is assumed that a uniform intensity is observed across the entire catalyst surface. The discrete ordinate method (DOM) was chosen in the software to provide more reliable results for solving radiation field problems with chemical reactions (de Oliveira et al., 2022).

2.1.2. Transport equations and kinetics

The fluid is assumed to be Newtonian, incompressible, and isothermal, having constant physical properties. The system simulation was conducted with a three-dimensional, steady-state, laminar flow model and photocatalytic surface reactions. The reaction involved in this scenario is the heterogeneous degradation of perfluorooctanoic acid (PFOA) over immobilized-titanium dioxide nanoparticles. The overall reaction was considered as a surface reaction causing the complete mineralization of PFOA ($\text{C}_8\text{HF}_{15}\text{O}_2$). To model the dependence of reaction rate on PFOA concentration and radiation, a user-defined function based a previous study (Nourizade et al., 2021) using slurry reactors. For systems having TiO_2 as the photocatalyst, the value of the order for the light intensity is equal to 0.5 (Peralta Muniz Moreira & Li Puma, 2021). A power-law model is employed to describe concentration profile, which can be accepted if the absorption on the catalytic surface is negligible (Alvarado-Rolon et al., 2018).

2.1.3. Geometrical model and grid generation

An annular reactor geometry based on a previous study (Kumar & Bansal, 2013) was considered. The middle length of the annular space is porous because this contains the TiO₂ photocatalysts. A cylindrical lamp was housed inside the tube at the center of the reactor.

2.1.4. Boundary Conditions and Physical Properties

Boundary conditions were also set to complete the CFD model, which was defined as follows. The inlet velocity of the fluid was set to 4.502×10^{-4} m/s. The direction of the flow was normal to the boundary, while the inlet mass fraction of PFOA was set to 1×10^{-6} (1 ppm). On another note, the boundary condition pressure-outlet used was 1 atm at the outlet. A no-slip boundary condition was utilized at the reactor walls. Aside from this, a zero diffusive flux of species was set at the walls, except for the part where the surface reaction was specified.

2.1.5. Computational Fluid Dynamics (CFD) Solution

The CFD code Fluent (ANSYS Inc., 2021) was used in the photocatalytic reactor simulation. PRESTO was utilized as the pressure discretization scheme, while the SIMPLE algorithm was used for the pressure-velocity coupling.

Effect of Process Variables

The length of packing material, initial PFOA concentration, Reynolds number, and surface irradiance were varied to determine its effect on the photocatalytic degradation efficiency.

Photocatalytic Activity

The degradation efficiency of the photocatalyst at varying conditions was determined. This is quantified by using the proceeding equation:

$$\text{Degradation (\%)} = \frac{C_o - C_t}{C_o} \times 100 \quad (10)$$

where C_o is the initial PFOA concentration, C_t pertains to PFOA concentration in the solution after time t .

3. RESULTS AND DISCUSSIONS

CFD Simulation Results

3.1.1. Velocity and Radiation Profile

The PFOA-contaminated water was incompressible, Newtonian, isothermal, and possessed constant physical properties. The fluid flow changed when it reached the middle part of the reactor. The velocity is reduced because it has a lower porosity compared to the two inert regions of the reactor since this is where the TiO₂ photocatalysts are immobilized (Shazly & Eletriby, 2014). The radiation profile inside the photocatalytic reactor was also observed. The incident radiation is the greatest in the inner region of the reactor where the UV lamp is placed. There is a decrease in the irradiance as the area went further from the radiation source (Moreno-SanSegundo et al., 2020).

3.1.2. Degradation of PFOA

With TiO₂ photocatalysts and light, the degradation of PFOA in the reactor with TiO₂ was determined. The decrease of the molar concentration of PFOA under Re = 20 and light intensity of 60 W/m² along the reactor length is presented in Figure 1.

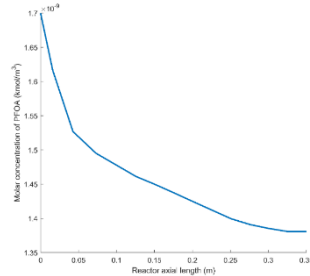


Figure 1. Molar concentration of PFOA along the axial length of the reactor.

As observed, the molar concentration decreases along the reactor length until it reaches the outlet of the annular reactor, indicating PFOA degradation. An efficiency of 22.38% was obtained. Apart from the TiO₂ photocatalysts at the middle part of the reactor, the presence of UV radiation along the whole reactor length also contributed to PFOA mineralization.

Effect of Process Variables in the Photocatalytic Degradation Efficiency

Figure 3 shows a comparison of the degradation efficiencies for each process variable studied.

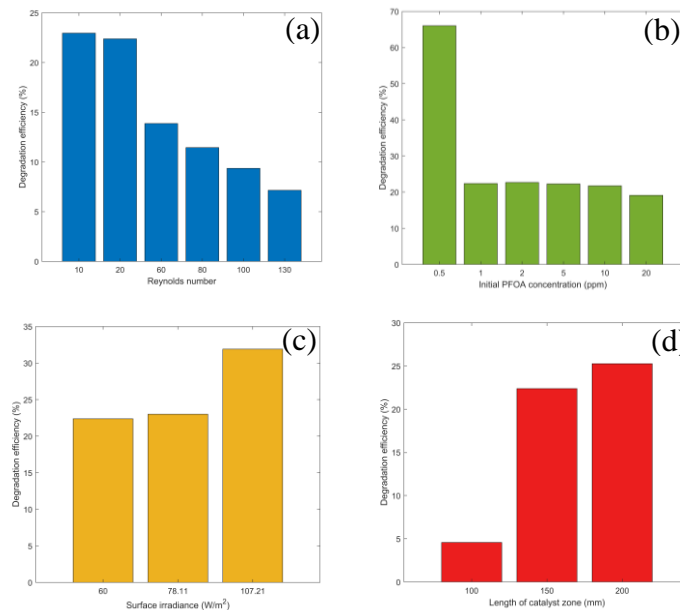


Figure 2. Effect of: (a) Reynolds number, (b) initial PFOA concentration, (c) surface irradiance, and (d) catalyst zone length on the degradation efficiency.

From Figure 2a, Re values of 10 and 20 resulted in the highest degradation efficiency of 22.96% and 22.38%, respectively. An increase of Re decreased the observed degradation of the target pollutant. These findings concur with a previous computational study (Periyathamby U, 1999). The highest efficiency was recorded when the PFOA initial concentration was 0.5 ppm (Figure 2b). This reduced as the pollutant became more concentrated in the fluid. A decrease in efficiency is expected since the amount of PFOA species to be broken down increased, but other factors affecting degradation remain unchanged (Rayalu et al., 2012). Results also show

that when the light intensity increases, the degradation of the pollutant also increases (Figure 2c). This result agrees with the previous studies (Jia et al., 2010; Reza et al., 2015). A higher light intensity leads to a greater electron excitation. This aids in generating free radicals that break down the pollutant. In Figure 2d, the effect of the catalyst zone length can be seen. It was observed that the decrease in PFOA concentration is greater for the reactor with the longest catalyst zone. There is an enhancement in the removal rate of PFOA when the catalyst dosage is increased and attributed this to increased quantities of photons adsorbed and a larger amount of active sites present for degradation (Yao et al., 2021).

Degradation of PFOA using Optimum Parameters

In the previous sections, the effect of several process variables was determined. The results obtained were used to determine the degradation efficiency of the modeled process when these optimum parameters are used. The observed rate constant is $1.301 \times 10^{-3} \text{ s}^{-1}$. This is the highest recorded rate constant when compared to the ones obtained previously. In line with this, 72.08% of PFOA degraded within 1000 seconds. This is expected since only a low concentration of PFOA is present in the solution, while the Reynolds number, surface irradiance intensity, and catalyst zone length utilized resulted in the highest degree of degradation.

4. CONCLUSIONS

In conclusion, we were able to simulate the degradation of PFOA in the modeled annular reactor with immobilized photocatalysts. According to the results, 22.38% of PFOA degraded within 1000 seconds with a reaction rate constant of $2.564 \times 10^{-4} \text{ s}^{-1}$. This is comparable to previous experimental studies on PFOA degradation. It was also found that the Reynolds number is inversely proportional to the degradation efficiency and rate of reaction. A low Re is more favorable since the modeled reaction incorporates the amount of absorbed radiation. A decrease in the efficiency was recorded at higher Reynolds number because of the lesser residence time of the fluid in the reactor. On the other hand, the efficiency decreases as the initial PFOA concentration increases because the capacity of the reactor to degrade PFOA molecules declines. But it can be concluded that TiO_2 photocatalysis has a potential in PFOA degradation at lower concentrations. Results also showed that the increase in light intensity causes an increased excitation of electrons, resulting in an enhanced degradation efficiency. The length of catalyst zone was also found to enhance the degradation efficiency of the reactor and the reaction rate because a longer catalyst zone length means more immobilized TiO_2 photocatalysts with active sites for degradation are available. Using the optimum conditions for each process variable, we were able to obtain the highest degradation efficiency.

Acknowledgements: The authors thank A.R. Caparanga, L.L. Tayo, and J.C. Millare for providing suggestions and feedback to improve the manuscript. This research received no specific grant from the public, commercial, or not-for-profit funding agencies.

REFERENCES

Alvarado-Rolon, O., Natividad, R., Romero, R., Hurtado, L., & Ramírez-Serrano, A. (2018). Modelling and

- Simulation of the Radiant Field in an Annular Heterogeneous Photoreactor Using a Four-Flux Model. *International Journal of Photoenergy*, 2018. <https://doi.org/10.1155/2018/1678385>
- ANSYS Inc. (2021). *ANSYS Fluent Tutorial Guide 2021 R1*.
- de Oliveira, G. X., Lira, J. O. de B., Riella, H. G., Soares, C., & Padoin, N. (2022). Modeling and Simulation of Reaction Environment in Photoredox Catalysis: A Critical Review. *Frontiers in Chemical Engineering*, 0, 77. <https://doi.org/10.3389/FCENG.2021.788653>
- Fàbrega, F., Kumar, V., Schuhmacher, M., Domingo, J. L., & Nadal, M. (2014). PBPK modeling for PFOS and PFOA: Validation with human experimental data. *Toxicology Letters*, 230(2), 244–251. <https://doi.org/10.1016/j.toxlet.2014.01.007>
- Gravelle, C. (2014). *A novel approach to reaction modeling for photocatalytic oxidation processes*. <https://knowledgecommons.lakeheadu.ca/handle/2453/4155>
- Jia, G., Wang, G., Zhang, Y., & Zhang, L. (2010). Effects of light intensity and H₂O₂ on photocatalytic degradation of phenol in wastewater using TiO₂/ACF. *Proceedings - 2010 International Conference on Digital Manufacturing and Automation, ICDMA 2010*, 1, 623–626. <https://doi.org/10.1109/ICDMA.2010.431>
- Kumar, J., & Bansal, A. (2013). Photocatalytic degradation in annular reactor: Modelization and optimization using computational fluid dynamics (CFD) and response surface methodology (RSM). *Journal of Environmental Chemical Engineering*, 1(3), 398–405. <https://doi.org/10.1016/J.JECE.2013.06.002>
- Loi, E. I. H., Yeung, L. W. Y., Taniyasu, S., Lam, P. K. S., Kannan, K., & Yamashita, N. (2011). Trophic magnification of poly- and perfluorinated compounds in a subtropical food web. *Environmental Science and Technology*, 45(13), 5506–5513. <https://doi.org/10.1021/es200432n>
- Moreno-SanSegundo, J., Casado, C., & Marugán, J. (2020). Enhanced numerical simulation of photocatalytic reactors with an improved solver for the radiative transfer equation. *Chemical Engineering Journal*, 388, 124183. <https://doi.org/10.1016/J.CEJ.2020.124183>
- Nourizade, M., Rahmani, M., & Javadi, A. (2021). Simulation of a Photocatalytic Reactor Using Finite Volume and Discrete Ordinate Method: A Parametric Study. *Amirkabir Journal of Mechanical Engineering*, 53(Issue 1 (Special Issue)), 573–588. <https://doi.org/10.22060/MEJ.2019.16699.6425>
- Pelch, K. E., Reade, A., Wolffe, T. A. M., & Kwiatkowski, C. F. (2019). PFAS health effects database: Protocol for a systematic evidence map. In *Environment International* (Vol. 130, p. 104851). Elsevier Ltd. <https://doi.org/10.1016/j.envint.2019.05.045>
- Peralta Muniz Moreira, R., & Li Puma, G. (2021). Multiphysics Computational Fluid-Dynamics (CFD) Modeling of Annular Photocatalytic Reactors by the Discrete Ordinates Method (DOM) and the Six-Flux Model (SFM) and Evaluation of the Contaminant Intrinsic Kinetics Constants. *Catalysis Today*, 361, 77–84. <https://doi.org/10.1016/J.CATTOD.2020.01.012>
- Periyathamby U, R. A. K. (1999). Computer Simulation of a Novel Photocatalytic Reactor Using Distributive Computing Environment - Periyathamby - 1999 - Chemical Engineering & Technology - Wiley Online Library. *Chem. Eng. Technol.*, 22(10), 881–888. <https://onlinelibrary.wiley.com/doi/abs/10.1002/%28sici%291521-4125%28199910%2922%3A10%3C881%3A%3Aaid-ceat881%3E3.0.co%3B2-x>
- Pino, E., Calderón, C., Herrera, F., Cifuentes, G., & Arteaga, G. (2020). Photocatalytic Degradation of Aqueous Rhodamine 6G Using Supported TiO₂ Catalysts. A Model for the Removal of Organic Contaminants From Aqueous Samples. *Frontiers in Chemistry*, 8, 365. <https://doi.org/10.3389/fchem.2020.00365>
- Rayalu, S. S., Mangrulkar, P. A., Kamble, S. P., Joshi, M. M., Meshram, J. S., & Labhsetwar, N. K. (2012). Photocatalytic degradation of phenolics by N-doped mesoporous titania under solar radiation. *International Journal of Photoenergy*, 2012. <https://doi.org/10.1155/2012/780562>
- Reza, K. M., Kurny, A., & Gulshan, F. (2015). Parameters affecting the photocatalytic degradation of dyes using TiO₂: a review. *Applied Water Science* 2015 7:4, 7(4), 1569–1578. <https://doi.org/10.1007/S13201-015-0367-Y>
- Shazly, Y. M. S. El, & Eletriby, S. W. (n.d.). *Finite Element Study of the Mass Transfer in Annular Reactor*.
- Yao, X., Zuo, J., Wang, Y. J., Song, N. N., Li, H. H., & Qiu, K. (2021). Enhanced Photocatalytic Degradation of Perfluorooctanoic Acid by Mesoporous Sb₂O₃/TiO₂ Heterojunctions. *Frontiers in Chemistry*, 9, 352. <https://doi.org/10.3389/FCHEM.2021.690520/BIBTEX>

APPLICATION OF MACHINE LEARNING CLASSIFICATION AND REGRESSION ALGORITHMS FOR QUANTIFYING NUTRIENT TRANSPORT CONSIDERING GROUNDWATER-SURFACE WATER INTERACTIONS IN AN AGRICULTURAL WATERSHED IN CANADA

Ahmed Elsayed^{1*}, Sarah Rixon¹, Jana Levison¹, Andrew Binns¹, Pradeep Goel²

¹ School of Engineering, University of Guelph, Guelph, Ontario, Canada

² Ministry of the Environment, Conservation and Parks, Etobicoke, Ontario, Canada

*Corresponding author (aelsay03@uoguelph.ca)

ABSTRACT

Elevated levels of nutrients (e.g., nitrogen and phosphorus) can cause algal bloom formation and eutrophication in surface water (e.g., streams, rivers, and lakes), leading to serious ecosystem changes that can impact human and aquatic life. For example, Lake Erie, one of the Laurentian Great Lakes in Canada and the United States, is experiencing high levels of phosphorus, leading to significant degradation in water quality. Moreover, nutrients can adversely impact groundwater quality, affecting both drinking and irrigation water sources. For humans, exposure to high concentrations of nutrients in drinking water can cause critical diseases such as cancer. To avoid these serious issues, water resources should be protected against receiving high concentrations of nitrogen and phosphorus. Agricultural fields are important non-point sources of nutrient release into surface water and groundwater receptors as a result of the introduction of excessive synthetic fertilizers and manure. Different factors can influence nutrient transport in agricultural fields such as climate conditions, land use and field properties. Therefore, continuous monitoring and quantification of nutrient loss to surface water and groundwater from agricultural lands is extremely important to ensure the protection of water resources. In addition, the application of optimal nutrient and crop management practices in agricultural watersheds is imperative for water protection. Determining the governing factors for nutrient loss from agricultural watersheds to surface and subsurface water is key to enhance water quality in receiving water bodies.

Typical field sampling approaches require considerable time and effort to obtain realistic measurements. In addition, measurement techniques for quantifying nutrient concentrations (e.g., nitrate and phosphorus) in field samples are time intensive and require specific procedures and kits. Typical sampling and measurement approaches of nutrient concentrations in surface and subsurface water can lead to noisy and inconsistent datasets due to human errors and variations in sampling techniques. Moreover, field sampling is not feasible in some cases due to field and climate conditions (e.g., winter season). In parallel, integrated numerical models that simulate nutrient transport in groundwater and surface water have not included all governing factors for nutrient transport processes. Many existing numerical models contain a large number of parameters with high non-linearity and uncertainties (e.g., soil properties) while the application of some more sophisticated numerical models may not be practical or cost-effective. Considering these challenges, the application of data-driven models using machine learning (ML) algorithms can be used as an effective approach to yield high performance for solving the complexity of transport processes since they can deal with different scales of datasets and parameter variability. Also, ML models can investigate the

interdependence between the involved process variables since ML models deal with the input (e.g., field and hydrological conditions) and output (e.g., nutrient concentrations) variables based on historical observations.

In the current study, different classification (e.g., decision trees and support vector machine) and regression (e.g., artificial neural network) ML algorithms were applied on a dataset of five observation sites in an agricultural watershed in Ontario, Canada to classify and predict nutrient concentrations in surface water and groundwater. In the structure of ML algorithms, the input variables included the weather conditions (e.g., precipitation), water chemistry parameters (e.g., temperature and pH) for surface and subsurface water, hydrogeological (e.g., groundwater elevations), hydrological (e.g., surface flow) and field (e.g., land use and nutrient application amounts) conditions while the main output variables were the nutrient concentrations in surface water and groundwater at the observation locations in the watershed. In addition, the interdependence and correlation between the variables involved in nutrient transport were determined where the governing factors of nutrient concentrations were specified. The ML model simulation results can be used by decision makers to recommend suitable nutrient management practices in agricultural watersheds to protect and improve groundwater and surface water quality. The results of this study can also be implemented to interpolate nutrient concentrations in the watershed from a series of point measurements and prediction of nutrient concentrations at new locations.

REAL TIME MONITORING OF TEMPERATURE STRATIFICATION TO RESPOND TO EUTROPHICATION

Özge Yücel-Bilen¹, Emrehan Berkay Çelebi¹, Utku Berkalp Ünalın¹, Emine Betül Şanlı², Serbay Şimşir², Süleyman Kazım Sömek³, Aydoğa Kallem², Reza Ahmadian⁴, Şimşek Demir^{2,5}, Ayşegül Aksoy^{1*}

¹ Department of Environmental Engineering, METU, 06800 Ankara, Turkey

² PRF R&D Inc, METU Technopark, Silicon Block No:19/ZK-9, 06800 Ankara, Turkey

³TUBITAK Uzay, 06800, Ankara, Turkey

⁴ Hydro-environmental Research Center, Cardiff University, Cardiff CF24 3AA, United Kingdom

⁵ Department of Electrical and Electronics Engineering, METU, 06800 Ankara, Turkey

*aaksoy@metu.edu.tr

ABSTRACT

Importance of autonomous systems to respond to acute environmental occurrences is increasing, as they provide swift and accurate reactions without the need of manual supervision. In this study, a real-time autonomous monitoring, warning, and emergency action system was developed to restore low dissolved oxygen concentrations that may occur in eutrophic lakes and minimize mass fish kills. The system includes two multiparameter sondes that measure temperature and water quality parameters at two different depths, an anemometer, a depth sensor, an aerator, data transfer equipment and energy systems. Real-time data transmitted to the server via 3G is visualized on the Grafana data visualization platform and can be monitored instantly. With the help of rule-based algorithms integrated into the system, the aerator works when necessary, providing oxygen to the water. The system was placed in Lake Eymir in April 2021. The data show that with the formation of temperature-dependent stratification, anoxic conditions occurred in the bottom layers of the lake, and dissolved oxygen was below saturation values at the surface. As the dissolved oxygen in the surface layer fell below the rule-based limit of 4 mg/L, the aerator started to operate autonomously, and the situation was notified to the center. The system evaluated instant information independently and successfully operated autonomously.

Keywords: *Eutrophication, autonomous systems, real-time monitoring, water quality management, temperature stratification*

1. INTRODUCTION

Eutrophication is a widespread problem in lakes and reservoirs caused by the excessive input of nutrients, mainly nitrogen and phosphorus, often as a result of human activities. This problem can lead to harmful algal blooms, fish kills, and the production of toxins. While there are many management strategies for mitigating the consequences of eutrophication, recovery is expensive and takes a long time (Wilkinson, 2017)

Development of autonomous systems capable of emergency response, along with the implementation of environmental control measures are of great importance in order to preserve environmental integrity and prevent the problem before it occurs. In cases such as mass fish kills, which may happen due to acute or instantaneous events, it is not always possible to detect and react with traditional water quality monitoring strategies. Additionally, technological advances and increasing environmental impact of climate change make it clear that new approaches that do not strictly depend on manual input will be preferred to conserve the existing environmental systems. In this regard, autonomous systems can provide innovative and robust solutions to overcome the limitations of traditional field data acquisition and consequent laboratory analysis (Barros et al., 2019). Furthermore, advanced autonomous systems that are already being used in lakes and reservoirs also allow the operators and researchers to monitor the conditions through inexpensive means (Park et al., 2020)

Primarily, autonomous systems in water bodies work based on the data acquired through submerged sensors. Devices that automatically track the water quality record the critical physical, chemical and biological water quality parameters at multiple measurement points and different times. These data which are then transferred through telemetry or internet servers, can be easily processed and broadcast, providing a continuous record of water quality (Wagner et al., 2000).

In this study, a real-time autonomous monitoring, warning and emergency response system was developed to mitigate the impact of reduced oxygen concentrations as a consequence of eutrophication and thermal stratification. This system consists of water quality, depth and wind-speed sensors, an internet-based real-time data transmitter, data visualization software and an on-site aerator. The novelty of this study is apparent in our real-time monitoring, warning and response system which decides on and implements the suitable action without requiring human input, based on its analysis of continuous data.

2. MATERIAL AND METHODS

This study is conducted in Lake Eymir (Figure 1) which is located 20 km to the south of Ankara, Türkiye. Lake Eymir has a surface area of 1.25 km² and is located 967 m above sea level. It is a relatively shallow lake, 4 km in length and 250 m in width. The maximum depth has been measured as 5.9 m as of April 2021. The primary input into the lake consists of the inflow from Lake Mogan, located in the same watershed. Additional inflow has been observed from Kislakci Creek during spring and groundwater aquifers. The only outflow is to the Imrahor Creek in a controlled manner (Beklioglu et al., 2017). Lake Eymir and Lake Mogan, along with surrounding residential and agricultural areas, grasslands, and forests form the “Golbasi Special Environmental Protection Zone” (Tabiat Varlıklarını Koruma Genel Müdürlüğü, 2020). In the past decade, mass fish kills and water quality problems have been observed in Lake Eymir, which is currently categorized as eutrophic. Because of this, constant monitoring of water quality parameters in Lake Eymir is of great importance.

The floating platform that was specially crafted for this study was designed to house and protect the related equipment. Energy required for the sensors, data transmission units and the aerator is provided through 8 rechargeable batteries powered by 4 photovoltaic cells located above the platform. Two multi-parameter sondes connected to the center of the platform are located 25 cm and 4 m below the water surface. They can continuously measure dissolved oxygen (DO), temperature, pH, electrical conductivity and salinity. Additionally, the sonde located at 25 cm below the surface can measure turbidity. When the autonomous system deems it necessary, the aerator is switched on to inject air into the water through two nozzles. The system also includes a sonar depth sensor which measures the depth of water and water surface temperature, along with an anemometer, recording the wind speed. Calibration and cleaning of the sensors are done through regular maintenance visits.



Figure 1. Location of Lake Eymir

Connection of the sensors to the data transmission equipment for real-time monitoring is achieved through a developed algorithm and combined electronic circuit modules. Data from the sensors are conveyed to a communication unit using a Modbus RTU protocol. Real-time transmission of the data measured in the field is achieved through a Raspberry PI which is connected to the internet via a 3G modem. This data is then stored on a web server designated for this study. To minimize the energy consumption, system is turned on every 15 minutes by an Arduino and the Raspberry PI transmits the measured data. Furthermore, software on the Raspberry PI is designed to enable update remotely. This way, required updates and corrections can be implemented without going to the site. In the case of a connection loss, the data are also

backed-up to a local SD card, connected to the Raspberry PI, which can then be accessed in-person to avoid loss of data. Data stored on the designated server is processed through Grafana data visualization tool and released to the end-user in the form of visual, graphics-based outputs, accessible via a web browser-based user interface.

Data from the sensors are analyzed by the system. When predetermined conditions occur, aeration is triggered autonomously. Currently, a rule-based algorithm tracks the DO concentration data from the sensor at 25 cm depth. If it falls below 4 mg/L, aeration starts to provide oxygen in order to sustain the necessary aquatic conditions. Modules of the system are shown in Figure 2.

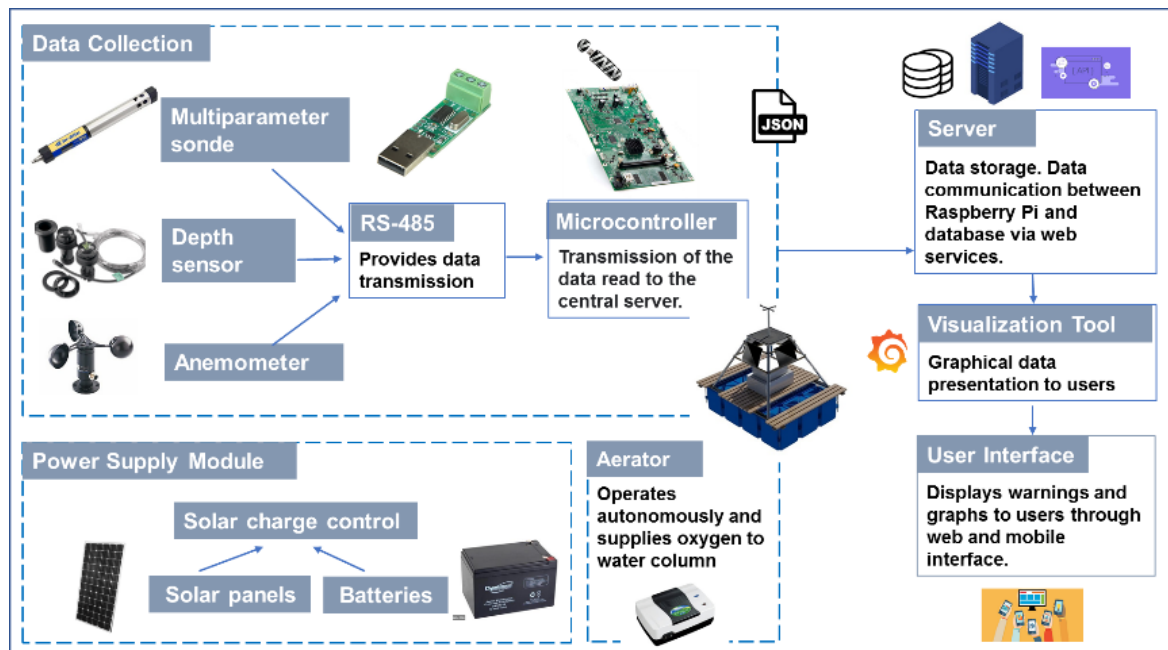


Figure 2. Framework of the autonomous monitoring, warning, and response system

3. RESULTS AND DISCUSSIONS

The system was placed in Eymir Lake in April 2021 after the design and production phases of the platform were completed. Since this date, the data obtained in real time are collected and the changes in the parameters are examined. The graphic given in Figure 3 shows the temperature data transmitted to the central server. The variation of the temperature values measured at 15- minute intervals at surface, 0.25 m, and 4 m depths for May, 2022 can be seen in the figure.

Looking at the data collected during this period, there is no significant difference in the temperature values measured at the surface and at a depth of 0.25 m. On the other hand, measured values at 4 m depth show the formation of temperature-dependent stratification clearly. Wind speed impacted temperature as well as DO concentrations, probably due to wind induced mixing and aeration. Wind speed reached up to 9.9 m/s during the observation time. During this period, very low DO concentrations were measured. Most of the time measured DO concentrations were below the 4 mg/L mark.

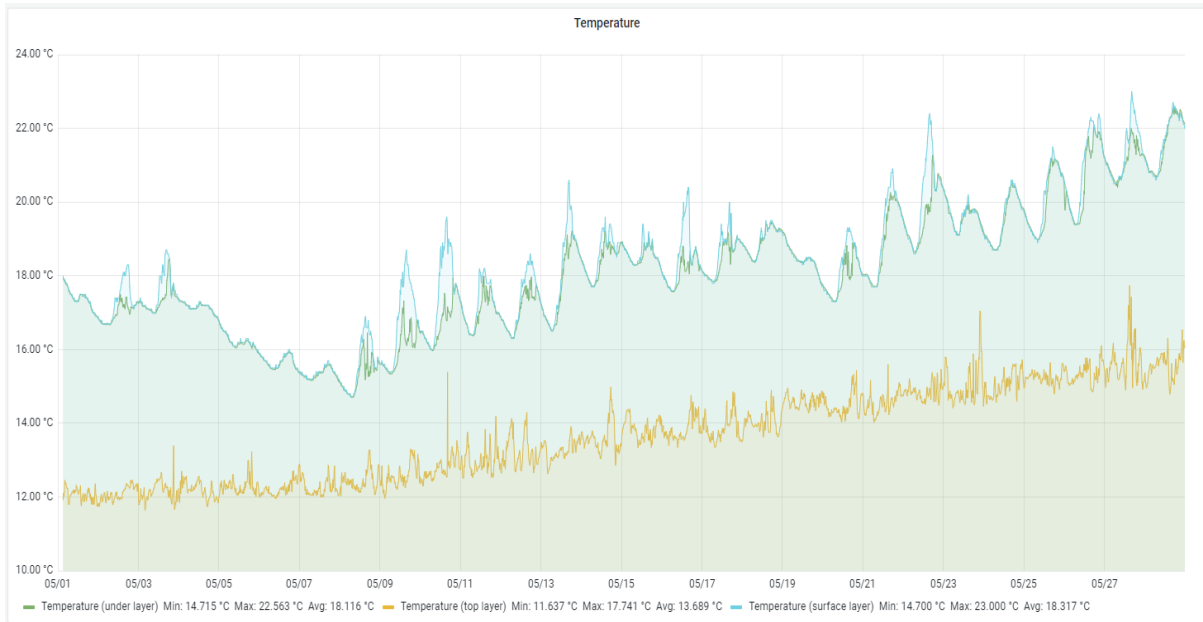


Figure 3. A screenshot from Grafana visualization tool for water temperature at surface, -0.25 m and -4m

In Figure 4, the variation of DO concentrations for this period is given. While the maximum DO concentration for the upper layer reached approximately 5 mg/l, the maximum concentration in the lower layer was measured around 1 mg/l during the same period, indicating surging of anoxic conditions and probable mixing from bottom sediments. These concentrations were also validated against an external DO probe.

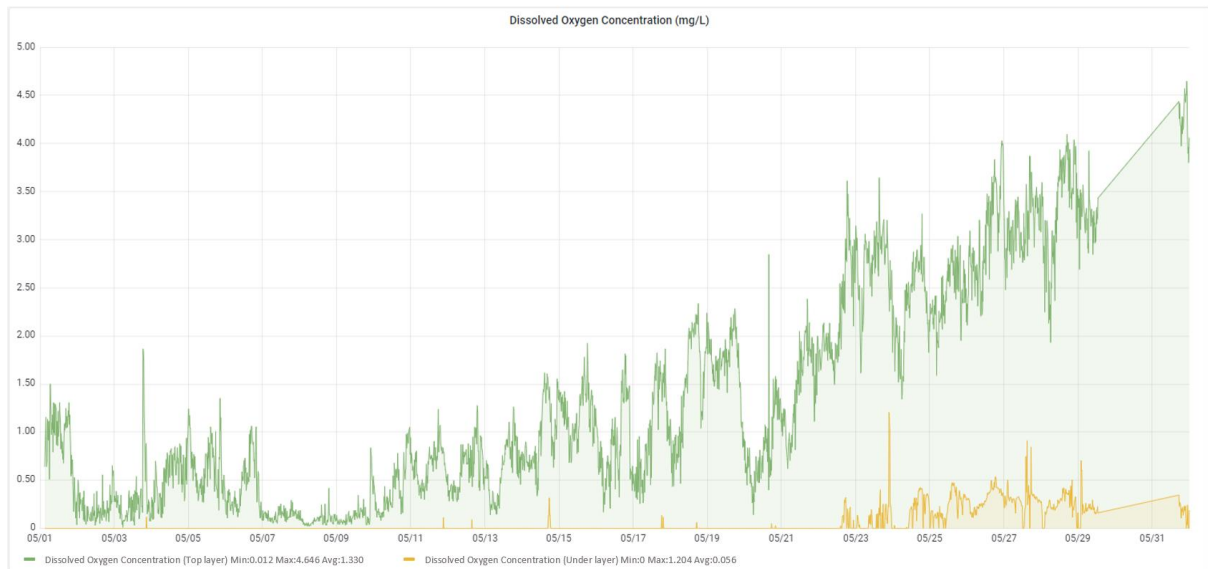


Figure 4. A screenshot from Grafana visualization tool for Dissolved Oxygen Concentration at -0.25 m and -4m

4. CONCLUSIONS

The developed system is expected to be an exemplary autonomous monitoring, warning and response tool that can accomplish i) real-time data acquisition from water bodies, ii) evaluation through algorithms and iii) accurate response implementation. Such systems can be used to

both track the progress of eutrophication in water bodies as well as trigger emergency response mechanisms when aquatic life is threatened. Up to this point, it has been successful in tracking changes in water quality parameters at different depths and real-time transmission of related data, as well as responding to critical situations autonomously. Gathered data shows that Lake Eymir is thermally stratified and DO concentrations are affected greatly by temperature and high wind speeds. Through further data acquisition, more in-depth analyses will be carried out.

Acknowledgements: This work was supported by the Royal Academy of Engineering under the Newton-Katip Çelebi Program.

REFERENCES

- Barros, M., Granchinho, P., Ferreira, C., Neves, P., Magalhaes, H., Santos, L., Lopes, B., Marques, J., Pinho, H., Mourato, S., & Martins, A. (2019). Study of the requirements of an autonomous system for surface water quality monitoring. *Renewable Energy and Power Quality Journal*, 17, 399–404. <https://doi.org/10.24084/repqj17.323>
- Beklioğlu, M., Bucak, T., Coppens, J., Bezirci, G., Tavşanoğlu, N., Çakiroğlu, A. I., Levi, E. E., Erdoğan, S., Filiz, N., Özkan, K., & Özen, A. (2017). Restoration of eutrophic lakes with fluctuating water levels: A 20-year monitoring study of two inter-connected lakes. *Water (Switzerland)*, 9(2). <https://doi.org/10.3390/w9020127>
- Park, J., Kim, K. T., & Lee, W. H. (2020). Recent advances in information and communications technology (ICT) and sensor technology for monitoring water quality. *Water (Switzerland)*, 12(2). <https://doi.org/10.3390/w12020510>
- Tabiat Varlıklarını Koruma Genel Müdürlüğü. (2020). *Gölbaşı Özel Çevre Koruma Bölgesi Yönetim Planı 2015-2019*. [https://webdosya.csb.gov.tr/db/tabiat/editordosya/golbasi_yonetim_plani\(1\).pdf](https://webdosya.csb.gov.tr/db/tabiat/editordosya/golbasi_yonetim_plani(1).pdf)
- Wagner, R., Matraw, H., Ritz, G., & Smith, B. (2000). ... standard procedures for continuous water-quality monitors: Site selection, field operation, *US Geological Survey Water-Resources Investigations* ... <http://scholar.google.com/scholar?hl=en&q=Guidelines+and+Standard+Procedures+for+Continuous+Water-Quality+Monitors:+Site+Selection,+Field+Operation,+Calibration,+Record+Computation,+and+Reporting&btnG=Search#0>
- Wilkinson, G. M. (2017). Eutrophication of Freshwater and Coastal Ecosystems. In *Encyclopedia of Sustainable Technologies* (pp. 145–152). Elsevier. <https://doi.org/10.1016/B978-0-12-409548-9.10160-5>

MODEL BASED EUTROPHICATION ASSESMENT OF KÖYCEGİZ LAKE

Elif Atasoy Aytış^{1}, Elif Soyer², Ali Ertürk³*

^{1.} Marmara University, Department of Environmental Engineering, İstanbul, TURKIYE

^{2.} Marmara University, Department of Environmental Engineering, İstanbul, TURKIYE

^{3.} İstanbul University, Faculty of Fisheries, Division of Freshwater Biology, İstanbul, TURKIYE

**Corresponding author (atasoy.e@gmail.com)*

ABSTRACT

In this study, a simple steady state eutrophication model system is developed for the Köyceğiz Lake. The model is applied using the simple available data published in the different literature. Our preliminary investigations have shown that the model is successfully calibrated, reproduced the eutrophic state of the Köyceğiz Lake and responded as expected to different nutrient management scenario simulations and climate change simulations. The first findings show that the Köyceğiz Lake would respond more sensitive to nutrient load increase than to the decrease of freshwater due to climate change

Keywords: *Köyceğiz Lake, Eutrophication, Diffuse pollution, Climate change*

1. INTRODUCTION

Köyceğiz Lake, which is located in the western Mediterranean part of Republic of Türkiye is one of the components of a complex lagoon system called Köyceğiz-Dalyan Lagoon system dominated by brackish water. Considering this fact and also that the lake is classified as a meromictic lake investigation of the lake is an interesting task. In the last decades many studies about the related lagoon system was conducted. Gürel (2000) studied nutrient dynamics of the lagoon system. Ertürk (2002) investigated the hydraulic behavior of the entire system. Yüceil's (2005) initial efforts together with the study conducted by Balloch (2009) resulted in the development of a hydrological modelling system covering most of the drainage area, whereas Güzel (2010) applied the SWAT model to the entire watershed. Further studies conducted by Erturk et al (2014) quantified the expected impact of climate change on the watershed on the hydrological process level. Another branch of studies initiated by Adalı (2004) aimed to investigate the nutrient loads in the watershed followed by the eutrophication model developed by Ekdal (2008) covering the southern waterbodies part of the lagoon ecosystem. Recently, Keskin (2019) studied eutrophication risk in the lagoon system and interpreted the total phosphorus to be the limiting nutrient. These studies and several more not mentioned here, clearly show that an ecological model that is investigating the eutrophication in the entire lagoon systems waterbodies has not been developed yet for the Köyceğiz Lake itself, in spite of being the largest waterbody in the system, at least has not been studied with some kind of mechanistic modelling approach. The aim of this study is to initiate the efforts to set up an eutrophication model for the Köyceğiz Lake which will help to close the gap towards a full scaled all-waterbody ecological model for the Köyceğiz-Dalyan Lagoon system.

2. MATERIAL AND METHODS

Case Study Area

The Köyceğiz Lake watershed 900 km² fairly large compared to the Lakes surface area that is 55 km². Since the population is estimated 43000 and most of the population is connected to advance biological wastewater treatment plants with nutrient removal, it can be assumed that the nutrient emissions are dominated by diffuse sources. This assumption is backed up by Adalı (2004), where the MONERIS model was applied for an initial estimate of diffuse nutrient loads. Köyceğiz Lake is 13 km long, 6 km wide, and with its average depth of 25 m it is a, meromictic lake. Several streams (such as Namnam Creek, Yuvarlakçay Creek and Kargıcak Creek.) discharge into the lake. The lake and its watershed are declared as a Special Environmental Protection Area. The overall watershed has a typical Mediterranean climate.

Hydrological Investigation

The first step in this study is to develop a simple-but realistic enough water budget system for the watershed of the Köyceğiz Lake, where the watershed was delineated using a digital elevation model (DEM) with a spatial resolution of 30 m x 30 m, considering the rivers draining into the Köyceğiz Lake as subwatersheds. An investigation related to the rivers based on monthly flow data and topographical information revealed that the water retention time in the rivers is mostly on a range of hours rarely closing a day so that the nutrient retention and transformation in the rivers are neglected at this level of the study and rivers were considered as conduits collecting and channeling the nutrient loads into the watershed. Water budget is constructed using the method developed by Thornwaite and Matter (1957) based on monthly meteorological information. The monthly potential evapotranspiration was estimated using the method proposed by Doğdu (2011) based on Thornwaite (1948) In this study that waterbudget method was modified to suit the project by introducing a more detailed algorithm that calculates the surface runoff and a more realistic representation of soil water storage by introducing the field capacity as well. The required information for water budget computations were land use and land cover information obtained from CORINE 2018 and soil related information from the Ministry of Agriculture and Forestry.

Estimation of Land Based TP Loads

Land based nutrient loads were calculated as agricultural fertilizer application, livestock and land use. The yearly commercial fertilizer application data were gathered from the Ministry of Agriculture and Forestry and excess nutrient loads the lake were then calculated with these data. Livestock based nutrient emissions were calculated using number of animals in the watershed was obtained from the same institution and the unit loads as assumed by Ayaz et. al. (2013). Land use-based background nutrient loads were calculated as in Gürel et al (2011).

The Lake Eutrophication Model System

A simple eutrophication model of the Köyceğiz Lake is developed for the initial studies. Considering that the lake is of meromictic character, the model developed in this study consists of two layers with a stable stratification. The steady-state approach is incorporated aiming to calculate the annually averaged nutrient concentrations for the epilimnion and hypolimnion. A non-steady state solution based on eigenvalue method where it is proven that for this problem a non-complex eigenvalues are always obtainable is also developed for further investigations

in future research. Such a solution is not considered for primary use due to the lack of time series (such as seasonal) based of nutrient load data. The necessary geometric information for the Köycegiz Lake was obtained from Ertürk (2002). The average annual inflow from the Mediterranean Sea into the Köycegiz Lake was estimated using the salt budget based on the data from Kazanci et al. (2004). The model was calibrated using the data published by Keskin (2019). A spreadsheet-based infrastructure for automatic construction of water budget, nutrient loads, the Lake Eutrophication Model and its optimization based calibration was developed as well. The calibration procedure is relatively simple from the computational point of view where the difference between the model results and the monitoring results were used as the objective function and the physical range of model constants were used as constraints.

3. RESULTS AND DISCUSSIONS

The model calibration, where the yearly averaged nutrient concentrations were compared with the monitoring published by Keskin (2019) based on an optimization algorithm aiming to minimize the residuals between the steady state model results and monitoring was successful with a relative error of less than 5% for nutrient concentrations. Based on the model results, Köycegiz Lake is considered as eutrophic and considerable efforts are needed to control the diffuse sources. The model is at this stage ready for investigating the general trophic state of Köycegiz Lake for different scenarios such as the management options related to diffuse pollution and water budget changes due to climate change, however since the framework is designed for steady state it is not ready to yield the time scale, when the positive or negative effects of the nutrient management or mis-management could be expected. From both scenarios, the initial findings show that the changes in nutrient emissions have more pronounced effect on the trophic state of the Köycegiz Lake than the climate change driven by freshwater inflow.

4. CONCLUSIONS

A model system was successfully developed for the Köycegiz Lake, providing results related to different management and climate change scenarios. More detailed information will be given in the presentation and full paper version of this extended abstract.

REFERENCES

- Ayaz, S. 2013. Aktaş, Ö., Dağlı, S., Aydöner, C., Aytış, E. A., Akça L. Pollution loads and surface water quality in the Kızılırmak Basin, Turkey. *Desalination and Water Treatment* 51 (7-9), 1533-1542, 2013
- Adalı, N. İ: (2004). Modeling of nutrient emissions in Köyceğiz Lake-Dalyan Lagoon watershed-application of the MONERIS model, Master Thesis, İTÜ Graduate School.
- Balooch, M.A. (2009)., Hydrological simulation program-Fortran (HSPF) model as a decision support tool for a developing country-A case study from Turkey PhD Thesis, İTÜ Grad. School.
- Doğdu, M.Ş. (2011). A computer program for water budget calculations used for hydrological studies, Stata Hydraulic Works, Technical Bulletin, No 112, 19-32.
- Ekdal, A. (2008). Water quality modeling of Köyceğiz-Dalyan Lagoon, PhD Thesis, İTÜ Grad. School.
- Ertürk, A (2002). Hydraulic modelling of Köyceğiz-Dalyan Lagoon system, Master Thesis, İTÜ Grad. School.
- Ertürk, A.,Ekdal, A. Gürel, M., Karakaya, N., Güzel, Ç., Gönen. İ.E., (2014). Evaluating the impact of climate change on groundwater resources in a small Mediterranean watershed, *STOTEN* 499, p 437-447
- Gürel M., Erturk A. , Şeker D. Z. , Tanik A., Ekdal A., Avsar C., Öztürk İ (2011). Estimation of monthly diffuse nutrient loads for a watershed in Turkey. *Water and Environment Journal* 25(2), 219-229.
- Gürel, M. (2000). Nutrient dynamics in coastal lagoons:Dalyan lagoon case study, PhD Thesis, İTÜ Grad. School.
- Güzel, Ç (2010).Applicaition of SWAT model in a watershed in Turkey, İTÜ Graduate School.

- Kazancı, N., İzbirak, A., Çağlar, S:S:, Gökçe, D. Hydrobiological Investigation of Köyceğiz-Dalyan Special Protection Area Aquatic Ecosystem, Imaj Publishing, Ankara, 165 p.
- Keskin, F. (2019). Determination of toxic metal and eutrophication risks in Köyceğiz lake dalyan lagoon system, Turkey PhD Thesis, Muğla Sıktı Koçman Universitu Grad. School.
- Thornwaite, C.W. 1948. An Approach Toward a Rational Classification of Climate. *Geographical Rev.*, 38:55-94.
- Thornwaite, C.W., and J.R. Mather, 1957. Instructions and Tables for Computing Potential Evapotranspiration and the Water Balance, Drexel Institute of Technology, Laboratory of Climatology, Publications in Climatology 10(3)
- Yüceil, K. (2005) Development of model support system for rural area non-point source modeling: Köyceğiz-Dalyan watershed case study, PhD Thesis, İTÜ Grad. School.

LONG-TERM SPATIAL-TEMPORAL MONITORING OF EUTROPHICATION IN LAKE BURDUR USING REMOTE SENSING DATA

Serra Salgut, Gizem Tuna Tuygun, and Alper Elçi*

Dokuz Eylul University, Department of Environmental Engineering, Izmir, Türkiye

*Corresponding author (alper.elci@deu.edu.tr)

ABSTRACT

Eutrophication caused by environmental changes and anthropogenic activities continues to be one of the major environmental challenges in lakes worldwide. Therefore, accurate spatial-temporal evaluations of algal blooms and determining chlorophyll-a (Chl-a) concentrations are key in mitigating eutrophication. This study uses a remote sensing approach to perform long-term Chl-a concentration and trophic state index (TSI) monitoring on Lake Burdur, Türkiye. Google Earth Engine (GEE), an effective tool for accessing and processing satellite data is used for data retrieval and analysis. Surface reflectances from Landsat 5, Landsat 7, and Landsat 8 satellite image collections are evaluated with an empirical model to estimate a 37-year long (1984 to 2021) time series of Chl-a concentrations. Images affected by cloud cover, icing, and other weather events are excluded from the analysis. Pixel quality masks are applied to retain only acceptable quality pixels that are evaluated to calculate Chl-a concentration. The data sets are analyzed based on annual, seasonal, and monthly temporal averages. Study results show that a statistically significant temporal trend for the entire study period could not be detected; only an increasing trend in Chl-a concentrations is apparent for the last 20 years. Landsat-derived TSI indicates that Lake Burdur has been mostly hypertrophic from 1984 to 2021. The results improve our understanding of the spatiotemporal variability of eutrophication to develop related strategies to mitigate eutrophication.

Keywords: *eutrophication, remote sensing, Google Earth Engine, surface water, Landsat*

1. INTRODUCTION

Freshwater lakes are for some areas in the world critical water resources that have various purposes. However, eutrophication threatens the sustainability of these lakes. Eutrophication trends in lakes are more pronounced in recent decades due to anthropogenic pollutant input and climate change (Smith, 2003; Le et al., 2010). Although the eutrophication process is a natural event of water body enrichment, it can cause significant environmental nuisances and can be a problem for water authorities. Long-term datasets of water quality variables causing lake eutrophication prove to be useful to develop effective water management strategies (Cao et al., 2022).

Traditionally, water-quality of a lake is determined with in-situ measurements and laboratory analysis. This approach leads to ground-based more or less accurate measurements that reflect

the actual water quality of the lake, however, it requires allocation of time and monetary resources. Furthermore, in-situ measurement cannot provide a large-scale spatial and temporal overview of the water quality (Gao et al., 2015; Li et al., 2017). Remote sensing with satellites offers efficiency and versatility that can be used to estimate water quality variables. It has the benefits of working with a much wider spatial and temporal coverage and being cost-effective and less time-intensive compared to ground measurements. For example, Landsat images have a spatial resolution of 30 m and a revisit cycle of 16-day, meeting the requirements of image quality and spectral range. The launch of the Landsat-5 Thematic Mapper (TM, 1984–2012), the Landsat-7 Enhanced Thematic Mapper Plus (ETM+, 1999~), and the Landsat-8 Operational Land Imager (OLI, 2013~) provided nearly 40 years of remote sensing data, enabling the extraction of historical water quality information (He et al., 2021). Landsat data is used to obtain trophic state index values (TSI) (Hu et al., 2022), Chl-a concentrations (Cardall et al., 2021; Cao et al., 2022), nutrient concentrations (Li et al., 2017), eutrophication status (Chen et al., 2020) in lakes. Among these variables, Chl-a is related to phytoplankton biomass and is an indicator of the trophic status of the lake. Although wide spectral bandwidths (> 50 nm) equipped with Landsat satellites diminish the features of the spectrum and limit the performance of estimating water substances in lakes (Cao et al., 2019), several studies have shown the potential for TSI retrievals in specific lakes and demonstrated reasonable accuracy (Iwashita et al., 2004; Lee et al., 2016; Ha et al., 2017). The trophic state of water bodies can be quantitatively evaluated with the TSI, which was first proposed by Carlson (1977). It provides practical information for lake management, which uses single or multiple water quality parameters, including Secchi disk depth, Chl-a concentration, total nitrogen, or total phosphorus. The TSI is considered an effective indicator for inland water quality and has been widely used for lakes worldwide (e.g. Hu et al., 2021).

In this study, the long-term (1984 to 2021) and high spatial resolution algae concentrations of Lake Burdur were obtained based on the application of an empirical model on the time series of Landsat imagery using Google Earth Engine (GEE) (Gorelick et al., 2017) as a cloud computing interface. Lake Burdur is under significant environmental stress and the shrinking rate of the lake is at an alarming level. TSI was also calculated based on Landsat-derived Chl-a concentrations. Interannual and seasonal patterns of the TSI and Chl-a concentrations were identified. This study aims to fill this gap by generating a 37-year (1984–2021) Chl-a and TSI dataset of Lake Burdur based on Landsat images.

2. MATERIAL AND METHODS

Study Area

The Lake Burdur river basin is situated in southwestern Türkiye, between 37.12°- 38.17° N and 29.52°-30.85° E (Figure 1), and in a climatic transition zone between the Central Anatolian and Mediterranean regions. The basin is also named the “Lakes Region” of Türkiye. The long-term mean annual precipitation in the river basin is 444 mm, which is low compared to the typical Mediterranean climate. The largest surface water body is Lake Burdur, which has a declining volume of water with the most recent estimate at 3900 m³, and a water surface area of 122.6 km² (SYGM, 2020). The water surface area of Lake Burdur decreased steadily from 1984 through 2018 (Elçi, 2019). The decrease in water levels is due to the construction of upstream

dams, increasing water evaporation, and decreasing water inflow to the lake. Lake Burdur is among Turkey's largest and deepest natural lakes and is located within a closed hydrological basin, which has a drainage area of 3211 km². The average and the maximum depths are 40 m and 100 m, respectively (Girgin et al., 2004). The lake is fed by intermittent flowing streams and sporadic groundwater seepage. Karstic aquifers in the basin are important water resources that strongly influence the water balances of the lakes.

The lake's ecosystem is threatened by organic carbon and nutrient influx originating from diffuse sources, and numerous discharges of industrial and urban wastewater. Based on a water quality modeling study by SYGM (2020) the average hydraulic retention time is estimated at 33.8 years.

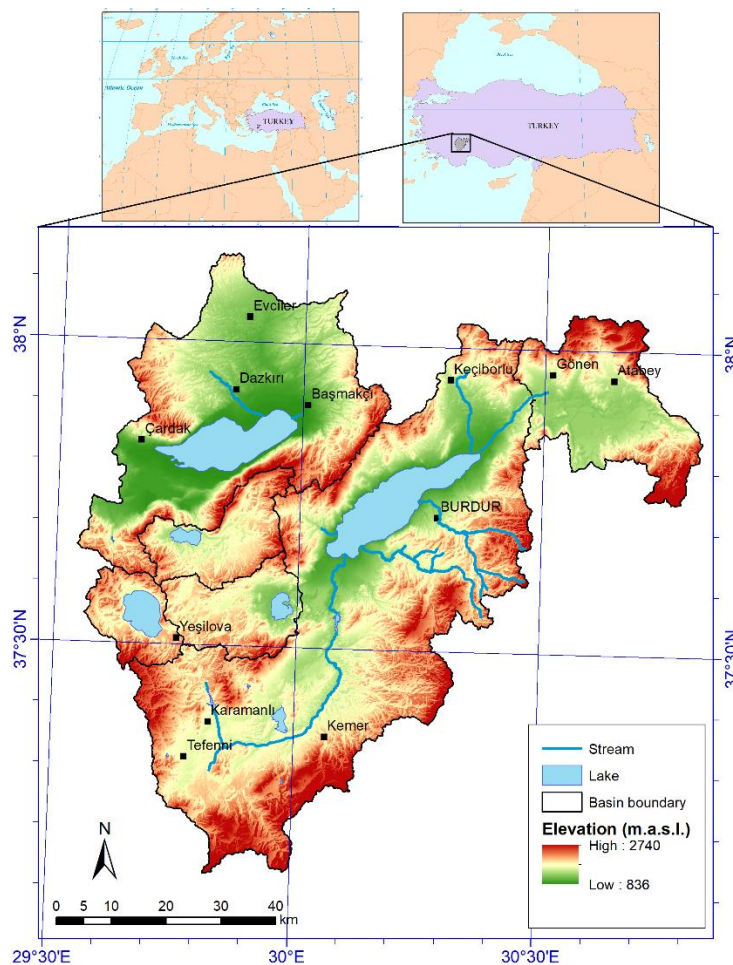


Figure 1. Location of the Lake Burdur watershed

Data Retrieval and Data Processing

This study is executed in three steps: 1) remote sensing data retrieval, 2) remote sensing data pre-processing, and 3) determining spatiotemporal distributions of Chl-a concentrations using the empirical model with Landsat images from 1984 to 2021. Surface reflectance images of Lake Burdur were obtained from the Landsat-5 TM, Landsat-7 ETM+, and Landsat 8 OLI sensors. Landsat data have the longest records and the highest consistency spectrum among the current satellites to obtain any surface water quality variable successfully. Simultaneously, some cloud computing systems were set up to handle petabytes of geospatial data. GEE is an

example of a cloud-computing platform that can efficiently provide access, manage and process big data due to the capabilities of high-performance computing. All data were collected and processed on the GEE platform.

After retrieval of all images for the study period, data was pre-processed. Firstly, images were cropped to fit the image coverage to the study area, thereby reducing data processing loads. Retrieved images represent data from 1984 until the present at 16-day intervals. A total of 1275 images were accessed although not all images are usable due to cloud, ice, and other issues. GEE commands were used to calculate the Modified Normalized Difference Water Index (MNDWI) (Xu, 2006) to mask off the pixels that do not represent water body pixels. Also, pixel quality masking was performed to exclude pixels with issues that affect data accuracy and/or are affected by cloud cover or shadowing. The pixel quality is represented as an integer number stored in a separate band of the Landsat data. After masking, the remaining pixels represent the extent of the visible water body at the time of the image.

In the next step, algae concentrations were computed. Algae concentrations are typically represented as Chl-a concentrations in water. Surface reflectance data from satellite images are used to estimate Chl-a concentrations by developing an empirical model that relates surface reflectances to the unique spectral signature of Chl-a (Hansen and Williams, 2018). The empirical model equation developed by Hansen and Williams (2018) was implemented to calculate the Chl-a concentration in each image pixel over the entire 37-year dataset in GEE. This equation represents the empirical relationship between Chl-a and various band surface reflectances from Landsat image data (Eq.1 and Eq.2). Finally, Chl-a spatial distribution maps and time series charts are created with R studio 3.5.2.

The Chl-a equation applied for Landsat 5 and 7 images:

$$Chla_{5_7} = e^{(7.33 - 0.004 * B1 - 0.05 * \frac{B2}{B7} + 0.01 * \frac{B3}{B5})} \quad (1)$$

Similarly, the following Chl-a equation is applied for the Landsat 8 images:

$$Chla_8 = e^{(1.64 - 1.58 * \log(B5) - 1.69 * \frac{B3}{B4} - 0.28 * \frac{B3}{B7} + 1.28 * \log(B3))} \quad (2)$$

B1: Band 1 (Blue) SR

B2: Band 2 (Green) SR

B3: Band 3 (Red) SR

B5: Band 5 (Short Wavelength Infrared 1) SR

B7: Band 7 (Short Wavelength Infrared 2) SR

After applying these equations to each pixel of the bands in an image, Chl-a concentrations in mg/m³ are calculated for each pixel. A few outlier values comprising 16% of all data are excluded from the analysis. Finally, spatially averaged annual, seasonal, and monthly Chl-a concentrations were calculated to obtain algae concentration time series for the period 1984 to 2021. Also, the distribution of algae concentrations over the lake is evaluated by computing a median concentration for each month.

In addition, seasonal TSI values were calculated based on Chl-a concentrations (Eq.3). TSI values can be classified into three levels: oligotrophic ($TSI < 30$), mesotrophic ($30 \leq TSI < 50$), and eutrophic ($TSI \geq 50$). The TSI equation that is related to Chl-a concentration in mg/m^3 was used in this study:

$$TSI(CHL) = 9,81 * \ln(CHL) + 30,6 \quad (3)$$

3. RESULTS AND DISCUSSIONS

Interannual Variation of Chl-a Concentrations and TSI over Lake Burdur

The long-term time series of spatially averaged Chl-a concentrations and related TSI values were obtained for Lake Burdur for the period 1984 – 2021 (Figure 2). Chl-a concentrations ranged between $58.7 mg/m^3$ and $196.4 mg/m^3$ over 37 years. Relatively higher values are observed in 2010 and 2021 and lower values are observed between 1991-1993. A significant increase is evident for the period 2002-2010. While the maximum Chl-a concentration reached $130 mg/m^3$ in the first two decades of the analysis period, it reached $200 mg/m^3$ in the recent two decades. Overall, an upward trend in algae concentrations can be observed in the last 20 years, although concentration is fluctuating between years.

The highest TSI (82.40) was calculated for the year 2010 and the lowest TSI (70.55) for 1992 (Figure 2b). The TSI values indicate that Lake Burdur's hypertrophic status from 1984 to 2021 did not change over the years.

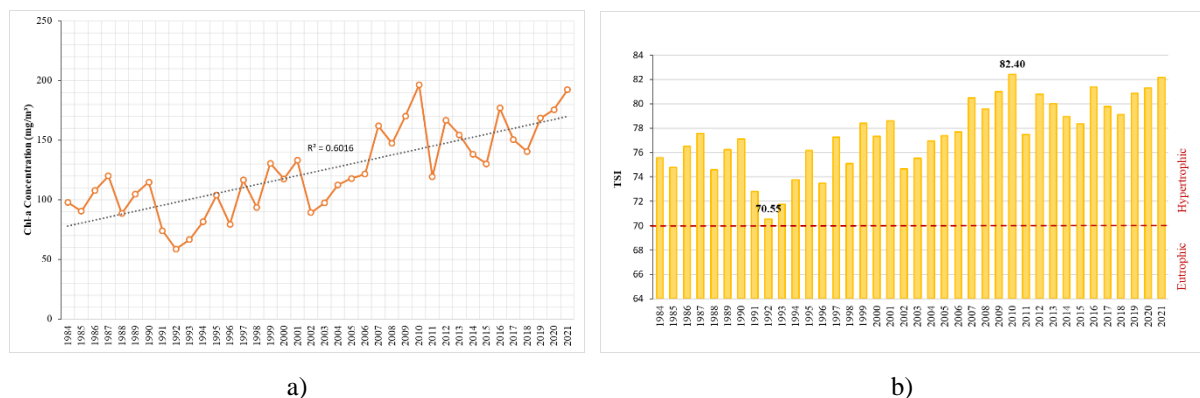


Figure 2. Interannual variation of a) Chl-a and b) TSI over Lake Burdur from 1984 to 2021

Seasonal Variation of Chl-a Concentrations and TSI over Lake Burdur

The seasonal changes in the trophic state of Lake Burdur over the past 37 years are shown in Figures 3 and 4. Seasons are defined here as the following: December–February as winter, March–May as spring, June–August as summer, and September–November as autumn. In the study period from 1984 through 2021, seasonal dynamics showed visible differences. Mostly, high Chl-a concentrations are pronounced during autumn and summer. Relatively high concentrations were observed in some years (e.g. 1997, 2010, and 2021) also for the winter months. Low concentrations are typically observed during spring. However, it is difficult to make a general conclusion about seasonal concentration patterns. In addition, the trophic state in winter is more variable than in other seasons. TSI values for spring and summer appear to be

more stable (Figure 4). According to TSI values, the lake is mostly in a hypertrophic state, except during the winter months of some years.

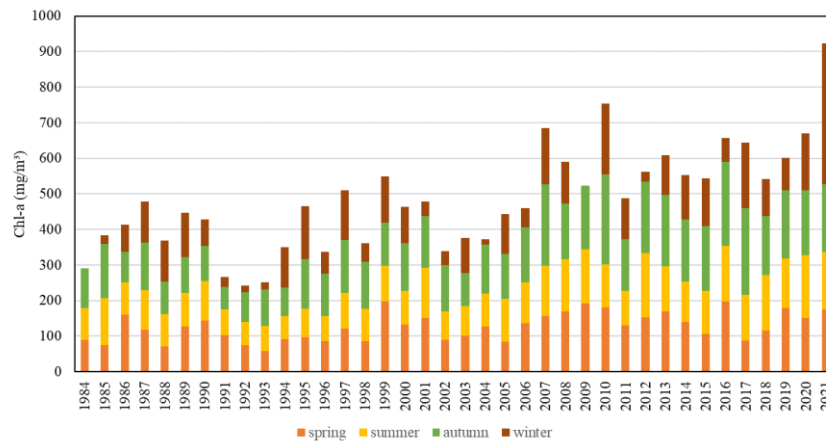


Figure 3. Seasonal variations of Chl-a concentrations for the period of 1984-2021

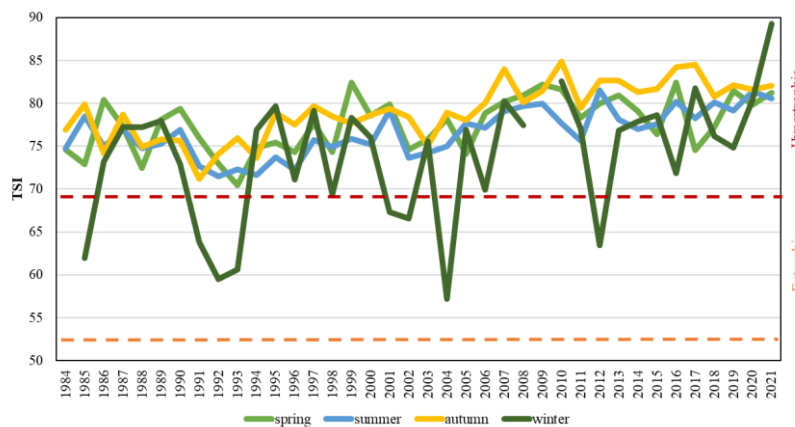


Figure 4. Seasonal variations of TSI values for the period 1984-2021

Spatial variations of multiannual monthly mean Landsat-derived Chl-a are also determined to further understand Lake Burdur's trophic state. Distribution maps of the multiannual monthly median Chl-a values from Landsat images are shown in Figure 5. Temporal variability and a fairly stable spatial distribution pattern of Chl-a concentrations can be observed. High and low concentration zones in the lake are consistent for all months. Higher algae concentration can be seen in the middle of the lake, where the lake is deep. Lower algae concentrations are typically visible in the riverine zones of the lake, where water levels are shallow and water currents more dominant than in other areas of the lake. The temporal rate of Chl-a concentration change appears to be higher in the middle of the lake compared to the nearshore areas. An explanation as to why this pattern is observed could be related to differences in lake hydrodynamics and variability of nutrient processing kinetics. More elaborate studies would be needed to reach a definite conclusion.

Figure 5 also shows that the spatial distribution patterns of temporally averaged Chl-a concentration are similar during a year. Although the Chl-a levels showed absolute differences between different months, the spatial variations displayed a similar pattern. A relatively stable and homogeneous distribution of the highest and lowest values is observed over the lake.

Median Chl-a values were highest during October and November, with Chl-a concentrations in the 450-500 mg/m³ range. Concentrations lower than 200 mg/m³ could be observed during the summer months. Overall, it appears that algae blooms in Lake Burdur are typically occurring from November to February and early spring (March) rather than during the late spring (April and May) and summer (June to August), and early fall (September).

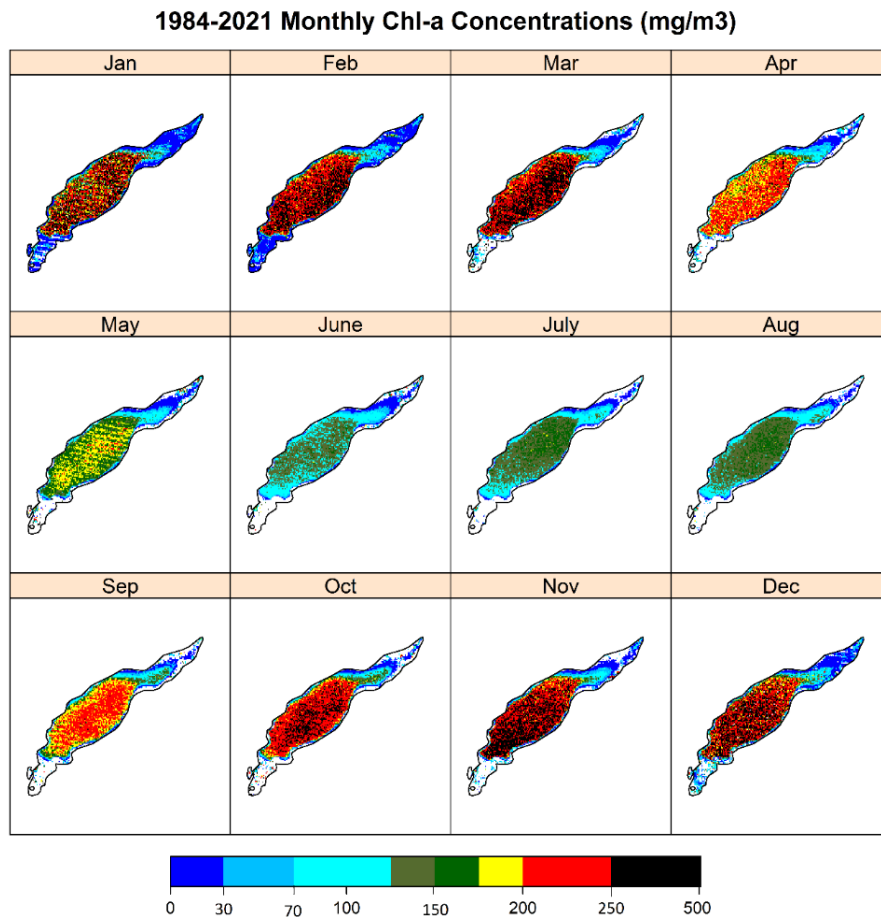


Figure 5. Spatial distribution of multi-annual monthly median Chl-a concentrations over Lake Burdur

Comparison with In-Situ Measurements

Due to the very limited availability of in-situ measurement data it was not possible to ground-truth our results. Nevertheless, the results were compared with the limited amount of measured Chl-a concentration data (Table 1) that was obtained for the years 1997 (Girgin et al., 2004) and 2018 (SGYM, 2020). All measured Chl-a concentrations reflect Chl-a content in surface water samples. Error bars for the measured concentration data were not available. It is evident that Chl-a concentrations were lower in 1997. Assuming that these concentrations are accurate results from Landsat data overestimated Chl-a levels at the lake surface. Measurements provided by SGYM (2020) show that Chl-a concentrations were significantly higher in 2018, which was partly confirmed by estimations from Landsat data. It is evident that measured concentration values for April 2018 are underestimated in the present study. It should be noted

that estimations given in Table 1 are spatially-averaged values and that concentrations over the lake area can vary considerably, as it was shown in Figure 5.

Table 1. Comparison of Chl-a concentrations with in-situ measurements in 1997 and 2018

Months	Chl-a Concentrations for the Year 1997 (Girgin et al. (2004))		Chl-a Concentrations for the Year 2018 (SYGM (2020))	
	Measured (mg/m ³)	Estimated monthly range in present study (mg/m ³)	Measured (mg/m ³)	Estimated monthly range in present study (mg/m ³)
Jan	-	-	718	66.8 – 1567
Apr	14.74	18.8 – 24.3	291	79.5 – 219
July	6.82	64.6 – 135	472	111 – 199
Oct	1.17	189	750	60.2 – 933

4. CONCLUSIONS

Long-term remote sensing-based Chl-a concentrations and related TSI datasets were obtained for Lake Burdur, Turkiye using an empirical model. A procedure is developed using GEE, and 37 years of Chl-a data is retrieved to explore the spatial-temporal patterns of algae concentrations and the evolution of eutrophication in the lake. The time series of Chl-a concentrations estimated for the period from 1984 to 2021 over Lake Burdur indicate apparent spatial-temporal differences. Spatially, higher Chl-a concentrations were observed in the middle of the lake, possibly associated with factors related to the water depth, and showed a clear decreasing gradient in nearshore regions. Further studies are needed to investigate the causes of the spatial variability of Chl-a. It is likely that anthropogenic organic carbon and nutrient influxes interacting with meteorological factors play a key role in the variability of the trophic state of the lake. From a seasonal perspective, Chl-a appeared to be higher during the late fall and winter and lower during the summer and spring. Further analysis should be performed to understand the driving factors, in particulate climate variables, affecting the trophic level by season in the lake. Also, the study can be extended to explore relationships of spatial-temporal trophic state with lake bathymetry, water temperature, point source locations and their discharge timings, and the influence of wind and temperature.

Due to the lack of an adequate data set of ground measurements, estimated Chl-a concentrations could not be verified. Therefore, the estimated concentration values might be different from actual historical concentrations although the fluctuations are expected to be consistent with actual observations. Conclusively, this non-invasive remote sensing approach can be applied also to other lakes to support strategies for effective watershed management and mitigate problems related to eutrophication.

REFERENCES

- Cao, Z., Ma, R., Duan, H., & Xue, K. (2019). Effects of broad bandwidth on the remote sensing of inland waters: Implications for high spatial resolution satellite data applications. *ISPRS Journal of Photogrammetry and Remote Sensing*, 153, 110–122.

- Cao, Z., Ma, R., Melack, J.M., Duan, H., Liu, M., Kutser, T., Xue, K., Shen, M., Qi, T., & Yuan, H. (2022). Landsat observations of chlorophyll-a variations in Lake Taihu from 1984 to 2019. *International Journal of Applied Earth Observation and Geoinformation*, 106, 102642.
- Cardall A., Tanner K., & Gustavious W. (2021). Google Earth Engine Tools for Long-Term Spatiotemporal Monitoring of Chlorophyll-a Concentrations, *Open Water Journal*, 7(1).
- Carlson, R.E. (1977). A trophic state index for lakes. *Limnology and Oceanography*, 22(2), 361–369.
- Chen, Q., Huang, M., & Tang, X. (2020). Eutrophication assessment of seasonal urban lakes in China Yangtze River Basin using Landsat 8-derived Forel-Ule index: A six-year (2013–2018) observation. *Science of the Total Environment*, 745, 135392.
- Elçi, A. (2019). Analysis of Satellite Imagery to Determine Spatial-Temporal Changes of Surface Water Bodies: A Case Study of Burdur River Basin, Turkey. In *Proceedings of the 38th IAHR World Congress, September 2019, Panama City, Panama* (pp. 840–845).
- Gao, Y., Gao, J., Yin, H., Liu, C., Xia, T., Wang, J., & Huang, Q. (2015). Remote sensing estimation of the total phosphorus concentration in a large lake using band combinations and regional multivariate statistical modeling techniques. *Journal of Environmental Management*, 151, 33–43.
- Girgin, S., Kazancı, N., & Dügel, M. (2004). On the limnology of deep and saline Lake Burdur in Turkey. *Acta Hydrochim. Hydrobiol.*, 32, 189–200.
- Gorelick, N., Hancher, M., Dixon, M., Ilyushchenko, S., Thau, D., & Moore, R. (2017). Google Earth Engine: Planetary-scale geospatial analysis for everyone. *Remote Sensing of the Environment*, 202, 18–27.
- Ha, N.T.T., Koike, K., Nhuan, M.T., Canh, B.D., Thao, N.T.P., & Parsons, M. (2017). Landsat 8/OLI Two bands ratio algorithm for chlorophyll-a concentration mapping in hypertrophic waters: An application to west lake in Hanoi (Vietnam). *IEEE Journal of Selected Topics in Applied Earth Observations and Remote Sensing*, 10, 4919–4929.
- Hansen, C.H. & Williams, G.P. (2018). Evaluating remote sensing model specification methods for estimating water quality in optically diverse lakes throughout the growing season. *Hydrology*, 5(4), 62.
- He, T., Xiao, W., Zhao, Y., Chen, W., Deng, X., & Zhang, J. (2021). Continues monitoring of subsidence water in mining area from the eastern plain in China from 1986 to 2018 using Landsat imagery and Google Earth Engine. *Journal of Cleaner Production*, 279, 123610.
- Hu, M., Ma, R., Cao, Z., Xiong, J., & Xue, K. (2021). Remote Estimation of Trophic State Index for Inland Waters Using Landsat-8 OLI Imagery. *Remote Sensing*, 13(10).
- Iwashita, K., Kudoh, K., Fujii, H., & Nishikawa, H. (2004). Satellite analysis for water flow of Lake Inbanuma. *Advanced Space Research*, 33, 284–289.
- Le, C., Zha, Y., Li, Y., Sun, D., Lu, H., & Yin, B. (2010). Eutrophication of lake waters in China: Cost, causes, and control. *Environmental Management*, 45, 662–668.
- Lee, Z., Shang, S., Qi, L., Yan, J., & Lin, G. (2016). A semi-analytical scheme to estimate Secchi-disk depth from Landsat-8 measurements. *Remote Sensing of Environment*, 177, 101–106.
- Li, Y., Zhang, Yunlin, Shi, K., Zhu, G., Zhou, Y., Zhang, Y., & Guo, Y. (2017). Monitoring spatiotemporal variations in nutrients in a large drinking water reservoir and their relationships with hydrological and meteorological conditions based on Landsat 8 imagery. *Science of the Total Environment*, 599–600, 1705–1717.
- Smith, V.H. (2003). Eutrophication of freshwater and coastal marine ecosystems: A global problem. *Environmental Science and Pollution Research*, 10, 126–139.
- SYGM (2020). *River Basin Management Plan for Lake Burdur River Basin*. General Directorate of Water Management, Ministry of Agriculture and Forestry, Ankara.
- Xu, H. (2006). Modification of normalised difference water index (NDWI) to enhance open water features in remotely sensed imagery. *Int. J. Remote Sens*, 27, 3025–3033.

EXAMINING THE USE OF GEMSTAT GLOBAL DATA SOURCE FOR A WATER QUALITY MODEL

Ismail Bilal Peker^{1}, Sezar Gülbaz¹*

¹ Istanbul University - Cerrahpaşa, Civil Engineering, Istanbul, Turkey

**Corresponding author (pekerbilal@iuc.edu.tr)*

ABSTRACT

Water quality model has an importance value to manage water resources. Soil and Water Assessment Tool (SWAT) is a hydrological and water quality model among several other software programs. SWAT is an effective ecosystem model and established tool for the studies on the water quality management. In this study, a hydrological and water quality model for the upper part of the Porsuk Basin were generated by using SWAT. In the model, the freely available instantaneous flowrate and nitrate (NO₃) data from the GEMStat portal in addition to flowrate data obtained by local institution in Turkey named General Directorate of State Hydraulics Works (DSI). The Global Freshwater Quality Database GEMStat provides a large variety of water quality data from countries worldwide. The main target of this study is to investigate the utility of GEMStat data for a water quality model. For this purpose, firstly, the SWAT model was developed by using global data sources such as SRTM for digital elevation map, CORINE for digital land use/cover map, FAO-DSMW for digital soil map. Then, the flowrate results obtained by the model were calibrated and validated for both measured data obtained from DSI and GEMStat in three different periods. Finally, the goodness of the calibration and validation results was assessed using statistical measure, including the Nash-Sutcliffe efficiency (NSE). On a daily basis, the value of NSE was 0.64 for calibration step with measured flowrate data obtained from DSI. And, the value of NSE for validation with GEMStat instantaneous flowrate data with calibrated parameters is 0.58. The model was also calibrated using GEMStat NO₃ data with a reasonable value (NSE = 0.45). Hence, the results show that GEMStat instantaneous flowrate and NO₃ data can be used as an auxiliary open-source data in the SWAT modeling process.

Keywords: *Upper Porsuk Basin, Water quality model, SWAT, GEMStat*

1. INTRODUCTION

Water quality control is very important in planning water resources and determining management strategies. Computer models are robust tools for predicting water quality in a region, but modeling in regions without data is challenging. Choosing an appropriate model and obtaining the necessary data is critical to construct a reliable model. In this scope, water quality in a region can be controlled by means of water quality models and a base is prepared for the necessary measures to be taken.

There are numerous water quality modelling tools (Ejigu, 2021, Bai et al., 2022). SWAT is an effective tool for both the water quantity and quality assessment, especially in agricultural watersheds. Costa et al. (2019) stated that SWAT is the most frequently used water quality model in the world. Besides, the supply of data required for modeling is as important as model selection. Researchers prefer to different data sources if there are no enough data measured in the region. Although physical-based (such as land use, soil type) and meteorological (such as precipitation and temperature) global data sources are accessible, it is relatively difficult to obtain measurement data on water quality. There are a few continental and global datasets such as CESI (Canadian Environmental Sustainability Indicators program), GEMStat (Global Freshwater Quality Database), GLORICH (GLOBAL RIVER CHemistry), Waterbase and WQP (Water Quality Portal) (Virro et al., 2021). Among these, the GEMStat provides datasets on water quality on several rivers in Turkey. Porsuk Stream is one of them with measurement data available on the GEMStat portal.

Studies in the Porsuk Basin (Güngör and Göncü, 2013; Celen et al., 2014; Köse et al., 2018), the researchers endeavored their own field measurements. In the present study, only free data sources that are open to access are used. Modeling was implemented by driving only freely accessible data that can be obtained from internet resources. Calibrating and testing outputs in water quality models is quite challenging. Studies on this require great effort and data archive. The aim of this study is to investigate the availability of the data on water quality provided globally, rather than to present a comprehensive water quality model. In this context, the flowrate and NO₃ obtained by the model were calibrated and validated for both DSI and GEMStat data source in three different periods. Hence, it is desirable to test the usability of GEMStat data in such a study. The signals of our results are intended to provide insight into the usability of GEMStat data in future studies.

2. MATERIAL AND METHODS

Study Area and Data

Porsuk Stream feeds the Sakarya River, which has an important water potential in Turkey. Especially the upper part of the Porsuk Basin (a part up to Eskişehir province) is used as a drinking and utility water basin (Köse et al., 2016). For this reason, it is of great importance to examine the water quality in this region in terms of the health of the ecosystems in the region.

For this study, the upper part of the Porsuk Basin is selected as the study area. The basin is located between 29°35' - 30°30' east longitudes and 38°43' - 39°38' north latitudes. The location of the basin is shown in the **Figure 1**. Upper Porsuk Basin covers an area of approximately 3,947 km². The mean elevation of the basin is 1,160 m, range between 904 and 2,184 m. Agricultural lands are dominant in the basin (about 47%). Besides, bare land (about 14%) and forests (about 13%) are the other land use classes. According to the FAO map, the soils in the basin are mostly (about 90%) Bk45-2bc coded, C group hydrological soil class.

The spatial data consists of digital elevation model (DEM), land use and soil type maps. 30 m cell sized the Shuttle Radar Topography Mission (SRTM) ([url-1](#)) data was utilized for watershed delineation and stream network process. The European Environment Agency - Coordination of Information on the Environment (EEA-CORINE) cell sized 100 m ([url-2](#)) and

the Digital Soil Map of the World (DSMW) scaled 1:5000000 by the Food and Agriculture Organization of the United Nations Educational, Scientific and Cultural Organization (FAO-UNESCO) ([url-3](#)) data were employed for generating land use and soil type, respectively. The meteorological data were gathered from global weather data derived from Climate Forecast System Reanalysis (CFSR) ([Fuka et al., 2014](#)). The available date range for this data is 1980-2013. Also, there are two flow stations on the river of upper part of the Porsuk: The first one (Station Code: E12A003) is located at the whole outlet of the basin and it has continuous discharge data at the period of 1980-2015. The second station (Station Code: D12A033) is located at the middle of the basin. The continuous discharge data of this station can be obtained between the years 1997-2006. The second station has also the discrete data for both discharge and NO₃ at the period of 1984-1987 water years. This data is gathered from monitoring indicators provided by the United Nations Environment Programme Global Environment Monitoring System (UNEP GEMStat) ([UNEP-GEMS/Water Programme, 2006](#)). Hence, the 1980-2006 time interval is selected as the modeling period.

Model Setup

The SWAT model is a physically-based, continuous and semi-distributed watershed model developed by the USDA (United States Department of Agriculture) ([Arnold et al. 1998](#); [Neitsch et al., 2009](#)). Successful applications of the SWAT model have been demonstrated by different disciplines in areas varying from field scale to basin scale, with different geographical conditions in different climatic zones throughout the world ([Gassman et al., 2007](#)).

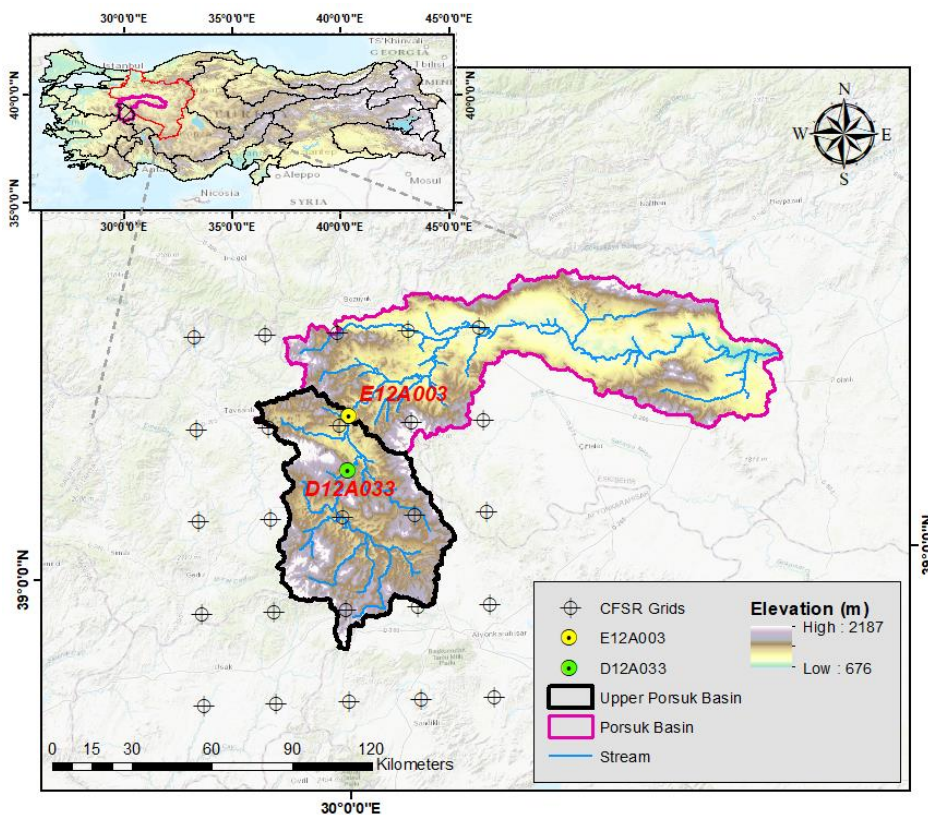


Figure1. Location of study area.

For the current study, the ArcSWAT extension is preferred for the setup the SWAT model for the Upper Porsuk Basin. Utilizing this interface used via ArcGIS, the inputs can be easily integrated into the model and it can be used in the GIS environment. In the first step, depending on the DEM, the Upper Porsuk Basin was subdivided into 20 subbasins. Then, 586 HRUs are automatically created by combining the spatial model inputs (DEM, land use and soil). Ten elevation bands were preferred. The meteorological data prepared in the appropriate format during the model period (1980-2006) can be entered into the model and the model can be run.

3. RESULTS

Flow Calibration and Validation

In the selected modeling period which is between 1980 and 2006, the simulation flowrate outputs were calibrated and validated with the data of the two stations (D12A033 and E12A003). Among these stations, the relatively more reliable one obtained from the sources provided by DSI (D12A033) was used for the calibration. The period 2002-2006, which contains the most up-to-date and continuous data, was determined as the calibration period. The other continuous period for the same station, between 1997-2000, was used in the first validation period. In addition, the continuous data of the other station coded E12A003 were run with calibrated parameters and the model was verified in the second time. Finally, another verification was realized using the instantaneous flow data for the same station gathered from GEMStat portal (D12A033-GEMStat) in the period 1984-1987 water years. In **Figure 2**, the selected calibration and validation periods are summarized.

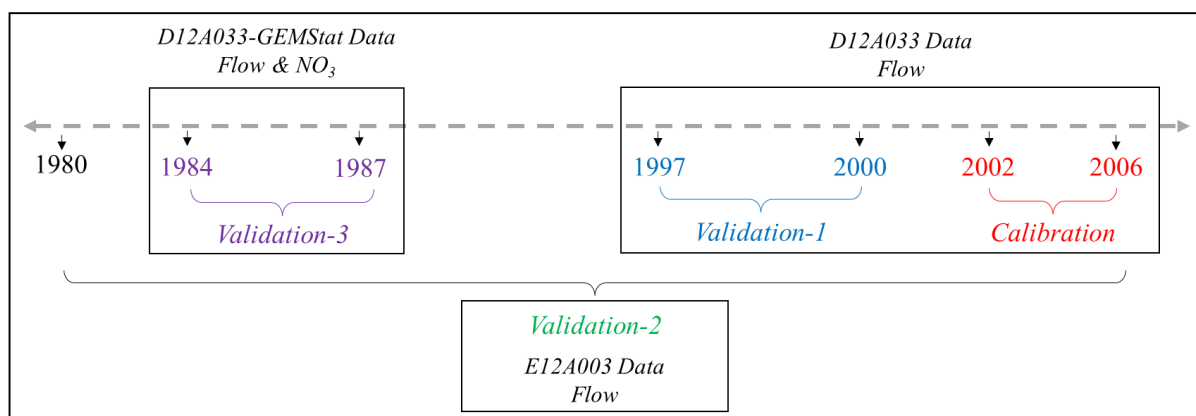


Figure 2. Calibration and validation periods.

The SWAT-CUP (SWAT-Calibration and Uncertainty Program) automatic calibration program (Abbaspour, 2012) was used to obtain optimized parameters. The SUFI-2 (Sequential Uncertainty and Fitting-version2) algorithm (McKay et al., 1979) in SWAT-CUP was preferred for calibration. As a result of the local sensitivity analysis performed manually before the calibration, 20 sensitive parameters were determined. The calibration process was utilized in daily time step and in 4 iterations with 500 simulations.

The success of the model was detected by the NSE (Nash-Sutcliffe Efficiency) value. Accordingly, the model calibration success is 0.64 and 0.44 of NSE values in calibration and

first validation periods, respectively (**Figure 3-a**). The calibrated model was also tested at a different station with the code E12A003 for a long and continuous period (1980-2006). This 26-years complete period is important in that it covers the entire time interval used in modelling. The success of the daily simulation performed here is 0.40 for NSE (**Figure 3-b**). Finally, the discrete data from station D12A033 in different time ranges were also tested to verify the calibration. The reason why these data, which were ranged in the 1984-1987 water years time period, are also used for modeling is that water quality data are also available in the same time period. In order to discuss the NO_3 outputs that will be presented in the following parts of the study, the flow data of this period should also be verified. As a result, the success of the model flow data with 50 measuring points for this period is 0.58 for NSE. The pictorial representation of the scattered points of the instantaneous flow data are given in the **Figure 3-c**. It presents a coherent trend image of measurement and simulation data in comparison. **Table 1** summarizes the NSE values according to the flow data for all periods.

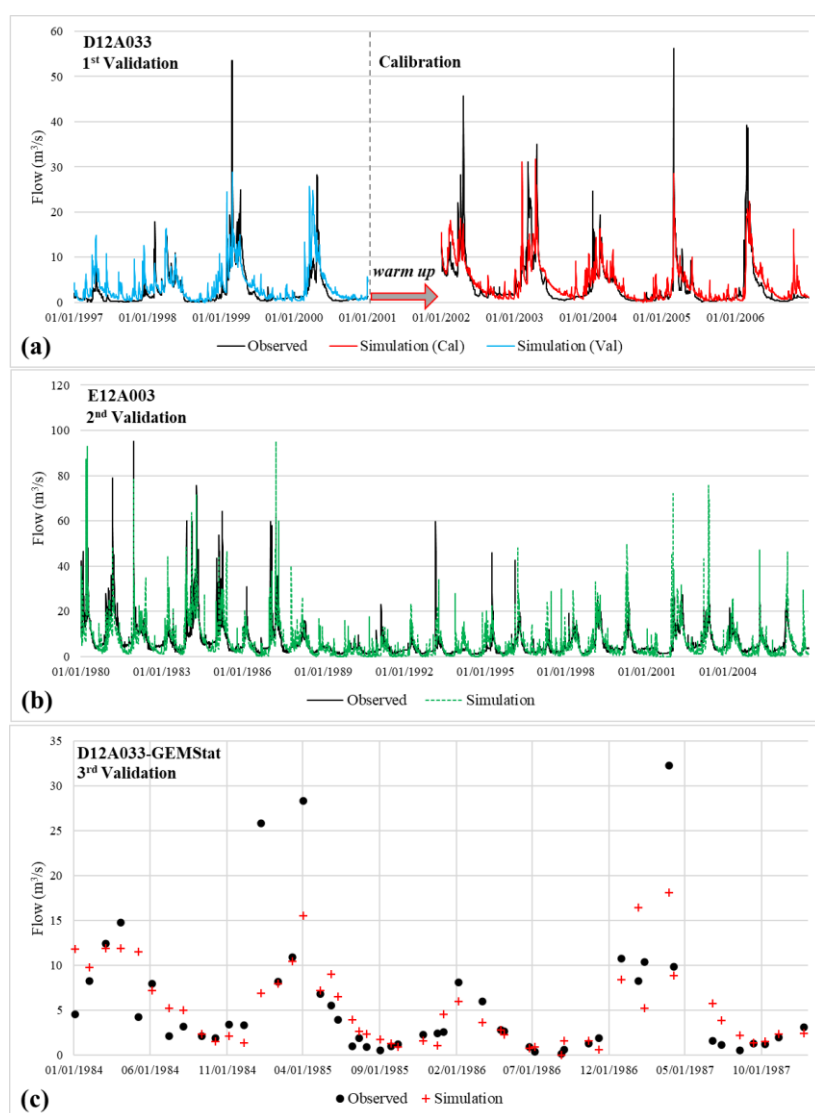


Figure 3. Hydrographs for (a) the calibration and the 1st validation, (b) the 2nd validation and (c) the 3rd validation periods.

Table 1. NSE values of the model in all periods according to the flow data.

Period	Time	Data Type	NSE
Calibration	2002-2006	Daily-Continuous	0.64
1st Validation	1997-2000	Daily-Continuous	0.44
2nd Validation	1980-2006	Daily-Continuous	0.40
3rd Validation	1980-1984 water years	Daily-Noncontinuous	0.58

NO₃ Calibration

After the flow calibration and validation process, simulation of the NO₃ data were examined. For this purpose, NO₃ data were obtained in the 1984-1987 water years period (3rd validation period) for station D12A033-GEMStat. Outputs for first impression were observed without first calibrating the water quality parameters. The NSE value is -0.25 as a poor performance.

The most effective parameters were adjusted as recommended in (Abbaspour et al., 2015) to improve performance. Four parameters were used, namely SOL_NO3, SHALLST_N, RCN and NPERCO as shown in the **Table 2**. As a result of this manual process, it was aimed to improve the NO₃ model values. As a result, the NSE value was improved to 0.45. This result can be improved by adding new parameters that may be effective and fine-tuning the four parameters tested. **Table 2** gives the information about the parameters and the calibrated values. Also, the calibrated NO₃ values are shown in the **Figure 4** comparing with measured values.

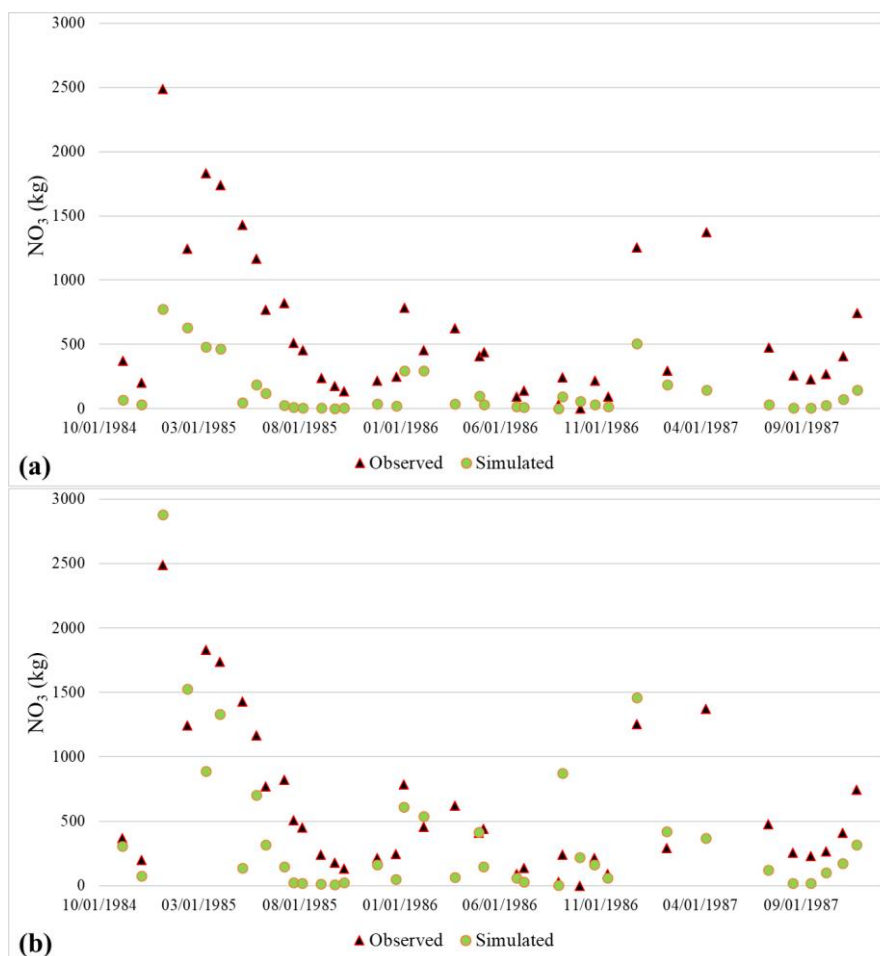


Figure 4. Observed and simulated NO₃ values (a) before and (b) after calibration

Table 2. Description for manually calibrated water quality parameters.

Parameter	Description	Unit	Default Range	Calibrated Value
SOL_NO3	Initial NO ₃ concentration in the soil layer	mg N/kg soil	0 - 100	20
SHALLST_N	Initial concentration of nitrate in shallow aquifer	mg N/L	0 - 1000	250
RCN	Concentration of nitrogen in rainfall	mg N/L	0 - 15	5
NPERCO	Nitrate percolation coefficient	unitless	0 - 1	0.7

4. CONCLUSIONS

Determining the hydrological behavior of the Upper Porsuk Basin is the important front step to assess the NO₃ outputs. For this purpose, the first step of this study was to examine the flow outputs with the basin modeling performed with SWAT. In the calibration and validation periods, the flow outputs were analyzed and the basin model was tested. Thus, a reasonable and trustable model for Upper Porsuk Basin is achieved in terms of the flow data. With this first step, a base was prepared for the water quality model. It is concluded that the NSE value, which is 0.64 in the calibration period, is lower in three validation periods, but at an acceptable level. Calibrating the NO₃ outputs was the second step of the study. Within this context, the obtained GEMStat NO₃ values were compared with the SWAT model outputs and the success of the simulation was interpreted. NO₃ values taken at 38 points (each for one day) in the 1984-1987 water years period were used. NSE value of 0.45 was obtained with manual calibration.

The scarcity of input data sets for water quality models and the difficulty of making measurements are obvious. Global or continental-scale data portals such as GEMStat assist researchers in meeting this challenge. Archiving of the data collected in the rivers is very important for the calibration and validation of water quality models. In this study, GEMStat global data was tested with SWAT as a water quality model in a basin in Turkey. Hence, NO₃ simulations could be validated with the help of a freely available data set. Our modeling results are consistent and successful. It shows that as a result of sharing the previous measurements over the internet free of charge, time and labor can be saved without re-doing the difficult field measurements for water quality models. We strongly recommend the development of open source and free data portals.

Acknowledgements: Thanks to GEMStat, an operational part of the GEMS/Water Program of the United Nations Environment Program (UNEP) for providing free data, the GEMS/Water Data Center (GWDC) within the International Center for Water Resources and Global Change (ICWRGC) in Koblenz, Germany.

REFERENCES

- (url-1) Shuttle Radar Topography Mission (SRTM) 1 Arc-Second Global doi: /10.5066/F7PR7TFT <https://www.usgs.gov/> (accessed on 29 December 2021).
- (url-2) CORINE Land Cover. *Copernicus Land Monitoring Service*; CORINE Land Cover: Copenhagen, Denmark, 2000; Available online: <https://land.copernicus.eu/pan-european/corine-land-cover> (accessed on 29 December 2021).
- (url-3) Food and Agriculture Organization of the United Nations. FAO Digital Soil Map of the World (DSMW). Available online: <http://www.fao.org/geonetwork/srv/> (accessed on 24 October 2020).

- Abbaspour, K. C., Rouholahnejad, E., Vaghefi, S., Srinivasan, R., Yang, H., Kløve, B. (2015) A continental-scale hydrology and water quality model for Europe: Calibration and uncertainty of a high resolution large-scale SWAT model. *Journal of Hydrology*, 524, 733–752. <https://doi.org/10.1016/j.jhydrol.2015.03.027>
- Abbaspour, K.C. (2012) SWAT-CUP-2012.SWAT Calibration and Uncertainty program—A User Manual. Swiss Federal Institute of Aquatic Science and Technology, Dübendorf.
- Arnold, J.G.; Srinivasan, R.; Mutiah, R.S.; Williams, J.R. (1998) Large area hydrologic modeling and assessment part I: Model development. *Journal of American Water Resources Association*, 34(1), 73–89. <https://doi.org/10.1111/j.1752-1688.1998.tb05961.x>
- Bai, J., Zhao, J., Zhang, Z. and Tian, Z. (2022) Assessment and a review of research on surface water quality modeling. *Ecological Modelling*, 466, 109888. <https://doi.org/10.1016/j.ecolmodel.2022.109888>
- Celen, M., Karpuzcu, M., Onkal Engin, G. et al. (2014) Modelling total phosphorus input pathways in the Porsuk reservoir catchment in Turkey. *Environmental Earth Sciences*, 72(12), 5019–5034. <https://doi.org/10.1007/s12665-014-3371-x>
- Costa, C.M.d.B., Leite, I.R., Almeida, A.K. et al. (2021). Choosing an appropriate water quality model - a review. *Environmental Monitoring and Assessment*, 193(1), 38. <https://doi.org/10.1007/s10661-020-08786-1>
- Fuka, D.R.; Walter, M.T.; MacAlister, C.; DeGaetano, A.T.; Steenhuis, T.S.; Easton, Z.M. (2014) Using the Climate Forecast System Reanalysis as weather input data for watershed models. *Hydrological Processes*, 28(22), 5613–5623. <https://doi.org/10.1002/hyp.10073>
- Gassman, P.W.; Reyes, M.R.; Green, C.H.; Arnold, J.G. (2007) The Soil and Water Assessment Tool: Historical Development, Applications, and Future Research Directions. *Transactions of the ASABE*, 50(4), 1211–1250. <https://doi.org/10.13031/2013.23637>
- Güngör, Ö. and Göncü, S. (2013), Application of the soil and water assessment tool model on the Lower Porsuk Stream Watershed. *Hydrological Processes*, 27(3), 453-466. <https://doi.org/10.1002/hyp.9228>
- Köse, E. , Çiçek, A. , Uysal, K. , Tokatlı, C. , Arslan, N. & Emiroğlu, Ö. (2016). Evaluation of Surface Water Quality in Porsuk Stream. *Anadolu University Journal of Science and Technology C - Life Sciences and Biotechnology*, 4(2), 81-93. <https://doi.org/10.18036/btdc.35567>
- Köse, E., Emiroğlu, Ö., Çiçek, A., Tokatlı, C., Başkurt, S., Aksu, S. (2018). Sediment Quality Assessment in Porsuk Stream Basin (Turkey) from a Multi-Statistical Perspective. *Polish Journal of Environmental Studies*, 27(2), 747-752. <https://doi.org/10.15244/pjoes/76113>
- Ejigu, M. T. (2021). Overview of water quality modeling. *Cogent Engineering*, 8(1), 1891711. <https://doi.org/10.1080/23311916.2021.1891711>
- McKay, M.D.; Beckman, R.J. and Conover, W.J. (1979) Comparison of Three Methods for Selecting Values of Input Variables in the Analysis of Output from a Computer Code. *Technometrics*, 21(2), 239–245. <https://doi.org/10.2307/1268522>
- Moriasi, D.N.; Arnold, J.G.; Van Liew, M.W.; Bingner, R.L.; Harmel, R.D. and Veith, T.L. (2007) Model Evaluation Guidelines for Systematic Quantification of Accuracy in Watershed Simulations. *Transactions of the ASABE*, 50(3), 885–900. <https://doi.org/10.13031/2013.23153>
- Neitsch, S.L.; Arnold, J.G.; Kiniry, J.R.; Williams, J.R. *Soil and Water Assessment Tool Theoretical Documentation Version 2009*; Texas Water Resources Institute: Forney, TX, USA, 2011; pp. 1–618.
- UNEP-GEMS/Water Programme (2006). UNEP Global Environment Monitoring System, Water Programme Available online: www.gemstat.org (accessed on 08 August 2022).
- Virro, H., Amatulli, G., Knoch, A., Shen, L. and Uemaa, E. (2021) GRQA: Global River Water Quality Archive. *Earth System Science Data*, 13(12), 5483-5507. <https://doi.org/10.5194/essd-13-5483-2021>

PARTICULATE PHOZZYLOGIC INDEX: TOWARDS A MORE ACCURATE AND TRANSPARENT IDENTIFICATION OF CRITICAL SOURCE AREAS TO MITIGATE PHOSPHORUS EMISSIONS

Gerold Hepp¹, Ottavia Zoboli¹, Eva Strenge¹ and Matthias Zessner^{1}*

¹ TU Wien, Institute for Water Quality and Resource Management, Karlsplatz 13, 1040 Wien,
Austria

* *Ottavia Zoboli (ozoboli@iwag.tuwien.ac.at)*

ABSTRACT

To cost-effectively mitigate the diffuse emissions of phosphorus from agricultural soils into surface waters, it is essential to identify critical source areas (CSAs) and to reduce the complexity of data-intensive fate and transport models to easy-to-use information for policy makers and water quality managers at field scale. In this context, we have developed the new Particulate PhozzyLogic Index (PPLI), by combining the results of the PhosFate model – a semi-empirical, spatially distributed P emissions and transport model - with fuzzy logic. To transform the outcome of PhosFate, namely PP loads at e.g. 10x10 m resolution, into usable information for decision makers, we calculated the total absolute PP contributions to surface waters for each field by means of zonal statistics and then applied fuzzy membership functions to such results.

The main advantage of this index is the possibility to transform the results of scenarios or even of different models into a map, which shows for all agricultural fields included in a catchment a ranking of the possibility that high PP emissions will actually reach surface waters. Further, we present an enhancement of the PhosFate model achieved by implementing a new algorithm, through which the model allocates the particulate phosphorus (PP) loads entering surface waters to their sources of origin.

Model calibration shows a Nash-Sutcliffe efficiency (NSE) of about 0.95 and a modified Nash-Sutcliffe efficiency (mNSE) of around 0.83. We have carried out a sensitivity analysis testing the impact of different factors, such as storm drains, flow directions or discharge frequencies, on the identification of CSAs. The results indicate that, despite uncertainties and potential deviations due e.g. to open furrows at field borders, the 80:20 rule (only about 20% of a watershed's area is responsible for approximately 80% of phosphorus emissions into surface waters) is largely confirmed in the study.

Keywords: *phosphorus emissions, fate model, index, field scale, fuzzy logic.*

1. INTRODUCTION

Critical source areas (CSAs) represent a fundamental concept in the field of diffuse pollution mitigation. They are defined as those areas within a watershed that contribute disproportionately to the pollution load in surface waters via one of many possible transport pathways. They are especially relevant for tackling emissions of particulate-bound pollutants, such as particulate phosphorus (PP). The goal of this contribution is to develop a novel semi-empirical “index” for PP by combining spatially distributed models, i.e. PhosFate in this case, with fuzzy logic. As a precondition to this step, it was necessary to completely redesign and improve the model's existing algorithm for allocating the PP emissions, which actually reach surface waters to their specific source areas, in a way that ensures the conservation of mass under all circumstances. Further, we conduct a sensitivity analysis to assess the impact of uncertain input data (e.g. flow directions) and model parameters (e.g. discharge frequencies) on the designation of CSAs for a case study catchment with an area of several hundred square kilometers.

2. MATERIAL AND METHODS

The study was conducted in the case study catchment of the river Pram, located in the federal state of Upper Austria, in the north-western part of Austria. This catchment was selected based on previous studies, which indicated the absolute dominance of agricultural erosion as pathway for diffuse PP emissions. The PhosFate model, a semi-empirical, spatially distributed P emissions and transport model, was originally developed by Kovacs et al. (2008, 2012) and was recently extended and improved by Hepp and Zessner (2019). In this study, PhosFate was coupled with the STREAM model (Cerdan et al., 2002a,b; Le Bissonnais et al., 2005). To transform the outcome of PhosFate, namely PP loads at e.g. 10x10 m resolution, into usable information for decision makers, we calculated the total absolute PP contributions to surface waters for each field by means of zonal statistics and then applied fuzzy membership functions to such results.

3. RESULTS AND DISCUSSIONS

Taking into consideration the range of uncertainty assessed via the sensitivity analysis, catchment-wide PP emissions into surface waters range between 8.0–8.7 Mg yr⁻¹ and 15.9–16.2 Mg yr⁻¹. The results indicate about one quarter to almost a half of all PP inputs enter surface waters via storm drains and road embankments. 96.6-98% of the PP inputs originate from arable land, while the contribution of grassland and forest soils is almost irrelevant. However, the model shows how forest soils act as important transfer zones for upstream PP loads, mainly via preferential flow pathways. Approximately 7% of the fields in the watershed are identified as part of CSAs. Figure 1 presents the final PPLI map. The fields colored in violet are the ones considered the most possible CSAs.

4. CONCLUSIONS

This study successfully developed and implemented into the PhosFate model a new algorithm for the allocation of PP emissions entering surface waters to their respective source areas. An innovative aspect of this algorithm is that in comparison to the existing one it guarantees the conservation of mass in every single cell and not only on the level of zero-order catchments. With the help of fuzzy logic, it was possible to translate the model results into a novel Phosphorus Index, which has both a sound mathematical foundation and a considerable value for management purposes. The Particulate PhozzyLogic Index (PPLI) ranks all agricultural fields of a potential large catchment with respect to their possibility of emitting high PP emissions actually reaching surface waters. Its range of possibility lies between zero (“not possible”) and one (“perfectly possible”). Possibility values of 0.5 or higher imply that a field belongs to the 20% of agricultural land responsible for 80% of the PP inputs into surface waters, which is also our definition of CSAs.

REFERENCES

- O. Cerdan, Y.L. Bissonnais, V. Souchère, P. Martin, V. Lecomte (2002a) Sediment concentration in interrill flow: Interactions between soil surface conditions, vegetation and rainfall. *Earth Surf. Process. Landforms*, 27, pp. 193-205, 10.1002/esp.314
- O. Cerdan, V. Souchère, V. Lecomte, A. Couturier, Y. Le Bissonnais (2002b) Incorporating soil surface crusting processes in an expert-based runoff model: Sealing and Transfer by Runoff and Erosion related to Agricultural Management. *CATENA*, 46, pp. 189-205, 10.1016/S0341-8162(01)00166-7
- G. Hepp, O. Zoboli, E. Streng, M. Zessner (2022). Particulate PhozzyLogic Index for policy makers—an index for a more accurate and transparent identification of critical source areas. *Journal of Environmental Management*, 307, 114514.
- G. Hepp, M. Zessner (2019) Assessing the impact of storm drains at road embankments on diffuse particulate phosphorus emissions in agricultural catchments. *Water*, 11 (2019), p. 2161, 10.3390/w11102161
- A. Kovacs, M. Honti, M. Zessner, A. Eder, A. Clement, G. Blöschl (2012) Identification of phosphorus emission hotspots in agricultural catchments. *Sci. Total Environ.*, 433, pp. 74-88, 10.1016/j.scitotenv.2012.06.024
- A.S. Kovacs, M. Honti, A. Clement (2008) Design of best management practice applications for diffuse phosphorus pollution using interactive GIS. *Water Sci. Technol.*, 57, pp. 1727-1733, 10.2166/wst.2008.264
- Y. Le Bissonnais, O. Cerdan, V. Lecomte, H. Benkhadra, V. Souchère, P. Martin (2005) Variability of soil surface characteristics influencing runoff and interrill erosion. *CATENA*, 62 (2005), pp. 111-124, 10.1016/j.catena.2005.05.001

META-RESEARCH ON NUTRIENT TRANSPORT IN SURFACE WATER AND GROUNDWATER USING A TEXT MINING ALGORITHM

Ahmed Elsayed^{1*}, Sarah Rixon¹, Christina Zeuner¹, Jana Levison¹, Andrew Binns¹, Pradeep Goel²

¹ School of Engineering, University of Guelph, Guelph, Ontario, Canada

² Ministry of the Environment, Conservation and Parks, Etobicoke, Ontario, Canada

*Corresponding author (aelsay03@uoguelph.ca)

ABSTRACT

Excessive release of nutrients (e.g., nitrogen and phosphorus) has a negative effect on environmental and human health. Elevated levels of nutrients can cause eutrophication and algal bloom formation in lakes and rivers, leading to serious threats to aquatic and human life. Therefore, quantification of nutrient transport in groundwater and surface water is essential to overcome the environmental concerns and better understand the remediation approaches. In the literature, different studies investigated nutrient dynamics in groundwater, surface water (e.g., lakes and streams), and impact of tile drains on nutrient transport. However, these studies were diverse because of the variety of the case studies and their surrounding conditions (e.g., metrological and hydrogeological conditions). There are numerous factors that can affect nutrient transport in surface and subsurface water. For example, soil characteristics, watershed size and land use activities (e.g., agricultural management practices) are unique characteristics for each watershed. Therefore, meta-research (research on research) is an effective technique to quantify the most significant topics related to nutrient transport in surface water and groundwater and identify current research trends and potential research challenges/gaps. This can be achieved through applying text mining algorithms and developing a systematic literature review. Meta-research can also be implemented to determine the main knowledge gaps in the field of nutrient dynamics in surface water and groundwater. Meta-research can also illuminate the most important factors that govern nutrient transport in surface water and groundwater.

In the current study, meta-research was implemented to extract the meaningful information and trends from previous studies related to nutrient dynamics in groundwater and surface water through a two-step analysis (i.e., quantitative and qualitative). In addition, a systematic literature review was constructed through applying topic modeling and text analysis on the abstracts (i.e., text dataset) of these studies. In the quantitative analysis, a text mining algorithm was used to determine the most frequently examined topics in the literature while these topics were comprehensively investigated in a qualitative analysis to highlight the strengths and weaknesses in these studies. Accordingly, more than 700 publications related to nutrient transport in surface and subsurface water were gathered to perform a meta-research approach on their abstracts. Following data processing, Latent Dirichlet Allocation (LDA), a text mining algorithm, was deployed on the text dataset to determine the most important topics covered in the literature. Also, different research gaps were illuminated based on the absence of these topics in the results of topic identification by the text mining algorithm and meta-research. The insights of the quantitative analysis can be used to define the knowledge gaps that should be investigated in future studies while the results of the qualitative analysis can be used as a

reference for the most important topics that were published in the field of nutrient transport processes in surface water and groundwater.

ASSESSMENT OF RUSLE'S COVER MANAGEMENT SUB-FACTORS FOR UNIDENTIFIED URBAN LAND-USE CLASSES

A. Eljamassi¹; O. Dawoud²; M. Davud³

¹ Associate Professor, Faculty of Engineering, Islamic University of Gaza, Gaza, Palestine.

ajamassi@iugaza.edu.ps

² Assistant Professor, Civil Engineering Department, Istinye University, Istanbul, Turkey

osama.dawoud@istinye.edu.tr

³ Assistant Professor, Software Engineering, Istanbul Sabahattin Zaim University, Istanbul, Turkey

muhammed.davud@izu.edu.tr

ABSTRACT

Insufficient resources can be found which guide the parameterization of the sub-factors of the cover management component of RUSLE for urban land-use classes. The current study investigates inclusion of the cover management sub-factors of unidentified urban land-use classes in the calibration process of a RUSLE-SDR model. The original form of the model assigned the magnitude of 0.5 for both of the unidentified classes which are in “developed” and “urbanized” zones. The current study conducted a sensitivity analysis of the two sub-factors. The model is tested for the behavior of the error of estimated delivered sediments at three different regions in the study area where field measurements were conducted. Results showed that the overall error in model estimations is sensitive to these sub-factors. The relaxation of the model and involvement of the sub-factors in the calibration process was found effective in approaching the most accurate global solution. This study paves the road for integrating different computational techniques that overcomes the uncertainty involved in parameterization of RUSLE-SDE models.

Keywords: *Urban Areas, RUSLE, Cover Management Factor*

Introduction

Cover management factor (C) is an essential component of the Revised Universal Soil Loss Equation (RUSLE) [1]. However, insufficient studies tackled the C-factor magnitudes for urban land-use classes [2]. The original concept of RUSLE was developed for estimation of the sediment's generation potential in arable lands or those of natural green cover [3]. However, the impact of the sediments erosion and deposition in poorly-developed regions necessitates through investigation of characterization techniques. Different approaches were employed aiming at enhancing prediction of the C-factor for urbanized land-use classes [4], [5].

The current study investigates parametrization of Cover management (C) sub-factor for unidentified urban classes in Gaza Governorate in Palestine. A GIS-based RUSLE that has been developed for mapping and characterization of the soil erosion and deposition in the governorate was used by the current study. The hydrological watersheds under concern involve a variety of land-use classes that has been assigned a C-factor guided by reference magnitudes from literature [6]. Accumulated sediments were measured at three stormwater detention and infiltration basins: Asqula, Sadaqa, and Shiekh Radwan for the years from 2018 to 2020. Each one of these three basins serve as the final drainage point for three watersheds highlighted in the *figure 1*. The data were used to validate a RUSLE model that was prepared by another study. The unidentified areas were classified

into two classes for the C-factor, which are: C1 and C2. The classification was based on the land-use map which identified the “urbanized” and “developed” zones. The current study investigates inclusion of those two factors into calibration process for the purpose of enhancing the accuracy of the model predictions.

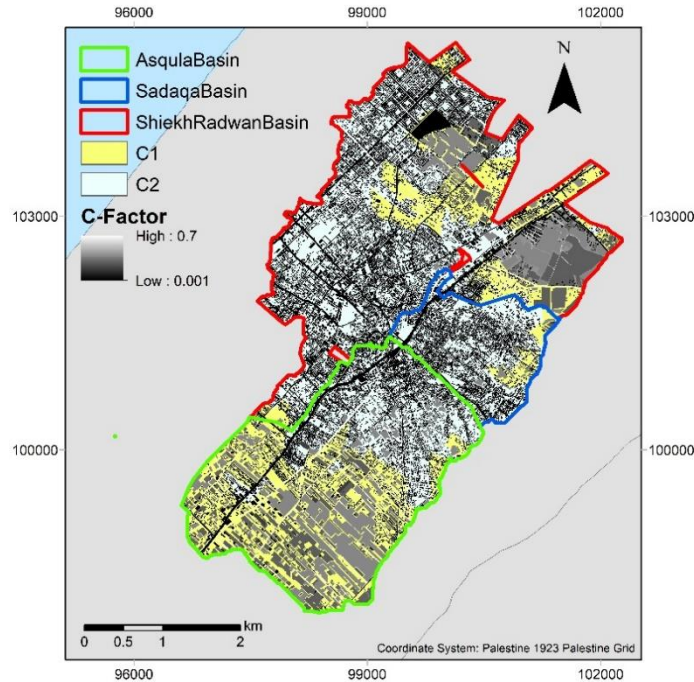


Figure1. A map of the study area. C1 and C2 shaded zones refer to the unidentified areas in the developed and the urbanized zones, respectively

Methodology

The Revised Universal Soil Loss Equation was employed as follows [1]:

$$A = R \times K \times LS \times C \times P \quad (1)$$

where, A is the soil loss ($t \text{ ha}^{-1}\text{yr}^{-1}$); R is the rainfall erosivity factor ($\text{MJ mm ha}^{-1}\text{h}^{-1}$); K is the soil erodibility factor ($\text{ton ha h MJ}^{-1}\text{mm}^{-1}$); L is the slope length factor; S is the slope steepness factor; C is the cover and management factor; P is the support and conservation practices factor.

The connectivity index developed by was employed, as follows [7]:

$$IC = \log_{10} \frac{\bar{C}\bar{S}\sqrt{A}}{\sum_i \frac{d_i}{C_i S_i}} \quad (2)$$

where, \bar{C} and \bar{S} are the average C-factor and slope gradient (m/m) for the upslope contributing area. d_i is the length of the flow path along the i^{th} cell according to the steepest downslope direction (m).

For the calculation of the sediments delivery ratio, the equation was used as follows [8]:

$$\text{SDR} = \frac{0.8}{1 + \exp\left(\frac{IC_0 - IC_i}{k}\right)} \quad (2)$$

Where IC_0 and k are calibration factors.

The model was automated such that it iterates for C_1 , C_2 . Data were used to conduct a sensitivity analysis of the cover-management sub-factors. Thereafter, the data was used to investigate the optimal combination of the two factors that attain the minimal residual.

Results

A sensitivity analysis for the two C_1 and C_2 factors was conducted fixing the SDR calibration parameters k and IC_0 at their magnitudes 1.0 and 3.0 which were calibrated based on the basic assumptions for the cover

management sub-factors. The analysis conducted by fixing one of the sub-factors at the average value, which is 0.5 since the C-factors ranges between 0 and 1 and iterating over this margin for the other factor in a change of $\pm 20\%$ of the total margin. The change in model estimations for the three basins are shown in **Error! Reference source not found.** for C1 and C2 respectively. The zero value was avoided expressing it as 0.001 to avoid error in calculation of the SDR.

Results showed differential sediments' yield from each one of the three basins in response to the changes tested parameters. Asqula basin was found highly sensitive to the changes to C1 that exceeded 100% change. In contrary, Asqula was the least sensitive basin to the changes in C2, where the maximum change did not exceed 10%. On the other hand, Shiek Radwan showed 115% increase in estimated yield when C2 was increased up to 1.

For every observation point, Equation 2 provide a solution function of IC and k. **Error! Reference source not found.** show a set of these functions for tested values of C1 and C2. These figures were developed by iterating for k and IC for each combination of C1 and C2 magnitudes. Although the process was automated, it was time consuming and required high computational resources. A set of selected magnitudes are published in the current paper for demonstration purposes.

Since each line of these represent the solution function for a single basin, the global solution is where all these functions intersect. However, due to the uncertainty involved in preparation of the RUSLE model, the global solution is considered at the point that represent the least standard deviation, as shown in **Error! Reference source not found.**. The least standard deviation would emerge in the least total residual for the model estimations.

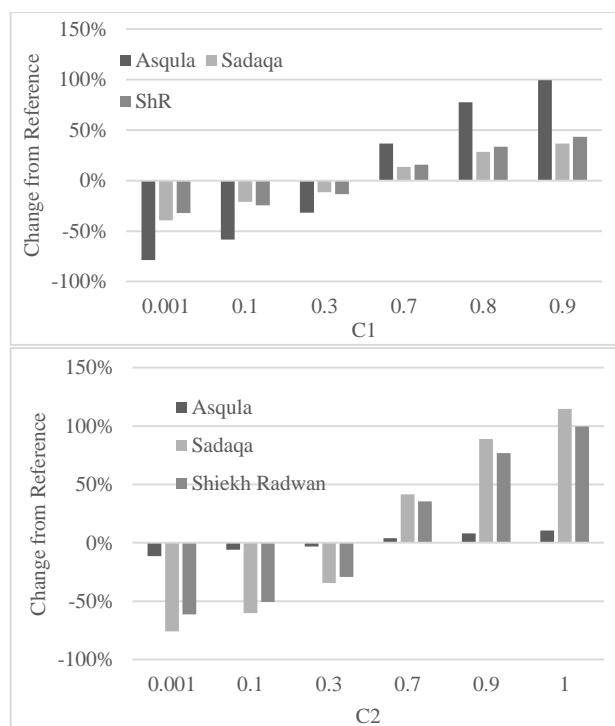


Figure2: Sensitivity Analysis of the RUSLE-SDR model for C1 and C2 for the year 2019. Reference is the model estimations at C1=C2=0.5

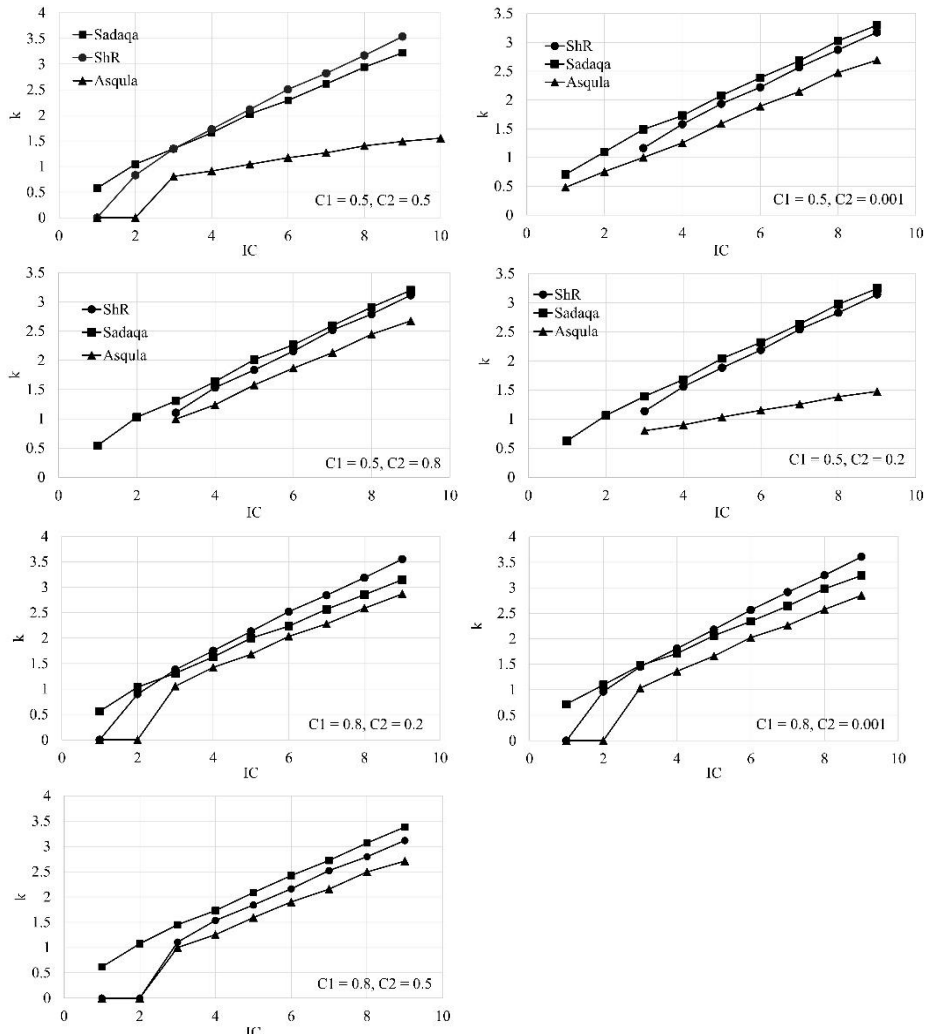


Figure3: Influence of C1 and C2 on solution Functions for the RUSLE-SDR model for the year 2019

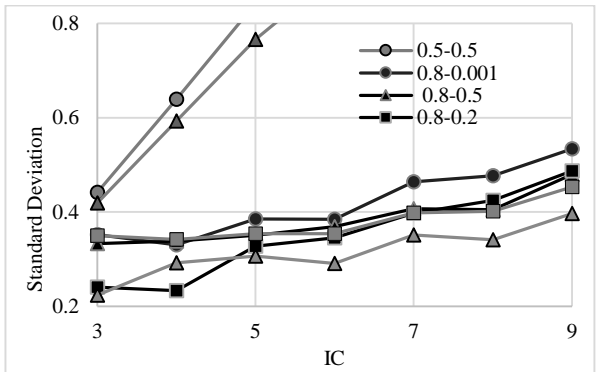


Figure4: Standard deviation of the solution functions

Discussion

The cover management factor was tested within the range of 0.001-1.0. The zero magnitude was avoided as it physically represents a sink or a sediments trap, which is not the case for the impervious surfaces. Therefore, the zero value was assigned to the soil erodibility factor instead. The zero value was also avoided as it produces erroneous results for the employed SDR model.

Error! Reference source not found. shows a highly differential sensitivity for each basin. Also, the sensitivity as found to be highly affected by the land-use characteristics for each basin. This indicates that the modelers should avoid any rough or arbitrary assumptions regarding the cover management factor.

This can also be concluded investigating the solution functions shown in **Error! Reference source not found.** They showed that the selected reference condition of $C1=C2=0.5$ does not provide the best global solution; and altering $C2$ towards 0.001 or 0.8 provided better proximity of the solution function to each other.

In general, setting $C1$ as 0.8 provided better global solution, as one can notice that the lines representing the solution function are approaching each other.

When plotting the standard deviation of the function magnitudes for different IC values, the highest standard deviation was noticed for the two cases when $C1=0.5$, and $C2=0.5$ and 0.2. In fact, such conditions are not matching the land-use conditions since $C1$ covers “developed” zones, and $C2$ cover the “urbanized” zones.

All results provided better solution compared to the one acquired by the reference condition (i.e. $C1$ and $C2$ were set to the average value of 0.5). The condition to provide the standard deviation is $C1=0.5$, and $C2=0.8$. Apparently, this assumption is not valid as it indicates higher sediments yield from urbanized regions compared to the developed regions. Thus, they were not considered despite they provided the lowest standard deviation.

Therefore, it can be inferred that the RUSLE-SDR model would achieve the least residual of the estimated global solution at the condition where $C1=0.8$, and $C2=0.2$. This is also available when IC is 4.0, and $k=1.64$.

The automated analysis is a time-consuming and computational resources. However, better results can be achieved densifying the incremental investigation of parameters. This can be also enhanced by applying different computational algorithms in the seek of the optimal solution.

The current study emphasized the critical consequences involved in the arbitrary assumption of cover management factors. It also showed that involving the sub-factors, which has no guiding reference, in the calibration process would provide more precise solutions.

Conclusions

Results showed that the arbitrary assumptions of no cover management by applying maximum magnitude of 1.0, average value of 0.5, or no-erosion condition of zero value is a critical common practice that emerges in overestimation or erroneous results for the generated sediments; and thus, this assumption should be carefully employed considering other human practices which are not explicitly implemented for sediments generation control. On the other hand, the zero magnitude that was assumed for specific land-use classes is not physically reasonable, and adversely affect the subsequent calculations for the sediment’s delivery ratio and sediments deposition.

The current study showed that the estimation of erosion is very sensitive to the cover management factor of bare (or undeveloped) lands existing in urbanized areas and developing areas. This urges the planners to carefully collate the cover management sub-factors into classes, and to seek the best parameterization possible. As demonstrated by the current study, considering this sub-factor in the calibration enhances the ability to approach a more precise global solution based on the local observation points.

Future research is recommended to develop an automated model for calibration of the RUSLE-SDR model involving all uncertain sub-parameters in addition to the regular k and IC calibration parameters. This model is advised to be applied to the

References

- [1] K. G. Renard, G. R. Foster, G. A. Weesies, D. K. McCool, and D. C. Yoder, Eds., *Predicting soil erosion by water: a guide to conservation planning with the revised universal soil loss equation (RUSLE)*. Washington, D. C, 1997.
- [2] M. Tshikeba Kabantu, R. Muamba Tshimanga, J. M. Onema Kileshye, W. Gumindoga, and J. Tshimpampa Beya, “A GIS-based estimation of soil erosion parameters for soil loss potential and erosion hazard in the city of Kinshasa, the Democratic Republic of Congo,” 2018, vol. 378, pp. 51–57. doi: 10.5194/piahs-378-51-2018.
- [3] W. H. Wischmeier and D. D. Smith, *Predicting rainfall erosion losses: A guide to conservation planning*. Washington, D.C., U.S.: United States Department of Agriculture, 1978.
- [4] S. Pandey, P. Kumar, M. Zlatic, R. Nautiyal, and V. P. Panwar, “Recent advances in assessment of soil erosion vulnerability in a watershed,” *Int. Soil Water Conserv. Res.*, Mar. 2021, doi: 10.1016/j.iswcr.2021.03.001.
- [5] H. P. Guy, “Sediment problems in urban areas,” U.S. Geological Survey, Reston, VA, USGS Numbered Series 601-E, 1970. doi: 10.3133/cir601E.
- [6] P. Panagos *et al.*, “Reply to the comment on ‘Rainfall erosivity in Europe’ by Auerswald *et al.*,” *Sci. Total Environ.*, vol. 532, pp. 853–857, Nov. 2015, doi: 10.1016/j.scitotenv.2015.05.020.
- [7] L. Borselli, P. Cassi, and D. Torri, “Prolegomena to sediment and flow connectivity in the landscape: A GIS and field numerical assessment,” *CATENA*, vol. 75, no. 3, pp. 268–277, Nov. 2008, doi: 10.1016/j.catena.2008.07.006.
- [8] O. Viggiak, L. Borselli, L. T. H. Newham, J. McInnes, and A. M. Roberts, “Comparison of conceptual landscape metrics to define hillslope-scale sediment delivery ratio,” *Geomorphology*, vol. 138, no. 1, pp. 74–88, Feb. 2012, doi: 10.1016/j.geomorph.2011.08.026.

MODELLING POTENTIAL IMPACTS OF CLIMATE CHANGE ON HEAVY METAL TRANSPORT IN DRAINAGE BASINS

Kamil Çöllü¹, Muhammed Aslan², Zeynep Akdoğan^{1*}, and Başak Güven¹

¹. Institute of Environmental Sciences, Boğaziçi University
34342 Istanbul, Turkey

². Civil Engineering Department, Boğaziçi University
34342 Istanbul, Turkey

*Zeynep Akdoğan (zeynep.akdogan@boun.edu.tr)

ABSTRACT

Modelling approaches have become necessary for better understanding of the links between climate-related drivers and pollutant transport to evaluate climate change impacts on water resources. This study aims to investigate the effect of future climate change on heavy metal loads in selected areas of the Marmara Region, Turkey between the years 2022 and 2049. For this purpose, surface runoff and soil moisture content of each selected area for 10 km resolution is estimated via Regional Climate Model (RegCM4) with Representative Concentration Pathway 4.5 (RCP 4.5) scenario using Max Planck Institute (MPI) dataset. The model is validated comparing the surface runoff values obtained by Rational Method and RegCM4 for the years 2006 and 2007. Finally, loads of heavy metals including Copper (Cu), Nickel (Ni) and Zinc (Zn) are simulated via MATLAB for the years from 2022 to 2049 using previously analyzed soil samples collected from the 8 different lands of the Marmara Region. The simulation results reveal that Zn has the greatest load values, especially in Kandıra, because of having the highest concentrations in soil. According to the RCP 4.5 scenario results, an increasing trend for the heavy metal loads is observed from the year 2022 to 2049.

Keywords: *Climate change, Heavy metals, Load, Surface runoff.*

1. INTRODUCTION

Future climate change is a significant environmental challenge, which has an interaction with land use changes. High population density and associated rapid growth of urbanization, industrialization and agriculture have become important drivers of increased number of contaminants in the environment. These contaminants affect the water quality and human health by being transported to surface and ground waters via runoff, which is highly affected by soil structure, climate and topography. Agricultural runoff has been identified as a critical nonpoint source of pollution, which transports some emerging contaminants, such as persistent organic pollutants (Bhaduri et al., 2000).

Heavy metal contamination in the environment is a major concern due to their toxicity, persistence, bioaccumulation potential, and resulting ecological risks to biota (Guo et al., 2015; Zhang et al., 2018). Certain heavy metals such as copper, lead and zinc are more soluble in water than others, and industrial and commercial land uses are the greatest contributors of those into the runoff (Reddy et al., 2014). This study aims to investigate the effect of future climate

change on heavy metal loads in selected areas of the Marmara Region, Turkey between the years 2022 and 2049. For this purpose, runoff production and soil moisture content of each selected area for 10 km resolution is estimated by the Regional Climate Model (RegCM4) with Representative Concentration Pathway 4.5 (RCP 4.5) scenario using Max Planck Institute (MPI) dataset. Transport of Copper (Cu), Nickel (Ni) and Zinc (Zn) from soil to surface runoff is predicted using initial concentrations of these metals in soil. Finally, heavy metal loads are simulated for the years from 2022 to 2049.

2. MATERIAL AND METHODS

Study Area

Marmara Region is situated in the northwest of Turkey with an area of 67000 km² approximately. Precipitation averages about 600-700 mm annually and mainly falls between November and January. Average annual temperature is between 14°C and 16°C and the mean monthly temperatures range from 5°C in the coldest months to 25°C in warm seasons (Munsuz and Ünver, 1999). Land use activities in the region mainly include residential, industrial and agricultural practices. Study area and sampling stations are given in Figure 1.

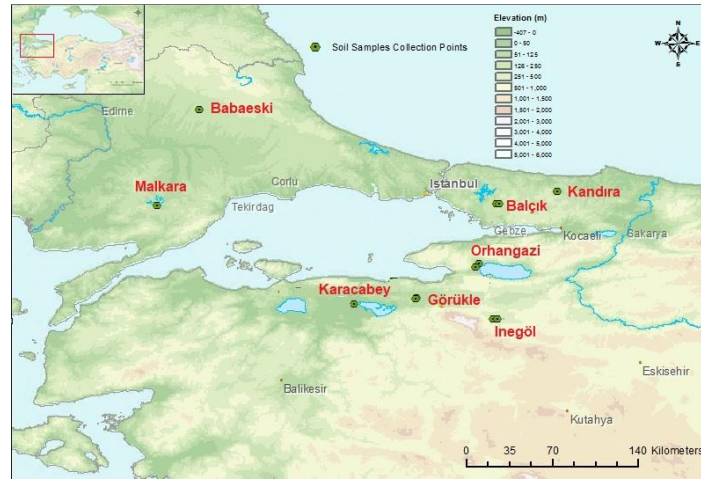


Figure 1. Study area and soil samples collection stations.

Model Description and Data Requirements

Surface runoff and soil moisture content of each selected area for 10 km resolution is obtained via RegCM4 with RCP 4.5 scenario using MPI dataset for the years 2022 to 2049. RCP 4.5 is a scenario that stabilizes radiative forcing at 4.5 W m⁻² in the year 2100 without ever exceeding that value. Transport model is developed using agricultural soil samples collected from 8 different areas (Figure 1) analyzed for metal concentration and soil characteristics (soil texture, pH, organic carbon and moisture content) (Balcıoğlu et al., 2007). Kinetic model equations are used in estimation of Cu, Ni and Zn concentrations in pore water and runoff (Montforts, 1999). In this study, soil partition coefficients of metals (K_p , m³ kg⁻¹) are obtained from the literature (US EPA, 2005). Subsequently, K_{sw} (m³ m⁻³) partition coefficients between soil and water for each heavy metal are calculated by equation 1.

$$K_{sw} = F_{ws} + (F_{ss} \times K_p \times \rho_{solid}) \quad (1)$$

where F_{ws} is fraction water in soil (m³ m⁻³), F_{ss} is fraction solids in soil (m³ m⁻³), and ρ_{solid} is density of soil solids (kg m⁻³). These parameters are estimated in MATLAB using the measured

data including mass of soil samples (M_s , kg) and fresh bulk density of soil (ρ_{soil} , kg m⁻³) (Balcioğlu et al., 2007) and simulated data, F_{ws} , obtained from RegCM4. Data requirements and algorithm of the model are shown in Table 1.

Predicted Environmental Concentrations of heavy metals in pore water (PEC_{pw}) (g m⁻³) transported from contaminated soil are found as below:

$$PEC_{pw} = \frac{MEC_s \times \rho_{soil}}{K_{sw}} \quad (2)$$

where MEC_s is Measured Environmental Concentration in the soil samples (g kg⁻¹), and ρ_{soil} is fresh bulk density of soil (kg m⁻³). Fraction of metals not adsorbed to soil particles, but existing in the soil water is transported to runoff water by precipitation. It is assumed that predicted metal concentration in runoff (PEC_r) (g m⁻³) is equal to PEC_{pw} diluted by one order of magnitude:

$$PEC_r = \frac{PEC_{pw}}{10} \quad (3)$$

Loads of heavy metals (g s⁻¹) are estimated by equation 4:

$$Load = Q \times PEC_r \quad (4)$$

where Q is the surface runoff (m³ s⁻¹).

The calculation of heavy metal loads is carried out using MATLAB as modelling environment.

Table 1. Data requirements for heavy metal transport modelling.

Data Type	Unit	Source
Mass of soil sample (M_s)	kg	Observed (Balcioğlu et al., 2007)
Bulk density of soil (ρ_{soil})	kg m ⁻³	Observed (Balcioğlu et al., 2007)
Measured Environmental Concentration of heavy metals in soil (MEC_s)	g kg ⁻¹	Observed (Balcioğlu et al., 2007)
Partition coefficients of heavy metals between soil and water (K_p)	m ³ kg ⁻¹	US EPA, 2005
Surface runoff (Q)	m ³ s ⁻¹	Simulated (RegCM4)
Soil moisture content (F_{ws})	m ³ m ⁻³	Simulated (RegCM4)

The validation of the climate model is undertaken based on the simulated runoff and the estimated values of Rational Method for the years 2006 and 2007. For this purpose, surface runoff and soil moisture content of each area for 10 km resolution is simulated via RegCM4 with RCP 4.5 scenario. Moreover, time series precipitation data for the years 2006 and 2007, topographical data, and land use information for the selected areas are entered to Storm Water Management Model (SWMM) to estimate the surface runoff values via Rational Method. Despite primarily use for urban areas; in this study, SWMM is preferred because of its convenience to clearly simulate surface runoff and operate with spatial interface. The map of the study area is transferred to SWMM and divided into manageable Hydrological Response Units (HRUs) for 10 km resolution to enter the input data. Meteorological data providing daily precipitation for each sampling station is obtained from the Turkish State Meteorological

Service. Slope of each selected area are obtained from Geographical Information Systems (GIS). Moreover, the percent imperviousness (% *I*) data are determined via land use and cover data of the year 2015, which is derived from the GIS-based maps, obtained from Republic of Turkey Ministry of Food, Agriculture and Livestock. % *I* for all HRUs are estimated using runoff coefficients corresponding to three land use classes; commercial, residential and agricultural lands (US EPA, 2009). SWMM applies Rational Method for each HRU using runoff coefficients produced by the model to establish a relationship between time-series precipitation and surface runoff (equation 5).

$$Q = C \times i \times A \quad (5)$$

where *C* is the runoff coefficient produced by SWMM, *i* is the daily precipitation (mm d⁻¹), and *A* is the area (m²). Estimated runoff values of rational method and RegCM4 are compared to demonstrate the model validation.

3. RESULTS AND DISCUSSIONS

Model validation results are given in Figure 2.

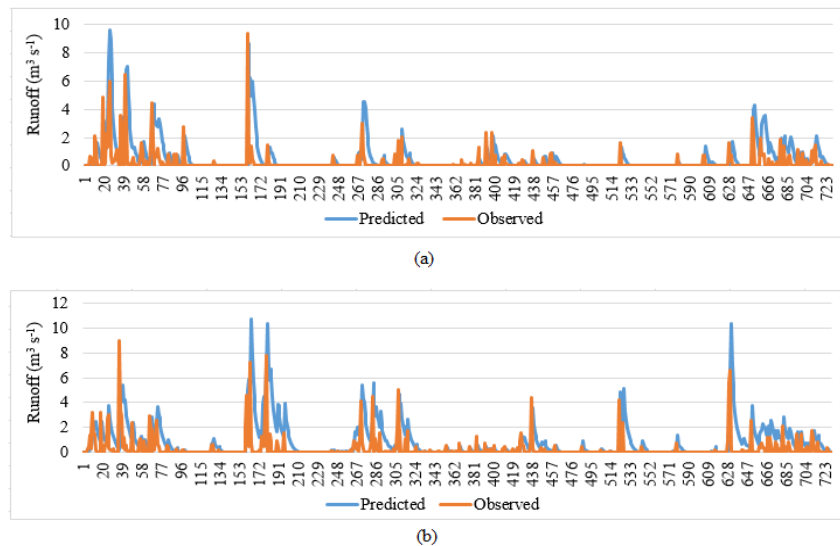


Figure 2. Model validation results for (a) Karacabey and (b) Görükle stations.

The monthly load of heavy metals is simulated via MATLAB for the years 2022, 2030, 2040 and 2049. The model outcomes are given for Cu (Figure 3), Ni (Figure 4) and Zn (Figure 5), respectively.

Although Zn has an average K_p (0.501 m³ kg⁻¹) amongst the other heavy metals, it has the greatest load values, especially in Kandıra. On the other hand, despite the smallest K_p (0.316 m³ kg⁻¹), which means the lowest sorption capacity in the soil, Cu has the lowest load in some locations of the region, such as Karacabey and Orhangazi. These results are attributed to differences between MEC_s , which are more effective than K_p in release of heavy metals to runoff and subsequent loads to outfall in the present study. In addition to initial concentrations in soil, transport of heavy metals to receiving waters depends on the rainfall intensity and runoff volume during the rainfall period. According to the RCP 4.5 scenario results, there is an increasing trend for the heavy metal loads from the year 2022 to 2049. The simulation outcomes demonstrate that the monthly load of Cu, Ni and Zn reaches its maximum in November and

December, while the lowest load is observed in July and August. These results reveal that rainfall intensity increase the release of contaminants into surface runoff.

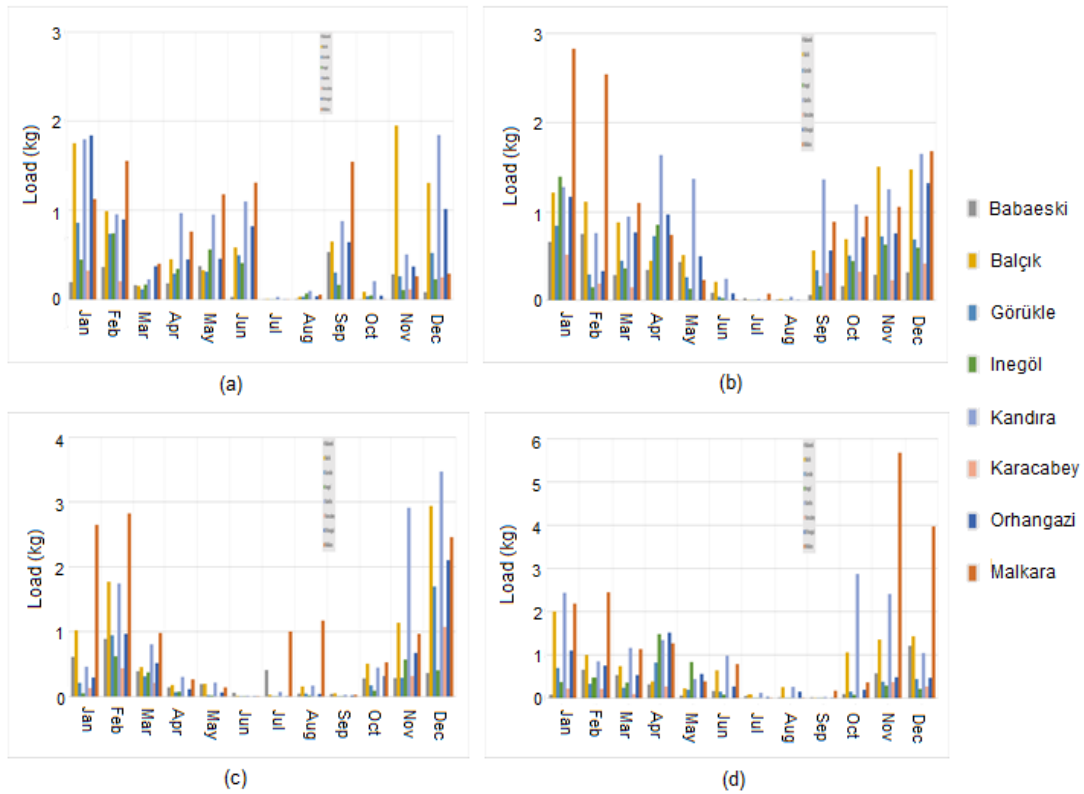


Figure 3. Monthly load of Cu for the years (a) 2022, (b) 2030, (c) 2040 and (d) 2049.

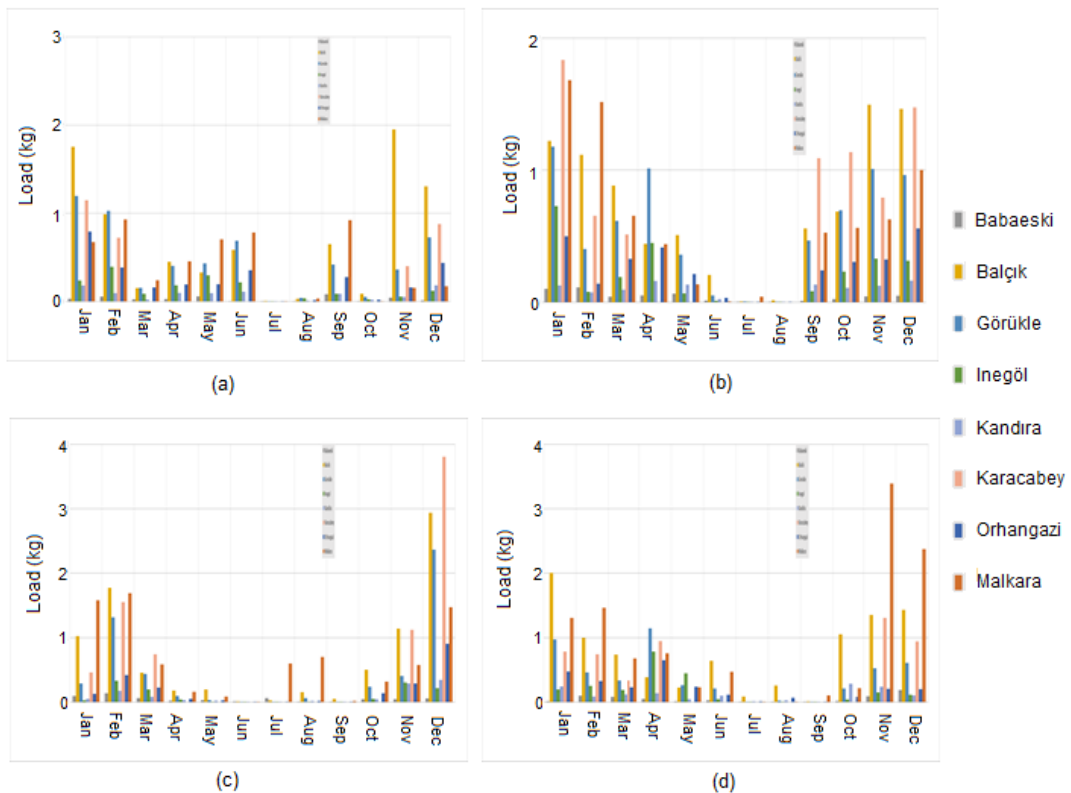


Figure 4. Monthly load of Ni for the years (a) 2022, (b) 2030, (c) 2040 and (d) 2049.

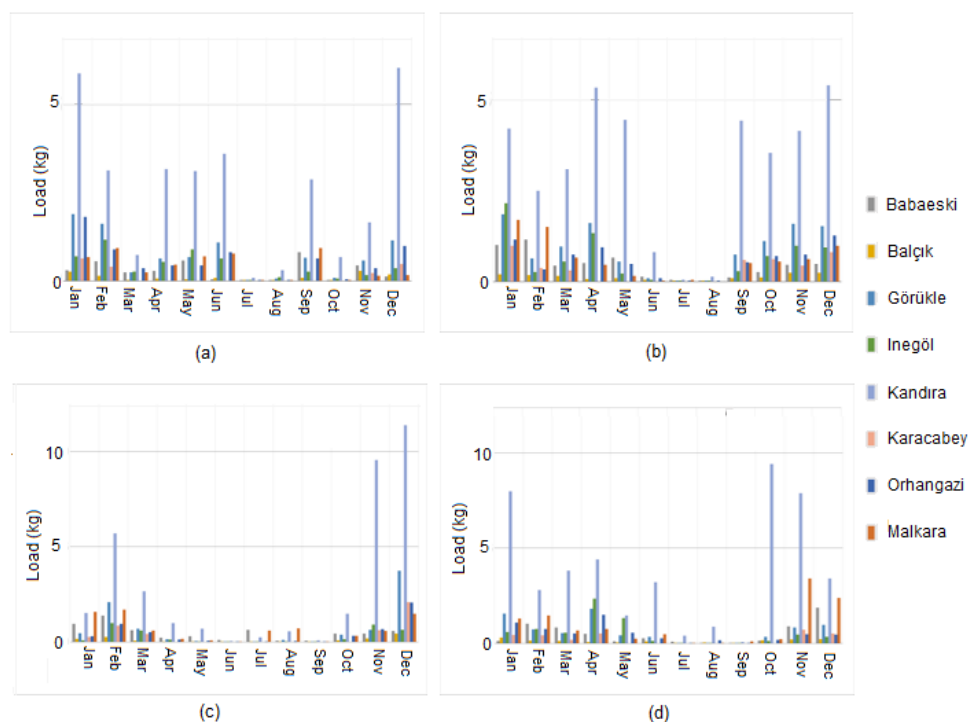


Figure 5. Monthly load of Zn for the years (a) 2022, (b) 2030, (c) 2040 and (d) 2049.

4. CONCLUSIONS

The present study investigates the effect of future climate change on heavy metal loads in the selected areas of the Marmara Region between 2022 and 2049. According to RCP 4.5 scenario results, an increasing trend for heavy metal loads is observed from the year 2022 to 2049. Each heavy metal reaches its maximum value in winter, which reveals that high rainfall events increase the release of contaminants into runoff. The results also reveal that Zn has the greatest load values because of having the highest concentrations in soil.

Acknowledgements: This research is supported by Boğaziçi University Research Fund Grant Number 6643.

REFERENCES

- Balcıoğlu, I., Ötker, M., Saraç, C., Şalcıoğlu, A., Cengiz, M., & Karıcı, A. (2007). Fate of veterinary drugs in the environment. TUBITAK report, Istanbul, Turkey.
- Bhaduri, B., Harbor, J., Engel, B., & Grove, M. (2000). Assessing watershed scale, long-term hydrologic impacts of land-use change using a GIS-NPS Model. *Environmental Management*, 26(6), 643–658.
- Guo, W., Huo, S., Xi, B., Zhang, J., & Wu, F. (2015). Heavy metal contamination in sediments from typical lakes in the five geographic regions of China: Distribution, bioavailability, and risk. *Ecological Engineering*, 81, 243-255.
- Montforts, M. H. M. M. (1999). Environmental risk assessment for veterinary medicinal products part 1. Other than GMO-containing and immulogical products first update. RIVM, Bilthoven, Netherlands.
- Reddy, K. R., Xie, T., & Dastgheibi, S. (2014). Removal of heavy metals from urban stormwater runoff using different filter materials. *Journal of Environmental Chemical Engineering*, 2(1), 282-292.
- US EPA (2005). Partition coefficients for metals in surface water, soil, and waste. US EPA, Washington, DC.
- US EPA (2009). Stormwater Management Model applications manual. US EPA, Cincinnati, OH.
- Zhang, H., Huo, S., Yeager, K.M., Xi, B., Zhang, J., He, Z., Ma, C., & Wu, F. (2018). Accumulation of arsenic, mercury and heavy metals in lacustrine sediment in relation to eutrophication: Impacts of sources and climate change. *Ecological Indicators*, 93, 771-780.

THE APPLICATION OF ATMOSPHERIC AND SOIL SENSORS FOR MONITORING NATURE-BASED STORMWATER TREATMENT FACILITIES

Minsu Jeon¹, Nash Jett Reyes¹, Hyeseon Choi², and Leehyung Kim^{1*}

¹ Department of Civil and Environmental Engineering, Kongju National University, 1223-24 Budaedong, Seobukgu, Cheonan city, Chungnamdo, 31080, Republic of Korea

² Univ Lyon, INSA Lyon, DEEP, EA7429, 11 rue de la Physique, F-69621, Villeurbanne cedex, France

*Corresponding author(leehyung@kongju.ac.kr)

ABSTRACT

Low impact development (LID) facilities are small-scale and decentralized technologies that require frequent monitoring and maintenance; however, these tasks are often limited by excessive manpower requirements. This study was conducted to assess the cost-effectiveness of using sensors to cost-effectively monitor and evaluate the overall performance of LID facilities. Atmospheric and soil sensors were installed in a rain garden to obtain pertinent information that can be used to predict the non-point pollution reduction efficiency of the facility. Throughout the data collection period, the recorded average rainfall depth, duration, intensity, and antecedent dry days were 5.9 mm, 6.95 hours, 0.87 mm/hr, and 7.3 days, respectively. During rainfall events, the average atmospheric concentration of PM₁₀ (74.7 µg/m³) was up to 10 times lower than the PM₁₀ concentration during dry day periods (744 µg/m³). The electrical conductivity in the inlet zone of the rain garden's filter bed was relatively higher than the succeeding portions since most of the particulate contaminants are adsorbed in the woodchip layers. The accumulation of ionic compounds in the filter bed's inlet generally resulted in elevated electrical conductivity measurements. Generally, the main factors that affected the stormwater quality were air temperature, fine dust concentration, vehicular traffic, anthropogenic activities, antecedent dry periods, and catchment area characteristics. Further studies and data collection are still recommended to assess the applicability of sensors as cost-effective means of monitoring LID facilities.

Keywords: *Low impact development, nature-based solutions, rain garden, sensors, stormwater*

1. INTRODUCTION

Low impact development (LID) technologies are commonly used to establish the natural water cycle, manage excessive flood volumes, and treat non-point source pollutants in stormwater. These nature-based facilities utilize soil, filter media, plants, and microorganisms in order to perform various processes that generally improve environmental quality. Monitoring LID facilities is necessary to determine the pollutant loads within the catchment area and assess the treatment efficiency of LID systems. Water samples are also manually collected and analyzed in the laboratory to obtain the physicochemical characteristics of pollutants in stormwater. LID

facilities are small-scale and decentralized systems that are distributed throughout the catchment area. Effective monitoring schemes also require the sample collection and hydraulic measurements in the inflow and outflow ports of the facility and thus, the manpower requirement is critical in the conduct of manual monitoring. Water quality sensors are often used as an alternative for manual monitoring; however, most LID facilities do not have a constant water level that will allow the effective use of water quality sensors. Therefore, this study was conducted to evaluate the applicability of atmospheric and soil sensors as cost-effective tools for monitoring the pollutant removal performance of LID facilities.

2. MATERIAL AND METHODS

The rain garden installed at the Kongju National University was designed to treat stormwater runoff from an impervious parking lot. Storm event monitoring and water quality sampling were conducted for a total of five years from 2014 to 2018. Water quality assessment was performed by collecting stormwater samples from the inflow and outflow ports of the facility. Water samples were collected at intervals of 0, 5, 10, 15, 30, and 60 minutes for the first hour of monitoring while succeeding samples were collected at an hourly interval. Flow measurements were also performed every five minutes as soon as the inflow and outflow were observed in the rain garden. Atmospheric and soil sensors were also installed in the rain garden to assess the correlation between various environmental parameters (i.e. soil moisture, electrical conductivity, ambient temperature, rainfall, fine dust concentration, etc.) and stormwater pollutant concentrations.

3. RESULTS AND DISCUSSIONS

The data used for model calibration and verification were obtained from the Korea Meteorological Administration (KMA). The coefficient of determination (R^2) and root mean square error (RMSE) were utilized as the metrics to determine the model accuracy. Continuous measurements of atmospheric and hydrologic parameters such as ambient temperature, humidity, fine dust (i.e. PM_{2.5} and PM₁₀) concentration, humidity, and precipitation depth and intensity, were obtained from the sensors. The data gathered from the period between February 2021 and September 2021 were utilized as model inputs.

The average PM₁₀ concentration measured throughout the monitoring period was 49.3 $\mu\text{g}/\text{m}^3$. During the summer season, the PM₁₀ concentration increased by up to 799 $\mu\text{g}/\text{m}^3$ due to the accelerated drying of particulates that can be dispersed in the atmosphere. The average temperature, moisture content, and electrical conductivity in the filter bed of the rain garden amounted to 20.5 °C, 20.3%, and 0.027 $\mu\text{s}/\text{cm}$, respectively. The soil layers surrounding the facility exhibited a relatively lower mean temperature (13.5°C) and electrical conductivity (0.023 $\mu\text{s}/\text{cm}$), but higher moisture content (24.1%) as compared with the filter bed of the rain garden. Since the rain garden is situated in an unshaded area, the facility receives direct heat from the sunlight. The direct exposure of the rain garden to sunlight ultimately resulted in high temperatures and lower moisture content inside the facility.

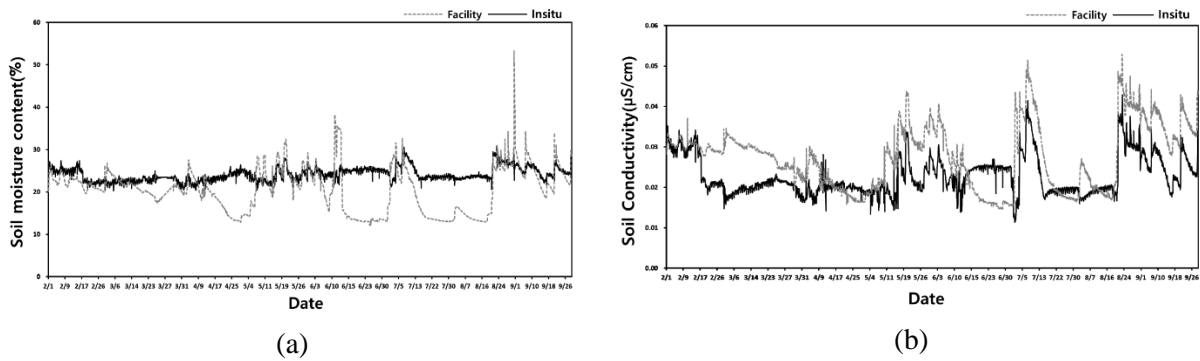


Figure 1. Fluctuations of moisture content and electrical conductivity measurements inside the filter bed of the rain garden

4. CONCLUSIONS

Monitoring and maintenance of LID facilities remain the biggest challenges in the utilization of nature-based technologies for stormwater management. This study explored the applicability of atmospheric and soil sensors for monitoring LID facilities in order to overcome the constraints in managing nature-based facilities. The following conclusions were drawn after the assessment of the results:

1. In cases where there are no observed changes in the moisture content and electrical conductivity inside the facility for four or more days after a rainfall event, the facility can either be damaged or dysfunctional. The excessive deposition and accumulation of sediments from stormwater can reduce the infiltration rate within the system due to pore blockage, thus resulting in the deterioration of the facility.
2. Based on the data collected from the sensors, air temperature, fine dust concentration, vehicular traffic, anthropogenic activities, antecedent dry days, and catchment area characteristics were the main factors affecting the pollutant concentrations in stormwater.
3. The filter media characteristics affect the moisture content and electrical conductivity recovery time inside the facility. It is, therefore, necessary to account for the filter media composition in order to adequately assess the overall status and performance of the nature-based system.

Acknowledgements: This research was supported by the National University Development Project by the Ministry of Education in 2022.

CORRELATION ANALYSIS BETWEEN WETLAND WATER LEVEL AND RAINFALL IN JANGGUN WETLAND

Junhyeong Lee¹, Jong-Gu Hwang Bo², Kisung Lee², and Soojun Kim^{2}*

¹ *INHA University, Program in Smart City Engineering, Incheon, Republic of Korea*

² *INHA University, Department of Civil Engineering, Incheon, Republic of Korea*

³ *INHA University, Department of Civil Engineering, Incheon, Republic of Korea*

**Corresponding author (sk325@inha.ac.kr)*

ABSTRACT

Since the water level of the wetland has a major influence on the area of the wetland and the maintenance of the wetland ecosystem, it is very important to identify the water level fluctuation and minimum appropriate water level of the wetland for efficient wetland management. In this study, we analyze the fluctuation of the water level due to rainfall using rainfall and water level gauging data of the Jangggun Wetland located in Geumjeongsan Mountain, South Korea. And discuss the minimum required water level for major biological groups in the wetland.

Keywords: *Jangggun wetland, Wetland water level, Rainfall.*

1. INTRODUCTION

Wetlands are areas where fresh water, brackish water, or salt water permanently or temporarily covers the surface, providing various functions to the ecosystem, such as climate control, biodiversity preservation, water purification, and flood reduction. Recently, the importance of the wetland environment has emerged due to climate change and regional development, and the importance of sustainable wetland management is emerging (Oh et al., 2018).

2. MATERIAL AND METHODS

First, rainfall and water level gauging systems were installed to collect rainfall and water level data in wetlands, and the observed time series data contains many types of noise. Therefore, it is necessary to determine the rainfall event among the time series, and to distinguish between the non-rainfall periods in which no rainfall occurs. In addition, the time interval and duration of the preceding rainfall affecting the wetland level, and the minimum appropriate level at which the Jangggun wetland can maintain its ecological function were analyzed. Major biological groups such as dominant species and endangered species were investigated living in the Jangggun wetland, and the minimum appropriate water level was analyzed through life cycle analysis of each biological group.

3. RESULTS AND DISCUSSIONS

Major biological group

The dominant species in the Jangggun wetland is "Molinia japonica", and it is a plant that

grows by absorbing water using its roots. "Molinia japonica" can grow and form colonies even in an environment with an underground water level of 120mm, and it is necessary to maintain the water level in June-August, the flowering season. The endangered species of Janggun wetland include "Nannophya pygmaea Rambur" and "Bombina orientalis", and since they spawning on or in the water, the appropriate water level for spawning should be maintained on the wetland surface. In addition, the main spawning period is May-July, and since about 60 days are required for the hatched juvenile to become an adult, the water level of 20mm should be maintained in May-September. As a result, it was investigated that the level of 20mm must be maintained during May to September for the growth of major biological groups in the Janggun wetland.

Rainfall and water level

We analyzed the change in the wetland water level according to the occurrence of rainfall using rainfall and water level data obtained from three gauging point in the Janggun wetland . If the water level before the rainfall occurred remained above 50mm, most of the rainfall was flow out to downstream of the wetland. In addition, when the wetland water level was increased due to the occurrence of rainfall, the water level maintained until about 8 days on average. On the other hand, when the rainfall inter-event time lasted more than 25 days, it was found that only the groundwater level increased and the surface water level did not recover even if the rainfall occurred thereafter.

4. CONCLUSIONS

An appropriate management plan was derived by investigating major biological groups such as dominant species and endangered species in the wetland and changes in the wetland water level due to the occurrence of rainfall in the Janggun wetland. In order to maintain the habitat environment of major biological groups, it should maintain the appropriate surface water level from May to September. In the case of the wetlands, the wetland water level is maintained for about 8 days thereafter the rainfall event when the total rainfall occurs 9.6mm or more, and the wetland water level cannot be restored if the inter-event time period lasts more than 25 days. Therefore, for sustainable wetland management, rainfall and water level changes in the Janggun wetland must be continuously monitored, and water level increasing management is necessary in consideration of factors other than rainfall in case the rainfall inter-event time period lasts for a long time.

Acknowledgements: This work was supported by Korea Environmental Industry&Technology Institute through Wetland Ecosystem Value Evaluation and Carbon Absorption Value Promotion Technology Development Project, funded by Korea Ministry of Environment(MOE)(2022003630001)

REFERENCES

Seunghyun, Oh, Jungwook, Kim, Myung-Byung, Chae, Younghye, Bae & HungSoo, kim. (2018). Case study: Runoff analysis of a mountain wetland using water balance method. *Journal of Wetlands Research*, 20(3), pp.210-218.

GROUNDWATER HYDROLOGY AND QUALITY

A LABORATORY SCALE EXAMINATION OF SALINITY INTRUSION USING UNDERGROUND DAM

Akif Epcin^{1*}, Ayse Nur Karayel¹, Babak Vaheddoost², Egemen Aras²

MSc student, Bursa Technical University, Department of Civil Engineering, Hydraulic Program.

PhD, Bursa Technical University, Department of Civil Engineering, Hydraulic Program.

** Corresponding author and the presenter*

Akif Epcin. Email: akifepcin@gmail.com

ABSTRACT

Freshwater is one of the most important natural resources that affect our lives to great extent. In this respect, underground water constitutes a large portion of available freshwater, that is vulnerable against pollution. Typically, the intrusion of brine to the coastal aquifer occurs when freshwater in the nearby aquifer is overused. Hence, in the following study a laboratory scale experiment is designed and conducted to study the role of the so-called underground dams on the intrusion of saline water into the aquifer. To do this, a sand box of 1300*200*400 mm made up of 10 mm Plexiglass is used. The box contained two reservoirs for the salt and fresh water of 229 and 225 mm height respectively. A uniform sand of 1~2 mm is used, and the brine (25 gr/l) is mixed with 2 gr/l food color to monitor the salt water movement through porous medium. The setup is then used and a set of different walls with 100, 150, and 200 mm height also made up of Plexiglass is used to study the spatial and temporal effect of underground dam on the salinity intrusion. Then, the movement of the salty water through the porous medium is monitored, and the coordinates of the saltwater movement is used to investigate the changes in the vertical and horizontal velocity and acceleration of the fluids. It is concluded that the underground dam decelerates the salt water intrusion, but this delay is not permanent and very sensitive to the condition.

Keywords: *Salinity intrusion, sand box, underground dam, coastal aquifers*

ASSESSING THE SPATIOTEMPORAL VARIABILITY OF GROUNDWATER LEVEL AND QUALITY USING HYBRID VMD-DSE-K-MEANS TECHNIQUE

Roghayeh Ghasempour¹, V. S. Ozgur Kirca^{2*}, Seyed Mahdi Saghebian³

¹. Division of Water Resource Engineering, Department of Civil Engineering, University of Tabriz, Tabriz, Iran.

². Division of Hydraulics, Department of Civil Engineering, Istanbul Technical University, Istanbul, Turkey.

³. Department of Civil Engineering, Ahar Branch, Islamic Azad University, Ahar, Iran

*Corresponding author (kircave@itu.edu.tr)

ABSTRACT

The study of spatiotemporal variations of groundwater levels (GWL) is an important factor in the management and planning of water resources. In this research, a multiscale method based on the Variational Mode Decomposition (VMD), Differential Symbolic Entropy (DSE), and K-means clustering approaches was developed to assess the monthly spatiotemporal variations of groundwater levels for Ardabil plain located in the Northwest of Iran. In this regard, the monthly time series of GWL were decomposed using VMD; then, the entropies of the subseries were calculated and used for zoning and classifying the basin in terms of GWL via the K-means method. Results showed that the excessive exploitation of groundwater resources in the basin caused a decrease in GWL. From the results, the optimal number of clusters for the selected aquifers was obtained as four. Results showed that increasing the DSE amounts of the subseries indicated a decrease in the mean GWL of the piezometers and there was an inverse relationship between these two parameters. The capability of the proposed methodology was also assessed for groundwater quality in terms of the Total Dissolved Solids (TDS) parameter. In general, the obtained results proved the efficiency of the applied multiscale method. Therefore, the developed method can be reliably used to assess spatiotemporal variations of groundwater quantity and quality.

Keywords: *Aquifer, Entropy, Groundwater level, Total dissolved solids, Spatiotemporal variations, Variational mode decomposition.*

1. INTRODUCTION

Groundwater, constituting 28.2% of available fresh water on the planet, is a major source of water for agriculture, industry, and drinking water (Shiati, 1999; Smedema and Shiati, 2002). This fact has increased the importance of studying the characteristics of groundwater (Reghunath et al., 2005). Groundwater quality is affected by ecological and anthropogenic activities such as urbanization, intensive irrigated agriculture, mining activities, disposal of untreated waste (domestic or otherwise), and lack of rational management. The groundwater contamination may lead to serious environmental sanitation problems. In many parts of the world, groundwater is at high risk of pollution due to urbanization, agricultural and industrial activities, as well as mining enterprises due to their overexploitation. Groundwater is the main

and more reliable resource of irrigation. Both overexploitation from aquifers to meet the irrigation needs and drought events have caused severe groundwater level drops in many regions of the world. Where groundwater is used for irrigation, aquifers are also being depleted at an alarming rate (Reghunath et al., 2005). Therefore, accurate estimation of quality and quantity parameters of groundwater has always been a research priority given its high importance. Due to the complexity of groundwater systems as well as the lack of historical datasets or statistics of ground water levels (GWL), spatial and temporal studies of GWL are difficult. Therefore, investigating the variation of groundwater resources has become a major issue in global hydrogeological studies (Dai et al. 2019; Liu et al. 2019).

Time series of groundwater characteristics show annual and inter-annual changes. In addition, they constitute complexly superimposed randomness and periodicity, as well as other nonlinear response characteristics due to internal and external factors (Li et al., 2020). In fact, most hydrological signals have seasonal fluctuations; so, it is important to use appropriate approaches to identify the dominant characteristics of signals. In this regard, the use of signal preprocessing methods can be useful. Variational Mode Decomposition (VMD) is a common approach which is used for non-stationary time series decomposition (Ghasempour et al., 2022). In addition, clustering techniques are applied to determine the pattern in unlabeled samples by organizing the samples into homogeneous classes. Since a clustering method considers both spatial and temporal domains of components, its results demonstrate temporary changes and local characteristics (Barton, 2016; Zhou and Chan, 2014). The K-means technique is one of the most widely used clustering techniques for such purposes.

Due to the non-stationary properties of GWL, and also, the necessity for identifying homogeneous GWL regions, a multiscale approach was developed in this research to assess the GWL properties in the Ardabil basin. In this regard, monthly GWL datasets from 26 piezometers covering the period of 1995 to 2019 were used and the spatiotemporal characteristics of GWL data were assessed for the selected basin. In the considered methodology, at first, time series were broken down into several subseries via VMD; then, the entropy values of obtained subseries were computed. The Differential Symbolic Entropy (DSE) was used as the governing parameter to determine the complexity of time series. The obtained DSE values were utilized for zoning the selected region and detecting the relationship between GWL data and DSE values. Finally, area clustering was performed using the K-means in order to recognize the homogenous GWL areas. In the final step of the research, the efficiency of the proposed method was assessed in the analysis of the spatiotemporal variations of groundwater quality. Total Dissolved Solids (TDS), which is a measure of the dissolved combined content of all inorganic and organic substances present in water, was used for the latter purpose.

2. MATERIAL AND METHODS

Study area and used datasets

The Ardabil plain aquifer is located in the Northwest of Iran in the province of Ardabil. There are long winters in this region and the average annual rainfall is 320 mm. The wettest and driest months of this region are May and August, respectively. The average temperature in Ardabil

basin is 9 °C. The location of the study area is shown in Figure 1. Agriculture is the main occupation of the people living in this area. In recent decades, the rapid development of cities, extensive agricultural activities, and some industrial activities have caused stress on the aquifers of the basin. The average use of water in this basin for drinking, industrial, and agricultural activities is about 200 (million m³/year) (Taie Semiromi and Koch, 2019). 89% of the total water demand is provided by groundwater and the remaining 11% by surface water (Ardabil Regional Water Authority, 2013; Aghbolagh and Fataei, 2016). Intense extraction of groundwater in this basin has reduced the groundwater level as much as 12 meters over the past 25 years (Aghbolagh and Fataei, 2016). In this study, the GWL and TDS datasets from 26 piezometers located over the basin, covering a time period between 1995 and 2019, were used.

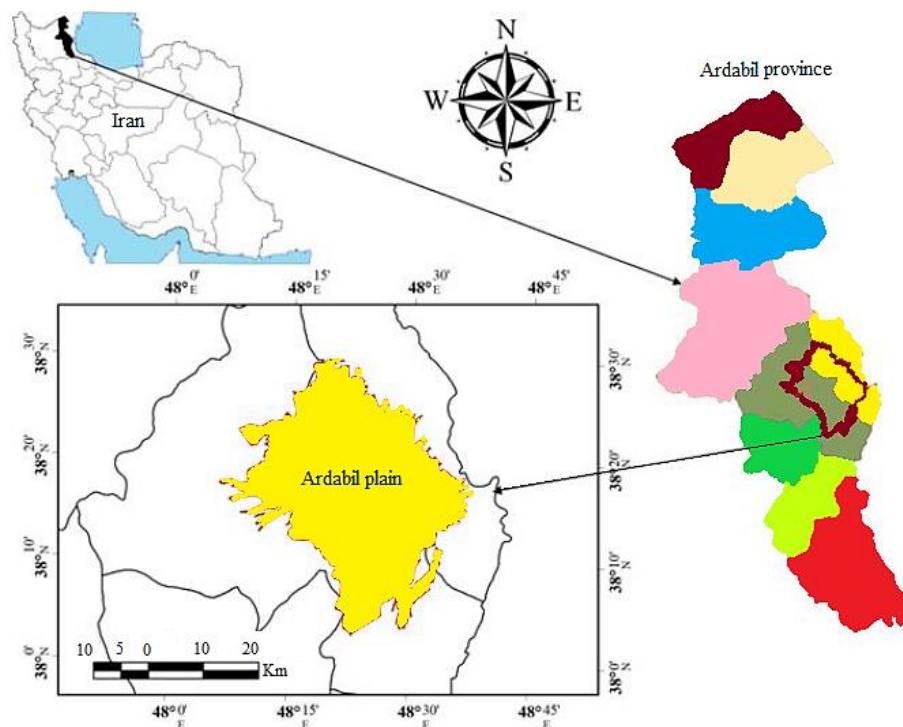


Figure 1. Map showing the study area (Ardabil basin).

Variational Mode Decomposition (VMD)

In this study, the new Variational Mode Decomposition (VMD) method was used for breaking down the original signal into more stationary and regular components. By signal decomposition, the irrelevant properties of the time series may be removed. Therefore, the quality of datasets is increased by removing the “noise” of the time series. VMD aims to decompose a real valued input signal into an ensemble of band-limited Intrinsic Mode Functions (IMF) with specific sparsity properties while reproducing the input signal. It is more effective than other signal decomposition methods as it is able to generate IMF components concurrently using an optimization method, which can avoid the error caused during the recursive calculating and ending effect. Consequently, the main purpose of VMD is the construction and solution of a constrained variational problem described below:

$$\min_{u_k(t), w_k} \left\{ \sum_{k=1}^K \left\| \partial_t \left[\left(\delta(t) + \frac{j}{\pi t} \right) * u_k(t) \right] e^{-jw_k t} \right\|_2^2 \right\} \quad s.t. \quad \sum_{k=1}^K u_k(t) = f(t) \quad (1)$$

in which K is the total number of IMFs and ∂_t is the partial derivative for time t . $\delta(t)$, j , $u_k(t)$, w_k , and $f(t)$ stand for the dirac distribution, imaginary unit, t th data in the k th IMF, center frequency of the k th IMF, and t th data in the original time series, respectively. For solving this constrained optimization problem, Zuo et al. (2020) introduced an approach as below:

$$u_k^{n+1}(w) = \frac{f(w) - \sum_{i=1, i \neq k}^K u_i(w) + 0.5\lambda(w)}{1 + 2a(w - w_k^n)^2}; \quad w_k^n = \frac{\int_0^{\frac{\pi}{2}} w |u_k^{n+1}(w)|^2 dw}{\int_0^{\frac{\pi}{2}} |u_k^{n+1}(w)|^2 dw} \quad (2)$$

$f(w)$, $u_i(w)$, $\lambda(w)$, and $u_k^{n+1}(w)$, and n are the Fourier transforms of $f(t)$, $u_i(t)$, $\lambda(t)$, $u_k^{n+1}(t)$, and the number of iterations, respectively.

Differential Symbolic Entropy (DSE)

Differential Symbolic Entropy (DSE), proposed by Yao and Wang (2017), is a physical quantity used to assess the complexity of time series. It considers the relationship of three consecutive elements in time sequences and introduces a control factor that can flexibly control the process of differential symbol transformation. This symbolic method is realized by detecting the local dynamic information of time sequences in detail. The calculation process of DSE is encoding the data sequence after symbolization. Then, get the final DSE by calculating the probability of each code. In this study, after data decomposition using VMD, the DSE values of IMFs were computed and used as the representative feature of IMFs to investigate the variations of the basin in terms of the GWL and TDS.

K-means algorithm

K-means is one of the clustering methods that has shown decent performance in hydrological research. In the K-means, the clustering may be performed with minimization or maximization of an objective function. This means that if the criterion is measuring the distance between samples, the objective function will be based on minimization, and the aim of the clustering operation will be to find clusters where the distance between samples in each cluster is minimal. Conversely, if the similarity function is used to measure the similarity of samples, the objective function is selected so that the clustering response maximizes its value in each cluster (Yang and Deng, 2010). Due to the simplicity of this method along with its ability in large datasets classifying and its fast implementation, it is a widely used method.

The results of spatial clustering were assessed using the Silhouette coefficient (SC) criterion. This index shows the degree of similarity for data placed in the same cluster. The values of SC vary between -1 and 1 and its optimal value is 1.

$$SC_i = \frac{b(i) - a(i)}{\max[a(i), b(i)]} \quad (3)$$

where $a(i)$ and $b(i)$ stand for the mean dissimilarity of i th sample with other samples of the same cluster and the lowest mean dissimilarity of i th sample with other clusters, respectively.

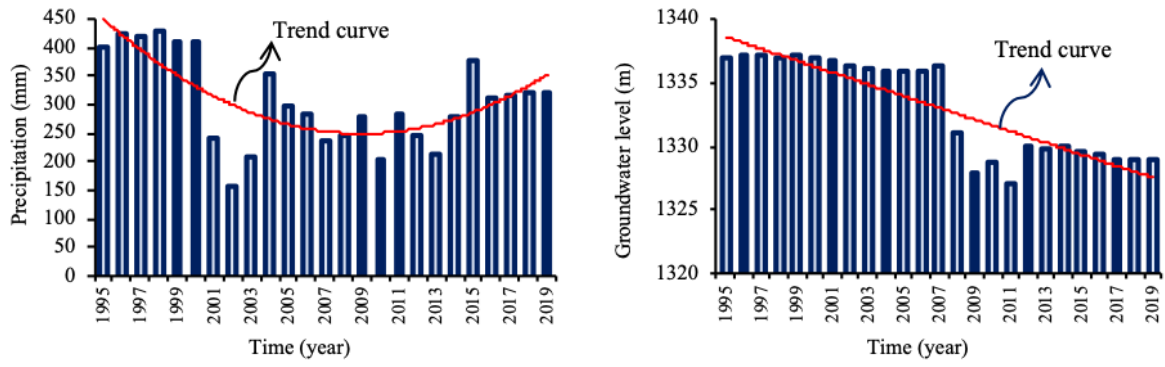
3. RESULTS AND DISCUSSIONS

Assessing the spatiotemporal variations of groundwater levels

In this section, the variations of GWL and precipitation in the selected time period were assessed. In this regard, for the study period, groundwater level time series of 26 piezometers and precipitation time series observed in five stations, distributed in the different parts of the basin, were used. Figure 2(a) shows the mean annual precipitation and groundwater levels for the selected basin. Based on this figure, at the beginning of the selected statistical period, the annual precipitation had a descending trend and then experienced an ascending trend. Furthermore, based on the results of groundwater level, it was observed that until 2007 the water level in the basin remained somewhat stable, but at 2008, a sharp drop in groundwater level of the basin occurred which continued until 2011. After this year, the groundwater level remained almost stable. However, the general trend of groundwater level was descending. Therefore, it can be deduced that precipitation cannot be taken as the sole reason behind the groundwater variations. Furthermore, human activities such as overexploitation of groundwater from the wells are the most probable reason behind these variations.

The variations of GWL for the years 1996, 2010, and 2019 are shown in Figure 2 (b). For calculating the GWL drop, at first, the absolute height of the groundwater, which shows the depth of water in a well from sea level, was obtained. Then, the amount of the GWL drop was calculated considering the year that had the highest GWL in a long period of time. It should be noted that due to the recording of consistent data from 1995 to 2019, this time period was selected for GWL analysis. However, the GWL drops of the selected piezometers were calculated based on the year with the highest GWL value during a long-time period (i.e. 1990 during the time period of 1980 to 2019). It can be seen that the GWL decreased during the selected period indicating the excessive exploitation of groundwater in different parts of the plain, especially in the Central parts. According to the distribution map of the existing wells, the highest concentration of wells is in the Eastern and Central areas of the plain; therefore, water exploitation is more intense in these areas and the drop in ground water level is more noticeable in the Central parts, as expected. In order to investigate the role of land use changes in groundwater exploitation, the land use maps for these years are shown in Figure 3. As seen, agricultural activities were increased over time, which had a noteworthy impact on the depletion of groundwater levels.

(a)



(b)

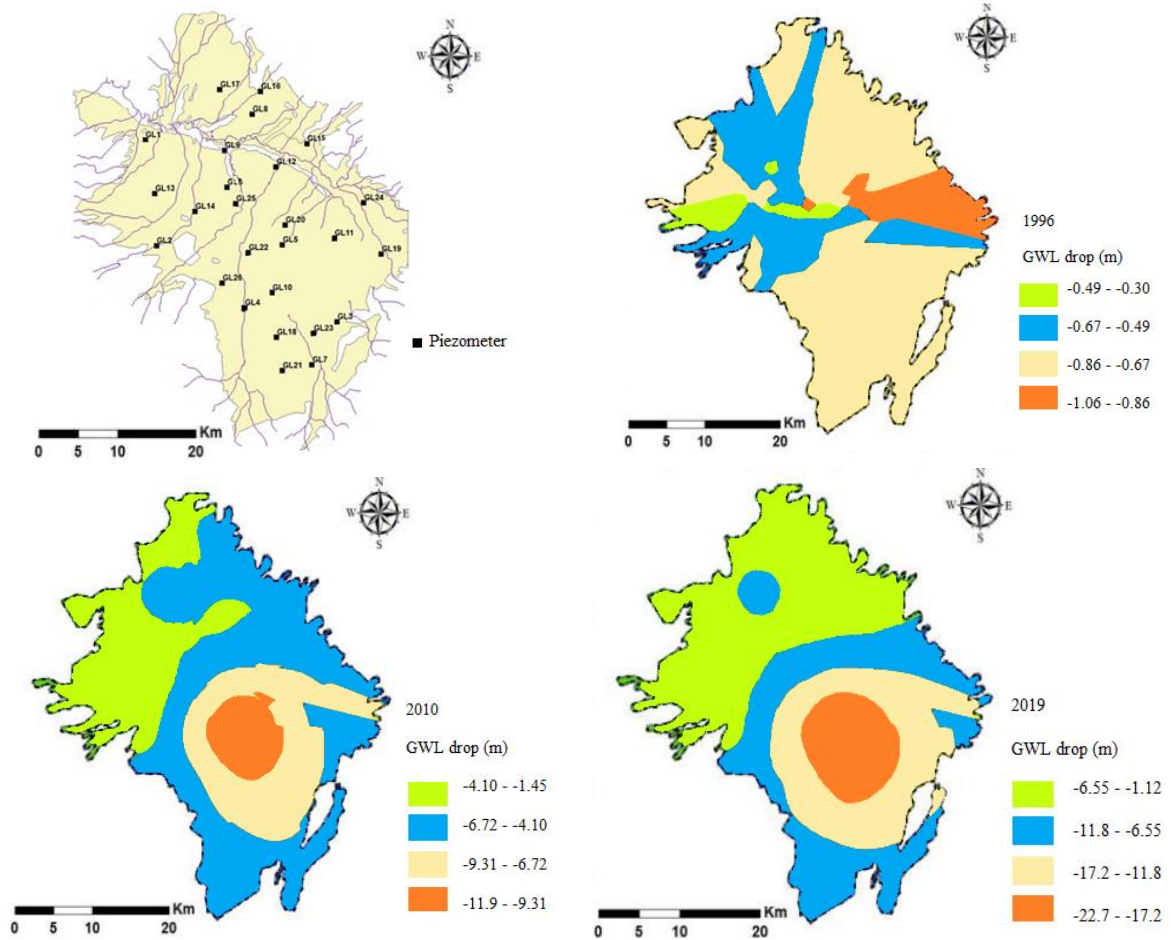


Figure 2. (a): Variations of the precipitation and GWL in the selected period and (b): zoning maps of GWL drop in Ardabil basin for 1996, 2010, and 2019.

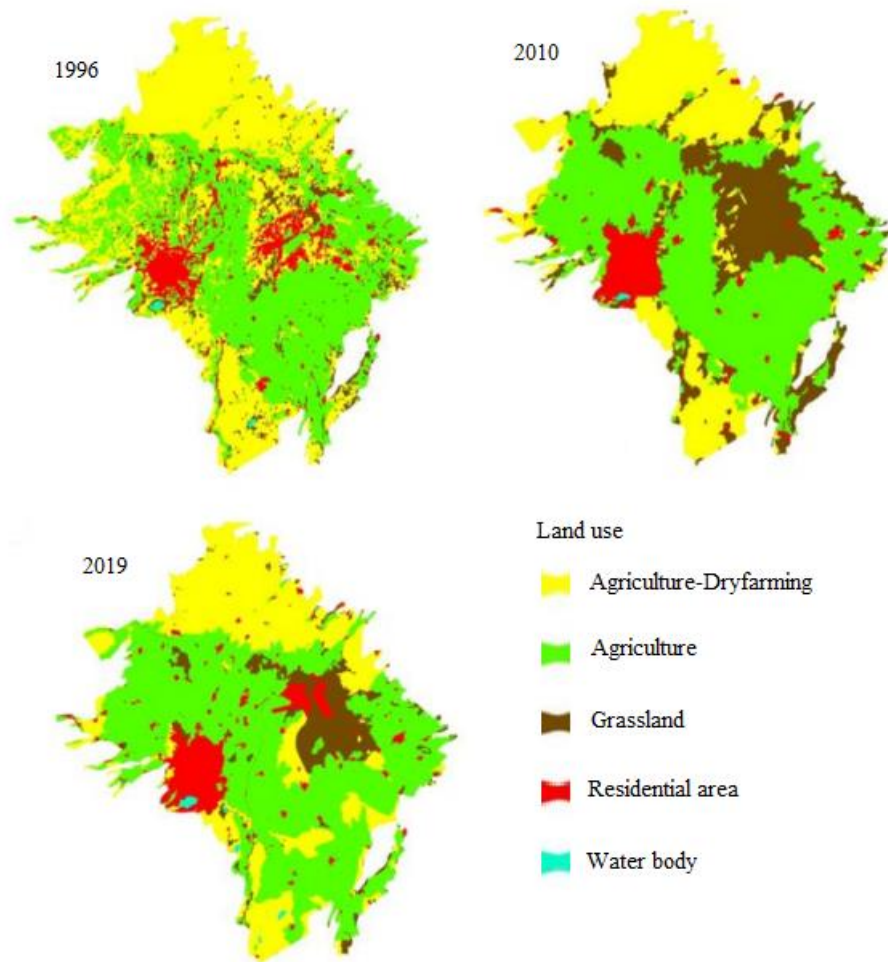


Figure 3. Land use maps of 1996, 2010, and 2019.

Time series analysis using VMD method and computing the DSE of the IMFs

For investigating the spatiotemporal variations of GWL using the proposed hybrid multiscale method, the GWL time series of each of the considered piezometers located in the Ardabil basin were decomposed. A multiscale method based on the VMD-DSE was developed to decompose the datasets and increase their ability in GWL assessment. The quality of the raw datasets can be affected during the data collection due to various external and internal factors. Accurate modeling of the intended variable becomes difficult with the integration of unrelated factors. Therefore, the VMD and DSE were used to break down the GWL raw datasets into several components in order to decrease the modeling complexity. The basis of the VMD method is the breakdown of a time series into several different IMFs (9 IMFs was extracted in this study). Evaluation of the complexity of each IMF was performed using the DSE. The DSE values for the IMFs obtained for one of the piezometers (P2) are shown in Figure 4 (a). According to this figure, the DSE from the IMF1 component to the last component (i.e. IMF9) has a downward trend indicating that the IMF1, having the largest entropy value, has the highest complexity. Due to the increase in the number of parameters that can be used for zoning of the area, the mean DSE values of the IMFs were selected for zoning the selected area.

The mean GWL and DSE values of the all IMFs were used to zone and classify the plain in terms of the GWL. The zoning maps of Ardabil basin based on the mean GWL and DSE values

are shown in Figure 4 (b). In this figure, an inverse relationship between entropy and GWL variables is evident. The Southern and Central parts of the basin had the highest GWLs and the lowest amounts were obtained for the Northern regions. Instead, higher values of entropy were observed in the Northern parts and the Southern parts had the lowest values of this parameter.

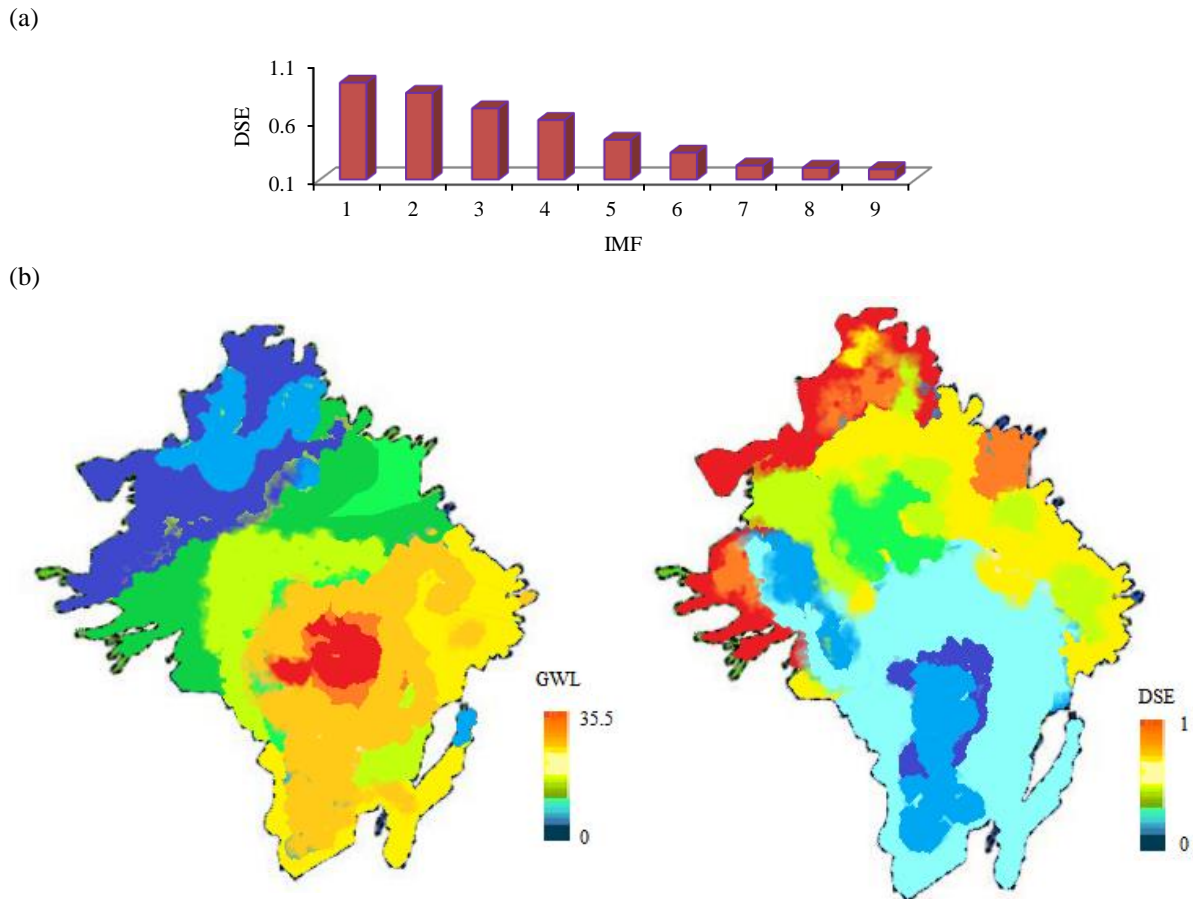


Figure 4. (a): DSE values for decomposed IMFs obtained for one of the piezometers and (b): zoning maps of the mean GWL and DSE variables for the selected area.

Clustering the selected basin based on VMD-DSE-K-means method

After computing the entropy values of the obtained subseries, clustering of the selected piezometers was performed. For the area clustering, firstly, the appropriate number of clusters (NC) is obtained considering the entropy values of the decomposed subseries. In this study, K-means operation was performed for the NC values between 2 and 10 to identify the optimum NC. This best NC was determined based on the Silhouette Coefficient (SC) value and dispersion of samples in the clusters. Accordingly, NC = 4 was selected as the optimum number of clusters.

The geographical locations of the piezometers clustered through the DSE values via the K-means approach are shown in Figure 5. For evaluating the efficiency of the clustering method, the SC was used. The higher the value of the SC for a sample, the more it belongs to that cluster, and vice versa. Additionally, the absence of a single-membered cluster indicates optimal clustering. The obtained results for area clustering, including the SC values, are listed in Table 1. The mentioned table shows the members of each cluster and their central piezometers (i.e.

the piezometer with higher SC_i). According to the results, the selected piezometers were divided into four clusters. By comparing Figures 4 (b) and 5, it could be seen that the piezometers with the same GWL or DSE values were located in the same group in most cases. For example, the Southwestern parts, which had the highest GWL and the lowest DES, were located in the Cluster 1, and the Northeastern parts with lower GWL values and higher DES values were located in the Cluster 3. Other regions of the basin were located in other separate clusters. Therefore, it can be deduced that the proposed method clustered the GWL piezometers into approximately identical clusters.

Table 1. The clustering results obtained for the GWL.

Cluster	Piezometer	SC_i	Central member
1	4, 10, 18, 22, 26	0.78, 0.79, 0.59, 0.69, 0.61	10
2	1, 2, 5, 6, 9, 11, 12, 13, 14, 20, 25	0.48, 0.69, 0.68, 0.78, 0.61, 0.59, 0.45, 0.68, 0.73, 0.65, 0.60	6
3	8, 15, 16, 17	0.81, 0.84, 0.55, 0.78	15
4	3, 7, 19, 21, 23, 24	0.49, 0.86, 0.77, 0.64, 0.65, 0.77	7

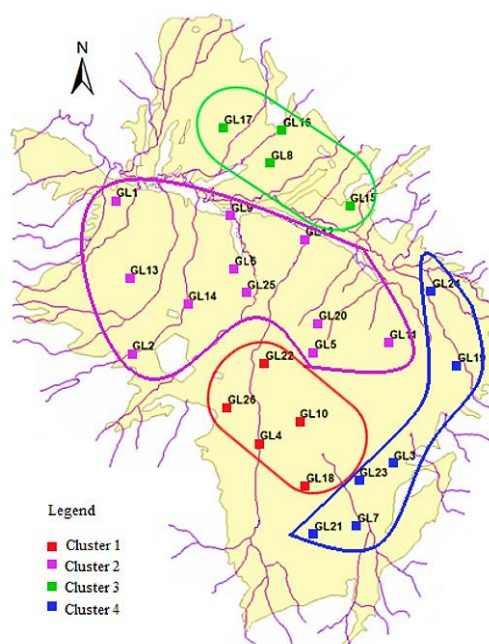


Figure 5. The results of the VMD-DSE-K-means clustering for GWL assessment.

Investigating the capability of the applied methodology in groundwater quality assessment in terms of TDS

In this section, the potential of the proposed method for evaluating the spatiotemporal variations of groundwater quality parameter was investigated. Total Dissolved Solids (TDS) parameter was used for this purpose. TDS, which shows the amount of material dissolved in water and indicates the "freshness" of water, is one of the most important parameters to quantify the water quality in an aquifer. Increased levels of TDS in an aquifer indicate poor quality of water and possible contamination. After the decomposition of data into several IMFs components via the VMD, the entropy values of the IMFs were calculated, and taken as inputs of the K-means method to generate the spatial maps of TDS over the study area. Figure 6 shows the obtained

results for area zoning and clustering in terms of TDS. From the results, it was observed that the Southern half of the basin had lower TDS (i.e. higher water quality) than the Northern half. By comparing Figures 4 and 6, it can be stated that there is a significant relationship between groundwater level and the water quality, so that the TDS value is the lowest in the areas where the groundwater level is higher. Based on the clustering results obtained for TDS, the basin was classified into four groups, which was very consistent with the clustering results obtained for GWL. Areas with different TDS values were placed in different groups. In general, results proved the appropriateness and efficiency of the applied method in assessing the selected basin in terms of the TDS.

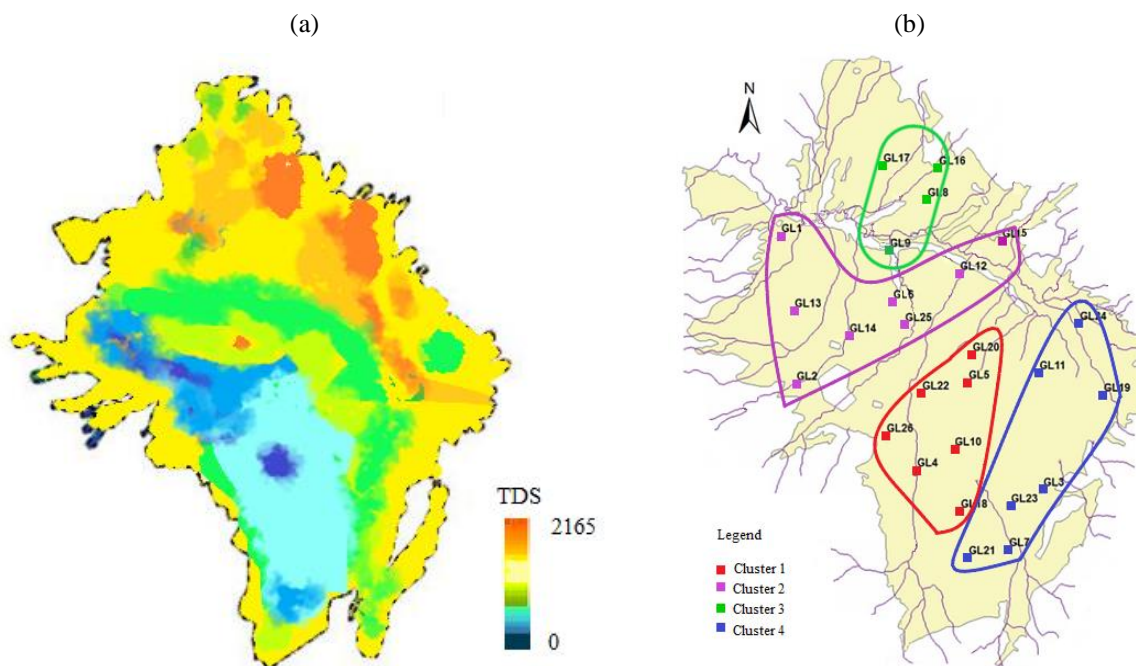


Figure 6. Zoning maps of the TDS (b): the results of the VMD-DSE-K-means clustering for TDS.

4. CONCLUSIONS

In the current study, the groundwater level fluctuations during a 25-year duration (1995-2019) in the Ardabil basin were investigated. Using the VMD method, the raw GWL time series were decomposed and the entropy values of the obtained subseries were calculated. Then, the selected piezometers were clustered by K-means method. The efficiency of the proposed method in spatial clustering was assessed via Silhouette Coefficient index.

Based on the results, it was found that an important governing factor in the dropping of GWL was the overexploitation of wells used to promote agriculture in the region. Although the rainfall in the study area increased in some years, the GWL had a downward trend during the selected time period, which was due to the excessive exploitation of water from wells. The groundwater level in the Southern half of the plain was higher than the Northern half. Also, an inverse relationship was found between DSE and GWL variables. According to the results obtained for area clustering in terms of GWL, the Central, Northern, and Southeastern parts with different levels of groundwater were placed in separate clusters. The capability of the proposed multiscale method was also evaluated in assessing the variations of groundwater

quality parameter (i.e. TDS). The latter results proved the desirable efficiency of the developed method. It was observed that the level and quality of groundwater are interrelated such that the TDS value was the lowest in the areas where the GWL was higher. The results of this study showed that using the developed methodology, the quality and quantity parameters of groundwater can be reliably assessed. Therefore, the proposed methodology can be applied other basins, as well, to investigate and manage groundwater resources.

REFERENCES

- Aghbolagh, J. Z., & Fataei, E. (2016). The study of changes in Ardabil plain groundwater level using GIS. *Advances in Science and Technology Research Journal*, 10(29), 109-115.
- Ardabil Regional Water Authority. (2013). Investigation of groundwater balance in Ardabil Plain. Ardabil: Ardabil Regional Water Authority.
- Barton, Y., Giannakaki, P., Von Waldow, H., Chevalier, C., Pfahl, S., & Martius, O. (2016). Clustering of regional-scale extreme precipitation events in southern Switzerland. *Monthly Weather Review*, 144(1), 347-369.
- Dai, L., Guo, X., Du, Y., Zhang, F., Ke, X., Cao, Y., Li, Y., Li, Q., Lin, L., & Cao, G. (2019). The Response of Shallow Groundwater Levels to Soil Freeze-Thaw Process on the Qinghai-Tibet Plateau. *Groundwater*, 57(4), 602-611.
- Ghasempour, R., Roushangar, K., Kirca, O. V. S., & Demirel, M. C. (2022). Analysis of spatiotemporal variations of drought and its correlations with remote sensing-based indices via wavelet analysis and clustering methods. *Hydrology Research*, 53(1), 175-192.
- Li, H., Lu, Y., Zheng, C., Zhang, X., Zhou, B., & Wu, J. (2020). Seasonal and inter-Annual variability of groundwater and their responses to climate change and human activities in arid and desert areas: a case study in Yaoba Oasis, Northwest China. *Water*, 12(1), p.303.
- Liu, Q., Chen, S., Jiang, L., Wang, D., Yang, Z., & Chen, L. (2019). Determining thermal diffusivity using near-surface periodic temperature variations and its implications for tracing groundwater movement at the eastern margin of the Tibetan Plateau. *Hydrology Process*, 33(8), 1276-1286.
- Reghunath, R., Murthy, T. R., & Raghavan, B. R. (2005). Time series analysis to monitor and assess water resources: A moving average approach. *Environmental Monitoring and Assessment*, 109(1), 65-72.
- Shiati, K. (1999). World Water Vision for Food: Country Case Study Iran. *Paper presented at the MENA Consultation Meeting*, Bari, Italy.
- Smedema, L. K., & Shiati, K. (2002). Irrigation and salinity: a perspective review of the salinity hazards of irrigation development in the arid zone. *Irrigation and drainage systems*, 16(2), 161-174.
- Taie Semiromi, M., & Koch, M. (2019). Reconstruction of groundwater levels to impute missing values using singular and multichannel spectrum analysis: application to the Ardabil Plain, Iran. *Hydrological Sciences Journal*, 64(14), 1711-1726.
- Yang, L., & Deng, M. (2010). Based on k-means and fuzzy k-means algorithm classification of Precipitation. *In 2010 International Symposium on Computational Intelligence and Design, IEEE*. 1, 218-221.
- Yao, W., & Wang, J. (2017). Double symbolic joint entropy in nonlinear dynamic complexity analysis. *AIP Advances*, 7(7), p.075313.
- Zhou, P. Y., & Chan, K. C. (2014). A model-based multivariate time series clustering algorithm. *In Pacific-Asia Conference on Knowledge Discovery and Data Mining (pp. 805-817)*, Springer, Cham.
- Zuo, G., Luo, J., Wang, N., Lian, Y., & He, X. (2020). Decomposition ensemble model based on variational mode decomposition and long short-term memory for streamflow forecasting. *Hydrology*, 585, p.124776.

ENGAGEMENT OF WASH ENTREPRENEUR TO ADDRESS GROUNDWATER CONTAMINATION

*Shah Riazur Rahman,
CARE Bangladesh, Programme Department, Shouhardo III program, Dhaka, Bangladesh*

ABSTRACT

Based on SDG 6, it's quite challenging to ensure sustainable access to water and sanitation for all in Bangladesh and to address groundwater quality and contamination issue. Based on data of Multiple Indicator Cluster Survey (MICS) of UNICEF and Govt. of Bangladesh 2019, 98.5 per cent of households have access to an improved source of drinking water whereas 21 percentage of rural household population (9.9 % in urban) with Arsenic in source water containing over 10 ppb Arsenic concentration (WHO standard) and 84.6 per cent of households have access to improved sanitation and these data represents the severity of arsenic concentration in the groundwater and contamination of groundwater due to use of unimproved sanitation. To cater the demand of safe drinking water and improved sanitation at the household level, CARE Bangladesh introduced market based WASH intervention in the SHOUHARDO III (Strengthening Household Abilities to Respond to Development Opportunities) program which encompassed the community based WASH management as a sustainability issue. The program conducted a situation analysis with the intention to assess the need of local service provider (LSP)-led water quality testing, production and selling of improved latrine products and repair of tube well with a specific focus on LSP's capacity building, the willingness of the community people to pay, and the potential challenges and then based on situation analysis report, program selected WASH entrepreneurs as LSP and facilitated five days long residential training with necessary tools and techniques so that they could start the business. The WASH entrepreneurs played a vital role to aware people on drinking arsenic free safe water and tested household tube well with arsenic kit box at a certain fee, repaired tube well to make functional of those tube well, constructed platform of Tube well to avoid contamination from groundwater and produced different latrine products and sold to the customer and all that happened due to conducting a baseline survey at the beginning of the business. The baseline survey benefitted them with creating linkage between local-level water and sanitation planning with larger level water resources through demand-supply interface of market strategy and ensured community managed services at the doorstep of the households. In each month all WASH LSP submitted their business data to local Govt. institution like DPHE (Department of Public Health Engineering) so that DPHE could take initiative with alternative mitigation option for arsenic affected tube well and LSPs communicated with VDC (village development communities) members to give pressure to the locally elected bodies like Union council to leveraging WASH services for the poor and the marginalized people in their annual plan and budget. In addition to demand creation, LSP made better linkage with WASH private sector actors to ensure supply chains of spare parts of water and sanitary materials in the last miles. Therefore, this type of market driven initiative will contribute to minimize the risk of groundwater contamination and to improve the groundwater quality and broadly to achieve SDG 6.

Keywords: *WASH entrepreneurs, arsenic, groundwater, latrines, demand, supply, SDG*

ON NUMERICAL MODELING OF GROUNDWATER FLOW IN STREAM-WETLAND-AQUIFER SYSTEMS

Uğur BOYRAZ¹, Cevza Melek KAZEZYILMAZ-ALHAN *

¹ Istanbul University-Cerrahpasa, Civil Engineering, Istanbul, Türkiye

*Corresponding author (meleka@iuc.edu.tr)

ABSTRACT

Groundwater resources are in interaction with the nearby surface water bodies. This interaction affects the hydrology of both water systems. Therefore, the determination of groundwater behavior is crucial for sustainable solutions in the water research area. In this study, a numerical algorithm called “Wetland Systems Finite Difference (WSF) Numerical Model” is developed using an explicit finite difference numerical scheme for a stream-wetland-aquifer system. 2 dimensional steady and transient flow conditions are considered. A homogeneous and isotropic aquifer is assumed and a sloped stream is defined as a boundary condition to the system to represent the stream effect on groundwater flow. The source/sink term is introduced into the groundwater flow equation using Darcy’s Law to represent the effect of wetland on groundwater flow. The groundwater head distributions and hyporheic exchange flow rates between stream & aquifer and wetland & aquifer are obtained. Moreover, this stream-wetland-aquifer system is modeled with Visual MODFLOW (VMOD) which is a 3-dimensional groundwater flow numerical model and is commonly used in groundwater-related problems. Modeling assumptions and capabilities of VMOD on a stream-wetland-aquifer system are investigated and compared with WSF. The comparison of the VMOD solutions with WSF solutions showed that both models calculate groundwater head distribution similarly. However, modeling algorithms and approaches are different to simulate streams and wetlands. While VMOD works with distinct modules to combine stream, wetland, and aquifer, WSF consists of one algorithm which considers them as a unique system. In addition, the basic differences, advantages, and disadvantages of VMOD and WSF are discussed.

Keywords: *Stream-wetland-aquifer system, hyporheic exchange, numerical solution, Wetland Systems Finite Difference (WSF) Numerical Model , Visual Modflow.*

INVESTIGATION OF LAKE-AQUIFER INTERACTIONS WITH EXPERIMENTAL METHODS

İnci Yalçın¹ and Cevza Melek Kazezyılmaz-Alhan^{1}*

¹ *İstanbul University-Cerrahpaşa, Department of Civil Engineering, İstanbul, Turkey*

^{*} *Corresponding author (meleka@istanbul.edu.tr)*

ABSTRACT

Groundwater is one of the largest freshwater reserves that needs to be protected and developed. Groundwater in unconfined aquifer is in constant interaction with surface water. This interaction has an impact on water supply and water quality, and the hydrological behavior of systems involving surface water-groundwater interactions needs to be investigated. In this study, the lake-aquifer system, in which the surface water-groundwater interaction is observed, was investigated by experimental methods. The effects of different parameters on the interactions were examined and the results were compared.

Keywords: *Lake-Aquifer System, Surface Water-Groundwater Interactions, Hydrology Apparatus.*

1. INTRODUCTION

Groundwater continuously interacts with surface water, affecting the water quantity and quality (Kazezyılmaz-Alhan ve Medina, 2008; Sophocleous, 2002). The importance of considering groundwater and surface water as a single resource has become increasingly evident (Winter et al., 1999). The interaction of different types of surface water with groundwater occurs differently. In this study, experiments were carried out with the Hydrology Apparatus in order to observe the surface water-groundwater interactions in the lake-aquifer system and the effects of different parameters on these interactions. The experiments were conducted with different hydraulic head differences, under different rainfall intensities and with and with no lake bed. The change in surface water and groundwater levels in the aquifer under different conditions was observed from piezometers located at different points in the system. The experimental results were compared and evaluated to present the impact of different parameters on the interactions.

2. MATERIAL AND METHODS

The experimental system, which simulates the lake-aquifer interaction, was developed by integrating the material representing the lake into the Hydrology Apparatus in the Hydraulics Laboratory. In addition, the suitable soil type and its properties for lake-aquifer interaction were determined.

The Hydrology Apparatus consists of a 2x1m storage filled with sand, which represents the aquifer, nozzles above the storage for simulation of rainfall, and a water tank at the bottom for the circulation of water through the system. The rainfall-runoff relation, infiltration and groundwater flow may be observed using the system.

In order to determine the proper soil type, observations on water flow were made with laboratory sand and natural washed sand in the aquifer. Based on the observations, natural washed sand provides a more suitable environment for the experiments. The grain size distribution and hydraulic conductivity tests for natural washed sand were carried out in order to determine its mechanical properties. Then, the storage, which represents the aquifer, was filled with the natural washed sand.

In order to simulate the lake in the experimental setup, a hemispherical material was designed which allows for water flow between lake and aquifer. Then, it was placed in the middle of the aquifer. In order to simulate the lakebed, which represents the transition between the aquifer and the lake, a mixture of sand and clay was applied. The lake-aquifer interaction experimental setup with Hydrology Apparatus is shown in Figure.



Figure1 Lake-Aquifer Interaction Experimental Setup with Hydrology Apparatus.

Eight scenarios were considered to investigate the effects of hydraulic head difference, rainfall and lake bed parameters on the lake-aquifer interactions. Two-dimensional flow in the horizontal plane was taken into account. The conditions chosen for each scenario are given in Table.

Table 1. Lake-aquifer system parameters.

Experiment No	Lake Bed Thickness (cm)	Groundwater Table (cm)	Lake Surface (cm)	Constant Boundary Condition (cm)	Recharge (cm/min)
1		-	-	17	-
2		3	-	-	0.07
3	0	-	18	-	-
4		-	18	-	0.07
5		-	-	17	-
6		3	-	-	0.07
7	0.5	-	18	-	-
8		-	18	-	0.07

3. RESULTS AND DISCUSSIONS

In the experiments carried out in the Hydraulics Laboratory of Istanbul University-Cerrahpaşa Civil Engineering Department, the groundwater table values during unsteady state conditions were observed with the piezometers and the results were compared. In order to determine the effect of hydraulic head on the interactions, experiments were carried out under two different conditions, i.e. the aquifer recharge and the aquifer discharge.

Then, rainfall was added to the experiments in order to determine the effect of the hydraulic head difference on the interaction under rainfall events. Rainfall resulted in an increase in the groundwater level in the system relatively faster than the experiments without rainfall.

In order to investigate the effect of the lake bed on the interaction between the lake and the aquifer, experiments with and with no lake bed were carried out. The lake bed partially prevented the water exchange between the two water sources and slowed down the water transition.

An example of the comparison of the experiments is given Figure 2. Figure 2 presents the results of Experiment 3 and Experiment 7, which are carried out without and with the lake bed under initially dry aquifer condition, respectively. The surface water flows towards aquifer representing aquifer recharge. The results of all experiments were similarly compared.

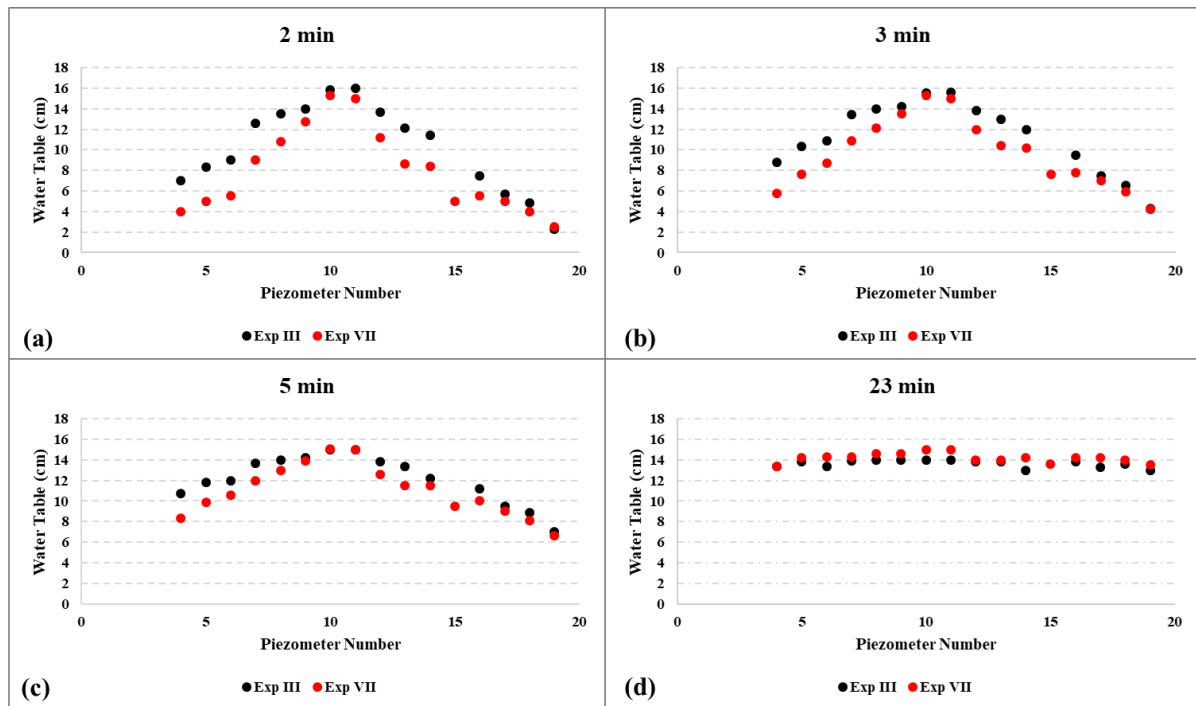


Figure 2. Comparison of the piezometer values of experiment 3 and 7 for different times (a) 2 min, (b) 3 min, (c) 5 min, (d) 23 min.

4. CONCLUSIONS

In this study, the effects of lake-aquifer interactions on groundwater flow were investigated by experimental methods. By establishing different models, the parameters affecting the groundwater level distribution were investigated and determined. As a result of the experimental studies, it has been determined that the lake-aquifer interactions can be observed under hydraulic head difference, rainfall and variable lake bed conditions with the Hydrology Apparatus. It has been observed that the hydraulic head difference, rainfall and lake bed have a significant effect on the lake-aquifer interaction, and these effects depend on time and location.

REFERENCES

- Kazezyilmaz-Alhan, C. M. & Medina, M. A. (2008). The effect of surface/ground water interactions on wetland sites with different characteristics. *Desalination*, 226, 298-305.
- Sophocleous, M. (2002). Interactions between groundwater and surface water: the state of the science. *Hydrogeology Journal*, 10, 348 (2002).
- Winter, T. C., Harvey, J. W., Franke, O. L. & Alley, W. M. (1999). Ground water and surface water: a single resource. *U.S. Geological Survey Circular 1139*, Denver, Colorado 1999.

NEXUS APPROACH

THE IMPACT OF RENEWABLE ENERGY ON ECONOMIC GROWTH IN CEE COUNTRIES

Author 1, Prof. Assoc. Dr. Doriana Matraku (Dervishi),
Author 2, Ph.D. student Kamela Selenica*

Lecturer of Economics, Economics Department, Faculty of Economy, University of Tirana (FEUT)

Albanian Development Fund, Tirana, Albania. Ph.D. student, Economics Department, FEUT, Tirana, Albania

**Corresponding author email: dorianadervishi@feut.edu.al.*

ABSTRACT

In recent years, climate change and global warming, limited reserves of natural gas and petrol sources, high and volatile energy prices, and technological change make it mandatory to replace traditional energy sources with alternative energy sources. Studies have shown that fossil fuel consumption is the largest contributor to global greenhouse gas emissions and that continued dependence on fossil fuels will only exacerbate the rate of environmental degradation. To reduce CO₂ emissions, many countries have shifted to using renewable energy sources. In this context, this study aims to explore and evaluate the relationship between renewable energy consumption and economic growth for 19 Central Eastern European countries, from the time interval 2000-2019, within the framework of a traditional production function.

The study was implemented via dynamic panel data estimation methods, to research the long-term relationship between renewable energy consumption and economic growth in CEE countries, by taking into consideration the cross-section dependence effect in the panel. The estimation of long-term parameters was conducted by implementing fully modified ordinary least squares (FMOLS) and dynamic ordinary least squares (DOLS), to increase the accuracy and efficiency of model estimation. In this study, we have also tested for the stability of the series with the panel unit root tests and analyzed the long-term co-integration relationship between the dependent and independent variables in the panel data set, by using the panel co-integration test. The results of panel unit root tests show that series are stable and don't have unit roots at the first difference. The study has also concluded that there is a long-term balance relationship between renewable energy consumption and economic growth and the empirical results suggest that renewable energy consumption has a positive impact on economic growth.

Keywords: *Economic Growth, Renewable Energy, Long-term relationship, CEE countries*

1. INTRODUCTION

Each stage of economic development has been accompanied by a characteristic energy transition, moving from one fuel source to another, as the main factor of energy production growth in developing economies. While the energy demand continues to increase everywhere in the world, the levels of carbon dioxide emitted into the atmosphere have also been increasing, which is negatively affecting efforts to combat climate change. Consumption of non-renewable energy can boost economic growth, but it is undoubtedly a significant source of environmental pollution and carbon dioxide emission. Since the pollution caused by fossil fuels has increased year by year and the economic situation has been worsening due to the COVID-19 and energy crisis, many countries have been forced to find alternative energy sources to conventional energy sources. With the aim of sustainable development for the future, most of them have started investing in new energy developments. Renewable energy sources as an alternative source present themselves with an important potential and perform a crucial role, by decreasing dependency on fossil fuels, which are very limited in supply. Due to climate change and the global warming situation, renewable energy could be the most attractive alternative to fossil fuels, reducing the CO₂ emission process (Bhuiyan et al., 2022).

The relationship between renewable energy and economic growth has created a large interest among researchers and policymakers worldwide. This interest has also been the motivation for our work and has led us to undertake this study. This study aims to explore the relationship between renewable energy consumption and economic growth for the time interval 2000-2019, for 19 Central Eastern European countries: Albania, Belarus, Bosnia and Herzegovina, Bulgaria, Croatia, Czech Republic, Estonia, Hungary, Latvia, Lithuania, Moldova, North Macedonia, Poland, Romania, Russia, Serbia, Slovak Republic, Slovenia, and Ukraine.

Most of the previous studies have shown a positive relationship between renewable energy consumption and economic growth, which is also called the *growth hypothesis* in literature. Bilgili and Ozturk (2015) found that renewable energy had a significant positive impact on economic growth in G7 and 51 sub-Saharan African countries using panel co-integration, panel OLS and panel DOLS for the 1980–2009 period. Inglesi-Lotz (2016) estimated the impact of renewable energy consumption on economic welfare by employing panel data techniques, including 34 OECD countries for the period from 1990 to 2010, and concluded that the influence of renewable energy consumption on economic growth is positive and statistically significant. Similarly, Koçak and Şarkgüneşi (2017) explored the relationship between renewable energy consumption and economic growth within the framework of the traditional production function for the period of 1990–2012 in 9 Black Sea and Balkan Countries and concluded that there exists a long-term balance relationship between renewable energy consumption and economic growth and renewable energy consumption has a positive impact on economic growth.

Some other studies have shown different results, supporting the *neutrality hypothesis* (energy consumption doesn't have any effect on economic growth). Menegaki (2011) analyzed the relationship between economic growth and renewable energy for 27 European countries in a multivariate panel framework over the period 1997–2007 using a random effect model and he

couldn't find a significant relationship between renewable energy and economic growth. Bhattacharya et al. (2016) in their study examined the possible effect on the economic growth of renewable versus non-renewable energy sources across 38 countries for the time period between 1991 and 2012 and concluded that renewable energy consumption has a positive impact on economic growth for 23 countries and a negative impact for 4 countries. This implies that those countries which had a negative impact on economic growth, need to increase capital for sustainable development of renewable energy consumption and follow a gradual process for deployment. Shahbaz et al. (2020) also examined the effect of renewable energy consumption on economic growth across 38 countries from 1990 to 2018 using DOLS, FMOLS, and heterogeneous non-causality approaches and confirmed the presence of a long-run relationship between renewable energy consumption and economic growth. They also found a positive impact of renewable energy on economic growth for 58% of the sample countries and a negative impact for 24% of the sample countries.

The organization of this paper is as follows: Section 2 discusses the model, data and describes the econometric methodology. Section 3 provides the estimation results, derived from the panel unit root test, the panel cointegration test, as well as the estimation of the long-run coefficients using the DOLS and FMOLS methods. Finally, Section 4 evaluates the main conclusions of our study and policy implications.

2. ECONOMETRIC METHODOLOGY

Model, data, and econometric methodology

In this paper, the linkages between renewable energy and economic growth will be examined using the neo-classical production function following Koçak and Şarkgüneşi (2017). The general type of production function that considers renewable energy, capital, and labor as individual inputs is defined as follows:

$$Y_{it} = f(RE_{it}, K_{it}, L_{it}) \quad (1)$$

In Eq. (1), Y stands for economic growth, RE stands for renewable energy, K stands for capital stock and L stands for labor, while i and t stand for nation and time. Thus, Equation 1 was transformed into a log-linear specification by taking all the variable's natural logarithms. The benefits we get from transforming the equation into logarithmic form are: a) the transformation of the variables into a natural logarithm provides efficient and consistent empirical results (Shahbaz et al., 2012); b) the transformation of data series into a natural logarithm avoids the problems associated with dynamic properties of the data series (Bhattacharya et al., 2016). The empirical equation of the production function is modeled as follows:

$$\ln Y_{it} = \beta_{1i} \ln RE_{it} + \beta_{2i} \ln K_{it} + \beta_{3i} \ln L_{it} + \varepsilon_{it} \quad (2)$$

where β_1 , β_2 and β_3 are elasticities of economic growth with respect to renewable energy consumption (RE), capital (K) and labor (L), respectively and ε is the error term.

Our study employs data for 19 Central Eastern European countries (Albania, Belarus, Bosnia and Herzegovina, Bulgaria, Croatia, Czech Republic, Estonia, Hungary, Latvia, Lithuania, Moldova, North Macedonia, Poland, Romania, Russia, Serbia, Slovak Republic, Slovenia, and

Ukraine) for the time period 2000-2019. We would like to highlight that one of the limitations of this paper is the lack of data availability for Kosovo, which is part of the CEE countries. The databases provided for this country are very truncated since it is considered a new country. For economic growth, we used GDP (constant 2015 US\$), for renewable energy consumption (RE) the share of renewable energy in total final energy consumption (%), for capital (K) we used gross fixed capital formation (constant 2015 US\$), and for labor (L) we used labor force participation rate (% of the total population for ages 15-64). All the data that we are using for our study is collected from the World Bank Database.

To study the long-term relationship between renewable energy consumption and economic growth in CEE Countries, we will use the panel data method. First, to test for the stability of the series and to ensure the robustness of our components we will use the panel unit root test. This test considers both heterogeneity and cross-sectional dependence across panels. The first generation of tests assumes that cross-section units are cross-sectionally independent; whereas the second generation of panel unit root tests relaxes this assumption and allows for cross-sectional dependence (Tugcu, 2018). Therefore, the empirical equation of the unit root test is modeled as follows:

$$\Delta y_{it} = \rho y_{it-1} + \sum_{L=1}^{pi} \theta_{iL} \Delta y_{it-L} + \alpha_{mi} d_{mt} + \varepsilon_{it}, \quad m = 1,2,3 \quad (3)$$

In equation (3) ε_{it} is uncorrelated throughout the units and follows an ARMA process. Δ shows the first differences d_{mt} shows dummy variables for each unit, α_{mi} shows their parameters (Koçak and Şarkgüneşi, 2017). We test the null hypothesis that each series in the panel dataset contains a unit root against the alternative, at least one of the individual series in the panel is stationary (no unit root) $H_0: \rho=0$ and $H_a: \rho < 0$. When the null hypothesis is rejected, it is determined that the series doesn't contain a unit root, so the series are stationary. If the results of the test show that the series are stable at level value, then the analysis will proceed with the traditional OLS method estimation, otherwise, if the series are stable at first differences, the panel cointegration test will be followed in our study.

Second, we use the Pedroni panel cointegration test, to examine if between variables exists a long-term cointegration relationship. Pedroni (2000) introduced seven test statistics that test the null hypothesis of no cointegration (in other words, the residuals are non-stationary) against the alternative hypothesis that approves there is a co-integration relationship. The seven test statistics are grouped into two categories: group-mean statistics that average the results of individual country test statistics and panel statistics that pool the statistics along the within-dimension (Neal, 2014). The first group of Pedroni's tests consists of panel semi-parametric v , ρ , and t-statistics which corresponds to the variance ratio, and Phillip-Peron ρ and t-statistics univariate analogues, respectively, and parametric panel ADF t-statistics. The second group consists also of Phillip-Peron ρ and t-statistics and ADF t-statistics, but is computed according to the group-mean principle (Mitić et al., 2017). If the results of the Pedroni test indicate that the null hypothesis is rejected, then it is determined that exists a long-term relationship among the variables.

The last step is estimating the long-run elasticity of output, by using Pedroni's (2000, 2001) Fully Modified OLS (FMOLS) and Dynamic OLS (DOLS) methods, since these two approaches account for serial correlation and endogeneity that may exist in our model. The equation is modeled as follows:

$$Y_{it} = \delta_{it} + \beta_i X_{it} + \varepsilon_{it} \quad (4)$$

where Y and X indicate the dependent variable and the corresponding vector of independent variables, while i, t, and ε stand for individuals, time, and the error term, under the assumption that there is no dependence between sections that consist of the panel. The DOLS estimator in a panel case can be derived by running the following regression:

$$y_{it} = \alpha_i + \beta_i x_{it} + \sum_{k=-Ki}^{Ki} \gamma_{ik} \Delta x_{it-k} + \varepsilon_{it}$$

where K denotes the number of lags/leads chosen using some info criterion and γ_{ik} is the coefficient of a lag or lead of the first differenced variables. The DOLS estimator also has an additional advantage in controlling the endogeneity in the model, as augmentation with the lead and lagged differences of the regressor suppresses the endogenous feedback (Lean & Smyth, 2010). Besides the DOLS method and considering that the properties of our data are first-order integrated, this study will also use the Pedroni (2000) FMOLS approach. FMOLS estimator eliminates the second order bias caused by the endogeneity of the regressors by incorporating the Phillips and Hansen (1990) semi-parametric correction into the OLS estimator.

Descriptive statistics of the variables

Table 1 presents the descriptive statistics for each of the variables in our model and correlations among these variables, to show some of the beginning information in our analysis. All the results shown in the tables in this paper are author calculations. In Table 1 we can notice that all descriptive statistics of lnGDP are greater than those of lnRE, lnK and lnL. From the correlation matrix, we can see that lnGDP is positively correlated with lnK and lnL and negatively correlated with lnRE. lnK is positively correlated with lnL and negatively correlated with lnRE. lnL is also negatively correlated with lnRE.

Table 1. Descriptive statistics and correlation matrix

Descriptive statistics	lnGDP	lnK	lnL	lnRE
Mean	24.63	23.11	14.96	2.61
Std. Dev	1.30	1.29	1.22	0.77
Min	22.08	20.23	13.39	-0.01
Max	28.01	26.49	18.14	3.75
Observations	380	380	380	380

Correlation matrix

lnGDP	1			
lnK	0.998	1		
lnL	0.873	0.847	1	
lnRE	-0.51	-0.496	-0.717	1

3. RESULTS AND DISCUSSIONS

We have applied LLC (Levin, Lin, and Chu) panel unit root tests to GDP, Renewable Energy, Capital and Labor levels and first differences. The results of panel unit root test are provided in Table 2.

Table 2. LLC panel unit root test

Variable	I(1)
GDP	-4.42***
Δ GDP	-5.18***
RE	-1.32
Δ RE	-8.25***
K	-4.00***
Δ K	-8.04***
L	-1.10
Δ L	-5.18***

*** Indicates the rejection of null hypothesis of unit root at 1% significance level.

As we see, the results of the panel unit root test are mixed, especially for GDP and capital, where the LLC test indicates stationarity in both levels in the first differences, while renewable energy consumption and labor are stable only at the first differences. However, the empirical results reported in Table.1 reveal that the null hypothesis of the panel unit root is rejected for all the variables after the first differencing, indicating that the series are stable at the first difference.

The next step is to examine the co-integration relationship between the variables since a long-term equilibrium relationship is possible to happen. Table 3 shows the findings of the panel co-integration test. According to the test results, out of seven test statistics, only five confirm the presence of a co-integration relationship among lnGDP, lnRE, lnK, and lnL. Therefore, we conclude that a balanced relationship in the long term between renewable energy consumption, capital, and labor seems possible.

Table 3. Pedroni panel co-integration test results

	Statistic	Probability
Within dimensions (common AR coefficients)		
Panel v-statistic	-4.439***	0.000
Panel rho-statistic	0.249	0.401
Panel PP-statistic	-3.325***	0.000
Panel ADF-statistic	-3.553***	0.000
Between dimensions (individual AR coefficients)		
Group rho-statistic	1.543*	0.061
Group PP-statistic	-4.740***	0.000
Group ADF-statistic	-4.382***	0.000

*** Indicates the rejection of the null hypothesis of unit root at 1% significance level.

* Indicates the rejection of the null hypothesis of unit root at 10% significance level.

Newey-West Bandwidth selection with Bartlett Kernel is used.

The last step is to estimate the long-term output elasticities, using panel dynamic OLS and panel fully modified OLS. The results of the estimation for both methods are presented in Table 4. As we can see, both panel DOLS and panel FMOLS give similar results, for each of the variables, in terms of sign and significance level. For the DOLS results, a 1% increase in renewable energy will increase GDP by 0.16%, while for the FMOLS results, a 1% increase in renewable energy will increase GDP by 0.17% and the coefficients are statistically significant at 1% level. Our findings also suggest that both capital and labor have a positive impact on economic growth, and coefficients are statistically significant at 1% and 5% level, respectively.

Table 4. Panel data analysis for CEE Countries (2000-2019)

Variable	Panel DOLS		Panel FMOLS	
	Coefficient	t-statistic	Coefficient	t-statistic
lnK	0.488***	0.000	0.536***	0.000
lnL	0.416**	0.022	0.327**	0.021
lnRE	0.163***	0.000	0.170***	0.000

*** Indicates the significance level at 1%.

** Indicates the significance level at 5%.

4. CONCLUSIONS

Nowadays the world attentions are focused towards sustainable development, which is possible to be achieved by using sustainable energy and by ensuring access to affordable, reliable, and

clean energy for citizens. The transition to an energy system based on renewable technologies will have very positive economic consequences on the global economy and it is considered essential to raise the standard of living. We conclude that our analysis showed that the series are stationary at the first differences by the panel unit root test. The results of the Pedroni cointegration test show that between the GDP, renewable energy consumption, gross fixed capital formation and labor force participation rate exists a long-term balance relationship. The estimation of the parameters of the relationship between renewable energy and economic growth indicate that renewable energy can be considered as a significant driver of economic growth. Specifically, the results of this study shows that a 1% increase in renewable energy consumption will increase GDP by 0.16% for DOLS method, while a 1% increase in renewable energy consumption will increase GDP by 0.17% for FMOLS method. Capital and labor also have a positive impact on economic growth, where a 1% increase in gross fixed capital formation will increase GDP by 0.48%, while a 1% increase in labor force participation rate will increase GDP by 0.41%.

The findings in this paper suggest that it is very important for government policies to support and promote the use of renewable energy sources in these CEE countries, replacing the use of traditional energy sources. To develop a sustainable economy, all the countries need a wide range of policy interventions and financing measures to support the transformation of energy and to improve energy efficiency. The government could promote innovation, providing fiscal incentives to companies investing in the R&D sector for finding more efficient solutions and clean-energy technologies that could be adopted. Governments could also decide to stimulate the use of renewable energy by lowering taxes, reducing investment costs through subsidies, loans, and grants, or by using sales tax exemptions for solar cells and feed-in tariffs. In those countries where the policies will be adopted, it will not only encourage them to export their technologies, but also lead them to share their policy experiences with other countries, creating renewable energy-oriented networks between their organizations.

Acknowledgments: The authors acknowledge the grant provided by IWA DIPCON 2022 and Cost Action CA 20138.

REFERENCES

- Bhattacharya, M., Paramati, S.R., Ozturk, I., Bhattacharya, S. (2016). The effect of renewable energy consumption on economic growth: evidence from top 38 countries. *Applied Energy*, 162, 733–741.
- Bhuiyan, M. A.; Zhang, Q.; Khare, V.; Mikhaylov, A.; Pinter, G.; Huang, X. (2022), Renewable Energy Consumption and Economic Growth Nexus—A Systematic Literature Review. *Frontiers in Environmental Science*, 10
- Bilgili, F. & Ozturk, I. (2015). Biomass energy and economic growth nexus in G7 countries: Evidence from dynamic panel data. *Renewable and Sustainable Energy Reviews*, 49, 132-138.
- Inglesi-Lotz, R. (2016). The impact of renewable energy consumption to economic growth: A panel data application. *Energy Economics*, 53, 58-63.
- Koçak, E. & Şarkgüneşi A. (2017). The renewable energy and economic growth nexus in Black Sea and Balkan countries. *Energy Policy*, 100, 51-57.
- Lean, H.H. & Smyth, R. (2010). CO2 emissions, electricity consumption and output in ASEAN. *Applied Energy*, 87, 1858–1864.

- Menegaki, A. N. (2011). Growth and renewable energy in Europe: A random effect model with evidence for neutrality hypothesis. *Energy Economics*, 33, 257-263.
- Mitić, P., Ivanović, O.M., Zdravković, A. (2017). A Cointegration Analysis of Real GDP and CO2 Emissions in Transitional Countries. *Sustainability*, 9(4), 1-18
- Neal, T. (2014). Panel cointegration analysis with xtpedroni. *The Stata Journal*, 14(3), 684-692
- Pedroni, P. (2000). Fully modified OLS for heterogeneous cointegrated panels. Nonstationary Panels, Panel Cointegration, and Dynamic Panels. *Advances in Econometrics*, 15, 93–130.
- Pedroni, P. (2001). Purchasing power parity tests in cointegrated panels. *Review of Economics and Statistics*, 83(4), 727-731.
- Phillips, P.C.B. & Hansen, B.E. (1990). Statistical inference in instrumental variables regression with I(1) processes. *Review of Economic Studies*, 57, 99-125
- Shahbaz M, Loganathan N, Zeshan M, Zaman K. (2015). Does renewable energy consumption add in economic growth? An application of auto-regressive distributed lag model in Pakistan. *Renewable and Sustainable Energy Reviews*, 44, 576-585.
- Tugcu, C. T. (2018). Panel Data Analysis in the Energy-Growth Nexus, in Menegaki, A.N. (ed). *The Economics and Econometrics of the Energy-Growth Nexus*, 255-271
- World Bank, URL: (<http://data.worldbank.org/indicator>) (accessed 19.07.22).

PROLONGED DROUGHTS EFFECTS ON STREAM NITROGEN DYNAMICS IN CENTRAL GERMANY

Seifeddine Jomaa^{1*}, Xiangqian Zhou¹, Xiaoqiang Yang¹ and Michael Rode¹
¹. Helmholtz Centre for Environmental Research - UFZ, Germany
*Corresponding author (Corresponding author's e-mail)

ABSTRACT

Germany has experienced prolonged summer droughts from 2015-2018, similarly to many other regions in Southern and Central Europe. Consequently, river nitrate concentrations have exhibited considerable alterations. However, the effects of prolonged drought conditions have been rarely explored using a process-based and fully distributed hydrological water quality model. This study examines the spatiotemporal effects of drought conditions on stream nitrate responses of the Bode catchment using the grid-based mHM-Nitrate model. The model was trained and tested using data from six gauging stations, reflecting the contrasting landscape and different runoff components and their associated nitrate-mixing from upstream to downstream of the Bode catchment. Results revealed that the model could reproduce the daily discharge and nitrate concentration well, reflected by Nash-Sutcliffe Efficiency ≥ 0.73 and Kling-Gupta Efficiency ≥ 0.50 for discharge and nitrate concentration, respectively. Notably, the model could significantly represent the distinct spatiotemporal trends of nitrate concentrations observed between upstream and downstream gauging stations. The decline of nitrate concentration in the lowland area in drought periods (2015-2018) was probably due to the limited terrestrial export loading (ca. 40% lower than that of average years 2004-2014) and increased instream retention efficiency (20% higher in summer within the whole river network). This study helped gain insights into the spatiotemporal effects of prolonged droughts on streamflow and nitrate dynamics at the catchment scale. Testing and assessing water quality models under real changing weather scenarios such as droughts is essential for developing scientific knowledge and enhancing science-based management on water-quality responses to future climate change.

Keywords: *Drought, Nitrate mixing, Catchment hydrology, Water quality model.*

FORECASTING THE WATER CONSUMPTION OF HYDROELECTRICITY POWER PLANTS IN THE CONTEXT OF THE WATER-ENERGY NEXUS BASED ON AN ARTIFICIAL INTELLIGENCE APPROACH

Cigdem Coskun Dilcan^{1,2}, and Merih Aydinalp Koksal¹*

¹ Hacettepe University, Environmental Engineering Department, Ankara, Türkiye

² Present address: Ankara University, Water Management Institute, Ankara, Türkiye

*Corresponding author Cigdem Coskun Dilcan (coskunc@ankara.edu.tr)

ABSTRACT

The global water and energy demand is expected to grow significantly, making them vital resources that must be managed wisely. The main objective of this paper is to investigate the nonlinear relationship between the water consumption and electricity generation of hydropower plants with dams using the Adaptive NeuroFuzzy Inference System model. The annual average electricity generation and basin-based meteorological parameters of 80 hydroelectric power plants with dams were used as the input parameters. Their water consumption was used as the output parameter in the model. The dataset is divided randomly into training and testing datasets with ratios of 65%-35%, 70%-30%, 80%-20%, and 85%-15%. The 85%-15% splitting gave the best results with 13.54 % MAPE of all datasets. The water consumption of hydropower plants was forecasted between 2023 and 2053 using the GFDL RCP 4.5 and 8.5 climate scenarios. The results show that water intensity (m^3/GWh) in 2023 will increase from 39,419 m^3/GWh and 38,663 m^3/GWh to 65,414 m^3/GWh and 63,768 m^3/GWh in 2053, respectively.

Keywords: *water consumption, hydroelectric powerplant, ANFIS, evaporation, water-energy nexus.*

1. INTRODUCTION

Power generation from hydroelectric plants has increased by 50% since 1990 as the largest renewable energy source worldwide. The global hydroelectricity production capacity is expected to increase up to 17% between 2021 and 2030 (IEA, 2021). The commonly used type of hydropower generation occurs at dams or rivers. "Run-of-the-river" hydropower plants (HPP) consume minimal water and do not require reservoirs. When associated with water storage in reservoirs, the amount of water consumed at the HPP is determined by leakage and evaporation. These depend on the climate and physical characteristics of the reservoir (McMahon and Price, 2011).

In the literature, there are some studies on determining the water consumption of HPP using linear estimations. A review study on water consumption from HPP by Bakken et al. (2013) indicated that the commonly used term for water consumption from HPP was evaporation. Besides this, it was stated that water loss via groundwater leakage could be negligible. Water consumption from HPP also depends on temperature, precipitation, reservoir surface area, etc.

Mekonnen & Hoekstra (2011) stated that reservoirs in tropical regions have higher evaporation rates than in mild regions.

Besides the linear estimations, artificial intelligence approaches are used to determine the water consumption of HPP. In the study of Allawi et al. (2019), an ANN prediction model was developed using hydrological parameters of reservoir systems. The parameters were inflow, the release of the dam, initial and final storage of the reservoir as input, and evaporation from the reservoir as output (Allawi, 2019). Also, some studies included different combinations of meteorological input parameters such as rainfall, minimum, mean, and maximum temperature, relative humidity, minimum, maximum, and mean wind speed, global solar radiation, sunshine hours, and surface pressure. The commonly used artificial intelligence approaches used to estimate the water consumption of HPP are Feed Forward Neural Network (FFNN), Adaptive Neuro-Fuzzy Inference System (ANFIS), Support Vector Regression (SVR), Multilinear Regression (MLR), FLANN (Functional link ANN), MLANN (Multilayer ANN), Linacre and Christiansen (Empirical models), Whale Optimization Algorithm (WOA), Grey Wolf Optimization (GWO) (Nourani et al., 2019, Seifi and Soroush, 2020, Majhi and Naidu, 2021). However, there is a lack of studies including the nonlinear relationship with the artificial intelligence approach, which can interconnect electricity production with the water consumption prediction of HPP and better work with nonlinear and limited data and error reduction. Thus, the main objective of this study is to determine the interaction between the water consumption of electricity generation of HPP with a new model approach via using ANFIS for sustainable resource management.

2. MATERIAL AND METHODS

The study area, data sources, model development, and statistical measurements involved in this study are summarized in the following sections.

Study Area and Data Sources

The input and output parameters of the developed model are obtained from the data of 80 hydroelectric plants with dams above 25 MW installed capacity in Turkey (TEIAS, 2022). The locations of the hydropower plants are presented in Figure 1.

The climate change projections data for 25 basins of Turkey was obtained from The Turkish State of Meteorological Service. The climate models selected are Geophysical Fluid Dynamics Laboratory Model (GFDL), The Hadley Centre Global Environment Model (HadGEM), and The Max Planck Institute for Meteorology-Earth-System Model (MPI). These models were developed based on the Representative Concentration Pathway (RCP) 4.5 and 8.5 future emissions scenarios on fine spatial resolution up to 10 km by 10 km. The reference meteorological data between 1990 and 2000 was used to develop the ANFIS model. The reason for choosing basin-based meteorological data was to be able to cover a large area depending on characteristic climatic features. The annual average evaporation and average electricity generation of 80 HPP with dams were gathered from the Basin-based Master Plan Reports of State Hydraulic Works, EUAS, and open sources.

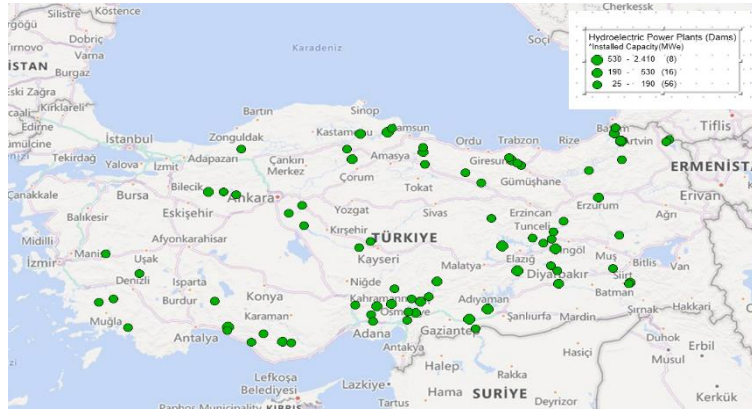


Figure1. Locations of the hydroelectric powerplants

The descriptive statistics of the input and output parameters of the developed model are given in Table 1.

Table 1. Descriptive statistics of the input and output parameters

		Statistical data			
	Parameters	Ranges	Mean	SD	Units
Input	Annual Avg. Sunshine Duration	8.64 - 9.61	9.12	0.23	(hours)
	Annual Avg. Precipitation	1.23 - 3.00	1.82	0.42	(mm)
	Annual Avg. Wind Speed	2.89 - 3.79	3.12	0.20	(m/s)
	Annual Avg. Generation	28.40 - 7485.50	658.90	1317.49	(GWh)
	Annual Avg. Temperature	2.51 - 11.29	7.37	1.99	(⁰ C)
Output	Annual Avg. Evaporation	200 - 1119	369.80	146.40	(Mm ³)

Adaptive Neuro-Fuzzy Inference System Model Development

The adaptive neuro-fuzzy inference system (ANFIS), proposed by Jang et al., is a method for tuning the existing rule base of a fuzzy inference system (FIS) whose membership functions are adjusted using the adaptive learning capability of an artificial neural network. An adaptive network is one type of neural network that includes multiple layers, and learning rules are applied to nodes in layers to reduce errors in the network's output. By combining FIS with adaptive networks, ANFIS models are trained faster and more accurately and can accelerate convergence faster than the conventional ANN (Jang et al., 1997). MATLAB Neuro-Fuzzy Designer Toolbox was used as a modeling tool for model development which supports easy creation and modifying the ANFIS model properties.

2.4 Statistical Measures

The three most commonly used statistical measures to determine the model's prediction accuracy are root mean square error (RMSE), mean absolute percent error (MAPE), and coefficient of determination (R-square). In the following formulas, X_i is the simulated variable, Y_i is the actual variable, and m is the number of variables.

$$RMSE = \sqrt{\frac{1}{n} \sum_{t=1}^n (X_t - Y_t)^2} \quad (1)$$

$$MAPE = \frac{100\%}{n} \sum_{t=1}^n \left| \frac{e_t}{y_t} \right| \quad (2)$$

The R-squared (Wright, 1921), ranging from zero to one, represents the square of the correlation (r) between two data sets. It can be defined as the convergence rate of the independent and predicted dependent variables.

$$R^2 = 1 - \frac{\sum_{i=1}^m (X_i - Y_i)^2}{\sum_{i=1}^m (\bar{Y} - Y_i)^2} \quad (3)$$

After each trial, suitable FIS parameters, such as the number and type of input membership functions, were evaluated based on the RMSE of the training and testing datasets.

3. RESULTS AND DISCUSSIONS

The dataset is divided into training and testing datasets by the ratio of 65%-35%, 70%-30%, 80%-20%, and 85%-15% randomly for all GFDL, HadGEM, and MPI climate scenarios, respectively. The prediction performances of the developed models are evaluated based on the RMSE and MAPE of dataset errors. The model parameters are presented in Table 2.

Table 2. ANFIS model development parameters

ANFIS Parameters	Value
Input Membership Function (MF) Type	gbellmf
Number of Input MF	[2 2 2 3 3]
Output MF Type	Constant
FIS Generation Method	Grid Partitioning
Learning Algorithm	Hybrid
Number of Epoch	300

MAPE of the training, testing, and all dataset errors are presented in Table 3. As can be seen here, the dataset separated as 85-15% resulted in the lowest testing dataset MAPEs with 9.37%, 9.59, and 9.87% for GFGL, HadGEM, and MPI weather estimates, respectively. The MAPE of the testing dataset is under and near 10% for the HPP ANFIS model, which can be considered a good prediction performance for this model (Gilliland. M., 2010).

Table 3. MAPE of HPP ANFIS Model

Data splitting ratio		Error Metric MAPE (%)		
		<i>GFDL</i>	<i>HadGEM</i>	<i>MPI</i>
65 % Training-35% Testing	Training	10.06	10.83	9.92
	Testing	44.67	33.97	31.24
	All Data	22.04	18.84	17.30
70 % Training-30% Testing	Training	12.51	12.79	12.60
	Testing	23.54	28.73	24.22
	All Data	15.76	17.49	16.03
75 % Training-25% Testing	Training	14.07	14.15	13.94
	Testing	21.87	30.90	19.94
	All Data	15.97	18.23	15.40
80 % Training-20% Testing	Training	14.04	14.28	13.55
	Testing	19.64	20.10	18.27
	All Data	15.19	15.47	14.52
85 % Training-15% Testing	Training	14.30	14.68	14.63
	Testing	9.37	9.59	9.87
	All Data	13.54	13.90	13.89

The model developed using the GFDL climate estimates resulted in the lowest MAPE (13.54%) for all datasets. Thus, it was selected for forecasting the water consumption of HPPs between 2023 and 2053. The actual and predicted water consumption of 80 HPPs using the GFDL model weather estimates with 85-15% dataset split is shown in Figure 2.

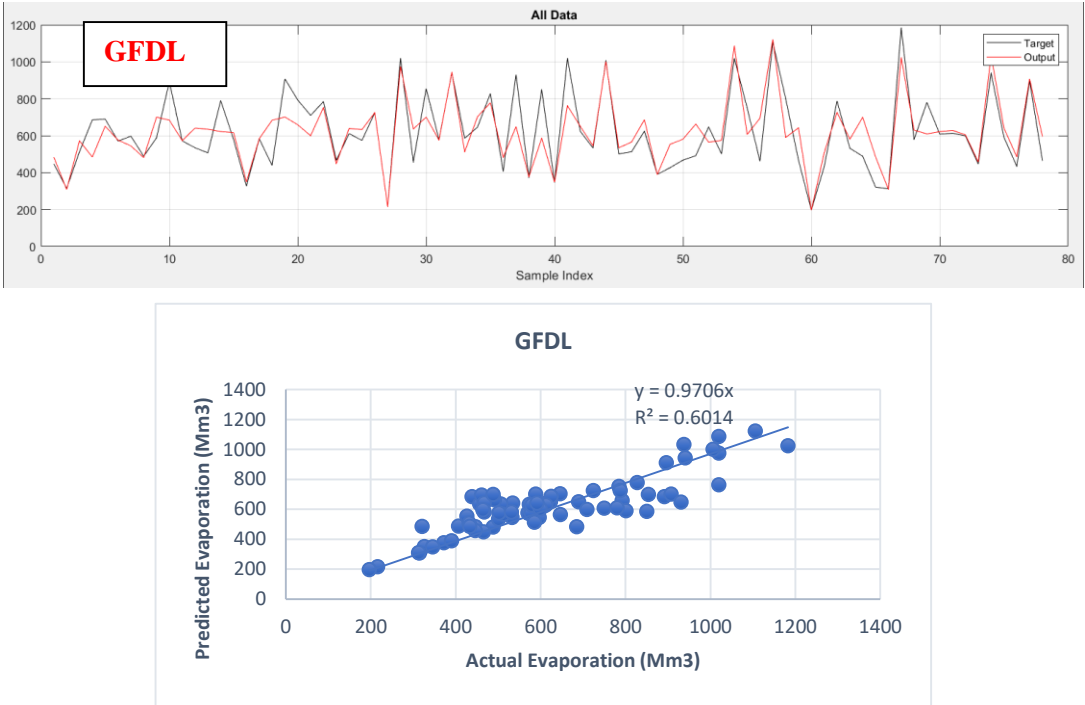


Figure 2. Actual and predicted HPP water consumption based on GFDL estimates

The water consumption of HPPs in 2053, estimated based on the GFDL 4.5 and 8.5 climate scenarios, will reach 10,963 Mm³ and 10,687 Mm³, respectively, as presented in Figure 3. Water intensity (m³/GWh) of the HPPs estimated based on GFDL 4.5 and 8.5 climate scenarios are expected to increase from 39,419 m³/GWh and 38,663 m³/GWh to 65,414 m³/GWh and 63,768 m³/GWh between 2023 and 2053, respectively. GFDL RCP 4.5 and 8.5 climate scenario estimates are very close. Water consumption of HPPs' will increase by nearly 80% in 2053 depending on the 2023 consumption levels for both GFDL RCP 4.5 and 8.5 climate scenario estimates.

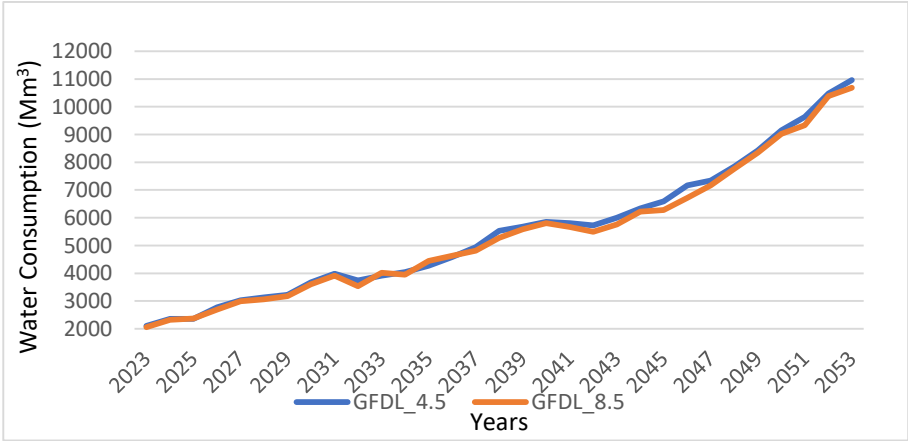


Figure 3. Forecasted water consumption between 2023 and 2053

4. CONCLUSIONS

ANFIS model could be considered a good prediction performance for estimating and forecasting the water consumption of the HPPs depending on the MAPE and R^2 results in the context of the water-energy nexus parallel to the aim of the study. GFDL RCP 4.5 and 8.5 climate scenario results show that water consumption of HPPs' will increase by nearly 80% in 2053 compared to 2023 consumption levels. Besides, the water consumption estimates based on GFDL RCP 4.5 and 8.5 scenarios are found to be very close to each other.

Acknowledgments: The authors acknowledge the support of the Turkish State of Meteorological Service, State Hydraulic Works, and The Electricity Generation Corporation (EUAS).

REFERENCES

- Allawi, M. F., Jaafar, O., Mohamad Hamzah F., Koting, S. B., Mohd N. S. B., and El-Shafie A., "Forecasting hydrological parameters for reservoir system utilizing artificial intelligent models and exploring their influence on operation performance," *Knowledge-Based Syst.*, vol. 163, pp. 907–926, Jan. 2019.
- Bakken, T. H., Engeland K., Killingtveit A., Alfredsen K., and Harby A., "Water consumption from hydropower plants – Review of published estimates and an assessment of the concept," *Hydrol. Earth Syst. Sci.*, vol. 17, no. 10, pp. 3983–4000, 2013.
- Gilliland M., *The Business Forecasting Deal Exposing Myths, Eliminating Bad Practices, Providing Practical Solutions*. John Wiley & Sons, Inc., 2010.
- International Energy Agency (IEA), *Key World Energy Statistics*, 2021. (<https://www.iea.org/fuels-and-technologies/hydropower>) Accessed Date: 01.08.2022
- Jang, J.S.R., Sun, C. T., and Mizutani, E., "Neuro Fuzzy and Soft Computing A Computational Approach to Learning and Machine Intelligence". Prentice Hall, pp: 1-607, 1997.
- Mekonnen M. M. and A Hoekstra. Y. "The water footprint of electricity from hydropower" *Value of Water, Research Report Series*, No:51, 2011.
- Majhi, B., Naidu, D. (2021). Pan evaporation modeling in different agroclimatic zones using functional link artificial neural network. *Information Processing In Agriculture* 8, 134– 147.
- McMahon J. and Price, S. K., "Water and Energy Interactions," *Annu. Rev. Environ. Resour.*, vol. 36, p. 163–91 First, 2011.
- Nourani. V., Elkiran. G., Abdullahi J. (2019). Multi-station artificial intelligence-based ensemble modeling of reference evapotranspiration using pan evaporation measurements. *Journal of Hydrology* 577, 123958. <https://doi.org/10.1016/j.jhydrol.2019.123958>.
- Seifi, A., Soroush, F. (2020). Pan evaporation estimation and derivation of explicit optimized equations by novel hybrid meta-heuristic ANN based methods in different climates of Iran. *Comput. Electron. Agric.* 173, 105418. <https://doi.org/10.1016/j.compag.2020.105418>.
- TEIAS,2022. <https://www.teias.gov.tr/turkiye-elektrik-uretim-iletim-istatistikleri> (Access Date: 14.07.2022)
- Wright S. 1921. Correlation and causation. *Journal of Agricul*

EVALUATION OF THE WATER-ENERGY-FOOD NEXUS IN THE CONTEXT OF PRECISION AGRICULTURE

Ezgi Özdemir¹, Emre Alp^{2*}

¹ Department of Environmental Engineering, Middle East Technical University, Ankara, Turkey

² Department of Environmental Engineering, Middle East Technical University, Ankara, Turkey

*Corresponding author (emrealp@metu.edu.tr)

ABSTRACT

Water, food, and energy nexus is a strategy to evaluate the interconnections and interdependencies between water, food, and energy while considering the positive and negative outcomes of managing these sources. The natural sources that are used in the elements of the nexus are limited. Water is a crucial element for living beings considering the direct or indirect usage of water in the production of food and energy. Agricultural water consumption is a significant part of global water withdrawals. Since the population and resource demand has drastically increased in the last centuries, the need to evaluate the relationship between water, food, and energy is essential, especially in water-scarce regions. Intelligent irrigation provides a sustainable solution to this problem. This study aims to estimate how much energy savings can be achieved using the water savings obtained by usage of intelligent irrigation systems instead of conventional irrigation in a semi-arid watershed, Ankara creek basin, Turkey. The climatic data is retrieved from CLIMWAT for CROPWAT database and soil characteristics are determined from literature survey. After collection of the data, water consumption is examined under two scenarios: conventional and intelligent irrigation using CROPWAT model. The results showed that both water and the energy savings that can be obtained by water savings is significant.

Keywords: *intelligent irrigation, water-energy-food nexus, precision agriculture*

1. INTRODUCTION

Water scarcity is a current challenge especially in developing countries which have become more crucial with rapid population growth and an increase in resource demand. In Turkey, agricultural water withdrawals are reported as approximately 85% of the total water withdrawals in the last decade (FAO, 2016). The considerable amounts of water used in production and processing food products may have adverse environmental impacts such as land degradation, changes in runoff and groundwater recharge, water quality, and availability (Finley and Seiber, 2014). Furthermore, the adverse impacts of climate change are expected to increase the pressure on the available freshwater resources (Tsakmakis et al., 2018). Hence, more efficient ways to use water in agriculture is a major concern since agricultural activities heavily depend on water.

According to the Food and Agricultural Organization of the United Nations (FAO), the production of food should rise 70% by 2050 to feed the projected future population that is 9 billion people. Therefore, producing more food products using less water is crucial. It is

reported that to increase crop production, arable lands must be expanded but also crop yields and cropping intensity must rise to meet food demands. Because of the uneven distribution of freshwater sources, even though the amount is sufficient, the water use efficiency must be increased for sustainable use of freshwater resources in agriculture (HLEF2050).

Technological innovations play a crucial role in the implementation of Sustainable Development Goals (SDGs) as stated in the 2030 Agenda for Sustainable Development (SDGs; UN Interagency Task Team on Science, Technology, and Innovation for the SDGs, 2018). Technological innovations such as intelligent irrigation systems can promote sustainable management of resources and can be beneficial for the implementation of SDG 2 (Zero Hunger) and SDG 6 (Clean Water and Sanitation) since intelligent irrigation aims to reduce water loss (SDG 6) and maintain crop yield (SDG 2) (Schwindenhammer and Gonglach, 2021).

Water, food, and energy nexus is a strategy to evaluate the linkages between water, food, and energy sectors. The natural sources that are used in the elements of the nexus are limited. In order to make an appropriate decision making in every sector separately, the interrelationships between water, energy and food sectors should be well-known. Water and energy security are closely connected to each other. 2-3% of the energy generated in the world is used for water supply and sanitation. In case of shortage of water due to recent environmental problems like drought and climate change, the needed amount of water by power plants can cause environmental damage or can be forced to shut down (Finley and Sieber, 2015). Exploration of fossil fuels is highly water consumptive process and also, the used water is polluted by tailings seepage, fracturing fluids, flow-back and produced water.

As explained in the previous paragraph, water needed for energy production is affected by several factors including agricultural water requirement. In irrigation systems, more effective use of rainfall and regulation of irrigation scheduling is needed to reduce water losses while maintaining crop yields (FAO, 2011). The timing and irrigation volume should be optimized so that water loss due to excessive irrigation is minimized and the reduction of crop yield is not observed due to the lack of irrigation (Mason et al, 2019). Intelligent irrigation systems are sensor network-based, knowledge- and technology-driven systems which have proven to be useful for the reduction of water loss. Intelligent irrigation systems use the real-time data gathered by sensor networks such as soil condition, water use by crop, and weather conditions to adjust irrigation schemes (Shi et al., 2021). By using real-time data collected by sensors, intelligent irrigation systems can regulate irrigation scheduling and the amount of water required by plants (Mohammed et al., 2013).

Agricultural water consumption is a major part of the global water withdrawals. Since the population and resource demand are drastically increased in the last centuries, the need for the evaluation of the relationship between the water and the production of food and energy is gained importance especially in water scarce regions. Intelligent irrigation provides a sustainable solution for this problem. The aim of this study is to estimate how much energy savings can be achieved using the water savings obtained by usage of intelligent irrigation systems instead of conventional irrigation in a semi-arid watershed, Ankara creek basin, Turkey.

2. MATERIAL AND METHODS

Irrigational use of water consists of evaporated water, transpired water, and water incorporated into crops (Rinaldi et al., 2014). To decrease the amount of water used for irrigational purposes, transpired water should be minimized to prevent losses. Intelligent irrigation systems are one method that can be used in precision irrigation practices. Precision irrigation is scheduling irrigation so that the amount of water given to the land should be precisely the same as the irrigation requirement of the plant at the time of irrigation. Therefore, precision irrigation practices are based on real-time data collection and are site-specific. To determine whether intelligent irrigation systems are feasible, all factors such as economic factors, farmers' attitudes and lifestyle, and environmental factors should be considered holistically (Jochinke et al., 2007). In this paper, the evaluation is based on environmental factors.

Study Area

Ankara Creek sub-basin is located in Ankara basin. Ankara basin is located to the east of Sakarya Basin. It is divided into two sub-basins named Ankara creek and Kirmir creek sub-basins. The total area covered by Ankara basin is 11778 km². Ankara creek and Kirmir creek sub-basins cover 7178 km² and 4600 km², respectively. In Ankara, 60% of the land is used as agricultural land and the most important field products are wheat, barley, and sugar beet. The Ankara basin has continental climate characteristics due to its location in the Central Anatolia Region.

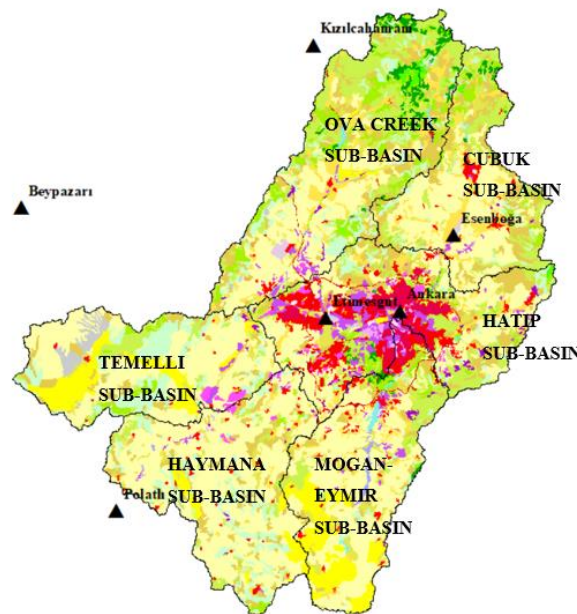


Figure 1. Land cover of sub-basins and location of stations-Ankara creek basin

Model Development

The CROPWAT 8.0 model was developed by the Land and Water Resources Development Department of Food and Agricultural Organization. In this study, CROPWAT version 8.0 for Windows is used to quantify water savings and crop yield for Ankara Creek sub-basin. CROPWAT is a decision support tool for the calculation of crop water requirements and

irrigation requirements with the inputs such as soil, climate, and crop data. CROPWAT model is a reliable tool to predict irrigational water requirement and has been used to estimate crop water demand and crop yield under different irrigation practices and climates (Zheng et al., 2012; Tan et al., 2019). It is verified that the model can simulate the potential evapotranspiration values for different crops with different meteorological conditions. The data sources will be given in the following section.

The procedure for calculation of potential evapotranspiration is explained in the FAO 56 Irrigation and Drainage Paper and FAO 33 Irrigation and Drainage Paper (Allen et al., 1998; Doorenbos and Kassam, 1979). CROPWAT model is a user-friendly model that can be used efficiently for preliminary analysis (Knezevic et al. 2013). The user-defined irrigation management and water supply options are the main reason for the selection of the model.

CROPWAT 8.0 is based on the FAO Penman-Monteith equation and crop coefficients for the estimation of the reference evapotranspiration (ET_0) (Allen et al., 2006). Where ET_0 is the reference evapotranspiration and K_c is the crop coefficient. Crop coefficients data is gathered from the Water Consumptions of Irrigated Plants in Turkey for crops in Ankara Creek sub-basin. Furthermore, CROPWAT calculates effective rainfall to account for the losses to runoff and percolation using the formula from USDA's Soil Conservation Service.

The output of the model is reference evapotranspiration, crop water requirements under different scenarios, net irrigation requirement, the yield of the crops, and the effective rainfall.

Data

CROPWAT 8.0 requires inputs such as climatic data like rainfall, minimum temperature, maximum temperature, humidity, wind speed, and sunshine hours; crop pattern in the bounded area; crop coefficients at initial, development, mid-season, and late-season for each crop; soil characteristics like total available soil moisture, maximum rain infiltration rate, maximum rooting depth, initial soil moisture depletion and initial available soil moisture (Elbeltagi et al., 2020). Data sources for the CROPWAT model are given in Table 3.

Table 3. Data sources for CROPWAT 8.0 model

Climatic Data	From the CLIMWAT for CROPWAT database which includes long term monthly mean meteorological data between 1971 and 2000 compiled by FAO
Crop patterns	From the Agricultural economics report prepared for Sakarya Watershed
Crop coefficients	From the Water Consumptions for Irrigated Plants in Turkey
Soil characteristics	From literature survey

The crop pattern of Ankara creek basin is determined from the Agricultural economics report prepared for the Sakarya watershed. The most dominant crop in Ankara Creek Basin is small grains which covers 41% of the irrigated area followed by small vegetables which covers 22%

of the area. Other main crops in the area are green beans, tomato, sugar beet, sunflower, maize, and table grapes.

The soil characteristic data in the CROPWAT model is determined as Calcic Xerosols from the FAO-UNESCO Soil map of the world report. Calcic Xerosols are classified as medium soil in CROPWAT model input.

3. RESULTS AND DISCUSSIONS

Calibration and Validation

Based on the meteorological data retrieved from CLIMWAT and soil characteristics from CROPWAT database, K_c values for each of the crop type is calibrated using the measured values.

Irrigation Scenarios

In this study, two irrigation scenarios that are conventional and intelligent are analyzed and compared. In the conventional irrigation scenario, existing irrigation systems are considered for each irrigation area. For the intelligent irrigation scenario, the usage of a drip irrigation system is assumed. The efficiencies of irrigation systems are retrieved from the Masterplan report prepared for Sakarya Watershed. For gravity flow and drip irrigation systems, efficiencies are selected as 85% and 98%, respectively.

In the conventional irrigation scenario, the crop is irrigated independently from soil moisture. The irrigation schedule, which is the main difference between scenarios, is determined by FAO instruction with a fixed amount of water given to the soil within a certain period of time. The values for irrigation scheduling are estimated based on the following steps: (i) irrigation requirement of each crop is determined using the CROPWAT model, (ii) irrigation requirement for every stage is determined (Initial, development, mid and late), (iii) application depth is determined by considering the rooting depth of the crop and soil characteristics, (iv) irrigation requirement is divided into application depth to determine the number of irrigation applications needed for each stage, and, (v) irrigation intervals are found by dividing the duration of each stage by the number of irrigation applications.

In the intelligent irrigation scenario, the crop is irrigated according to the available moisture of the soil. To represent this dynamic, in this study, the crop is irrigated when depletion reaches 105% and filled 50% of the field capacity. Therefore, using this method, the soil water retention is always below the field capacity. Percentages are found by the trial-and-error method. The main consideration in this method was that there were no crop yield losses.

The CROPWAT model is constructed for each crop for two different scenarios. Water consumptions for each scenario are calculated considering the efficiency of irrigation systems between 2012-2018. The model outputs for each crop and each scenario are total net irrigation and efficiency of rain. The average increase in efficiency of rain and the average decrease in total net irrigation is found as 5.3% and 33.1% respectively.

The production of 1 kWh electricity by hydropower plants requires approximately 245 liters of water (Mekonnen and Hoekstra, 2011). Using the given statistics, the amount of electricity that can be produced using the water savings from precision agriculture can be calculated as a part of the Water-Food-Energy Nexus evaluation.

4. CONCLUSIONS

In this study, a preliminary analysis is conducted to determine how much water savings can be achieved using intelligent irrigation systems and how much electricity can be produced using these water savings. The CROPWAT model is used to determine crop water requirements under different irrigation schedules to represent the effectiveness of intelligent irrigation systems. Considering each crop in the study area, an average of 5.3% increase in the efficiency of rain is observed. This analysis showed that using intelligent irrigation systems precipitation periods can be used more beneficially in irrigation areas. Furthermore, an average of 33.1% decrease in total net irrigation is achieved according to the model which indicates that in semi-arid areas, intelligent irrigation can be effectively used to decrease the water amount that is used in the agriculture sector. However, the cost is a very essential part of this study. The water savings may not compensate for the cost of intelligent irrigation system implementation. Therefore, a cost-benefit analysis should be conducted.

Using intelligent irrigation systems provides significant amount of water savings in the basin which is important because of the semi-arid property of the region. One of the benefits of the water savings is that since less amount of water will be used in irrigation, energy production will be affected considering the interlinkages in the nexus concept. Furthermore, hydropower generation in the Orta Sakarya Basin which is located in the upstream of Ankara creek basin will be affected positively.

REFERENCES

- Agricultural Development Economics Division Economic and Social Development Department. (2009). High Level Expert Forum - How to Feed the World in 2050.
- Allen, R. G. (Rick G.), & Food and Agriculture Organization of the United Nations. (1998). Crop evapotranspiration: guidelines for computing crop water requirements. Food and Agriculture Organization of the United Nations.
- Doorenbos J., & Kassam A.H. (1979). FAO Irrigation and Drainage Paper 33: Yield Response to Water.
- Elbeltagi, A., Zhang, L., Deng, J., Juma, A., & Wang, K. (2020). Modeling monthly crop coefficients of maize based on limited meteorological data: A case study in Nile Delta, Egypt. *Computers and Electronics in Agriculture*, 173(August 2019), 105368. <https://doi.org/10.1016/j.compag.2020.105368>
- FAO-Unesco. (1981). Soil map of the world.
- Finley, J. W., & Seiber, J. N. (2014). The nexus of food, energy, and water. In *Journal of Agricultural and Food Chemistry* (Vol. 62, Issue 27, pp. 6255– 6262). American Chemical Society. <https://doi.org/10.1021/jf501496r>
- Jochinke, D. C., Noonon, B. J., Wachsmann, N. G., & Norton, R. M. (2007). The adoption of precision agriculture in an Australian broadacre cropping system-Challenges and opportunities. *Field Crops Research*, 104(1–3), 68–76. <https://doi.org/10.1016/j.fcr.2007.05.016>

KNEŽEVIĆ Mirko, PEROVIĆ Natalija, ŽIVOTIĆ Ljubomir, & TOPALOVIĆ Ana. (2013). SIMULATION OF WINTER WHEAT WATER BALANCE WITH CROPWAT AND ISAREG MODELS. *Agriculture & Forestry*, 59(1), 41–53.

Mason, B., Rufí-Salís, M., Parada, F., Gabarrell, X., & Gruden, C. (2019). Intelligent urban irrigation systems: Saving water and maintaining crop yields. *Agricultural Water Management*, 226. <https://doi.org/10.1016/j.agwat.2019.105812>

McCready, M. S., Dukes, M. D., & Miller, G. L. (2009). Water conservation potential of smart irrigation controllers on St. Augustinegrass. *Agricultural Water Management*, 96(11), 1623–1632. <https://doi.org/10.1016/j.agwat.2009.06.007>

Rinaldi, M., & He, Z. (2014). Decision Support Systems to Manage Irrigation in Agriculture. In *Advances in Agronomy* (1st ed., Vol. 123). <https://doi.org/10.1016/B978-0-12-420225-2.00006-6>

Schwindenhammer, S., & Gonglach, D. (2021). Sdg implementation through technology? Governing food-water-technology nexus challenges in urban agriculture. *Politics and Governance*, 9(1), 176–186. <https://doi.org/10.17645/pag.v9i1.3590>

Shi, J., Wu, X., Zhang, M., Wang, X., Zuo, Q., Wu, X., Zhang, H., & Ben-Gal, A. (2021). Numerically scheduling plant water deficit index-based smart irrigation to optimize crop yield and water use efficiency. *Agricultural Water Management*, 248. <https://doi.org/10.1016/j.agwat.2021.106774>

Tan, M., & Zheng, L. (2019). Increase in economic efficiency of water use caused by crop structure adjustment in arid areas. *Journal of Environmental Management*, 230, 386–391. <https://doi.org/10.1016/j.jenvman.2018.09.060>

Tsakmakis, I. D., Zoidou, M., Gikas, G. D., & Sylaios, G. K. (2018). Impact of Irrigation Technologies and Strategies on Cotton Water Footprint Using AquaCrop and CROPWAT Models. *Environmental Processes*, 5, 181–199. <https://doi.org/10.1007/s40710-018-0289-4>

THE WEF NEXUS APPROACH TO ACHIEVE THE SUSTAINABLE DEVELOPMENT GOALS

Alexandra E. Ioannou¹, Chrysi S. Laspidou^{1*}

¹ University of Thessaly, Department of Civil Engineering, Volos, Greece

*Corresponding author (laspidou@uth.gr)

ABSTRACT

To achieve global sustainability, we need to meet the needs of the present without endangering the needs of the future generations. The 17 SDGs were constituted to address global sustainability. Water, energy and food are inextricably linked, affecting not only each other in multiple ways but also the whole system. In this analysis, we tried to quantify the impact of water-energy-food nexus as a multi-dimensional approach on the 17 SDGs, aiming to promote integrating planning and policymaking.

Keywords: *water-energy-food nexus, sustainable development goals, Sankey diagram, circular bar plot, k-means clustering.*

1. THE WEF NEXUS APPROACH TO SUSTAINABLE DEVELOPMENT

Considering that environmental exploitation will increase in the future due to overpopulation and lack of resource efficiency, in 2015 the United Nations has set the 2030 Agenda for Sustainable Development, consisting of 17 Sustainable Development Goals (SDGs) (UN, 2015). In order to achieve the SDGs, all relevant stakeholders should collaborate and succeed in managing the synergies and trade-offs across individual management and governance sectors (Stein et al., 2014). Nexus approach aims at enhancing WEF security and thus contributing to CO₂ emissions decrease by achieving resource efficiency increase and integrating management and governance at all sectors and scales (Hoff, 2011).

In this analysis, 20 applicable water-, energy- and food-related indicators were used, following the work by Simpson et al., 2020 that used these indicators to constitute the [WEF Nexus Index](#). This index aims at providing a quantitative perspective and offering a lens for the evaluation of trade-offs to be considered in pursuit of sustainable development. We also selected two indicative SDG indicators per SDG, to quantify how they are influenced by the 20 nexus indices representing the three nexus pillars – water, energy and food. We explore how and in what way (positively or negatively) the three WEF Nexus pillars, affect the 17 SDGs. Quantifying these interlinkages, we can identify which SDGs are more influenced – either positively or negatively – by the three WEF Nexus pillars and thus help policy makers and stakeholders understand the interdisciplinary connection of the 17 SDGs through WEF nexus and their interactions and to help finding the best-fitting solution achieving the goals and obtain worldwide sustainability.

2. RESULTS AND DISCUSSIONS

Impact quantification

Nilsson et al., 2016, proposed a kind of impact quantification that aims at measuring the influence among SDG indicators with values varied from -3 to +3. In this analysis we attempt to quantify the influence that WEF indices have on the selected SDG indicators. We quantified the WEF nexus impact – through the 20 nexus pillars indices – on the 17 SDGs – through the 34-selected SDG indicators. The values, as aforementioned, are distributed from -3 to +3; The strongest negative impact is quantified with -3, whereas the strongest positive impact is quantified with +3. Zero values indicate no impact.

Visualization of the results

The results could not be easily read and analyzed, so, to facilitate understanding, explaining, and analysis of the results, we chose to visualize the results through advanced visualizing diagrams, specifically that being *Sankey diagram* and *Circular bar plot*. Both diagrams depict how the three sectors constituted by their respective nexus indices, affect the 34 SDG indicators making up the 17 SDGs.

To form Sankey diagram, the absolute values (positive and negative ones) are summed to have the input data needed. Figure 1a shows the flows that link the three Nexus Pillars with the 17 SDGs, and the wider a flow is the more related the pillar with the respective SDG is. The *Water sector* seems to most influence SDG6, 7, 2, and 8. The *Food sector* according to Sankey diagram mostly affects the SDG5, 2, 16, 14, and 3. Lastly, the *Energy sector* affects the SDG11, 12, 13, and 9 the most.

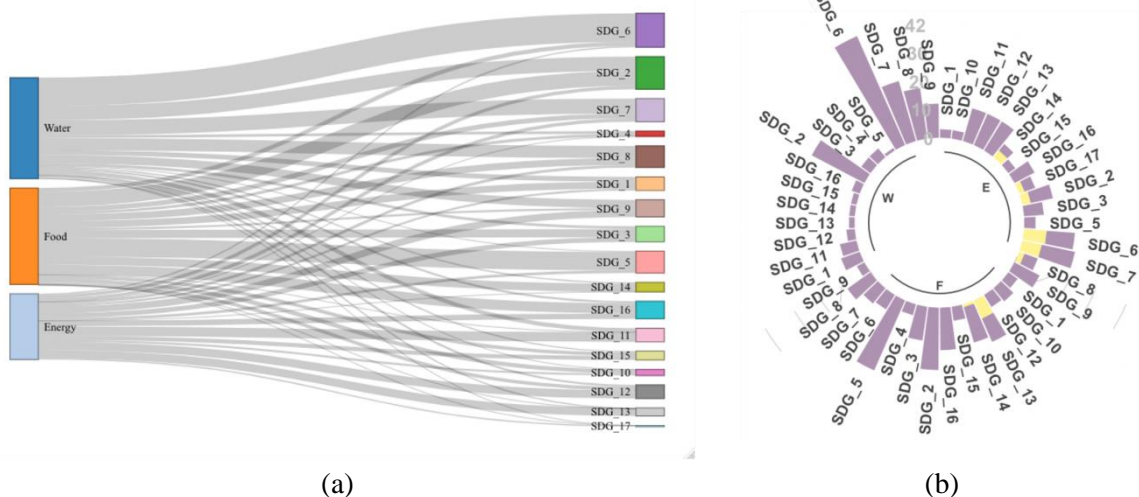


Figure1. (a) The Sankey diagram showing with flows how the three WEF pillars affect the 17 SDGs. (b) The circular bar plot indicating how the 17 SDGs are affected by the 20 WEF Nexus indices.

In circular bar plot there are different bars for the positive and negative values; Purple bars represent positive sum of values, while yellow bars represent negative ones. This diagram has a privilege over Sankey since, we can observe whether an SDG is affected either positively (synergies) or negatively (trade – offs). In figure 1b, we observe that water sector has the greatest impact on the same SDGs (SDG7, 2, and 8) as in Sankey diagram; this could be attributed to the fact that the specific sector revealed only synergies with the SDGs. As far as the energy sector is concerned, we realize that except from SDG11, 12, 13 and 9, this sector has also a significant impact on SDG7, 2, and 6, since there are both synergies and trade-offs.

Also, according to the circular bar plot, the food sector additionally to SDG5, 2, 16, 14, and 3, affects also SDG13.

Clustering Analysis

A k-means clustering algorithm was applied to the values of WEF Nexus Pillars impact, thus allowing the 17 SDGs to be grouped according to these values. The analysis revealed four clusters, i.e., SDGs that are mostly affected by Energy Pillar (CL_1 [E]), SDGs mostly affected by Food Pillar (CL_2 [F]), SDGs mostly affected by Water Pillar (CL_3 [W]), and the least influenced SDGs generally (minimum values) by all three Pillars (CL_4 [M]). The results are shown in Figure 4 and the clustering accuracy is 94%, indicating that we obtained clusters with well grouped data. The results are shown in Table 1.

Table 1: The four clusters obtained by k-means clustering algorithm.

Cluster_1 (red) Energy	Cluster_2 (green) Food	Cluster_3 (blue) Water	Cluster_4 (purple) Minimum
SDG_9	SDG_2	SDG_6	SDG_1
SDG_11	SDG_3	SDG_7	SDG_4
SDG_12	SDG_5	SDG_8	SDG_10
SDG_13	SDG_16		SDG_14
			SDG_15
			SDG_17

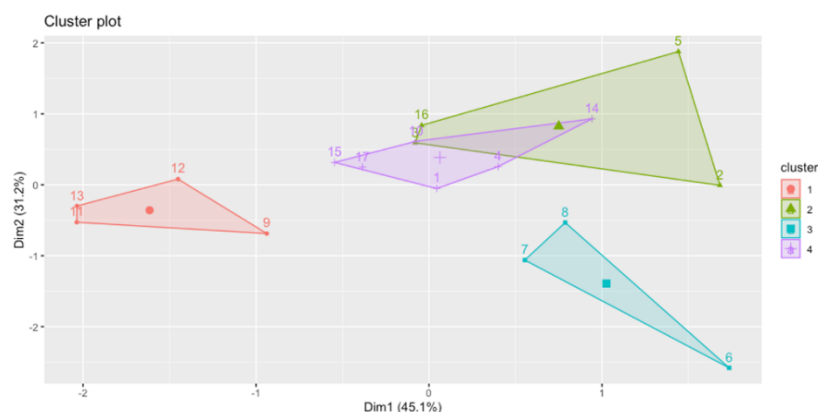


Figure 2: The four clusters of the 17 SDGs, obtained with k-means algorithm.

REFERENCES

- Hoff, H. (2011). Understanding the Nexus. Background Paper for the Bonn 2011 Nexus Conference: The Water, Energy and Food Security Nexus. Stockholm: Stockholm Environment Institute.
- Nilsson, M., Griggs, D., & Visbeck, M. (2016). Policy: map the interactions between Sustainable Development Goals. *Nature*, 534(7607), 320-322.
- Simpson G.B., Jewitt G.P.W., Becker W., Badenhorst J., Neves A.R. , Rovira P. and Pascual V. (2020). The Water-Energy-Food Nexus Index, Jones & Wagener <<https://www.wefnexusindex.org>> doi: 10.31219/osf.io/tdhw5.
- Stein, C., Barron, J., Nigussie, L., Gedif, B., Amsalu, T., & Langan, S. J. (2014). Advancing the water-energy-food nexus: social networks and institutional interplay in the Blue Nile. WLE Research for Development (R4D) Learning Series.
- United Nations (UN) (2015). Transforming Our World: The 2030 Agenda for Sustainable Development. United Nations, New York. Available at <https://sustainabledevelopment.un.org/post2015/transformingourworld/publication>

THE IMPACT OF RENEWABLE ENERGY ON ECONOMIC GROWTH IN CEE COUNTRIES

Author 1, Prof. Assoc. Dr. Doriana Matraku (Dervishi)*,
Author 2, Ph.D. student Kamela Selenica

1. Lecturer of Economics, Economics Department, Faculty of Economy, University of Tirana (FEUT)
2. Albanian Development Fund, Tirana, Albania. Ph.D. student, Economics Department, FEUT, Tirana, Albania

*Corresponding author email: dorianadervishi@feut.edu.al

ABSTRACT

In recent years, climate change and global warming, limited reserves of natural gas and petrol sources, high and volatile energy prices, and technological change make it mandatory to replace traditional energy sources with alternative energy sources. Studies have shown that fossil fuel consumption is the largest contributor to global greenhouse gas emissions and that continued dependence on fossil fuels will only exacerbate the rate of environmental degradation. To reduce CO₂ emissions, many countries have shifted to using renewable energy sources. In this context, this study aims to explore and evaluate the relationship between renewable energy consumption and economic growth for 19 Central Eastern European countries, from the time interval 2000-2019, within the framework of a traditional production function.

The study was implemented via dynamic panel data estimation methods, to research the long-term relationship between renewable energy consumption and economic growth in CEE countries, by taking into consideration the cross-section dependence effect in the panel. The estimation of long-term parameters was conducted by implementing fully modified ordinary least squares (FMOLS) and dynamic ordinary least squares (DOLS), to increase the accuracy and efficiency of model estimation. In this study, we have also tested for the stability of the series with the panel unit root tests and analyzed the long-term co-integration relationship between the dependent and independent variables in the panel data set, by using the panel co-integration test. The results of panel unit root tests show that series are stable and don't have unit roots at the first difference. The study has also concluded that there is a long-term balance relationship between renewable energy consumption and economic growth and the empirical results suggest that renewable energy consumption has a positive impact on economic growth.

Keywords: *Economic Growth, Renewable Energy, Long-term relationship, CEE countries*

1. INTRODUCTION

Each stage of economic development has been accompanied by a characteristic energy transition, moving from one fuel source to another, as the main factor of energy production growth in developing economies. While the energy demand continues to increase everywhere in the world, the levels of carbon dioxide emitted into the atmosphere have also been increasing, which is negatively affecting efforts to combat climate change. Consumption of non-renewable energy can boost economic growth, but it is undoubtedly a significant source of environmental pollution and carbon dioxide emission. Since the pollution caused by fossil fuels has increased year by year and the economic situation has been worsening due to the COVID-19 and energy crisis, many countries have been forced to find alternative energy sources to conventional energy sources. With the aim of sustainable development for the future, most of them have started investing in new energy developments. Renewable energy sources as an alternative source present themselves with an important potential and perform a crucial role, by decreasing dependency on fossil fuels, which are very limited in supply. Due to climate change and the global warming situation, renewable energy could be the most attractive alternative to fossil fuels, reducing the CO₂ emission process (Bhuiyan et al., 2022).

The relationship between renewable energy and economic growth has created a large interest among researchers and policymakers worldwide. This interest has also been the motivation for our work and has led us to undertake this study. This study aims to explore the relationship between renewable energy consumption and economic growth for the time interval 2000–2019, for 19 Central Eastern European countries: Albania, Belarus, Bosnia and Herzegovina, Bulgaria, Croatia, Czech Republic, Estonia, Hungary, Latvia, Lithuania, Moldova, North Macedonia, Poland, Romania, Russia, Serbia, Slovak Republic, Slovenia, and Ukraine.

Most of the previous studies have shown a positive relationship between renewable energy consumption and economic growth, which is also called the *growth hypothesis* in literature. Bilgili and Ozturk (2015) found that renewable energy had a significant positive impact on economic growth in G7 and 51 sub-Saharan African countries using panel co-integration, panel OLS and panel DOLS for the 1980–2009 period. Inglesi-Lotz (2016) estimated the impact of renewable energy consumption on economic welfare by employing panel data techniques, including 34 OECD countries for the period from 1990 to 2010, and concluded that the influence of renewable energy consumption on economic growth is positive and statistically significant. Similarly, Koçak and Şarkgüneşi (2017) explored the relationship between renewable energy consumption and economic growth within the framework of the traditional production function for the period of 1990–2012 in 9 Black Sea and Balkan Countries and concluded that there exists a long-term balance relationship between renewable energy consumption and economic growth and renewable energy consumption has a positive impact on economic growth.

Some other studies have shown different results, supporting the *neutrality hypothesis* (energy consumption doesn't have any effect on economic growth). Menegaki (2011) analyzed the relationship between economic growth and renewable energy for 27 European countries in a multivariate panel framework over the period 1997–2007 using a random effect model and he couldn't find a significant relationship between renewable energy and economic growth.

Bhattacharya et al. (2016) in their study examined the possible effect on the economic growth of renewable versus non-renewable energy sources across 38 countries for the time period between 1991 and 2012 and concluded that renewable energy consumption has a positive impact on economic growth for 23 countries and a negative impact for 4 countries. This implies that those countries which had a negative impact on economic growth, need to increase capital for sustainable development of renewable energy consumption and follow a gradual process for deployment. Shahbaz et al. (2020) also examined the effect of renewable energy consumption on economic growth across 38 countries from 1990 to 2018 using DOLS, FMOLS, and heterogeneous non-causality approaches and confirmed the presence of a long-run relationship between renewable energy consumption and economic growth. They also found a positive impact of renewable energy on economic growth for 58% of the sample countries and a negative impact for 24% of the sample countries.

The organization of this paper is as follows: Section 2 discusses the model, data and describes the econometric methodology. Section 3 provides the estimation results, derived from the panel unit root test, the panel cointegration test, as well as the estimation of the long-run coefficients using the DOLS and FMOLS methods. Finally, Section 4 evaluates the main conclusions of our study and policy implications.

2. ECONOMETRIC METHODOLOGY

Model, data, and econometric methodology

In this paper, the linkages between renewable energy and economic growth will be examined using the neo-classical production function following Koçak and Şarkgüneşi (2017). The general type of production function that considers renewable energy, capital, and labor as individual inputs is defined as follows:

$$Y_{it} = f(RE_{it}, K_{it}, L_{it},) \quad (1)$$

In Eq. (1), Y stands for economic growth, RE stands for renewable energy, K stands for capital stock and L stands for labor, while i and t stand for nation and time. Thus, Equation 1 was transformed into a log-linear specification by taking all the variable's natural logarithms. The benefits we get from transforming the equation into logarithmic form are: a) the transformation of the variables into a natural logarithm provides efficient and consistent empirical results (Shahbaz et al., 2012); b) the transformation of data series into a natural logarithm avoids the problems associated with dynamic properties of the data series (Bhattacharya et al., 2016). The empirical equation of the production function is modeled as follows:

$$\ln Y_{it} = \beta_{1i} \ln RE_{it} + \beta_{2i} \ln K_{it} + \beta_{3i} \ln L_{it} + \varepsilon_{it} \quad (2)$$

where β_1 , β_2 and β_3 are elasticities of economic growth with respect to renewable energy consumption (RE), capital (K) and labor (L), respectively and ε is the error term.

Our study employs data for 19 Central Eastern European countries (Albania, Belarus, Bosnia and Herzegovina, Bulgaria, Croatia, Czech Republic, Estonia, Hungary, Latvia, Lithuania, Moldova, North Macedonia, Poland, Romania, Russia, Serbia, Slovak Republic, Slovenia, and Ukraine) for the time period 2000-2019. We would like to highlight that one of the limitations

of this paper is the lack of data availability for Kosovo, which is part of the CEE countries. The databases provided for this country are very truncated since it is considered a new country. For economic growth, we used GDP (constant 2015 US\$), for renewable energy consumption (RE) the share of renewable energy in total final energy consumption (%), for capital (K) we used gross fixed capital formation (constant 2015 US\$), and for labor (L) we used labor force participation rate (% of the total population for ages 15-64). All the data that we are using for our study is collected from the World Bank Database.

To study the long-term relationship between renewable energy consumption and economic growth in CEE Countries, we will use the panel data method. First, to test for the stability of the series and to ensure the robustness of our components we will use the panel unit root test. This test considers both heterogeneity and cross-sectional dependence across panels. The first generation of tests assumes that cross-section units are cross-sectionally independent; whereas the second generation of panel unit root tests relaxes this assumption and allows for cross-sectional dependence (Tugcu, 2018). Therefore, the empirical equation of the unit root test is modeled as follows:

$$\Delta y_{it} = \rho y_{it-1} + \sum_{L=1}^{pi} \theta_{iL} \Delta y_{it-L} + \alpha_{mi} d_{mt} + \varepsilon_{it}, \quad m = 1,2,3 \quad (3)$$

In equation (3) ε_{it} is uncorrelated throughout the units and follows an ARMA process. Δ shows the first differences d_{mt} shows dummy variables for each unit, α_{mi} shows their parameters (Koçak and Şarkgüneşi, 2017). We test the null hypothesis that each series in the panel dataset contains a unit root against the alternative, at least one of the individual series in the panel is stationary (no unit root) $H_0: \rho=0$ and $H_a: \rho < 0$. When the null hypothesis is rejected, it is determined that the series doesn't contain a unit root, so the series are stationary. If the results of the test show that the series are stable at level value, then the analysis will proceed with the traditional OLS method estimation, otherwise, if the series are stable at first differences, the panel cointegration test will be followed in our study.

Second, we use the Pedroni panel cointegration test, to examine if between variables exists a long-term cointegration relationship. Pedroni (2000) introduced seven test statistics that test the null hypothesis of no cointegration (in other words, the residuals are non-stationary) against the alternative hypothesis that approves there is a co-integration relationship. The seven test statistics are grouped into two categories: group-mean statistics that average the results of individual country test statistics and panel statistics that pool the statistics along the within-dimension (Neal, 2014). The first group of Pedroni's tests consists of panel semi-parametric v , ρ , and t-statistics which corresponds to the variance ratio, and Phillip-Peron ρ and t-statistics univariate analogues, respectively, and parametric panel ADF t-statistics. The second group consists also of Phillip-Peron ρ and t-statistics and ADF t-statistics, but is computed according to the group-mean principle (Mitić et al., 2017). If the results of the Pedroni test indicate that the null hypothesis is rejected, then it is determined that exists a long-term relationship among the variables.

The last step is estimating the long-run elasticity of output, by using Pedroni's (2000, 2001) Fully Modified OLS (FMOLS) and Dynamic OLS (DOLS) methods, since these two

approaches account for serial correlation and endogeneity that may exist in our model. The equation is modeled as follows:

$$Y_{it} = \delta_{it} + \beta_i X_{it} + \varepsilon_{it} \quad (4)$$

where Y and X indicate the dependent variable and the corresponding vector of independent variables, while i, t, and ε stand for individuals, time, and the error term, under the assumption that there is no dependence between sections that consist of the panel. The DOLS estimator in a panel case can be derived by running the following regression:

$$y_{it} = \alpha_i + \beta_i x_{it} + \sum_{k=-Ki}^{Ki} \gamma_{ik} \Delta x_{it-k} + \varepsilon_{it}$$

where K denotes the number of lags/leads chosen using some info criterion and γ_{ik} is the coefficient of a lag or lead of the first differenced variables. The DOLS estimator also has an additional advantage in controlling the endogeneity in the model, as augmentation with the lead and lagged differences of the regressor suppresses the endogenous feedback (Lean & Smyth, 2010). Besides the DOLS method and considering that the properties of our data are first-order integrated, this study will also use the Pedroni (2000) FMOLS approach. FMOLS estimator eliminates the second order bias caused by the endogeneity of the regressors by incorporating the Phillips and Hansen (1990) semi-parametric correction into the OLS estimator.

Descriptive statistics of the variables

Table 1 presents the descriptive statistics for each of the variables in our model and correlations among these variables, to show some of the beginning information in our analysis. All the results shown in the tables in this paper are author calculations. In Table 1 we can notice that all descriptive statistics of lnGDP are greater than those of lnRE, lnK and lnL. From the correlation matrix, we can see that lnGDP is positively correlated with lnK and lnL and negatively correlated with lnRE. LnK is positively correlated with lnL and negatively correlated with lnRE. LnL is also negatively correlated with lnRE.

Table 1. Descriptive statistics and correlation matrix

Descriptive statistics	lnGDP	lnK	lnL	lnRE
Mean	24.63	23.11	14.96	2.61
Std. Dev	1.30	1.29	1.22	0.77
Min	22.08	20.23	13.39	-0.01
Max	28.01	26.49	18.14	3.75
Observations	380	380	380	380
Correlation matrix				
lnGDP	1			

lnK	0.998	1		
lnL	0.873	0.847	1	
lnRE	-0.51	-0.496	-0.717	1

3. RESULTS AND DISCUSSIONS

We have applied LLC (Levin, Lin, and Chu) panel unit root tests to GDP, Renewable Energy, Capital and Labor levels and first differences. The results of panel unit root test are provided in Table 2.

Table 2. LLC panel unit root test

Variable	I(1)
GDP	-4.42***
Δ GDP	-5.18***
RE	-1.32
Δ RE	-8.25***
K	-4.00***
Δ K	-8.04***
L	-1.10
Δ L	-5.18***

*** Indicates the rejection of null hypothesis of unit root at 1% significance level.

As we see, the results of the panel unit root test are mixed, especially for GDP and capital, where the LLC test indicates stationarity in both levels in the first differences, while renewable energy consumption and labor are stable only at the first differences. However, the empirical results reported in Table.1 reveal that the null hypothesis of the panel unit root is rejected for all the variables after the first differencing, indicating that the series are stable at the first difference.

The next step is to examine the co-integration relationship between the variables since a long-term equilibrium relationship is possible to happen. Table 3 shows the findings of the panel co-integration test. According to the test results, out of seven test statistics, only five confirm the presence of a co-integration relationship among lnGDP, lnRE, lnK, and lnL. Therefore, we conclude that a balanced relationship in the long term between renewable energy consumption, capital, and labor seems possible.

Table 3. Pedroni panel co-integration test results

Statistic	Probability
Within dimensions (common AR coefficients)	

Panel v-statistic	-4.439***	0.000
Panel rho-statistic	0.249	0.401
Panel PP-statistic	-3.325***	0.000
Panel ADF-statistic	-3.553***	0.000
Between dimensions (individual AR coefficients)		
Group rho-statistic	1.543*	0.061
Group PP-statistic	-4.740***	0.000
Group ADF-statistic	-4.382***	0.000

*** Indicates the rejection of the null hypothesis of unit root at 1% significance level.

* Indicates the rejection of the null hypothesis of unit root at 10% significance level.

Newey-West Bandwidth selection with Bartlett Kernel is used.

The last step is to estimate the long-term output elasticities, using panel dynamic OLS and panel fully modified OLS. The results of the estimation for both methods are presented in Table 4. As we can see, both panel DOLS and panel FMOLS give similar results, for each of the variables, in terms of sign and significance level. For the DOLS results, a 1% increase in renewable energy will increase GDP by 0.16%, while for the FMOLS results, a 1% increase in renewable energy will increase GDP by 0.17% and the coefficients are statistically significant at 1% level. Our findings also suggest that both capital and labor have a positive impact on economic growth, and coefficients are statistically significant at 1% and 5% level, respectively.

Table 4. Panel data analysis for CEE Countries (2000-2019)

Variable	Panel DOLS		Panel FMOLS	
	Coefficient	t-statistic	Coefficient	t-statistic
lnK	0.488***	0.000	0.536***	0.000
lnL	0.416**	0.022	0.327**	0.021
lnRE	0.163***	0.000	0.170***	0.000

*** Indicates the significance level at 1%.

** Indicates the significance level at 5%.

4. CONCLUSIONS

Nowadays the world attentions are focused towards sustainable development, which is possible to be achieved by using sustainable energy and by ensuring access to affordable, reliable, and clean energy for citizens. The transition to an energy system based on renewable technologies will have very positive economic consequences on the global economy and it is considered essential to raise the standard of living. We conclude that our analysis showed that the series are stationary at the first differences by the panel unit root test. The results of the Pedroni co-

integration test show that between the GDP, renewable energy consumption, gross fixed capital formation and labor force participation rate exists a long-term balance relationship. The estimation of the parameters of the relationship between renewable energy and economic growth indicate that renewable energy can be considered as a significant driver of economic growth. Specifically, the results of this study shows that a 1% increase in renewable energy consumption will increase GDP by 0.16% for DOLS method, while a 1% increase in renewable energy consumption will increase GDP by 0.17% for FMOLS method. Capital and labor also have a positive impact on economic growth, where a 1% increase in gross fixed capital formation will increase GDP by 0.48%, while a 1% increase in labor force participation rate will increase GDP by 0.41%.

The findings in this paper suggest that it is very important for government policies to support and promote the use of renewable energy sources in these CEE countries, replacing the use of traditional energy sources. To develop a sustainable economy, all the countries need a wide range of policy interventions and financing measures to support the transformation of energy and to improve energy efficiency. The government could promote innovation, providing fiscal incentives to companies investing in the R&D sector for finding more efficient solutions and clean-energy technologies that could be adopted. Governments could also decide to stimulate the use of renewable energy by lowering taxes, reducing investment costs through subsidies, loans, and grants, or by using sales tax exemptions for solar cells and feed-in tariffs. In those countries where the policies will be adopted, it will not only encourage them to export their technologies, but also lead them to share their policy experiences with other countries, creating renewable energy-oriented networks between their organizations.

Acknowledgments: The authors acknowledge the grant provided by IWA DIPCON 2022 and Cost Action CA 20138.

REFERENCES

- Bhattacharya, M., Paramati, S.R., Ozturk, I., Bhattacharya, S. (2016). The effect of renewable energy consumption on economic growth: evidence from top 38 countries. *Applied Energy*, 162, 733–741.
- Bhuiyan, M. A.; Zhang, Q.; Khare, V.; Mikhaylov, A.; Pinter, G.; Huang, X. (2022), Renewable Energy Consumption and Economic Growth Nexus—A Systematic Literature Review. *Frontiers in Environmental Science*, 10
- Bilgili, F. & Ozturk, I. (2015). Biomass energy and economic growth nexus in G7 countries: Evidence from dynamic panel data. *Renewable and Sustainable Energy Reviews*, 49, 132-138.
- Inglesi-Lotz, R. (2016). The impact of renewable energy consumption to economic growth: A panel data application. *Energy Economics*, 53, 58-63.
- Koçak, E. & Şarkgüneşi A. (2017). The renewable energy and economic growth nexus in Black Sea and Balkan countries. *Energy Policy*, 100, 51-57.
- Lean, H.H. & Smyth, R. (2010). CO2 emissions, electricity consumption and output in ASEAN. *Applied Energy*, 87, 1858–1864.
- Menegaki, A. N. (2011). Growth and renewable energy in Europe: A random effect model with evidence for neutrality hypothesis. *Energy Economics*, 33, 257-263.
- Mitić, P., Ivanović, O.M., Zdravković, A. (2017). A Cointegration Analysis of Real GDP and CO2 Emissions in Transitional Countries. *Sustainability*, 9(4), 1-18
- Neal, T. (2014). Panel cointegration analysis with xtpedroni. *The Stata Journal*, 14(3), 684-692

- Pedroni, P. (2000). Fully modified OLS for heterogeneous cointegrated panels. Nonstationary Panels, Panel Cointegration, and Dynamic Panels. *Advances in Econometrics*, 15, 93–130.
- Pedroni, P. (2001). Purchasing power parity tests in cointegrated panels. *Review of Economics and Statistics*, 83(4), 727-731.
- Phillips, P.C.B. & Hansen, B.E. (1990). Statistical inference in instrumental variables regression with I(1) processes. *Review of Economic Studies*, 57, 99-125
- Shahbaz M, Loganathan N, Zeshan M, Zaman K. (2015). Does renewable energy consumption add in economic growth? An application of auto-regressive distributed lag model in Pakistan. *Renewable and Sustainable Energy Reviews*, 44, 576-585.
- Tugcu, C. T. (2018). Panel Data Analysis in the Energy-Growth Nexus, in Menegaki, A.N. (ed). *The Economics and Econometrics of the Energy-Growth Nexus*, 255-271
- World Bank, URL: (<http://data.worldbank.org/indicator>) (accessed 19.07.22).

SOIL CONTAMINATION

PESTICIDES AND CHEMICAL ELEMENTS IN BRAZILIAN PANTANAL SEDIMENTS

Silvio César Sampaio^{1}, Kathleen Jeniffer Model^{1*}, Plínio Emanuel Rodrigues Silva¹, Floriano Luiz Suszek¹,
Cleuciane Tillvitz do Nascimento¹, Natalia Pereira¹, Marcelo Bevilacqua Remor¹*

¹ Western Paraná State University, Department of Agricultural Engineering, Cascavel, Brazil

**Corresponding author (Silvio.sampaio@unioeste.br)*

ABSTRACT

The Pantanal is the largest wetland in the world and is recognized for its biodiversity and for providing various environmental services. However, the Brazilian Pantanal is being impacted by human activities, especially agriculture and urbanization. In this sense, the objective of the study was to quantify the concentration of organochlorine and organophosphate pesticides, in addition to chemical elements in the sediment of the Brazilian Pantanal. Bottom sediment samples were collected at 30 points equally divided into three lagoons. Pesticides were extracted from the matrix using the QuEChERS method and quantified in GC/MS. The chemical elements were extracted in hydrofluoric acid and quantified in ICPMS. The pesticide concentrations in the bottom sediment samples were lower than the detection limit of the method. The chemical elements in the sediment were lower than the reference geochemical values, which indicates that human activity is not influencing the concentrations of chemical elements and pesticides in the sediment of the analyzed lakes.

Keywords: *Trace elements, Geochemical background, Organochlorine, Organophosphate.*

1. INTRODUCTION

The Pantanal is recognized as the largest wetland area on the planet, covering 195,000 km², with 140,000 km² in Brazilian territory (Roque et al., 2021). It is recognized for its biodiversity and for providing various environmental services. UNESCO recognized it as a Biosphere Reserve in 2000 (Faria et al., 2021). However, only about 10% of the Pantanal is designated as protected areas, despite evidence that agricultural and other human activities in the Pantanal are negatively impacting ecosystem functions (Schulz et al., 2019). Among the human activities that most impact the Pantanal are agricultural activities (Lacerda, 2017) and urbanization (Schulz et al., 2018).

Inadequate agricultural practices negatively impact water systems through the removal of native vegetation and soil erosion, which increase the amount of sediment in rivers, causing silting of water bodies (Gazolla and Gonçalves, 2017). As a consequence of the silting of the main channel of the rivers, permanent flooding of land occurred, including about 180 farms and the homes of 1000 families in the Upper Taquari Basin (Schulz et al., 2019). Eutrophication is also a problem caused by agriculture that uses nutrients to increase production and through leaching or surface runoff ends up increasing the concentrations of phosphorus and nitrogen in the

aquatic system (Anderson et al., 2020). Another problem arising from agriculture is the entry of pesticides into water bodies through leaching, surface runoff or even drift (Roque et al., 2021).

Urbanization contributes to the eutrophication of water systems through the entry of domestic and industrial sewage with high concentrations of phosphorus and nitrogen (Barile, 2018). In addition to nutrients, domestic and industrial sewage is often contaminated with chemical elements that end up contaminating water bodies (Conceição et al., 2018).

In aquatic ecosystems, sediments play a vital role in nutrient recycling (Hasimuna et al., 2021). In addition to nutrients, sediment acts as a scavenger of micro pollutants such as chemical elements and pesticides (Zhuang et al., 2021). Pollutants enter the water system through surface runoff, leaching or atmospheric deposition, eventually binding with suspended sediment particles and settling in lower energy environments (Ashayeri and Keshavarzi, 2019). When environmental conditions change, chemical elements accumulated in the sediment are desorbed and distributed in the water column resulting in secondary pollution (Li et al., 2020). Therefore, sediment is not only the sink, but also the source of chemical elements in the water (Almeida et al., 2020). In the last decades, pollution of sediments by micropollutants has become one of the most prominent problems in the aquatic environment and many studies have shown that the concentration of chemical elements are sensitive indicators of pollutants in the aquatic ecosystem (Ustaoğlu and Islam, 2020; Zhuang et al., 2021). In this context, the objective of the study was to quantify the organochlorine and organophosphate pesticides and chemical elements in the bottom sediment of the Brazilian Pantanal.

2. MATERIAL AND METHODS

Study area

The lakes that were analyzed are: Collection area S1 – Baía Nova Salina (20°37'50" S/ 57°58'25" W) located on the left bank of the Paraguai river, downstream of the Taquari rivers outlet, Negro and Miranda, 180 km south of the city of Corumbá – MS. Collection area S2 – Lagoa Mandioré (18°09'02" S/ 57°32'31" W), located in the center of the Pantanal, on the right bank of Paraguay, 70 km north of the city of Corumbá – MS. Collection area S3 – Chacororé Bay (16°14'47" S/ 55°52'49" W), located on the left bank of the Cuiabá River, upstream of the Itaquira River outlet, close to the city of Barão de Melgaço, 70 km south of the city of Cuiabá – MT. Figure 1 demonstrates the study area.

Samples preparation and collection

Sediment collection was carried out in three lakes, in the superficial fraction of the bottom sediment (SSF). The SSF collection was performed at 10 points, randomly distributed within each lake, with the aid of an Ekman-type dredger. The collection took place from May 10 to 25, 2016. The samples were packed in plastic packaging and stored at a temperature of 4 °C, until arrival at the laboratory. The SSF samples were oven-dried at 60 °C and sieved through a 63 µm mesh to perform the analyzes as recommended by Remor et al., 2018a and Model et al., 2018.

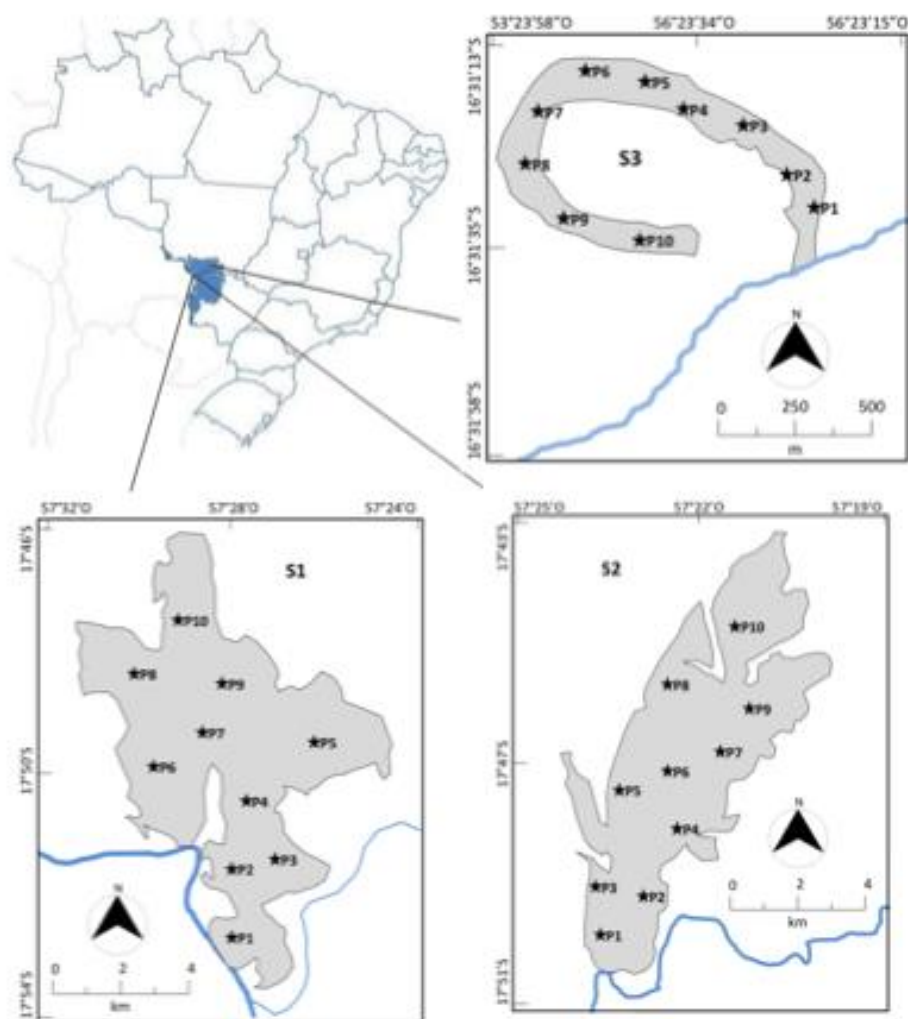


Figure 1. Study area, Brazilian Pantanal.

Analytical procedures

Pesticides were extracted from sediment samples using the QuEChERS method, described by Fernandes et al. (2013). This technique, which is based on extraction with acetonitrile, has been shown to be effective when compared to others, as it reduces or replaces many of the complex analytical steps of traditional methods. The method provides results with high quality, high yield, low consumption of solvents and glassware, low laboratory costs and low cost (Model et al., 2018). The analytes were analyzed by gas chromatography coupled to mass spectrometry (Shimadzu, GCMS-QP2010 SE) and separated in a Restek RTX® - 5MS capillary column (30 m x 0.25 mm x 0.25 μ m). The column oven temperature started at 150 $^{\circ}$ C increasing to 300 $^{\circ}$ C at the rate of 4 $^{\circ}$ C min^{-1} and held for 4 min, with a helium entrainment rate of 1.08 mL min^{-1} . Ion source temperature of 280 $^{\circ}$ C, injected volume of 1 μ L and runtime with gas of 41.50 min (Cembranel et al., 2017).

The organochlorines analyzed were α -BHC, β -BHC, γ -BHC, δ -BHC, aldrin, DDD, DDE, DDT, dieldrin, endosulfan I (α), endosulfan II (β), endosulfan sulfate, endrin, endrin aldehyde, heptachlor, heptachlor epoxide and methoxychlor, with detection limit of 0.02 ng g^{-1} and quantification limit of 0.03 ng g^{-1} (Model et al., 2018). The organophosphates analyzed were azinphos-methyl, chlorpyrifos, disulfoton, ethoprophos, methyl parathion, O (2,4-

dichlorophenyl) and ronnel (fenchlorphos), with a detection limit of 0.1 ng g⁻¹ and a limit of quantification of 0.2 ng g⁻¹ (Model et al., 2018). The accuracy of the method was determined by adding the pesticide standards to uncontaminated sediment samples from 1876 (Remor et al., 2015), as established by Silva et al. (2021). Pesticide recovery was 98% (average of 3 samples).

Total organic carbon (TOC) analysis was performed using a CNS LECO® elemental analyzer, using 250 mg aliquots of dry sediment. The accuracy of the analysis was determined with the aid of ISE 921 certified reference materials (river sediment) and 98.5% recovery was obtained. The extraction of chemical elements in the sediment samples was performed wet, with hydrofluoric acid (HF). This method allowed the extraction of the metals bound even in the primary structures of the sediment, such as quartz.

The quantification of chemical elements in the extract for each sample was performed using inductively coupled plasma mass spectrometry (ICP-MS). The chemical elements analyzed were: Na/23, Mg/26, Al/27, P/31, K/39, Ca/44, Cr/52, Mn/55, Fe/57, Ni/60, Cu/63, Zn/66, As/75, Se/82, Cd/114, Hg/204 and Pb/208. The accuracy of the analysis was determined using certified reference materials (Table 1).

Table 1. Recovery percentage average (n = 5) of the chemical elements in reference material ISE 921

Element	Recovery %	Element	Recovery %
Na	99.1	Ni	98.8
Mg	99.8	Cu	99.6
Al	100.2	Zn	100
P	99.7	As	99.9
K	99.2	Se	100.4
Ca	100.1	Cd	100.1
Cr	100.1	Hg	100
Mn	98.3	Pb	99.4
Fe	100.2		

Data analyses

The set of sediment chemical variables were simultaneously summarized in a single Principal Component Analysis (PCA). This reduction is done by transforming the set of original variables into a new set of variables (Principal Components – CPs), which maintains, as much as possible, the variability of the original set. The PCA was performed on the correlation matrix (Pearson) of the variables and the CP retention criterion adopted was the “broken-stick”, that is, with eigenvalues greater than those expected by chance (Jackson, 1993). In order to interpret the meaning of the retained CPs of the original variables, only Pearson's correlation coefficients greater than 70% were considered.

The Contamination Factor (CF), the Degree of Contamination (DC), the Sedimentological Sensitivity Factor (SSf) and the Index of Potential Ecological Risk (IPER) were applied to identify and quantify the contamination of the sediment by heavy metals. The equations for calculating CF, DC, SSF and IPER are described in Fiori et al. (2013). The geochemical reference values used for the application of the index were established by Remor (2017).

3. RESULTS AND DISCUSSIONS

Sediment samples collected in the Brazilian Pantanal showed concentration of organochlorine and organophosphate pesticides below the detection limit of the analytical method used (0.02 ng g^{-1} for organochlorines and 0.10 ng g^{-1} for organophosphates). In this sense, we can infer that the sediment of the analyzed lakes has a concentration of pesticides not detectable by the method used.

The principal component analysis (PCA) of the set of chemical variables of the sediment is represented in Figure 2. Only one principal component was considered capable of being evaluated according to the "broken-stick" criterion, totaling 81.19% of the variability of the set of sediments. Dice. The PCA shows that the variability in the concentration of trace elements between the collection sites (Lagoons) is greater than the variability between the points (Figure 2). The main component is composed of the elements described in Figure 2. The only variable that does not make up the main component is the COT CPs not interpretable according to the "broken-stick" test. Thus, it has variability, between the collection points and between the collection sites (Lagoons), smaller than those generated by chance, therefore, there is no statistically significant difference between the factors and their levels (Jackson, 1993).

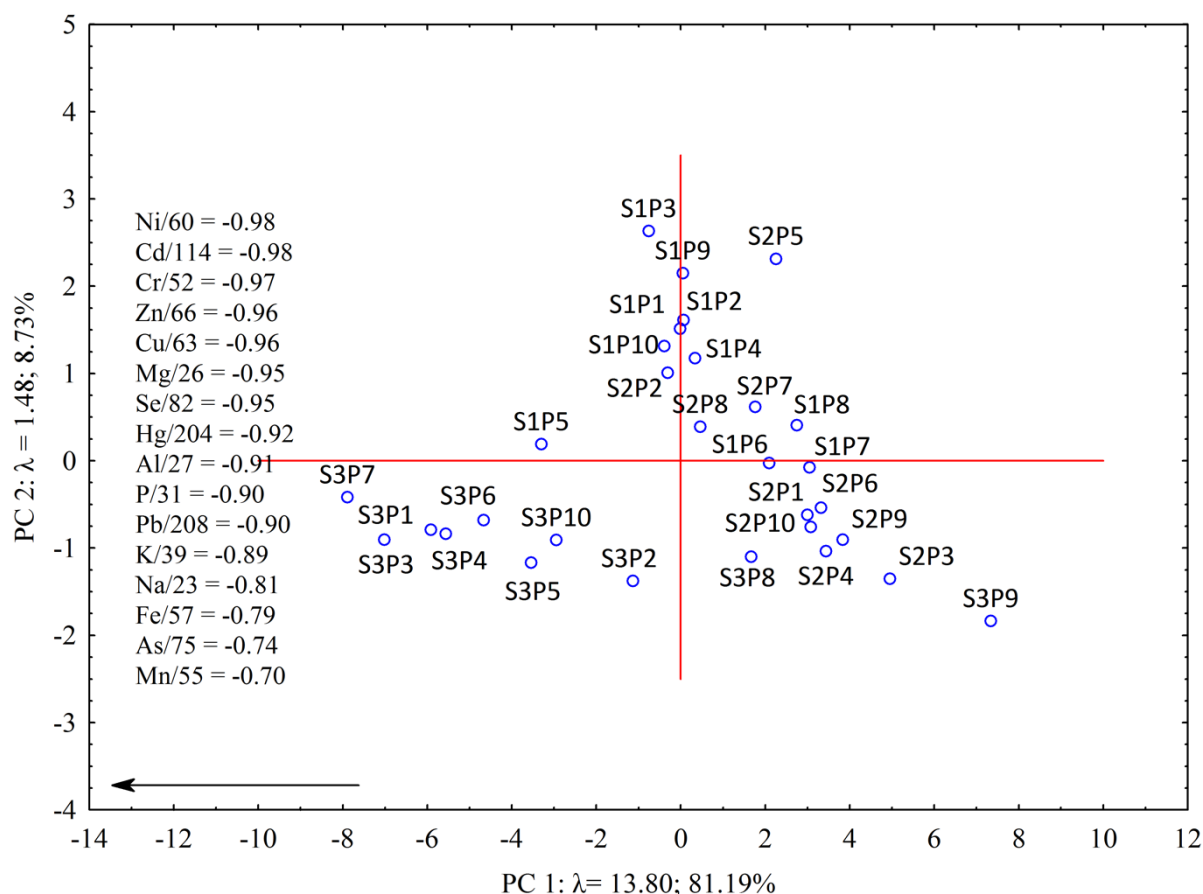


Figure 2. Principal components analysis of the chemical variables in the Brazilian Pantanal sediments.

The PCA demonstrates that there is a difference in the concentration of chemical elements in the sediment of the analyzed sites. The S3 site presented the highest concentrations of chemical elements in the sediment when compared to the S1 and S2 sites. This fact can be explained by

the fact that the river that supplies the S3 site is the Cuiabá River. This river has a lower flow than the Rio São Lourenço (site S2) and the Rio Paraguai (site S1). In this sense, the Cuiabá River has less diluting power than the others, concentrating more chemical elements per particle of sediment (Nanos and Martín, 2012).

The application of the contamination factor, degree of contamination and potential ecological risk index (Table 2) shows that the sediment of the studied lakes does not present anthropic interference. All index values at all points and all sites were classified as low.

Table 2. Brazilian Pantanal sediments Contamination Factor (CF), Contamination Degree (CD), Sedimentological Sensitivity Factor (SSF), and Index of Potential Ecological Risk (IPER)

IC	Sampled Lagoons		
	S1	S2	S3
Cr/52	0.53±0.14	0.39±0.12	0.64±0.26
Ni/60	0.38±0.13	0.32±0.10	0.67±0.29
Cu/63	0.40±0.11	0.42±0.15	0.67±0.24
Zn/66	0.52±0.15	0.51±0.19	0.63±0.26
As/75	0.56±0.13	0.54±0.26	0.85±0.32
Cd/114	0.50±0.11	0.43±0.10	0.76±0.28
Hg/204	0.54±0.11	0.45±0.10	0.57±0.19
Pb/208	0.51±0.11	0.54±0.13	0.69±0.25
CD	3.93±0.90	3.59±0.95	5.48±2.06
SSF	29.87±13.39	28.64±15.08	32.96±14.46
IPER	30.68±18.14	25.16±6.02	33.17±11.82

Contamination Factor classes: $CF < 1$: Low; $1 \leq CF < 3$: Moderate; $3 \leq CF < 6$: Considerable; $CF \geq 6$: Very high. Contamination Degree classes: $CD > 8$: Low; $8 \leq CD < 16$: Moderate; $16 \leq CD < 32$: Considerable; $CD \geq 32$: Very high. Index of Potential Ecological Risk classes: $IREP < 150$: Low; $150 \leq IREP < 300$: Moderate; $300 \leq IREP < 600$: Considerable; $IREP \geq 600$: Very high (Fiori et al., 2013).

The values of the contamination indices of the bottom sediment of the lakes evaluated in the study were low. This fact can be explained because the indices take into account the natural concentration of chemical elements in the sediment. These concentrations are known as geochemical reference values – GRV (Remor et al., 2018b). The GRV was determined specifically for each sampled site, and as the concentrations of chemical elements were below the GRV, it indicates that human activities are not interfering with the concentration of chemical elements in the sediment of the studied lakes (Crespo and Martín, 2015). In this sense, we can infer that the concentrations of chemical elements found in the sediment of the studied lakes are of natural origin.

4. CONCLUSIONS

During the study it was not possible to identify the presence of organochlorines and organophosphates in the sediment of the evaluated lakes. In this sense, it is concluded that the lakes evaluated in the study did not show interference from human action in relation to the increase in the concentration of organochlorines, organophosphates and chemical elements in the sediment. Being, the concentrations of chemical elements found coming from the natural composition of the soil.

Acknowledgements: The authors acknowledge the grant provided by Araucária Foundation (Protocol number 47376, agreement 003/2017).

REFERENCES

- Almeida, L. C., Júnior, J. B. S., Santos, I. F., Carvalho, V. S., Santos, A. S., Hadlich, G. M., & Ferreira S. L. C. (2020). Assessment of toxicity of metals in river sediments for human supply: Distribution, evaluation of pollution and sources identification. *Mar. Pollut. Bull.*, 158, 111423.
- Anderson, N. J., Heathcote, A. J., & Engstrom, D.R. (2020). Anthropogenic alteration of nutrient supply increases the global freshwater carbon sink. *Sci. Adv.*, 6(16).
- Ashayeri, N. Y., & Keshavarzi, B. (2019). Geochemical characteristics, partitioning, quantitative source apportionment, and ecological and health risk of heavy metals in sediments and water: A case study in Shadegan Wetland Iran. *Mar. Pollut. Bull.*, 149, 110495.
- Barile, P. J. (2018). Widespread sewage pollution of the Indian River Lagoon system, Florida (USA) resolved by spatial analyses of macroalgal biogeochemistry. *Mar. Pollut. Bull.*, 128, 557-574.
- Cembranel, A. S., Frigo, E. P., Sampaio, S. C., Mercante, E., Dos Reis, R. R., & Remor, M. B. (2017). Residue analysis of organochlorine and organophosphorus pesticides in urban lake sediments. *Engenharia Agrícola*, 37(6):1254-1267.
- Conceição, K. Z., Vilas Boas, M. A., Sampaio, S. C., Remor, M. B., & Bonaparte, D. I. (2018). Statistical control of the process applied to the monitoring of the water quality index. *Engenharia Agrícola*, 38(6), 951-960.
- Crespo, C. H., & Martín, M. (2015). Determination of background levels and pollution assessment for seven metals (Cd, Cu, Ni, Pb, Zn, Fe, Mn) in sediments of a Mediterranean coastal lagoon. *CATENA*, 13, :206–214.
- Da Silva, K. A., Nicola, V. B., Dudas, R. T., Demetrio, W. C., Maia, L. S., Cunha, L., & de Oliveira, C. M.R. (2021). Pesticides in a case study on no-tillage farming systems and surrounding forest patches in Brazil. *Scientific Reports*, 11(1).
- Faria, E., Girard, P., Nardes, C. S., Moreschi, S., Christo, S. W., Ferreira Junior, A. L., & Costa, M. F. (2021). Microplastics pollution in the South American Pantanal. *Case Studies in Chemical and Environmental Engineering*, 3, 100088.
- Fernandes, V. C., Domingues, V. F., Mateus, N., & Delerue-Matos, C. J. (2013). Multiresidue pesticides analysis in soils using modified QuEChERS with disposable pipette extraction and dispersive solid-phase extraction. *Journal Separation Science*, 36, 376-382.
- Fiori, C. S., Rodrigues, A. P. C., Santelli, R. E., Cordeiro, R. C., Carvalheira, R. G., Araújo, P. C., Castilhos, Z. C., & Bidone. E. D. (2013). Ecological risk index for aquatic pollution control: a case study of coastal water bodies from the Rio de Janeiro State, southeastern Brazil. *Geochim. Bra.*, 27, 24-36.
- Gazolla, B. L., & Gonçalves, F. V. (2017). Caracterização do processo de erosão das margens do Rio Miranda na região do Passo do Lontra, Corumbá, Mato Grosso do Sul. *Anuár. Inst. Geociênc.*, 40(2), 144-152
- Hasimuna, O. J., Chibesa, M., Ellender, B. R., & Maulu, S. (2021). Variability of selected heavy metals in surface sediments and ecological risks in the Solwezi and Kifubwa Rivers, Northwestern province. *Zambia. Scientific African*, 12, e00822.
- Jackson, D. A. (1993). Stopping rules in principal components analysis: A comparison of heuristical and statistical approaches. *Ecology*, 74, 2204-2214.
- Lacerda, A. R. (2017). Mudanças em desejos e oportunidades no status de pecuarista pantaneiro. *Rev. Estud. Pesqui. Admin.*, 1(1), 30-40

- Li, M., Zhang, Q., Sun, X., Karki, K., Zeng, C., Pandey, A., Rawat, B., & Zhang, F. (2020). Heavy metals in surface sediments in the trans-Himalayan Koshi River catchment: Distribution, source identification and pollution assessment. *Chemosphere*, 244, 125410.
- Model, K. J., Sampaio, S. C., Remor, M. B., Mercante, E., & Vilas Boas, M. A. (2018), Organoclorated and organophosphorus pesticides in the Pelotas River sediment. *Engenharia Agrícola*, 38(1), 124-134.
- Nanos, N., & Martín, J. A. R. (2012), Multiscale analysis of heavy metal contents in soils: spatial variability in the Duero river basin (Spain). *Geoderma*, 189-190, 554–562.
- Remor, M. B. (2017). *Geoquímica do sedimento do Pantanal brasileiro*. PhD thesis, Universidade Estadual do Oeste do Paraná, Engenharia Agrícola.
- Remor, M. B., Sampaio, S. C., Damatto, S. R., Castilhos, A. C., Stevaux, J. C., & Vilas Boas, M. A. (2015). Geochemistry of the Upper Paraná River floodplain: Study of the Garças Pond and Patos Pond. *J. Radioanal. Nucl. Chem.*, 305, 409-418.
- Remor, M. B., Sampaio, S. C., de Rijk, S., Vilas Boas, M. A., Gotardo, J. T., Pinto, E. T., & Schardong, F. A. (2018b). Sediment geochemistry of the urban Lake Paulo Gorski. *International Journal of Sediment Research.*, 33(4), 406-414.
- Remor, M. B., Sampaio, S. C., Model, K. J., Falco, T. D., & Prudente, V. H. R. (2018a). Mercury in the sediment of the upper Parnaíba River. *Engenharia Agrícola*, 38(5), 760-767.
- Roque, F. O., Guerra, A., Johnson, M., Padovani, C., Corbi, J., Covich, A. P., & Yon, L. (2021). Simulating land use changes, sediment yields, and pesticide use in the Upper Paraguay River Basin: Implications for conservation of the Pantanal wetland. *Agriculture, Ecosystems & Environment*, 314, 107405.
- Schulz, C., Martin-Ortega, J., & Glenk, K. (2018). Value landscapes and their impact on public water policy preferences. *Glob. Environ. Chang.*, 53, 209-224
- Schulz, C., Whitney, B. S., Rossetto, O.C., Neves, D. M., Crabb, L., Oliveira, E. C., Lima, L. T., Afzal, M., Laing, A. F., Fernandes, L. C. S., Silva, C. A., Steinke, V. A., Steinke, E. T., & Saito, C. H. (2019). Physical, ecological and human dimensions of environmental change in Brazil's Pantanal wetland: Synthesis and research agenda. *Science of The Total Environment*, 687, 1011-1027.
- Silva, K.A., Nicola, V.B., Dudas, R.T., Demetrio, W.C., Maia, L.S., Cunha, L., Bartz, M.L.C., Brown, G.G., Pasini, A., Kille, P., Ferreira, N.G.C., & Oliveira, C.M.R. (2021). Pesticides in a case study on no-tillage farming systems and surrounding forest patches in Brazil. *Scientific Reports*, 11, 9839.
- Ustaoğlu, F., Islam, M.S. (2020). Potential toxic elements in sediment of some rivers at Giresun, Northeast Turkey: A preliminary assessment for ecotoxicological status and health risk. *Ecological Indicators*, 113, 106237.
- Zhuang, S., Lu, X., Yu, B., Fan, X., & Yang, Y. (2021). Ascertain the pollution, ecological risk and source of metal(loid)s in the upstream sediment of Danjiang River, China. *Ecological Indicators*, 125, 107502.

OCURRENCE OF HAZARDOUS SUBSTANCES IN SOILS AND RIVER SUSPENDED SEDIMENT IN 7 RIVER CATCHMENTS WITHIN THE DANUBE RIVER BASIN

Zsolt Jolankai^{1*}, Adrienne Clement¹, Mate Kardos¹, Steffen Kittlaus², Nikolaus Weber², Ottavia Zoboli², ,
Oliver Gabriel³, Martina Broer³, Florentina Soare⁴ Carmen Hamchevici⁴, Radoslav Tonev⁵, Dimitar Mihalkov⁵,
Radmila Milacsic⁶, Katarina Markovic⁶, Lucija Levstek⁶, Orsolya Szomolanyi¹, Matthias Zessner²

¹. Budapest University of Technology and Economics, Department of Sanitary and Environmental Engineering,
Budapest, Hungary

². Technical University Vienna, Department, Vienna, Austria

³. Umwelt Bundesamt Austria, Vienna, Austria

⁴. National Administration Romanian Waters, Bucharest, Romania

⁵. Bulgarian Water Association

⁶. Jožef Stefan Institute

*Corresponding author (jolankai.zsolt@emk.bme.hu)

ABSTRACT

An extensive monitoring programme has been carried out on 7 river catchments across the Danube River Basin to investigate sources and pathways of a diverse spectrum of hazardous substances. The one-year long monitoring campaign was designed to be cost-effective and used spatially or temporally aggregated composite samples of soil, atmospheric deposition, waste water, suspended sediment and river water (low- and high flow samples). Heavy metals, PFCs, PAHs and several widely used organic compounds have been analysed in this study and found similar spatial patterns for most substances.

Keywords: PAH, Heavy metals, PFCs, soil contamination, composite soil sampling.

1. INTRODUCTION

Hazardous substances (HS) pose a risk to human health and to maintaining or achieving good ecological status of European Rivers, which is the main objective of the Water Framework Directive. The number of substances that are harmful or potentially harmful in a mixture are increasing as it can be learned from scientific works (Kortenkamp et al., 2019) or from the increasing list of priority substances used in the EU legislation. As the number of substances increase, the associated costs of monitoring and measures also increase.

The sampling programme delivered in the Danube Hazard m3c project aimed to increase the efficiency of monitoring and therefore reduce the costs by applying sampling methodologies that reduce labour cost while maintaining the information value of sampling. The sampling aimed to collect information about emissions in waste water treatment plants, atmospheric deposition, soils, suspended sediments and river water at low and high-flow conditions. This paper focuses on the methods and initial results of the soil sampling.

2. MATERIAL AND METHODS

An extensive soil sampling campaign have been carried out on seven pilot catchments across the Danube River Basin (DRB) (Ybbs and Wulka catchments in Austria, Koppány and Zagyva

catchments in Hungary, Somesul Mic and Viseu in Romania, Vit in Bulgaria, the area of which varies from ~400 to 2200 km²). The soil sampling targeted all the major land uses on the catchments with special focus on agriculture, but forests and pastures were also sampled in a quantity relevant to their share in the total catchment area. Beside land use, soil information was also taken into account, using soil texture maps and organic matter content maps of the area, where available. 20 samples have been located with random sampling within 10 spatial units that were determined with GIS applications.

The sampling have been carried out using hand held auger probes. The samples were collected from the upper 30 cm in case of arable land, and the upper 10 cm in case of pastures and forests. At each spots the samples were taken from further 3-5 subsamples, which were mixed on site. At each spot 50 g of sample were collected into a glass jar, which was held in cool place until delivery to the preparation lab, where the samples were homogenized, sieved on 2mm sieve and lyophilized. Samples were sent to three labs in the DRB to measure for different set of substances. The analysis of the samples targeted 16 PAH compounds, a group of other organic substances including two pharmaceuticals (Diclofenac and Carbamazepine), two pesticides (Tebuconazole, Metolachlor), several perflourinated compounds (PFC), other industrial substances (phenols), and 8 potentially toxic elements (PTEs) (Cd, Cr, Cu, Hg, Ni, Pb, Zn, As).

3. RESULTS AND DISCUSSIONS

Spatial distribution of six out of 8 measured substances (heavy metals and As) is shown in **Figure**. The relations of concentrations between the pilot catchments are similar for most substances (slightly different for arsenic). The Vit, the Somes and Viseu catchments shows somewhat higher concentrations for most metals. There is a clear difference in the source and delivery mechanisms of the different metals in suspended sediment sample as Cr, Ni has lower concentration than in soils, while Zn, Pb and Cu has in much higher concentrations in suspended matter (based on sediment results for Hungary only). According to the first analysis, concentrations in forest and pasture soils show similar concentration ranges to agricultural soils.

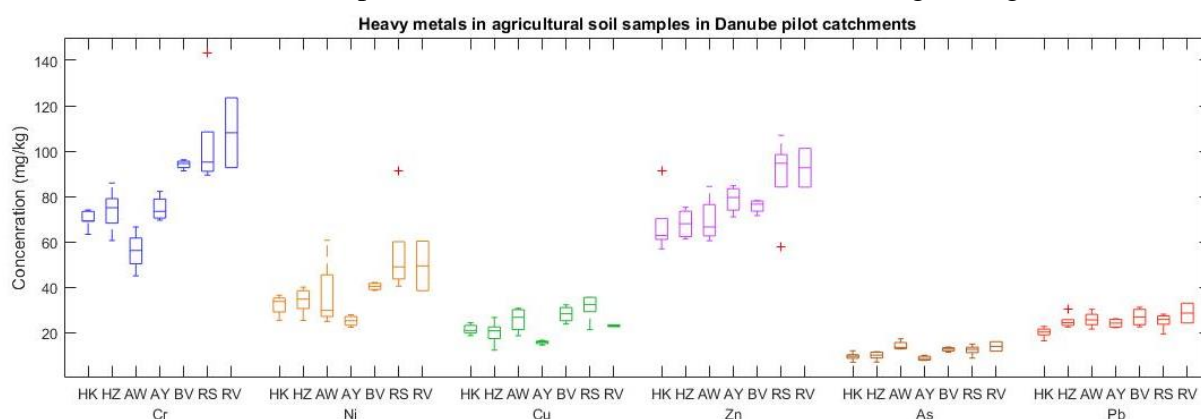


Figure1. Concentration ranges of 5 heavy metals and arsenic in the seven pilot regions (K – Koppány , Z - Zagyva , W – Wulka , Y – Ybbs, BV - Vit, S – Somes, RV – Viseu)

Out of the 16 measured PAH compounds, 11 have been found in substantial quantities (**Figure**.). Just like in the case of heavy metals, the spatial pattern across the pilot regions are similar in case of all the PAH compounds. Looking at the mean of the sum of 16 PAH compounds across the pilots, it becomes apparent that forest soils have higher concentrations

(84.2 $\mu\text{g}/\text{kg}$) than soils with agricultural (59.7 $\mu\text{g}/\text{kg}$) and pasture (49.8 $\mu\text{g}/\text{kg}$) land uses, which is in alignment with some previous studies e.g.(Łyszczarz et al., 2021)

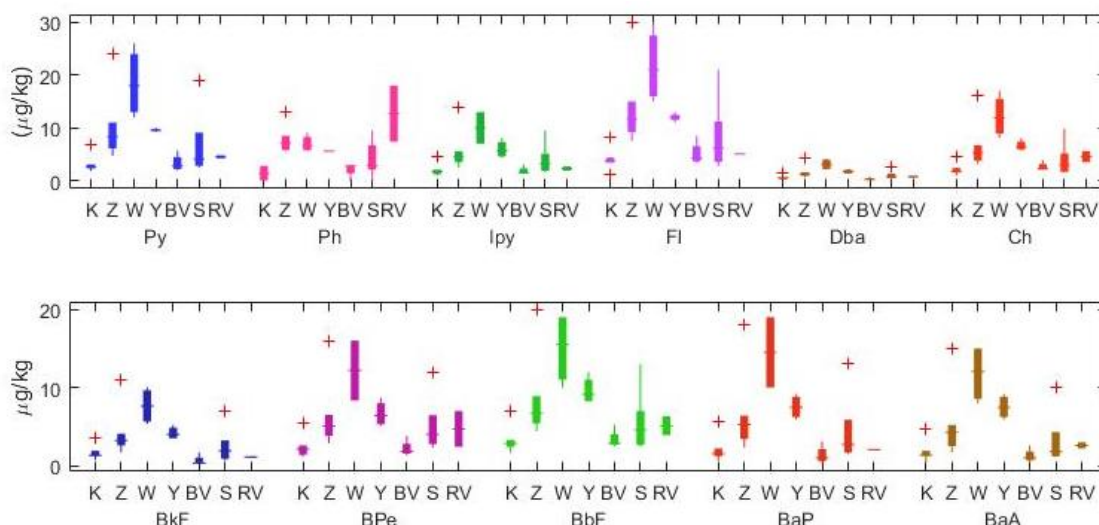


Figure 2. Concentration ranges in agricultural soils of 11 PAH compounds that were found in relevant quantities in the 7 pilot catchments (See abbreviations for Figure 1.) Py – Pyrene, Ph – Phenanthrene, Ipy – Indeno(1,2,3-c,d)pyrene, Fl – Flouranthene, DbA – dibenzo(a,h)anthracene, Ch – Chrysene, BkF – Benzo(k)flouranthene, BPe – Benzo(g,h,i)perylene, BbF – Benzo(b)flouranthene, BaP – Benzo(a)pyrene, BaA – Benzo(a)anthracene

The preliminary analyzes of perfluorinated compounds show heterogeneity of the occurrence in soils across the DRB and across land uses. The total concentrations of the 12 analyzed variants were in the range of 0.35-4 $\mu\text{g}/\text{kg}$. The highest concentrations were found from perfluorooctanesulfonic acid (PFOA) with 0.4 $\mu\text{g}/\text{kg}$ on average. Out of the remaining analyzed organic compounds only pesticides were found in detectable amounts in agricultural soils of three catchments with an average concentration of 0.06 mg/kg.

4. CONCLUSIONS

Gaining concentration ranges of a large group of chemicals from soils representing three different land uses across seven pilot areas of the DRB proved that there is a clear spatial heterogeneity for heavy metals and PFC across the basins. PAH concentrations for forests tend to be higher than for agricultural soil samples.

Acknowledgements:

The research has been supported primarily by the Danube Hazard m3c project (DTP3-299-2.1), co-financed by the WFD monitoring KEHOP-1.1.0-15-2016-00002, project no. BME-NVA-02, financed under the TKP2021 funding scheme, and the Széchenyi Plan Plus program with the support of the RRF 2.3.1 21 2022 00008 project.

REFERENCES

- Kortenkamp, A., Faust, M., Backhaus, T., Altenburger, R., Scholze, M., Müller, C., Ermler, S., Posthuma, L., & Brack, W. (2019). Mixture risks threaten water quality: the European Collaborative Project SOLUTIONS recommends changes to the WFD and better coordination across all pieces of European chemicals legislation to improve protection from exposure of the aquatic environment to multiple pollutants. *Environmental Sciences Europe*, 31(1), 69. <https://doi.org/10.1186/s12302-019-0245-6>
- Łyszczarz, S., Lasota, J., Staszal, K., & Błońska, E. (2021). Effect of forest and agricultural land use on the accumulation of polycyclic aromatic hydrocarbons in relation to soil properties and possible pollution sources. *Forest Ecology and Management*, 490, 119105. <https://doi.org/https://doi.org/10.1016/j.foreco.2021.119105>

IMPACT OF THE SOIL STRATIFICATION AND SATURATION ON THE PERFORMANCE OF INFILTRATION BOREHOLES

Ziyad Abunada¹, Wafa Alijla² and Osama Dawoud^{3*}

¹. CQ University, Australia

². Durham University, United Kingdom

³. İstinye Üniversitesi, Turkey

*Corresponding author (dawoud.ps@gmail.com)

ABSTRACT

Infiltration boreholes are of the common practices for stormwater harvesting. However, the capacity of these boreholes is highly dependent on the soil stratification characteristics and saturation conditions. This hinders the wide-scale planning and preliminary designs which rely on limited geotechnical information. The current study considered the case of a borehole that penetrates an upper clay layer to reach a sandy aquifer where the water level is located below an unsaturated zone. The analysis showed that the impact of the available infiltration depth is highly significant compared to the depth to the water table. The study also showed that the formation of the saturated field under the borehole maximizes the infiltration rate. This indicates that priority should be given to the maximization of the depth of aquifer penetration regardless of the hydrogeological conditions. This study helps planning wide-scale infiltration projects in a way that maximizes the infiltration capacity at the minimal cost.

Keywords: Infiltration, Borehole, Stratification, Unsaturated flow

EFFECT OF SOIL MICROPLASTICS ON SEED GERMINATION OF HELIANTHUS ANNUUS L. AND SORGHUM BICOLOR L.

Mehmet Meric TUNALI¹, Merve TUNALI^{1,2}, Başak GÜVEN¹, Orhan YENİGÜN^{*,1,3}

¹ Boğaziçi University, Institute of Environmental Sciences, Bebek 34342, Istanbul, Turkey

² Empa, Swiss Federal Laboratories for Materials Science and Technology, Lerchenfeldstrasse 5, 9014 Sankt Gallen, Switzerland

³ European University of Lefke, School of Engineering, Gemikonagi, Lefke, North Cyprus, Turkey

*yeniguno@boun.edu.tr

ABSTRACT

Microplastic (MP) particles and fibers can be found in different ecosystems including soils. Effects of MPs in soil can vary depending on their abundance, types, and environmental conditions. Plants are known to be affected by MPs presence; plant growth parameters and seed germination performance are generally used as endpoints to assess the impact of MPs on plants. In addition, the role of soil microorganisms –such as Arbuscular Mycorrhizal Fungi (AMF) species can differ in relation with plant species and microplastic presence. In this study, germination capacity of sunflower (*Helianthus annuus L.*) and sorghum (*Sorghum bicolor*) seeds in the presence of MPs on 3 different levels; 0.4%, 0.8%, and 1.6% and with/without Arbuscular Mycorrhizal Fungi (*Glomus mosseae*) inoculation were assessed. as a preliminary step prior to plant growth experiments.

Sunflower seeds' germination was increased by 8% for 0.4% MPs compared to control group and with increasing level of MPs germination rate of sunflower were decreased by 6%, 17% for 0.8%, 1.6% MPs, respectively. Whereas Sorghum seeds germination decreased by 10%, 11% and 24% for the same range of microplastic fibers present in the system.

AMF inoculation (Control +) showed 4% better germination rate compared to sunflower control group without inoculation; for MP levels of 0.8% and 1.6% the rate was increased by 2% and 26%, respectively. Sorghum seeds germination rates were decreased with AMF presence by 22% for control group and 13.3%, 15.6%, and 12.2% for increasing MP levels present in the system.

Keywords: microplastic, soil, germination, plant, mycorrhiza.

1. INTRODUCTION

Plastic materials can remain for centuries in ecosystems due to their chemical compositions and characteristics, and can affect soil organisms including plants. Microplastics; defined as tiny plastic fragments, fibers, and granules particles that are <5 mm in diameter (Thompson et al., 2004) have been identified in different environmental systems including lakes, rivers, surface waters, reservoirs, sediments of rivers, and terrestrial environments (Zbyszewski and Corcoran, 2011; Klein et al., 2015).

In addition to microplastics that may be present in the soil bodies, plastic residues can also disintegrate into micro- and nano-plastics, which pose potential risks to soil biology and human health (Kasirajan and Ngouajio, 2012; Steinmetz et al., 2016; Wang et al., 2016). MPs entering in the soil systems are estimated to be 4 to 23 times higher than in oceans (Horton et al., 2017). Microplastics can damage the structure of soil (e.g. reducing soil bulk density increasing

porosity) (Jiang et al., 2017), limit soil permeability and reduce water holding capacity (Zeng et al., 2013), negatively influence soil aggregation (Lozano et al. 2021). By affecting soil properties, MP can also effect root growth of the plants and overall plant productivity; as roots of plants can grow more freely with increased porosity resulting in more plant biomass on both roots and shoots (Lozano et al, 2021). Effects on plant growth can vary depending on several factors such as polymer type, MP abundance, seed type.

On the other hand, Arbuscular Mycorrhizal Fungi (AMF) family can form symbiosis with plants and help their host to resist harsh conditions as well as increasing soil quality and stability through protein production named "Glomalin Related Soil Protein". Interactions between microplastics and AMF community in soil bodies and their effect on plant growth as well as in the presence of other soil pollutants such as microplastics have been confirmed. Wang et al (2016) revealed that the AMF genera highly affected with microplastic presence (type and concentration).

This research was conducted as a preliminary step prior to plant growth experiments (in same conditions, gives a general idea on the potential impact of microplastics in soils on seed germination and the role of mycorrhiza species, if any, on sunflower and sorghum seeds' germination capacity.

2. MATERIAL AND METHODS

Differentiation on the plant growth was determined by the comparison of the respective control groups; first control group is maintained to observe the seed germination without any stress from MPs and AMF. Second control group was the AMF control group to identify the AMF influence without MP presence. Through MP groups 1 and 2 on the effects of microplastics on plant growth with/without AMF were obtained. Experiments were conducted in following groups:

- Control group (without MPs, and AMF)
- AMF Control Group (without MPs, with AMF)
- MP Group1 (with MPs, without AMF)
- MP Group2 (with MPs, and AMF)

Glomus mosseae was adapted local climate over the past few years and supplied from Ege University, Turkey. Sunflower and sorghum seeds were supplied from Turkish commercial farming business located in Tekirdağ and İzmir, respectively. Seeds were treated with distilled water and ethanol sequentially. Germination tests were conducted in petri dishes using (*Helianthus annuus L.*) and sorghum (*Sorghum bicolor*) seeds in the presence of microplastic fibers. Manual cutting of commercial polyester rope "Paraloc rope, Mamutec, Switzerland, product number: 8442171" followed by sieving process (<1mm) was used to generate microplastic fibers. Obtained fibers were incorporated into petri dishes in accordance with relative weights of petri dishes and stirred with distilled water to ensure homogeneity within each petri dish prior to the placement of plant seeds. 3 different levels of microplastic fibers were monitored; 0.4% (w:w), 0.8% (w:w), and 1.6% (w:w), respectively.

Arbuscular Mycorrhizal Fungi (*Glomus mosseae*) along with proper control groups all treatment levels had 3 parallels. 48 sterile petri dishes were prepared to conduct the germination test. Planted numbers of seeds in petri dishes were 5 for sunflower, and 10 for sorghum seeds for each petri dish.

Introduction of the Arbuscular Mycorrhizal Fungi; *Glomus mosseae*, into the germination system, was conducted as following procedure; 30.002 g of Glucose Hydrate ($C_6H_{14}O_7$) was dissolved in 100 ml distilled water. Afterwards, 1.8 g of AMF spores was added to the prepared solution. 5 ml of this mixture was added to each petri dishes prior to the plantation of seeds. Initial concentration of the AMF spores was 100 mg mycorrhizal fragments including spores

and hyphae per petri dish (Brundrett, 2002). Germination of seeds were monitored for 5 days and results were reported as cumulative sum for each group.

3. RESULTS AND DISCUSSIONS

To determine plant seeds' germination performance obtained seeds were tested with microplastic fibers and AMF presence in petri dishes. According to germination rates, sunflower had higher germination rate compared to sorghum variation, 91.1% and 63.33% for control groups, respectively. Germination rates over time is detailed in Table 1.

Germination study results were consistent within their own categories, it can be argued that microplastic presence affects the germination capacity with high level of MPs. Only sunflower seeds treated with low amount of MP -0.4% had better germination rate compared to control group of the same category by 8%. With increasing MP levels number of germinated seeds have decreased for both plants. Sunflower seeds' germination went down by 6% for 0.8% MPs and 17% for 1.6 MPs, respectively. Whereas Sorghum seeds germination decreased by 10%, 11.11% and 24.55% for the same range of microplastic fibers present in the system.

Additionally, AMF introduction to the system seems to have helped with germination of seeds with relatively high level of microplastics especially for sunflower species. Sunflower control group with AMF inoculation (Control +) has 4.4% better germination rate compared to sunflower control group without inoculation; MP level of 0.4% was not affected by AMF presence since all sunflower seeds were germinated in both sets; for MP levels of 0.8% and 1.6% the germination rate was increased by 2.22% and 26.66%, respectively.

Sorghum seeds have not benefited from AMF inoculation in terms of their germination rates. Overall germination rate decreased by 22% for control group and 13.3%, 15.6%, and 12.2% for increasing microplastic levels present in the system.

Table 1. Germination ratio of Sunflower and Sorghum species

Sunflower	Day 3	Day 4	Day 5	Sorghum	Day 3	Day 4	Day 5
Control	80%	80%	80%	Control	80%	80%	80%
	80%	100%	100%		50%	50%	50%
	100%	100%	100%		60%	60%	60%
0.4% MP	100%	100%	100%	0.4% MP	40%	40%	50%
	100%	100%	100%		60%	60%	60%
	100%	100%	100%		50%	60%	60%
0.8% MP	100%	100%	100%	0.8% MP	50%	50%	50%
	60%	80%	80%		60%	60%	60%
	80%	80%	80%		40%	50%	50%
1.6% MP	40%	60%	60%	1.6% MP	40%	40%	40%
	60%	100%	100%		30%	40%	40%
	80%	80%	80%		30%	30%	30%
Control + <i>G.mossaea</i>	80%	80%	80%	Control + <i>G.mossaea</i>	40%	40%	40%
	100%	100%	100%		50%	30%	50%
	80%	100%	100%		40%	40%	40%
0.4% MP + <i>G.mossaea</i>	100%	100%	100%	0.4% MP + <i>G.mossaea</i>	40%	40%	40%
	100%	100%	100%		30%	30%	30%

	100%	100%	100%		50%	50%	50%
0.8% MP + <i>G.mossaea</i>	80%	80%	80%	0.8% MP + <i>G.mossaea</i>	30%	30%	30%
	100%	100%	100%		50%	50%	50%
	80%	80%	80%		30%	30%	30%
	100%	100%	100%		50%	50%	50%
1.6% MP + <i>G.mossaea</i>	100%	100%	100%	1.6% MP + <i>G.mossaea</i>	10%	10%	10%
	100%	100%	100%		50%	50%	50%
	80%	100%	100%		20%	20%	20%
	100%	100%	100%		50%	50%	50%

4. CONCLUSIONS

Findings of this study supports that microplastic presence inhibits the seed germination rate for sorghum and sunflower plants noticeably, and beneficial soil organisms such as AMF can relatively help with germination of these seedlings and can potentially support their growth depending on microplastic levels in soil, species involved, and other stress conditions such as climate conditions, salinity levels, any other contamination that may be present in soil body including heavy metals during germination and growth phase of the respective plants. It should also be noted that these results constitute primary findings and data obtained was not sufficient for full factorial statistical comparison; yet, it can be utilized as a primary step for further research on this topic.

REFERENCES

- Brundrett, M.C., 2002. Co-evolution of roots of mycorrhizas of land plants, *New Phytologist*, 154, 275-304.
- Horton, A.A., Svendsen, C., Williams, R.J., Spurgeon, D.J., Lahive, E., 2017. Large microplastic particles in sediments of tributaries of the River Thames, UK – Abundance, sources and methods for effective quantification. *Mar. Pollut. Bull.* <https://doi.org/10.1016/j.marpolbul.2016.09.004>
- Jiang, X.J., Liu, W., Wang, E., Zhou, T., Xin, P., 2017. Residual plastic mulch fragments effects on soil physical properties and water flow behavior in the Minqin Oasis, northwestern China. *Soil Tillage Res.* <https://doi.org/10.1016/j.still.2016.10.011>
- Kasirajan, S., Ngouajio, M., 2012. Polyethylene and biodegradable mulches for agricultural applications: A review. *Agron. Sustain. Dev.* <https://doi.org/10.1007/s13593-011-0068-3>
- Klein, S., Worch, E., Knepper, T.P., 2015. Occurrence and spatial distribution of microplastics in river shore sediments of the rhine-main area in Germany. *Environ. Sci. Technol.* <https://doi.org/10.1021/acs.est.5b00492>
- Lozano, Y., Lehnert, T., Linck, L.T., Lehmann, A., Rillig, M.C., 2021. Microplastic Shape, Polymer Type, and Concentration Affect Soil Properties and Plant Biomass. *Front. Plant Sci* <https://doi.org/10.3389/fpls.2021.616645>
- Steinmetz, Z., Wollmann, C., Schaefer, M., Buchmann, C., David, J., Tröger, J., Muñoz, K., Frör, O., Schaumann, G.E., 2016. Plastic mulching in agriculture. Trading short-term agronomic benefits for long-term soil degradation? *Sci. Total Environ.* <https://doi.org/10.1016/j.scitotenv.2016.01.153>
- Thompson R C, Olsen Y, Mitchell R P, Davis A, Rowland S J, John A W, McGonigle D and Russell A E 2004 Lost at sea: where is all the plastic? *Science* 304 838. <https://doi.org/10.1126/science.1094559>
- Wang, J., Lv, S., Zhang, M., Chen, G., Zhu, T., Zhang, S., Teng, Y., Christie, P., Luo, Y., 2016. Effects of plastic film residues on occurrence of phthalates and microbial activity in soils. *Chemosphere.* <https://doi.org/10.1016/j.chemosphere.2016.02.076>
- Zbyszewski, M., Corcoran, P.L., 2011. Distribution and degradation of freshwater plastic particles along the beaches of Lake Huron, Canada. *Water. Air. Soil Pollut.* <https://doi.org/10.1007/s11270-011-0760-6>
- Zeng, L.S., Zhou, Z.F., Shi, Y.X., 2013. Environmental problems and control ways of plastic film in agricultural production, in: *Applied Mechanics and Materials.* <https://doi.org/10.4028/www.scientific.net/AMM.295-298.2187>

FATE AND TRANSPORT OF SOME COMMONLY USED PESTICIDES IN THE KONYA PLAIN, TURKEY

Yağmur Ongar^{*1}, Ulaş Tezel¹, Burak Demirel¹, and Nadim K. Coptý¹
¹Institute of Environmental Sciences, Boğaziçi University, İstanbul, Turkey
^{*}Corresponding author (yagmurongar@gmail.com)

ABSTRACT

Pesticides are widely used in agriculture to combat a variety of pests and increase crop yields to meet expanding global nutritional needs. It is estimated that more than 2 million tons of pesticides are used worldwide annually. However, besides their benefits, there are some detrimental side effects on both living organisms and the environment. The purpose of this study is to examine the fate and potential transport of two herbicides (2,4-dichlorophenoxyacetic acid and fenoxaprop-p-ethyl) widely used in the Konya Plain, one of the major agricultural areas of Turkey. Soil samples were first collected and screened for a wide range of pesticides using liquid chromatography coupled with tandem mass spectroscopy (LC-MS/MS). Extraction of target pesticides from the soil samples was performed using “quick, easy, cheap, effective, rugged, and safe” QuEChERS method. Both kinetic and equilibrium sorption tests along with column transport experiments were performed to evaluate the sorption and potential mobility of the target herbicides. Results show that a wide range of insecticides, herbicides and fungicides were detected in the collected soil samples. The 24h distribution coefficient (K_d) value of Fenox was calculated as 297 mL g^{-1} , while no significant sorption was observed for 2,4-D. Overall, the experiments demonstrated that the transport potential of 2,4-D is high while Fenox mobility is limited due to its high sorption. On the other hand, Fenox has higher potential for accumulating in the soil.

Keywords: *QuEChERS, soil, adsorption, pesticide, fate and transport*

1. INTRODUCTION

By the end of 2022, the world population is estimated to reach 8 billion people; this figure is expected to reach 8.5 billion in 2030, and 10 billion in 2050 (UN, 2022). This expeditious population growth places global food demand and trading of agricultural products at the heart of national economies (Kummu et al., 2020). Consequently, increasing agricultural productivity by controlling crop pests and diseases has also gained tremendous emphasis in recent decades.

In 2019 roughly 2 million tons of pesticides were applied with an estimated budget of 50 billion USD. Among these two million tons of pesticides used, herbicides account for about half of this consumption (Akanksha Sharma et al., 2020; Anket Sharma et al., 2019).

Agrochemicals have been quite successful in the control of crop pests and diseases. However, these chemicals are associated with many potential side effects. This study aims to investigate

the fate and transport potential of some commonly used herbicides agricultural soils of Turkey by conducting batch and column experiments.

5. MATERIAL AND METHODS

4) Chemicals

All the target herbicides (2,4-D and Fenox) and surrogate standards were purchased at their purest grade from Sigma Aldrich Chemicals Company for the development of the analytical method and for the quantification of these chemicals in the soil samples. Stock solutions of the chemicals were individually prepared at 10 or 1 g L⁻¹ in methanol and stored at -20°C in 10-mL amber vials until use.

2.2. Soil sampling and characterization

Soil samples that used in the experiments were collected from a field located in Karaman, near the district of Karapınar, Konya. For the extraction, batch and column experiments, a total of 17 soil samples (from depths of about 10 to 20 cm) were collected on March 25, 2021 from five different fields. The collected samples were air-dried, passed through a 2 mm sieve and stored in zip-lock bags at +4°C.

The sieve analysis was done by using the Endecotts EFL 2000 vibrating shaker. The pH of the soil samples was measured in a pH meter, the EC was determined by conductivity meter, and CEC was determined using sodium acetate (NH₄OAc) solution. Duplicate samples were used for the characterization of the soil samples.

2.3. Pesticide extraction from the soil samples

In order to analyze the pesticide levels in the soil samples QuEChERS (quick, easy, cheap, effective, rugged, and safe) method was performed. The AOAC method was selected as a pesticide extraction method for the soil samples.

2.4. Batch and Column Experiments

For the batch and column experiments, air-dried and sieved soil samples were used. Five different concentrations of working solution were prepared for both target pesticides.

3. RESULTS AND DISCUSSIONS

3.1. Soil Characterization

The pH_(KCl) of the soil mixture was measured as 8.07±0.01 at 20.0±1°C, which could be classified as moderately alkaline soil. The moisture content of the soil mixture was found to be 13.7 % while the organic content was found to be 3.0 %. The EC of the soil mixture (#12,13,14) was determined as 142.6±2.9 µs cm⁻¹ and CEC of it was determined as 29.08 mEq 100 g⁻¹.

Table 1. Characterization of the soil samples used for the batch and column experiments (mean standard dev., n=2)

Sample	CEC (mEq 100 g ⁻¹)	EC (μs cm ⁻¹)	pH (KCl)	Soil texture	Moisture content (%)	Organic content (%)
#12,13,14	29.08	142.6±2.9	8.07±0.01	Loamy sand	13.7±0.57	3.0±0.06

3.2. Pesticide Extraction from the Soil Samples

The mean recovery of surrogate standards and target herbicides from the soil by AOAC and BS methods were 45.4 14.1 and 51.6 28.2% (n=21), respectively. No significant difference of recovery efficiency was detected between the two methods used for the extraction. According to the recovery results, it is observed that the target herbicides can be absorbed by the soil and their sorption behavior can be accurately determined by using the selected surrogate standards.

3.3. Sorption Kinetics

In order to establish the sorption behavior of the selected herbicides, sorption batch experiments were conducted. Over time, it is expected to observe a decrease in the initial pesticide concentrations in the aqueous phase due to sorption process. For 2,4-D and all initial concentrations, it was observed that the concentration remained constant over the duration of the tests, indicating that there was very limited sorption. On the other hand, a clear reduction was observed for Fenox concentration in the aqueous phase for all the prepared concentrations. As a final step for the investigation of sorption behavior, equilibrium sorption isotherms were constructed for both herbicides and for the hour 24 (Figure 1.).

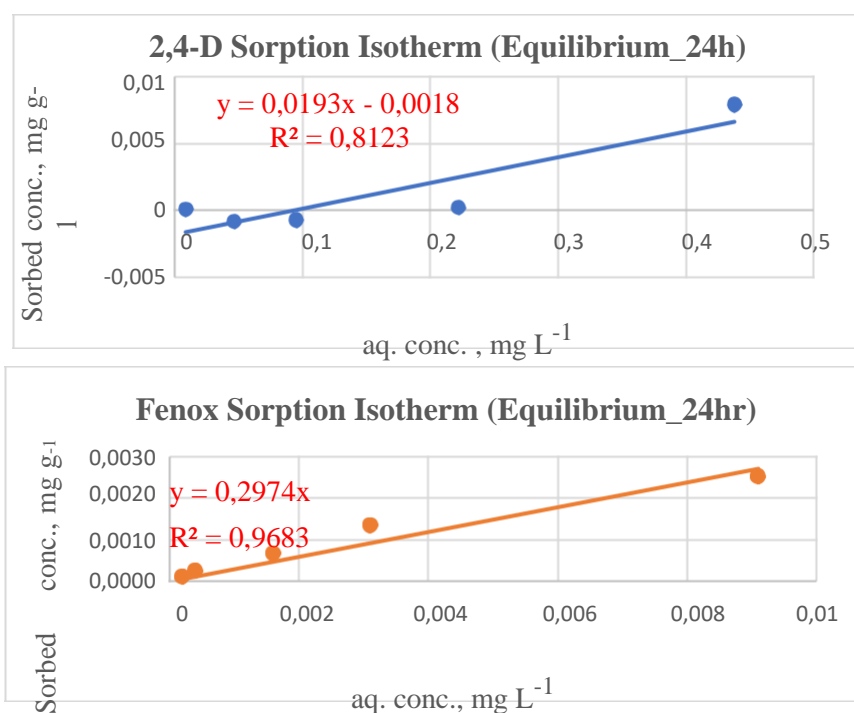


Figure 1. Sorption isotherms of 2,4-D and Fenox for the hour 24 respectively

3.4. Column Experiments

For the column transport experiments a concentration of $500 \mu\text{g L}^{-1}$ working solution was prepared for both of the target pesticides. The dispersion coefficient of the column experiments was calculated as $7.71 \text{ cm}^2 \text{ min}^{-1}$ for 2,4-D and $44.74 \text{ cm}^2 \text{ min}^{-1}$ for Fenox, respectively. In addition, the breakthrough time was calculated as roughly 21 min for 2,4-D and 250 hours for Fenox, respectively. Breakthrough of Fenox on the other hand, was not observed over the duration of the test (8 mL pore volume), confirming its high sorption potential and low mobility.

4. CONCLUSIONS

This laboratory scale study aimed to investigate the fate and transport behavior of some commonly used pesticides in the Konya Plain, Turkey. 2,4-D and Fenox were selected as the target since they are widely used in the farmlands of the Konya Plain. The objective of these batch tests were to examine the sorption kinetics and to determine K_d values for the isotherm constant 2,4-D and Fenox. As a result of batch sorption experiments, no significant sorption was observed for 2,4-D. On the other hand, significant Fenox sorption was achieved after 24 hour equilibration. The K_d value for Fenox was calculated as 297.4 mL g^{-1} . The high sorption potential of Fenox observed from the batch sorption tests show that this pesticide has a very low leaching potential compared to 2,4-D. It means that Fenox has a higher tendency to accumulate in soil and plants. On the other hand, 2,4-D poses a greater risk for the contamination of groundwater and nearby surface water resources. Future studies will examine the potential biodegradation of these two herbicides.

Acknowledgements: The authors acknowledge the financial support provided by Boğaziçi University Research Fund Grant Number 16865.

REFERENCES

- Kummu, M., Kinnunen, P., Lehtikoinen, E., Porkka, M., Queiroz, C., Rööös, E., Troell, M., & Weil, C. (2020). Interplay of trade and food system resilience: Gains on supply diversity over time at the cost of trade independency. *Global Food Security*, 24(November 2019), 100360.
- Sharma, Akanksha, Shukla, A., Attri, K., Kumar, M., Kumar, P., Suttee, A., Singh, G., Barnwal, R. P., & Singla, N. (2020). Global trends in pesticides: A looming threat and viable alternatives. *Ecotoxicology and Environmental Safety*, 201(March), 110812.
- Sharma, Anket, Kumar, V., Shahzad, B., Tanveer, M., Sidhu, G. P. S., Handa, N., Kohli, S. K., Yadav, P., Bali, A. S., Parihar, R. D., Dar, O. I., Singh, K., Jasrotia, S., Bakshi, P., Ramakrishnan, M., Kumar, S., Bhardwaj, R., & Thukral, A. K. (2019). Worldwide pesticide usage and its impacts on ecosystem. *SN Applied Sciences*, 1(11).
- United Nations Department of Economic and Social Affairs, Population Division (2022). World Population Prospects 2022: Summary of Results. UN DESA/POP/2022/TR/NO. 3.

ASSESSMENT OF SURFACTANT-ENHANCED IN SITU CHEMICAL OXIDATION OF DNAPL SOURCE ZONES

Zeynep Demiray^{1*}, Nihat Hakan Akyol² and Nadim Copty¹

¹ Bogazici University, Turkey

² Kocaeli University, Turkey

*Corresponding author (zeynep.demiray@boun.edu.tr)

ABSTRACT

The presence of chlorinated solvents in the subsurface in the form of dense non-aqueous phase liquids (DNAPL) often leads to long-term contamination of large portions of groundwater resources. In this study, the synergetic effects of combined surfactant-enhanced dissolution with in-situ permanganate oxidation of a DNAPL source zone entrapped in heterogeneous porous media are investigated. Flow cell experiments were conducted using silica sand and natural calcareous soil. Although high fractions of DNAPL PCE source zones in heterogeneous porous media were removed by non-ionic surfactant, Tween 80, enhanced flushing, the heterogeneous system exhibited an extended multi-step concentration behavior. The results emphasized that when Tween 80/MnO₄⁻ were applied with sufficient dosage and provided enough contact time, pool-dominated source zones could be remediated more efficiently compared to surfactant flushing or permanganate oxidation independently. The experiments are also used to numerically model the interaction of the Tween 80-enhanced permanganate oxidation processes for DNAPL PCE in both porous media configurations. UTCHEM, a multiphase model, was successfully adapted to simulate the oxidation process in the presence of a surfactant. The model results demonstrated that the low reaction rate constants of oxidations with Tween 80 indicate that Tween 80 may interfere with the reaction rate. On the other hand the increase in the solubility of PCE in the presence of Tween 80 more than compensates for the decrease in reaction rate constant.

ESTIMATING THE CONTRIBUTION OF ROAD SWEEPING IN THE NON-POINT POLLUTANT LOAD REDUCTION IN HIGHWAYS AND EXPRESSWAYS

Nash Jett DG. Reyes¹, Heeman Kang², Minsu Jeon¹, and Leehyung Kim^{1*}

¹ Kongju National University, Department of Civil Engineering, Cheonan-si, South Korea

² Korea Expressway Corporation, Environment Research Division, Gyeonggi-do, South Korea

*Corresponding author (leehyung@kongju.ac.kr)

ABSTRACT

Stormwater runoff from highways and expressways are large contributors of non-point pollutant loads in natural environments. Specifically, road-deposited sediments (RDS) can serve as a primary vessel for the transport of pollutants during the washoff process. It is necessary to investigate the characteristics of RDS collected from road sweeping since it can serve as fundamental data for estimating the non-point pollutant loads on highways. Chemical analyses were performed to determine the pollutant concentrations in the RDS. The amount of RDS collected on highways through road sweeping amounted to 18,381 tons/year. Based on the rate of sediment accumulation on highways, it was estimated that road sweeping can generally reduce the TOC, T-N, and T-P loads by 275,652.5 kg/year, 15,399.1 kg/year, and 11,095.6 kg/year, respectively. RDS collected from the highway also contained considerable heavy metal concentrations. Estimates revealed that the removal of sediments along highways can reduce non-point Cu, Pb, Zn, and Ni loads by 1,902.6 kg/year, 575 kg/year, 6,011.8 kg/year, and 352.9 kg/year, respectively.

Keywords: *Non-point source pollution, road-deposited sediment, road sweeping, stormwater*

1. INTRODUCTION

Significant amounts of road-deposited sediments (RDS) can accumulate on the surface of highways and expressways pollutants due to the high traffic volume. Among the best management practices (BMPs) for highway pollution management, road sweeping is commonly regarded as an effective way to prevent pollutant washoff and deposition in natural environments. It is necessary to investigate the characteristics of RDS since it can provide fundamental data for estimating non-point pollutant loads from highways and expressways. This study was conducted to determine the concentration of various pollutants in RDS. A countrywide evaluation and data collection were also performed to estimate the overall effectiveness of road sweeping in reducing the non-point pollutant loads on major highways in South Korea.

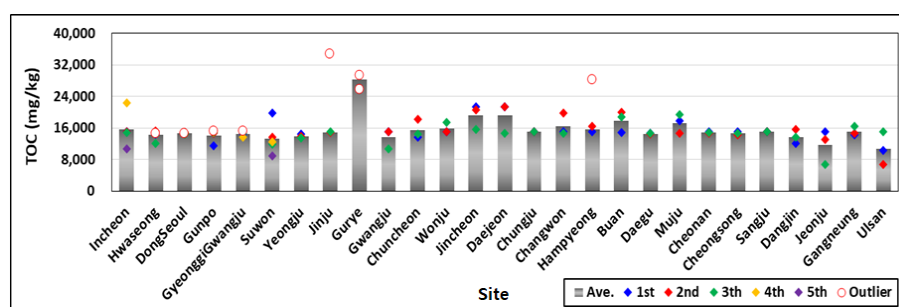
2. MATERIAL AND METHODS

Sampling was conducted three times at the 21 highways managed by the Korea Expressway Corporation (KEC). Additionally, monitoring was conducted five times at six highways located

in a metropolitan area. A total of 93 RDS samples were obtained from the sediment storage yard of KEC. The storage yard serves as a temporary holding facility where street sweepers unload the RDS collected from the 27 highways and expressways managed by the KEC. The sediment samples collected from a particular site were mixed thoroughly to achieve an accurate representation of the sediments deposited along the whole stretch of the highway. The samples, which weighed approximately 3kg each, were stored in the refrigerator (4°C) and transported to a laboratory for analysis. The samples were dried at 105 to 110°C for more than four hours. The remaining concomitants, such as fallen leaves, grasses, branches, cigarette butts, gravel, glass, and plastic pieces, were also removed after drying. The parameters included in the sediment analyses were moisture Content, total nitrogen (T-N), total phosphorus (T-P), total organic carbon (TOC), and heavy metals (i.e. Zn, Cr, Cu, Pb, and Ni). The sediments were analyzed in accordance with the Korean Standards for Water Quality Testing (Korea Ministry of Environment, 2018). Statistical analyses were conducted using the SPSS program. The sets of data that can be considered as outliers were excluded from the analyses.

3. RESULTS AND DISCUSSIONS

The concentration of some typical non-point pollutants in the RDS samples collected from different highways and expressways in Korea were exhibited in Figure 1. The result of the T-test analysis revealed that there were no significant differences in the sediment pollutant concentrations collected from different sites. Moreover, the data collected followed a normal distribution, indicating that the arithmetic mean can be used to represent a reasonable estimate of the pollutant concentrations in the sediments. The heavy metals concentration in the sediments collected from six highways in metropolitan areas were shown in Figure 2. The average moisture content, TOC, TN, and TP in the sediment samples amounted to 11.6±4.4%, 14,996.6±2,749.8 mg/kg, 837.8±46 mg/kg, and 603.6±182.4 mg/kg, respectively. In the case of heavy metals, relatively high concentrations of Cu (103.5±45.6 mg/kg), Pb (31.3±15.4 mg/kg), Zn (327.1±104.5 mg/kg), and Ni (19.2±6.7 mg/kg) were measured in the RDS. The contribution of road sweeping to the non-point source pollutant load reduction in highways was estimated through the annual sediment accumulation rate in highways and expressways. The recorded annual rate of sediment accumulation along the studied highways and expressways amounted to 18,381 tons/year. Based on the amount of sediments recovered through road sweeping, it was estimated that non-point TOC, T-N, and T-P loads can be reduced by 275,652.5 kg/year, 15,399.1 kg/year, and 11,095.6 kg/year, respectively. Moreover, the annual load of heavy metals from RDS can be reduced by approximately 352.9 kg/year to 6,011.8 kg/year through road sweeping.



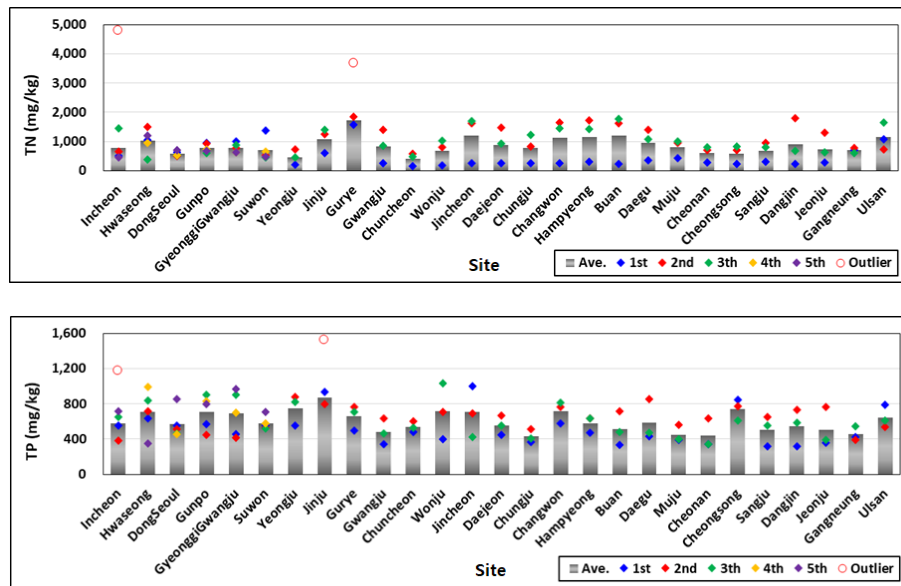


Figure 1. Concentration of typical non-point source pollutants in RDS collected from major highways and expressways

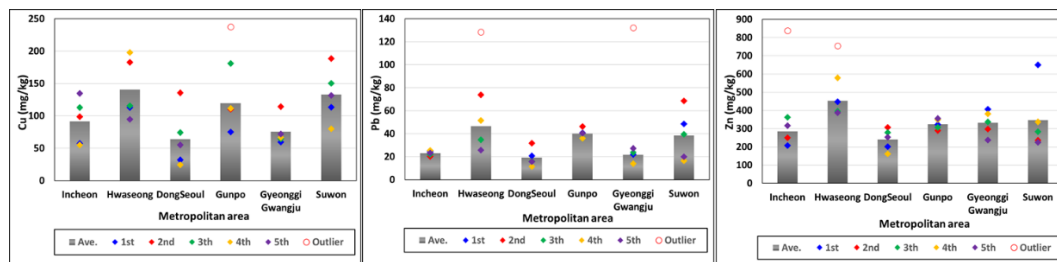


Figure 2. Concentration of heavy metals in RDS in metropolitan highways

4. CONCLUSIONS

This study assessed the effectiveness of road sweeping in reducing the non-point pollutant loads on highways and expressways. High vehicular traffic on major highways and expressways generates significant loads of particulate matter that can accumulate on impermeable surfaces. Specifically, RDS containing considerable amounts of pollutant loads can greatly contribute to environmental degradation. Cleaning operations are necessary to reduce non-point pollutant loads from highways and expressways with heavy vehicular traffic.

Specifically, road sweeping can contribute to the removal of excessive RDS that are heavily contaminated by various NPS pollutants.

Acknowledgements: This work was supported by Korea Environmental Industry&Technology Institute (KEITI) through Wetland Ecosystem Value Evaluation and Carbon Absorption Value Promotion Technology Development Project, Funded by Korea Ministry of Environment (MOE)(2022003630005)

EXTREME HYDROLOGIC EVENTS

REGIONAL FLOOD LOSS MODELLING OF THE TOWN OF BOZKURT IN KASTAMONU, TURKEY

Fidence Cyizere Rukundo, Ms. Candidate¹; Derya Deniz, Ph.D.^{2}; Yiğit Can Altan, Ph.D.³
Civil Engineering Department, Özyeğin University
[*derya.deniz@ozyegin.edu.tr](mailto:derya.deniz@ozyegin.edu.tr)*

ABSTRACT

Flooding is one of the most devastating natural disasters, and its effects are exacerbated by the current unprecedented climate change and population growth. Particularly in Turkey, time and time again, the frequency of floods has resulted in significant economic losses. There have been a few studies to assess and attenuate the loss effects of floods by different researchers in Turkey, but more research is still needed to understand and quantify these effects. This is especially essential for preparing appropriate flood mitigation and emergency plans. This study proposes a regional flood loss framework for the case study of Bozkurt, Kastamonu, located in the Western Black Sea Basin of Turkey. The framework has been tested to estimate regional economic loss estimates of the Bozkurt town for the August 2021 flooding event. The key factors that govern the loss estimates are also identified and integrated into the proposed framework. The framework can be used to assess future potential flood losses for the Bozkurt town.

Keywords: *Bozkurt Town, Flood Hazard, Flood Loss Modelling.*

1. INTRODUCTION

Turkey has suffered a spate of flood events over the last few decades, and their economic losses are enormous, second only to earthquakes (Koç et al., 2020). According to the Turkish Disaster Database, the recent floods have caused more than 700 hundred deaths and US\$800 million of economic losses over the past eight decades (Koç et al., 2020). While there have been many studies about earthquake events, little was done to analyze and mitigate the effects of flood disasters in Turkey. Most attention has been given to hazard modeling for the flood studies conducted for Turkey. It is rare to find comprehensive flood studies for Turkey considering economic flood losses, except a few ones (Beden and Ulke, 2021).

In the wake of the destructive flood event in Bozkurt in August 2021, our study aims to create a regional flood loss approach for the case study of Bozkurt, located along the Ezine river subbasin in the Western Black Sea Basin of Turkey. Some researchers have already started investigating the causes of the 2021 flood (Kelesoglu et al., 2022). Therefore, this paper further extends these studies by estimating the incurred flood losses in the region through the proposed loss framework. The framework can also be used to assess future flood losses that may occur for the town of Bozkurt.

2. THE CASE STUDY

Bozkurt is a town located in the city of Kastamonu, a part of Turkey's Western Black Sea Basin. It covers an area of roughly 280 km². According to the 2010 census, the district's population is 8945, of which 5074 live in downtown Bozkurt. The region is drained mainly by Ezine Stream, whose mouth empties into the Black Sea (see Figure 1).

In August 2021, alongside other parts of the Black Sea region, Bozkurt was ravaged by devastating flooding due to a two-days of torrential rain. According to the Turkish disaster agency AFAD, the death toll was 71 people in the city of Kastamonu alone, and approximately 685 buildings were affected by the flood in Bozkurt town (Kelesoglu et al., 2022).

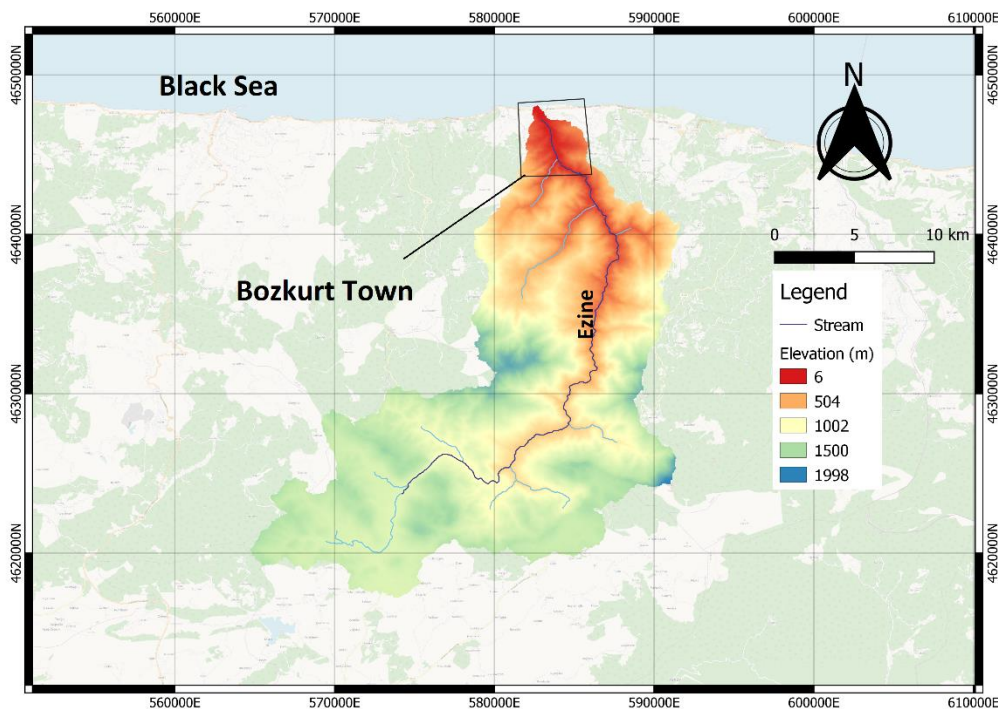


Figure 1: Locations of the case study area (shown in a box) and Ezine stream in Kastamonu, Turkey

3. MATERIAL AND METHODS

As the study's main purpose is to establish a regional flood loss model for the town of Bozkurt, the flood hazard map of the town is first required to be established. Following several studies on flood hazard modeling (Gülbaz et al., 2019; Hoseinil et al., 2017; Yuan et al., 2011), the Watershed Modeling System (WMS, 2018), a software program that combines both hydrologic and hydraulic models, is used to create the flood map. A Digital Elevation Model (DEM) of Ezine Stream Watershed is first prepared using the topographical data inside the program's Geographical Information System (GIS). The hydrological model is then prepared through the Hydrologic Modeling System (HEC-HMS) incorporated in the WMS, using the meteorological information collected from the stations in the Bozkurt district. Next, by taking advantage of the

River Analysis System available in WMS (HEC-RAS), a hydraulic model is established to obtain a flood hazard map for Bozkurt using the flow hydrographs obtained from the hydrologic analyses as boundary conditions.

Using flood hazard maps obtained from the WMS, estimates of flood losses are then calculated using the flood depth-damage functions provided for the European Countries (Huizinga et al., 2017; see Figure 2). Though many factors contribute to building flood damage, water depth is generally agreed to be the main contributing factor (Deniz et al., 2017; Ceyhan et al., 2021). This study thus takes the flood depth and also building use types and building floor areas as the key factors to perform damage and loss analyses through the flood depth-damage functions.

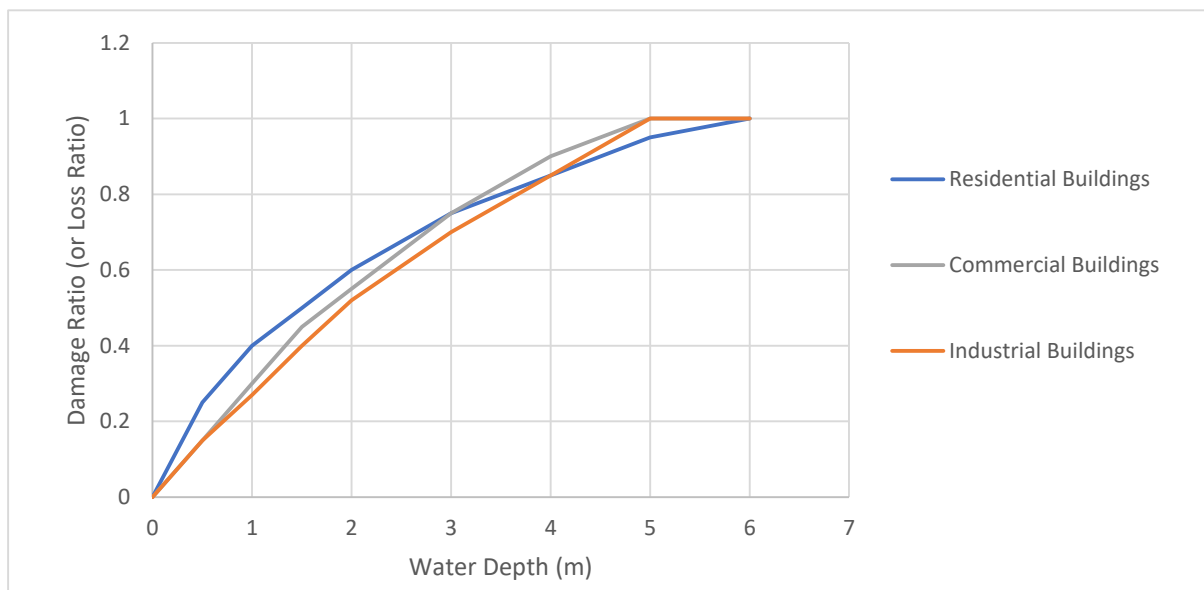


Figure 2: The flood depth-damage curves assumed in the study (Huizinga et al., 2017)

4. RESULTS AND DISCUSSIONS

The results obtained from the hydrological and hydraulic analyses performed in WMS are used to establish a flood hazard map for the town of Bozkurt in Figure 3. Next, the affected buildings are put into their corresponding categories of building use, most of which are either residential buildings or commercial buildings, and their footprint areas are calculated. For residential buildings, the affected area is found to be 37,184 m², and for commercial buildings, a total of 6,494 m² is affected.

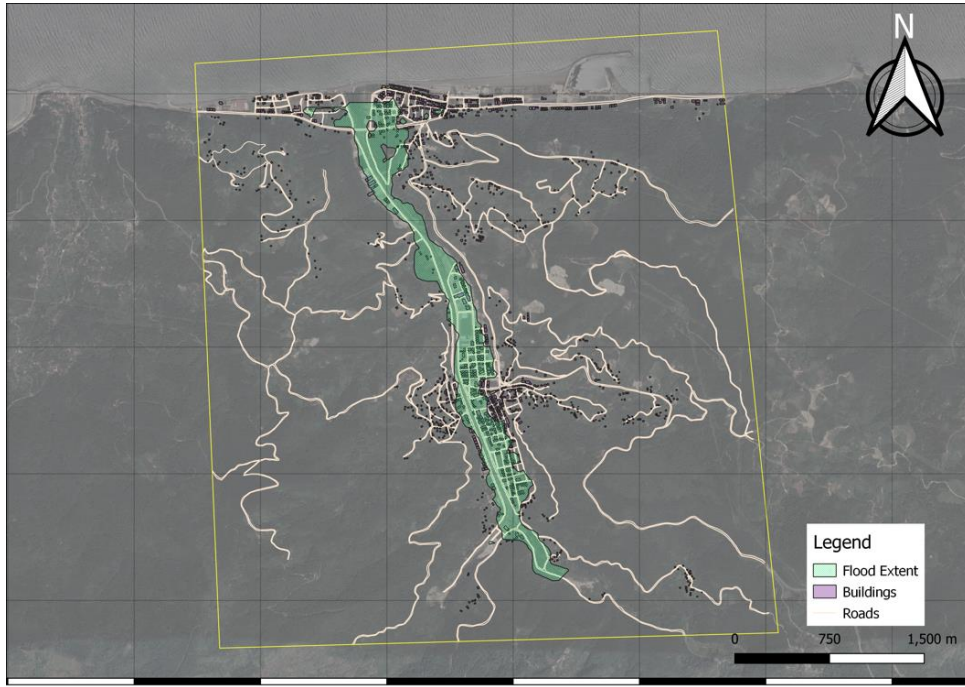


Figure 3: The August 2021 flood hazard model obtained for the town of Bozkurt

Using the depth-damage curves by Huizinga et al., (2017), the damage percentage on each building is calculated. According to Huizinga et al. (2017), Turkey's unit building value is £454/m² for residential buildings and £656/m² for commercial buildings (based on the year 2010). Considering the inflation rate, an estimated total building repair cost of around £15 million is calculated based on the year 2021. Approximately 77% of this total estimate corresponds to repair costs of residential buildings. It is worth mentioning that the calculated cost does not include the financial loss on infrastructures and other economic activities like agriculture. Moreover, it is noticed that calculated cost values give reasonable results compared to the flood damage data reported in the literature (Kelesoglu et al., 2022; Baycan et al., 2022; Ankara, 2021).

The flood analysis results show that Bozkurt is a very vulnerable region exposed to frequent potential flooding. Given the increasing threat of climate change, with a significant number of buildings located in or near flood-prone areas, significant losses can be expected in future flooding events if immediate and appropriate measures are not taken.

5. CONCLUSIONS

This paper establishes a flood loss approach that can estimate flood losses for Bozkurt Town for future flooding events. The approach is tested and validated with the collected data for the catastrophic flood event that took place on 11th August 2021. Flood depth, type of building use, and building area are identified as the key factors in the flood loss estimates. This paper is among the few studies conducted on regional flood loss modeling for Turkey, considering the

case study of Bozkurt. This work will shed light on future research to conduct flood loss studies for other flood-prone areas in Turkey.

6. ACKNOWLEDGMENTS

One of the authors, Dr. Derya Deniz, acknowledges the support provided by the European Union's Horizon 2020 research and innovation program under the Marie Skłodowska-Curie grant agreement No. 893147.

REFERENCES

- Baycan, H., Ciner, M. İ. R. A. Ç., Gök, C., Peker, İ. S. M. A. İ. L., & Gülbaz, S. E. Z. A. R. FLOOD MODELING OF EZINE AND AYANCIK STREAM WATERSHEDS IN WESTERN BLACK SEA BASIN, TURKEY.
- Beden, N., & Ulke Keskin, A. (2021). Estimation of the local financial costs of flood damage with different methodologies in Unye (Ordu), Turkey. *Natural Hazards*, 108(3), 2835-2854.
- Brunner, G. W. (2020). *HEC-RAS river analysis system. Hydraulic reference manual. Version 6.0*. Hydrologic Engineering Center Davis CA.
- Ceyhan, A.B., Deniz, D. (2021). "Flood loss and functionality models for single-family homes", 14th International Congress on Advances in Civil Engineering (ACE), Istanbul, Turkey.
- Deniz, D., Arneson, E. E., Liel, A. B., Dashti, S., & Javernick-Will, A. N. (2017). Flood loss models for residential buildings, based on the 2013 Colorado floods. *Natural Hazards*, 85(2), 977-1003.
- Gülbaz, S., Kazezyılmaz Alhan, C. E. V. Z. A., Bahceci, A., & Boyraz, U. (2019). Flood modeling of Ayamama river watershed in Istanbul, Turkey. *Journal of Hydrologic Engineering*, 24.
- Hoseini, Y., Azari, A., & Pilpayeh, A. (2017). Flood modeling using WMS model for determining peak flood discharge in southwest Iran case study: Simili basin in Khuzestan Province. *Applied Water Science*, 7(6), 3355-3363.
- Huizinga, J., De Moel, H., & Szewczyk, W. (2017). *Global flood depth-damage functions: Methodology and the database with guidelines* (No. JRC105688). Joint Research Centre (Seville site).
- Kelesoglu, M. K., Temur, R., Gülbaz, S., Apaydin, N. M., Kazezyılmaz-Alhan, C. M., & Bozbey, I. (2022). Site Assessment and Evaluation of the Structural Damages After the Flood Disaster in the Western Black Sea Basin on August 11, 2021.
- Ankara, İnşaat Mühendisleri Odası (2021). 11 Ağustos 2021 Bozkurt taşkın felaketi değerlendirme raporu.
- Kelesoglu, M. K., Temur, R., Gülbaz, S., Apaydin, N. M., Kazezyılmaz-Alhan, C. M., & Bozbey, I. (2022). Site Assessment and Evaluation of the Structural Damages After the Flood Disaster in the Western Black Sea Basin on August 11, 2021.
- Koç, G., Petrow, T., & Thieken, A. H. (2020). Analysis of the most severe flood events in Turkey (1960–2014): which triggering mechanisms and aggravating pathways can be identified? *Water*, 12(6), 1562.
- Watershed Modelling System (WMS) 2018. Reference manual, user manual (v10.1). Provo, UT: Environmental Modeling Research Laboratory of Brigham Young Univ.
- Yuan, Yongping, and Kamal Qaiser. Floodplain modeling in the Kansas river basin using hydrologic engineering center (HEC) models: impacts of urbanization and wetlands for mitigation. US Environmental Protection Agency, Office of Research and Development, 2011.

INVESTIGATION OF FLOOD MITIGATION IN BOZKURT DISTRICT

Hayri BAYCAN¹, Uğur BOYRAZ^{2*},

¹ Author_1's Istanbul University-Cerrahpasa, Civil Engineering, Istanbul, Türkiye

² Author_2's Istanbul University-Cerrahpasa, Civil Engineering, Istanbul, Türkiye

*Corresponding author (uboyraz@iuc.edu.tr)

ABSTRACT

Flood control structures and improvements of the natural open channels play an important role in flood management. A flood may be a fatal event without a control strategy. One of the latest events in the Western Black Sea region occurred in Bozkurt, Kastamonu, which is located in the Ezine stream watershed, on August 11, 2021. As a result of this flood, 72 people died and dozens were injured. In addition, many buildings were damaged, and the Bozkurt district was declared a “disaster area” by the state because of the substantial damages. This study aims to evaluate how to minimize the current flood risk in the Bozkurt district. For this purpose, a hydrological model was built by using US Environmental Protection Agency’s Storm Water Management Model (EPA SWMM) to determine the effects of the flood event and evaluate the flood control scenarios. Two different flood control options were considered. First, a new channel that is designed by the state was integrated into the model and the capacity of the channel during the same flood event was determined. The model results showed that the new channel was still insufficient to carry the massive amount of water routed along the catchment. Therefore, a dam was proposed to be built in the catchment. The location, water volume, and height of the dam structure were determined and defined in the EPA SWMM model. The hydrographs and the water depths were obtained before and after the dam and the results were compared. It was observed that the dam decreased the peak flow rate by 55% and the water depth in the channel by 34.2%.

Keywords: *Ezine stream watershed, flood control dams, flood mitigation, US Environmental Protection Agency’s Storm Water Management Model (EPA SWMM), Hydrodynamic model.*

1. INTRODUCTION

Floods may cause serious damage to urbanized and agricultural areas such as the destruction of buildings, roads, bridges, contamination of groundwater, environmental harm, etc. To prevent these damages, flood control structures should be constructed by considering the local requirements and applicability. Structural flood control systems include dams, channels, levees, and flow-diversion regulations (Abdella and Mekuanent, 2021; Heidari, 2009). The basic strategy in these systems is to keep water away from the areas with high flood risk by controlling the hydrograph, i.e. collecting the water in reservoirs, and delaying/reducing the peak (Ghosh, 2017). Dams are one of the most common structures not for just reducing the flood risk but also for collecting water for domestic and agricultural demands. They also have a range of economic, environmental, and social benefits (Takezawa, et al., 2007).

Determining the properties of a dam is crucial for preventing floods effectively. The reservoir capacity, location, dam height, weir capacity, and operational procedures should be determined

optimally for the best performance. Schumann and Sieber (2006) examined the role of the dams on preventing floods and showed the importance of the dam operational process on performance, by demonstrating a specific flood event. Karakuş and Yıldız (2022) showed how to select the most optimum dam location by using 9 parameters (elevation, slope, distance to roads, rainfall, lineament density, distance to residential areas, land use/land cover, soil types, and stream density) via Geographical Information Systems (GIS). They also obtained the dam site selection suitability map as a result of the study. Han et al. (2022) investigated the flood control capacities of several dams using the inlet and outlet flow rates based on weather forecasts. They determined the flood control capacity of 12 dams in South Korea and proposed a method to estimate the water level.

In this study, the flood-preventing solutions were studied in Bozkurt district, Kastamonu, Türkiye. The great amount of rainfall caused a flood greater than 500 years period in this region on August 11, 2021. The Bozkurt district had serious damages and 72 people lost their lives. The stream channel was broken after the flood. A new channel, which is under construction, was modeled to determine the flood prevention capacity. Moreover, a dam was defined in the model and its effect on flood mitigation was investigated. The hydrographs and the flow depths were obtained for different scenarios created by combining the effects of the dam and the new channel. The performance of the flood prevention solutions was discussed.

2. MATERIAL AND METHODS

Study Area

The Ezine Stream Watershed is located in Kastamonu, Türkiye. The drainage area of the watershed is 375 km² approximately. The watershed is located between 33°–34° east longitudes and 41°–42° north latitudes (Figure 1). The basin is mountainous. Forests and agricultural areas cover the drainage area.

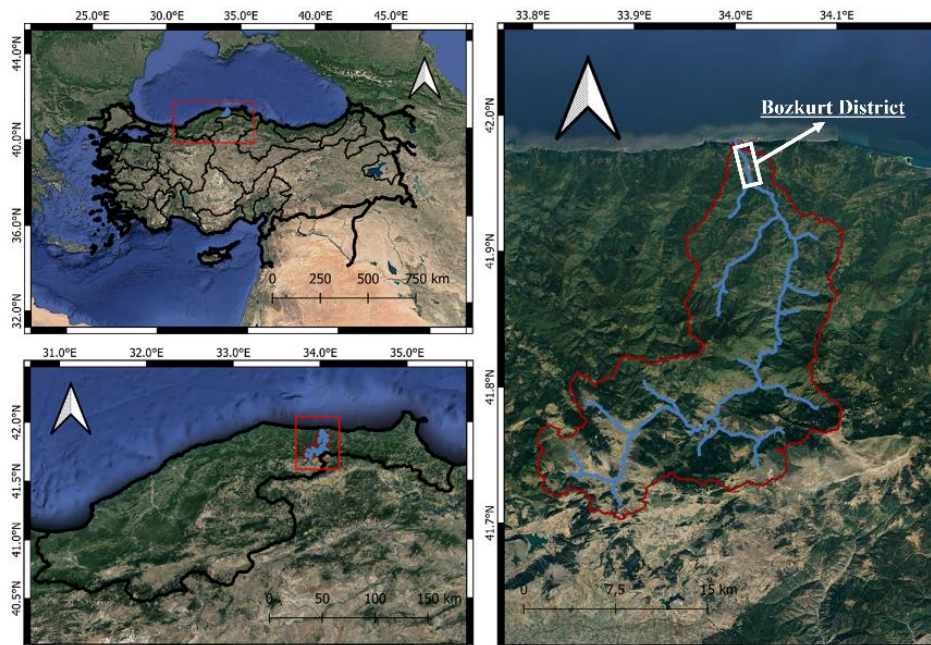


Figure 1 Location of the Ezine Stream Watershed

The Ezine Stream begins from the Devrekani district, then passes through the Küre mountains and Bozkurt district respectively. Finally, the stream reaches the Black Sea from Abana district. The total length of the stream is 60 km. Bozkurt district is 2 km south of the Black Sea coast and 95 km north of the Kastamonu city center. The population of the district is 9170 (Turkish

Statistical Institute, 2021). Since the Bozkurt district is located downstream of the watershed and is urbanized in the embankments, the flood risk of the region is high.

Flood event in Bozkurt district on August 11, 2021

As a result of the massive amount of precipitation volume that dropped on August 10-11, 2021, the Ezine Stream flooded. The Bozkurt district was highly damaged. 72 people died and hundreds of people were affected physically, psychologically, and also economically owing to this catastrophic event. Many buildings and bridges were damaged or collapsed. The infrastructure and electricity networks had become inoperable in the city. After the flood, a big amount of debris littered the streets, especially in the coastal area.

Storm Water Management Model (SWMM)

SWMM is a dynamic rainfall-runoff-subsurface runoff simulation program that consists of hydraulics, hydrology, and water quality modules. The program was developed by Environmental Protection Agency in 1971. SWMM is often used for urban areas, sewer systems, and drainage systems. It is also capable of simulating flood, groundwater flow, and LID controls (Rossman, 2010).

SWMM calculates the surface runoff that occurred after a rainfall event on a subcatchment. The program is capable to route the flow using steady flow conditions, kinematic wave equation, and dynamic wave equation. The flow is routed through the elements such as closed pipes, open channels, reservoirs, water tanks, pumps, etc. The program calculates the depth, velocity, and hydrograph as outputs. The flow calculations are done using the Manning equation. Moreover, infiltration can be determined using 4 different models such as Horton, Modified Horton, Green Ampt, and Curve Number methods.

Model Inputs and Data Collection

To model the Ezine Stream basin, parameters such as topographic maps, river cross sections, slope and width values of subcatchments, and the soil properties of the study area are required. Most of the data and the information about the study area were obtained by using the Quantum Geographical Systems (QGIS). The soil maps and information were obtained by using Harmonized World Soil Web Database (HWSD) viewer application, which is improved by the Food and Agriculture Organization of the United Nations (FAO). The soil type of the Ezine Stream Basin was determined as sandy clay. The Green-Ampt method was chosen as the infiltration method, and it requires the following parameters: hydraulic conductivity, suction head, and initial deficit. The suction head and the hydraulic conductivity were determined considering the typical values of sandy clay loam (Rawls et al. 1983). In addition, the initial deficit was provided from the reports of the European Environment Agency (EEA, 2021). There are 4 rain-gauge stations in the study area. These stations are the Abana station, the Mamatlar Village station, the Kuz Village station, and the Devrekani station. The precipitation data measured at these stations were obtained from the Turkish State Meteorological Service (MGM) and the hyetograph was calculated. Figure 2 shows the hyetograph of the 10-11 August rainfall event. The rest of the model parameters are selected by matching the study site properties with the typical values reported in the literature (McCuen et al. 1996; ASCE, 1982; Rawls et al. 1983; EEA, 2021). All model parameters were summarized in Table 1.

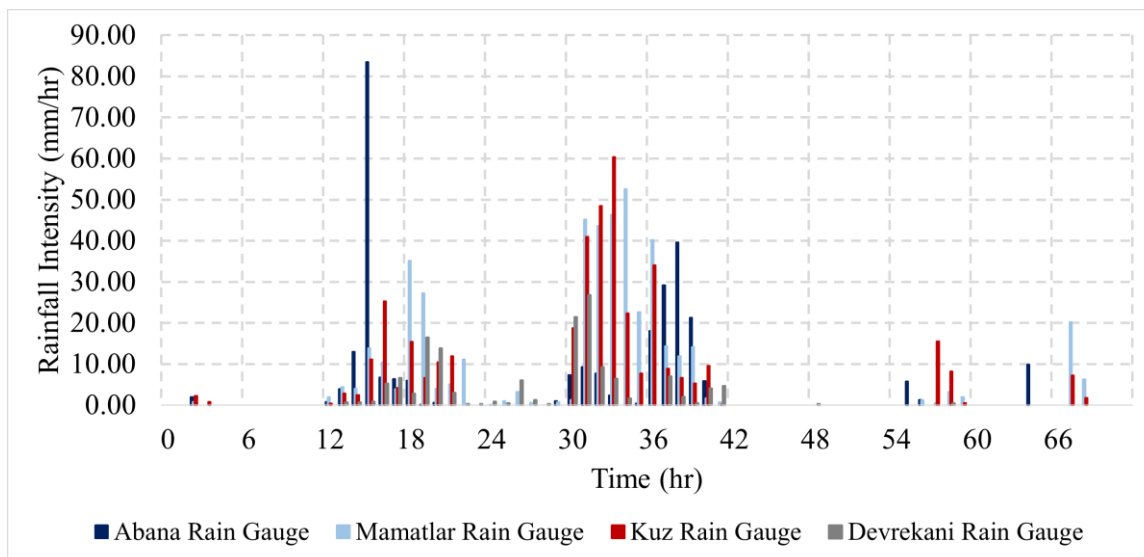


Figure2. Precipitation data of the August 10-11, 2021.

Table 1. Parameters for subcatchments, conduit and soil used in EPA SWMM

<i>EPA SWMM elements</i>	<i>Parameters</i>	<i>Value</i>
<i>Subcatchment</i>	Manning's roughness coefficient	0.5
	Manning's roughness coefficient for the naturel stream	0.1
<i>Conduit</i>	Manning's roughness coefficient for the improvement channel	0.041
	Suction Head	219.964
<i>Soil</i>	Hydraulic Conductivity	1.584
	Initial Deficit	0.02

Model Setup

The Ezine Stream Basin was delineated using the DEM data in QGIS. The delineated watershed boundaries were imported into the EPA SWMM. The watershed was divided into 29 subcatchments. Then, the stream was defined by using 34 conduits, and the cross-sections of each conduit were assigned to the model through the data obtained from the QGIS program.

A new channel project was developed and the construction of the new channel began in the Bozkurt district. The cross-section of the new channel is rectangular in the stream sections nearby the city center and trapezoidal in the upstream and downstream parts of the stream. The width of the rectangular channel is 71 m and the depth is 3.5 m. The bottom width of both trapezoidal channels is 75 m. The upper width of the upstream channel is 85.5 m and the depth is 3.5 m. The upper width and the depth of the downstream channel are 88.5 m and 4.5 m, respectively. The total length of the channel is 4.7 km. These data were defined to the SWMM model. Moreover, Manning's roughness coefficient of the channel was defined as 0.41 according to the project design.

In addition, a dam was defined in the SWMM model for flood control purposes. In the SWMM model, a storage unit was used to define the dam. The height-area curve was calculated using the topographical map obtained from QGIS. The total height of the dam was chosen as 50 meters, and the maximum storage volume was calculated as 35810000 m³. Finally, the kinematic wave method was chosen as the routing method, and the flood event of the 10-11 August storm was simulated.

3. RESULTS AND DISCUSSIONS

Since the Bozkurt district is placed downstream of the watershed, the surface runoff gathered from the whole watershed passes throughout the district and the flood risk is quite high for the region. The urbanization on the banks of the Ezine stream also increases the risk. Unfortunately, there were serious damages in the mentioned flood disaster due to the urbanization in the floodplain. Therefore flood prevention precautions should be taken to prevent or minimize the damages in the future in the Bozkurt district. Here, two different structural precaution performances were presented. First, the performance of the new channel was discussed. Then, a dam was proposed for flood control, and its performance in flood mitigation was evaluated.

In Figure 3, the flood hydrographs were presented for two cases. In the first case, there is no flood control dam in the catchment. In the second one, there is a 50 m dam to prevent flooding. Moreover, the new channel's cross-section is considered for both cases. The hydrographs were obtained at the entrance point of Bozkurt. In the first case, the maximum flow rate was calculated as 320 m³/s on August 10, and 1670 m³/s on August 11. After the dam was defined, the maximum flow rate was calculated as 270 m³/s on August 10 and 750 m³/s on August 11. Results show that the dam decreased the maximum flow rate by 15.6 % on August 10 and 55 % on August 11. The dam did not affect the peak flow rate between the 18th and 22nd hours of the analysis (day 1), since the precipitation was heavier in the downstream part of the dam and the runoff that occurred on the upstream watershed did not reach the Bozkurt, yet. After the 22nd hour, the effect of the dam is seen. The dam completely stored the runoff that came from the upstream part of the dam and the flow rate started to decrease earlier. On the second day of the analysis, the precipitation was heavy in the whole watershed. The total rainfall duration was 12 hours and the rainfall intensity exceeded 40 mm/hr for the 3-5 hours at the upstream stations (Mamatlar and Kuz stations). The peak runoff reached Bozkurt at the 39th hour without the dam. After the dam application, the peak flow was controlled between the 36th and 46th hours. During this time, the dam stored the incoming flow from upstream. The fluctuations occurred due to the weir activity.

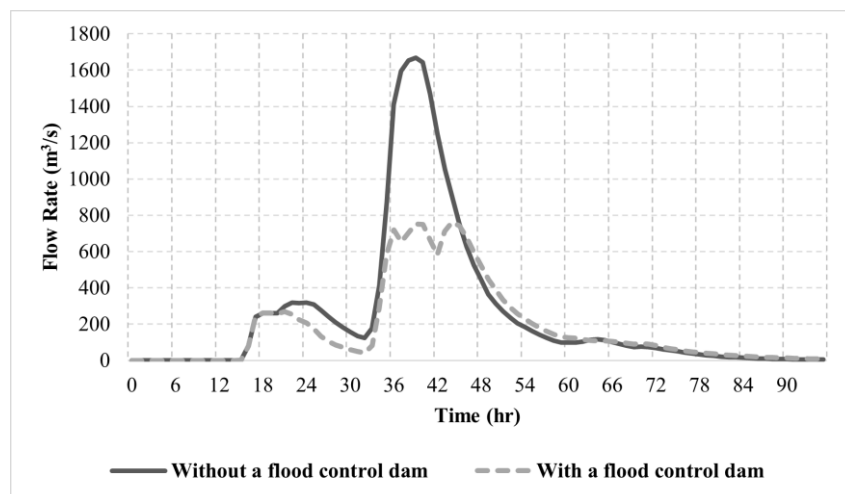


Figure 3 The hydrographs of the city center before and after the flood control dam application.

In Figure 4, the water depth-time graph was presented for both cases. The water depth was calculated as 1.4 m on August 10, and 3.8 m on August 11. Since the capacity of the new channel is 3.5 m, the stream is still flooding in case 1. When the dam was defined in the model, the water depth in the channel dropped to 1.3 meters on the first day. Moreover, the water depth dropped to 2-2.5 meters on August 11.

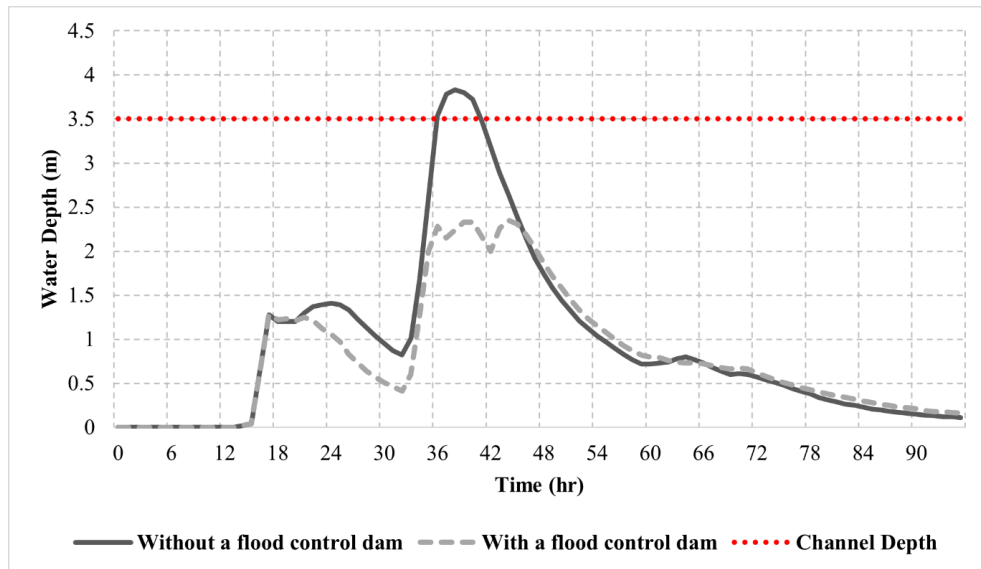


Figure4. The water depth obtained in the stream sections nearby the Bozkurt district.

4. CONCLUSIONS

In this study, the hydrodynamic model of the Ezine Stream Watershed, located in Kastamonu, Türkiye, is established by using EPA SWMM. Two scenarios for flood control measures were integrated into the hydrodynamic model. In the first scenario, the new channel, which is under construction at the stream sections nearby the Bozkurt district, was defined in the hydrodynamic model and the flood control capacity was evaluated. In the second scenario, a dam for flood control purposes was defined in the model. The water depth and the peak flow rate were obtained for both cases i.e. before and after the dam application. According to the results, the following conclusions are obtained:

- The capacity of the new channel is investigated. It is observed that it may be insufficient to carry the peak flow. There may be several circumstances during a flood event that decrease the channel capacity. Therefore, an improvement on the channel design should be made to stay on the safe side. Alternative measures such as increasing the channel depth, flood walls, or flood control dams should be taken in the region.
- A 50 meters high dam is integrated into the hydrodynamic model and a significant reduction in the maximum flow rate is obtained. A flood control dam is a preferable choice considering the other benefits such as domestic/agricultural water supply, electricity generation, etc.

- The height of the dam may be optimized by taking into account various operating conditions such as weir type, capacity, storage, and discharge rate of the dam. Therefore, the dam design can be improved as a future study.

REFERENCES

- Abdella, & Mekuanent, F. (2021). Application of hydrodynamic models for designing structural measures for river flood mitigation: the case of Kulfo River in southern Ethiopia. *Modeling Earth Systems and Environment*, 7(4), 2779–2791.
- ASCE (1982) “Gravity Sanitary Sewer Design and Construction,” ASCE Manual of Practice No. 60, New York, NY. [Preprint].
- Environmental European Agency (EEA) (2021) Soil moisture deficit, <https://www.eea.europa.eu/ims/soil-moisture-deficit>.
- Han, H.; Kwak, J.; Kim, D.; Jung, J.; Joo, H.; Kim, H.S. Development of Simple Method for Flood Control Capacity Estimation of Dam in South Korea. *Water* 2022, 14, 1366.
- Heidari, A. (2009). Structural master plan of flood mitigation measures. *Natural Hazards and Earth System Sciences*, 9(1), 61–75. doi:10.5194/nhess-9-61-2009
- Karakuş, C.B., Yıldız, S. 2022 Gis-multi criteria decision analysis-based land suitability assessment for dam site selection. *Int. J. Environ. Sci. Technol.*
- McCuen, R. et al. (1996) “Hydrology,” FHWA-SA-96-067, *Federal Highway Administration*, Washington, DC.
- Rawls, W.J., Brakensiek, D.L. and Miller, N. (1983) “Green-ampt Infiltration Parameters from Soils Data,” *Journal of Hydraulic Engineering*, 109(1), pp. 62–70. doi:10.1061/(ASCE)0733-9429(1983)109:1(62).
- Rossman, L. A. (2010). Storm water management model, user’s manual, version 5. EPA/600/R-05/040. Cincinnati: Water Supply and Water Resources Division, National Risk Management Research Laboratory, USEPA.
- S.N. Ghosh (2017) *Flood Control and Drainage Engineering*. 4th edn. CRC Press.
- Schumann, A. & Sieber, H. -U (2006, June) Expectations and reality about the role of dams for flood control - experience of the extreme flood in August 2002 in Saxony. In *Proceedings of the June 18, 2006, Dams and Reservoirs, Societies and Environment in the 21st Century, Vols 1 and 2*
- Takezawa, M, Gotoh, H. & Takeuchi, Y (2007). Mitigation of flood hazards in Japan *Proceeding of the May, 2007, 4th International Conference on River Basin Management Vols 104* (pp. 271-282)
- Turkish Statistical Institute (TURKSTAT), 2021, <https://www.tuik.gov.tr/>
- Uşkay, S., Aksu, S., (2002). “Floods in Our Country, Causes, Damages and Measures to be Taken ”, *Proceedings of the 2002 Turkey Engineering News* 420-421-422 (pp. 133-136)
- Wisner, P. E. (1976). ENGINEERING IN FLOOD CONTROL. *Canadian Water Resources Journal*, 1(1), 75–89. doi:10.4296/cwrj0101075

ELMALI DAM FAILURE ANALYSIS AND FLOOD DISASTER SIMULATION WITH DIFFERENT SCENARIOS USING HEC-RAS 2D

İsmail Bilal Peker⁽¹⁾, Abdülbaki Hacı⁽²⁾, Yasin Paşa⁽³⁾, Sezar Gülbaz⁽⁴⁾

⁽¹⁾ Faculty of Engineering, Civil Engineering Department, Istanbul University - Cerrahpaşa, Avcılar, Istanbul, Turkey

E-mail: pekerbilal@iuc.edu.tr

⁽²⁾ Faculty of Engineering, Civil Engineering Department, Istanbul University – Cerrahpaşa, Avcılar, Istanbul, Turkey

E-mail: abdulbakhaci0@gmail.com

⁽³⁾ Faculty of Engineering and Architecture, Civil Engineering Department, Istanbul Gelişim University, Avcılar, Istanbul, Turkey

E-mail: yabdullahzade@gelisim.edu.tr

⁽⁴⁾ Faculty of Engineering, Civil Engineering Department, Istanbul University - Cerrahpaşa, Avcılar, Istanbul, Turkey

E-mail: sezarg@iuc.edu.tr

ABSTRACT

Dams, essential hydraulic structures in water planning and management, have several benefits for a society like providing irrigation, electricity generation, flood control, water supply and recreation. However, many dams have almost reached or exceeded the estimated construction life; thus they risk structure stability. Even though it is comparatively rare, dam failures resulting from flood wave propagation can cause immense damages. Although dams are trustworthy, many disasters that occurred in the past show that a dam can fail in different ways, such as piping or overtopping. Since the collapse of a dam will directly affect most people's lives, analyzing the dam failure and determining the flood area caused by the failure becomes significant. Two-dimensional (2D) numerical simulation proved to be an effective tool for understanding flood events caused by dam failure. HEC-RAS 2D, one of the most popular hydraulic models, is implemented to estimate the breaching parameters and flow conditions. In this study, the downstream of a consecutive dam system, consisting of Elmalı 2 concrete-buttruss dam, which is unique among dam failure studies located upstream and Elmalı 1 earth-fill gravity dam located downstream of the watershed is selected as the study area. Since heavy traffic highway and densely residential regions are located just around the downstream of the consecutive dam system, this vulnerable study area is preferred. The study aims to evaluate the dam failure analysis of Elmalı 2 dam with more water holding capacity under different scenarios. Moreover, the inundation regions are also evaluated visually, and areal differences are analyzed comparatively. The dam failure simulation scenarios are examined for three significant criteria: breach formation time (BFT), the number of failed buttresses for Elmalı 2 and reservoir volume rate of Elmalı 1 (RVR). Therefore, peak water depth (H_p), peak flow rate (Q_p), peak velocity (V_p) and time to reach the peak (t_p) are discussed for the study area by comparing the scenarios. The results show that breach formation time and the number of failed

buttresses effectively affect the peak flow rate, peak velocity, peak depth and time to reach the peak. On the other hand, it has been observed that there is no severe effect of the reservoir volume rate of Elmalı 1 in the consecutive dam system. Hence, the effects of these criteria on the susceptible city area located downstream of the possible failure of Elmalı 2 is presented.

Keywords: *Dam Failure Analysis, Consecutive Dam, Buttress Dam, HEC-RAS 2D, Flood Risk*

1. INTRODUCTION

Dams benefit societies in many different ways (e.g., water to drink, water supply, irrigation, hydroelectric power production and so forth); on the other hand, complete or partial failure of dams for different reasons can cause critical problems for the same societies (Singh and Scarlatos, 1998; Altinbilek, 2002). As a result of any dam failure, it is vital to determine the flood in case any possible collapsing of structures especially in areas close to the settlements. More than one hundred dam failures have occurred since the 1700s, and thousands of people have died including environmental damages worldwide (URL-1, 2021). For this reason, studies on dam-break modellings are of great importance as they directly affect human life and property (Fread, 1996).

The main causes of dam failure are overtopping and piping (Costa, 1985; Foster et al., 2000). Even if the reason is different, almost all failures begin with a breach formation. The breach is defined as an opening formed in the dam body, and gradual expansion results in a large volume of water in the reservoir propagating to the downstream parts destructively (Wahl, 1998). Breach geometry (breach depth and width, breach side slope factor), timing (initial breach time, breach formation time, etc.), failure mode, and breach progression need to be estimated well in dam-break modelling. Also, flow conditions and dam body type can affect estimation peak hydrograph, which occurs after the breach progress (Brunner, 2014). All in all, there are two fundamental tasks in dam break analysis: the prediction of the reservoir outflow hydrograph and the routing of that hydrograph through the downstream (Wahl, 1998).

The primary purpose of the present study is to reveal and evaluate the flood mitigation that will occur due to the possible dam failure in Istanbul, Turkey. Analyzes are evaluated for the study area includes the downstream regions consisting of high-populated residential areas and dense traffic highway of two consecutive dams named as Elmalı 2 (a concrete-buttress dam) and Elmalı 1 (an earth-fill gravity dam in the upstream part of Elmalı 2). It is a critical situation that the dams are consecutive, and these dams cause risks by being located in the upstream part of the residential area. In this study, Dam break simulations are performed with three criteria: Breach formation time and the number of failed buttresses of Elmalı 2 and the reservoir volume rate of Elmalı 1. The simulations are realized as 88 runs under three different simulation sets based on these criteria. The results provide information like the peak values of the water depth, the flow rate and the velocity, the time to reach the peak, and flood maps for the scenarios. Flood maps in the simulation results are compared spatially and the effect of the three criteria on the flood is analyzed. It is aimed to compare the results of the possible dam failure disaster that may occur in the study area under different criteria by examining the simulation results. Within this scope, evaluating the effects of different criteria on the results is essential in the

operation methods of dams and taking measures to reduce the harmful effects of dam failure. In addition, determining the areas affected by dam failure is of great importance in taking precautions to mitigate flood hazards.

2. MATERIAL AND METHODS

2.1. Study Area

The study area is located in Istanbul, Turkey as shown in Figure 1. The residential areas likely to be affected by the flood are located around the Göksu River flowing into the Bosphorus located downstream of the dam (Figure 1). There are two dam bodies: The first one, named Elmalı 1, was operationalized in 1907, and the second one, named Elmalı 2, was constructed in 1955. Elmalı 2 is located 1.2 km ahead towards the upstream of the first one. Elmalı 1 is a type of earth-fill gravity dam, and the height of the dam body from the foundation is 22 m. Elmalı 2 is a buttress dam, and the height from the foundation is 49 m. The total drainage area of the two dams is 81.5 km². Also, maximum water surface elevations of the dams are 32.4 and 67.5 m for Elmalı 1 and Elmalı 2, respectively. At these water surface elevations, the reservoir storage capacities are 1.7 x 10⁶ m³ for Elmalı 1 and 17.0 x 10⁶ m³ for Elmalı 2 (Ağralıoğlu et al., 2015).

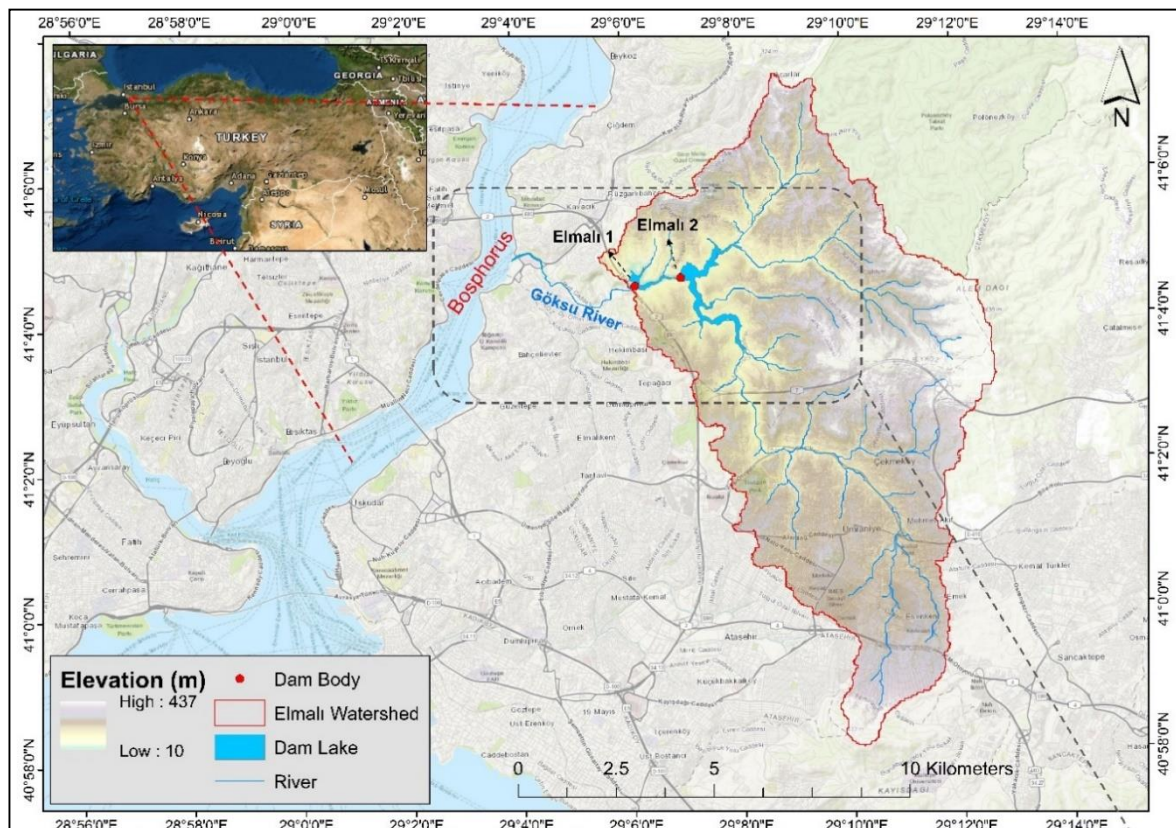


Figure 1. Location of the Elmalı 1 and Elmalı 2 Dams with the drainage area and stream network

3. RESULTS AND DISCUSSIONS

The model results are presented under three criteria as 1) the effects of the breach formation time, 2) the number of failed buttresses and 3) the reservoir volume rate of Elmalı 1. The effects of three different criteria, which are thought to be effective in dam failure, are presented as four different model outputs: the peak values of the water depth (h_p), the flow rate (Q_p) and the velocity (v_p), and the time to reach the peak (t_p). The model outputs obtained are taken from the cross-section downstream of the Elmalı 1 dam body. Hence, the effects of three different criteria are investigated on the graphs comparatively. Also, as a spatial output of the flood that will occur due to possible failure, flood maps are given for visual inspection in the study area (Figure 2).

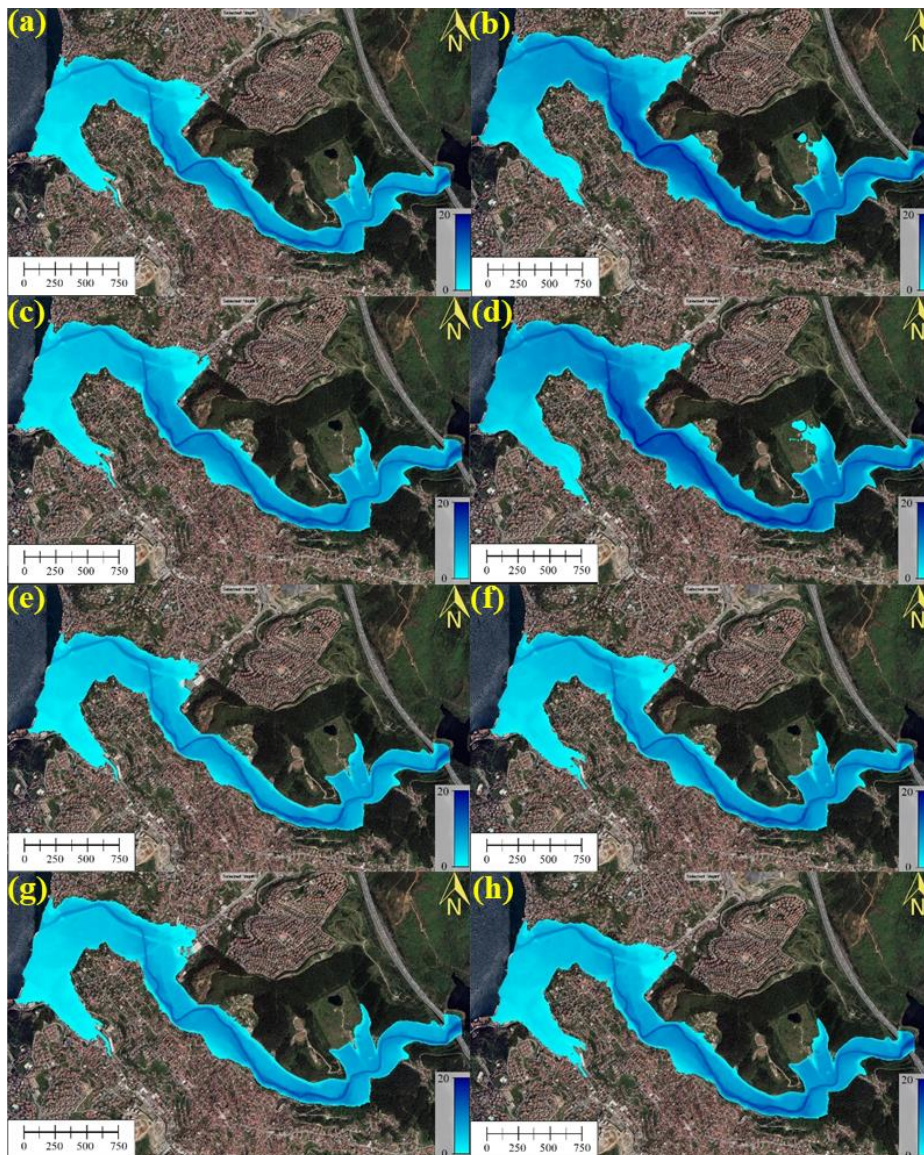


Figure 2. Flood inundation maps with water depths under Scenarios (a) BFT: 0.1- RVR: 0% - Failed Buttresses: 6, (b) BFT: 0.1 - RVR: 0% - Failed Buttresses: 11, (c) BFT: 0.1 - RVR: 100% - Failed Buttresses: 6, (d) BFT: 0.1 - RVR: 100% - Failed Buttresses: 11, (e) BFT: 0.5 - RVR: 0% - Failed Buttresses: 6, (f) BFT: 0.5 - RVR: 0% - Failed Buttresses: 11, (g) BFT: 0.5 - RVR: 100% - Failed Buttresses: 6, (h) BFT: 0.5 - RVR: 100% - Failed Buttresses: 11.

4. CONCLUSIONS

In this study, dam failure analysis is developed and possible scenarios are presented. For this purpose, consecutive dams named Elmalı 1 and Elmalı 2 located in residential areas and close to a heavy-traffic highway are selected. Elmalı 2, a concrete buttress dam located upstream of a consecutive dam system, has a possible flood risk for the residential area and highway in Istanbul, Turkey. When the simulations of failure of the buttresses under different criteria such as breach formation time, number of failed buttresses for Elmalı 2 and reservoir volume rate of Elmalı 1 are examined, it is observed that the study area where has high density residential area will be seriously affected by the possible dam failure. This conclusion is reached by peak values of hydraulically important parameters and visual inspection of inundation areas.

The most effective criterion is the breach formation time between 0.1 hr and 0.5 hr. Furthermore, the second effective criterion is the number of failed buttresses for Elmalı 2 which are between 6 and 11. The reservoir volume rate of Elmalı 1 is the most ineffective criterion. Empty or full of Elmalı 1, which is located upstream of the consecutive dams, almost does not affect the flood wave due to the possible failure of Elmalı 2. Therefore, it is deduced that the operating volume of Elmalı 1 has no effect in order to prevent the adverse effects of a possible dam failure. The dam break model developed can provide a pretty good idea of what areas would flood in the event of a dam failure. Hence, in the operation of these consecutive dams, it can be concluded that keeping Elmalı 1 Dam in the upstream section empty may not prevent the negative consequences of the possible failure of the Elmalı 2.

Moreover, the time to peak value is a crucial parameter to take precautions such as early warning systems to diminish flood effects on residential areas. The flood on the highway, which will be the first affected area, will reach its maximum level in 13-34 minutes at the earliest. Therefore, the systems to be taken to reduce the effect of flood should be taken by considering this period to prevent life and property loss. Moreover, the flood map determined in this study can be used to plan new residential areas and identify buildings that need to be moved to safer areas.

Acknowledgements: The authors would like to thank Republic of Turkey Ministry of National Defence General Directorate of Mapping (HGM), General Directorate of State Hydraulic Works (DSI), and Istanbul Water and Sewerage Administration (ISKI) for their data support and valuable discussions in undertaking this work.

REFERENCES

- Ağralıoğlu, N., Altunkaynak, A., & Özger, M., (2015)., “Elmalı - I and II dams engineering studies technical report.” Istanbul Water and Sewerage Administration (ISKI) (In Turkish).
- Altınbilek, D. (2002). The role of Dams in Development. *Water Resources Development*, 18(1), 9-24. <https://doi.org/10.1080/07900620220121620>
- Brunner, G. (2014). Using HEC-RAS for Dam Break Studies. U.S. Army Corps of Engineers, Hydrologic Engineering Center, TD-39, 609 Second Street, Davis, CA.
- Costa, J. E. (1985). Floods from dam failures. *U.S. Geological Survey Open-File Rep. No. 85-560*, U.S. Geological Survey, Denver
- Foster, M., Fell, R., & Spannagle, M. (2000). The statistics of embankment dam failures and accidents. *Canadian Geotechnical Journal*, 37(5), 1000-1024. <https://doi.org/10.1139/t00-030>

- Fread, D.L. (1996). Dam-Breach Floods. In: Singh V.P. (eds) Hydrology of Disasters. *Water Science and Technology Library*, vol 24. Springer, Dordrecht. https://doi.org/10.1007/978-94-015-8680-1_5
- Singh, V.P., & Scarlatos, P.D. (1988). Analysis of Gradual Earth-Dam Failure. *Journal of Hydraulic Engineering*, 114(1), 21-42. [https://doi.org/10.1061/\(ASCE\)0733-9429\(1988\)114:1\(21\)](https://doi.org/10.1061/(ASCE)0733-9429(1988)114:1(21))
- URL -1: https://en.wikipedia.org/wiki/Dam_failure, Wikipedia, Dam Failure, 09.11.2021.
- Wahl, T.L. (1998). Prediction of Embankment Dam Breach Parameters–A Literature Review and Needs Assessment, DSO-98-004, *Dam Safety Research Report*, U.S. Department of the Interior Bureau of Reclamation, Dam Safety Office (DSO), Water Resources Research Laboratory.

FLOOD MANAGEMENT FOR İSTANBUL MEGA-CITY

Tunay ÇARPAR¹, Mohsen Mahmoody VANOLYA^{2*}, Bulent KOCAMAN², Ali Osman ILGAZ², H. Kürşat TÜRKMEN², Tuğba ÖLMEZ HANCI¹, Şafak BAŞA¹

¹ İSKİ, İstanbul, Türkiye

² Yüksel Proje, Ankara, Türkiye

*Corresponding author (mmahmoody@yukselproje.com.tr)

ABSTRACT

İstanbul Mega-city is located between Marmara and Karadeniz seas with numerous short streams and rivers in North-South or South-North directions. These streams' flash floods recently hit urban areas by extreme increasing storms which increase the risk of loss of life and property in this metropole. This study proposes a methodology for flood management based on the type of storms, land use, floods, and urban problem to reduce economic damage and risk to urban areas. A strategy is developed for long-term flood management based on the vision and mission of sustainability and water-sensitive cities. Based on the scope of the current situation, the risk to inhabitants and economic damage are extracted for the urban and rural streams. Various structural and non-structural measures were considered for solving the flood problems. The measures were prioritized by a multi-criteria analysis including sustainability pillars (Social, economic, and, environmental). In addition, water quality and wastewater discharge remediation were considered to the improvement of the stream's environment. The prioritization is extended as a flood action master plan for the 2053 horizon.

Keywords: *Urban flood, Flood Damage, Flood Measures, Multi-Criteria Analysis, Master Plan*

1. INTRODUCTION

Urban floods are ranked as one of the main disasters among natural and unnatural disasters. The increase of impervious surfaces and the development of various structures along urban streams and rivers sometimes lead to the clogging of waterways and the consequences will be the loss of life and property. Urban flood management is inevitable, and it dates back thousands of years (Luo et al., 2015). In the past, flood control was accomplished by structural methods such as flood walls and dikes, but nowadays, non-structural measures such as flood warning systems and watershed runoff management are also being considered for sustainable long-term performance.

The megacity of İstanbul, with a population of about 16 million, is not an exception to urban flood risk, particularly since the city is located under the influence of hydrometeorology and climate change in two big water bodies (the Black and the Mediterranean Sea). In addition, the geomorphology of İstanbul allows streams and rivers to flow in the north-south (outlet to the Marmara) and south-to-north directions (outlet to the Black Sea) where heavy rains from the hills quickly transfer downstream of the city on the low coastal area. This process generates the great potential for flash fluvial flooding as well as pluvial flooding from heavy rain

downstream. In recent years, heavy storms caused by climate change in summers (17 July 2017 and 15 August 2022) had significant damage to the infrastructure and economic activities of the historic part of the metropole. Therefore, urban flood management in İstanbul is one of the priorities of long-term urban planning, which is being conducted by the İstanbul Water and Sewerage Administration (İSKİ) for the 2053 horizon. This research is a part of the flood management studies conducted in line with the drinking water, sewage, and drainage of rainwater and floods in the İstanbul Drinking Water and Sewerage Master Plan Project. In this research, the methodology and criteria of flood planning for streams and rivers (macro-scale drainage systems) are considered. The urban drainage network and rainwater collection (micro-scale drainage system) have been investigated separately in another methodology. This methodology is proposed for flood management based on the type of storms, land use, floods, and urban problem to reduce loss of life and economical damage to urban areas. This methodology is derived and adapted from the flood directive (EC Flood Directive 2007) and flood management law prepared by the general directorate of water management (SYGM, 2016), with extra parts for special and local conditions of the İstanbul Megacity. Particularly the stakeholders and role of watershed management are considered in the methodology.

2. MATERIAL AND METHODS

Study Area

This study was applied to the streams and rivers inside İstanbul province. The province of İstanbul is separated by the Bosphorus, the western part is located on the European continent (Europe Side), while the eastern part is located on the Asian continent (Asian Side). While the surface area of İstanbul is approximately 5435 km² since the flood study area was created by considering the stream watersheds which were determined as approximately 6420 km². The study area including 18 main watersheds is shown in Figure. The study area including 18 main watersheds is shown in Figure. This study considered 218 sub-watersheds in the flood risk management plan.

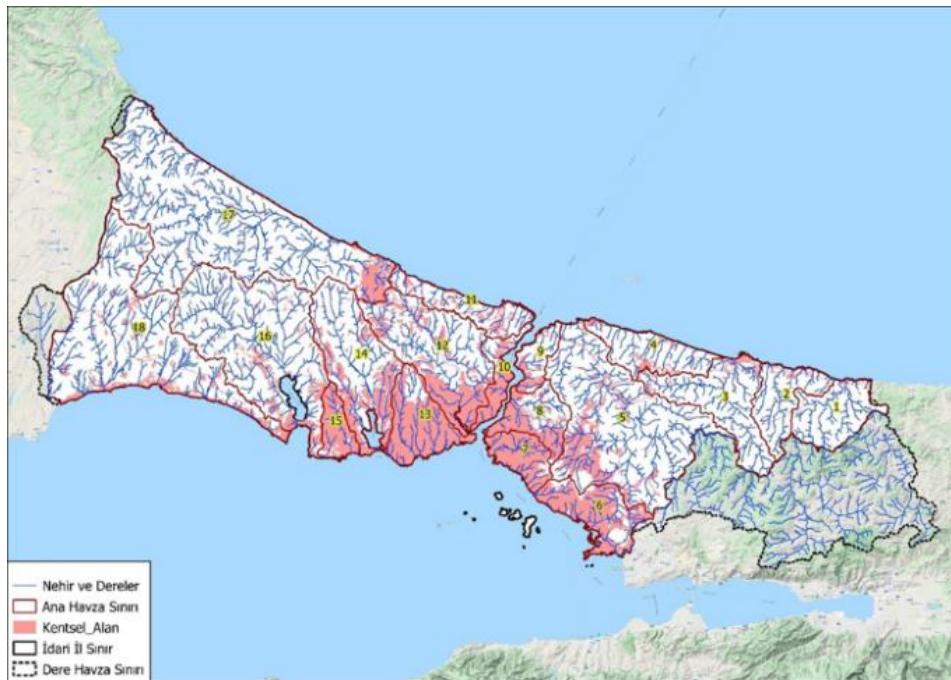


Figure1. İstanbul administrative border and working area

Evaluation of Flood Risks

Flood risk evaluation is a combination of hydrology and hydraulic modelling with the people at inundation risk and asset pricing on the flood zones. The flood hazard and risk maps are prepared based on the outputs of these studies (SYGM 2016, FD 2007). These maps were used to estimate the loss of life and property in the risk-prone areas. The flood hazard ratio (FHR) is calculated by the following Equation:

$$FHR = d \times (v + n) + EF \quad (1)$$

Here;

d = Flood depth (m)

v = Velocity of flood waters (m/sec)

FHR = Flood hazard ratio

EF = Debris factor (0, 0.5, 1 depending on the likelihood that debris will cause a hazard)

n = 0.5 constant

The debris factor is taken as zero in flood hazard ratio calculations. In addition, at a given recurrence (T) the probability (p) of floods with specific recurrence (n) is calculated using the following equation:

$$p = 1 - (1 - 1/T)^n \quad (2)$$

In addition to observing historic damages of floods, various methods and curves have been used to calculate the risk to people at risk (PAR) and their properties and the economic risk of flooding. One common formula is the expected annual damage (EAD) calculation which is given below:

$$EAD = \int_0^1 \text{Damage}(p) dp \quad (3)$$

Damage (p) in Equation 3 is the human or economic damage that occurs at p probability. For human damage (loss of life), the generated curves by Shand et al., (2011) are used in this study. According to these curves, loss of life is predicted to occur at current depths above 1.2 and when $d_{\text{housing}} \times v_{\text{housing}}$ is greater than 1.2. A physical loss rate was also estimated for human injuries (yellow zone).

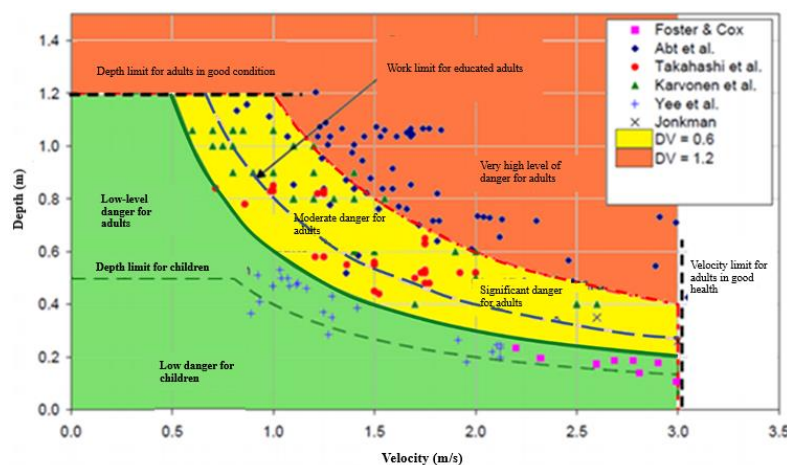


Figure2. Current velocity and depths are used for estimating the potential loss of life (Shand et al., 2011).

The economic damages were obtained from the values given in the "Global flood depth-damage functions database (Huizinga et al., 2017)" based on the flow depths. Indirect flood damages consist of damage to daily activities during the flood period, such as ordinary business activities and household chores, damage to service systems after flooding, and psychological effects of flooding on people. As indirect losses are difficult to calculate, they are accepted as a proportion (up to 30%) of direct risks.

Flood Risk Management Plan (FRMP)

After the determination of flood risk, the perspective of a convenient flood risk management plan includes the minimization of human and economic losses of floods and the use of flood waters for different purposes are considered. Such a plan requires both strategic planning and water-sensitive city planning. In strategic planning, the vision, mission, goals, and plans are determined, and the water-sensitive city determines the trend and the horizon reach the vision. The water-sensitive city is a wider vision based on the holistic management of the integrated water cycle and seeks to protect and promote the health of receiving waterways, reduce flood risk, and create public spaces that capture, clean, and recycle water. The water-sensitive city vision integrates water and urban planning to facilitate better liveability outcomes more broadly, by increasing biodiversity and providing public green space, healthy waterways, and connected communities (Wong, 2006). Based on these strategies, the proposed FRMP implementation approach is presented in Figure. The proposed FRMP serves to reduce the existing flood risks during and after floods, strengthen resilience, raise awareness of flood risks, and implement the principle of solidarity, avoiding new flood risks (EC, FD, 2007). In the FRMPs four priorities for flood risk management objectives have been identified as protection of human health, environmental, cultural heritage, and socio-economic activities. Based on status, a catalogue of measures for flood management and improvement of streams is provided in Table . Various structural and/or non-structural measures are mandatory to eliminate or minimize risks.

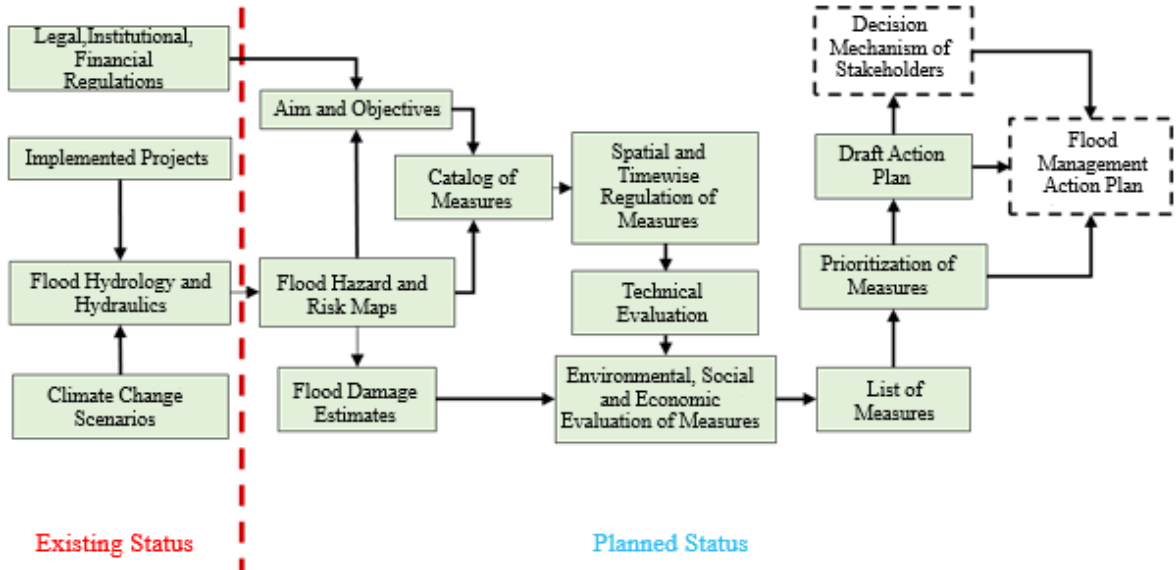


Figure3. Draft Flood Risk Management Plan approach.

Table 1. The vision, main objectives, targets, and measures for İstanbul.

Visions	Main Objectives	Objectives	Measures
The ability of the stream to support habitat for biodiversity development	1. Authority Management	1. Regulations and Responsible Institutions for Areas Affected by the Stream	Legislation
			Stream Corridor and Flood Spread Maps
			Expropriation
			Institutional Stream Cleaning
			Development of İSKABİS
	2. Flood Management	2.1 Flood Management - Non-structural Measures	Watershed Management
			Flood Early Warning System
			Spatial Planning (Land Use)
			Flood Insurance
			Crisis Management and Evacuation
			Dynamic Retention and Reservoir Operation
		2.2 Flood Management - Structural Measures	Micro-scale Drainage System
			Natural Water Retention Methods
	3. Water Quality in Flood Management	3. Wetlands Restoration	Local Protection and Regulation
			Coastal Flood Management
Pond, Lakes, and Reservoir Restoration			
Stream Restoration			

Since there are some overlaps/uncertainties regarding the authorities and responsibilities of the institutions within the scope of flood management, a separate group is presented for institution management. This group of measures is closer to the non-structural part and should be considered emergency measures. The measures and their alternatives have been selected by determining the level of effectiveness in reducing flood risk for streams or sub-watersheds.

Measures Prioritization and Action Plan

Enormous costs require to implementation of various measures of flood management. Unlike other water resources development plans, FRMPs have no income and the profit of these types of plans is calculated from the amount of reduced damage. On the other hand, the calculation of the amount of damage reduction is not calculated with the necessary accuracy due to the uncertainties related to indirect and intangible damages. Also, the cost of non-structural measures and institutional measures cannot be accurately measured. Therefore, in flood risk management plans, only the reduction of direct and tangible structural damage is considered. Therefore, measures based on the severity and reduction of the maximum flood risk have been considered and prioritized. Within the scope of this study, in line with the disaster and flood action plan principles used and implemented by the Federal Emergency Management Agency (FEMA) and the European Commission (EC), a flow diagram summarizing the selection of measures for sub-watersheds by multiple criteria analysis is given in Figure.

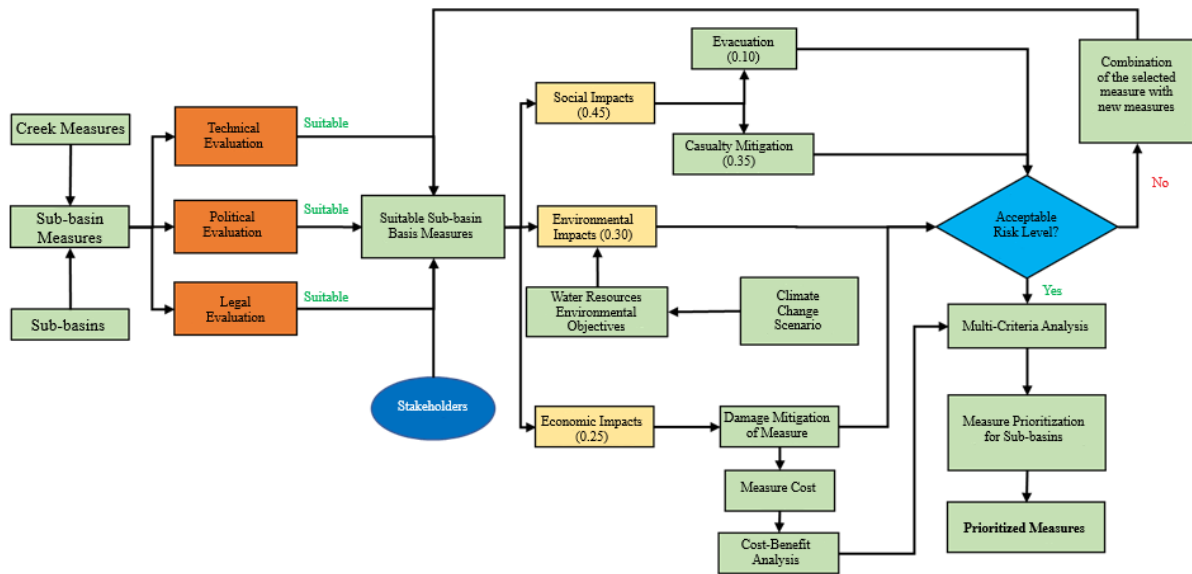


Figure4. Selection of measures for sub-watersheds through multiple criteria analysis.

The proposed measures were subjected to a technical, political, and legal evaluation process and suitable alternatives were identified on a sub-watershed basis. Suitable alternatives were evaluated in terms of their social, environmental, and economic impacts, and because of the evaluation, the option that was found to have an acceptable risk level was recommended as a measure. The typical table of scoring the MCA is presented in

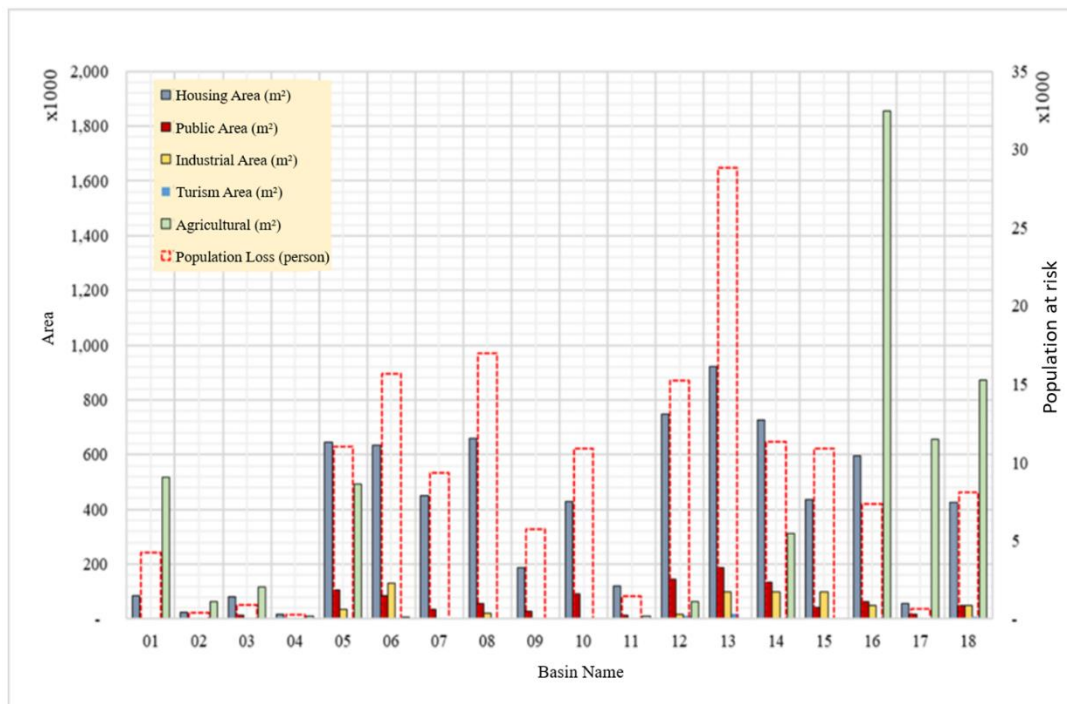


Figure6. Economic damage and People at risk in the 18 main watersheds of İstanbul megacity

. The measure that was not found to be suitable for the acceptable risk level was evaluated and made suitable within the framework of the impacts by combining the measure in question with other measures. Selected suitable measures (those with an acceptable level of risk) were assigned various weighting coefficients according to social, environmental, and economic

impacts and these coefficients were used in the multiple criteria analysis to prioritize the measures.

Cost-Benefit Analysis (CBA)

Economic analysis in the context of flood risk management plans is different from economic analysis of other water resources projects such as water supply, irrigation, drainage, and dam construction. In flood risk management projects, there is no revenue, and the benefit value is derived from the reduction of damage (the difference between damage with and without the project). The flood risk reduction benefit is calculated by Equation 4:

$$Benefit = EAD_b - EAD_a \quad (4)$$

Where EAD_b and EAD_a are expected annual damage before and after implementation of a measure. To the direct cost of each measure, the following costs need to be added (Equation 5).

- (A) Procurement and administrative expenses (10%)
- (B) Engineering (20%)
- (C) Physical flexibility (10%)
- (D) Expropriation (depending on location)
- (E) Operation and maintenance (10%)

$$Total\ Measure\ cost\ (P) = Measure\ cost \times \frac{(100+A+B+C)}{100} \times \frac{(100+E)}{100} + D \quad (5)$$

Table 2. Criteria and scoring for prioritization of measures.

Criteria		Unit	Quality and Score (0-100)			Account Transaction type	Weight
Main Criteria	Sub Criteria						
Suitability and Justification	Technical		Rare failure with adequate hydraulic and structural performance	Limited hydraulic capacity or structural performance	Unacceptable hydraulic and structural performance		
	Legal		Quite easy to expropriate	Easy to expropriate	Exceedingly difficult to expropriate		
	Political and Social acceptance		Implemented in the public interest and without conflict	In the interest of a group but does not contradict the public interest	One group has a personal stake and is in complete conflict with the public interest		
Social Impacts	Reducing Flood Risk to People	%	>80 (100)	50-80 (50)	<50 (0)	+	0,35
	Evacuation and Relocation		No need for Evacuation and Relocation (100)	People have influence over their property (50)	Evacuation and relocation needed (0)	+	0,10
Economic Impacts	Material Damage Mitigation	%	>80 (100)	50-80 (50)	<50 (0)	+	0,10
	Benefit/Cost Ratio		>2 (100)	1-2 (50)	0-1 (0)	+	0,15
	Measure Cost	M\$	<K* (1,3)	K-O (1,0)	>O** (0,9)	x	
	Measure Type		Planned (1.3)	Restoration (1.2)	New applications (1)	x	
Environmental Impacts	Water Quality		Improving water quality (100)	No impact on water quality (50)	Reducing Water Quality (0)	+	0,10
	Ecology		Protected areas accounted for (100)	A large proportion of protected areas accounted for (50)	Most protected areas not accounted for (0)	+	0,10
	Climate Change	%	30% measures adapting to increasing climate change impact (100)	Measures to adapt to increasing climate change impact between 15-30% (50)	Measures adapting to less than 15% climate change impacts (0)	+	0,05

	Cultural Impact	Fully protects cultural and historical sites (100)	No protection of cultural and historical sites (50)	Damage to cultural and historical sites (0)	+	0,05
--	-----------------	--	---	---	---	------

* Threshold price of small measures: 70 M€ ** Threshold price of intermediate measures: 70-280 M€

The expected annual cost of the project is calculated by Equation 6:

$$EAD = \frac{r(P)}{1-(1+r)^{-n}} \quad (6)$$

Here, the EAC is the annual expected cost, r is the average interest rate over the project life of n years, and P is the value of the baseline precautionary cost. Using the previous calculations, benefit/cost ratios are calculated with Equation 7:

$$\frac{Benefit}{Cost} = \frac{EAD_b - EAD_a}{EAC} \quad (7)$$

A benefit/cost ratio greater than 1 indicates that the project is economic. If this ratio is less than 1, the benefit should be justified by showing that the measure reduces intangible harm or improve other environmental and social benefits. The following data are important in these calculations.

- Project duration: The project duration for flood risk management projects has been accepted as 30 years.
- Inflation or interest rate is assumed to be 10%.

3. RESULTS AND DISCUSSIONS

The people at flood risk and the potential for economic damages are estimated and are shown in Figure. In the figure area and person at risk are selected because of uncertainty in price estimation. This figure shows that watershed 13 (Ayamama and Tavukçu streams located in Bağcılar, Davutpaşa, Bakırköy, Zeytinburnu, and Fatih) has the highest risk for people, and watershed 16 has the largest economic losses due to its size.

According to land use, İstanbul streams are divided into urban and rural (agriculture, forest) reaches, and proposed suitable measures for each part are guided by the catalogue of measures. Measures are proposed according to flood types (fluvial floods, flash floods, pluvial floods, and, coastal floods). The streams were divided into upstream, middle, and downstream sections. Water storage and retention measures are considered suitable for the upstream section of the watershed. While determining the measures, watershed management and the effects of the measures on each other were evaluated on a stream-by-stream basis. It is aimed to establish a balance between structural and non-structural measures in flood management. It is proposed to harmonize the structural solution zones in urban areas, which were previously built using concrete materials, with the green corridor. Institutional flood management legislation and implementation, stream protection and flood propagation maps, and the development of İSKABİS are recommended for the whole of İstanbul. Flood insurance is also proposed for all regions, except for forests.

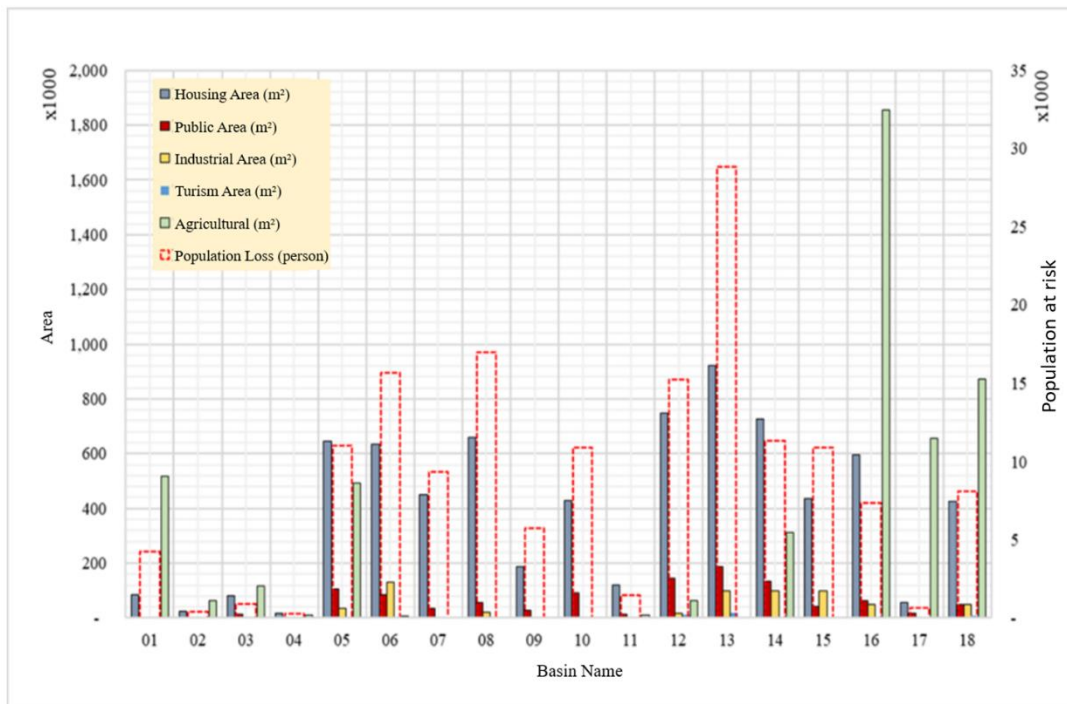


Figure6. Economic damage and People at risk in the 18 main watersheds of İstanbul megacity

In the case of flood governance, determining the boundaries and bed of the river is of immense importance. This method helps the safe passage of floods in the coming years of development. Therefore, for institutional objective, a graph was developed for the protection of stream corridor widths as shown in **Figure**. The curves show the upper bound of the graph considered by the eye. Here, B is the stream corridor width (m) and Q is the flow rate of Q_{100} (m^3/s).

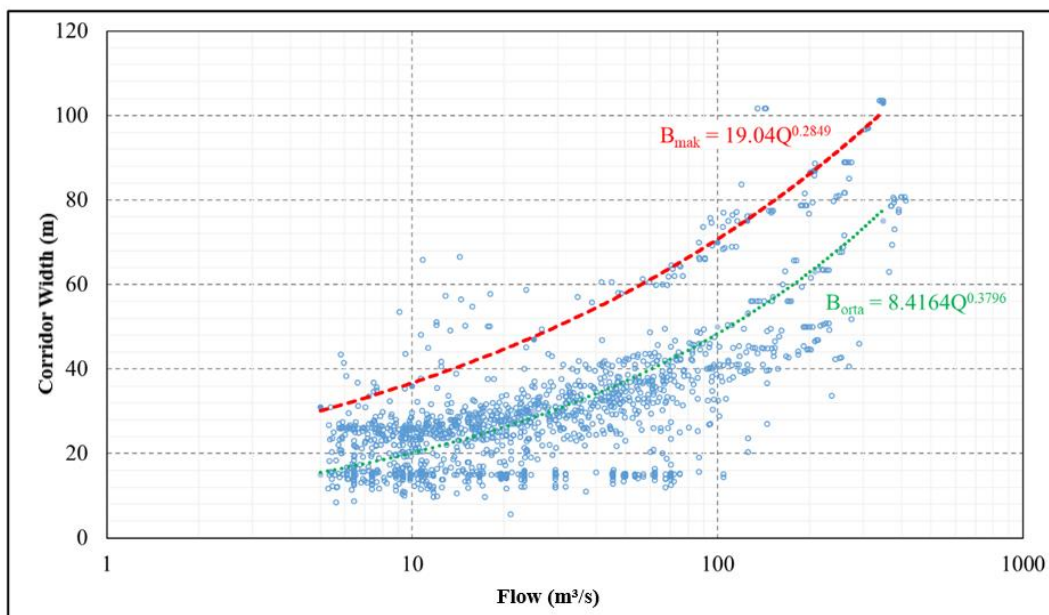


Figure7. Relationship between flow rate and stream corridor width.

Regarding the non-structural measures, the development of the existing flood warning system and measuring and monitoring of the flow of floods is considered as one crucial measure. In addition, watersheds management of runoff and erosion reduction and dynamic retention and reservoir operation were also considered for the study area. The proper operation of flood

control reservoirs is a fundamental non-structural solution for this region with the capability of recreation and tourism which are considered in the measures.

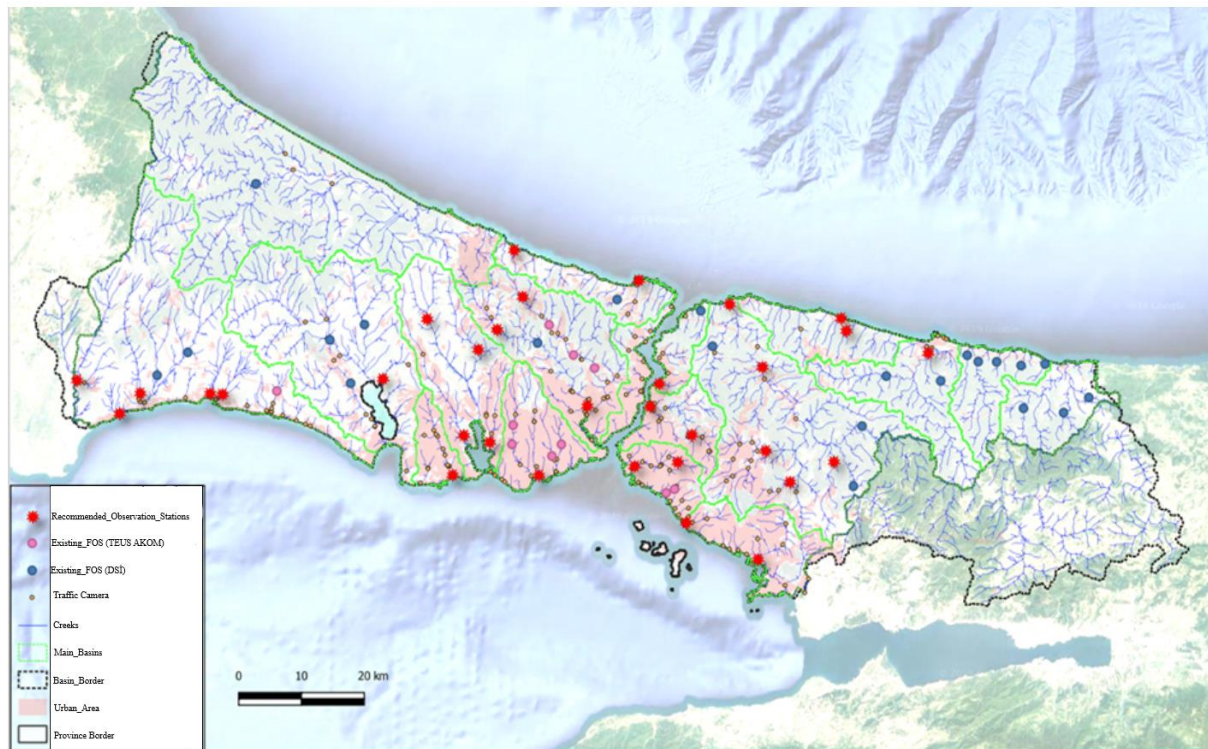


Figure8. Existing stream gages and proposed stream gages in the urban area for the flood warning system

The basis of this operation is to maximize the use of available storage during flood events. Although reservoirs are not designed to provide complete protection against all possible floods, efficient use of their storage capacity can prevent major flood disasters by significantly reducing flood levels in downstream streams.

Structural measures include local protection, flood walls, weirs, and bypass channels. Structural measures can never eliminate the risk of flooding. In addition, due to their physical presence, they have the potential to create a false sense of security, which can lead to misuse of land in protected areas. Structural measures to be implemented in İstanbul streams within the scope of this study are micro-scale drainage systems, natural water retention methods, local protection, and regulation, and coastal flood management. Descriptions of these measures are presented below. For this reason, innovative approaches are required to implementation of Low Impact Development (LID). These approaches protect against flooding in urban areas and provide treatment benefits by reducing the pollution load in stormwater. The local protection measure is one of the fastest structural measures implemented in the world. This measure was one of the first methods used for flood control. However, because of climate change and human interventions, these measures have proven to be inadequate at times. To date, concrete, stone, and inflexible materials have been used as part of these measures. However, it is recommended to keep the measures more flexible by using new approaches such as green waterways, which are now being implemented. These structural measures were widely used in İstanbul and proposed in the FRMPs by considering green space corridors and stream restoration. Since this study is conducted within the scope of the Master Plan, the measures recommended in this report should only be used in preliminary design and route identification studies.

By considering various measures from the catalogue, their efficiency and cost are extracted and used for prioritization. In this framework, small (<25 M€), medium (25-150 M€), and large

measures (>150 M€) were considered. For small measures, it is assumed that expenditures will be made from the annual budgets of İSKİ and its stakeholders, while for large measures, planning is considered with financing tools to be provided by ministries or from abroad. In the Master Plan studies, the investment programs and budgets of other sections will be taken into consideration, and these values will be revised and finalized. As a sample, the prioritization of measures for implementation is shown for sub-watersheds of main watershed No.8.

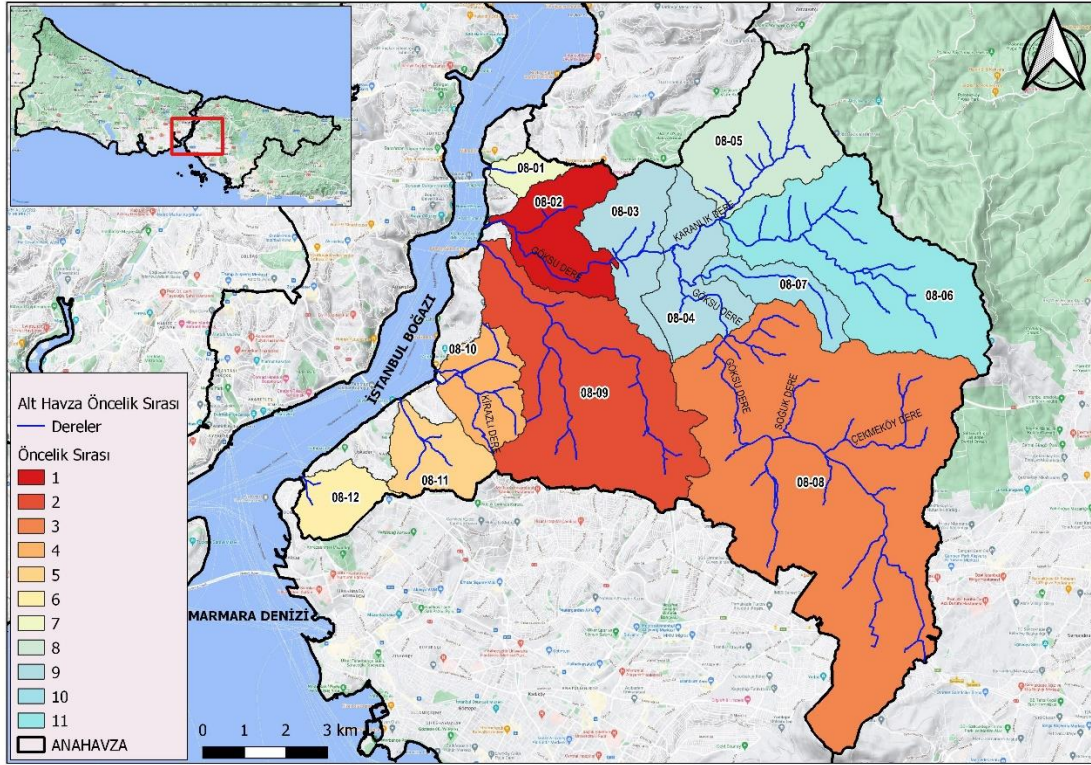


Figure9. Sub-watersheds prioritization of Watershed 8 in the Flood Risk Management Plan for İstanbul

4. CONCLUSIONS

In this study, a combination of various methods is considered for extracting the draft of the flood risk management plan for İstanbul Megacity. first, vision and objectives were determined, and a catalogue of flood measures was created accordingly. There is a total of 17 measures in this catalogue. These measures are well practiced in İstanbul and around the world. Using the catalogue of measures, suitable measures were selected for streams at risk of flooding, and their spatial and temporal assessment for preliminary design was conducted on a sub-watershed basis. While some of the measures apply to all İstanbul streams, others are appropriate for stream-specific applications. Cost analysis of these proposed measures was also conducted.

The selection of measures for the Draft Flood Action Plan was based on multi-criteria analysis and sustainability principles (environmental, social, economic). The multi-criteria analysis was carried out in two stages: selection of good practices among the measures for each sub-watershed and prioritization of sub-watersheds based on İstanbul. Since the measures proposed in this report are the result of a large-scale study, they should be confirmed and implemented in the field.

Acknowledgments:

REFERENCES

- Defra and Agency** (2006) The Flood Risks to People Methodology, Flood Risks to People Phase 2, FD2321 Technical Report 1, HR Wallingford et al. did the report for Defra/EA Flood and Coastal Defence R&D Programme,
- Dinç, H.** (2019). Analysis of the physical impact of land use decisions on stream systems and its reflection on urban life - Inundation, flood and flood risk evaluation in İstanbul. *Journal of Planning*, 29(2), 147-170.
- Luo, Pingping, et al.** (2015), "Historical assessment of Chinese and Japanese flood management policies and implications for managing future floods." *Environmental Science & Policy* 48 (2015): 265-277.
- Ministry of Environment and Urbanization** (2021). 2021 construction and installation unit prices. Directorate of High Technics Board, Ankara.
- Ministry of Agriculture and Forestry General Directorate of State Hydraulic Works (2021)**. DSİ unit price book for 2021. Ankara
- Huizinga, J., de Moel, H., Szewczyk, W.** (2017). Global flood depth-damage functions: Methodology and the database with guidelines (No. JRC105688). Joint Research Center (Seville site). EUR 28552 EN. DOI: 10.2760/16510
- İLBANK İller Bankası A.Ş.** (2021). 2021-unit prices for infrastructure facilities. Department of Investment Coordination, Ankara.
- İMP-JV** Joint Venture for the Preparation of Drinking Water and Sewerage Master Plan, 2020. Existing Streams Interim Report. İstanbul, Türkiye
- İMP-JV** Joint Venture for the Preparation of Drinking Water and Sewerage Master Plan, 2021a. Streams Optional Planning Interim Report. İstanbul, Türkiye
- İMP-JV** Joint Venture for Preparation of Drinking Water and Sewerage Master Plan, 2021b. Stormwater Collection System Optional Planning Interim Report. İstanbul, Türkiye
- Ramirez, H. D. R.** (2004). Flood control reservoir operations for conditions of limited storage capacity. Texas A&M University.
- Samsunlu, A.** (2020). İstanbul streams and their problems, section 2. Water and environmental technologies. August 2020 Year: 15, Issue: 145
- Shand, Tom & Smith, Grantley & Cox, R. & Blacka, Matt.** (2011). Development of appropriate criteria for the safety and stability of persons and vehicles in floods. In Proceedings of the 34th World Congress of the International Association for Hydro-Environment Research and Engineering: 33rd Hydrology and Water Resources Symposium and 10th Conference on Hydraulics in Water Engineering (p. 404). Engineers Australia.
- Shrestha, A.B., Shah, S. H. and Karim, R.,** (2008): Resource manual on flash flood risk management- Module 1: Community-based Management. Kathmandu, Nepal: International Centre for Integrated Mountain Development (ICIMOD).
- General Directorate of Water Management** (2017). Flood Management. Ankara, Türkiye. 248 pp. <http://taskinyonetimi.tarimorman.gov.tr/engine//engine/file.axd?file=/Dokumanlar/Task%C4%B1nYonetimi.pdf>
- IPCC**, 2007: Climate Change 2007: Synthesis Report. Contribution of Working Groups I, II, and III to the Fourth Assessment Report of the Intergovernmental Panel on Climate Change [Core Writing Team, Pachauri, R.K and Reisinger, A. (eds.)]. IPCC, Geneva, Switzerland, 104 pp.
- WMO World Meteorological Organization** (2006). Environmental aspects of integrated flood management, APFM Technical Document No 3, Flood Management Policy Series. Geneva, Switzerland. 71 pp.
- Wong, T. H.** (2006). The water-sensitive urban design-the journey thus far. *Australasian Journal of Water Resources*, 10(3), 213-222.

MODELLING AND SIMULATION OF FLOODS IN A RIVER BASIN: FIRST PHASE TOWARDS FLOOD MANAGEMENT USING NBS IN THE OITAVEN-VERDUGO RIVER BASIN (NW SPAIN)

Carolina Acuña Alonso^{1*}, Lucia Martínez Portabales¹, Enrique Valero¹ and Xana Álvarez¹,
¹. Agroforestry Group, Department of Natural Resources and Environmental Engineering, School of Forestry Engineering, University of Vigo, 36005 Pontevedra, Spain
^{*}Corresponding author (carolina.alonso@uvigo.es)

ABSTRACT

Floods are recurrent phenomena with significant environmental and socio-economic impacts. The risk of flooding increases when land use changes. The objective of this research has been to obtain an integrative methodology based on the development of a model in HEC-HMS, calibrated and validated from events between 2018-2022, and to apply simulations employing the use of Nature-Based Solutions (NBS) tools, in this case reforestation, to reduce flood hazard. This model has been applied in a basin in Galicia (NW Spain), a basin that periodically floods. Focusing on how forest use and NBS can reduce the risk of flooding in cities and crops that are in the high-risk area. It was obtained that by changing the CN in sub-basin 3 from 77 to 50, the volume in this sub-basin, where flooding occurs, is reduced by 19%. It has been found that the use of reforestation in the sub-basin located in the middle is more beneficial than reforestation upstream.

Keywords: *Nature-based solutions, Flood hazard management, Curve number*

1. INTRODUCTION

Globally, floods are one of the natural phenomena that affect the most people in the world, generating a large number of fatalities and a high socio-economic impact. In addition, climate change has caused hydrological changes around the world, increasing the likelihood of extreme weather events such as floods (Rajkhowa and Sarma 2021). Hydrological modelling is another tool with great potential in land management. The Hydrologic Modelling System (HEC-HMS), a software app developed by the US Army Corps of Engineers Hydrologic Engineering Center (HEC), is a numerical, semi-distributed hydrologic model used for event-based and continuous runoff simulation (Ford et al., 2002).

The purpose of this study is firstly to model the Verdugo and Oitavén River Basin (northwest Spain). This study is due to the risk that some of its areas are at risk of flooding, as it also has a large surface area of urban centres and floods usually entail many economic costs. A simulation will be carried out in an event testing the use of Nature Based Solutions (NBS).

2. MATERIAL AND METHODS

Study area

The areas to be studied are the Verdugo River and the Oitavén River, which belong to the Province of Pontevedra, Galicia, Spain, and both join in a common final stretch of 7 km, flowing into the Vigo estuary. They are considered a single hydrographic system, the so-called Verdugo-Oitavén. The Verdugo River is identified as the main riverbed. It rises on the slope of Outeiro Grande, in the village of Cernadelo (Forcarei, Pontevedra) at an altitude of 760 m. As it descends, the river flows through deep V-shaped valleys for most of its 41 km long course, and gradually narrows. The River Oitavén, which is the main tributary of the Verdugo, rises at the confluence of the waters of the Regato de las Ermitas (at an altitude of 720 m) and the River Xesta (at an altitude of 920 m). It runs for approximately 32 km to its mouth, on the right bank of the Verdugo at Ponte da Barca (Soutomaior, Pontevedra) and has a V-shaped riverbed with valleys along all its stretches. Its channelling system supplies water to the city of Vigo, as well as to Mos, Porriño, Redondela and Salceda. The total size of the Verdugo-Oitavén Basin is approximately 335 km², of which 177 km² correspond to the Oitavén Basin. The absolute flow at the mouth of the Verdugo River is 17 m³/s, while the flow of the Oitavén River before its confluence reaches 10.5 m³/s. Both are rain-fed rivers, including their tributaries, and the average annual rainfall in their basins is approximately 1890 mm.

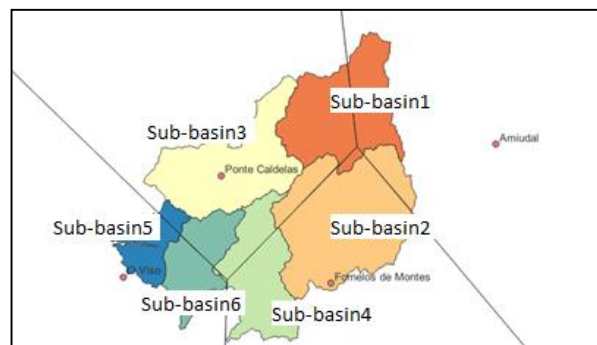


Figure 1. Calculated sub-basins in the study area

Model simulations

In this study, different simulations based on a hydrological model of the Verdugo-Oitavén River Basin are run and analysed. These simulations are calculated from a hydrological model obtained with the HEC-HMS software (V.4.9.0), calibrated and validated with data from 2017 to 2019. To obtain the hydrological model of the study area, a digital terrain model was obtained from the National Centre for Geographic Information, specifically from the National Aerial Orthophotography Programme (PNOA) (Spanish National Geographic Institute 2021). Land uses were obtained from SIOSE (Gobierno de España 2016). Precipitation and evaporation data were obtained from Meteogalicia (Xunta de Galicia 2021), calculating the weighted average precipitation of each station using the Thiessen polygon method. Flow data were obtained from the website of the Ministry for Ecological Transition (2020). The model was calibrated using two different methods, but on the same dates, to check which gave better results. The two methods used were the Soil Conservation Service-Curve Number Method and the Clark Method. Other parameters were calculated: The time of concentration was added to the data for the corresponding sub-basin (hours), while the lag time was added to the data for each

corresponding reach (minutes). Finally, a robustness check of the developed model was performed to confirm that the results obtained were reasonable and consistent with expectations. The HEC-HMS model was calibrated and validated using the calibration and validation strategy of calibrating model parameters by sub-basin from upstream to downstream according to Zhang et al. (2022). For the simulations the infiltration capacity was quantified in a parameter derived by the Soil Conservation Service (SCS) called CN (Curve number). This parameter determines the runoff over an area based on soil type, soil cover and the hydrological group of the soil (Cronshey 1986).

3. RESULTS AND DISCUSSIONS

The calibration process using the SCS curve number method gives a result of $R^2 = 0.96$, while Clark's method gives $R^2 = 0.91$. Both figures are very high. In the validation check for the SCS curve number method $R^2 = 0.99$, while in the Clark method $R^2 = 0.99$. Different studies suggested this common method for the assessment of time series agreement by examining the sum of squared differences (Najimn et al., 2006). The results indicate that the HEC-HMS model is well optimised in this study and that the HEC-HMS model is generally reliable and robust for flood simulation in this study area.

First, a simulation was carried out by changing the land use from agricultural to forestry in sub-basin 1, which is further upstream. Forestation was simulated, however, the results obtained, although good, did not practically change the flow volume of sub-basin 3, where the municipality of Ponte Caldelas is located, which is the urban nucleus that tends to suffer severe flooding. Therefore, by changing the curve number in sub-basin 3 from 77.26 to 50 and subsequently carrying out these simulations we can see that in the results both the peak flow and its volume decrease. For the precipitation event studied, the volume in sub-basin 3 decreases from 62.92 to 51.14 mm, with a change in its land use; and the peak flow also decreases from 16.5 to 13.2 m³/s. These two values also decrease as you go downstream.

4. CONCLUSIONS

The land cover change in the Verdugo-Oitavén River Basin, composed of very small and heterogeneous plots of (0.26 ha on average) allowed to simulate the reduction of the flow rate. The use of reforestation as NBS is effective in reducing flood hazard in the catchment. The use of NBS tools to increase water retention in watersheds is considered as a sustainable tool to improve territorial planning. All this through an integrated approach supported by new coordinated and multi-sectoral policies.

Acknowledgements: This research was funded by the Universidade de Vigo (convocatoria de axudas propias á investigación da Uvigo para o ano 2021) under project 21VI-01.

REFERENCES

- Cronshey, Roger. 1986. *Urban Hydrology for Small Watersheds*. US Department of Agriculture, Soil Conservation Service, Engineering Division.
- Ford, David, Nathan Pingel, and J J DeVries. 2002. *Hydrologic Modeling System HEC-HMS: Applications Guide*. US Army Corps of Engineers, Hydrologic Engineering Center.
- Gobierno de España. 2016. "SIOSE. Sistema de Información de Ocupación Del Suelo de España." *Ministerio de Transportes, Movilidad y Agencia Urbana*, <https://www.siose.es/>.
- Najim, Mohamed Mujithaba Mohamed, Mukand Singh Babelb, and Rainer Loofb. 2006. "AGNPS Model

- Assessment for a Mixed Forested Watershed in Thailand.”
- Rajkhowa, Sanchayita, and Jyotirmoy Sarma. 2021. “Climate Change and Flood Risk, Global Climate Change.” In *Global Climate Change*, 321–39. Elsevier.
- Spanish National Geographic Institute. 2021. “Spanish National Plan for Orthophotography (PNOA).” 2021.
- Xunta de Galicia. 2021. “Meteogalicia.” https://www.meteogalicia.gal/Caire/index.action?request_locale=gl.
- Zhang, Ke, Md Halim Shalehy, Gazi Tawfiq Ezaz, Arup Chakraborty, Kazi Mushfique Mohib, and Linxin Liu. 2022. “An Integrated Flood Risk Assessment Approach Based on Coupled Hydrological-Hydraulic Modeling and Bottom-up Hazard Vulnerability Analysis.” *Environmental Modelling & Software* 148: 105279. <https://doi.org/https://doi.org/10.1016/j.envsoft.2021.105279>.

RESERVOIR AND SURFACE WATER BODIES

MODELLED NITRATE CONCENTRATIONS IN THE LEACHATE OF GERMANY - COMPLIANCE CHECKING AND GAP ANALYSIS FOR REACHING WFD TARGETS FOR GROUNDWATER -

Kunkel Ralf, Wolters Tim and Wendland Frank*

¹Forschungszentrum Jülich, Agrosphere Institute (IBG-3), 52425 Jülich, Germany

**Corresponding author (t.wolters@fz-juelich.de)*

ABSTRACT

In the project AGRUM-DE the mean long-term nitrate concentration in leachate was modelled from Germany based on the model system RAUMIS-mGROWA-DENUZ and validated with observed groundwater data. For this purpose, monitoring stations were preselected with respect to the oxidizing properties of aquifers, near to the surface and shallow springs. Comparisons between modelled and observed mean concentrations have been carried out for all major land use classes (arable land, forest, grassland and urban areas). The agreement between modelled nitrate concentrations in the leachate and measured nitrate concentrations in groundwater showed that the model system was able to reliably represent interrelationships and influencing factors that determine simulated nitrate concentrations in the leachate. On the other hand, it has been proven that observed nitrate concentrations in groundwater may provide a solid data source for checking the plausibility of modelled nitrate concentrations in leachate in cases where certain preselection criteria are applied.

Keywords: *nitrate; groundwater; leachate; modelling; validation; state scale*

1. INTRODUCTION

Since the nitrate threshold limit value for groundwater of 50 mg NO₃/L is continuously exceeded in some regions of Germany, general administrative regulations for standardized designation of nitrate polluted and eutrophicated areas in Germany have been issued. Amongst others, the nitrate concentration in the leachate is used a decisive indicator to assess a potential reduction requirement for N-surpluses from agriculture to make to ensure that the nitrate concentration in the leachate does not exceed 50 mg NO₃/L.

We used the model system RAUMIS-mGROWA-DENUZ consisting of a nutrient balance model, a nutrient balancing model (RAUMIS, Gömann et al., 2020), a water balance model (mGROWA, Hermann et al., 2015) and a nitrate transport model in soil (DENUZ, Wendland et al., 2009) to predict the nitrate concentrations in the leachate throughout Germany. This was done using the water balance for the time period 1981-2010, N-deposition data from the PINETI 3 data set (Schaap et al. 2018) and the nutrient balance from agriculture for the period 2014-2016 with a spatial resolution of 100x100 m grids. Figure 1 shows that the calculated nitrate concentrations in the leachate display high values above 50 mg NO₃/L in regions either characterized by high nitrogen inputs due to high stock densities (e.g., in the northwestern part of Germany) or by low leachate rates (e.g., northeastern part of Germany). Forested areas

usually show low nitrate concentrations. To be able to use these results for the development of policy measures to improve groundwater quality it is necessary to check the results for compliance by comparison with observation data.

2. MATERIALS AND METHODS

We used observed nitrate concentrations from groundwater monitoring wells and springs for the comparison with modelled nitrate concentrations in the leachate. To make sure that the concentrations in groundwater can be assumed to correspond to the concentrations in the leachate, several constraints have been considered (Wolters et al., 2021).

- Modelled results represent temporal averages whereas observations are related to a specific point in time and usually show great variabilities over time. Therefore, no exact agreement can generally be expected when modelled long-term mean nitrate concentrations in leachate are compared with individual observed nitrate concentrations in groundwater. However, mean or median values of the observed data can be used at least in terms of magnitude.
- Since only near-surface groundwater reflects the quality of the leachate that has infiltrated into an aquifer, only data from upper aquifers or shallow sources only should be included in the validity check.
- The correlation of nitrate concentrations in the leachate and in groundwater may be lost at least partially by denitrification processes in the groundwater. Therefore, an evaluation of local denitrification conditions by assessing the most important indicators for denitrification – Fe, Mn, O₂, NO₃ and DOC (Wendland et al., 2020) – and disregarding stations with reduced groundwaters is required.
- Due to lateral flow in the aquifer the entire inflow area of a groundwater monitoring site contributes to the observed nitrate concentration at that site. Therefore, the inflow area of each site is assessed using the groundwater flow directions derived from a model of the groundwater surface. Median nitrate concentrations for the whole inflow areas are calculated from the modelled values and compared to the observed concentrations.

3. RESULTS AND DISCUSSIONS

Groundwater quality data have been provided by the federal states of Germany via the LAWA Groundwater Committee. For nitrate, 204000 observations from 22000 groundwater measuring points from the period from 2006 to 2018 are available in this way. From this database those observations have been selected, which are from the time period 2014-2018, originating from less than 10 m below the groundwater surface and display mostly oxidized groundwater conditions. By this, the usable number of groundwater monitoring sites was reduced to 3391. Median values for each monitoring station were calculated and compared to the median modelled nitrate concentration of the respective inflow area.

Figure 1 shows the locations and observed nitrate concentrations used for the comparison. The spatial distribution of the data is quite inhomogeneous. In the northern part of Germany, reduced conditions in groundwater are quite common, leading most of the observations data to be disregarded. For one federal state (Bavaria) no groundwater data could be used.

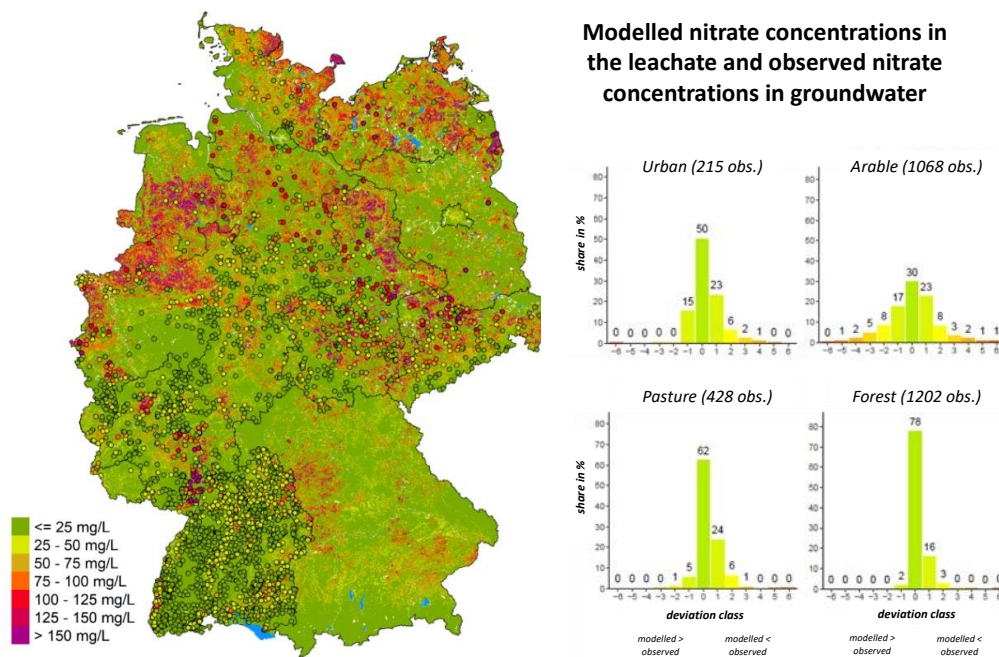


Figure 1. Calculated nitrate concentration in the leachate, observed nitrate concentrations in groundwater and deviation between observed and modelled values for different land use classes.

Since a simple comparison of measured point values and modelled raster values is misleading, it must be defined how a “good” or “bad” match can be defined. As a minimum requirement, it can certainly be stated that a large-scale model should primarily reflect the spatial patterns. In terms of absolute values, however, it is acceptable if there are significant differences. From a first optical assessment of figure 1, the compliance of observed and modelled concentrations seems to be quite good. For a more objective comparison, modelled and observed data have been categorized in classes of 25 mg NO₃/L each and compared to each other. The agreement is considered as being good, if observed and measured concentrations are in the same category; fair to bad, there is a deviation of one to more categories. The four histograms of the deviations classes in figure 1 illustrate, that the compliance is mostly good or at least fair and that the modelled nitrate concentrations are not over- or underestimated systematically. However, the deviations of individual data values may be quite significant, in particular for arable land, indicating that the compliance is good in general and on a level of regions and classes but on a level of individual wells. Nevertheless, it can be stated that the model system was able to reliably represent interrelationships and influencing factors that determine simulated nitrate concentrations in the leachate and that preselected observed nitrate concentrations in groundwater may provide a solid data source for checking the plausibility of modelled nitrate concentrations in leachate.

REFERENCES

- Gömann, H., Kreins, P., Brandes, E. and Pfingsten, T. (2020): Regionalisierte Quantifizierung der landwirtschaftlichen Flächenbilanzüberschüsse in Nordrhein-Westfalen, Teilbericht I zum Vorhaben GROWA+ NRW 2021, Köln/Braunschweig, 85 p.
- Herrmann, F.; Keller, L.; Kunkel, R.; Vereecken, H.; Wendland, F. (2015): Determination of spatially differentiated water balance components including groundwater recharge on the Federal State level—A

- case study using the mGROWA model in North Rhine-Westphalia (Germany). *J. Hydrol. Reg. Stud.* 2015, 4, 294–312.
- Schaap, M.; Hendriks, C.; Kranenburg, R.; Kuenen, J.; Segers, A.; Schlutow, A.; Nagel, H-D; Ritter, A.; Banzhaf, S. (2018): PINETI-3: Modellierung atmosphärischer Stoffeinträge von 2000 bis 2015 zur Bewertung der ökosystem-spezifischen Gefährdung von Biodiversität durch Luftschadstoffe in Deutschland; Umweltbundesamt, Dessau, Germany; *UBA-Texte* 79/2018, 149p.
- Wendland, F., Kunkel, R. and Voigt, H.-J. (2004): Assessment of groundwater residence times in the pore aquifers of the River Elbe Basin, *Environmental Geology* Vol. 46, pp. 1-9.
- Wolters, T.; Cremer, N.; Eisele, M.; Herrmann, F.; Kreins, P.; Kunkel, R.; Wendland, F. Checking the Plausibility of Modelled Nitrate Concentrations in the Leachate on Federal State Scale in Germany. *Water* 2021, 13, 226. <https://doi.org/10.3390/w13020226>

INVESTIGATING DIFFUSE POLLUTION DYNAMICS IN AN URBAN CATCHMENT AREA USING FIRST FLUSH ANALYSIS

Gil Cruz^{1,2}, Miguel Enrico Robles¹, Rommel Glenn Mendova² and Marla Maniquiz-Redilla^{1}*

1 Department of Civil Engineering, De La Salle University, 2401 Taft Avenue, Malate, Manila 1004, Philippines

2 Office of Environmental Sustainability, Bataan Peninsula State University, Capitol Compound, Tenejero, Balanga, Bataan, 2100, Philippines

**Dr. Marla Maniquiz-Redillas (marla.redillas@dlsu.edu.ph)*

ABSTRACT

Pollutants present in urban stormwater runoff pose an environmental threat to the natural receiving water bodies. However, diffuse pollution has not yet been investigated in the Philippines. First flush is an important phenomenon commonly used in stormwater treatment system design where only the highly concentrated initial part of the runoff hydrograph is subject to treatment. Hence, understanding the water quality and the duration of the first flush in an urban catchment area that is to be diverted for treatment will be beneficial for transitioning to Low Impact Development (LID) approach in stormwater management. This study aims to investigate the diffuse pollution dynamics by analyzing the occurrence of first flush of urban stormwater runoff from actual rainfall events in Balanga City, Bataan, Philippines and use it as an evidence-based criteria to design low impact development controls. Water quality analysis for total suspended solids (TSS), total dissolved solids (TDS), chemical oxygen demand (COD), nitrate, phosphate, ammonia, and chloride were conducted. It was found that most commonly, the first flush can exist through the initial 10%–30% of the runoff for storm event with an average rainfall intensity of 5mm/hr. Hence, to effectively treat the stormwater runoff with minimum risk of discharging significant high loads of pollutants to natural receiving water bodies, it is recommended that at least the initial 30% of the runoff should be subject to treatment. Results of this study provide a localized framework for designing and implementing options for robust urban water management especially in designing appropriate LID controls that will address non-point source pollution in developing countries like the Philippines.

Keywords: *First flush analysis, diffuse pollution, water quality volume, low impact development, urban runoff*

1. INTRODUCTION

Rapid urbanization alters the function and structure of natural landscapes as it transforms pervious surfaces into impervious surfaces. Water pollutants are commonly characterized as point or diffuse, according to their source and pathway to the receiving environment. Urban stormwater runoff usually exhibits the ‘first flush’ effect, wherein the discharge in the initial stage of a runoff event contains considerably higher amounts of pollutants as compared with

the latter phase of the event (Jeung et al., 2019). Accordingly, these pollutants are essential to be investigated in the management of stormwater runoff in order to protect and conserve the environment (Ahmed et al., 2016). Several factors have also been identified including hydrologic process features such as rainfall intensity, rainfall duration, rainfall pattern, season fluctuation. Lastly, anthropogenic activities such as land-use patterns and farmland management ways constitute a bigger part in contribution to non-point source pollution (Xiang et al., 2013). This study aims to investigate the occurrence of diffuse pollution dynamics and analyze the occurrence of first flush of urban stormwater runoff from actual rainfall events in Balanga City, Bataan, Philippines.

2. MATERIAL AND METHODS

The rainfall depth and intensity were determined by installing a rain gauge in the site study area (5.828 ha) in Balanga City, Bataan. Meanwhile, runoff flow rate, was measured using a handheld flowmeter during the actual sampling. Individual samples during the four (4) rainfall events were collected from the identified outflow of the catchment area. Samples were collected every 5 min for the first 30 min, every 10 min between 30 and 60 min, every 30 min between 60 and 120 min, and every 60 min until rainfall stopped. The samples were stored in 500-mL polyethylene bottles at the site. They were placed in containers with ice bags and transported to the laboratory the same day. Heavy metal analysis on road-deposited sediments were conducted in a commercial laboratory and correlated with actual traffic volume count. The FF was found to be occurring when the slope of normalized cumulative mass emission plotted against normalized cumulative volume is greater than 45°.

3. RESULTS AND DISCUSSIONS

This study verified that large values of mean rainfall intensity (up to 10mm/hr) are related to the occurrence of First Flush (FF) for most pollutants especially for TSS and PO₄ (Figure 1). The concentration of chemical constituent in early runoff can be 10 times higher than the concentration of runoff at the end of rainfall. It is important to note that the design of LID relatively considers frequent events, usually rainfall events during wet season. Accordingly, these smaller, more frequent storms significantly represent the majority of rainfall events in terms of both the number of rain events and the total runoff volume. Antecedent dry days (ADD) was found to significantly influence build-up processes in the collection point and with strong correlation to FF occurrence. ADD and traffic volume also affected the heavy metals present in road deposited sediments. Figure 2 shows that the most abundant heavy metals include Fe, Ca, Ti, K, Sr, Mo, and Mn based on XRF analysis conducted.

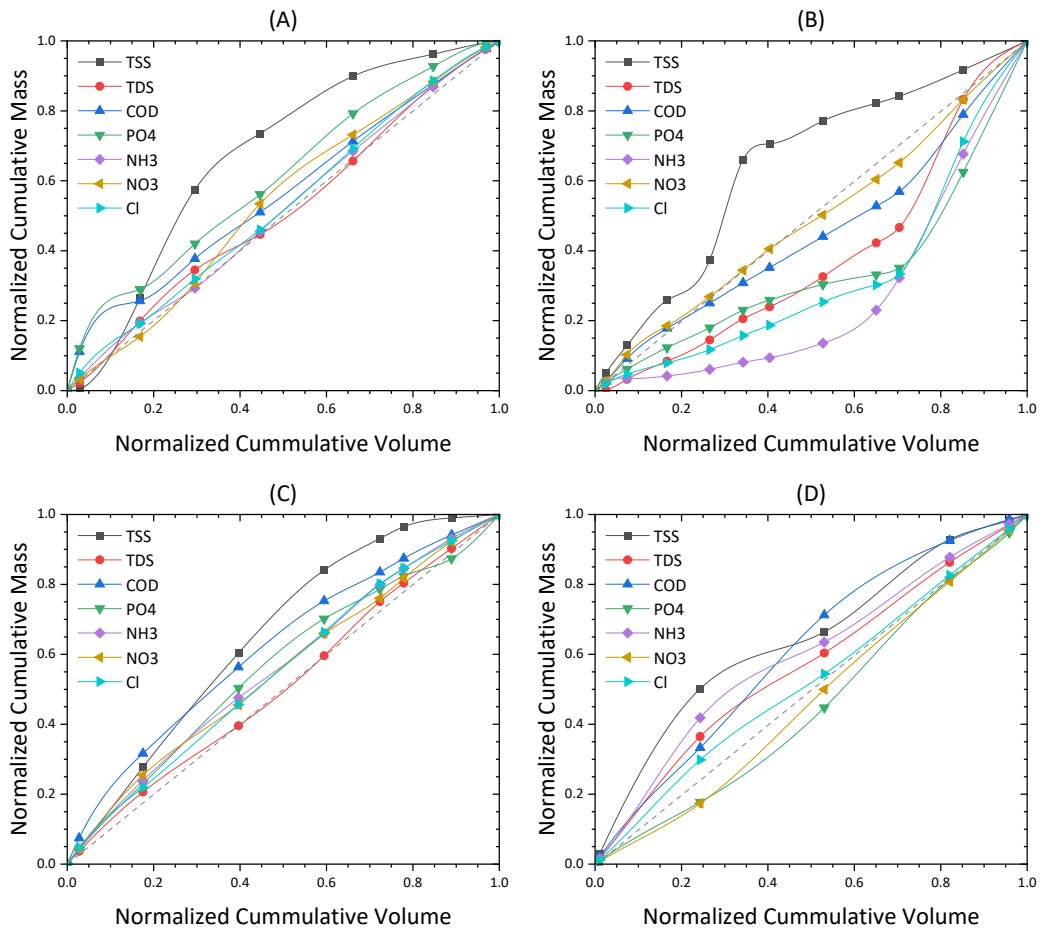


Figure 1. Normalized cumulative pollutant mass vs Normalized cumulative runoff volume for four (4) rainfall events

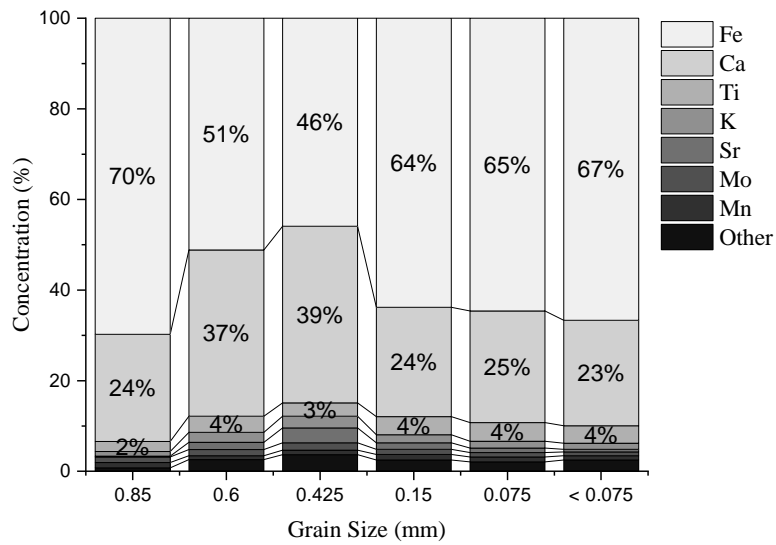


Figure 2. Plotted heavy metal concentration (%) in collected road-deposited sediments

4. CONCLUSIONS

First flush effect of water quality parameters and chemical constituents can be evaluated both qualitatively and quantitatively. In this study, first flush exists through the initial 10%–30% of the runoff for storm event with an average rainfall intensity of 5mm/hr. Hence, to effectively treat the stormwater runoff with minimum risk of discharging significant high loads of pollutants to natural receiving water bodies, it is recommended that at least the initial 30% of the runoff should be subject to treatment. Results of this study provide a localized framework for designing and implementing options for robust urban water management especially in designing appropriate LID controls that will address non-point source pollution in developing countries like the Philippines.

Acknowledgements: This research was supported by Department of Science and Technology Philippine Council for Industry, Energy and Emerging Technology Research and Development (DOST-PCIEERD) under the Human Resource Development Program with grant number PMIS#9755

REFERENCES

- Ahmad, Z. U., Sakib, S., Gang, D. D. (2016). Nonpoint Source Pollution. *Water Environment Research*, 88(10), 1594–1619. doi:10.2175/106143016X14696400495497
- Jeung, M.; Baek, S.; Beom, J.; Cho, K. H.; Her, Y.; Yoon, K. Evaluation of Random Forest and Regression Tree Methods for Estimation of Mass First Flush Ratio in Urban Catchments. *J. Hydrol.* 2019, 575, 1099–1110. <https://doi.org/10.1016/j.jhydrol.2019.05.079>.
- Stenstrom, M.; Kayhanian, M. First Flush Phenomenon Characterization. 2005.
- Xiang, L., Zhou, P.F., Chen, X. G., Zhu, Y. S., Yu, Z. B., Chen, X. (2013). Study on Non-Point Source Pollution in the Agricultural Watershed. *Advanced Materials Research*, 765-767(), 2926–2929. doi:10.4028/www.scientific.net/AMR.765-767.2926

ANTALYA WATER AND WASTE WATER AUTHORITY (ASAT) ACTION PLAN FOR WATER SCARCITY CAUSED BY CLIMATE CHANGE

Cem Çakmak

Antalya Water and Wastewater Authority, Antalya, TURKEY

ABSTRACT

Various negative situations caused by climate change affect negatively Turkey and Antalya province like the whole world. With this study, it is aimed to create a scientific and original document for the strategic decisions, actions and solution proposals regarding the detection of adverse situations caused by climate change and prevention and/or minimization of their consequences within the scope area of duty, authority and responsibility of Antalya Water and Wastewater Administration. In this study; the effects of climate change in Antalya: Drought Effect, Salinity Formation in Groundwater and Deterioration of Water Quality, Outdated Water Supply Projections, Emerging Need for Relatively More Investments, Emerging Need for Additional Water Resources will be discussed under the main headings. In this study; the measures implemented by the ASAT for the consequences of climate change: Reducing Water Losses, Prevention of Use of Drinking Water for Other Purposes, Department of Subscriber Affairs and Evaluation of Meter Reading performances, Control of Local Wells, Basin Protection Works, Water Saving Campaigns, System Efficiency Studies will be examined under the main headings. In this study; the measures planned to be implemented in the short and medium term by the ASAT for the consequences of climate change: Wild Flooding Irrigation, Preparation of Integrated Urban Water Management Plan, Preparation of Potable Water Master Plan, Increasing the number of physical leak detection equipment, Evaluation of rain water and wastewater from Treatment Plants, Development of Customer Relationship Management (CRM) software, Water Saving Campaigns will be examined under the main headings.

Keywords: *Climate Change, Drought, Water Losses, Water Saving Campaigns, System Efficiency*

1. THE EFFECTS OF CLIMATE CHANGE ON ANTALYA:

Drought:

Drought analysis information published by the Turkish State Meteorological Service reveals the extent of the drought threat awaiting Turkey. In addition to the actions to be taken by the central government for fighting drought, ASAT should take various measures. Signs of drought in Antalya can be listed as follows: Reduction of rain and snowfall in the basins that feed the regions where water supply is provided to the city of Antalya, The static water levels in the deep wells have decreased in the water production facilities, therefore it has become necessary to lower the submersible pumps deeper. Decreased water levels in springs where groundwater comes to the surface and river, lake, pond, reservoirs.

Salinity and Deterioration of Water Quality in Groundwater:

As a result of the decrease in groundwater a relatively large amount of seawater is mixed into the groundwater, increased movement of sea water to continent.

Outdated Projections for Water Supply:

ASAT measures the water demands of the constantly developing city of Antalya with the studies determined according to the population projections and sets strategic targets according to the results, makes budget studies and makes investments. However, due to this latest situation caused by climate change, it has become necessary to update the current projections and to carry out a drinking water master plan study for the whole of Antalya Province.

Need for More Investment:

This extraordinary new situation due to climate change makes it more difficult to use limited resources and invest.

Need for Additional Water Resources:

When considering the latest situation in Turkey and Antalya of climate change will bring, it will be necessary to research and determine new drinking and utility water resources in Antalya. The production of fresh water from the sea (desalination) which is currently being practiced in desert countries, is the worst possible situation and the most expensive for our province. This and all alternatives should be determined by a water master plan.

2. MEASURES IMPLEMENTED BY ANTALYA WATER AND WASTE WATER AUTHORITY FOR THE RESULTS OF CLIMATE CHANGE:

Reducing Water Losses:

Reducing of water losses that does not rise to the surface in the Antalya drinking water network is one of the most important working areas of the institution. Within the scope of this effort the following studies are carried out. “Basic Strategy and Responsibilities Report for the Management and Reduction of Water Losses in the Antalya Potable Water Network” was prepared and the short, medium and long-term actions to be taken to reducing against water loss and leakage were revealed. All kinds of components constituting the drinking water network and all kinds of data associated with them are saved in the GIS database. So the existing infrastructure has been made questionable and workable. Field control and calibration works are continuing to determine the accuracy of the infrastructure information saved in the GIS database. Standards have been developed to up-to-date the infrastructure information saved in the GIS database and how new manufacturing works by the contractor and the company will be transferred to GIS database. Flow meters have been installed at unmeasurable water production points. Thus, studies are continuing to determine the overall loss of the water system. General and local pressure management and optimization works are continuing in the network in order to reduce losses and leakages and pipe damages. The history of the urban pipe damages was revealed using the GIS infrastructure. As a result of revealing the pipe damages history, the condition grades of the network pipes were determined. The pipes in the streets where the damage repairs exceeded the amount determined by the company were took to the investment program and replaced. District Meter Areas (DMA) have been designed and determination of the water loss amounts in these regions has begun for reducing the amount of water loss in the city-wide. The amount of water supply is compared with the consumption in DMAs created as a result of network design studies and the items of losses are determined specifically for the area. The flow meters and other measurement devices installed in the DMAs has been connected to the operation center with SCADA. Alarms has been set for night flows

exceeding the determined seasonal limits, thus Leak Detection Teams have performed acoustic listening in the area. The reaction of the water network in existing and extraordinary situations has been simulated by using hydraulic modeling software. The water network is listened and water leakages are founded by using portable listening devices installed on metal network accessories and other leak detection equipment. The areas including physical water leaks are narrowed by performing step tests in DMAs. After the physical connections between private wells and water network are determining the water flowing into these wells is prevented by canceling these connections. Unmetered usage points (mosques, parks, gardens, cemeteries etc.) are determined and the water consumption found by installing meters in these points is added to the relevant part in the water budget. "Building Main Meter Subscription" application and accruing the differences to the subscribers was started for preventing the losses on the pipes between the subscriber branch connection and the meter collector. Thus, the visible and invisible leaks in this area will be repaired and the water treatment equipment backwash water will be accrued to the users. The conformity of the goods received to the institution to the relevant standards was started to be checked. Controls for the detection of illegal usages and penalties for detected users are continued. Necessary studies are continuing to prevent the using of fire hydrants for other than intended use. Building improvement, repair, maintenance and construction works continue in order to prevent water losses in drinking water tanks.

Prevention of Use of Drinking Water for Other than Purpose:

In rural areas transferred to the company by law, rural water tariffs determined by same law are relatively much cheaper than urban water tariffs. For this reason, the behavior of people living in rural areas to use drinking water for agricultural irrigation has emerged. This behavior should be strictly prevented. Due to the chlorine used for disinfection in content, ASAT drinking water is not suitable for agricultural irrigation. Water stress is frequently seen due to excessive agricultural irrigation in some regions. In order to meet the increasing water demand especially in summer season, pumps must be run for more hours or spare pumps must be put into operation. Thus, an excessive amount of groundwater is used and an excessive amount of electrical energy is consumed. For these reasons, an upper limit has been set showing the normal water consumption for people living in rural areas. High cost bills have been calculated for water consumption above this limit. Thus, the usage of drinking water for agricultural irrigation was prevented.

Evaluation of Meter Reading and Other Fieldwork Performances:

Meter reading, consumption, collection, debt follow-up, detection of illegal uses, energy usage, performance and efficiency studies are reviewed at monthly evaluation meetings with the participation of senior management. Necessary actions are taken for optimum use of available resources.

The Controlling of Local Wells:

The private wells in the regions where the ASAT sewerage network is located are checked and meters are installed in their outlet pipes. Thus, the water coming from the private wells to the ASAT sewerage network and from there to the ASAT wastewater treatment plants is accrued to the users. The central government should give the authority to inspect local wells to the ASAT, which is the local water authority. Thus, ASAT can penalize the inappropriate situations that will arise as a result of the inspection for the license and water amount allocation.

Basin Protection Studies:

All kinds of inspections and sanctions are carried out for the protection of the basins feeding the reservoirs of the Antalya city.

Water Saving Campaigns:

With the “Water is Life” project; the water cycle, the place of ASAT in the water cycle on Antalya scale, water leaks, need for water saving and its methods were explained to primary school students through 3D movies, education, study visit etc. techniques. With the "Repair Project", schools and mosques in Antalya were visited and faulty faucets and plumbing were repaired free of charge by ASAT's crew. With the posters hung in these places, it was tried to draw the attention of the public to water saving. With the "ASAT Whatsapp Chat Line", it was ensured that the public could share the water faults with company without giving an address, by simply sharing a location, thus to respond to the faults more quickly.

3. MEASURES PLANNED IN THE SHORT AND MEDIUM TERM TO BE IMPLEMENTED BY ASAT FOR THE RESULTS OF CLIMATE CHANGE:

Preventing Wild Flooding Irrigation:

One of the most important things to be done to prevent the drought caused by climate change is the prevention of Wild Flooding Irrigation. 70% of the fresh water in the world is used for irrigation Agricultural irrigation is not under control in Antalya. In addition, water wells should be inspected by looking to their license at what purpose they are drilled and how much water is allocated. It is necessary to give power of supervision and sanction to ASAT for resolving of lack of authority.

Preparation of Integrated Urban Water Management Plan:

With this report, the urban water management plan will be presented regarding the current situation and what needs to be done in drinking water, sewage, wastewater treatment and solid waste management.

Preparation of Potable Water Master Plan:

The amount of water that many settlements of Antalya need and will need will be calculated. Water demands will be determined. With the help of hydraulic modelling software; calculations, hydraulic analysis and design of drinking water networks will be made and current status will be update. It will be prepared all kinds of scientific documents for the regulation of water production and management activities. All necessary actions to reduce the amount of water loss in the network will be linked to a strategy. In this master plan, which is planned to be made in the medium term, the negative effects of climate change will definitely be examined.

Increasing the number of physical leak detection equipment:

Physical water leak detection equipment will be provided in the short term for the use of ASAT Branch Offices.

Reuse of stormwater and wastewater:

Necessary studies will be carried out to collect rainwater in various places and to feed groundwater. The effluent of treatment plants is used for the landscape irrigation of the plants. In addition, studies will be carried out for the use of the effluent of the treatment plants in parks, turf fields and ornamental pools.

EVALUATING THE PROPOSED CHECK DAMS PERFORMANCES ON FLOOD MITIGATION IN BOZKURT DISTRICT

Hayri BAYCAN¹, Uğur BOYRAZ^{2*},

¹ Author_1's Istanbul University-Cerrahpasa, Civil Engineering, Istanbul, Türkiye

² Author_2's Istanbul University-Cerrahpasa, Civil Engineering, Istanbul, Türkiye

*Corresponding author (uboyraz@iuc.edu.tr)

ABSTRACT

In recent years, the frequency and intensity of floods have increased considerably because of uncontrolled urbanization and climate change. Especially, the areas urbanized on the flood plain are at high flood risk. Flood damages can be substantially reduced by using flood control structures in these areas. Flood control structures play an important role in decreasing the maximum flow, controlling the surface runoff, trapping sediment, and increasing the lag time of the peak flow. This study aims to evaluate the effect of the check dams on flood prevention in the Bozkurt district. 11 check dams were designed and proposed in Ezine Stream Catchment for flood mitigation purposes. The check dams are defined in the hydrodynamic model of the catchment. The rainfall-runoff simulation was done using the August 10-11 flood event data. As result, the maximum flow rate in the region was reduced by 23.5% and the water level by 15.3% by using these 11 check dams.

Keywords: *Check dams, flood prevention, EPA SWMM, hydrodynamic model, flood.*

1. INTRODUCTION

Check dams are operative structures that are widely used in flood management. They help to control surface runoff, peak channel flow, and concentration time. The check dams also trap sediments and prevent reductions in channel capacity due to the sediment load (Abbasi et al., 2019). Designing check dams and determining their location in a catchment are crucial for the best flood mitigation performance. Yazdi et al. (2018) developed a model to optimize the design of check dams for flood control purposes in mountainous catchments. Wang et al. (2021) captured 74 percent of the incoming precipitation volume using check dams. Thus, they reduced the amount of the surface stored water by 3 times compared to the model without the check dams. For the best performance, it is important to accurately determine the storage capacity, weir properties, and effective dam height of check dams (Hassanli and Beecham., 2013). Huang et al., (2021) developed a method based on high-resolution topogrammetry besides traditional calculation methods by using a geographical information system to calculate storage capacity. Bozkurt, which is located in north Türkiye, is subjected to heavy rainfalls and flooding in recent years. One of the major flood events occurred on August 11, 2021, and caused serious damage in the Bozkurt city center. In this study, the check dams are proposed as a flood precaution in Bozkurt and the performance on flood mitigation is investigated. 11 check dams are proposed considering their effects on peak flow and concentration time. The effects on maximum flow rate and water depths are discussed.

2. MATERIAL AND METHODS

Model Development

Environmental Protection Agency Storm Water Management Model (EPA SWMM) was used to create a hydrodynamic model, and the required topographical data were obtained through the Quantum Geographical Information System. EPA SWMM is a dynamic simulation program that is used to model the rainfall-runoff relationship (Rossman, 2010). The channel, which is currently in construction, and 11 check dams were defined to the hydrodynamic model. Then, the characteristics such as height, depth, and location of the check dams were investigated for the best performance. While determining the potential dam locations, the factors such as the slope of the land and the storage volume were taken into consideration. Firstly, contour maps are created using QGIS. Then, the possible locations to build the check dams were selected. A total of 11 check dam locations were selected and defined as storage units in the SWMM model. The height-area curves of the check dams were determined. The maximum height of the check dams ranges from 13 m to 15 m. A weir structure was defined for each check dam to drain excess water. The orifices were defined to ensure continuous flow from the upstream to the downstream. The orifices were also used to apply the operating conditions of the check dams.

3. RESULTS AND DISCUSSIONS

In Figure 1 (a), the hydrographs obtained from the SWMM model were presented for two cases. In the first case, there are no check dams in the catchment, and in the second case, there are 11 check dams for flood control purposes. The hydrographs were obtained at the entrance of the Bozkurt city center. In both cases, the maximum flow rates were calculated at approximately 320 m³/s on the first day between the 8th and 20th hours. To be able to control the second peak, the orifices of the check dams operated to allow the upstream flow to pass through downstream; which also means that the check dams did not keep the water on the first day between the 8th and 20th hours.

In the first case, the maximum flow rate was calculated as 1684 m³/s on the second day of the analysis. In the second case, the maximum flow rate was calculated as 1288 m³/s, which shows that using check dams decreased the maximum flow rate by 23.5%. The orifices of the check dams were operated with a capacity varying between 10% and 50% during the 22nd-26th hours. This situation helped to control the check dams' storage volume and the weirs' load for reducing the peak flow.

In Figure 1 (b), the water depth-time graphs were presented for both cases. On the first day, water depth did not change in both cases due to the operating conditions of the check dams. On the second day, the maximum water depth was calculated as 3.84 m in the first case. Since the channel has a capacity of 3.5 m, flooding occurs. After using the check dams, the maximum water depth was calculated as 3.25 which means that the maximum water depth decreased by 15.3% and there is no flooding in the channel.

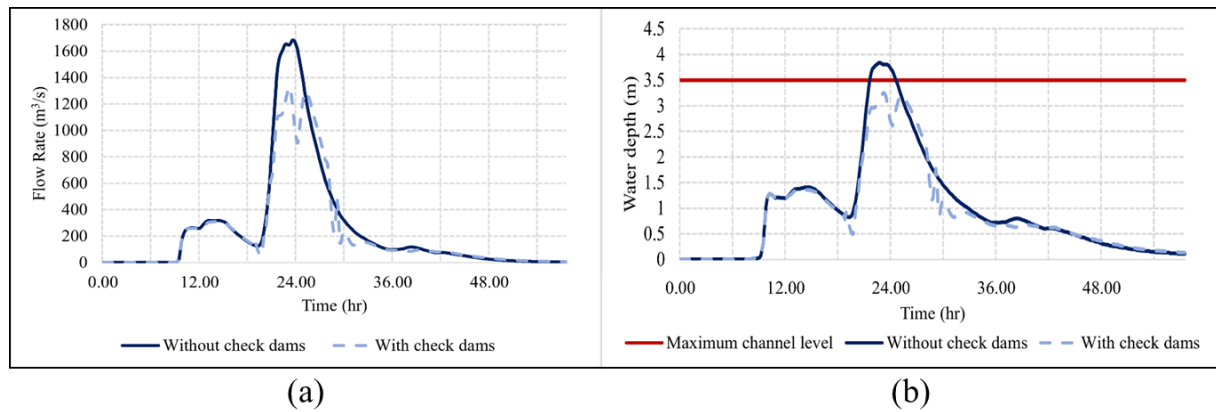


Figure 1. (a) The hydrographs at the entrance of the city center before and after check dams' applications. (b) The water depth obtained at the entrance point of the city center.

4. CONCLUSIONS

In this study, the hydrodynamic model of the Ezine Stream Catchment in Kastamonu, Türkiye, was created by using EPA SWMM. Since the previous improved channel was damaged due to the destructive flood on 11 August 2021, the new channel that is in construction was considered. Moreover, 11 check dams were defined in the model for flood control purposes. The hydrographs and the water depth-time graphs were obtained from both the check dam and non-check dam models. Additionally, the effect of check dams on peak flow is discussed. As result, flooding is still observed in the SWMM model without the check dams. The minimum number of 11 check dams, whose height is not greater than 15 m, helped to prevent the flood. According to the results obtained, it has been seen that check dams play a critical role in reducing the peak flow and controlling the flood. Moreover, the use of check dams by adjusting the operating conditions through orifices has enabled more productive usage of storage volumes to reach the best performance on peak flow reduction. Thus, the maximum flow rate and water depth have reduced significantly. For further research, the design/number/locations of the check dams may be improved using optimization tools in the study area according to the catchment characteristics.

REFERENCES

- Abbasi, N. A., Xu, X., Lucas-Borja, M. E., Dang, W., & Liu, B. (2019). The use of check dams in watershed management projects: Examples from around the world. *Science of The Total Environment*.
- Hassanli, A.M.; Beecham, S. (2013) Criteria for Optimizing Check Dam Location and Maintenance Requirements. Ph.D. Thesis, University of South Australia, Centre for Water Management and Reuse, Adelaide, SA, Australia,
- Huang, T., Ding, M., Gao, Z., & Téllez, R. D. (2021). Check dam storage capacity calculation based on high-resolution topogrammetry: Case study of the Cutou Gully, Wenchuan County, China. *Science of The Total Environment*, 790, 148083.
- Rossman, L. A. (2010). Storm water management model, user's manual, version 5. EPA/600/R-05/040. Cincinnati: Water Supply and Water Resources Division, National Risk Management Research Laboratory, USEPA.
- Wang, T., Hou, J., Li, P., Zhao, J., Li, Z., Matta, E., ... Hinkelmann, R. (2021). Quantitative assessment of check dam system impacts on catchment flood characteristics – a case in hilly and gully area of the Loess Plateau, China. *Natural Hazards*, 105(3), 3059–3077.
- Yazdi, J., Sabbaghian Moghaddam, M., & Saghafian, B. (2018). Optimal Design of Check Dams in Mountainous Watersheds for Flood Mitigation. *Water Resources Management*.

DERIVATION OF DAM BREAK EMPIRICAL EQUATION FOR DARLIK DAM IN ISTANBUL, TURKEY

Abdülbaki Hacı⁽¹⁾, Ezgi Selen Tilav⁽²⁾, İsmail Bilal Peker⁽³⁾, Rasim Temur⁽⁴⁾, Yasin Paşa⁽⁵⁾, Sezar Gülbaz⁽⁶⁾

⁽¹⁾ Faculty of Engineering, Civil Engineering Department, Istanbul University – Cerrahpaşa, Avcılar, Istanbul, Turkey

E-mail: abdulbakhaci0@gmail.com

⁽²⁾ Faculty of Engineering, Civil Engineering Department, Istanbul University - Cerrahpaşa, Avcılar, Istanbul, Turkey

E-mail: selentilav@gmail.com

⁽³⁾ Faculty of Engineering, Civil Engineering Department, Istanbul University - Cerrahpaşa, Avcılar, Istanbul, Turkey

E-mail: pekerbilal@iuc.edu.tr

⁽⁴⁾ Faculty of Engineering, Civil Engineering Department, Istanbul University - Cerrahpaşa, Avcılar, Istanbul, Turkey

E-mail: temur@iuc.edu.tr

⁽⁵⁾ Faculty of Engineering and Architecture, Civil Engineering Department, Istanbul Gelişim University, Avcılar, Istanbul, Turkey

E-mail: ypasa@gelisim.edu.tr

⁽⁶⁾ Faculty of Engineering, Civil Engineering Department, Istanbul University - Cerrahpaşa, Avcılar, Istanbul, Turkey

E-mail: sezarg@iuc.edu.tr

ABSTRACT

This study aims to investigate the effects of a possible dam failure under various likely scenarios and to derive an empirical formula for estimating peak flood flowrate at the downstream of the dam body after dam failure. Darlık Dam is located in Istanbul, Turkey and an earth-fill gravity dam. The downstream area of Darlık Dam is selected as the study area since this region has a high-density residential area. The dam failure scenarios are examined under three criteria which are the most sensitive parameters for the dam failure analysis. These parameters are bottom breach width (BBW), side slope (SS), and the breach development time (BDT). It is seen that the BBW is the most sensitive parameter among them. On the other hand, SS affects the peak values of dam breach scenarios slightly. Furthermore, the empirical formula is derived to predict the peak outflow occurred after dam break as a function of SS, BDT, and BBW. In this study, Hydrologic Engineering Center-River Analysis System (HEC-RAS) software program is used for dam break analysis. Coefficients of the empirical formula are determined by using meta-heuristic algorithms. For analyses, 840 simulations are performed in this study to develop empirical formula. The reliability of the empirical formula is evaluated by calculating the absolute per cent error between the peak value of the simulation results obtained by HEC-RAS and the calculated peak flowrate obtained by empirical formula. The results show that the performance of the empirical formula is satisfactory.

Keywords: Dam Failure Analysis, Flood, Darlık Dam, Empirical Formula, HEC-RAS 2-D.

1. INTRODUCTION

Dams are important structures for the economy of the country and provide the need for continuous water supply, which is essential for human life. However, the volume of water

stored in a dam always poses a risk to the downstream part of the dam (Bharath et al., 2021). The flood wave, which is caused by the dam collapse and spreads rapidly in the downstream direction, can cause the release of large amounts of water, serious material damage, and loss of life (Galoie et al., 2012). The magnitude of the flood wave, which is generally formed as a result of dam failure, is greater than the normal flood, the time to reach the peak flow period is shorter, and the time required for warning and evacuation of the people living in the residential areas downstream of the dam is very less (Kocaman, 2002). Therefore, evaluating the effects of different criteria on flood parameters is essential for the operation of dams and taking necessary measures to minimize the harmful effects of a dam failure. Moreover, estimating peak flood flowrate is of great importance in taking proper precautions to mitigate flood hazards.

2. MATERIAL AND METHODS

Darlık Dam is located between 41°08' and 40°50' north latitudes and 29°30' and 29°42' east longitudes. Darlık Basin is located within the administrative borders of both Istanbul and Kocaeli provinces in the Marmara Region in Turkey (Figure 1). Darlık Dam was constructed on Darlık Stream by the Turkish State Hydraulic Works (DSI) in 1989 (DSI, 2016). This dam, which provides both drinking and irrigation water, is the 5th largest dam reservoir in Istanbul (Cüceloğlu, 2013).



Figure 1. Location of Darlık Dam.

3. RESULTS AND DISCUSSIONS

The effect of the breach bottom width, breach development time, and side slope on the peak flow is shown in Figure 2. It is observed that BBW and BDT are sensitive parameters in dam failure analysis. On the other hand, the effect of the side slope is very low in the large breach bottom width and very high in the small breach bottom width. Moreover, the structure of the empirical formula is developed to predict the peak flood flow after dam break. The suggested empirical equation is shown in Equation 1.

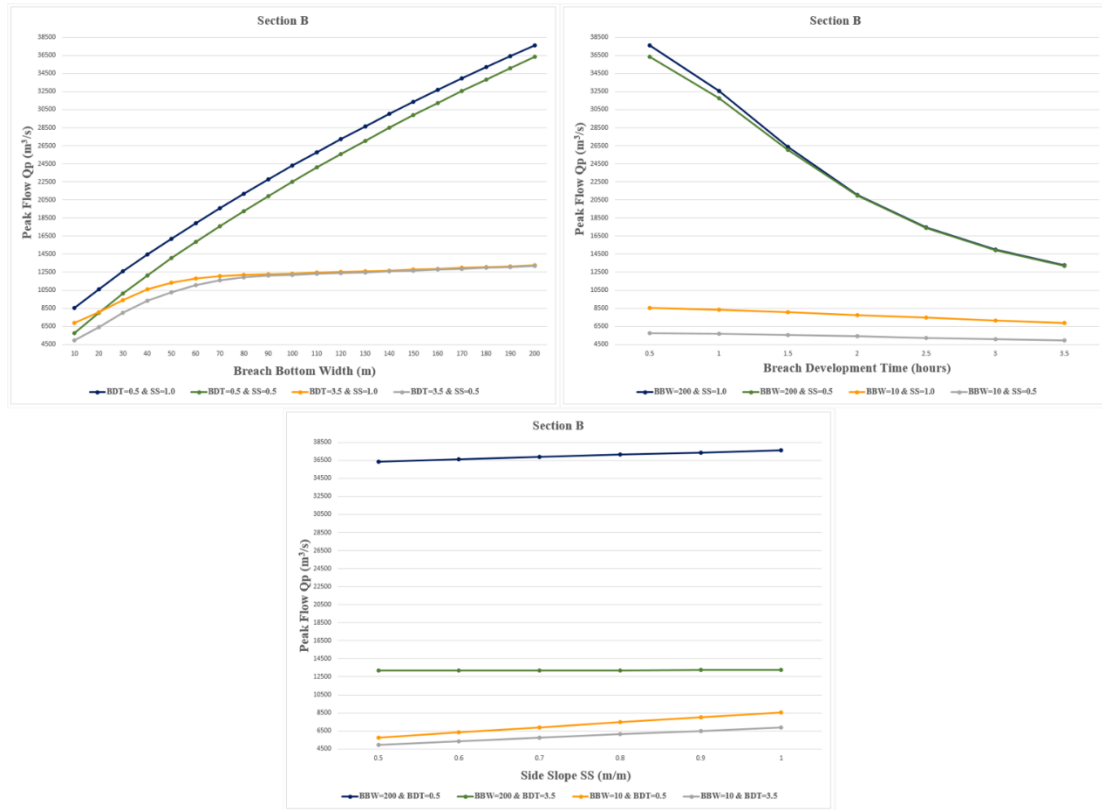


Figure 2. Q_p charts by criteria

$$Q_p = 2683.96 * \frac{(BBW)^{0.43} * (SS)^{0.11}}{(BDT)^{0.32}} \quad (Eq. 1)$$

4. CONCLUSIONS

In this study, BBW, SS, and BDT, are used to analyze dam break formation. It is observed that BBW and BDT are sensitive parameter in dam break analysis. On the other hand, SS affects the peak values of dam breach scenarios slightly. Furthermore, the empirical formula is developed depending on SS, BDT, and BBW. The results of the empirical formula developed herein are in good agreement with the simulated data obtained by HEC-RAS.

REFERENCES

- Bharath, A., Shivapur, A. V., Hiremath, C. G., & Maddamsetty, R. (2021). Dam break analysis using HEC-RAS and HEC-GeoRAS: A case study of Hidkal dam, Karnataka state, India. *Environmental Challenges*, 5, 100401.
- Galoie, M., Zenz, G., Eslamian, S., Motamedi, A. (2012). Numerical simulation of flood due to dam-break flow using an implicit method. *International Journal of Hydrology Science and Technology*, 2(2), 113–117.
- Kocaman, S. (2002). Dam break analysis and a case study, Master Thesis, Çukurova University, Institute of Science and Technology, Adana, Turkey.
- Cüceloğlu, G. (2013). Model supported hydrological analysis of Darlik watershed, Master Thesis, Istanbul Technical University, Institute of Science and Technology, Istanbul, Turkey.
- DSI, (2016). Turkish State Hydraulic Works (DSI) 2016 Official Water Resources Statistics.